

IAEA TECDOC SERIES

IAEA-TECDOC-1972

Benefits and Challenges of Small Modular Fast Reactors

Proceedings of a Technical Meeting



IAEA
International Atomic Energy Agency

BENEFITS AND CHALLENGES OF SMALL MODULAR FAST REACTORS

The following States are Members of the International Atomic Energy Agency:

AFGHANISTAN	GEORGIA	OMAN
ALBANIA	GERMANY	PAKISTAN
ALGERIA	GHANA	PALAU
ANGOLA	GREECE	PANAMA
ANTIGUA AND BARBUDA	GRENADA	PAPUA NEW GUINEA
ARGENTINA	GUATEMALA	PARAGUAY
ARMENIA	GUYANA	PERU
AUSTRALIA	HAITI	PHILIPPINES
AUSTRIA	HOLY SEE	POLAND
AZERBAIJAN	HONDURAS	PORTUGAL
BAHAMAS	HUNGARY	QATAR
BAHRAIN	ICELAND	REPUBLIC OF MOLDOVA
BANGLADESH	INDIA	ROMANIA
BARBADOS	INDONESIA	RUSSIAN FEDERATION
BELARUS	IRAN, ISLAMIC REPUBLIC OF	RWANDA
BELGIUM	IRAQ	SAINT LUCIA
BELIZE	IRELAND	SAINT VINCENT AND THE GRENADINES
BENIN	ISRAEL	SAMOA
BOLIVIA, PLURINATIONAL STATE OF	ITALY	SAN MARINO
BOSNIA AND HERZEGOVINA	JAMAICA	SAUDI ARABIA
BOTSWANA	JAPAN	SENEGAL
BRAZIL	JORDAN	SERBIA
BRUNEI DARUSSALAM	KAZAKHSTAN	SEYCHELLES
BULGARIA	KENYA	SIERRA LEONE
BURKINA FASO	KOREA, REPUBLIC OF	SINGAPORE
BURUNDI	KUWAIT	SLOVAKIA
CAMBODIA	KYRGYZSTAN	SLOVENIA
CAMEROON	LAO PEOPLE'S DEMOCRATIC REPUBLIC	SOUTH AFRICA
CANADA	LATVIA	SPAIN
CENTRAL AFRICAN REPUBLIC	LEBANON	SRI LANKA
CHAD	LESOTHO	SUDAN
CHILE	LIBERIA	SWEDEN
CHINA	LIBYA	SWITZERLAND
COLOMBIA	LIECHTENSTEIN	SYRIAN ARAB REPUBLIC
COMOROS	LITHUANIA	TAJIKISTAN
CONGO	LUXEMBOURG	THAILAND
COSTA RICA	MADAGASCAR	TOGO
CÔTE D'IVOIRE	MALAWI	TRINIDAD AND TOBAGO
CROATIA	MALAYSIA	TUNISIA
CUBA	MALI	TURKEY
CYPRUS	MALTA	TURKMENISTAN
CZECH REPUBLIC	MARSHALL ISLANDS	UGANDA
DEMOCRATIC REPUBLIC OF THE CONGO	MAURITANIA	UKRAINE
DENMARK	MAURITIUS	UNITED ARAB EMIRATES
DJIBOUTI	MEXICO	UNITED KINGDOM OF GREAT BRITAIN AND NORTHERN IRELAND
DOMINICA	MONACO	UNITED REPUBLIC OF TANZANIA
DOMINICAN REPUBLIC	MONGOLIA	UNITED STATES OF AMERICA
ECUADOR	MONTENEGRO	URUGUAY
EGYPT	MOROCCO	UZBEKISTAN
EL SALVADOR	MOZAMBIQUE	VANUATU
ERITREA	MYANMAR	VENEZUELA, BOLIVARIAN REPUBLIC OF
ESTONIA	NAMIBIA	VIET NAM
ESWATINI	NEPAL	YEMEN
ETHIOPIA	NETHERLANDS	ZAMBIA
FIJI	NEW ZEALAND	ZIMBABWE
FINLAND	NICARAGUA	
FRANCE	NIGER	
GABON	NIGERIA	
	NORTH MACEDONIA	
	NORWAY	

The Agency's Statute was approved on 23 October 1956 by the Conference on the Statute of the IAEA held at United Nations Headquarters, New York; it entered into force on 29 July 1957. The Headquarters of the Agency are situated in Vienna. Its principal objective is "to accelerate and enlarge the contribution of atomic energy to peace, health and prosperity throughout the world".

IAEA-TECDOC-1972

BENEFITS AND CHALLENGES OF SMALL MODULAR FAST REACTORS

PROCEEDINGS OF A TECHNICAL MEETING

INTERNATIONAL ATOMIC ENERGY AGENCY
VIENNA, 2021

COPYRIGHT NOTICE

All IAEA scientific and technical publications are protected by the terms of the Universal Copyright Convention as adopted in 1952 (Berne) and as revised in 1972 (Paris). The copyright has since been extended by the World Intellectual Property Organization (Geneva) to include electronic and virtual intellectual property. Permission to use whole or parts of texts contained in IAEA publications in printed or electronic form must be obtained and is usually subject to royalty agreements. Proposals for non-commercial reproductions and translations are welcomed and considered on a case-by-case basis. Enquiries should be addressed to the IAEA Publishing Section at:

Marketing and Sales Unit, Publishing Section
International Atomic Energy Agency
Vienna International Centre
PO Box 100
1400 Vienna, Austria
fax: +43 1 26007 22529
tel.: +43 1 2600 22417
email: sales.publications@iaea.org
www.iaea.org/publications

For further information on this publication, please contact:

Nuclear Power Technology Development Section
International Atomic Energy Agency
Vienna International Centre
PO Box 100
1400 Vienna, Austria
Email: Official.Mail@iaea.org

© IAEA, 2021
Printed by the IAEA in Austria
August 2021

IAEA Library Cataloguing in Publication Data

Names: International Atomic Energy Agency.
Title: Benefits and challenges of small modular fast reactors : proceedings of a technical meeting / International Atomic Energy Agency.
Description: Vienna : International Atomic Energy Agency, 2021. | Series: IAEA TECDOC series, ISSN 1011-4289 ; no. 1972 | Includes bibliographical references.
Identifiers: IAEAL 21-01435 | ISBN 978-92-0-124021-7 (paperback : alk. paper) | ISBN 978-92-0-124121-4 (pdf)
Subjects: LCSH: Nuclear reactors. | Fast reactors — Safety measures. | Sodium cooled reactors. | Liquid metal cooled reactors.

FOREWORD

The IAEA usually defines small and medium sized or modular reactors (SMRs) as reactors producing up to 300 MW(e) (small sized or small modular) and reactors producing 300–700 MW(e) (medium sized). There has been increasing interest in SMRs globally owing to their various benefits, such as flexible power generation options, the wide range of applications, enhanced safety resulting from inherent passive safety features, reduced upfront capital investment, and possibilities for cogeneration and non-electrical applications. At the same time, SMRs face various technical and economic challenges to their development and wide-scale deployment.

To understand the current status of the research and development in this area and to provide a forum to exchange information on related topics, the IAEA organized the Technical Meeting on Benefits and Challenges of Fast Reactors of the SMR Type in September 2019. The meeting brought together designers and researchers to discuss possible benefits of these reactors and the associated innovative systems that will help in their safe, secure, economical and early deployment, and to identify challenges that might impede the development of fast SMRs and find possible solutions to address the related issues.

A total of 23 peer reviewed papers were presented during the technical meeting, which was divided into four main technical sessions: (i) sodium cooled fast SMRs, (ii) heavy liquid metal cooled fast SMRs, (iii) safety aspects of fast SMRs and (iv) technology and research in support of SMR development. Three group discussions — on (i) in-factory construction, (ii) technological challenges to be resolved and (iii) benefits of fast SMRs including market needs — provided a comprehensive understanding of the most relevant topics in this area. All papers were peer reviewed by an international advisory group prior to the event. This publication presents the proceedings of the technical meeting and summaries of the technical and group discussion sessions, conclusions and recommendations discussed at the meeting, as well as the papers presented at the event.

The IAEA expresses its appreciation to all the contributors to this publication. The IAEA officers responsible for this publication were V. Kriventsev and C. Batra of the Division of Nuclear Power.

EDITORIAL NOTE

This publication has been prepared from the original material as submitted by the contributors and has not been edited by the editorial staff of the IAEA. The views expressed remain the responsibility of the contributors and do not necessarily represent the views of the IAEA or its Member States.

Neither the IAEA nor its Member States assume any responsibility for consequences which may arise from the use of this publication. This publication does not address questions of responsibility, legal or otherwise, for acts or omissions on the part of any person.

The use of particular designations of countries or territories does not imply any judgement by the publisher, the IAEA, as to the legal status of such countries or territories, of their authorities and institutions or of the delimitation of their boundaries.

The mention of names of specific companies or products (whether or not indicated as registered) does not imply any intention to infringe proprietary rights, nor should it be construed as an endorsement or recommendation on the part of the IAEA.

The authors are responsible for having obtained the necessary permission for the IAEA to reproduce, translate or use material from sources already protected by copyrights.

The IAEA has no responsibility for the persistence or accuracy of URLs for external or third party Internet web sites referred to in this publication and does not guarantee that any content on such web sites is, or will remain, accurate or appropriate.

CONTENTS

1.	INTRODUCTION	1
1.1.	BACKGROUND	1
1.2.	OBJECTIVE	1
1.3.	SCOPE	2
1.4.	STRUCTURE	2
2.	SUMMARY OF MEETING SESSIONS	3
2.1.	SESSION I: SODIUM COOLED FAST SMRS	3
2.2.	SESSION II: HEAVY LIQUID METAL COOLED FAST SMRS	6
2.3.	SESSION III: SAFETY ASPECTS OF FAST SMRS	8
2.4.	SESSION IV: TECHNOLOGY AND RESEARCH IN SUPPORT OF SMR DEVELOPMENT	10
3.	SUMMARY OF GROUP DISCUSSIONS	13
3.1.	GROUP DISCUSSION I: IN-FACTORY CONSTRUCTION	13
3.2.	GROUP DISCUSSION II: TECHNOLOGICAL CHALLENGES TO BE RESOLVED	14
3.3.	GROUP DISCUSSION III: BENEFITS OF FAST SMRS INCLUDING MARKET NEEDS	14
4.	CONCLUSIONS AND RECOMMENDATIONS	15
	REFERENCES	17
	ABBREVIATIONS	19
	PAPERS PRESENTED AT THE MEETING	25
	SESSION I: SODIUM COOLED FAST SMRS	27
	LARGE-EDDY SIMULATION OF THERMAL STRIPING IN THE UPPER INTERNAL STRUCTURE OF THE PROTOTYPE GEN-IV SODIUM- COOLED FAST REACTOR: DETAILED MODELLING AND SIMULATION WITH OPTIMAL FLOW REGION AND INTEGRATED SIMULATION WITH COMPONENT SIMPLIFICATION	28
	SMR CADOR: A SMALL SFR WITH INHERENT SAFETY FEATURES	40
	EVALUATION OF POTENTIAL SAFETY AND ECONOMIC BENEFITS AND CHALLENGES OF MODULAR SODIUM-COOLED FAST REACTORS	59
	FEASIBILITY STUDY OF SMALL SODIUM COOLED FAST REACTORS ..	73
	A PRELIMINARY STUDY OF AUTONOMOUS AND ULTRA-LONG LIFE HYBRID MICRO-MODULAR REACTOR COOLED BY SODIUM HEAT PIPES	90
	SESSION II: HEAVY LIQUID METAL COOLED FAST SMRS	101
	VALIDATION OF THERMAL HYDRAULIC DESIGN SUPPORT AND SAFETY METHODOLOGY AND APPLICATION SEALER	103
	LFR-SMR: AFFORDABLE SOLUTIONS FOR MULTIPLE NEEDS	118

INHERENT SELF-PROTECTION, PASSIVE SAFETY AND COMPETITIVENESS OF SMALL POWER MODULAR FAST REACTOR SVBR-100.....	131
CLFR-300, AN INNOVATIVE LEAD-COOLED FAST REACTOR BASED ON NATURAL-DRIVEN SAFETY TECHNOLOGIES	144
CONCEPTUAL DESIGN OF CHINA LEAD COOLED MINI-REACTOR CLEAR-M10D.....	152
LEAD FAST REACTOR TECHNOLOGY: A PROMISING OPTION FOR SMR APPLICATION	162
PRELIMINARY CONCEPTUAL DESIGN OF LEAD-COOLED SMALL FAST REACTOR CORE FOR ICEBREAKER	172
SEALER-UK: A 55 MW(E) LEAD COOLED REACTOR FOR COMMERCIAL POWER PRODUCTION.....	187
 SESSION III: SAFETY ASPECTS OF FAST SMRS.....	 195
EXPERIENCE IN THE PHYSICS DESIGN AND SAFETY ANALYSIS OF SMALL AND MEDIUM SIZED FBR CORES.....	197
INNOVATIVE MODELLING APPROACHES FOR MOLTEN SALT SMALL MODULAR REACTORS	212
NUMERICAL ASSESMENT OF SODIUM FIRE INCIDENT	224
ALFRED PROTECTED LOSS OF FLOW ACCIDENT EXPERIMENT IN CIRCE FACILITY	235
A PASSIVE SAFETY DEVICE FOR SFRS WITH POSITIVE COOLANT TEMPERATURE COEFFICIENT	250
 SESSION IV: TECHNOLOGY AND RESEARCH IN SUPPORT OF SMR DEVELOPMENT	 263
MYRRHA TECHNOLOGY AND RESEARCH FACILITIES IN SUPPORT OF HEAVY LIQUID METAL SMR FAST REACTORS.....	264
A MULTIPHYSICS APPROACH TO LFR ANALYSIS.....	280
ESTIMATION OF MINIMAL CRITICAL SIZE OF BARE ISO-BREEDING CORE FOR EIGHT SELECTED FAST REACTORS IN TH-U AND U-PU CYCLES	292
INTRODUCTION OF THE U.S. DOE VERSATILE REACTOR PROJECT...	305
A CHARACTERIZATION OF THE FINANCIAL RISK PROFILE OF FAST SMRS.....	316
 MEETING PROGRAMME	 341
MEETING ORGANIZATION	341
MEETING SESSIONS	341
GROUP DISCUSSIONS	344
INTERNATIONAL ADVISORY GROUP.....	344
 LIST OF PARTICIPANTS	 345
 CONTRIBUTORS TO DRAFTING AND REVIEW	 349

1. INTRODUCTION

1.1. BACKGROUND

There are several different small and medium sized or modular reactor (SMR) designs currently under development, which combine the benefits of operating a reactor in a fast neutron spectrum with the added benefits of SMR flexibility. For example, a fast reactor, in addition to its efficient use of fuel, can operate either as breeder to create more fissile fuel, or as a burner of plutonium and/or long-lived minor actinides. Combining this capability with the benefits of SMR power generation flexibility could produce additional advantages. However, it also introduces new challenges, technological and others, such as non-proliferation issues. Therefore, there is a need to identify such benefits and challenges of fast SMRs.

Currently, there are many state-of-the-art fast SMR designs with different features and systems under development and consideration, having both near and long-term deployment aspects. Modelling and simulation of advanced reactors are always challenging. One specific challenge is the development of new reactor simulation codes, physical and mathematical models and numerical techniques to address the issues specific to particular designs. Advanced fuel cycle options and actinide management can also have coupled challenges with the designs. Fast neutron spectrum reactors can use very different coolants including, but not limited to, liquid sodium, lead, lead-bismuth eutectic, molten salt, and helium, which might significantly challenge the structural integrity of the fuel and other reactor components. Several such issues were addressed by the fast reactor community through the presentations and the subsequent discussions during the IAEA technical meeting on *Benefits and Challenges of Fast Reactors of the SMR Type*, held in Milano, Italy in September 2019. The purpose of the meeting was to discuss both experiences and the latest innovations and technological challenges related to fast reactors of the SMR type. The meeting provided a forum to promote and facilitate the exchange of information on SMR fast reactors at the national and international levels and to present and discuss the current status of R&D in the field.

Taking recent developments into consideration, and in order to identify gaps and needs in fast SMR technology, the IAEA Technical Working Group on Fast Reactors (TWG-FR) recommended this meeting following Member States' request for information exchange in the area. The meeting, and hence the document, focuses on fast reactors of the SMR type and does not cover other large fast reactors or SMRs designed for the thermal neutron spectrum.

1.2. OBJECTIVE

In the world market of power-producing nuclear reactors, there is growing interest towards the so-called small and medium sized or modular reactors (SMRs). These reactors size is no larger than 300 MW(e); they can be assembled in workshop (in-factory construction), transported by ship or train, installed on site and connected to the electricity grid in a short time, significantly reducing the financial burden of the investment. Interest in SMRs is particularly strong in the European Union and the United States, Russia, Japan and Korea.

The first studies on SMR date back to the late 1980s and were mainly related to the light water cycles. Today, the various technologies of fast reactors have also undergone an improvement, so it seems plausible to conduct a critical overview even on the different concepts of Fast SMRs. It is meant to be noted that fast reactors offer the opportunity, thanks to breeding, to achieve very long production time before refuelling, making these machines very similar to “nuclear batteries”.

The objective of the present TECDOC is therefore to highlight and deepen the technological, economic and safety potential of Fast SMRs as well as the still open challenges that needs to be overcome in order to achieve sufficient credibility for market entry. The TECDOC also provides to the Member States a reference document, summarizing the work presented, including the full contribution, by the meeting participants.

1.3. SCOPE

This TECDOC is not only intended to overview engineering analyses of Fast SMR reactor concepts. Although it is mainly aimed to present innovative reactor solutions aimed to increase safety and simplicity of design, the parameters that contribute to the final cost of the plant are also considered. These additional elements help to verify the Fast SMRs market attractiveness.

The papers presented in the four sessions and the panel discussions are intended to provide an up-to-date picture of the benefits and challenges that industrial operators can encounter when addressing Fast SMR design concepts.

The scope of the present document is to present the state-of-the art of technology and discuss the benefits and challenges of fast SMRs.

This TECDOC presents the Proceedings of the Technical Meeting on Benefits and Challenges of Fast Reactors of the SMR Type, which was held in September 2019 in Milan. It includes summary of technical sessions, group discussions and includes the full papers which were submitted to and presented at the meeting.

1.4. STRUCTURE

Section 1 provides the introduction to the document, Section 2 summarizes the technical meeting session and discussions from the technical meeting, Section 3 provides a summary of group discussions, and Section 4 highlights conclusions and recommendations from the meeting. Full papers submitted to the meeting are also included in this document, categorized by technical sessions.

2. SUMMARY OF MEETING SESSIONS

2.1. SESSION I: SODIUM COOLED FAST SMRS

V. Kriventsev (International Atomic Energy Agency), A. Yamaguchi (Japan Atomic Energy Agency)

In Memoriam: Yury Ashurko[†] (IPPE, Russia)

The IAEA received a peer-review paper submitted by Dr Yury Ashurko (IPPE, Russia) who was planning to participate in the meeting in Milan but, sadly, passed away just a few days after the meeting. The deceased was a great professional who devoted all his life to studying and promoting the peaceful use of nuclear energy. Yury has published numerous publications on sodium cooled fast reactors technology, including reactor designs, safety features and regulatory issues. Ashurko, a brilliant nuclear engineer, was also a long-term member and frequent contributor of the IAEA Technical Working Group on Fast Reactors designated by Russian Federation. His contributions to the IAEA activities in the area of fast reactors technology development are hard to overstate. The IAEA includes his last scientific contribution in dedication to the memory of Dr Yury Ashurko.

In his paper, Y. Ashurko (IPPE, Russia, Paper ID #16) provides recommendations on improving safety characteristics of modular SFRs in order to reduce both cost of electricity production and the specific capital cost per reactor unit. In particular, an approach to improve capacity of a decay heat removal system (DHRS) is proposed that allows increasing rated thermal and electrical reactor power. It is shown that one of the most promising measures to improve economic performance of modular SFRs is to transition away from an expensive and complex DHRS, which is used in large sized SFR. Instead, a simple system of passive decay heat removal through the reactor vessel wall reduces cost, as well as raises nominal reactor power by increasing capacity of the DHRS. The proposed approach considers the cost due to beyond-design basis accidents (BDBA) occurrence frequency, and its consequences on economic performance of the nuclear power unit. A method for comparing impact of the change to cost of electricity is described. The author provides calculations that show the contribution to component of specific cost of electricity caused by possible expenses for eliminating BDBA consequences. It is shown that higher safety characteristics of a modular SFR against severe BDBA alone do not reduce the value of levelized cost of electricity (LCOE) to a level comparable to a large sized SFR. The author defines the values of probability of BDBA occurrence where modular SFR contribution to LCOE due to expenses on elimination of BDBA consequences does not exceed the same contribution for large sized SFRs as from $4 \cdot 10^{-8}$ to $1 \cdot 10^{-6}$ per reactor-year.

The analysis shows the impossibility of reaching the same economic indicators for modular SFRs as for large SFRs by only simplifying and improving safety systems and characteristics of modular SFRs. However, improving safety characteristics of modular SFRs in combination with measures taking advantage of its factory manufacturing can create good conditions for closing the gap in economic performance between modular and large sized SFR.

In Session I, participants presented and discussed four papers devoted to implementing sodium technology to small and medium sized fast reactors. Sodium has been used as a coolant for

[†] Deceased

nuclear reactors since Experimental Breeder Reactor EBR-I, which generated the first electricity produced by nuclear energy in 1951. The sodium technology is in its mature stage while sodium cooled fast reactors (SFRs) operation history includes about 500 reactor-years of successful operation worldwide. Many of the existing and past SFRs are small (experimental and test reactors) or medium-sized prototypes and could be formally classified as SMRs by their rated power. Nevertheless, small and medium power SFRs were not real SMRs but rather prototypes and demonstrators to test the technology with the final goal to build larger power reactor, similar to water cooled reactors. The development of advanced sodium small and medium sized reactors has attracted attention very recently following the global interest in SMRs. The main problem that designers of sodium cooled SMRs must address is that a typical SFR design includes intermediate coolant loop that is required to avoid aggressive chemical reaction of radioactive sodium in the primary circuit with water that is supplied to generation turbine. In comparison, the lead and lead-bismuth eutectic cooled fast reactors (LFRs), which were discussed at the following session, eliminate the need for a intermediate circuit and thus, radically decrease the capital cost. Nevertheless, several sodium cooled SMR designs have been proposed where the intermediate sodium circuit is either eliminated by replacing water with gas in Brayton cycle or the number of circulation loops in all three circuits are reduced. Sodium cooled SMRs can benefit from the proven mature technology but further researches are necessary to close technological gaps.

P. Gauthé (CEA, France, Paper ID #10) proposed a new concept of the sodium cooled loop-type reactor Core with Amplified DOppleR effect (CADOR) that combines SMR and SFR safety advantages to simplify the design in order to make these reactors affordable from the technical and economical point of view. CADOR provides inherent resistance to all accidents including unprotected reactivity insertions, which are a typical weakness in the SFR safety demonstration. The CADOR design allows eliminating the total meltdown of the core for all situations, including unprotected reactivity insertions. The target power of the CADOR reactor is 200 – 400 MW(th), i.e. 75 – 150 MW(e). The reactor is designed to remove the decay heat in natural convection with one system through the primary vessel without the sodium circuit. The reactor vessel diameter is less than 6m to allow road transportation. Depending on the selected reactor power, the vessel height is estimated between 10 and 20 meters. The intermediate coolant circuit is eliminated by applying the supercritical CO₂ Brayton conversion system, also increasing the efficiency of the plant. The feasibility of this type of cycle is not guaranteed for large power unit but can be envisaged for a SMR. However, additional studies are needed, including the choice of the fluid in the Brayton cycle. Further safety evaluations need to also include all classical transient analysis like the ULOF and local faults. The cost evaluation to assess the pros and cons of this new sodium cooled SMR are obliged to be also confirmed.

H. Hayafune (JAEA, Japan, Paper ID #23) presented a feasibility study of a new concept of sodium cooled, medium-sized, modular, one-primary-loop reactor of 300 MW(e) power. The reactor requires refuelling with metallic fuel once in 30 years. This SMR is compared with the other SFR designs, including pool-type reactors. One innovation that allows cost reduction is using a single sodium loop with two independent electromagnetic pumps arranged sequentially. The reactor vessel is dramatically simplified by eliminating a fuel handling system. There are two direct reactor auxiliary cooling systems (DRACS) and one intermediate reactor auxiliary cooling system (IRACS) for reactor decay heat removal. They are circulated by natural convection enhancing passive safety features in the decay heat removal operation. The evaluation of nuclear steam supply system mass shows that proposed one-loop-type concept can incorporate dramatically reduced material mass. Nuclear fuel cycle strategy with the modular reactor and recycle concept is thought to reduce R&D and financial risk since the

amount of budget for demonstration stage is relatively small and the facilities for demonstration are directly appropriated to commercial use. The authors study suggests that a total USD 1900 M budget for a set of a first-of-a-kind (FOAK) reactor and recycle plant can demonstrate fast reactor fuel cycle. The demonstration plant can be directly appropriated for commercial use without any significant design change. The rough estimation of the electricity costs shows that non-refuelling concept has competitiveness in remote areas.

S. Jang (KAIST, Rep. of Korea, Paper ID #27) introduced a conceptual design of the innovative micro-modular reactor cooled by sodium heat pipes. Twelve MW(th) hybrid micro modular reactor (H-MMR) are designed for autonomous continuous operation without refuelling over 20 years. The traditional SFR primary circuit where heat is removed from the reactor core by sodium flowing inside the fuel assemblies is replaced by the heat pipes with natural circulation of sodium. In this study, to enhance a neutron economy over an ultra-long core lifetime, the inverted FA concept using a low-density uranium mono-nitride (U15N) fuel with graphite moderator is adopted. The graphite is introduced to maintain mitigated excess reactivity by reducing the conversion ratio. The speaker explained that, in spite of using graphite moderator, the neutron spectrum in the core remains fast. Authors presented results of neutronics simulations that have been performed by Monte-Carlo code Serpent 2, using ENDF/B-VII.1 cross-sections library. It was found that the effect of the U15N-based inverted fuel assembly design allows achieving around 100-years reactor lifetime without refuelling, while the reactivity swing over the whole core lifetime is less than one dollar. The speaker noticed that H-MMR is in a preliminary conceptual design and future studies are required on optimization of the core design through the coupled analysis combined with the secondary system.

D. Kim (KAERI, Rep. of Korea, Paper ID #6) presented results of the numerical modelling of thermal striping in the upper internal structure of Prototype Gen-IV Sodium-cooled Fast Reactor (PGSFR). PGSFR is a 150 MW(e) medium sized reactor. Authors show that thermal striping phenomenon that may occur at the upper internal structure (UIS) above the core exit cannot be predicted by simple one-dimensional system codes and requires computational fluid dynamics (CFD) simulation in three dimensions. A large-eddy simulation (LES) model has been applied in the STAR-CCM+ CFD code. The model was first validated versus a triple jet experiment that modelled sodium mixing from the three-assembly core outlet. Then the LES model was extended to thermal striping at the UIS of the PGSFR. Meeting participants challenged the speaker with questions on applicability of the 3D CFD codes to the whole reactor core and primary system. It is obvious that thermal hydraulic simulations in 3D can be applied to the particular domain of the interest, the authors also proposed a coupling technique and conducted an integrated simulation that included all of the flow regions in the primary heat transport system was carried out to evaluate the performance of reactor vault cooling system (RVCS). The refined simplification models for the upper shield structure, heat exchangers, and core were developed. Simulations show that temperature distributions in the head access area, reactor, RVCS, and reactor support structures can be clearly resolved.

Presentations were followed by the discussion where participants reached consensus that sodium cooled SMRs could be safe and competitive, if optimized properly. The total structure mass can be reduced by either eliminating intermediate sodium circuit completely, by introducing Brayton conversion system, or by reducing the number of circulating loops. For SMRs, loop-type design seems preferable compared to traditional pool-type large SFR. However, in spite of the proven maturity of sodium technology, a lot of future researches are needed to reach economic competitiveness and, at the same time, to ensure the safety of sodium cooled fast SMRs.

2.2. SESSION II: HEAVY LIQUID METAL COOLED FAST SMRS

D. De Bruyn (SCK-CEN), J. Wallenius (KTH)

Eight of the twenty-three presentations were delivered in this session, which highlights the importance of heavy liquid cooled fast SMRs for many countries. Presentations on several designs ranging from 3 MW(e) up to 300 MW(e) were shared by Europe (SEALER, HYDROMINE and FALCON), two designs from China, Russia, and Republic of Korea. Two different coolants (Lead and Lead-Bismuth) are considered; we will not enter the now classical debate on the respective (dis)advantages of both coolants, as this debate has been published several times. The designs are considering single-unit reactors, even very small, as well as multiple-unit reactors (to fully use the “modular” aspect of the SMRs). We have classical reactors, sited on land, but also marine reactors, to be installed on icebreakers.

The paper presented by K. Zwijsen (NRG, Netherlands, Paper ID #1) focused on thermohydraulic design and validation of a small lead cooled nuclear power plant. The reactor operates at 8 MW(th) and is aimed at replacing diesel generators in remote Canadian regions, where fuel transport becomes expensive.

L. Cinotti (HYDROMINE, Luxemburg, Paper ID #2) presented the design of two related lead-cooled reactors. AS-200 is a 200 MW(e) compact and easy-to-operate installation, designed to reduce maintenance and inspection costs. The second design, TL-X, is a reduced version of the AS-200, aimed at providing a modular, plug-and-play battery reactor. Its power ranges from 5 up to 20 MW(e).

G. Toshinsky (IPPE, Russia, Paper ID #4) presented the concept of a 100 MW(e) Pb-Bi cooled reactor. This design prioritizes a higher standard of safety enabling it to be installed in the close vicinity of the consumer where a large amount of electricity is needed, like the mining industry. The installation must also be cost-competitive when compared to more classical alternatives.

Z. Chen (China Nuclear Power Technology Research Institute, China, Paper ID #7) presented the design of a 300 MW(e) reactor cooled with lead. However, Pb-Bi is currently envisaged as coolant for the smaller-size prototypes. Two inherent safety systems are implemented in the reactor. The aim is to improve simultaneously the economic performances and the safety; specifically, avoiding the necessity of evacuating the local population in severe accidents.

C. Liu (Institute of Nuclear Energy Safety Technology, China, Paper ID #15) presented the current design of the CLEAR-M (M for Mini) reactor, ranging from 1 to 100 MW(e) and cooled by lead. This reactor is proposed to cover a broad range of applications like remote regions or islands. Today, the design efforts are concentrating on the CLEAR-M10d and the prototype CLEAR-M10a, both having two independent residual heat removal systems and being designed for a long refuelling period.

G. Grasso (ENEA, Italy, Paper ID #24) presented how the design of the ALFRED reactor could be extended to the SMR topic. ALFRED is the result of several EC projects like ELSY (FP6) and LEADER (FP7). The current design is a 125 MW(e) reactor cooled by Lead. It is intended to be the demonstrator of LFR technology as the prototype of a commercial Lead cooled SMR (currently with a power around 250 MW(e)).

T.D.C Nguyen (Ulsan National Institute of Science and Technology, Rep. of Korea, Paper ID #29) presented the design of a reactor called SMLFR, to be installed on an icebreaker. Nuclear reactors in the marine industry are not limited to aircraft carriers or submarines. This requires an easy installation of the core on the ship, as well as easy removal after many years, 40 years in the present design. The reactor has a power of 15 MW(e), is cooled by Pb-Bi, and is using uranium nitride fuel. While this contribution was not presented during the workshop, it was considered useful to keep in the proceedings because of the good quality of the draft version and because it presented a different approach to land-based reactors.

J. Wallenius (KTH, Sweden, Paper ID #30) presented the current design of the lead-cooled 55 MW(e) SEALER-UK reactor. The reactor uses uranium nitride fuel, with no refuelling planned during the life of the plant. The global concept foresees blocks of four units, with the reactor vessels installed underground and only one turbine building for the four units. The aim is to reach a competitive cost and a reduced investment risk compared to either large nuclear power plants or more conventional reactors. Therefore, a large use of automatization is foreseen in factory, reducing the time for on-site construction.

2.3. SESSION III: SAFETY ASPECTS OF FAST SMRS

L. Longo (POLIMI), H. Hayafune (JAEA), P. Gauthe (CEA)

The session originally consisted of 4 papers:

- Experience in physics design and safety analysis of small and medium sized FBRs
- Numerical assessment of sodium fire incident
- ALFRED protected loss of flow accident experiment in CIRCE facility
- A Passive Safety Device for SFRs with Positive Coolant Temperature Coefficient
A fifth work
- Innovative modelling approaches for molten salt small modular reactors was instead presented in session IV, but following the discussion held at that session, it was decided to include in here

The session was opened by Mr Riyas Abdul Salim (Indira Gandhi Centre for Atomic Research (IGCAR), India, Paper ID #3), with the presentation “Experience in physics design and safety analysis of small and medium size FBRs”.

This research work stems from the observation that the increase in energy demand can be met by the use of fast reactors with high breeding ratio and low doubling time. The report describes the pros and cons in terms of safety of a small fast reactor compared to a medium size reactor. It highlights how, under the assumption that several active safety systems would fail, if an unprotected loss of flow accident (ULOFA) occurs, a passive heat removal system in a small reactor is more efficient than in a medium size reactor.

The second presentation, “Numerical assessment of sodium fire incident” was prepared at the Japan Atomic Energy Agency (JAEA) and presented by Mr Takashi Takata (Paper ID #25). In the article, reference is made to a verifiable accident in any type of sodium reactor, however, it is shown for the case of small reactors, where a ratio of the area of concrete wall surface to compartment volume increases in accordance with a decrease of the reactor dimensions. The case studied is a sodium leakage from a pipe. The article shows how, due to the heat released by the liquid metal in the surrounding environment, the temperature increases and the hydrogen in the walls can evaporate from the concrete and diffuse. In addition to this, the document discusses the difficulties and challenges of some calculation codes in simulating hydrogen generation during such an accident.

The third paper was presented by Mr Fabio Giannetti (Sapienza University of Rome, Italy, Paper ID #26). The presentation shares both experimental and numerical results from the European demonstration reactor ALFRED. ALFRED is a lead-cooled fast reactor and could be considered a prototype for an LFR commercial unit SMR. The purpose of the paper is to investigate the thermohydraulic behaviour of a steam generator for one of ALFRED's configurations: Steam Generator Bayonet Tube. The paper presents the main results obtained from the experimental reproduction of a Protected Loss of Flow Accident. A second part of the document is dedicated to the analysis of the characteristic parameters during the transient and the evolution of the thermal stratification in a large Heavy Liquid Metal pool.

The fourth contribution of the session was presented by Mr Yonghee Kim (Korea Advanced Institute of Science & Technology (KAIST), Paper ID #28). The study presents research on a Floating Absorber for Safety at Transient, FAST, that is able to insert negative reactivity in the case of increase in temperature of the coolant, which has a positive thermal coefficient of

reactivity. The study considers three anticipated transients without scram scenarios in which the performance of FAST has been analysed: (ULOF) unprotected loss of flow (ULOF), unprotected loss of heat sink (ULOHS) and the unprotected transient overpower (UTOP). The paper concludes that the feasibility of FAST is demonstrated by assuming severe ULOF, ULOHS and UTOP transients, with differing performance and results depending on the case. In perspective, the study suggests the use of more accurate simulation codes for a better evaluation of the FAST device performance.

As mentioned earlier, the last work of this session has been migrated from Session III. The research was presented by Mr Eric Cervi (Polytechnic School of Milan, Italy, Paper ID #8). The paper examines the case of a molten salt SMR and highlights the impact of system size on phenomena such as vacuum effects and fuel compressibility during fast transients driven by reactivity. A multiphysical model is proposed that considers a two-phase compressible model and a multi-group neutron diffusion model. The observed phenomena are typical of molten salt reactors of all sizes, however, they are amplified in small reactors due to increased neutron losses and therefore stronger vacuum and density reactivity feedbacks. Given the results, the work is a significant step forward in molten salt SMR modelling.

Each presentation was followed by 10 minutes of discussion with the whole audience. These discussions focused on the safety aspects of Fast SMRs. Different types of SMRs are taken for example covering lead, molten salts and sodium coolants. The safety aspects of SMRs are covered in all the work, but the studies also lead to differing results on larger reactors or subjects that do not concern safety. In general, this double aspect of works aimed at safety of both large reactors and SMRs, and in any case not only at fast-SMRs, raised criticism and appreciation addressed to all research without highlighting particular advantages and challenges.

Session 3 ended with 5 works and this is a good result not to be underestimated. All next generation reactors but SMRs in particular, are necessary to overcome challenges such as large-scale production and distribution of electricity, even in remote areas. Additionally, the importance of public opinion of nuclear power must be considered. In this sense, studies on safety aspects for new types of reactors are even more important because of their opportunity to gain public support.

2.4. SESSION IV: TECHNOLOGY AND RESEARCH IN SUPPORT OF SMR DEVELOPMENT

K. Tucek (EC/JRC), Z. Chen (CGN), L. Ren (CIAE)

Session IV discussed aspects related to the technology and research in support of the development of fast neutron spectrum SMRs. The session consisted of presentations from four IAEA Member States. This included: (i) two overview presentations on the development of flexible fast neutron spectrum irradiation facilities to support the assessment and qualification of fuels, materials, structures, and components for fast SMRs; and (ii) two detailed technical presentations related to multi-physics, neutronics, and thermal-hydraulic studies facilitating development and deployment of fast SMRs. In addition, it was decided to include in Session IV a single paper on financial risks of fast SMRs presented by S. Boarin (POLIMI, Italy, Paper ID #22) originally submitted to the planned session on Economic Aspects and Fuel Cycle of Fast SMRs that was excluded from the final meeting programme as it did not receive enough contributions.

The first presentation of R. Fernandez (SCK•CEN, Belgium, Paper ID #5) introduced the roadmap and development plan for the lead cooled SMR based on the MYRRHA technology. At the same time, it discussed the existing experimental facilities, including the thermal hydraulic bench, component research bench, material research facilities, as well as chemistry and coolant conditioning test rigs. MYRRHA (Multi-purpose hYbrid Research Reactor for High-tech Applications), currently being developed at SCK•CEN, will allow the demonstration of the accelerator-driven system (ADS) concept at pre-industrial scale, demonstration of transmutation of high-level nuclear waste, fuel developments for innovative reactor systems, material developments for Generation IV and fusion reactors, as well as radioisotope production for medical and industrial applications. To support the MYRRHA development, SCK•CEN has launched a strong and comprehensive R&D programme to address the main design and licensing challenges, in particular those related to the use of liquid lead-bismuth eutectic (LBE) as reactor coolant. In this frame, SCK•CEN has constructed, commissioned, and operates various LBE test facilities, including for: (i) the heavy liquid metal chemistry and conditioning research; (ii) the heavy liquid metal corrosion and mechanical property research for materials of advanced fast reactors; (iii) the testing of rotating components in heavy liquid metals; (iv) the reactor component hydraulic and hydrodynamic testing in a heavy liquid metal loop; and (v) the validation of complex flows in heavy liquid metal pool systems.

The second presentation by F. Heidet (ANL, USA, Paper ID #18) provided an overview of the development of the U.S. Department of Energy (DOE) Versatile Reactor Project (VTR). The project aims at addressing the domestic industry needs to deploy a fast neutron spectrum test reactor in order to accelerate irradiation testing and qualification of candidate fuels, materials, instrumentation, and sensors for fast SMRs. The construction of the reactor and start of its operation is envisioned by 2026. The VTR is designed to be a pool-type sodium-cooled fast reactor (based on the PRISM Mod-A plant layout) with a thermal power of 300 MW and fuelled by U-10Pu-10Zr ternary metallic fuel, using reactor-grade plutonium and low-enriched uranium with 5% ²³⁵U. The reactor is designed to offer peak fast fluxes and DPA levels in excess of 4.3×10^{15} n/cm²/s and 30 dpa/year, respectively, with up to 30 test locations concurrently available for irradiations (each having several litres of available testing space). In the designated test locations, VTR will also allow testing of fuels and materials in prototypical environments other than sodium including, but not limited to, lead, lead-bismuth eutectic, helium and molten salts. To optimise the reactor design, several trade-off studies were performed to determine the relationship between the maximum achievable peak fast flux (> 0.1 MeV) as a function of the

core power, while respecting basic thermal-hydraulic and temperature limits. The specific technology and siting of VTR will be selected by U.S. DOE following the methodology of the Analysis of Alternatives (AoA) and pursuant to the National Environmental Policy Act (NEPA).

The third technical presentation (PSI, Switzerland, Paper ID #21) by J. Křepel first introduced drivers behind the development of fast SMRs, discussing three pillars of sustainability (environment, economics, and social development), and the related potential advantages/features of fast SMRs. Furthermore, the study comprehensively analysed characteristics of the breeding and bare core size for eight fast core designs considered for SMRs (SFRs, LFRs, GFRs, and MSR), operating in the equilibrium U-Pu and Th-U cycle. The equilibrium fuel composition was evaluated assuming an infinite lattice configuration, with fission products neglected. Despite these simplifications, the results are quite indicative for the performance of each reactor concept and regarding the fuel composition in the equilibrium, the latter represented by an eigenvector of the Bateman matrix. The resulting system parameters were also subsequently used to estimate the minimum critical size of bare cores. Several other system performance parameters (such as the specific density of actinides and migration area) were also compared.

The fourth presentation (University of Bologna, Italy, Paper ID #9) by M. Sumini explained the development of the coupled multi-physics (neutronics-thermal-hydraulic) modelling tool, including the DRAGON lattice code, DONJON full core simulation code, and FEMUS 3D-porous media thermal-hydraulic CFD code, integrated in the SALOME platform. Both DRAGON-DONJON and FEMUS are open source simulation tools, developed by Polytechnique Montréal and University of Bologna, respectively. The modelling tool has been used to perform a preliminary study of a fast SMR, based on the ALFRED LFR concept. The lattice code was used to evaluate the macroscopic cross sections, collapsing the microscopic cross section data to 33 groups, and parametrizing them as a function of temperature and density. Using these macroscopic cross sections for the lattice cells, the distribution of neutron flux in the core was then obtained by the full core simulation with the DONJON code, while the thermal-hydraulic module (FEMUS) estimated the distribution of the coolant velocities, pressures, and temperatures in the reactor core. Preliminary results of the developed multi-physics approach were presented, which included the comparison of calculated k_{eff} -values during burn-up (vs. ERANOS and MCNPX) as well as estimations of 3D flux, power, and temperature distributions in the nominal operating conditions.

S. Boarin (POLIMI, Italy, Paper ID #22) presented a paper on “A characterization of the financial risk profile of fast SMRs: Comparison with SMRs of the PWR type”. The contribution was initially submitted to the planned session on Economic Aspects and Fuel Cycle of Fast SMRs that was excluded from the final meeting programme. The speaker reasonably concluded that financial risk is one of the reasons why SMRs are becoming more and more attractive in energy markets, despite a higher estimated levelized cost of energy (LCOE). Lower plant overnight cost reduces the financial risk of a project and makes the consequences of the risk manageable. The analysis of risks is carried out by means of an Analytical Hierarchy Process, which is suitable to the evaluation of factors with different metrics and/or which are not fully quantifiable. A comparative assessment of risk of Fast SMRs versus PWR SMRs is based on the opinions of the 18 experts in the nuclear industry. The expert panel included a range of individuals with different roles in the industry: from engineering, to safety and licensing, and including experts in nuclear economics. Some are entrepreneurs and NPP developers. Some are involved in fast reactor technology, others are generalists. The general results of the study show that Fast SMRs pay for the novelty of their concept in terms of higher financial risk perception.

During the discussion, several meeting participants indicated that a weak point of the presented approach is that some of the experts have limited or no knowledge of Fast SMR design features or phenomenology. The opinion of the selected experts is that PWR SMRs can rely on the experience of PWR technology and keep a competitive advantage in terms of risk perception over Fast SMRs. The higher risk perception associated with Fast SMRs in the critical construction phase is due to the lack of experience in project management of similar projects. Market strategy favours short-term return and lower risk projects. It is important to reduce the financial risk perception of an investment in Fast SMRs, at least for the deployment of the first units of this new technology. It is important to consider that financial risk assessment leads to general conclusions about Fast SMRs as a whole category. However, each fast reactor system has its own specific benefits and challenges that has a different impact on the financial risk perception.

Thematically, the Session also included the presentation of Dehee Kim (KAERI, Rep. of Korea, Paper ID #6), entitled “Large Eddy Simulation of Thermal Striping in the Upper Internal Structure of the Prototype Gen-IV Sodium-cooled Fast Reactor”. This presentation was given on the first day of the meeting during Session I (Sodium Cooled Fast SMR).

The Session highlighted the general lack of fast spectrum irradiation facilities for accelerated testing and qualification of new fuels, materials, and components for fast SMRs. This need is being addressed by the development and planned deployment of flexible fast neutron spectrum irradiation facilities, including MYRRHA (in Europe) and VTR (in US). These facilities will also provide unique capabilities for the qualification and further development of multi-physics tools for design, safety assessments, and licensing of fast SMRs. While fast SMRs are expected to be favoured in general public opinion, benefitting from their improved sustainability, intrinsic safety, better use of resources, and lower waste inventory, it appears necessary to reduce the perceived higher financial risk associated with fast SMRs. This may involve improved information and communication efforts, as well as the representative technology demonstration programs to increase the knowledge on performance characteristics of these innovative systems and gain the necessary experience feedback. In addition, appropriate, simplified regulatory frameworks are needed to mitigate the investment risks and accelerate the deployment. Complementary, new public policy and business models ought to be considered to decrease the financial risk and secure the necessary cash inflows. All these efforts require long-term strategic foresight, planning, and allocation of adequate resources by Member States.

3. SUMMARY OF GROUP DISCUSSIONS

3.1. GROUP DISCUSSION I: IN-FACTORY CONSTRUCTION

J. Wallenius (KTH)

The chair of the discussion (J. Wallenius) initiated the discussion by introducing an estimated breakdown of costs for recent construction of large PWRs in Europe with the following distribution:

- Direct construction cost: 20 %
- Indirect construction costs: 20 %
- Other costs, including licensing: 20 %.
- Financial costs: 40 %

Comparing to a published DOE benchmark on costs for building 1140 MW(e) PWRs in the US [1], the major difference is the financial cost, which historically has been smaller than direct and indirect constructions costs. However, increasing the average time for construction is associated with an increase in the risk of investment, both of which result in a higher financial cost. Hence, whereas publicly available databases quote the average WACC for a power utility in Western Europe at 5.7% [2], the WACC paid by EDF Energy for construction of Hinkley Point C is 9.2% [3].

Another point of concern, which was already pointed out in the early DOE study is the continuous increase in indirect construction costs during the US PWR build programme. These were mainly due to reduction in on-site labour productivity, caused by changing design, changing regulation and increasingly strict quality control measures. Hence, the rising costs for on-site field work is directly related to the increase in financial costs.

Several of the benefits resulting from in-factory-construction of SMRs are foreseen to address the above problems, namely:

1. Quality control is more easily implemented in factory environment than in-field.
2. Design changes due to teething problems of an immature design can be eliminated for the majority of the fleet
3. The time for construction can be reduced thanks to automated manufacturing procedures.

Consequently, factory production could potentially result in a significant reduction of capital costs for constructing new nuclear power plants.

During the discussion, the question was raised how many units a factory must produce to be able to provide the aforementioned benefits. Namely, in previous studies of costs for NOAK units, it has been indicated that cost reductions are mainly significant for the first few units of a series. J. Wallenius here stated, based on his conversations with Canadian automotive industry, that automated factory manufacture only becomes profitable when much larger series are produced. For reference, the intention of LeadCold is that its factories each would manufacture one reactor unit per month, for a total life-time production of 200 units. The cost of constructing such a factory has been estimated by partners of LeadCold to be about 300 M€.

Since small countries with a need of much less than 100 SMR units are among those interested in introducing SMRs, the question was raised whether such factories could be licensed for export of reactors. For this to happen, could a regulator from that small country accept or recognize a license issued by the regulator of the exporting country? This question relates to the ongoing attempts to harmonize regulation for large LWR designs, e.g. in Europe, which so far have been unsuccessful.

Another opportunity for cost reduction that was pointed out is the potential standardization of site preparation, which was successfully implemented in Japan.

3.2. GROUP DISCUSSION II: TECHNOLOGICAL CHALLENGES TO BE RESOLVED

V. Kriventsev (IAEA)

The discussion focused on several technical challenges that need to be resolved in order to achieve early deployment of fast SMRs. The main points are summarized in the Table 1

3.3. GROUP DISCUSSION III: BENEFITS OF FAST SMRS INCLUDING MARKET NEEDS

M. Ricotti (POLIMI)

The participants discussed key benefits of fast SMRs taking into consideration the needs of the market. The main points are summarized in the Table 1

4. CONCLUSIONS AND RECOMMENDATIONS

The presentations delivered at the Meeting and following discussions focused on the following basic question:

- Can fast SMR reactors gain a niche in the international market by ensuring greater safety at lower costs?

Considering the global level of this question, participants agree that answering the question is a real challenge for the technology. However, when the global problem is broken down into a series of specific technical and commercial aspects, it is shown that already some sub-challenges, if analysed individually by experts, can turned into benefits. Optimistically, it should be noted that during the four days of intense and stimulating discussions, no insurmountable challenges against fast SMR technology were identified.

Following these summaries, more detail about the aspects within this TECDOC, aimed to increase safety and reduce costs, are available. The comparison references for these potential benefits are both large size fast reactors and light water SMR. The resulting picture cannot offer a quantification of the human and financial resources that are required to address all unresolved challenges, but it will offer a qualitative image that could attract investors and interest engineers.

For sake of simplicity the main features, in term of safety enhancement and cost reduction, are labelled as benefits or challenges in the following table.

TABLE 1 SAFETY ENHANCEMENT AND COST REDUCTION BENEFIT-CHALLENGE ANALYSIS

Safety enhancement		Cost Reduction	
No off-site reactivity release	<i>Challenge</i>	Simple components	<i>Challenge</i>
Inherent safety	<i>Challenge</i>	Compact layout	<i>Challenge</i>
Large Doppler reactivity feedback	<i>Benefit</i>	Enhanced breeding	<i>Benefit</i>
Low coolant density reactivity effect	<i>Benefit</i>	Higher burnup	<i>Benefit</i>
Negative void reactivity feedback (in small cores)	<i>Benefit</i>	Long operation without refuelling	<i>Challenge</i>
Practical elimination of the core melting	<i>Challenge</i>	Modular construction + learning curve	<i>Challenge</i>
Natural circulation (without tall chimney)	<i>Benefit</i>	In-factory construction	<i>Challenge</i>
Fully passive DHR	<i>Challenge</i>	Easy transportation	<i>Benefit</i>
High or very high boiling temperature	<i>Benefit</i>	Reduced construction time accelerating pay-back	<i>Benefit</i>
Low coolant density reactivity effect	<i>Benefit</i>	Reduction of financial risks	<i>Challenge</i>
Passive radiation of primary vessel	<i>Benefit</i>	Reduced cost of decommissioning	<i>Benefit</i>
Code benchmark and code validation on UTOP, ULOF, ULOHS	<i>Benefit</i>	Lower capital cost	<i>Benefit</i>
Low operational pressure (except from gas cooled)	<i>Benefit</i>		
Elimination of population evacuation	<i>Challenge</i>		
No risk of hydrogen release (apart from sodium cooled)	<i>Benefit</i>		

Most of the meeting participants explained how they intend to address some, or all the challenges listed in the above table by wisely using the inherent benefits offered by the various fast SMR concepts. For this purpose, innovative reactor configurations have been described which can make the best use of the small core size and of specificities of the selected coolants. Engineering solutions have also been presented to simplify manufacturing, to implement passive actuation systems for enhanced safety, to reduce management costs through innovative fuels for extended life of the core. In addition, decay heat removal devices have been presented, together with calculations, that demonstrate effectiveness of these systems even in the worst operating conditions, guaranteeing the highest degree of the reactor safety. Additionally, several presentations also included interesting cost assessments.

REFERENCES

- [1] Phase VIII update (1986) report for the Energy Economic Data Base Program EEDB-VIII, DOE/NE-0079, Department of Energy, 1986.
- [2] ASWATH DAMODORAN, http://people.stern.nyu.edu/adamodar/New_Home_Page/datacurrent.html. New York University, 2020
- [3] JONATHAN FORD, <https://www.ft.com/content/f9a96304-e980-11e8-885c-e64da4c0f981>, Financial Times, November 22nd 2018.

ABBREVIATIONS

ADS	accelerator driven system
AFA	alumina-forming austenitic
ALFRED	advanced lead fast reactor european demonstrator
ALIP	annular linear induction pump
ANL	Argonne National Laboratory
ASTRID	advanced sodium technological reactor for industrial demonstration
ATWS	anticipated transients without scram
BDBA	beyond design basis accidents
BOP	balance of plant
BOC	beginning of cycle
BOL	beginning of life
BP	british petroleum
CADOR	Core with Amplified DOppleR effect
CC	cold collector
CFD	computational fluid dynamics
CGN	China General Nuclear Power Corporation
CHPCIT	combined heat and power generation
CLEAR-M	core inlet coolant temperature
COMLOT	China lead-based mini-reactor
CRDM	components loop testing
CTC	control rod drive mechanism
CV	coolant temperature coefficient
CVR	control volume
	coolant void reactivity
DHX	decay heat exchanger

DHRS	decal heat removal system
DRACS	direct reactor auxiliary cooling system
EBR	experimental breeder reactor
EFPD	equivalent full-power days
EFPY	equivalent full power year
ELSY	European lead-cooled system
EMP	electromagnetic pumps
EOC	end of cycle
EOL	end of life
E-SCAPE	European scaled pool experiment
ESS	energy storage system
FA	fuel assembly
FAST	floating absorber for safety at transient
FASTER	fast test reactor
FBR	fast breeder reactor
FDS	fast reactor structural design standard
FFT	fast Fourier transform
FFTF	fast flux test facility
FOAK	first of a kind
FTC	fuel temperature coefficient
GEC	gas-enhanced circulation
HAA	head access area
HC	hot collector
HERO	heavy liquid metal pressurized water cooled tubes
HEXACOM	heat exchanger at complot
HLM	heavy liquid metal
HMMR	hybrid micro modular reactor

HRS	heat removal system
HTR	high temperature reactor
IHX	intermediate heat exchanger
IFR	integrated fast reactor
IMR	integrated modular water reactor
INL	Idaho national laboratory
IRACS	intermediate reactor auxiliary cooling system
IV	internal vessel
IVS	in-vessel storage
JAEA	Japan Atomic Energy Agency
KAERI	Korea Atomic Energy Research Institute
LBE	lead-bismuth eutectic
LCOE	levelized cost of electricity
LES	large eddy simulations
LFR	lead-cooled fast reactor
LOCA	loss of coolant accidents
LUEC	levelized unit electricity cost
LWR	light water reactor
MA	minor actinides
MMR	micro-modular reactor
MOC	middle-of-cycle
MOX	mixed oxide
MSR	molten salt reactor
MV	main vessel
MYRRHA	multi-purpose hybrid research reactor for high-tech applications
NDDHRS	natural driven decay heat removal system
NDS	natural-driven safety

NDSS	natural driven shutdown system
NOAK	Nth-of-a-kind
NP	nuclear power
NSSS	nuclear steam supply system
ODE	ordinary differential equations
ODS	oxide dispersion strengthened
ORNL	Oak Ridge national laboratory
PGSFR	prototype gen-IV sodium-cooled fast reactor
PRACS	primary reactor auxiliary cooling system
PRISM	power reactor inherently safe module
PSA	probabilistic safety analysis
PV	primary vessel
PWR	pressurized water reactor
RANS	Reynolds-averaged Navier-Stokes
RCP	reactor coolant pumps
RMB	reactor monoblock
RMS	root mean square
RV	reactor vessel
RVACS	reactor vessel auxiliary cooling system
RVCS	reactor vault cooling system
SASS	self-actuated shutdown systems
SCWR	Super critical water reactor
SEALER	Swedish Advanced Lead Reactor
SFR	sodium cooled fast reactors
SG	steam generator
SGS	sub-grid-scale
SGTR	steam generator tube rupture

SMLFR	small modular lead fast reactor
SMR	small and medium-sized or modular reactor
SNF	spent nuclear fuel
STGS	spiral-tube steam generators
TFM	turbine flow meter
TRU	transuranic
TWG-FR	technical working group on fast reactors
UIS	upper internal structure
UN	uranium nitride
ULOF	unprotected loss of flow
ULOHS	unprotected loss of heat sink
UTOP	unprotected transient overpower
vSMR	very small reactor
VTR	versatile test reactor
XS	cross sections

PAPERS PRESENTED AT THE MEETING

SESSION 1: SODIUM COOLED FAST SMRS

LARGE-EDDY SIMULATION OF THERMAL STRIPING IN THE UPPER INTERNAL STRUCTURE OF THE PROTOTYPE GEN-IV SODIUM-COOLED FAST REACTOR: DETAILED MODELLING AND SIMULATION WITH OPTIMAL FLOW REGION AND INTEGRATED SIMULATION WITH COMPONENT SIMPLIFICATION

Paper ID #6

D. KIM
Korea Atomic Energy Research Institute
Daejeon, Republic of Korea
Email: dehee@kaeri.re.kr

S.R. CHOI, J.W. HAN, S. YEOM
Korea Atomic Energy Research Institute
Daejeon, Republic of Korea

S.H. RYU
Korea Electric Power Research Institute
Daejeon, Republic of Korea

Abstract

Small and medium-sized or modular reactors (SMRs) are becoming the centre of interest in the nuclear field due to their improved safety features and merits in cost. Most of the SMRs employ passive safety systems, and their components are installed in an integrated arrangement for compactness. The SMRs' design features require more specific modelling and simulation. In order to evaluate the design performance at the component level, a detailed modelling and simulation capability has to be provided since conventional 1D system codes cannot provide a sufficient resolution for thermal-hydraulic phenomena. For the detailed modelling and simulation on a SMR, computational fluid dynamics (CFD) is an essential tool. The SMRs' design features have to meet design requirements for thermal-hydraulic transients. Multi-dimensional multi-physics phenomena such as coolant mixing and heat transfer, including convection, conduction, and radiation, need to be investigated thoroughly from a design stage through performance evaluation and safety analysis. However, detailed modelling of the entire reactor requires too heavy computing load. Therefore, compromising approaches are necessary. The paper presents a systematic approach for accurate modelling and simulation with a reduced computing load. The necessity of a large eddy simulation for thermal striping analysis in a sodium-cooled fast reactor (SFR) and its efficient application technique are presented to assess the thermal fatigue's probability. Another case is an integrated simulation of the SFR reactor's entire primary heat transport system, where it is evaluated through the integrated modelling design performance of a reactor vault cooling system.

1. INTRODUCTION

Most of the small and medium-sized or modular reactors (SMRs) employ more secure design features such as passive safety systems, and their components are installed in an integrated arrangement for compactness and modularization. Some fast SMRs adopt a long-life core design. The system features of SMRs require detailed multi-dimensional multi-physics assessment for safe design and operation. In order to evaluate the design performance at a component or reactor level, detailed modelling and simulation have to be carried out since conventional 1D system codes [1, 2] cannot provide a sufficient resolution for thermal-hydraulic phenomena. Computation fluid dynamics (CFD) [3, 4] is an essential tool for detailed modelling and simulation. When applying CFD to a SMR, the computation domain for 3D CFD is reduced dramatically because of its smaller inventory compared to the conventional large-

sized reactors. However, even if a small-sized reactor is simulated, solving full-scale Reynolds-averaged Navier-Stokes (RANS) equations with a complete conjugate heat transfer or full-scale large eddy simulation (LES) is not yet affordable considering the computing resources. The paper presents a systematic approach for an affordable LES as well as for an efficiently integrated thermal-hydraulic simulation of the entire PHTS.

At the Korea Atomic Energy Research Institute (KAERI), a sodium-cooled fast reactor (SFR) named the Prototype Gen-IV Sodium-cooled Fast Reactor (PGSFR) was designed [5]. The PGSFR is a small-sized fast neutron reactor with a capability of 150 MW(e) electricity generation. The PGSFR aims to verify the TRU metal fuel performance, stable reactor operation, and transmutation ability of high-level radioactive wastes.

For the reactor core of the PGSFR, sodium coolant flowing inside a subassembly is not mixed with the sodium of neighbouring subassemblies and the flow rate through each subassembly is assigned separately from the other subassemblies. Therefore, core exit temperatures from the subassemblies become different from each other. In particular, the temperature difference between the hot sodium discharged from the fuel subassembly and the relatively low temperature sodium exiting from the control subassembly is definite. The coolant mixing with different temperatures draws temperature fluctuations at the structure's surfaces located near the core exit. This phenomenon is called thermal striping, which can induce periodic thermal fatigue and consequently deteriorate the integrity of the structures that are important for reactor safety.

The thermal striping mainly occurs at the upper internal structure (UIS) located right above the core exit. It is well-known that the thermal damage caused by the thermal striping tends to increase as the structure's location approaches the core exit. The bottom plate of the UIS is located at a sufficiently high level from the core exit to avoid severe effects from the thermal striping. However, the control rod drive mechanism (CRDM) guide tubes and thermocouples to monitor the subassembly temperatures locate closely to the core exit. Therefore, the CRDM guide tubes may suffer from severe thermal striping due to the strong inflow from the fuel subassemblies.

In this work, a numerical analysis was carried out to analyse the thermal striping phenomena in the UIS of the PGSFR. LES was applied to predict the temperature fluctuations in the UIS region because the popular RANS model is not adequate to capture rapidly oscillating turbulent flow physics. Before applying the LES to the UIS, the numerical approach utilizing the LES model was applied to a triple jet experiment to validate the capability of predicting the key flow physics. Further, in order to avoid a huge computing load required for the LES computation, the computational domain was reduced by a systematic approach in which the boundary conditions were modelled elaborately.

A passive decay heat removal system is more important in SMRs to enhance the reactor's safety. A high temperature operating condition for SFR draws concerns about thermal fatigue damage to the reactor vessel, containment vessel, and reactor support structures, including concrete cavity structures. The PGSFR employed a reactor vault cooling system (RVCS), which is an engineering feature that removes the heat released from the core through the containment vessel via a natural convection to protect the concrete cavity during normal operation and to remove the decay heat in the case of severe accidents [6].

The key structures of the RVCS are ducts, an air separator between the containment vessel and the concrete wall, and air stacks. Air comes down along the outer surface of the air separator, and the air turned to the opposite direction at the air separator bottom. Then it rises, removing the heat from the containment's outer surface. The heated hot air is discharged through the air stacks. Over the heat transfer path from the core to the RVCS' air flow, the heat transfer mechanisms of conduction, convection, and radiation are involved in a coupled manner. In order to design the RVCS, the temperature distribution over the support structures, the vessels, and the concrete wall has to be closely observed. Therefore, the thermal-hydraulic behaviour in the RVCS, sodium pools inside the reactor vessel, and head access area (HAA) also needs to be calculated in a coupled manner. The paper presents an integrated thermal-hydraulic modelling of such regions. However, the configuration of the entire geometry is difficult for detailed simulation. Therefore, simplified models have to be developed. The paper presents a refined model that can reduce the computing load and yet reproduce accurate results.

2. LARGE EDDY SIMULATION OF THE UPPER INTERNAL STRUCTURE

For a reactor utilizing a high coolant temperature, the creep-fatigue is a mechanism that can deteriorate the structural integrity. Repeated thermal cycles by thermal striping can accelerate the creep-fatigue's damage on the structures. In a thermal striping region, the turbulent flow fluctuates with high frequencies. The RANS approach is not sufficient to resolve the flow physics. The LES adopts a spatial filter to divide the eddies into larger and smaller eddies, in which the larger eddies are resolved without artificial modelling, and the smaller eddies are modelled by sub-grid-scale (SGS) stresses. Compared to the general purpose RANS turbulence models, which are time-averaged models, the LES can resolve time dependent fluctuations of flow variables more accurately. However, it is difficult to apply the LES to the entire domain inside the reactor vessel due to the enormous number of meshes. The paper represents a way to set up a computational domain that is reasonable for affordable LES simulation by pre-evaluation using RANS simulation.

2.1. Preliminary simulation

Before applying the LES to thermal striping in the PGSFR UIS region, the LES model was validated through a triple jet experiment [7]. The jets were discharged from three slots that were composed of a central slot for feeding hot air and both-sided slots for feeding cold air. The three slots had the same dimensions of which the width (W) and length were 0.015 m and 0.15 m, respectively. Each slot was separated by $2.5W$. The duct into which the jets enter had dimensions of a cross sectional area of $24W \times 24W$ and a stream-wise length of $133W$. The mesh size was 2.5 mm around the slots and 5 mm for the remaining region by which the total number of grids reached about 4 million.

Jets composed of 65°C hot air and 41°C cold air were injected into an air duct with the same velocity of 10 m/s. The LES with the WALE SGS model [8] and RANS with a realizable $k-\epsilon$ model were carried out for comparison purposes. STAR-CCM+ [9] was utilized for numerical simulations. The unsteady time step size was set to 0.0002 s. At a measuring position, a comparison between the simulation results and experimental data is summarized in Table 1, in which the differences between the LES and experiment were 1.3% by the mean value and 6.1% by the root mean square (RMS) value, respectively.

TABLE 1. COMPARISON OF TEMPERATURE AT A POINT (15W AWAY FROM SLOT CENTRE)

	Mean Temp. [°C]	RMS Temp. [°C]
Experiment	46.5	3.3
LES	47.1	3.1

Instantaneous temperature distributions at the mid plane obtained from the RANS and LES models are shown in Fig. 1. Both models produced different flow patterns. Complicated temperature fluctuations by turbulence mixing were only observed in the LES model. The LES apparently showed that large eddies started to shed near the jet slots, and the fluctuations disappeared as the flow went downstream. The time-averaged temperature profiles were compared with the experimental data in Fig. 2. The RANS model over-predicted the fluid temperature at the centre line but underestimated it at both sides. The LES gave more accurate results than the RANS model. The RANS model could not resolve the temporal and spatial temperature variations of the thermal striping generated from the triple jet.

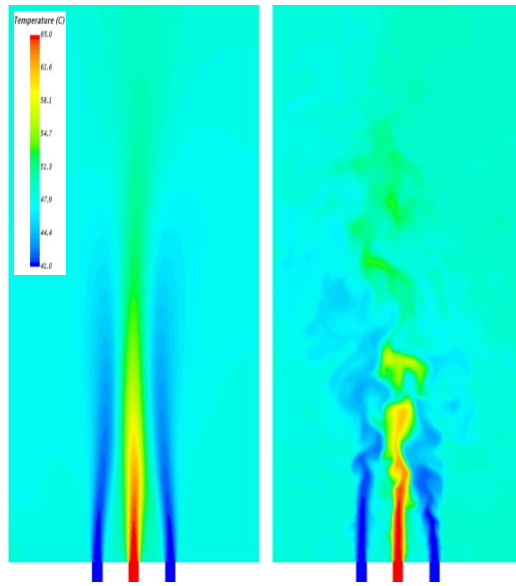


FIG. 1. Instantaneous fluid temperature contours at the mid plane (Left: RANS, Right: LES)

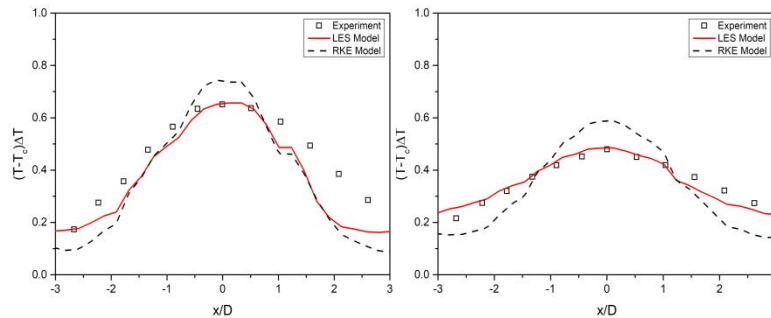


FIG. 2. Time-averaged temperature profiles along the mid plane (Left: 12W, Right: 18W away from the slot centre)

2.2. Simulation setup and numerical methods for the LES of the UIS

Through the thermal striping simulation for a triple jet, the necessity of employing the LES model over the RANS model for the flow mixing cases was demonstrated. The LES model proven by a simple test case was extended to thermal striping at the UIS of the PGSR. The UIS faced directly the hot sodium discharged from the core exit, and temperature differences between the neighbouring subassemblies induced thermal striping on the UIS surface. In order to characterize the striping at the UIS, numerical simulations were performed using STAR-CCM+. To reduce the computing load of the LES, the computational domain size was optimized using the RANS simulation. The full computational domain of the hot pool region is illustrated in Fig. 3. Three cases of the reduced domain were considered as shown in Fig. 4. The RANS simulation results for reduced domains such as velocity and temperature distributions along the horizontal sections above the core exit were compared with the results obtained from the full domain of Fig. 3. It was found that the geometry of the IHX inlet region and the upper core shield structure did not affect the flow characteristics of the core exit region while the UIS geometry was found to be crucial for thermal striping. If an appropriate pressure outlet condition could be given, a simulation of a reduced domain can give very similar results to the simulation of the full domain. After a detailed study using reduced computational domains, the middle case in Fig. 4 was chosen for the LES simulation, in which the 120° region of the core, UIS, and hot sodium plenum were included. In addition, 18 fuel subassemblies and 3 control rod subassemblies were involved. The pressure outlet condition was given by mapping the data obtained from the RANS simulation.

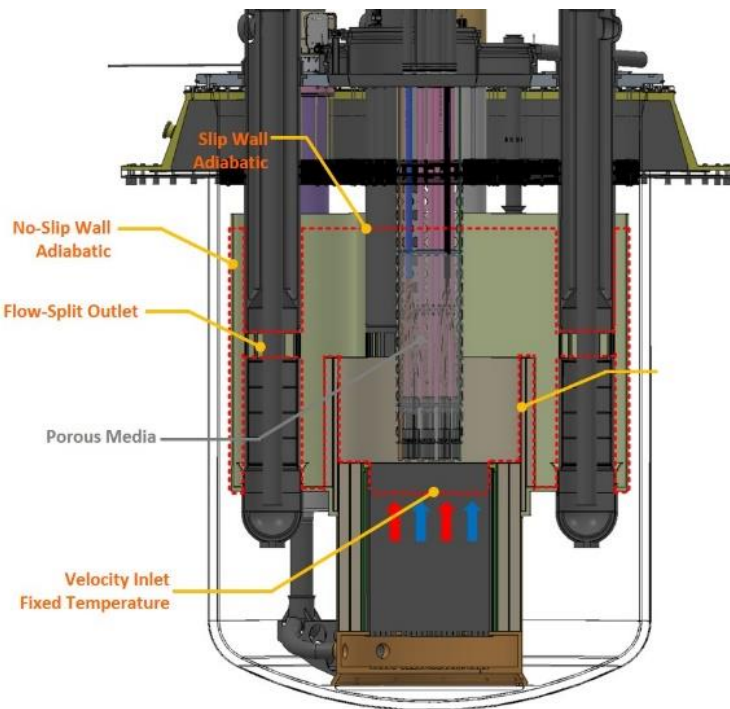


FIG. 3. Computational domain of hot pool region

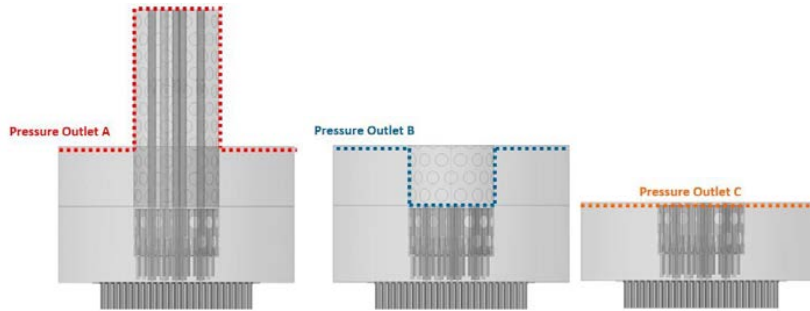


FIG. 4. Reduced computational domains from full hot pool domain

In order to determine the appropriate mesh size, a sensitivity study for mesh sizes was carried out, and about 7.9 million polyhedral grids were generated. The sensitivity of time steps was also studied, and 0.0001 seconds were chosen. The main parameters of the numerical methods are summarized in Table 2. The flow data were sampled from 1 to 5 seconds.

TABLE 2. NUMERICAL SCHEMES

Parameter	Numerical Methods
Time integration	Implicit unsteady (dt=0.0001 s, t=5 s)
Flow solver	Segregated flow solver (Bounded-central differencing)
Heat transfer	Segregated fluid enthalpy (2 nd order)
Turbulence model	LES with WALE SGS model
Wall function	All Y+ wall treatment
Buoyancy	Polynomial density with gravity

The flow rate through each control subassembly during normal operation was 2.11 kg/s, which was 1/5 ~ 1/10 of fuel subassemblies. The large temperature differences between the two neighbouring subassemblies ranged from 50 to 55°C. The coolant flow rates, core exit temperatures, and symmetric planes are displayed in Fig. 5. At a horizontal plane around the tip of the CRDM guide tubes, which were located 50 mm away from the core exit, the temperature and velocity distribution is displayed in Fig. 6. The high temperature sodium entered into the CRDM guide tube (CR #2) near the core centre. The flow rate was about 6.3 kg/s, and it was greater than that of the control subassemblies. For the CRDM guide tubes (CR #1, CR #3), the low temperature sodium rose. The flow rate was about 1.6 kg/s and 1.0 kg/s, respectively, and it was smaller than that of the control rod subassemblies. Around the CR #2, the temperature fluctuation amplitude was smaller than the CR #1 and CR #3. This is because the surrounding massive flow with the high temperature discharged from the fuel subassemblies was prevalent at the flow region around the CR #2 while the low temperature flow from the control subassembly at CR #1 and CR #3 mixed with the hot sodium from the fuel subassemblies, whose flow rates were at a similar range to the control subassembly. Around the CR #1, the instantaneous temperature and velocity distribution are shown at a vertical plane in Fig. 7. Since the flow rates from the neighbouring fuel and control subassemblies were similar for the CR #1, the flow instability was higher than the CR #2. Fluctuating vortices formed strongly around the tip of the CR #1. Fig. 8 shows temperature fluctuations at the CR #1, from which the amplitude of the oscillating temperature was found to be about 40°C. The RMS of the temperature fluctuation was calculated to be 9.39 °C, which was 18.3% of the maximum temperature difference of the inlet condition.

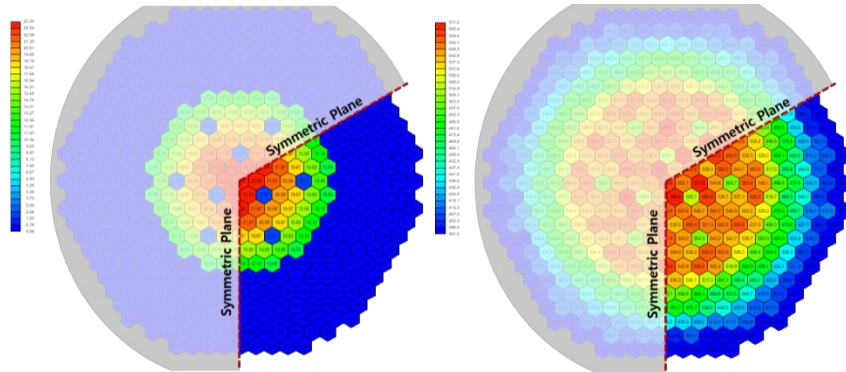


FIG. 5. Core exit flow conditions of computation region (Left: Flow rates, Right: Temperatures)

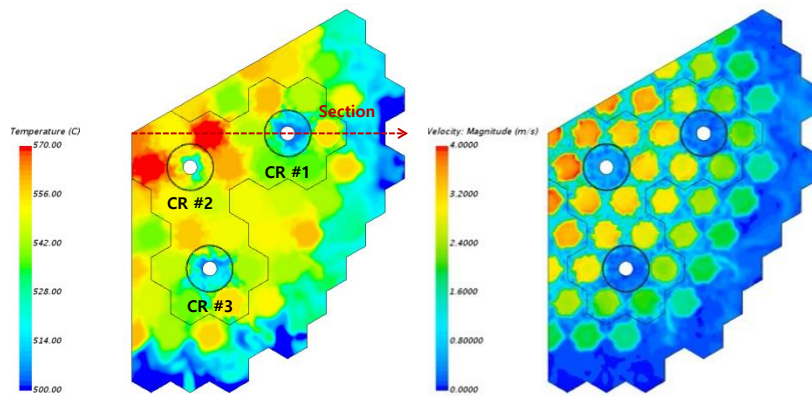


FIG. 6. Temperature and velocity distribution at the horizontal section (50 mm off from the core exit)

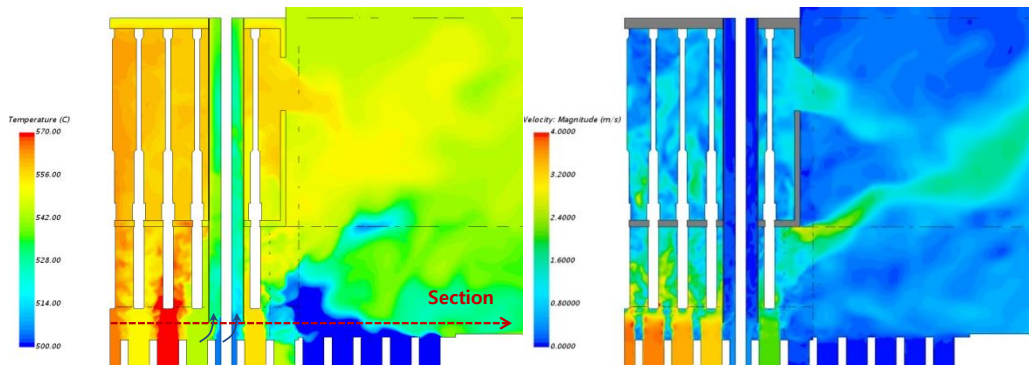


FIG. 7. Temperature and velocity distribution at the vertical section through CR #1

Fast Fourier transform (FFT) produced frequencies of temperature fluctuations, as in Fig. 8 ~ Fig. 10. The temperature fluctuations were negligible for the CR #2, while dominant frequencies were found in the CR #1 and CR #3. Along the axis of the CR #1, the normalized average and RMS of the fluid temperature were calculated for 5 seconds. The maximum RMS value was calculated to be 26.3% of the initial maximum temperature difference between the control subassembly and fuel subassembly. The temperature fluctuation calculation results will be provided for the thermal-fatigue assessment of the UIS.

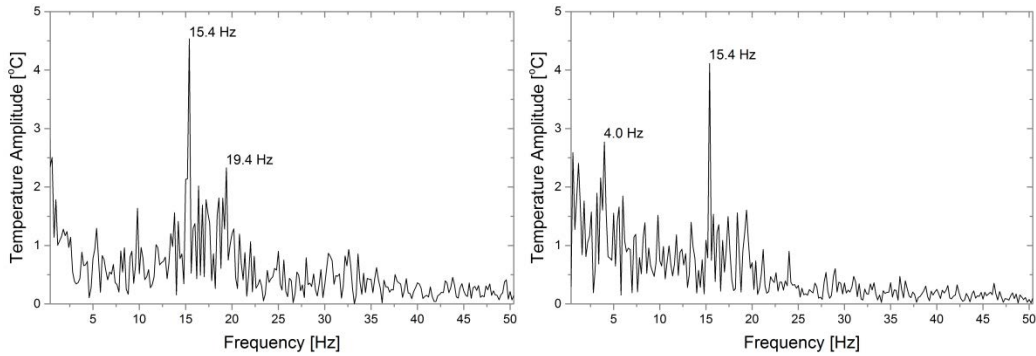


FIG. 8. FFT of the temperature difference fluctuation at the CR #1 (Left: Inner wall, Right: Outer wall)

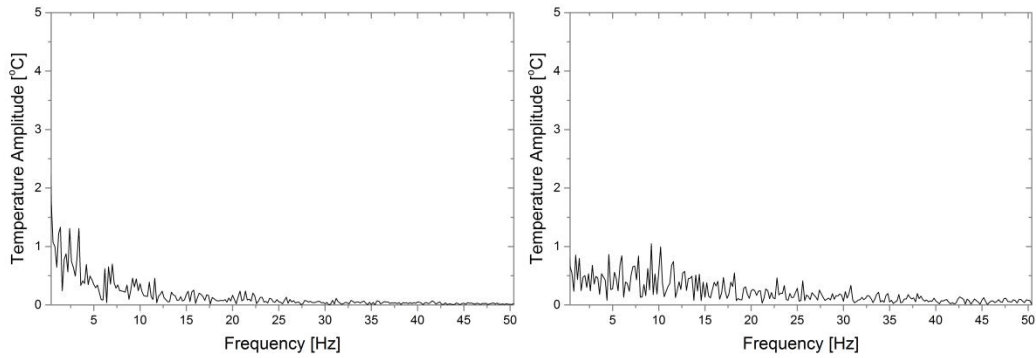


FIG. 9. FFT of the temperature difference fluctuation at the CR #2 (Left: Inner wall, Right: Outer wall)

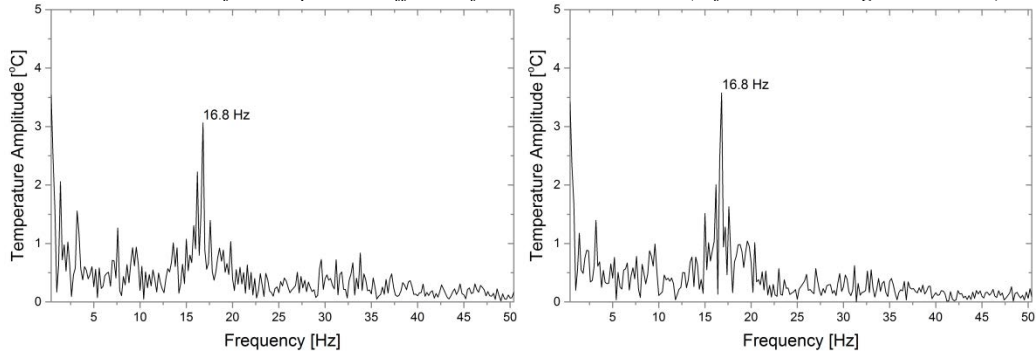


FIG. 10. FFT of the temperature difference fluctuation at the CR #3 (Left: Inner wall, Right: Outer wall)

3. INTEGRATED MODELLING AND SIMULATION OF THE ENTIRE PHTS FOR RVCS DESIGN

The reactor vault cooling system (RVCS) of the PGSFR is a passive heat removal system that operates during normal operation and severe accidents. The RVCS protects the vault and concrete cavity from the core heat during normal operation and removes the decay heat in the case of severe accidents. The containment and reactor vessels of the PGSFR are supported by the structure connected to the reactor head. The temperature of the reactor support structure and the vessels are critical for the reactor integrity. For thermal-hydraulic analysis, the thermal boundary conditions for only a local region cannot be given accurately without considering the connected regions. Thus, the entire reactor needs to be modelled and simulated to assess the RVCS' performance and examine the temperature of the reactor support structure and the vessels. However, full-scale simulation that reflects exact physics and geometries is not practical. To this end, simplified models for the components inside the reactor vessel were applied.

Intermediate heat exchangers (IHxs), decay heat exchangers (DHxs), and the reactor core inside the reactor vessel were simplified as porous media. For the porous media treatment of the core region, several flow groups for subassemblies were reflected. The upper shield structure in the cover gas region that protects the reactor head from the high temperature of the hot pool sodium was simplified by a conductive material after detailed analysis, as shown in Fig. 11. This technique holds the heat transfer rate difference between the two models within 1% and dramatically reduces the number of computational meshes.

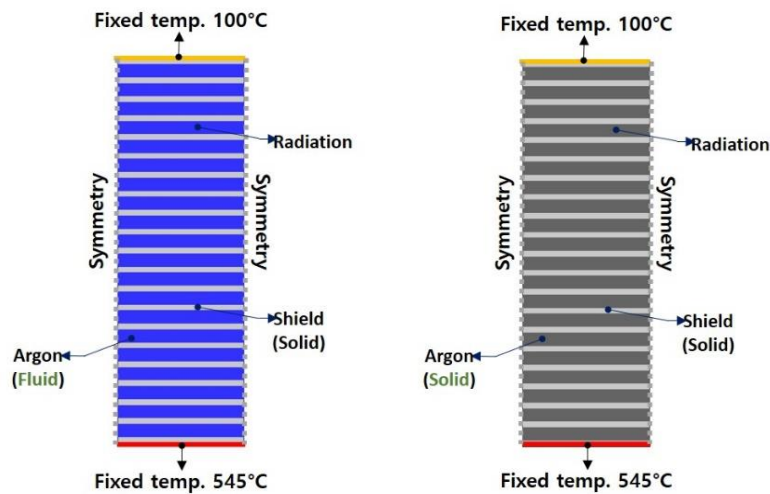


FIG.11. Simplified modelling of the upper shield structure (Left: Original, Right: Argon region as solid)

The concrete floor and other wall boundaries in the computational domain were set to be adiabatic. The computational domain, including the HAA, RVCS, and reactor, is shown in Fig. 12. The grid generation options such as polyhedral mesh and prism layers at solid walls were utilized, and 36 million cells were generated, as shown in Fig. 12. For turbulent modelling, the $k-\omega$ SST was employed with all Y^+ wall treatment functions. The conjugate heat transfer, including conduction, convection, and radiation, was activated.

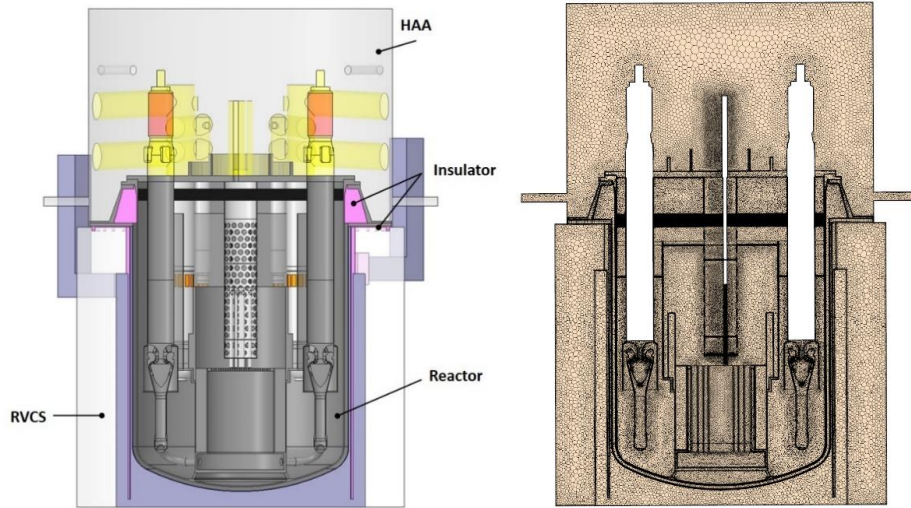


FIG.12. Computational domain (left) and grid system (right)

The temperature and velocity distributions at a vertical section are shown in Fig. 13, and the average temperatures of the main flow paths such as the core inlet and outlet were in good agreement with the design values within less than 1% difference. 20°C air feeds into the HAA area was discharged with a rising temperature of 43°C~ 47°C, which was the result of heat transfer from the reactor head and the pump motors. Hot pool sodium temperature decreased to below the design limit 150°C at the reactor head by successful functioning of the upper shield structure. The temperatures of the vessels and support structures were calculated within the design limits.

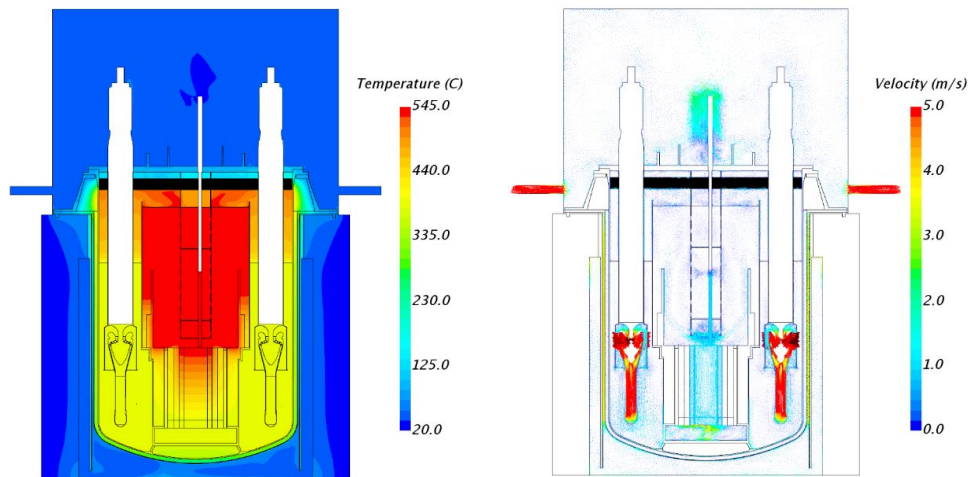


FIG.13. Temperature distribution (left) and velocity distribution (right)

For the RVCS, the mass flow rate and temperature at each stack exit were calculated to be around 6.4 kg/s and 168°C, respectively. The temperature at the concrete wall of the RVCS supposed to be below the ASME limit of 65°C during the plant’s normal operation. The concrete wall temperatures at different vertical planes are displayed in Fig. 14. The concrete wall temperatures were around 40°C, except for the upper and lower regions. The temperature of the upper region was caused by contact with the insulator. Through the simulation, it was found that for the lower region, an insulator needs to be added to eliminate hot spots. The findings will be applied during design modification.

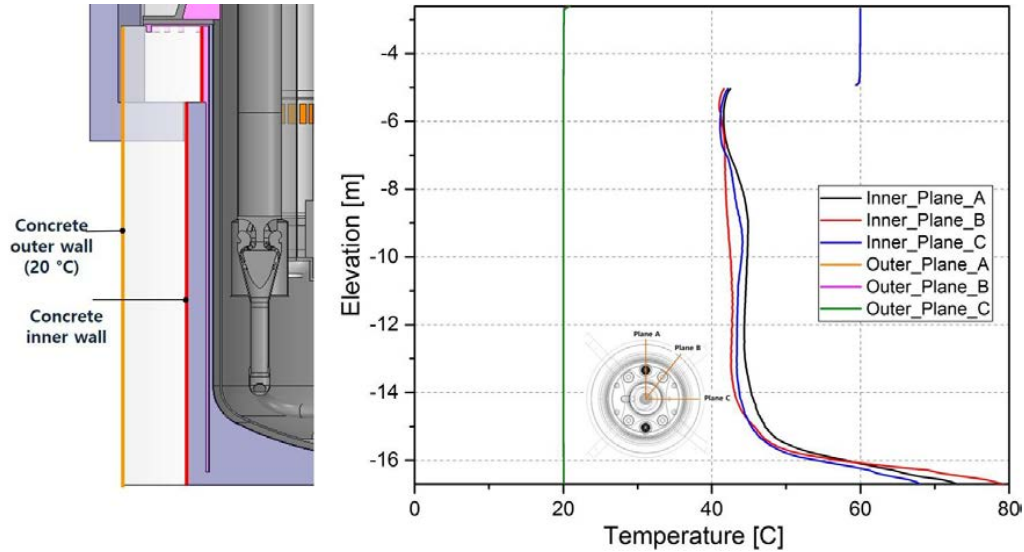


FIG.14. Vertical temperature distribution of inner & outer concrete in the RVCS

4. CONCLUSION

Generally, SMRs utilize a passive heat removal system, and components are arranged compactly inside the reactor vessel for modularization. A smaller inventory, but complicated arrangement requires detailed modelling and simulations. A multi-dimensional CFD can be more efficiently applied with the aid of refined simplification models.

The thermal striping phenomena in the UIS region of the PGSFR was investigated by using the LES model with an optimally reduced computational domain. Temperature fluctuations due to thermal striping in a short time scale were well resolved.

An integrated simulation that included all the flow regions in the primary heat transport system was carried out to evaluate the RVCS performance. To this end, refined simplification models for the upper shield structure, heat exchangers, and core were developed. Through this work, temperature distributions in the HAA, reactor, RVCS, and reactor support structures were clearly resolved.

ACKNOWLEDGEMENTS

This work was supported by the National Research Foundation of Korea (NRF) grant funded by the Korean government (MSIP) (No. NRF-2012M2A8A2025624).

REFERENCES

- [1] Idaho National Laboratory, RELAP5-3D Code Manuals Revision, 2017.
- [2] Argonne National Laboratory, The SAS4A/SASSYS-1 LMR Analysis Code System, 1996.
- [3] D'AURIA, F., Thermal Hydraulics in Water-Cooled Nuclear Reactors, Woodhead Publishing Series in Energy (2017).
- [4] NEA, Computational Fluid Dynamics for Nuclear Reactor Safety-5, NEA/CSNI/R(2016)1.
- [5] YOO, J. et al., Overall system description and safety characteristics of prototype gen IV sodium cooled faster reactor in Korea, Nucl. Eng. Technol. **48** (2016) 1059–1070.
- [6] CHOI, C., JEONG, T., AN, S., Thermal-hydraulic analysis of passive reactor vault cooling system (RVCS) in PGSFR using MARS-LMR, Ann. Nucl. Energy **117** (2018) 333–342.
- [7] NAM, H., KIM, J., Thermal Striping Experimental Data, LMR/IOC-ST-002-04-Rev.0/04, KAERI, 2004.
- [8] NICOUD, F., DUCROS, F., Subgrid-scale stress modelling based on the square of the velocity gradient tensor, Flow Turbul. Combust. **62** (1999) 183-200.
- [9] CD-adapco, STAR-CCM+ User's Manual, 2017.

P. GAUTHÉ
CEA Cadarache
St-Paul-Lez-Durance, France
Email: paul.gauthe@cea.fr

A. PANTANO
CEA Cadarache
St-Paul-Lez-Durance, France
Email: alessandro.pantano@cea.fr

Abstract

Competitiveness and safety of future reactors has to improve in order to be acceptable by the population and decision-makers. Unfortunately, the nuclear industry faces a major issue: for now, safety means costs and the safer the reactor is, the more expensive it is. Research in advanced reactors needs to tackle this dilemma by promoting inherent safety and simplified design.

In this context, Small Modular Reactors (SMR) show promise for addressing the energy challenges in terms of flexibility, cost, safety, manufacturability, ease of operation, integration in electricity networks, and coexistence with renewable energies. Besides, SFR allows also to close the fuel cycle by using the plutonium coming from LWR and to minimize final wastes. Specificities of SFR are also favourable for include inherent safety features : no pressure of the coolant in normal operation, good natural behaviour of the core during unprotected transients, a more effective decay heat removal in natural convection, air as a heat sink.

The paper develops the idea to combine SMR and SFR advantages in terms of safety to simplify the design in order to make these reactors affordable from the technical and economical point of view. The reactor called “SMR CADOR”, with a core concept featuring a reinforced Doppler reactivity feedback (CADOR stands for Core with Amplified DOPpleR effect), providing inherent resistance to all accidents including unprotected reactivity insertions, which are a typical weakness in the SFR safety demonstration. The design includes also the possibility to achieve the decay heat removal function by a system through the reactor vault and in natural circulation, which is a key feature to reach a high level of safety, only achievable with SMR but not for higher nominal power SFR.

The guiding principle is to develop intrinsic safety of the reactor and to simplify the system design at the same time. Besides the core and decay heat removal systems, the design includes innovative features regarding maintenance and fuel handling, energy conversion system, cogeneration possibilities. An enhanced safety level can be achieved with such a reactor type thanks to the integration of these innovative design options on the one hand, and the simplification of the reactor general design, on the other hand.

1. INTRODUCTION

Enhancement of safety in a nuclear reactor often leads to an increase of the overall investment cost for the construction of a nuclear power plant. A breakthrough design approach is needed, combining simplification and inherent safety features (resilient natural core behaviour, efficient natural convection, grace time & autonomy). It will build a path to both a robust safety demonstration, more convincing for people and decision-makers, and a less expensive design, essential for a realistic deployment. Besides, sustainability is still a key issue for the nuclear industry of the future, so the development of fast reactors still has to be promoted.

The paper shows how a SMR of SFR-type with inherent safety could be a good candidate to fulfil these ambitious objectives.

2. CONTEXT FOR GEN-IV SMR DEVELOPMENT

Nowadays, designers show more and more interest in development of Gen-IV SMR. For Gen-IV designs with low maturity, the development at first of a small reactor is less risky than developing directly a FOAK with large power. Apart from the SFR, there is no significant proof of large power re-actor based on Gen-IV technology. So, starting by SMR is common sense. Besides, SMR enables simpler design and some economics advantages. Mixing the ambitious objectives of Gen-IV designs and the benefits of SMR could be a game-changing choice for the future of nuclear industry.

2.1. General interest in SMR

Most of economic studies show the reduction of the investment cost expressed in € / MW(e) installed when the power of the reactor increases. However, SMR-type reactors aims to compensate for these penalties by simplifications related to factory manufacturing of components, reduced construction time, and reduced financial costs. Lot of doubts remains open on competitiveness between SMR and bigger classical reactors, it is clear that the SMR may be more favourable for the adoption of simplifications in their design which would allow them substantial savings in terms of economy. Moreover, we believe that the benefits in terms of safety and cost of a single unit enable to regain the public acceptance and the trust of the decision-makers.

2.2. Gen-IV objectives

Gen-IV objectives are ambitious: the perfect advanced reactor is safe, cheap, resistant to proliferation, sustainable, flexible and compatible with the intermittency of renewable energies. For now, one can say that it does not exist. Fulfil all these objectives in one “perfect” reactor is an unsolved challenge. For example, HTR and SCWR may be good candidates for economy but bring no solution for sustainability. Dealing with economics, safety and sustainability together is a challenge. Sustainability means fast reactors, so SFR, LFR and MSR are good candidates. A large SFR unit may be as safe as a similar GenIII PWR, but with a higher investment cost, that can only be compensated with an important increase of the uranium price. Theoretically, MSR could fulfil all the objectives but a lot of questions are remaining about the feasibility, especially with materials and chemistry issues, so MSR stands for a long-term solution. Another track is to consider the well-known SFR but with a small power to consider its potential in terms of cost-reduction, safety improvement and public acceptance.

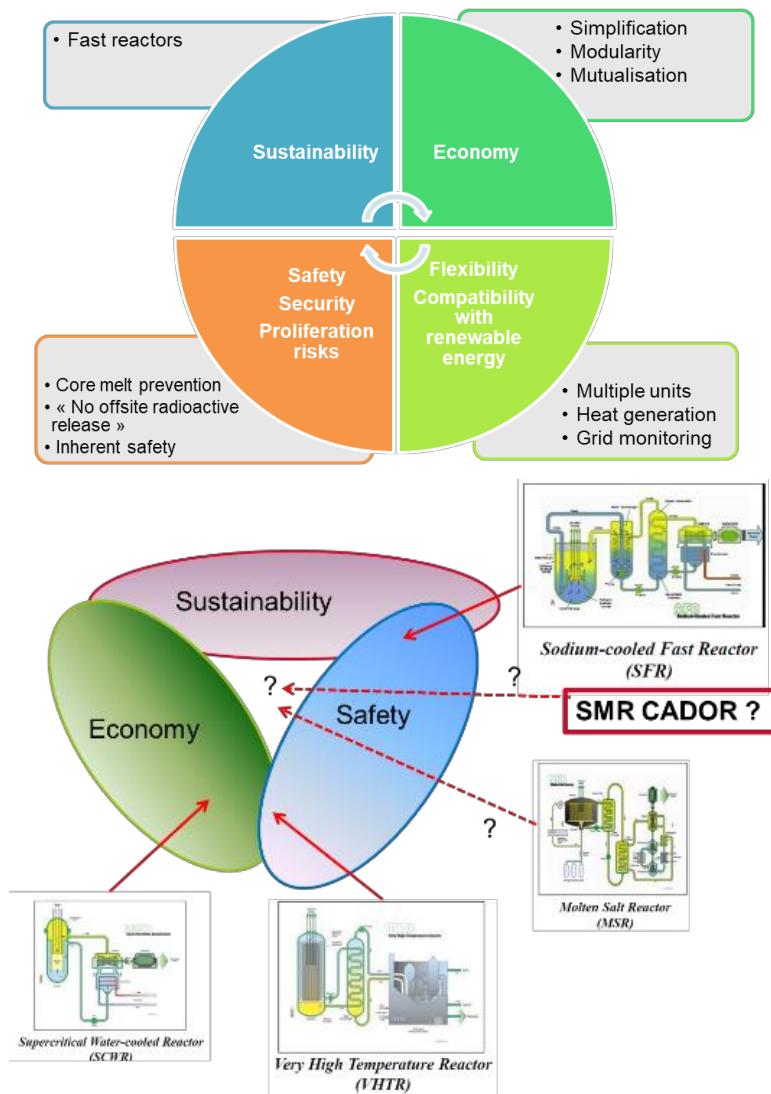


FIG. 1. Overview of GenIV SMR objectives

2.3. Inherent safety for Gen-IV SFR

For SFR type SMRs, we consider that a major breakthrough is the improvement of the prevention of the core melting prevention to an extent that can lead to the practical elimination of the whole core melting accident. It is a big challenge, but the advantages represent a game-changing track for advanced reactors. First, the debate on the acceptability is not the same. It could be more convincing to say that large radioactive releases are impossible than they likelihood is very low with a high degree of confidence. Eradicate the risks rather than dealing with the consequences is the key philosophy of inherent safety. Besides, this design approach may be fruitful to reduce the overall cost. Does reactor need core catcher? What are the confinement features? Not taking into account the whole core melting accident does not mean that we don't consider severe plant conditions. What is left in the 4th level of defence-in-depth is still an issue to figure and is not the goal of the paper. For that kind of SFR without whole core melting, the safety philosophy may be closer to HTR or MSR. To reach this objective, the design has to focus on the most challenging weakness of SFR design: reactivity insertion accidents and the decay heat removal function.

2.3.1. Reactivity insertions

Most of current designs of Gen-IV SFR focus on dealing with unprotected transients with combination of neutronic feedbacks and passive safety systems for the loss of flow or the loss of heat sink. These are good safety features, but this combination cannot avoid the core melting in case of unprotected reactivity insertion. Some of possible reactivity injection accidents are the flow of a large gas bubble through the core, the significant core compaction, the sudden break of the core support structure, leading to the withdrawal of all the control and safety rods from the core. The time needed to detect the problem and trigger the automatic shutdown system by gravity drop of the safety rods is too long, for this type of sequences, to be effective, i.e. about one second, compared with a tenth of a second for the duration of this type of accident. So these situations cannot be mitigate and have to be practically eliminated, and that requires a difficult and costly demonstration. The “practically eliminated” approach involves demonstrating that the implementation of a sufficient number of prevention lines of defense can guarantee that the occurrence of the event becomes highly improbable or physically impossible.

A first design objective is to design a core able to cope with these unprotected transients by its natural behaviour. The design approach of this CADOR core-type is to rely on a sufficiently large Doppler reactivity feedback effect in order to preclude any excessive power excursion following a prompt critical reactivity insertion. Starting from the CFV core-type, used in the ASTRID project, we introduce the following modifications to get to the CADOR one:

- Reduce the fuel temperature at nominal power by decreasing the mean linear power density by a factor of three, increasing the margin with respect to the melting point.
- Insert Beryllium metal pins within fuel subassemblies in place of fuel pins. The selected volume fraction of beryllium in the sub-assembly is 11%, which represents a compromise between a higher $K_{Doppler}$ value and penalties in terms of neutronic parameters, such as breeding gain and reactivity loss during irradiation.

Preliminary design and calculations on Unprotected Transient Over Power show that a CADOR core could avoid the core disruptive accident in case of unprotected accidents of reactivity

insertions. Nevertheless, more accurate calculation will be performed in the next future in order to demonstrate the elimination of the core melting due to the greater Doppler effect.

2.3.2. Decay heat removal

Decay heat removal is a key safety function. The Fukushima accident has shown the damages caused by a loss of this safety function. At least two safety systems ensuring this function, designed with redundancy and diversification preoccupations, have to be implemented. For SFR, we could take benefits of a lot of intrinsic features: high thermal inertia, natural convection capabilities, using air in natural convection as a heat sink for Na/air heat exchangers. On the other hand, the two main DHR systems are usually both composed by sodium circuits, with Na/Na exchangers in the hot or cold pools connected to Na/air heat-exchangers. These sodium circuits are both passing through the reactor slab. As a consequence, it is very difficult to exclude all common cause of failure between the two main DHR systems and to prove the total mutual independence. A solution is to implement a third system that extracts heat at the outer surface of the primary vessel (Reactor Vault Auxiliary Cooling System - RVACS), but this kind of system cannot fulfil the decay heat removal function by itself for large SFR, with a large decay heat. In this context, a SMR with its smaller power could provide an advantage by implementing an RVACS as one of the main DHR safety system, sufficiently efficient even just after the reactor shutdown. Moreover, if the system could operate in a passive way, with natural circulation in the primary circuit and in the RVACS, it could be a significant safety improvement.

3. OBJECTIVES OF THE SMR-CADOR

Safety

Two strong main objectives are the guidelines of the design:

- Avoid the core disruptive accident of the core for all postulated accidental scenarios, including unprotected reactivity insertions. The CADOR core is selected for this purpose.
- Remove the decay heat in natural convection with a DHR system through the surface of the Primary Vessel (PV). This objective has clearly the most impact on the design and will be the main topic of the paper.

Economy

The goal is to investigate promising design features to reduce the cost:

- Vessel diameter less than 6m to allow road transportation of the vessel. This assumption is consistent with large diameter road transportation found in France (ITER, Airbus...) The consequence is the choice of a LOOP-type reactor to reduce the size of the vessel.
- Removal of the intermediate sodium circuit. One of the over costs of SFR in comparison of PWR is the need of an intermediate circuit, to prevent the damage to the core in case of sodium-water (or gas) reaction. Considering that the CADOR core can cope with reactivity insertion due to an unprotected gas flow through the core, the design option of the removal of the intermediate loop can be envisaged. That

implies to design appropriate a sodium/gas heat exchanger and means of leakage detection.

- Simplified fuel handling systems, due to a low decay heat per subassembly for the SMR-CADOR core.
- Supercritical CO₂ Brayton conversion system to increase the efficiency of the energy conversion system. The feasibility of this type of cycle is not guaranteed for large power unit but can be envisaged for a SMR. This choice for the conversion system has to be confirmed by dedicated studies..
- Suppression of the safety vessel. A liner directly in the reactor pit is a design option suitable for a SMR.

The target power of the SMR CADOR reactor is between 200MW(th) to 400MW(th), meaning a range of [75MW(e) - 150MW(e)]. Another design track is to investigate the design of SMR-CADOR only for production of heat, operating in natural convection for normal operation. In this case, the target power is 50MW(th).

All these design options are not yet evaluated for the SMR-CADOR design. In this paper, in fact, we focus only on the primary system and the RVACS, taking care of the feasibility of a PV design due to the application of a passive radiative heat removal system. Hence, all the aspects related to the architecture of the system itself will be carried out later on.

Sustainability

The CADOR core needs to be able to use the plutonium coming from the spent MOX fuel of the PWR. The goal is not to be isogenerator but to burn some plutonium coming from the PWR in operation nowadays.

4. GOVERNING EQUATIONS OF THE PROBLEM

This paper introduces the concept of a fully passive decay heat removal system, in order to provide a breakthrough concept to minimize the cost and enhance the safety. The pre-design of a fully passive Decay Heat Removal System (DHRS), on the left in FIG. 1, presupposes a large number of variables to take into account in order to achieve a final design that complies with the physical constraints. In this specific application, the geometries of the Primary Vessel (PV) and the DHRS are the variable parameters, as well as the materials to use. However, this paper does not focus on the second field, even if this topic has an extreme importance. The pre-design problem is hence analysed in successive steps.

The first one consists on identifying the physical constraints, to be fulfilled by the whole system in order to confine the radioactivity and ensure the core cooling by a natural convection regime, summarized as;

$$1^{\text{st}} \text{ barrier integrity} \quad T_{clad} < T_{clad_{max}} = 825^{\circ}\text{C} \quad (1)$$

$$2^{\text{nd}} \text{ barrier integrity} \quad T_{PV} < T_{PV_{max}} = 700^{\circ}\text{C} \quad (2)$$

$$\text{Natural circulation} \quad \Delta p_{net} = \Delta p_{nat_{conv}} - \Delta p_{tot} > 0 \quad (3)$$

In fact, these equations ensure the integrity of the first (cladding) and second (PV) barriers for the radioactivity confinement, as well as the initiation of the natural circulation in an accidental situation. A $T_{PV_{max}}$ equal to 700°C has been considered as a value for more resisting steels

deployable in the next future. However, also lower $T_{PV_{max}}$ equal to 650°C has been considered later in the final section of this paper.

The third equation ensures that the natural convection initiated by the buoyancy forces can overcome the overall pressure drop in the circuit. Its first term can be written as;

$$\Delta p_{nat_conv} = g H_{nat_conv} (\rho_c - \rho_h), \quad (4)$$

where the g is the constant of the gravity acceleration, H_{nat_conv} and $(\rho_c - \rho_h)$ are respectively the geometrical height between the barycenters and the difference of the average densities between the cold and hot control volumes, i.e. CC and HC in FIG. 1. The second term Δp_{tot} represents the sum of all the concentrated and distributed pressure losses [3] of the primary circuit and of the core.

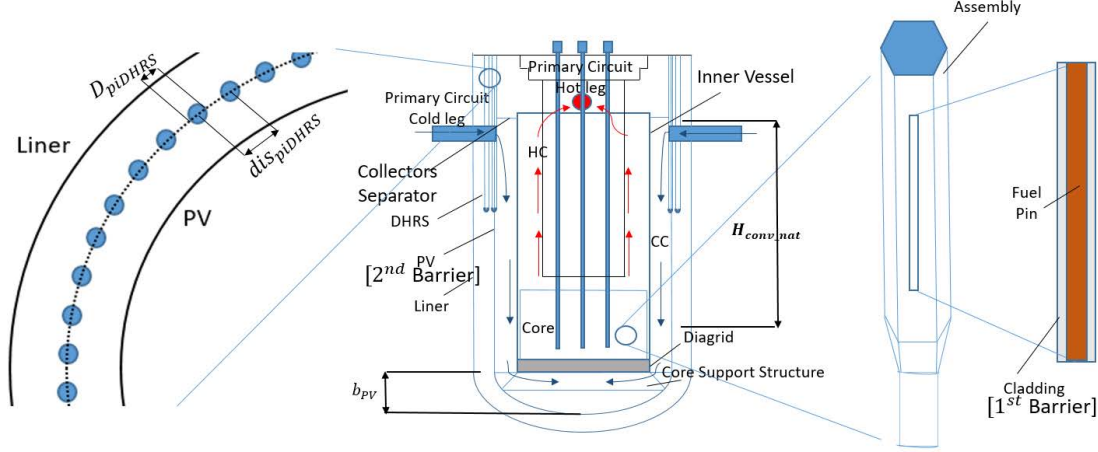


FIG. 1. On the left, placement of the DHRS. Zoom on the U-shape tubes (more than 100 couples) located on the average distance between liner and PV. On the centre, scheme of basic components of the primary geometry of the PV and DHRS. The control volumes considered in the simplified mathematical model are the Hot (HC) and Cold Collector (CC), the PV and the pit. On the right, zoom on the assembly and fuel pin schemes

In a second step, a calculation of a preliminary geometry is done, basing on the pre-design COPERNIC code [4], where only the main components are included in the global system. In order to determine the minimum height of the PV (H_{PV}), we ensure the continuity of the primary sodium flowrate in the primary circuit, in case of leakage from the PV and covering the level of the hot leg. This is done imposing the equation;

$$V_{LiNa} = V_{PVNa} = \frac{D_{int\ PV}^2 \pi}{4} (H_{PV} - b_{PV}) + V_{int\ Ellip_{PV}}, \quad (5)$$

where H_{LiNa} and D_{LiNa} are respectively the height of the retention liner and its internal diameter, while $V_{int\ Ellip_{PV}}$ is the volume of the elliptical bottom part of the PV. These parameters are already known and calculated in COPERNIC, in order to leave 25 cm of space between the PV and the liner and place the DHRS. The b_{PV} parameter is the vertical axe of the ellipsoid on the bottom of the PV, already fixed in the COPERNIC code. Therefore, the H_{PV} can be calculated as;

$$H_{PV} = \frac{4 (V_{LiNa} - V_{int\ Ellip_{PV}})}{D_{int\ PV}^2 \pi} + b_{PV}. \quad (6)$$

At this point the physical problem is posed through a set of governing equations, based on the geometry calculation previously made. The system has been divided in Control Volumes (CV), where for each one a temperature evolution is computed. We take into account six CV to find the solution of the problem, from the outer layer to the inner one: pit, liner, DHRS, PV, Cold Collector (CC) and Hot Collector (HC).

Unfortunately, it is possible to write only four Ordinary Differential Equations (ODE) for the HC, CC, PV and the pit as;

$$\frac{dT_{hc}}{dt} I_{hc} = [P_{res} - (K_{cond_{IV}} + (Q_{tot}c_p)) (T_{hc} - T_{cc})]; \quad (7)$$

$$\frac{dT_{cc}}{dt} I_{cc} = [(K_{cond_{IV}}) (T_{hc} - T_{cc}) + (Q_{tot}c_p)(T_{hc} - T_{cc}) - K_{conv_{Na}} (T_{cc} - T_{PV})]; \quad (8)$$

$$\frac{dT_{PV}}{dt} I_{PV} = [K_{conv_{Na}} (T_{cc} - T_{PV}) - K_{conv_{N_2}}(T_{PV} - T_{N_2}) - P_{PV}]; \quad (9)$$

$$\frac{dT_{pit}}{dt} I_{pit} = [K_{cond_{Li}} (T_{Li} - T_{pit}) - P_w]. \quad (10)$$

Where the in I are the thermal inertia of the CVs, calculated as;

$$I_{CV} = I_{CV_0} = \sum_{i=0}^N c_{p_{CV_i}} M_{CV_i}. \quad (11)$$

The coefficients $K_{cond_{IV}}, K_{cond_{Li}}$ are respectively the conduction coefficients in $\left[\frac{MW}{K}\right]$ of the Internal Vessel (IV) and of the liner. They can be calculated since the surfaces, the thickness and the thermal conductivities are already known. In addition, the coefficients $K_{conv_{Na}}, K_{conv_{N_2}}$ are respectively the convection coefficients in $\left[\frac{MW}{K}\right]$ of the sodium in the CC and of the gas between vessel and liner. They are estimated according to the correlations proposed by [5] and [6], while the temperature of the nitrogen T_{N_2} in the space between the liner and the PV is considered to be;

$$T_{N_2} = \frac{T_{PV} + T_{Li}}{2} \quad (12)$$

The physical properties, as well as the mass flowrate are known at the initial time. Nevertheless, the system of ODEs presented above introduces other unknowns, added to the problem, such as the decay heat P_{res} , the heat radiated by the PV (P_{PV}) and the heat removed by a pit coolant system from the pit P_w . Taking into account the value of $P_{nom} = 400 MW_{th}$, we adopt a decay heat equation of the type

$$P_{res} = P_{nom} * \left(K + \sum_{i=0}^6 e^{\lambda_i - \alpha_i t} \right), \quad (13)$$

where all the terms like K and all the exponents λ_i and α_i can be deduced. A tolerance of 10% has been adopted in order to have some physical margin.

The term P_w for the moment is set equal to $K_{cond_{Li}}(T_{Li} - T_{pit})$ in order to consider

$$\frac{dT_{pit}}{dt} I_{pit} = 0 \quad (14)$$

This choice has been taken because in this paper we focus only on the pre-design of the DHRS, neglecting the one of the pits. The term P_{PV} derives from the radiometric calculation between the DHRS, liner and PV. To determine the heat released by radiation from a surface we generally write

$$P_{PV} = A_{PV} \frac{\varepsilon_{PV}}{1 - \varepsilon_{PV}} (\sigma T_{PV}^4 - J_{PV}), \quad (15)$$

where σ is the Boltzmann constant. To compute the P_{PV} we need to know the area A_{PV} of the emitting surface, its emissivity ε_{PV} and its radiosity J_{PV} . All these magnitudes are known, except for the last one. However, its calculation involves also the radiosities of the other surface, hence the system reads

$$\begin{cases} J_{PV} = \varepsilon_{PV} \sigma T_{PV}^4 + (1 - \varepsilon_{PV})(J_{PV} F_{PV-PV} + J_{DHRS} F_{PV-DHRS} + J_{Li} F_{PV-Li}); \\ J_{DHRS} = \varepsilon_{DHRS} \sigma T_{DHRS}^4 + (1 - \varepsilon_{DHRS})(J_{PV} F_{DHRS-PV} + J_{DHRS} F_{DHRS-DHRS} + J_{Li} F_{DHRS-Li}); \\ J_{Li} = \varepsilon_{Li} \sigma T_{Li}^4 + (1 - \varepsilon_{Li})(J_{PV} F_{Li-PV} + J_{DHRS} F_{Li-DHRS} + J_{Li} F_{Li-Li}), \end{cases} \quad (16)$$

where for the calculation of the view factors F in the case of a bundle of pipes in front of a cylinder, we refer to [5]. However, these three supplementary equations add three other unknowns to the problem.

In conclusion, we count in total 11 equations describing the thermal behaviour of the physical system. Nonetheless, there are in total 13 unknown variables: the six temperatures of the CVs, the temperature of the nitrogen T_{N_2} , the powers P_{res}, P_{PV}, P_w , and the radiosities J_{PV}, J_{DHRS}, J_{Li} .

Therefore, we need 2 additional equations for the T_{DHRS} and the T_{Li} . The first one is supposed to be constant for all the duration of the transient and equal to 120°C. This value has been given in order to estimate the average DHRS temperature. It has to be verified in a second moment through an iterative calculation between the PV and the DHRS, once this last system will be modelled. The choice of the inner fluid of the DHRS has not been already made but liquid metals are good candidates. Nevertheless, the first performed calculations report some results that can slightly confirm this hypothesis. The reason is related to the low heat flux per pipe, due to the presence of more than 100 couples of U pipes belonging to the DHRS. On the other hand, for the liner we impose an adiabatic boundary condition, hence

$$T_{Li} = \sqrt[4]{\frac{J_{Li}}{\sigma}} \quad (17)$$

The mathematical problem is now well posed and the system of 13 equations, describing the thermal behaviour of the domain, can be solved for each time step.

However, only the first two constraints can be verified at each time step. For the third one, we evaluate the evolution of the mass flowrate of the primary sodium using a definition taken by [7],

$$Q_{nat_conv} = Q_0 \left(\frac{\rho_m \beta_m p_{res} \Delta T_0 C p_0 g H_{nat_conv}}{2 \Delta p_0 C p_m} \right)^{4/11}, \quad (18)$$

where the ρ_m is the average density between the cold and hot collectors in $\left[\frac{kg}{m^3}\right]$, β_m is the thermal expansion coefficient in $[K^{-1}]$, p_{res} is the fraction of the decay heat, the ΔT_0 and Δp_0 the temperature difference and the pressure drop across the core.

Since the mass flowrate evolution is known, the flow velocity can be found in each point of the circuit, hence also the third constraint can be verified at each time step.

5. DESIGN OF THE DECAY HEAT REMOVAL SYSTEM

The geometry of the DHRS is strongly dependent on the height of the PV, H_{PV} . Since this minimum length has been determined, its design can be performed. This system consists on a series of U-shape pipes surrounding the PV as in the left part of FIG. 1. The position of the pipes, located on the average distance between the PV and the liner maximizes the D_{PV} in a range between 5.48 m and 6 m, allowing its transportability. The pipes of the DHRS are made of the same stainless steel used for the PV with NaK or a thermal oil as internal fluid. They have a diameter $D_{pi\ DHRS} = 5\ cm$ and the mutual distance between them is $dis_{pi\ DHRS} = 10\ cm$. This distance has been fixed in order to comply with the construction feasibility, maximizing the heat transferred to the system and reducing the radiation reflections to the PV. Among the hypothesis done in pre-design phase, we mainly consider an average homogeneous temperature for all the bodies involved. To simplify the problem, also the emissivity has been considered as a constant, not dependent on the temperature of the material, nor from the direction. This approach is not very accurate, but still a good approximation to adopt for a pre-design phase.

Transient calculation

The fulfilment of the thermal and mechanical constraints is verified in a shutdown transient of almost 3 days. The geometries of DHRS and PV have to be integrated in a model that considers the temperature evolutions for the volumes considered in this analysis. For this reason, all the properties of the major components are calculated in the COPERNIC code and finally integrated in a 0D model, as the ODEs presented in the previous section. This approach is very simple, but gives reliable ideas about the order of magnitudes, ensuring the global energy conservation and a reasonable computational cost, necessary for a preliminary analysis. At time $t = 0\ s$ the control rods fall down and the power immediately decreases from $P_{nom} = 400\ MW_{th}$ according to the definition of P_{res} previously introduced. Considering the expression of the residual power, as well as all the governing equation, we can solve the set of ODEs previously presented. All the thermal inertia is calculated in the COPERNIC code at the initial time and they are considered as constant during the transient, since we assume a negligible variation of the mass in the collectors and the c_p almost independent on temperature. Being aware of all the simplifications, we solve the proposed ODEs adopting a Runge-Kutta4 scheme [8] implemented on a self-developed MATLAB script. The choice to deal with an explicit scheme is because all the thermal properties of the material depend on temperatures that are known just at the initial time. Moreover, we remark a rapid change of the power leading to an abrupt variation on temperature, thus possible discontinuities on the properties. On the other hand, an explicit scheme implies a smaller time step, hence a higher computational cost. In fact,

a convergence study has been performed at the beginning of the analysis, finding 0.2 s as the value of Δt corresponding to a good compromise between accuracy and computational cost. During the transient, both the thermal and the mechanical constraint need to be verified, ensuring the integrity of the first and second barrier, and a natural cooling of the core. The verification of these conditions at the same time is not trivial and the geometry of the PV, as well as the one of the DHRS plays a key role.

Influence of the geometry on the fulfilment of the physical constraints

The considerations presented in the previous sections have been applied in the pre-design COPERNIC code in order to determine the geometry of the PV, DHRS and liner fulfilling the physical constraints. We remind the reader that, in this paper, the DHRS is considered as a cold source at constant temperature of 120°C for the duration of the transient. Based on this consideration, the shutdown transient is studied with a first preliminary geometry.

This one has to be modified in order to comply with the physical constraints imposed. If we look at a physical parameter, for example the T_{PV} during the transient, it is a function of several factors as

$$T_{PV} = T(\epsilon_{DHRS}, \epsilon_{PV}, D_{PV}, H_{PV}, dis_{pi}, c_{pPV}, T_{in_{DHRS}}, fluid_{DHRS}, \dots). \quad (19)$$

Now we try to focus more on the parameters that could influence the design, having a strongest impact on it. The kind of fluid in the DHRS, as well as the inlet temperature can influence the design, but so far, we prefer to keep the problem of the real design of the DHRS aside in order to focus more on different design possibilities for the vessel. This choice will be reviewed when some useful PV configurations will be fixed. The geometrical distance between the pipes of the DHRS has been considered as a constant either for construction reasons and to trap the radiation between the liner and the PV. One important parameter is undoubtedly the emissivity of the external surfaces of the DHRS and PV. In fact, the higher the emissivity, the more heat can be removed, ensuring a proper cooling of the PV. Another important factor is the height of the PV and of the relative DHRS. The increase of the H_{PV} leads to a double advantage due to the simultaneous increase of the thermal inertia of the control volume as well as the surface exposed to the radiation. Although the thermal constraints could be already fulfilled through the increase of the H_{PV} , as shown in FIG. 2, the mechanical constraint is not verified for the present geometry. In order to respect this requirement, two different ways are proposed in this paper.

The first one supposes a configuration with passive system, which allows the sodium of the hot collector to bypass the IV, creating a sort of internal loop, bypassing the primary circuit. On the other hand, the other choice allows the sodium to pass through the primary loop, but extremely compact. In fact, in this configuration, the flowrate is split in several under loops in order to decrease the mass flowrate per loop, hence the overall pressure drops. Moreover, when the H_{PV} is increased, simultaneously, the DHRS is moved up with respect to the height of the core. This operation is performed in order to increase the H_{nat_conv} , useful to respect the mechanical constraint. Anyway, for both the cases, we need a double IV in order to isolate the hot collector to the cold one, increasing the difference of densities between the two collectors and the natural circulation of the primary sodium. The effect of the thermal insulation of the hot collector has been taken into account in this analysis through a coefficient $K_{isol} = 0.1$ that multiplies the calculated value of $K_{cond_{IV}}$.

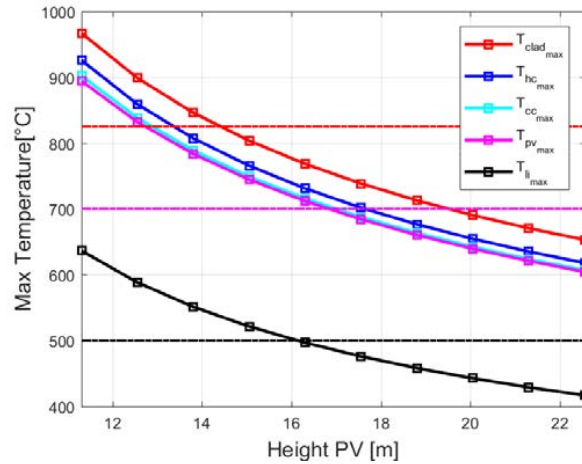


FIG. 2. Variation of the maximum CV average temperatures as a function of the H_{PV} . The dashed lines represent the thermal limits for the cladding, PV and liner

The results in FIG. 3 and

FIG. 4 show that the temperatures undergo an initial steep decrease in the first 15 minutes, due to the drop of the thermal power of the core. This phenomenon is followed by the shutdown of the EMP, which implies the immediate drop of the mass flowrate and a consequent increase of the sodium temperature. The maximum power evacuated by the DHRS corresponds to the moment when the maximum temperature is reached, due to the hypothesis of the constant T_{DHRS} . In addition, the DHRS supposed to work also during normal operating conditions, because of the continuous temperature difference between the DHRS and the PV, implying an evacuation of almost 0.5 MW or more according to the design. The two proposed configurations present two different geometries with advantages and drawbacks. The one with a passive bypass in the IV has a shorter geometry, with an 18 m height PV, and longer primary loops. This concept introduces a kind of breakup technology based on an internal bypass concept. On the other hand, the one without bypass has a compact primary loop and a 30 m height PV. It is important to remark that for both the geometries the same approach has been applied, adjusting the H_{PV} and the length of the DHRS in order to find a compromise for the fulfillment of the two types of constraints.

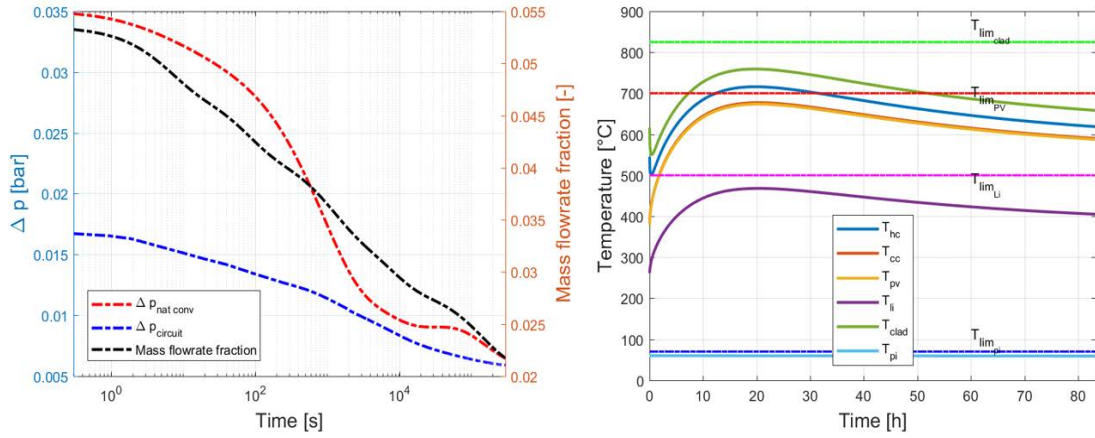


FIG. 3. Respect of the mechanical and thermal constraint for a configuration with a passive mechanical bypass. For a geometry of $D_{PV} = 5.48$ m and $\epsilon_{PV} = 0.5$, only in case of $H_{PV} > 18$ m both the thermal and mechanical constraints can be fulfilled

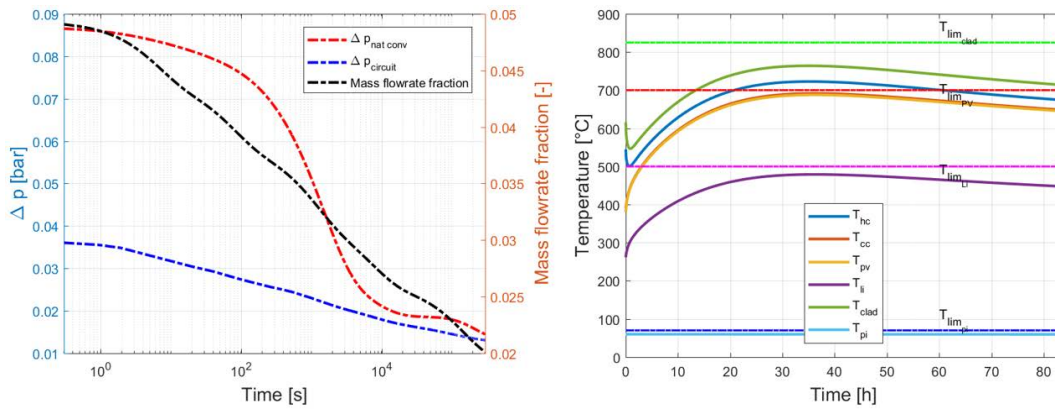


FIG. 4. Respect of the mechanical and thermal constraint for a configuration without a passive mechanical bypass. For a geometry of $D_{PV} = 5.48$ m and $\epsilon_{PV} = 0.5$, only in case of $H_{PV} > 30$ m both the thermal and mechanical constraints can be fulfilled

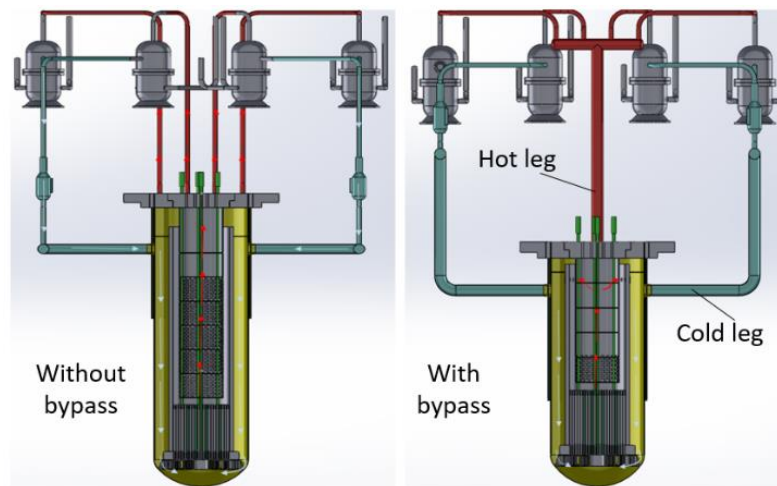


FIG. 5. Two different predesign schemes according to the natural circulation. The scheme on the right allows a strong reduction of the H_{PV} using a passive bypass device

6. COMPLETE PRE-DESIGN SCHEME

The conducted analysis about this loop type SMR shows up several potential configurations of the design of PV and DHRS. However, only the general components have been represented in this section, neglecting a part of the internal instrumentation, maintenance system, etc. Both the configurations present a common structure for what concerns almost all the internals and stratigraphy of the components outside the PV, as shown in FIG. 6. The core is surrounded by an IV, which separates the CC to the HC. The fuel assemblies are embedded in a diagrid made of steel, that allows a proper mass flowrate repartition. All the structure, including the IV, leans on the Core Support Structure (CSS), which is held by the PV. A massive lid embeds the top of the PV, leaving the place for the Upper Support Structure (UCS) and the few control rods penetrating inside the core. All the weight of the PV and its internals is maintained by the lid, which in turn is supported by the concrete structure of the pit.

The decay heat removal function, discussed in this paper, is performed only by one system, which is separated and independent from the pit cooling system (HRS in FIG. 6), and connected to a different sink to model. The DHRS, in dark green in FIG. 6, removes the heat in a fully-passive mode only by radiation, and it is located in between of the PV and the metallic liner. On the other hand, the cooling system embedded in the concrete pit, is not considered for the present phase of the pre-design, but it will work based on the same passive principle of the DHRS : the internal fluid flows from the sink to the heat source thanks to the difference of density between the colder and warmer parts of the U pipe. The physical working principals of the DHRS, as well as the application with an internal fluid will be tested in the next future. Both the two proposed configurations have an inner chrone-shape separator for the two collectors, which allows the hot sodium to get out the PV from the hot leg, located above the cold one. Moreover, the primary loops end with a separation of the primary circuit in several pipes, each one with an EMP and a modular IHX. In conclusion, the distinction of the two types (bypass and without bypass) leads to a net split of two kinds of concepts about the geometry of the PV and the primary loop.

The configuration without bypass has a more compact design of the circuit, in order to reduce the pressure drop as much as possible. Differently, on the configuration with a passive bypass system, the circulation towards the primary circuit is avoided, then the two primary loops present a more standard design.

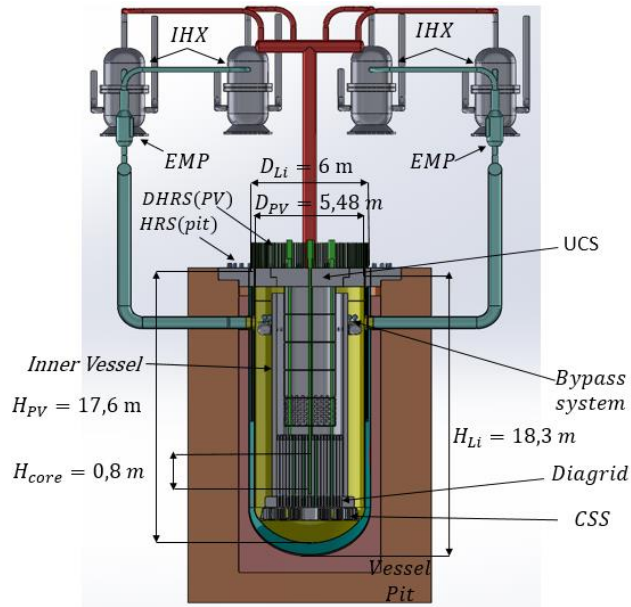


FIG. 6. Illustration of the reactor vessel, primary circuit and the main components in an axial cut. In this configuration, the diameter of the primary vessel has been fixed at 5.48 m. The pipes in red represent the hot branches, the cold ones are in teal

The primary circuit is not the only main difference between the two designs. In fact, also the shorter PV is a peculiar characteristic of the configuration adopting a bypass, due to the reduced overall pressure drops. Nevertheless, this innovative technology deserves a further investigation and test in order to ensure its feasibility in case of a reactor shutdown.

7. PRE-DESIGN OPTIONS

All the degrees of freedom introduced in the previous section, allow different possibilities for several options of pre-design. The effect to count two different ways to stand a natural circulation loop results on two different branches of design, each one entailing advantages and drawbacks. In addition, for each of these pre-design branches, we can remark a strong dependence on the emissivity of the PV and of the pipes of the DHRS. As demonstrated so far in [9] the effect of the application of a chromium oxide or graphite coating could largely improve the emissivity of the steel, hence the heat emitted by the body. However, this application is likely to be further investigated. In fact, the available results are valid for a restricted range of temperature and for a fresh material. The dependence on the emissivity, as well as the influence of a bypass system are valid for whatever power of the core. For this purpose, the reduction of the core power could be an important parameter to consider, in order to accomplish the thermal and the mechanical constraints too.

Let us consider now the same inlet and outlet temperatures of the sodium across the core, that results in a constant ΔT_{out-in} . With this condition, a reduction of the power leads to a proportional decrease of the nominal mass flowrate, thus the pressure drops too. Therefore, all the previous considerations can be applied for a lower power core of $300 MW_{th}$ and $200 MW_{th}$. The results in

FIG. 7 show a pivotal dependence on the use or not of the passive bypass system in order to initiate the natural convection regime. The greater D_{PV} influences the final height, due to the greater thermal inertia. However, its dependence is not very remarkable. Another important factor is $T_{PV,max}$ adopted for the primary vessel. In fact, to maintain a lower $T_{PV,max}$, a greater

radiative surface is needed. Finally, among the 72 different predesign configurations (24 for each value of core power), an optimum supposed to be found according to a techno-economical evaluation, accounting also the feasibility of a possible bypass system, as well as a chromium oxide or graphite coating for the PV.

WITH PASSIVE BYPASS

WITHOUT PASSIVE BYPASS

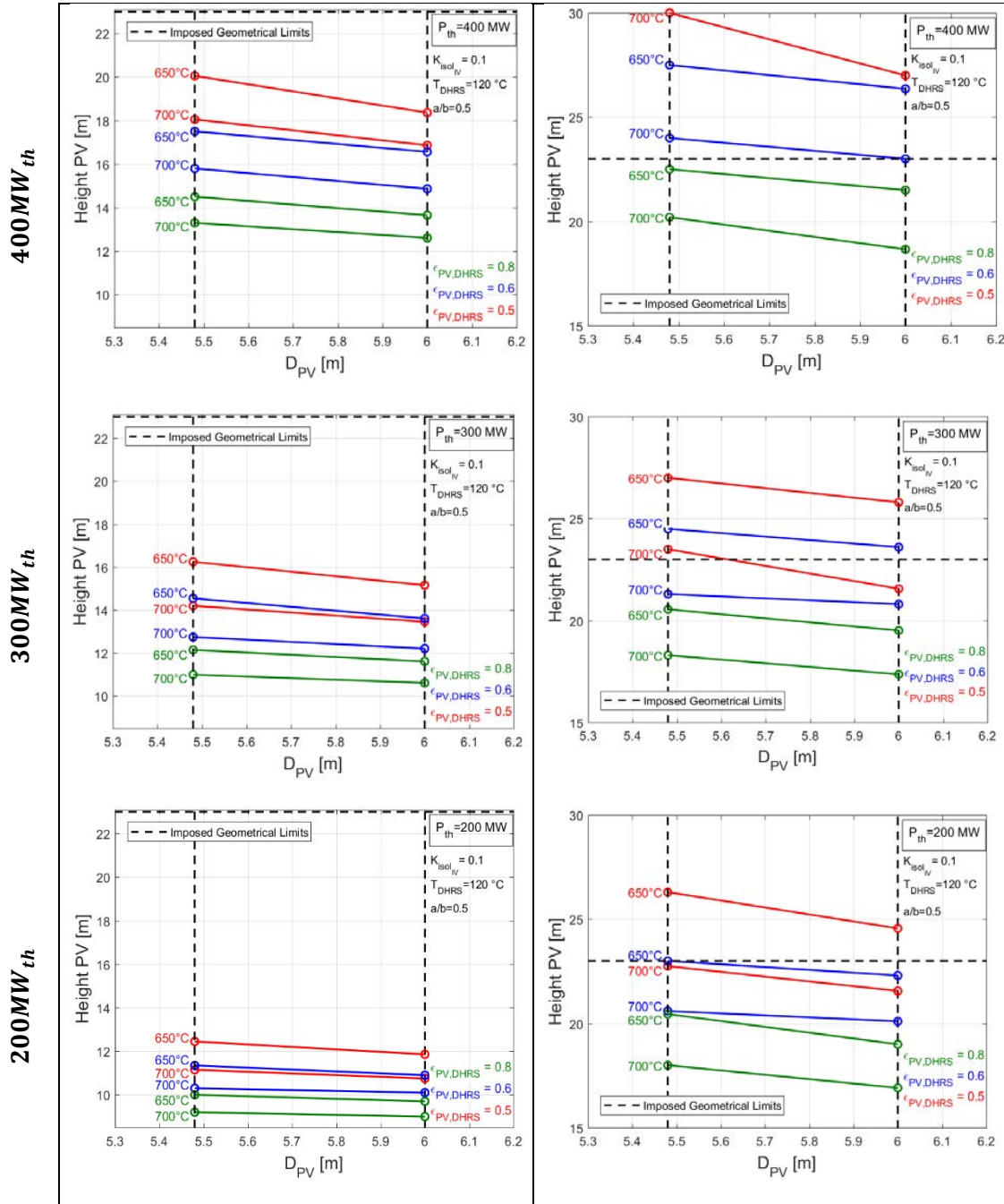


FIG. 7. Abacus of suitable configurations respecting the thermo-mechanical constraints. This analysis has been performed for the core powers of 400, 300 and 200 MW_{th}. The results remark a strong dependence on the use of the bypass system.

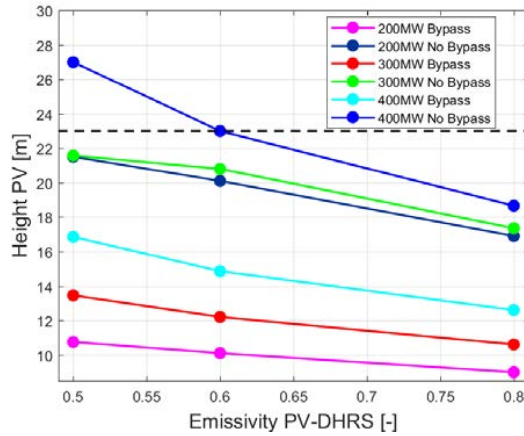


FIG. 8. Different options of configurations according to the emissivity, power and choice of natural convection loop to pursuit. The $T_{PV_{max}}$ is fixed at $700^{\circ}C$, for a D_{PV} of 6 m. The emissivity has a stronger impact for greater core power values.

8. CONCLUSIONS

This preliminary work shows different possible configurations for the SMR CADOR loop-type reactor. The objective to design a DHR system through the vessel able to operate in natural convection has an important impact on the design. For a vessel diameter of 6m and a nominal power between 200 and 400 MW_{th} , several designs are suitable with a vessel height between 10 and 20 meters. The key parameter is the flow path in natural convection in the primary circuit. The design of a by-pass of the primary loops is necessary to reduce the height of the vessel. Another key parameter is the emissivity of the vessel. Reaching a value of 0.8 would also enable the reduction of the size of the reactor.

A particular focus on the present DHR system has to be made in the next future, in order to assess its working principle. The future work will be the design of secondary loops, power conversion system, main DHR system, fuel-handling systems. After that, a preliminary evaluation of transient behaviour will be made to assess pros and cons of each design option and to choose the best nominal power for the reactor. It is advised that the design and the global reliability of the DHR architecture is assessed.

Further safety evaluations have to include all classical transient analysis like the ULOF and local faults. Finally, the work needs to include cost evaluation to assess the pros and cons of this new SFR design.

REFERENCES

- A., Q. (2013). *Scientific Computing with MATLAB and Octave*. Lausanne and Milan: Springer.
- Boarin S., L. G. (2014). Economics and financing of Small Modular Reactors (SMRs). In M. a. Carelli (Ed.), *Handbook of Small Modular Nuclear Reactors* (pp. 239-277). Cambridge, UK: Woodhead Publishing.
- Boarin, S. L. (2012, May). Financial Case Studies on Small- and Medium-Size Modular Reactors. *Nuclear Technology*, 178, 218-232.
- Bodi J., G. E. (2019). ESFR SMART Organization of a pit justifying the option of safety vessel suppression. *ICAPP*.
- Brookes, N. a. (2015). Power plants as megaprojects: Using empirics to shape policy, planning, and construction management. *Utilities Policy*, 36, 57–66.
- Canadian Small Modular Reactor (SMR) Roadmap Steering Committee. (2018). *A Call to Action: A Canadian Roadmap for Small Modular Reactors*.
- E. Dahlgren, K. L. (2012). *Small Modular Infrastructure*. Decision, Risk & Operations Working Papers Series, Columbia Business School.
- Finon, D. &. (2010). Contractual and financing arrangements for new nuclear investment in liberalized markets: Which efficient combination? In J.-M. G. François Lévêque (Ed.), *Security of Energy Supply in Europe: Natural Gas, Nuclear and Hydrogen* (pp. 117-135). Cheltenham, UK: Edward Elgar Publishing Limited.
- Group, E. F. (2018). *Market framework for financing small nuclear*. A report to Her Majesty's Government by the Expert Finance Working Group on Small Nuclear Reactors, UK Government, Department for Business, Energy and Industrial Strategy (BEIS).
- Grubler, A. (2010). The costs of the French nuclear scale-up: A case of negative learning by doing. *Energy Policy*, 38, 5174–5188.
- Incropera. (2013). *Foundation of Heat Transfer* (Sixth ed.). Wiley.
- Kuznetsov, N. K. (2012). Small modular reactors for enhancing energy security in developing countries. *Sustainability*, 4(8), 1806–1832.
- Locatelli, G. a. (2010, October). Competitiveness of Small-Medium, New Generation Reactors: A Comparative Study on Decommissioning. *Journal of Engineering for Gas Turbines and Power*, 132.
- M. Bernadete Junkesa, A. P. (2015). The Importance of Risk Assessment in the Context of Investment Project Management: a Case Study. In P. C. Science (Ed.), *Conference on ENTERprise Information Systems / International Conference on Project MANagement / Conference on Health and Social Care Information Systems and Technologies (CENTERIS / ProjMAN / HCist)*. 64, pp. 902-910. Elsevier.
- M.D.Carelli, B. C. (2007). Smaller sized reactors can be economically attractive. *International Congress on Advances in Nuclear Power Plants (ICAPP)*. Nice (France).
- Maynard R., M. N. (2017). Hemispherical Total Emissivity of Potential Structural Material for VHTR systems: Haynes 230. 179.
- Morin F., B. O. (2017). Copernic, a new tool based on simplified calculation methods for innovative LWRs conceptual design studies. *ICAPP*.
- Munson, O. H. (2013). *Fluid Mechanics, 7th Edition*. Wiley.
- N., S. (2011). *PhD Thesis, Etude conceptuelle d'un coeur de quatrième génération, refroidi au sodium, à combustible de type carbure*. UNIVERSITE D'ORSAY, PARIS XI.
- NAGENDRAT H. R., T. M. (1970). Free convection heat transfer in vertical annuli. *Chemical Engineering Science*, 25(pp. 605-610).
- OECD/NEA. (2015). *Nuclear New Build: Insights into Financing and Project Management*. Paris: OECD.
- (n.d.). *Rapport de sûreté Superphenix, Chapitre II 13.3.3*.
- World Nuclear Association. (2019, April). *Economics of Nuclear Power*. Retrieved from <https://www.world-nuclear.org/information-library/economic-aspects/economics-of-nuclear-power.aspx>
- World Nuclear Association. (2019, April). *Fast Neutron Reactors*. Retrieved from <https://www.world-nuclear.org/information-library/current-and-future-generation/fast-neutron-reactors.aspx>
- World Nuclear News. (2017, August 01). US nuclear construction project to be abandoned. *World Nuclear News*.
- Zaetta, A. e. (n.d.). - *Cador "Core with Adding DoppleR effect" concept - Application to Sodium Fast Reactors - submitted to EPJN*.

EVALUATION OF POTENTIAL SAFETY AND ECONOMIC BENEFITS AND CHALLENGES OF MODULAR SODIUM-COOLED FAST REACTORS

Paper ID #16

Y. M. Ashurko[†]
State Scientific Centre of the Russian Federation –
Institute for Physics and Power Engineering
(SSC RF-IPPE)
Obninsk, Russian Federation

Abstract

The report is devoted to evaluation of impact of safety systems and characteristics on economic performance of modular sodium-cooled fast reactors (SFRs) related to small and medium sized reactors (SMR). The comparison of modular SFRs with large sized ones is implemented. Based on analysis done, recommendations on ways to improve safety characteristics of modular SFRs in order to reduce cost of electricity, as well as capital cost are carried out. In particular, approach to improve capacity of a decay heat removal system through the reactor vessel wall is proposed that permits to increase rated thermal and electrical reactor power. Probability of practical occurrence of severe beyond-design basis accidents (BDBAs) increases in conditions of large-scale nuclear power growth with a significant increase of number of nuclear power units. In this regard, a special attention is paid to evaluation of economic indicators, taking into account the risk-informed factors associated with elimination of consequences of possible severe BDBAs. It is proposed an approach for considering influence of cost due to BDBA occurrence and its consequences on economic performance of nuclear power unit and corresponding method is developed. A parametric analysis of the nature and degree of influence of BDBA conditions and its consequences on value of specific cost of electricity is carried out. The values of probability of BDBA occurrence, when unfavourable influence of severe accidents and their consequences on value of specific cost of electricity is negligible, are determined. It is shown that higher safety characteristics of modular SFR against severe BDBA do not allow to reduce value of specific cost of electricity to level related to large sized SFR. The values of probability of BDBA occurrence for modular SFR, when contribution to specific cost of electricity due to expenses on elimination of BDBA consequences does not exceed the same contribution for large sized SFR, are defined.

1. INTRODUCTION

Prospects of development and implementation of every reactor technology are determined by its economic performance and competitiveness with other power sources. However, considering specific features of nuclear energy, safety issues are of paramount importance, which require an unconditional solution within framework of designs being developed.

At the same time, the implementation of necessary safety measures has an impact on all aspects of reactor technology, including its economic performance. The requirement to ensure normal operation of the power unit causes the presence of numerous safety systems in it. The presence of such safety systems leads to increase of the power unit cost, firstly, due to additional systems and equipment, and, secondly, due to need for their maintenance throughout the power unit lifetime.

However, safety aspects related to possibility of BDBA occurrence and necessity of elimination of its consequences, as a rule, were not taken into account when evaluating economic

[†] Deceased

performance of the power unit. This is justified at initial stage of nuclear power development with a small number of power units due to low probability of BDBAs. At the stage of large-scale development of nuclear power, characterized by a significant increase of the number of operated power units, total probability of BDBA that can be realized on these units is already a noticeable value. Therefore, the potential risks associated with possibility of severe BDBA occurrence and need to eliminate its consequences supposed to be considered when calculating specific cost of electricity used as a universal economic indicator in predicting competitiveness of reactor technology.

This paper analyses how safety issues are solved in modular SFRs and what impact decisions made have on their economic performance in comparison with performance of large sized SFRs.

An approach to evaluation of impact of safety aspects associated with possibility of BDBA occurrence on economic performance of the power unit is proposed and an appropriate method is developed. The parametric analysis of the nature and degree of influence of BDBA conditions and their consequences on value of the specific cost of electricity is carried out.

2. MODULAR SFR AND ITS FEATURES

The category of SMRs includes reactors with appropriate values of electrical power. Nevertheless, the key characteristic of this category of reactors is not power level, but modular principle of their manufacture. In other words, modular concept of the reactor is determinant attribute for SMRs.

The modular concept of the reactor involves its serial manufacture in factory conditions, transportation in form of complete modules to NPP site and its serial construction. This approach leads to restriction of modular reactors size (first of all, diameter of main and guard reactor vessels) and, as a consequence, to power limitation.

The limited power of modular reactor causes higher specific costs for its construction and operation per unit of electrical power compared to large sized reactor.

Improving economy of modular SFR can be achieved by:

- shortening construction time;
- reducing cost and improving quality of equipment manufacturing in factory conditions, in particular, due to larger seriality effect, that increases its reliability;
- facilitating its delivery to the site in comparison with large-dimensioned equipment for large sized SFRs;
- excluding long and expensive installation of this equipment in site conditions;
- simplification of safety systems and improving their reliability;
- enhancing safety against accidents, etc.

There are great prospects for combining modular units, for example, with placement of several modules in one reactor building, using a common refuelling system, connecting them to a common turbine, etc.

The report is restricted by consideration of impact of safety characteristics of modular SFR on its economic performance. The task is to assess how improvement of safety characteristics of modular SFR allows to bring its economic performance to indicators of large sized SFR.

3. ANALYSIS OF INFLUENCE OF MODULAR SFR SAFETY CHARACTERISTICS ON ITS ECONOMIC INDICATORS

The following main safety systems and characteristics are analysed in the report:

- Reactor core safety features;
- Reactor shutdown system;
- Decay heat removal system;
- Localizing safety system;
- Severe beyond-design basis accidents.

3.1. Reactor core safety features

Reactor core safety characteristics are important to avoid core damage in various transient and emergency modes. And, first of all, here it is necessary to point at accidents caused by failure of reactor shutdown systems, when change of reactor power is driven by reactivity feedback only.

Thus, impact of core safety characteristics on economic performance of a power unit can be estimated through cost associated with elimination of consequences of severe BDBA caused by failure reactor shutdown systems.

Here, ULOF accident caused by shutdown of all primary pumps without reactor scram is the most unfavourable one.

Let us compare behaviour of modular and large sized SFRs in this BDBA and evaluate its consequences.

The analysis performed for modular sodium-cooled fast reactor PRISM demonstrates a high level of its self-protection against this accident. The reactor overcomes the ULOF accident quite smoothly without core damage and coolant boiling [1].

At the same time, coolant boiling and, as a rule, reactor core damage in such an accident cannot be excluded for large sized SFR [2].

Thus, it can be argued that modular SFR has higher core safety characteristics compared with large sized SFR.

The main way of improving reactor core safety characteristics is to reduce severity of consequences of BDBA caused by failure of reactor shutdown systems. The impact of these accidents on economic performance of modular SFR is discussed below.

3.2. Reactor shutdown system

Besides standard emergency protection system which is qualitatively approximately the same in modular SFR and large sized one, additional reactor shutdown systems are used, as a rule, based on passive principle of operation. These systems are designed to reduce probability of occurrence of severe BDBA resulting in reactor core damage, as well as unacceptable radioactivity release outside site.

As a rule, passive reactor shutdown systems with absorbing rods based on various physical principles to hang on them in sodium flow are planned to be used in large sized SFR [3]:

- hydraulically suspended absorbing rods in sodium flow;
- absorbing rods based on temperature principle of action (magnets holding absorbing rods in sodium flow up to a certain temperature level, so-called Curie point; fusible inserts that ensure retention of absorbing rods until their melting temperature is reached, etc).

Regarding modular SFR, in particular, PRISM reactor design, it is proposed to use [4]:

- gas expansion modules;
- ultimate shutdown system (device with active principle of operation).

The failure probability is a defining characteristic for reactor shutdown systems. It can be reduced by replacing solid moving elements in them, which can cause device fault, for example, due to jamming solid absorbing rods because of core distortion or fuel pins swelling, etc., by devices using a liquid or gas medium as moving elements, such as in gas expansion modules.

As an example, it can be mentioned a device in which a liquid absorber is used as absorbing material and liquid that boils at a certain temperature and thereby pushes liquid absorber into reactor core space is applied as a working fluid [5].

Thus, the main direction of improvement of passive reactor shutdown systems is to reduce their failure probability, in particular, by diversification of devices provided for in the reactor design based on different operating principles, that decreases probability of severe BDBAs accompanied with failure of emergency protection and additional reactor shutdown systems.

3.3. Decay heat removal system

Decay heat removal in accident conditions it is easier to provide in modular SFR than in large sized one.

The relatively low level of decay heat allows to decline from expensive decay heat removal system (DHRS) with independent sodium loops, dipped autonomous heat exchangers (DHX) and air heat exchangers (AHX) in modular SFR. So, it is proposed to use a passive reactor vessel auxiliary cooling system (RVACS) for decay heat removal through the reactor vessel wall in the PRISM reactor [1],[4]. This DHRS has a low capacity, which imposes restriction on the value of nominal reactor thermal power. So, initial design of the PRISM reactor had thermal power of 471 MW. In this regard, an urgent task is a maximum possible increase of reactor thermal power by improving efficiency of the DHRS mentioned. In the latest version of the PRISM reactor design, so-called ALMR concept, reactor thermal power was raised to 840 MW by increasing reactor vessel size: diameter from 5.74 m to 9.118 m and height from 16.9 m to 19.355 m. In addition to increase of reactor vessel size, RVACS capacity can be raised by lengthening height of exhaust chimneys, as well as by increase heat transfer surface to the air in the gap between the guard vessel and the reactor silo and optimization of the gap width. The results of studies dedicated to this problem, given in [6], in which semipermeable grids or fin collectors were used for intensification of heat transfer surface to the air, show possibility of a significant increase of the RVACS capacity. The proposed measures make it possible to provide a safe decay heat removal for reactors with a thermal power up to 1000 MW. It is important to emphasize there is no need to make changes in designs of the guard vessel and the reactor silo.

RVACS is a completely passive system that does not require any switching on and functioning of the equipment, moreover, it does not have any moving elements. Therefore, probability of a complete failure of such a system is near zero. It is possible to speak only about decrease in efficiency of this system, for example, owing to destruction of exhaust chimneys. A complete blockage of the air flow cross-section is eliminated. Even when blocking 90% of the air flow cross-section, the DHRS capacity is sufficient to maintain coolant temperature within safe range [7]. Thus, application of the RVACS in modular SFR can significantly reduce probability of severe BDBA caused by DHRS failure in comparison with large sized SFR, which uses traditional DHRS.

Now it is recommended to provide alternative system in modern SFR designs for increasing reliability of implementation of decay heat removal function. As such a system it can be used, for example, DHRS through the surface of pipelines and equipment of the secondary circuit, proposed in [8]. This system provides for safety jacket for pipelines and equipment of the secondary circuit and creates air natural circulation in the gap between safety jacket and pipelines and equipment. In addition to decay heat removal, this system performs a containment function, restricting sodium combustion in case of sodium leak.

Thus, it is possible application of two variants of DHRS in modular SFR:

- the first option is conventional DHRS with heat dissipation through special heat transfer equipment (DHX, AHX). In this case, reactor power is limited only by reactor vessel size (firstly, diameter);
- the second variant assumes application of passive RVACS for heat removal through reactor vessel wall. For this option, acceptable reactor power level is limited not only by reactor vessel size, but also by RVACS capacity.

In the first case, modular SFR is practically reduced copy of large sized SFR: a) with decreased power due to limited reactor vessel size and b) with the same expensive DHRS, which requires significant volume of reactor building and operational maintenance. This approach seems to be unpromising, as it makes difficult to achieve economic indicators corresponding to large sized SFR, basing on the following considerations:

- it does not allow to simplify safety systems and reduce the list of expensive equipment manufactured;
- it requires additional volumes of the reactor building for DHRS placement, its special installation on site and maintenance during power unit operation.

In our opinion, it is preferable and promising to refuse from expensive DHRS by means of application of simple and reliable decay heat removal systems through walls of reactor vessel, pipelines and equipment of the secondary circuit. It can significantly reduce the amount of capital costs for construction of DHRS, operational cost for its maintenance, reduce volume of the reactor building, as well as decrease probability of severe BDBAs caused by DHRS failure, which may require significant costs for elimination of their consequences.

At the same time, attention is required to be paid to maximum increase of capacity of proposed DHRS and the corresponding increase of reactor thermal and electrical power while maintaining modular principle of manufacturing reactor vessel, that helps to reduce specific capital cost per unit of installed reactor power as well as reduce specific cost of electricity.

3.4. Localizing safety system

In SFR, localization functions are performed by sodium systems and equipment, including reactor vessel, guard vessel, as well as gas communications of the primary circuit, containment, sodium fire extinguishing systems, including passive fire extinguishing ones, emergency ventilation systems. The performance of localizing functions in modular SFR is provided in the same way as in large sized SFR and does not have any specific features. Failure to perform localizing functions leads either to power unit outage or to occurrence of beyond-design basis accidents. And consequences for modular SFR and large sized one are approximately the same.

Simplification of localizing safety systems can be achieved by placing all systems and equipment containing radioactive sodium inside reactor vessel.

Failure to perform localizing functions is mainly caused by breakdown of integrity of localizing systems, in particular sodium systems. In this respect, probability of such events in modular SFR is lower than in large sized SFR. This is due to the following circumstances:

- probability of breakdown of integrity of sodium and gas communications, guard vessel, containment elements is directly proportional to their surface, which is less in modular SFR than in large sized one;
- quality of manufacturing and control of modular SFR equipment in factory conditions is higher than that of large sized SFR equipment in site conditions, therefore, probability of its failure in modular SFR is lower than in large sized one.

Thus, impact of failures in localizing systems on economic performance of power unit is realized through costs associated with elimination of consequences of accidents resulting from these failures. It is shown below how costs associated with accidents, including those caused by failures in localizing safety systems, are considered when calculating specific cost of electricity.

3.5. Severe beyond-design basis accidents

This section evaluates a degree of impact of severe beyond-design basis accidents on economic performance of power unit and presents an appropriate method of accounting for this impact. At the same time, issues related to social, humanitarian and reputational aspects of the BDBAs remain outside scope of consideration.

Until now, consequences of such beyond-design basis accidents, as a rule, were not considered when evaluating economic performance of power units due to low probability of their implementation. However, experience of already occurred severe accidents shows that probability of practical occurrence of such accidents increases in conditions of a large-scale nuclear power development accompanied with a significant growth of power units number, requiring large financial costs to eliminate accident consequences even in case of occurring single accident. Accordingly, this can lead to a noticeable increase in cost of operation of each power unit on average.

In this regard, it is advisable to carry out economic assessments for nuclear power facilities, taking into account risk-informed factors associated with elimination of consequences of possible severe beyond-design basis accidents. Namely, it is proposed to include in the methodology for calculating specific cost of electricity of power unit a component of anticipated cost for eliminating consequences of severe beyond-design basis accidents, considering possible probability of their occurrence. This component can be included in cost of electricity as insurance premiums.

3.5.1. Method for accounting of possible BDBA consequences in cost of electricity

As noted above, impact of safety aspects related to BDBA occurrence has not yet been considered in evaluation of economic indicators of the power unit.

This section is devoted to description of the approach proposed to evaluate impact of BDBA and its consequences on value of specific cost of electricity, and the methodology developed on its basis.

The proposed method considers both direct cost for eliminating severe BDBA consequences in case of its occurrence, and cost caused by possible premature decommissioning of the power unit.

Specific cost of electricity under normal operation conditions of the power unit is calculated according to formula:

$$C_0 = \frac{S_{\Sigma} + S_D}{Q_{\Sigma}} = \frac{(S_0 + D_0) \cdot N}{W_0 \cdot DLT \cdot LF \cdot 8760 \cdot N} = \frac{S_0 + D_0}{W_0 \cdot DLT \cdot LF \cdot 8760} \quad (1)$$

where C_0 – specific cost of electricity, not including possible cost on elimination of BDBA consequences, USD/kW·h;

W_0 – nominal electrical power of a single power unit, kW;

N – number of operating power units, pcs;

LF – load factor, rel. unit;

DLT – design lifetime of the power unit, year;

S_{Σ} – total cost on construction and operation of N power units, excluding decommissioning, USD;

S_D – total cost on decommissioning of N power units, USD;

S_0 – cost on construction and operation of a single power unit, excluding decommissioning, USD;

D_0 – cost on decommissioning of a single (non-emergency) power unit, USD;

Q_{Σ} – total planned electricity production at N power units during DLT , kW·h.

It is assumed that BDBA occurs in the middle of the design lifetime of emergency power unit. Considering cost of eliminating possible consequences of severe BDBA and losses due to reduced electricity production caused by premature decommissioning of emergency power unit, the expression for specific cost of electricity is written in the following form:

$$C_{mod} = \frac{S_{\Sigma} + S'_D + S_{BDBA}}{Q_{\Sigma}^W} = \frac{S_0 + D_0 - D_0 \cdot DLT \cdot \sum_{i=1}^M P_{BDBAi} + DLT \cdot \sum_{i=1}^M P_{BDBAi} \cdot C_{BDBAi}}{W_0 \cdot DLT \cdot LF \cdot 8760 \cdot \left(1 - \frac{DLT}{2} \cdot \sum_{i=1}^M P_{BDBAi}\right)} \quad (2)$$

where C_{mod} is the specific cost of electricity, including cost on elimination of BDBA consequences, USD/kW·h;

M – number of various types of BDBAs, pcs;

S'_D – total cost on decommissioning of operating power units, USD;

S_{BDBA} – total cost on elimination of consequences of M severe accidents, USD;

Q_{Σ}^W – total reduced electricity production at N power units during DLT due to BDBAs, kW·h;

P_{BDBAi} – probability of BDBA of i type, 1/reactor·year;

C_{BDBAi} – possible cost on elimination of consequences of BDBA of i type, USD.

As a result, we get:

$$C_{mod} = \frac{C_0}{\left(1 - \frac{DLT}{2} \cdot \sum_i P_{BDBAi}\right)} - \frac{D_0 \cdot DLT \cdot \sum_{i=1}^M P_{BDBAi}}{Q_0 \cdot \left(1 - \frac{DLT}{2} \cdot \sum_{i=1}^M P_{BDBAi}\right)} + \frac{DLT \cdot \sum_{i=1}^M P_{BDBAi} \cdot C_{BDBAi}}{Q_0 \cdot \left(1 - \frac{DLT}{2} \cdot \sum_{i=1}^M P_{BDBAi}\right)} \quad (3)$$

where

Q_0 – planned electricity production at single power unit during DLT, kW·h.

Since $\sum_{i=1}^M P_{BDBAi} \ll 1$, therefore, losses caused by reduced electricity production at emergency power units can be neglected.

With this in mind, formula (3) for calculation of specific cost of electricity can be converted to the form:

$$C_{mod} \approx C_0 + \frac{DLT \cdot \sum_{i=1}^M P_{BDBAi} \cdot C_{BDBAi}}{Q_0} = C_0 + C_{BDBA} \quad (4)$$

where

$$C_{BDBA} = \frac{\sum_{i=1}^M P_{BDBAi} \cdot C_{BDBAi}}{W_0 \cdot LF \cdot 8760} - \text{component of specific cost of electricity caused by elimination of BDBA consequences, USD/kW}\cdot\text{h.}$$

3.5.2. Analysis of impact of BDBA conditions on specific cost of electricity

Scale of BDBA impact on cost of electricity is estimated by using the developed technique.

As a basic value for specific cost of electricity produced at large sized SFR during normal operation of power unit (C_0), take the value equal to 0.017 USD/kW·h.

The component of specific cost of electricity caused by BDBA influence ($LUEC_{BDBA}$) is directly proportional to values of probability of BDBAs that are characteristic of the power unit, and cost of their elimination and is inversely proportional to nominal electrical power and load factor of the power unit.

The parametric analysis of specific cost of electricity is performed, considering possible cost for BDBA elimination, depending on values of nominal electrical power of the power unit and BDBA probability.

Three categories of severe BDBAs can be selected in accordance with their consequences:

- accidents with reactor core damage excluding further operation of the power unit, but not accompanied by radioactivity release from containment;
- accidents with reactor core damage excluding further operation of the power unit, and with radioactivity release outside containment, which do not impact on the environment and do not require measures to protect the population;
- accidents with reactor core damage and with radioactivity release outside the plant site exceeding permissible level, which require measures on deactivation of area neighbouring upon the emergency power unit and, if necessary, measures to protect the population until its evacuation.

The first category of accidents requires mainly cost for decommissioning power unit, for the second and the third categories of BDBAs there are additional expenses for elimination of consequences of radioactivity release beyond established boundaries. These expenses include additional cost for cleaning and re-cultivation of area around the emergency power unit, for evacuation of the population, etc., and considerably exceed cost related to the first BDBA category.

Therefore, parametric analysis is applied to the third BDBA category, as the most unfavourable regarding its consequences.

Estimates of possible cost for elimination of consequences of severe accidents, made by various experts, differ significantly from each other [9]. Therefore, available information on the Chernobyl accident is taken as reference data on cost of eliminating BDBA consequences [9]. For this accident, cost is estimated equal to USD 358 billion. This value is used in calculations.

Data on cost of eliminating the Fukushima accident consequences is significantly less than cost of the Chernobyl accident, but it is still far from its final value. So according to [10], cost of eliminating the Fukushima accident consequences is currently equal to USD 41 billion and will reach USD 195 billion.

Fig. 1 presents dependence of C_{BDBA} on nominal electrical power of the power unit at various values of BDBA probability. The range of nominal electrical power is varied from 10 MW to 1200 MW, i.e. from SMRs to large sized reactors.

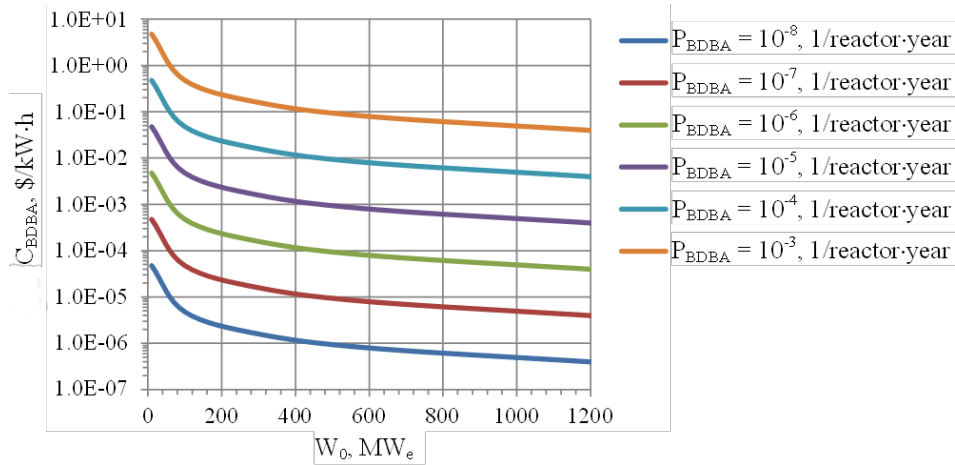


FIG. 1. Dependence of component of specific cost of electricity caused by BDBA influence on nominal electrical power of the power unit

Fig. 1 demonstrates that, all things being equal, component of specific cost of electricity caused by BDBA is raised with decrease of nominal electrical power of the power unit. Thus, addition of specific cost of electricity caused by BDBA is significantly higher for modular SFR than for large sized one. Note that value of component of specific cost of electricity caused by BDBA for modular SFR is lower than appropriate value for large sized SFR, if ratio of probability of BDBA occurrence in modular SFR to BDBA probability in large sized SFR is less than ratio of values of their nominal electrical power.

Fig. 2 shows dependence of C_{BDBA} on BDBA probability for various values of nominal electrical power of the power unit. Values of BDBA probability are ranged from 10^{-3} 1/reactor·year to 10^{-8} 1/reactor·year.

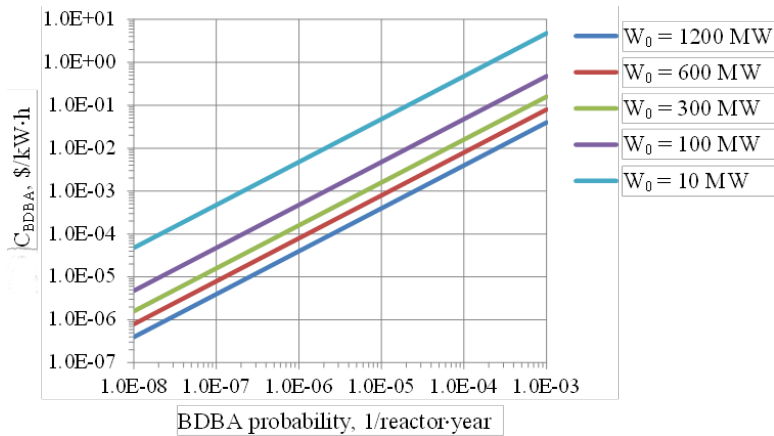


FIG. 2. Dependence of component of specific cost of electricity caused by BDBA influence on probability of its occurrence

The results, presented in Fig. 2, allow determining values of probability of BDBA occurrence, those limit its impact on specific cost of electricity by reasonable level. So, increase of specific cost of electricity due to BDBA does not exceed 1% of its total cost at probability of BDBA occurrence less $4 \cdot 10^{-8} - 1 \cdot 10^{-6}$ 1/reactor-year for modular SFR (depending on value of its rated electrical power) and less $4 \cdot 10^{-6}$ 1/reactor-year for SFR with electrical power of 1200 MW. Therefore, it is meant to be emphasized that, from this point of view, more rigid safety requirements are imposed on modular SFR than on large sized one.

Probability of severe BDBA, which is accompanied by an unacceptable radioactivity release outside the NPP site, is estimated to be no higher than $1 \cdot 10^{-6}$ 1/reactor-year in modern designs of large sized SFR. However, influence of BDBA on value of specific cost of electricity for large sized SFR is not much for this range of probability of BDBA occurrence.

The main share of spectrum of possible severe accidents is so-called heat sink accidents caused by failure of decay heat removal systems. Therefore, probability of BDBA occurrence for modular SFR is generally lower than for large sized one due to application of more reliable DHRS. This reduces impact of BDBA on value of specific cost of electricity for modular SFR too.

The enhancement of inherent core safety characteristics of modular reactor and its reactor shutdown systems can significantly decrease probability and severity of consequences of so-called reactivity accidents that lead to core damage, and thus reduce degree of influence of such BDBA on economic performance of modular SFR compared with large sized one.

The improvement of localizing safety systems mainly affects probability of occurrence of severe BDBS associated with their failure, which is a small share among all beyond-design basis accidents. In this regard, potential of these safety systems to improve economic performance of the power unit is limited.

4. RECOMMENDATIONS ON WAYS OF IMPROVEMENT OF MODULAR SFR

The below recommendations relate to proposed measures on enhancement of safety of modular SFR, which allow to improve its economic performance.

If exclude modular SFR designs with a fixed electrical power from consideration, one of the most effective measures to improve economic performance of modular SFR is to increase as much as possible its rated thermal and electrical power, while remaining within framework of the modular concept, based on factory manufacture of reactor equipment. The increase of power of modular reactor helps to reduce specific capital cost per unit of installed power of the facility, as well as reduce specific cost of electricity.

As noted above, two different approaches are possible here. The first option – traditional DHRS with heat removal through special heat exchange equipment (DHX, AHX). In this case, reactor power is limited only by reactor vessel size (its diameter). In the second variant – a passive decay heat removal system through the wall of reactor vessel RVACS is used for emergency heat removal. For this option, permissible reactor power is limited not only by reactor vessel size, but also by the RVACS capacity.

Thus, one of the fundamental and priority issues is the choice of DHRS concept. According to the author opinion, a more preferable and promising option is the system of decay heat removal through the wall of reactor vessel RVACS, considerations in favour of which are expressed in section devoted to description of DHRS for modular SFR. The conducted researches testify to significant potential of this system, the capacity of which due to optimization of width of the gap between guard vessel and reactor silo, increase of heat transfer surface to air and height of exhaust chimneys can provide a safe heat sink for modular reactors with a rated thermal capacity of up to 1000 MW.

In addition, application of fully passive DHRS significantly increases its reliability compared to traditional DHRS and, accordingly, reduces probability of severe BDBAs caused by DHRS failure, which prevail in BDBA spectrum.

However, the study revealed a limited potential of impact of measures to improve modular SAFR safety against severe BDBAs on its economic performance. More reliable DHRS and higher core safety characteristics can significantly reduce probability of severe BDBA occurrence in modular SFR compared with large sized one. But this advantage is neutralized by two circumstances. Firstly, component of specific cost of electricity caused by possible expenses on elimination of BDBA consequences is normalized to nominal electrical power of the power unit. Accordingly, to ensure the same value of this component of specific cost of electricity in modular SFR as in large sized one, provided the same cost for elimination of BDBA consequences for modular and large sized SFR, it is necessary that ratio of probability of severe BDBA occurrence in these reactors does not exceed ratio of their nominal electrical power. Secondly, contribution to specific cost of electricity of component caused by possible cost for eliminating BDBA consequences is minor for range of probabilities typical for severe BDBAs.

The influence of severe BDBAs on value of specific cost of electricity becomes insignificant with probability of BDBA occurrence in modular SFR lying in range of $4 \cdot 10^{-8} - 1 \cdot 10^{-6}$ 1/reactor-year depending on rated power of the reactor unit. Further reduction of probability of BDBA occurrence does not lead to any significant reduction in specific cost of electricity. At the same time, it is important that simplification and reduction of safety systems do not lead to an increase in probability of BDBA occurrence.

For a more accurate calculation of specific cost of electricity, special attention supposed to be paid to ensuring correct data on probability of occurrence of possible BDBAs and on cost of eliminating their consequences.

The analysis shows impossibility of closing the gap in economic indicators between modular SFR and large sized SFR only through measures to improve safety characteristics, as well as through simplification and improvement of safety systems in modular SFR. However, this gap seems to be, in principle, possible to eliminate in combination with measures that take advantage of modular SFR due to factory manufacturing principle. The final conclusion can be made only on results of comparison of concrete SFR designs taking into account the whole complex of their characteristics.

5. CONCLUSION

The report analyses how enhancement of safety systems and characteristics of modular SFR can improve its economic performance in relation to large sized SFR. Specific cost of electricity, which considers all other economic characteristics, such as metal consumption, capital cost, fuel cost and personnel cost, construction time, etc., is chosen as universal indicator for comparison of economic indicators of modular and large sized SFR.

The method is developed to consider risk-informed factors associated with elimination of possible severe BDBA consequences in specific cost of electricity. Calculations done by this method show that contribution to specific cost of electricity of component caused by possible expenses for eliminating BDBA consequences is negligible at the range of probability of BDBA occurrence in modular SFR equal to $4 \cdot 10^{-8} - 1 \cdot 10^{-6}$ 1/reactor·year depending on rated power of the reactor unit.

It is shown that one of the most promising measures to improve economic performance of modular SFR is transition from an expensive and complex decay heat removal system, which is used in large sized SFR, to a simple system of passive decay heat removal through the reactor vessel wall, as well as to raising nominal reactor power by increasing capacity of this DHRS.

The analysis shows impossibility of reaching the same economic indicators for modular SFR as for large SFR only by implementing safety measures, in particular by simplifying and improving safety systems and characteristics of modular SFR.

However, improving safety characteristics of modular SFR in combination with measures that take its advantage due to factory manufacturing principle can create good conditions for closing the gap in economic performance between modular and large sized SFR. In this regard, it is necessary to compare economic indicators for specific SFR designs, considering the whole complex of their characteristics.

REFERENCES

- [1] PLUTTA, P., TIPPETS, F., “General Electric Innovative Liquid Metal Reactor Plant Concept PRISM”, Fast Breeder Reactors: Experience and Trends (Proc. Int. Symp. Lyons, 1985), IAEA, Vienna (1986) IAEA-SM-284/61P.
- [2] KRÜSSMANN R., PONOMAREV A., PFRANG W., SCHIKORR M., STRUWE D. “Comparison of Results of SAS-SFR Calculations of the CP-ESFR Working Horse and Optimized Core Designs during the Initial Phase of an ULOF Accident”, Fast Reactors and Related Fuel Cycles: Safe Technologies and Sustainable Scenarios (FR13) (Proc. Int. Conf. Paris, 2013), IAEA, Vienna (2013) Paper T1-CN-199/320.
- [3] BOLSHOV, L., KLINOV, D., KAMAEV, A., LEMEKHOV, V., MOISEEV, A., SHEPELEV, S., VASILIEV, B., “Safety assurance of the new generation of the Russian fast liquid metal reactors”, Fast Reactors and Related Fuel Cycles: Next Generation Nuclear Systems for Sustainable Development (FR17) (Proc. Int. Conf. Yekaterinburg, 2017), IAEA, Vienna (2018) Paper CN245-577.
- [4] Fast Reactor Database: 2006 Update. IAEA-TECDOC-1531, IAEA, Vienna (2006).
- [5] ASHURKO, Yu., KUZNETSOV, I., Device for safety protection of a nuclear reactor. Certificate of authorship No 1618174 (priority date 28.12.1987) issued on 01.09.1990, G 21 C 9/02.
- [6] ASHURKO, Yu., LAZARENKO, G., “Characteristics of systems of emergency decay heat removal through reactor vessel wall and possible ways of their efficiency increase”, Sodium Cooled Fast Reactor Safety (Proc. Int. Top. Mtg. Obninsk, 1994), IPPE, Obninsk (1994).
- [7] BOARDMAN, C., HUNSBEDT, A., “Performance of ALMR Passive Decay Heat Removal System”, Passive and Active Safety Features of LMFBRs (Proc. Spec. Mtg. Oarai, 1991), IAEA, Vienna (1992) IWGFR/85.
- [8] ASHURKO, Yu., Decay Heat Removal System in the Secondary Circuit of the Sodium-Cooled Fast Reactor and Evaluation of its Capacity, Atomic Energy, Vol. 124, Issue 1 (2018) 3-8.
- [9] Greenpeace Russian branch. Who will pay for accidents? (2011), <https://www.greenpeace.org/russia/ru/campaigns/nuclear/accidents/chernobyl/25yrs/responsibility>
- [10] Ministry of Economy of Japan announced the cost of elimination of the NPP Fukushima-1 accident (2016), <https://ria.ru/20161209/1483182700.html>

FEASIBILITY STUDY OF SMALL SODIUM COOLED FAST REACTORS

Paper ID #23

H. HAYAFUNE
Japan Atomic Energy Agency
Oarai, Higashi-ibaraki-gun, Japan
Email: hayafune.hiroki@jaea.go.jp

Y. CHIKAZAWA
Japan Atomic Energy Agency
Oarai, Higashi-ibaraki-gun, Japan

Abstract

A small reactor has the potential to be utilized as a power source to meet the diverse social needs and reduce capital risks. In the previous feasibility study, two types of small sodium cooled fast reactors: #1 modular concept competitive to other larger reactors for base load power generation and #2 non-refuelling concept for remote power source whose capacity less than 50 MW(e) were investigated.

1. INTRODUCTION

A feasibility study on commercialized fast reactor cycle systems in Japan Atomic Energy Agency (JAEA) aims to clarify various perspectives for commercialization of fast reactor cycle systems that correspond flexibly to diverse future needs. In the JAEA feasibility study, various fast reactors with different sizes, fuel and coolant have been investigated. In this study, a small sized metal fuel sodium cooled reactor was studied as one of candidates for next generation reactors. Though a large-scale sodium cooled reactor (JSFR [1]) was selected to a reference design in the JAEA feasibility study, a small modular reactor still has attractiveness to achieve requirements for future energy resources with low R&D risk. A modular power source with a small electric power can reduce capital and R&D risks since such a small reactor needs a low construction cost per unit and can be demonstrated in small scale experimental facilities. Small light water reactors such as International Reactor Innovative and Secure (IRIS) [2], Integrated Modular Water Reactor (IMR) [3] and small BWR [4] whose electric outputs are around 300 MW(e) have been developed for diversified or modular power sources. As regards fast reactors, Integrated Fast Reactor (IFR) for a modular power source was proposed [5].

From the viewpoint of FR cycle commercialization, a low-cost demonstration including economic performance of the whole fuel cycle system is desirable. Previous studies on small reactors showed that a reactor whose electric power is approximately 300 MW(e) balances economic performance with reduction of capital and R&D risk [6]. From the point of fuel cycle, metal fuel cycle using electrometallurgical pyro processing has high economic potential in a small capacity. A previous study on IFR showed commercialization and safety potential of metal fuel cycle using modular reactors [5].

In the feasibility study, a new metal fuel sodium cooled reactor with 300 MW electric has been developed enhancing further cost reduction [7]. And economical potential at demonstration stage is emphasized. As a plant design, a minimum configuration with a compact reactor vessel, one-loop main cooling system and simple fuel handling system are adopted enhancing cost reduction. Besides, construction cost of a set of a first-of-a-kind reactor and small fuel cycle plant is evaluated to show budget requirement for demonstration of whole fuel cycle. A major advantage of the present modular concept is that the demonstration reactor and fuel cycle plant

can be directly appropriated for first commercial modules and the power plant can easily increase its capacity by adding reactor and electro refiner modules. Commercialization of nuclear fuel cycle using the present modular concept is thought to reduce R&D risk since the total budget for demonstration is small and the facilities for demonstration are directly appropriated to commercial use.

In a remote site with a small population, a small capacity power source with 50 MW-electric that does not require refuelling is attractive since fuel transfer costs to such a site are expensive. A super-safe, small, and simple reactor (4S) has been developed by the Central Research Institute of Electric Power Industry [8]. The 50 MW(e) 4S has a tall metal fuel core controlled by movable reflectors. The movable reflectors burn the core from the bottom to the top for 30 years without refuelling. Basic experiments of reflector control neutronics, the tall fuel assembly, and the reflector driver system have been performed [9].

In the present study, a new metal fuel core concept with 50 MW(e) and a core life of 30 years has been developed [10]. A single Pu enrichment plural Zr content regions core concept [11,12] is adopted to reduce local burn-up reactivity changes, achieving a high core outlet temperature of 550 degrees Celsius. In the present core concept, the fuel volume fraction is increased to achieve small burn-up reactivity suitable for a core life of 30 years. One attempt to increase the fuel volume fraction involves larger diameter fuel pins. Other attempts include thinner wrapper tube ducts and narrower inter-wrapper gaps that can be introduced particularly with a non-refuelling core. With the high fuel volume fraction, the burn-up reactivity is reduced to be approximately 1 percent of (dk/kk') , which is much smaller than that of the 4S value (9 percent of (dk/kk') [8]); thus, a conventional control rod system can be adopted for reactivity control while the 4S can adopt a movable reflector control.

In the plant design, a new compact loop-type plant for the new 50 MW(e) long-life core has been designed. The reactor vessel is minimized by considering a non-refuelling system that does not have a fuel handling machine, fuel transfer port, or rotating plug. In a loop-type reactor, the reactor vessel diameter is dramatically reduced by eliminating the fuel handling system. The loop number of the main cooling system is reduced to one by adopting two series of electromagnetic pumps (EMP), which are arranged in the intermediate heat exchanger. Dimensions of the major components and the total material mass of the nuclear steam supply system (NSSS) have been determined to estimate the economic potential of the non-refuelling concept.

2. MODULAR CONCEPT

2.1. Core design

The single plutonium enrichment plural zirconium content regions core concept proposed by Sugino et al [11,12] is adopted to the core design. In that core concept, breeding and burning in every core region are balanced by optimizing zirconium content and smear density of each core region to achieve small power distribution changes. Therefore, the core outlet temperature can be designed to be as high as 550 °C, which is a high value against the cladding temperature limitation of 650 °C of the metal fuel. For the present 300 MW(e) plant, a core with thermal output 714 MW has been designed by Sanda et al. [13]. The major parameters of the core are shown in Table 1.

The zirconium content is 10% and 6% in the inner and outer region. The smear densities are 70 and 75 % in the inner and outer region, respectively. The zirconium content and the smear density are selected from the range which has experience in the metal fuel irradiation test in EBR-II [14]. Fuel pin cladding and subassembly materials are oxide dispersion strengthened (ODS) martensitic steel [15] and PNC-FMS (Ferritic/Martensitic Steel) [16] which have high temperature strength and dimensional stability with high energy neutron fluence.

TABLE 1. CORE PARAMETERS [7]

Item	Unit	Value
Thermal Output	MW	714
Electric Output	MW	300
Operation Cycle	months	24
Batch Quantity	-	4
Temperature (Outlet/Inlet)	°C	550/395
Fuel Type	-	U-Pu-Zr
Plutonium Content	%	12.33
Smear Density (Inner/Outer)	%	70/75
Zirconium Content (Inner/Outer)	%	10/6
Subassembly Quantity (Inner/Outer)	-	81/162
Control Rod Quantity (Main/Backup)	-	7/3
Core Height	cm	100
Gas Plenum Height	cm	170
Core Equivalent Diameter	cm	263
Subassembly Pitch	mm	157.2
Duct Thickness / Subassembly Gap	mm	5/4.2
Fuel Pin Quantity per Subassembly	-	217
Fuel Pin Diameter	mm	8.5
Cladding Thickness	mm	0.5
Inter Fuel Pin Gap	mm	1.0
Average Discharge Burnup	GWd/t	80
Burnup Reactivity	dk/kk'	0.46
Breeding Ratio	-	1.03
Maximum Fast Neutron Fluence (E>0.1MeV)	n/cm ²	5.2x10 ²³

2.2. Plant design

A sketch of the reactor vessel is shown in Fig.1. The reactor vessel is minimized by adopting an upper inner structure with a slit (slit UIS) which is also adopted to the JSFR [1]. The slit UIS can reduce the distance between the centre of the core and the rotating plug since a fuel handling machine can access every fuel subassembly through the UIS slit. The hot and cold leg piping of the main cooling system enters from the top of the vessel without any nozzle on the vessel wall. The space outside the core barrel is utilized for the fuel transit point, piping entrances, the in-vessel storage (IVS) of the spent fuel assemblies, etc. Four-year decay storage is required for spent fuels to reduce the decay heat level up to 2 kW/subassembly with which a

spent fuel subassembly can be treated by gas cooling. In the modular concept, the minimum capacity for four-year storage is 122 subassemblies (2 batches) and the IVS can store more than 140 subassemblies. The IVS is separated into four regions as shown in Fig. 1 and each region has a coolant inlet whose coolant flow rate was controlled by orifices. An ex-vessel storage facility which could increase the plant construction cost is not need in the modular concept.

In the present design, hot sodium directly contacts with the primary vessel wall. A similar hot vessel design is adopted in the JSFR. The preliminary evaluation of the JSFR thermal transient analysis showed that the thermal shield inside the primary vessel wall could maintain the material damage below the design limit [1]. Fast Reactor Structural Design Standard (FDS) which includes new evaluation methods considering inelastic deformation is under developing for the next generation fast reactors [17]. The same measure and evaluation methods are thought to be applicable to the present 300 MW(e) design.

Major parameters and a schematic illustration of the main cooling system are shown in Table 2 and Fig. 2. The loop number is one by adopting two independent electromagnetic pumps (EMP) arranged in series. Electric power for the two EMPs is supplied independently and the stator casings have separated each other to keep redundancy of the primary circuit. But cold leg pipes are separated into two to mitigate reduction of the core flow rate in case of a pipe break accident. From the viewpoint of large flow rate and high efficiency, an annular linear induction pump (ALIP) with sodium cooled coils is applicable. There were two large scale demonstration tests of ALIP type EMPs. One is with 44 m³/min flow rate and 0.1 MPa pump head for 10000 hours operation [18]. The other is with 160 m³/min flow rate and 0.25 MPa pump head [19] for 2550 h operation. The 160 m³/min EMP was operated showing stable flow rate and pump head with 40 % efficiency. The practical efficiency becomes higher since the EMP loss is regained by coolant sodium and recycled in the real plant.

From the viewpoint of reliability, flow security in case of offsite power down is important since EMP coast down is maintained electrically. In the previous study on a small tank type reactor, a reliable EMP power source was proposed [20]. In the normal operation, a synchronous motor connected with EMP is operated without load and EMP coast down power is stored as mechanical inertia of a synchronous motor flywheel. When the offsite power is down and the power supply for a synchronous motor is stopped, the synchronous motor automatically switches into generator mode for EMP coast down power supply. The major feature of the EMP power source system with a synchronous motor provides passive EMP coast down without requiring any active signal. Reliability of EMP coast down with synchronous motors was evaluated in the previous study. In the case of an EMP served by double synchronous motors, failure probability of a single EMP coast down was evaluated to be 3.87×10^{-7} /demand and failure frequency of emergent loss of reactor flow was evaluated to be 3.39×10^{-8} /reactor-year showing enough reliability.

A system which adopts EMPs as main pumps has a possibility to reduce maintenance compared to the system which is equipped with mechanical pumps. A durability test of the coil insulation showed that it could be used for 100 years at 600 °C [21]. It means that EMPs can operate without coil exchanges in the plant lifetime. Monitoring of coil temperature and insulation test at annual inspection can confirm coil reliability.

For intermediate heat exchanger, the tube type is straight and the primary sodium flows inside the tubes. Material of the tubes, shell, and piping is 12Cr steel which has high thermal conductivity and low thermal expansion. The main EMPs of the primary sodium circuit are installed in the IHX to reduce sodium boundary and arrangement space for the primary sodium

circuit. The material of the EMP duct is made of austenitic stainless steel since ferritic steel cut off the electromagnet field from the EMP stators. The dissimilar material welds between 12Cr steel and the EMP duct are located at the top of the plug with thermal shield. Therefore, the temperature of the dissimilar welds is low and the access for maintenance is convenient.

For steam generator, tubes are helical coil type which has experience in Monju and Superphenix. The SG upper plenum contains a sodium purification system and a heat exchanger of a decay heat removal system to eliminate external branching of the sodium flow to reduce opportunities for sodium leak.

There are two direct reactor auxiliary cooling systems (DRACS) and one intermediate reactor auxiliary cooling system (IRACS) for reactor decay heat removal. They are circulated by natural convection enhancing passive safety features in the decay heat removal operation. The DRACS removes the decay heat from the reactor vessel by heat exchangers arranged in the reactor vessel. The IRACS heat exchanger is in the SG upper plenum. The DRACS heat exchangers are connected with the lower plenum by in-vessel pipes. Hot sodium from the core is cooled at the DRACS heat exchangers and goes down through the in-vessel pipes to the lower plenum by natural convection force. There are flow diodes at the penetration between the upper and the lower plenum to reduce reverse flow in the normal operation. In the future study, the performance of the flow diode will be tested in water experiments and transient analyses will be performed to show consistency of the whole decay heat removal system.

The view of main components and reactor building arrangement are shown in Fig. 3. The arrangement of the reactor components is simple adopting one loop system and the reactor building can be compacted without any ex-vessel fuel storage system. The volume of the reactor building is evaluated to be 66,000 m³ which is dramatically smaller than that of Monju (207,000 m³ for 280 MW(e)).

TABLE 2. MAJOR PARAMETERS OF COOLING SYSTEM [7]

Item	Unit	Value
Thermal Output	MW	714
Electric Output	MW	300
Primary Sodium Loop	-	1loop
Primary Sodium Temperature	°C	550/395
Primary Sodium Flow Rate	kg/h	1.3x10 ⁷
Secondary Sodium Loop	-	one loop
Secondary Sodium Temperature	°C	520/335
Secondary Sodium Flow Rate	kg/h	1.1x10 ⁷
Steam/Feed Water Temperature	°C	497/233
Steam Pressure	MPa	17.2
Steam Flow Rate	kg/h	1.2x10 ⁶
Thermal Efficiency *	%	42

*: thermal efficiency of steam cycle excluding plant load and heat loss.

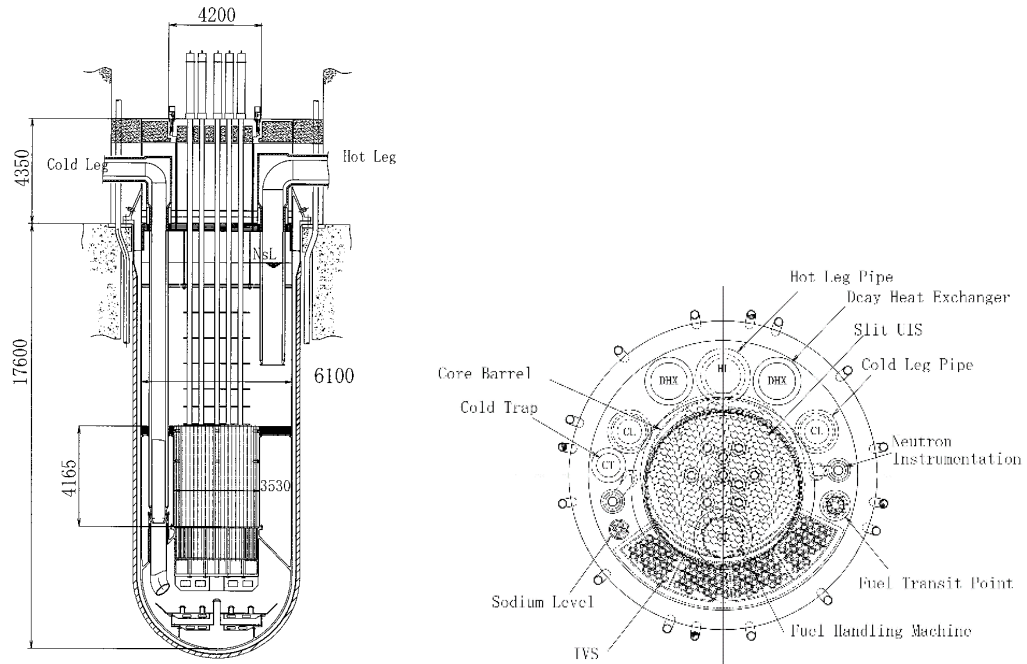


FIG. 1. Sketch of Reactor Vessel (modular concept) [7]

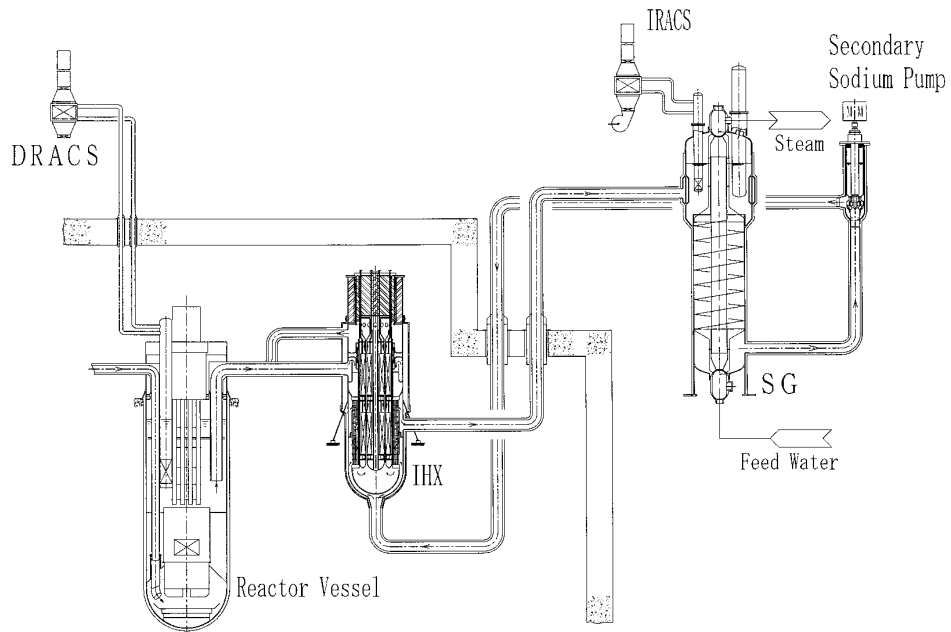


FIG. 2. Schematic Illustration of Cooling System (modular concept) [7]

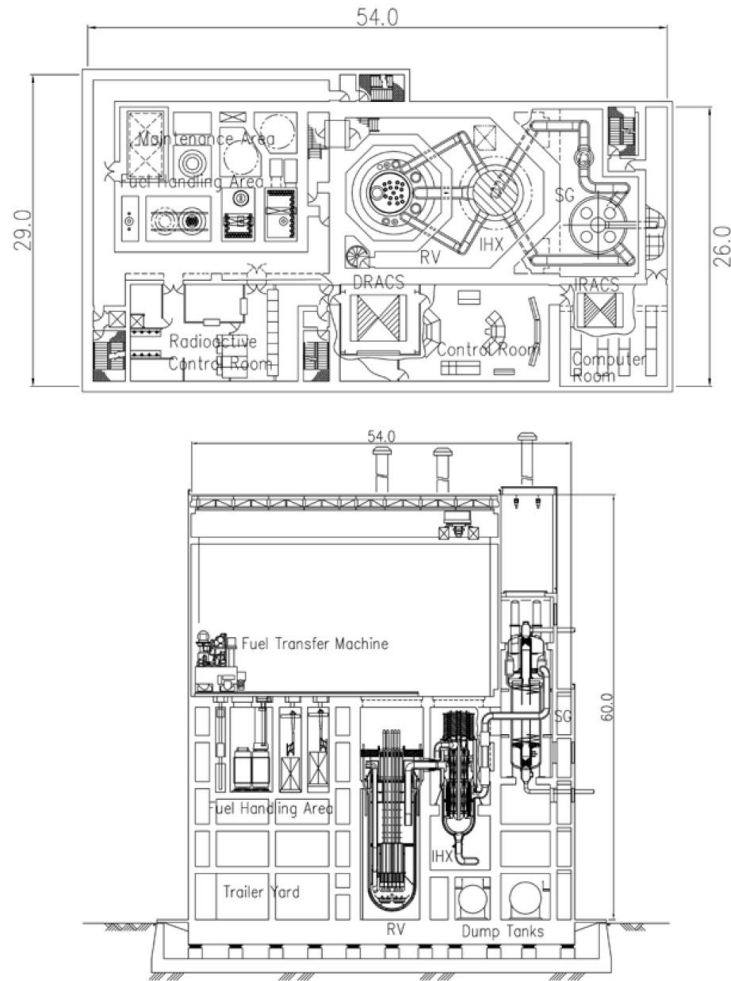


FIG. 3. Reactor Building Arrangement (modular concept) [7]

2.3. Economic evaluation

In the JAEA feasibility study, various concepts for commercialized fast reactor were designed and their economical potentials were estimated. In the economic evaluation, direct costs of NSSS and BOP (Balance of Plant) are classified into each component and facility, respectively. Direct cost of each component or facility was estimated based on the material weight or other major specifications. Indirect cost is estimated considering field cost, engineering cost, owners cost and interest during construction. Economic competitiveness of large and medium scale reactors with various coolants was summarized by Kotake et al. [22].

In the present study, the same database is used to evaluate construction cost of each component in the NSSS. The direct cost of NSSS components are evaluated based on each component mass. The direct cost of BOP and the indirect cost are roughly extrapolated from that of the medium scale reactor since the method for large scale reactors cannot be directly applied to small reactors. In the present estimation, the direct cost of BOP is assumed to be in proportion with the 0.6 power to the thermal output. Indirect cost is roughly evaluated on the assumption that the ratio of the indirect cost to the total cost was the same as that of the medium scale sodium cooled reactor.

The steel mass in the NSSS is shown in Table 3. The mass of the present loop type is evaluated to be 1191 tons including EMP stators of 154 tons. The total construction cost including indirect cost is evaluated to be 190 % of the target cost of 2,000 USD/kW(e) (1USD=100JPY). In the case of Nth-of-a-kind (NOAK) reactor, the construction cost can be reduced to be 115% of the target cost assuming learning effect ratio of 0.6. In order to evaluate electricity cost, a total fuel cycle system including reprocessing and fuel fabrication needs to be considered. Reprocessing and fuel fabrication suitable for metal fuel are pyrochemical processing with electrorefining and injection casting, respectively which have experiences in EBR-II [23]. In the JAEA feasibility study, a metal-fuel recycle plant combined a pyrochemical reprocessing facility with an injection casting fuel-fabrication facility for commercial base with 38tHM/y (heavy metal tons per year) capacity were designed showing that the fuel cost achieved 94% of the target cost of 8 USD/MWh [24,25]. Therefore, the electricity cost with the present modular concept in NOAK still has a possibility to achieve the target of 40 USD/MWh as a whole nuclear cycle system.

For the FR cycle commercialization, a demonstration with a small budget, low risk and high economic performance is desirable. According to previous studies [26], a reactor with electrical output more than 300 MW(e) is thought to be a minimum reactor size to show economic performance of power generation. In the present study, a minimum set of FR cycle demonstration facilities is assumed to be composed by a 300 MW(e) reactor and a small recycle plant for the 300 MW(e) reactor. The same components designed for the 38tHM/y commercialized facilities were equipped for demonstration of each component and capacity-increment potential. The fuel storages for new and spent fuels in the recycle plant are only temporary, assuming the reactor and its recycle plant are co-located in a site.

In the present modular concept, there are 243 subassemblies in the core with 26tHM/y and the mass flow of heavy metal is 3.3 tHM/y with the batch quantity of four and reactor operation cycle of two years. In the reprocessing facility, the electro refiner has two sets of electrodes and its capacity is approximately 4tHM/y. Other components have larger capacities since they are designed for commercial base. Therefore, the capacity of the fuel recycle plant can increase its capacity by adding electro refiner modules. Construction costs for a reactor and a small recycle plant in FOAK are estimated to be 1200 M\$ and 700 M\$ respectively. It means that a budget of 1900 M\$ can demonstrate whole FR fuel cycle with commercial based components. Besides, the demonstration plant can be easily commercialized since it can increase its capacity by adding reactor and electro refiner modules.

TABLE 3. NSSS MASS EVALUATION [7]

item	value (tonne)
primary vessel	107
inner structure	125
upper structure	122
guard vessel	72
primary cooling system *	276
secondary cooling system	335
total (tonne)	1037

*: Except EMP stator mass 154 tonnes

3. NON REFUELING CONCEPT

3.1. Core design

A new core concept that provides a 30-year life for a non-refuelling reactor has been developed. For a long operation cycle core, small burn-up reactivity is required to reduce the control reactivity of the core. Therefore, ternary metal fuel (U-Pu-Zr) is selected to achieve a high heavy metal density that results in smaller burn-up reactivity. In addition, a single Pu enrichment plural Zr content regions concept whose basic concept for large scale reactors is proposed by Sugino et al. [11,12] is adopted. In that core concept, breeding and burning in every core region are balanced by optimizing Zr content and smear density of each core region to achieve small power distribution changes. Therefore, the core outlet temperature can be designed to be as high as 550 degrees Celsius, which is a high value against the cladding temperature limitation of 650 degrees Celsius of the metal fuel. In the present study, the single Pu enrichment plural Zr content regions concept is adopted, since a small burn-up reactivity change is desirable for a long core life. In a long core life design, a large fuel volume fraction is important for achieving small burn-up reactivity. In that core concept, a large fuel pin diameter is applied to increase the fuel volume fraction. As further efforts for high fuel volume fraction, thinner wrapper duct thickness and narrower inter-wrapper gap are adopted. In an ordinary sodium-cooled reactor design, wrapper duct thickness and inter-wrapper gap are designed according to the load in the refuelling operation since the new fuels are pushed into the burned core in which subassemblies are in contact with each other for irradiation bowing. In the case of the non-refuelling concept, the inter-wrapper gap can be reduced since strong contact among subassemblies is acceptable. In addition, the wrapper duct thickness can also be reduced since it is only restricted by the normal operating condition.

In the metal fuel irradiation test in EBR-II [14], increased smear density results were reported in higher cladding strains, but lower cladding wastage was reported from fuel/cladding chemical interactions; the optimal fuel smear density fell between 75 and 85 percent. Therefore, both conventional and aggressive concepts are utilized in the present study. Specifications of the cores are shown in Table 4. Fuel pin cladding and subassembly materials are oxide dispersion strengthened (ODS) martensitic steel [15] and PNC-FMS (Ferritic/Martensitic Steel) [16], which have high temperature strength and dimensional stability with high energy neutron doses. The power distribution and fuel cycle were evaluated using the MOSES code [27], CITATION code [28], and SLAROM code [29] based on ADJ2000R [30]. Maximum smear densities in conventional and aggressive cores are limited to up to 75 percent and 85 percent respectively. A variation in Zr content is set to be 6 and 10 percent, considering irradiation experience in EBR-II [14].

The major difference between the two concepts is the gas plenum height. The gas plenum height of the conventional concept is 2.45 meters, which is much longer than that of the aggressive concept at 1.51 meters, since thin clad is adopted to increase the fuel volume fraction. The core equivalent diameters of the two concepts are both approximately 1.82 meters, with the same fuel subassembly quantities and similar subassembly pitches. Other differences in the core specifications include a slight pin diameter difference and spacer type; however, these have no major impact on the plant design. Therefore, in the following part of this paper, the aggressive core is selected as a temporal reference.

The core configuration of the aggressive design is shown in Figure 4. The fuel pin diameter and gap are 15 millimetres and 1 millimetre, respectively. The fuel pin quantity in a subassembly is 127, with the subassembly pitch approximately 188 millimetres. The wrapper duct thickness and gap are 2 millimetres and 1 millimetre. Three regions, according to the zirconium content and smear density and subassembly quantities, in the inner, middle, and outer cores are 15, 21 and 42, respectively. The zirconium content is 10 percent in the inner and middle cores and 6 percent in the outer core. The smear densities of the inner, middle, and outer cores are 70, 79, and 85 percent, respectively. The fuel volume fraction in each region is evaluated to be high—in the range from 41 to 50 percent.

Extremely small power distribution changes occur during the life of the core. The results indicate that plutonium burning and breeding in every core region are successfully balanced by optimizing zirconium content and smear density in the three separated regions, which allows the core outlet temperature to reach 550 degrees Celsius, with a maximum clad temperature limit of 650 degrees Celsius, since the flow distribution of the core can be optimized with the small radial power swing. The burn-up reactivity is estimated to be 1.11 percent of (dk/kk') , thereby achieving a 30-year core life with the average burn-up of 77 MWd/t. The core life is limited by the maximum high energy neutron fluence (>0.1 MeV) on fuel cladding. The resistance of ODS steel against fast neutron irradiation is still being tested, but the experiment indicated the possibility of ODS steel resisting a fluence of 5×10^{23} n/cm². Therefore, the maximum neutron fluence in this design is limited to approximately 5×10^{23} n/cm² [31].

Shielding is optimized with a combination of stainless-steel pins and zirconium hydride pins in one shielding subassembly. The stainless-steel pins are arranged inside, while the zirconium hydride pins are outside. The neutron fluence at the core formerly made by 9Cr ferritic steel is estimated to be 1.5×10^{22} n/cm² for >0.1 MeV, which is lower than that of the limit of ferritic steel at 4×10^{22} n/cm² [32].

A conventional control rod system using B4C pellets is selected to be used for main, backup, and self-actuated shutdown systems (SASS). The control rod quantities of main and backup systems are 5 and 2 respectively. The ¹⁰B content of the main system, which controls core reactivity in normal operations, is that of natural boron; the lifetime of the control rods is estimated to be more than 30 years. The ¹⁰B content of the backup control rods, which are located above the top of the active core, is 30 percent, thus keeping enough shutdown reactivity of one rod became stuck. The SASS is composed of curie point electromagnets arranged at the backup control rods. When the temperature at the curie point electromagnets surpasses the threshold temperature, the magnet force decreases rapidly. In addition, the backup control rods are dropped, resulting in a passive reactor shutdown.

TABLE 4. CORE DESIGN PARAMETERS [10]

Items	Units	Conventional	Aggressive
Output (Thermal/Electric)	MW	120/50	<<
Temperature (Outlet/Inlet)	°C	550/395	<<
Core Life Time	year	30	<<
Pin Diameter	mm	14.4	15
Clad Thickness	mm	0.55	0.78
Pin Gap	mm	1.6	1.0
Number of Pins	-	127	<<
Spacer	-	Grid	Wire
Fuel Assemblies (In/Mid./Out)	-	6/24/48	15/21/42
CR/RF Assemblies	-	7/42	<<
Pu Enrichment	%	approx. 12	<<
Zr Contents (In/Mid./Out)	%	10/10/6	<<
Smear Density (In/Mid./Out)	%	70/75/75	70/79/85
Lattice Pitch	mm	187.7	188.3
Duct Wall/Gap	mm	2/1	2/1
Core Height	m	1.18	1.01
Gas Plenum Height	m	2.45	1.51
Core Equivalent Diameter	m	1.82	<<
Core barrel Inner Diameter	m	2.31	<<
Pressure Drop (Bundle)	MPa	0.021	0.026
Average Discharge Burnup	MWd/t	74	77
Burnup Reactivity	%dk/kk'	1.24	1.11
Maximum Fast Neutron Fluence	n/cm ²	5.5x10 ²³	5.3x10 ²³

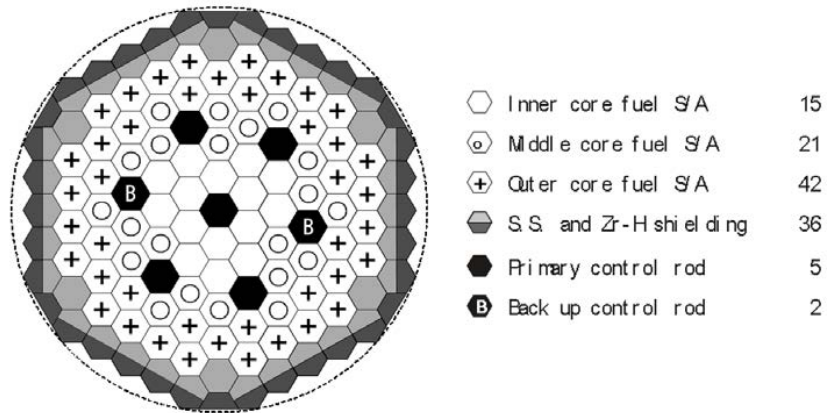


FIG. 4. Core Configuration (non-refuelling concept)

3.2. Plant design

Figure 5 illustrates the reactor vessel; whose basic features include a simplification of adopting a non-refuelling concept with the long-life core. The ordinary loop-type sodium-cooled reactor with refuelling uses a fuel transfer port, heat exchangers for decay heat removal, and sodium purification components between the core barrel and primary vessel. Therefore, the diameter of the primary vessel of the ordinary loop type is larger than that of the core barrel by approximately 3 meters. In the present non-refuelling concept, the core can be horizontally supported by the primary vessel directly without a core barrel since no components are arranged between the core and primary vessel—neither a fuel handling machine nor fuel transfer port in the primary vessel adopting the non-refuelling concept. The primary sodium purification during reactor operation can be eliminated since impurities from the outside are negligible without a refuelling operation. The volume of the reactor's upper plenum is reduced, moving the decay heat exchangers from the upper plenum to the cover gas area. The nozzle-type sodium inlet and outlet are also adopted to save in-vessel piping space. The reactor vessel nozzles have been in long-term operation in Joyo (an experimental fast reactor in Japan) and Monju (a prototype fast breeder reactor in Japan), demonstrating reliability. Adopting these simplifications, the inner diameter of the primary vessel is designed to be 2.8 meters, with the shielding circumscription diameter of 2.3 meters.

In the ordinary loop-type reactor with refuelling, the reactor vessel height is determined by the need to maintain the sodium level beyond subassemblies, which are transported above the core by the fuel handling machine in the refuelling operation. In the present non-refuelling concept, the height of the reactor vessel is reduced since the sodium level is determined only according to normal and decay heat removal operations. Another effort to reduce the reactor vessel height involves the arrangement of the decay heat exchangers in the cover gas. The coolant paths for the decay heat removal systems are always maintained by in-vessel piping. Therefore, no requirement exists for the sodium level in regard to the decay heat removal operation. The height of the reactor vessel, therefore, is finally designed at 13.4 meters after considering the sodium level reduction in case of primary vessel leakage. The upper structure of the reactor vessel is a dome without a rotating plug for fuel handling operation. The elimination of the rotation plug also allows the simplification of the roof deck without a cooling system for rotation plug.

The main cooling system loop number adopts two independent electromagnetic pumps arranged in a series. Electromagnetic pumps can be arranged in a series because they have no mechanical parts that can cause flow path blockage in pump failure. In the case of mechanical pumps, an impeller causes flow path blockage if the pump becomes stuck. When one electromagnetic pump is tripped during an accident, the other pump can maintain the core flow to reach a safe reactor shutdown. The reliability and R&D status of the EMP will be discussed in Section 2.2

In the case of primary sodium leakage, the sodium level is maintained by double-walled piping and guard vessels of the primary vessel as well as the intermediate heat exchanger. The primary circuit material is 316FR stainless steel, which is the same as in the reactor vessel, to eliminate dissimilar material welds in the primary system. The main pumps in the primary cooling system are arranged in the shell of the intermediate heat exchanger (IHX) to simplify the primary cooling system.

The secondary cooling system loop number also minimizes the material mass. The steam generator (SG) is a helical coil type that has been used in Super Phoenix and Monju. The SG tube material is 12Cr steel, which has high heat conductivity to reduce the heat exchange area.

The main steam temperature is 495 degrees Celsius in 16.7MPa, with the core outlet sodium temperature of 550 degrees Celsius. The steam cycle efficiency with this steam condition is estimated to be 42 percent when using a conventional steam turbine [1]. The SG upper plenum contains a sodium purification system and a heat exchanger of a decay heat removal system to eliminate any branch in the major cooling system, thus reducing sodium leak probability.

The decay heat removal system is composed of two direct reactor auxiliary cooling systems (DRACS) and one intermediate reactor auxiliary cooling system (IRACS), each with 50 percent heat capacity. They are operated using natural convection to enhance passive safety. Two DRACSs are suitable for a one-loop main cooling system since primary reactor auxiliary cooling system (PRACS) and IRACS has to depend on only one main circuit. In case of pipe break accidents in the main cooling system, the decay heat is removed directly from the reactor vessel by DRACSs. The DRACSs have penetrations between high and low pressure plenums to enhance natural circulation. Flow diodes at penetration reduce the bypass flow in the normal operation. The IRACS's heat removal coil is arranged at the SG plenum. These decay heat removal systems are circulated by natural convection forces during emergency operations, pursuing passive safety features.

The arrangement of the reactor building is shown in Figure 6. The compact arrangement is achieved adopting the compact reactor vessel, one loop main cooling system, and no fuel handling system so that the volumes of the confinement and the reactor building are evaluated to be 2530 meters³ and 21,000 meters³, respectively. An additional guard is located outside the double wall primary piping. This guard pipe is installed to maintain the sodium level against physical attack on the primary piping, such as a carried component drop.

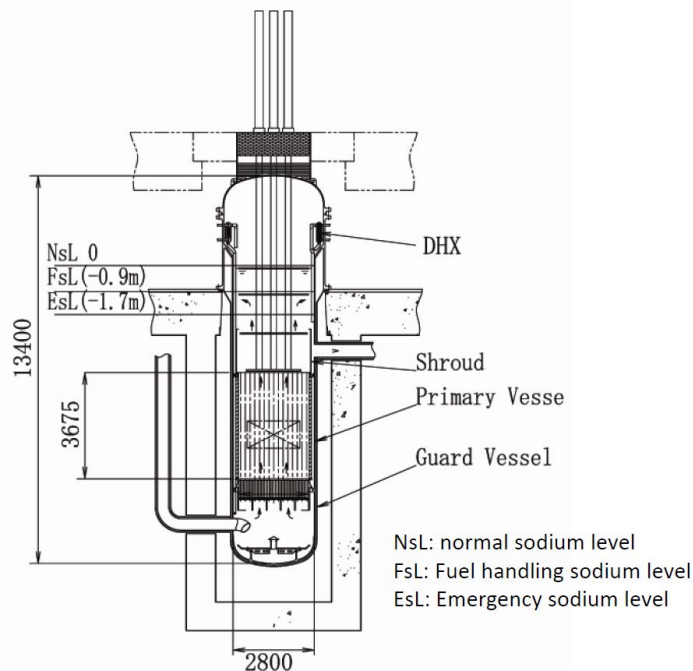


FIG. 5 Sketch of Reactor Vessel (non-refuelling concept) (unit: mm) [10]

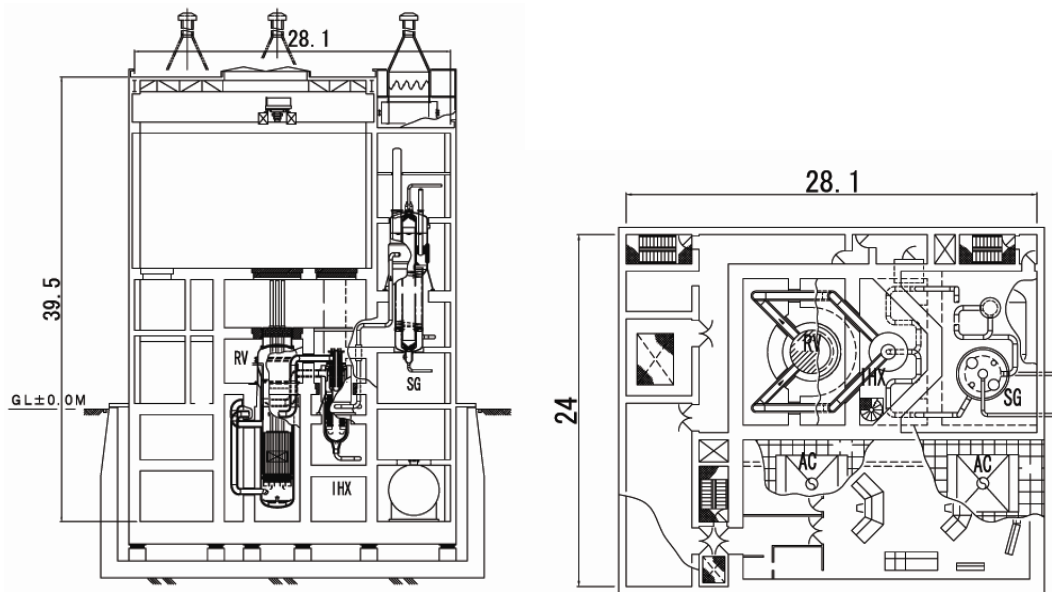


FIG. 6 Sketch of Reactor Building (non-refuelling concept) (unit: m)

3.3. Economic Evaluation

In the JAEA feasibility study, various commercialized fast reactors were designed, and their economical potentials estimated. In the economic evaluation, direct costs of NSSS and balance of plant (BOP) were classified according to each component and facility, respectively. The direct cost of each component or facility is assumed to be a product of the unit cost multiplied by the material mass or another major specification. Indirect cost is estimated considering field cost, engineering cost, owner's cost, and interest during construction. The economic competitiveness of large and medium scale reactors with various coolants was summarized by Kotake et al. [22].

In the present study, the same database is used to evaluate small reactor construction costs. The direct costs of NSSS components are evaluated using each component mass based on the database. The direct cost of BOP and the indirect cost are roughly extrapolated from that of medium scale reactors since the method for large and medium scale reactors cannot be directly applied to a small reactor. In the present estimation, the direct cost of the BOP is assumed to be in proportion to the 0.6 power to thermal output. The indirect cost is roughly evaluated assuming the ratio of the indirect cost to the total cost is the same as in the case of the medium scale sodium-cooled reactor.

The steel mass in the NSSS is shown in Table 5 compared to a pool-type reactor, which is a 50 MW(e) scale down concept of JAEA's 165 MW-electric reactor [20]. The 105-ton reactor structure includes a reactor vessel of 38.5 tons, an inner structure of 28 tons, an upper structure of 18 tons, and guard vessel of 20.5 tons. The total NSSS mass of the present loop type is evaluated to be 309 tons, much lower than that of the pool type's 484 tons. Unless the aggressive core design with an 85 percent smear density fuel is revealed to be feasible in the future study, the conventional design with a 75 percent smear density fuel has to be selected. In that case, the reactor vessel and guard vessel heights increase approximately 1 meter and the total mass increases approximately 5 tons. This value is negligible for the following economic evaluation.

The construction cost of a first of a kind (FOAK) is evaluated to be 8200 USD/kW(e) (1USD=100JPY) based on the above evaluation method. This value is 410 percent of the target construction cost for large scale reactors at 2000 USD/kW(e). In the JAEA feasibility study, the target electricity cost of a large-scale reactor for future Japan is 40 \$/MWh including capital, operations, and fuel cycle costs of 14, 15, and 11 \$/MWh, respectively [33]. The construction cost of nuclear power plant in regard to capital and related costs is roughly proportional. Therefore, the capital cost of the present non-refuelling concept is roughly estimated to be approximately 60 USD/MWh. The electricity cost is estimated to be 90 USD/MWh using the target costs for operation and fuel cycle. This value is too high for a power source in a city connected to a power grid, but it is still attractive for remote sites, such as Alaska and Hawaii, where electricity costs were reported to be in the range of 59 to 360 USD/MWh [34]; further cost reduction is expected in the case of an Nth of a kind (NOAK), considering the learning effect.

TABLE 5. STEEL MASS OF NSSS (TONNE) [10]

Items	Tank	Loop
Reactor Structures	345	105
Primary Cooling System	-	65
Secondary Cooling System	139	139
NSSS Total	484	309

4. CONCLUSIONS

A 300 MW(e) fast reactor with a compact reactor vessel, one-loop main cooling system and simple fuel handling system is proposed enhancing cost reduction. Economical evaluation shows that there is a possibility to achieve target electricity cost as a whole fuel cycle system in the commercial phase with plural reactors, though the reactor construction cost is slightly higher than that of the target. A major feature of the modular concept is that the demonstration reactor and recycle plant can be directly appropriated for first commercial modules and the power plant can easily increase its capacity by adding reactor and electro refiner modules. The present study suggests that a total 1900 M\$ budget for a set of a first-of-a-kind reactor and recycle plant can demonstrate fast reactor fuel cycle and the demonstration plant can be directly appropriated for commercial use without any significant design change. Nuclear fuel cycle strategy with the modular reactor and recycle concept is thought to reduce R&D and financial risk since the amount of budget for demonstration stage is relatively small and the facilities for demonstration are directly appropriated to commercial use.

A compact loop-type sodium-cooled reactor without refuelling for 30 years has been developed. A metal fuel core with a 30-year life and a simple plant system without refuelling has been proposed. The local burn-up reactivity change in every core region is minimized by adjusting zirconium content and smear density of the three core regions to achieve a 550-degree Celsius core outlet temperature. The burn-up reactivity at the end of the cycle is evaluated to be 1.1 percent of (dk/kk'), achieving a 30year core life. The reactor vessel is dramatically simplified by eliminating a fuel handling system. The number of the main cooling loops is reduced to one by adopting two series of electromagnetic pumps for primary sodium circulation. The nuclear steam supply system mass, 309 tons, shows that the present loop-type concept can incorporate a dramatically reduced material mass, more so than that of the previous pool-type concept of 484 tons. The rough estimation of the electricity costs shows that non-refuelling concept has competitiveness in remote areas.

REFERENCES

- [1] Y. SHIMAKAWA, S. KASAI, M. KONOMURA AND M. TODA, , “An innovative concept of sodium-cooled reactor pursuing high economic competitiveness”, Nucl. Tech., Vol.140, No. 1, (2002).
- [2] M.D. CARELLI, “IRIS Reactor Design Overview and Status Update”, ICAPP’05, No. 5059, Seoul, Korea, May, (2005)
- [3] T. KANAGAWA, K. HIBI, A. SERIZAWA, T. KUNUGI, T. MATSUMURA AND T. HIDA, “Development Status of Integrated Modular Water Reactor (IMR)”, ICAPP’05, No. 5204, Seoul, Korea, May, (2005)
- [4] H. HEKI, M. NAKAMURAM, M. TSUTAGAWA, M. KUROKI, K. ARAI AND T. HIDA, “Development Status of Compact Containment BWR Plant”, ICAPP’05, No. 5174, Seoul, Korea, May, (2005)
- [5] Y.I. CHANG, “The Integrated Fast Reactor”, Nucl. Tech., Vol. 88, (1989)
- [6] Y. CHIKAZAWA, T. HORI, M. KONOMURA, H. SHIOTANI, K. ONO, “System Design Study of a Small Sodium Cooled Reactor”, JNC TN9400 2002-055, (2002), in Japanese
- [7] Y. CHIKAZAWA ET AL., “A modular metal-fuel fast reactor with one-loop main cooling system”, Nucl. Tech., Vol. 159, p267-278, (2007)
- [8] N. UEDA ET AL., “Current status of sodium cooled super-safe small and simple reactor,” ICONE-10, No. 22353, Arlington, USA, April, (2002).
- [9] I. KINOSHITA, T. KOGA, T. TAKEDA, T. HIGUCHI, AND S. OKAJIIMA, “Development of an advanced controlling system for non-refueling reactors,” ICAPP’2005, No. 5115, May, (2005).
- [10] Y. CHIKAZAWA, ET AL., “A compact loop-type fast reactor without refuelling for a remote area power source”, Nucl. Tech., Vol. 157, p120-131, (2007)
- [11] S. SUGINO, T. OGAWA, Y. OKANO AND T. MIZUNO, “Advanced metal fuel core design study for SFR in the Feasibility Study in Japan”, GLOBAL 2005, No. 399, Oct., (2005)
- [12] T. MIZUNO, T. OGAWA, K. SUGINO AND M. NAGANUMA, “Advanced core design studies with oxide and metal fuels for next generation sodium cooled fast reactor”, ICAPP’05, No.5195, Seoul, Korea, May, (2005)
- [13] T. SANDA, Y. OKANO, M NAGANUMA AND T. MIZUNO, “Design Studies on Small Fast Reactor Cores IV”, JNC TN9400 2005-035,(2005)
- [14] H. TSAI, A.B. COHEN, M.C. BILLONE AND L.A. NEIMARK, “Irradiation performance of U-Pu-Zr Metal Fuels for Liquid-Metal-Cooled Reactors”, The 3rd JSME/ASME Joint International Conference on Nuclear Engineering, S210-2, Kyoto Japan, April, (1995)
- [15] UKAI, S., ET. AL., “Tube manufacturing and characterization of oxide dispersion strengthened ferritic steels ”, J. Nucl. Matter., vol. 283-287, pp.702-706, (2000).
- [16] UEHIRA, A., ET. AL., “Tensile properties of 11Cr-0.5Mo-2W,V,Nb stainless steel in LMFBR environment”, J. Nucl. Science and Tech., vol.37, No. 9, pp.780-786, (2000).
- [17] KASAHARA, N., ANDO, M. AND MORISHITA, M., “Research and development issues for fast reactor structural design standard (FDS)”, Proc. of the ASME PV&P Conf., PVP vol. 472, San Diego, USA, July, (2004)
- [18] W. KWANT, A.W. FANNING, Y. DAYAL, H. IKEDA, J. TAGUCHI, M. NAKAZAKI AND J.M. BOGGIO, “In-sodium and performance of a 43.5m³/min electromagnetic pump for LMR application”, ICONE-5, No. 2553, Nice, France, May, (1997)
- [19] H. OTA, K. KATSUKI, M. FUNATO, J. TAGUCHI, A.W. FANNING, Y. DOI, N. NIBE, M. UETA, T. INAGAKI, “Development of 160m³/min Large Capacity Sodium-Immersed Self-Cooled Electromagnetic Pump”, J. of Nucl. Sci. and Tech., vol. 41, No. 4, p511-523, (2004)
- [20] Y. CHIKAZAWA, Y. OKANO, T. HORI, Y OHKUBO, Y, SHIMAKAWA AND T. TANAKA, “A feasibility study on a small sodium cooled reactor as a diversified power source”, J. of Nucl. Sci. and Tech., vol. 43, No. 8, p. 829, (2006)
- [21] H. MITSUI, R. KUMAZAWA, R. AIZAWA, ET AL, “Study on the voltage endurance life of mica alumina compound insulation at elevated temperature”, Trans. IEEJ A, vol. 117[8], 839 (1997)
- [22] KOTAKE, S., SAKAMOTO, Y., ENUMA, Y., ANDO, M., NISHIKAWA, A. AND SAGAYAMA, Y., “The promising Fast reactor systems and their development plans in Japan”, Proc. if ICAPP’05, Seoul, Korea, paper 5466, (2005)
- [23] S.X. LI, T.A. JOHNSON, B.R. WESTPAL. K.M. GOFF AND R.W. BENEDICT, “Electrorefining Experience for Pyrochemical Processing of Spent EBR-II Driver Fuel”, Proc. of GLOBAL 2005, Tsukuba Japan, Oct, (2005).
- [24] K. SATO, T. FUJIOKA, H. NAKABAYASHI, S. KITAJIMA, T. YOKOO, T. INOUE, “Conceptual Design on an Integrated Metal Fuel Recycle Plant”, Proc. of GLOBAL 2003, New Orleans, LA, USA, Nov. 16-20, p756, (2003).

- [25] K. SATO, I. AMAMOTO, A. INOUE, Y. KOMA, S. YONEZAWA, T. TAKATA, K. FUJII, H. NAKABAYASHI, "Design Study and Evaluation of Advanced Reprocessing Systems for FR Fuel Cycle", JNC Technical Review, No. 24, Extra Edition, JNC TN1340 2004-003, (2004)
- [26] T. HORI, Y. CHIKAZAWA, M. KIDA, M. KONOMURA, "System Design Stud" on a Sodium-Cooled Small-Scale Reactor -Study Result in JFY2002-", JNC TY9400 2003-013, (2003) (in Japanese).
- [27] A. HARA, S. SUZUKI, T. IKEGAMI, S. NAKANISHI, AND H. TANIYAMA, "Development MOSES code for three dimensional diffusion analysis," PNC TN9520 89-002, (1989), in Japanese.
- [28] T. B. FOWLER, D. R. VONDY, AND G. W. CUMMINGHAM, "Nuclear Reactor Analysis Code; CITATION," ORNL-TM-2496, (1969).
- [29] M. NAKAGAWA AND K. TSUCHIHASHI, "SLAROM: A code for cell homogenization calculation of fast reactor," JAERI 1294, (1984), in Japanese.
- [30] T. HAZAMA, G CHIBA, K. NUMATA, AND W. SATO, "Development of the unified cross-section set ADJ2000R for fast reactor analysis," JNC TN9400 2002-064, (2002), in Japanese.
- [31] A. KIMURA, H. CHO, N. TODA, R. KASADA, H. KISHIMOTO, N. IWATA, S. UKAI, S. OHTSUKA, AND M. FUJIWARA, "Fuel Cladding Materials R&D for High Burn-up Operation of Advanced Nuclear Energy System," Proc. of ICAPP'06, Reno, USA, June, (2006).
- [32] C. KELLER AND R. A. STRUB, paper #167, the 7th World Power Conference, p. 55 (1968).
- [33] M. KONOMURA ET AL., "Feasibility study on commercialization of fast breeder reactor cycle systems, Interim report of phase II, Technical study report for reactor plant systems," JNC TN9400 2004-035, (2004) in Japanese.
- [34] "Report to congress on small modular nuclear reactors," U.S. Department of Energy, Office of Nuclear Energy, Science and Technology, May, (2001).

A PRELIMINARY STUDY OF AUTONOMOUS AND ULTRA-LONG LIFE HYBRID MICRO-MODULAR REACTOR COOLED BY SODIUM HEAT PIPES

Paper ID #27

Seongdong Jang
Korea Advanced Institute of Science and Technology (KAIST)
291 Daehak-ro, Yuseong-gu, Daejeon, 34141, Republic of Korea
Email: seongdong@kaist.ac.kr

Yonghee Kim
Korea Advanced Institute of Science and Technology (KAIST)
291 Daehak-ro, Yuseong-gu, Daejeon, 34141, Republic of Korea
Email: yongheekim@kaist.ac.kr

Abstract

A concept of hybrid micro modular reactor (H-MMR) aimed for autonomous operation and ultra-long core lifetime has been introduced. The H-MMR integrates an MMR developed by KAIST and renewable energy through a common thermal energy storage system (ESS). The reactor power is 12 MW(th) and it is designed for continuous operation without refuelling over 20 years. A unique feature of the H-MMR is that it is comprised of 18 hexagonal fuel assemblies (FAs) with sodium heat pipes cooled system, which are inserted into the FAs like a conventional fuel pin design. All the heat transfer is only through the heat pipes by natural circulation of sodium, while there is no direct flowing coolant through the FAs during both normal and transient conditions. The H-MMR core has a thick PbO radial-reflector and an oxide dispersion-strengthened steel (ODS) axial-reflector with a B₄C shielding layer in the outer region. The drum-type reactivity control system is in the radial-reflector as the primary reactivity control system, and a conventional secondary reactivity control device is placed in the central non-fuel region of the core. In this study, to enhance a neutron economy over an ultra-long core lifetime, the inverted FA concept using a low-density uranium mono-nitride (U¹⁵N) fuel with graphite moderator is adopted. All neutronic analyses were performed by Serpent 2 code, which is based on continuous energy Monte Carlo method, with ENDF/B-VII.1 data library. It was found that the effect of the U¹⁵N-based inverted FA design achieves around 100-years reactor lifetime without refuelling, while the reactivity swing over the whole core lifetime is less than one dollar. These results imply that the safe and long-life fast reactor can be realized, and it has a chance to achieve a very efficient autonomous load-following operation without any active controls.

1. INTRODUCTION

The interest in the sustainable development has been gradually increased owing to increasing the needs of the leaving pleasant environment to next generation. As part of the sustainable development in nuclear fields, the attention of the small and medium sized or modular reactors (SMRs) have been on the rise due to the benefits such as inherent passive safety, various applications and reduced capital cost. In this regard, the concept of the coexistence of SMRs with renewable energy via energy storage system (ESS) is highlighting for achieving substantive sustainability.

Recently, a micro-modular reactor (MMR) was developed by KAIST, which is the fast reactor using UC fuel with supercritical CO₂ gas cooled power conversion unit [1, 2, 3 and 4]. It has 36 MW(th) power with 34 % thermal efficiency, passive safety features, and over 20 years lifetime. The main objective of the MMR was to be able to be transported by a truck to the isolated sites by focusing on reducing the weight of the MMR module.

The purpose of the present study was to develop the hybrid micro modular reactor (H-MMR), which is the integrated concept with modified MMR and renewable energy through the ESS. The main objectives of this preliminary study were to achieve ultra-long lifetime around 100-years and ascertain the possibility of the autonomous load follow operation. The main feature of the H-MMR is the inverted fuel assembly (FA) using a homogeneous [5] or heterogeneous enriched uranium nitride ($U^{15}N$) fuel with a graphite moderator. Moreover, the heat transfer is only through the heat pipes, which are inserted into the inverted FAs, just by natural circulation of sodium without any forced circulation. All neutronic analyses were carried out by Serpent 2 code with the ENDF/B-VII.1 library [6].

2. CONCEPTUAL DESIGN OF H-MMR CORE

The conceptual design of the H-MMR core has two different types which are homogeneous and heterogeneous moderator configuration in the FA as shown in Fig.1. Note that all the main design parameters are same for both of types except for the detailed FA configuration and active core height. The H-MMR comprises of 18 FAs which are arranged as two rings without FA at the centre. A thick PbO radial-reflector and an oxide dispersions-strengthened steel (ODS) axial-reflector with a B_4C shielding layer are in periphery region of the active core. As the primary control systems, the drum-type reactivity control system is installed into the radial-reflector region, and a conventional secondary reactivity control device is in the central non-fuel region. The gas plenum region is in the above the active core and the bottom reflector consists of ODS.

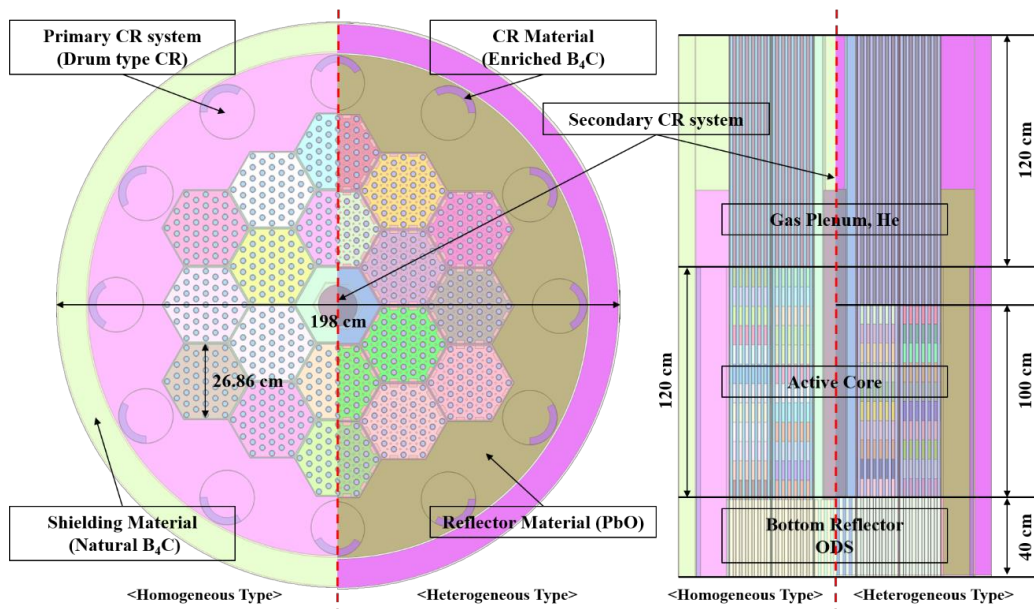


FIG. 1. Radial and axial configuration of H-MMR

The specific design parameters are in the TABLE 1. The reactor power is 12 MW(th) and the power density is 8.89 W/cc. Regarding $U^{15}N$ inverted FA, 99.9% ^{15}N enriched fuel material is adopted to avoid the decrease of the neutron economy due to the neutron capture by ^{14}N . To maintain mitigated excess reactivity by reducing the conversion ratio, the graphite moderator is inserted into the FA as both homogeneous and heterogeneous configuration. The active core height is 120 cm for the homogeneous type, and it is reduced to 100 cm for heterogeneous type in order to increase axial neutron leakage.

The concept of the inverted FA is that the fuel medium is filled into the hexagonal duct with the cylindrical heat pipes. In case of the homogeneous FA type, the fuel material consists of $U^{15}N$ fuel and graphite as a homogeneous mixture. On the other hands, rectangular parallelepiped and cylindrical graphite are inserted into the FA in case of heterogeneous type. The rectangular parallelepiped graphite moderators are in periphery region bordering the duct to reduce the maximum temperature at the edge of the FA while the cylindrical graphite moderators are inserted into the FA between heat pipes uniformly as shown in Fig.2.

TABLE 1. DESIGN PARAMETERS OF H-MMR

Parameters	Values
Reactor power	12 MW(th)
Number of fuel Assemblies	18
Active core equivalent radius hom. height het. height	61.46 cm 120 cm 100 cm
Whole core equivalent radius height	99 cm 280 cm
Power density	8.89 W/cc

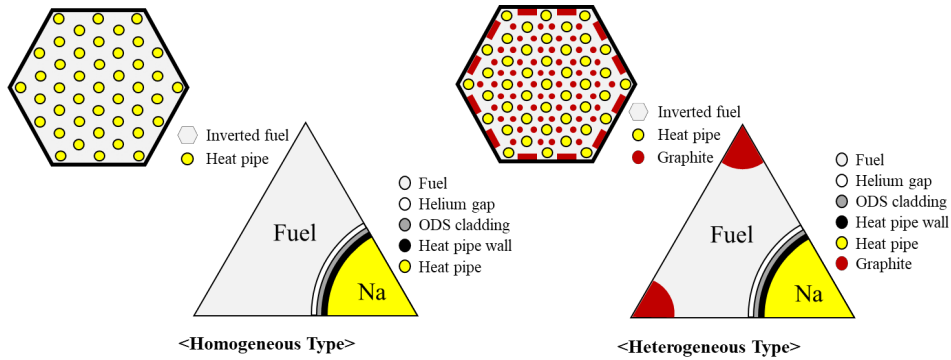


FIG. 2. Configuration of inverted fuel assembly cooled by heat pipes

The sodium heat pipes are covered by heat pipe wall, ODS cladding and He gap. The specific configuration of the heat pipe consists of liquid sodium region, wick structure and vapor sodium region as shown in Fig.3. All of temperature distribution were analysed by simplified 1- and 2-D model to obtain average temperature for Monte Carlo simulation. As part of results, the average fuel temperature was 1290 K and the average heat pipe temperature was 1122 K. All specific parameter of the inverted FA is shown in TABLE 2.

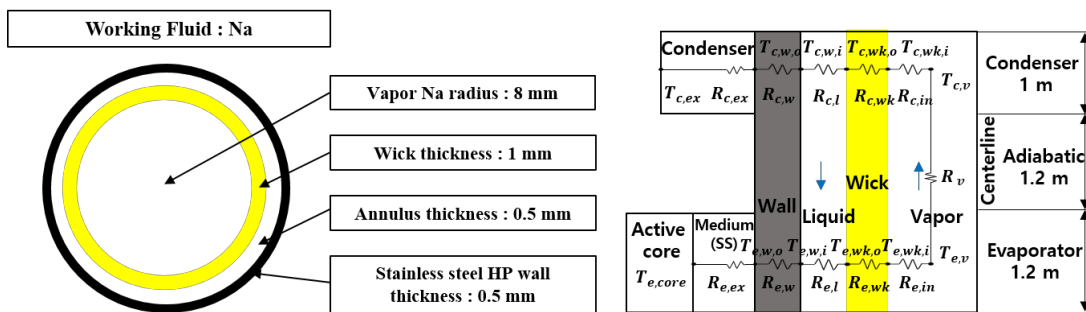


FIG. 3. Configuration of sodium heat pipe

TABLE 2. DESIGN PARAMETERS OF INVERTED FUEL ASSEMBLY

Parameters	Homogeneous Type	Heterogeneous Type
Fuel material (density)	U ¹⁵ N + C (11.53 g/cc)	U ¹⁵ N (13.5 g/cc)
Fuel volume fraction	82.5% (U ¹⁵ N) 17.5% (C)	87.8% (U ¹⁵ N) 12.2% (C)
Fuel enrichment (²³⁵ U)	11.67 w/o	11.60 w/o
Graphite moderator (rectangle circle)	-	2.95 cm × 1.00 cm 0.31
N-15 enrichment	99.9 %	
Cladding material (density)	ODS (7.2 g/cc)	
Gap material	Helium	
Number of heat pipes	43	
Radial and axial heat flux of heat	14.69 W/cm ² 2.5 kW/cm ²	
Heat pipe radius	0.95 cm	
Heat pipe wall thickness	0.05 cm	
Heat pipe cladding thickness	0.05 cm	
Heat pipe gap thickness	0.01 cm	
Fuel assembly pitch	26.86 cm	
Fuel assembly duct thickness	0.3 cm	
Inter-assembly gap	0.25 cm	
Average fuel temperature	1290 K	
Average heat pipe temperature	1122 K	

3. NUMERICAL RESULTS

In Serpent 2 Monte Carlo analyses, the condition of the depletion calculation was 200 inactive and 300 active cycle with 50,000 neutron histories per cycle. Especially for the reactivity feedback coefficients, 500,000 neutron histories were carried out with the same inactive and active cycle to obtain accurate results.

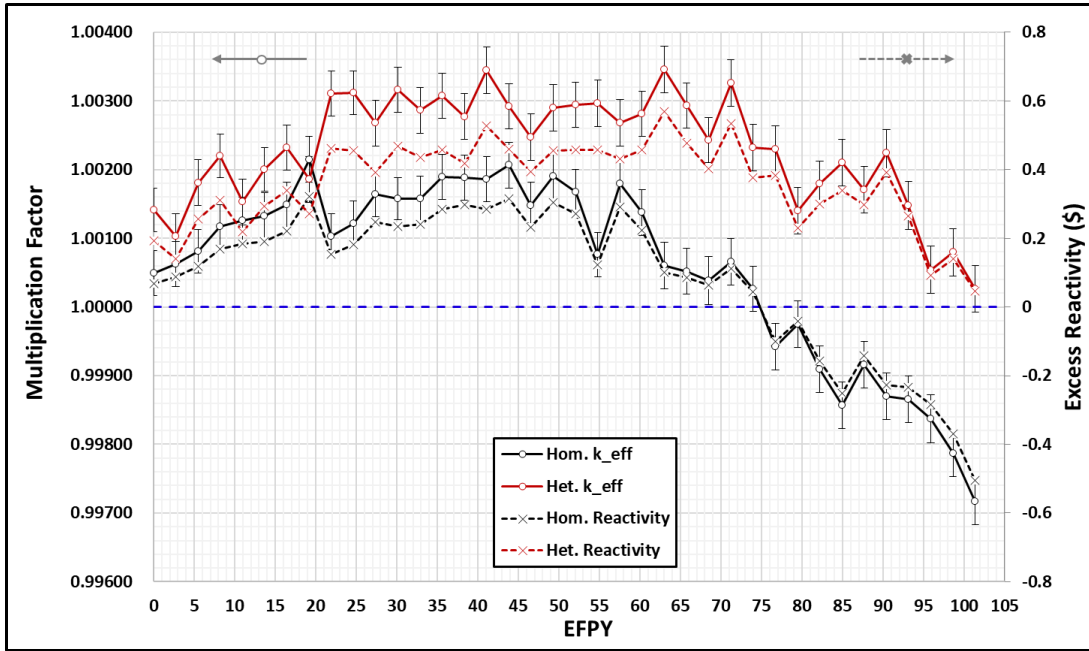


FIG. 4. Excess reactivity depending on effective full-power years (EPFY)

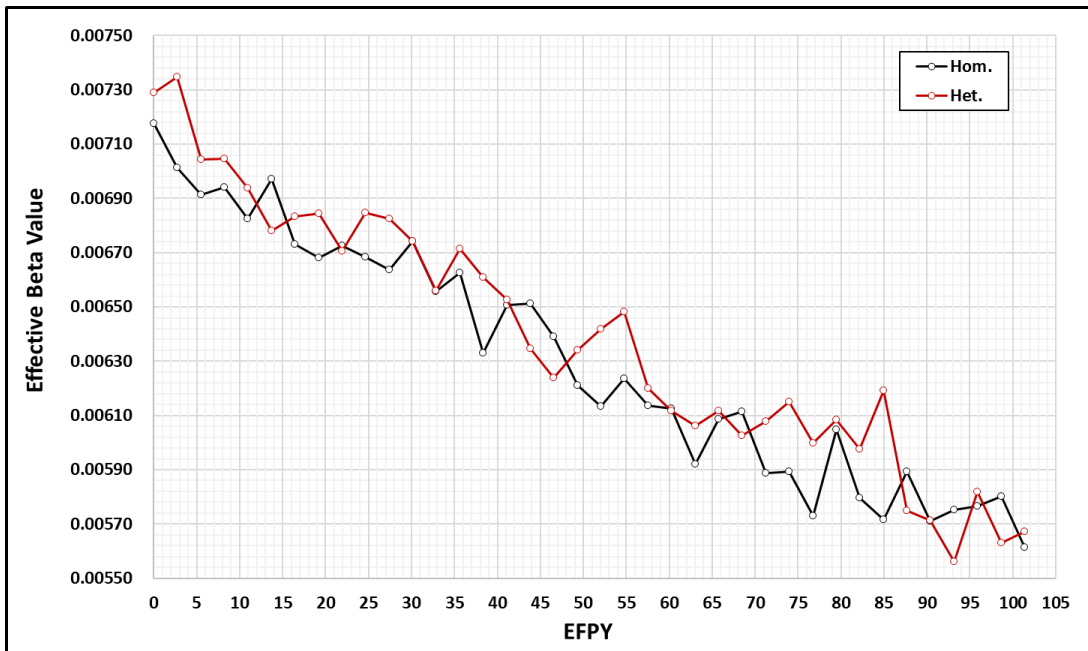


FIG. 5. Effective fraction of delayed neutrons (effective beta value) depending on EPFY

The excess reactivity depending on burnup for both homogeneous and heterogeneous type are shown in Fig. 4. The results of both types are optimized to accomplish the design objective such as autonomous and ultra-long life reactor by adjusting the fuel enrichment and moderator fraction. Especially, the main consideration of the moderator design is mainly focused on achieving less than one dollar excess reactivity since the prompt criticality incident could be happened when the excess reactivity is over a one dollar. Due to the composition change of the fuel material, especially the accumulation of Pu, the effective beta values keep reducing along with lifetime as shown in Fig.5. The results showed that the lifetime is around 75 years with less than 0.4 dollar excess reactivity for the homogeneous type. In case of the heterogeneous type, the lifetime is obtained as around 100 years with less than 0.6 dollar excess reactivity. The discharge burnup is evaluated as 33.45 GWd/MTU (3.56 % burnup) for homogeneous type and 50.31 GWd/MTU (5.36 % burnup) for heterogeneous type.

The reactivity feedback coefficients are arranged as shown in TABLE 3. The results showed that fuel temperature coefficient (FTC) values are dominant and negative depending on the burnup. In case of coolant temperature coefficient (CTC) values, they are slightly negative or negligible since the fraction of the liquid sodium in the heat pipe is quite small. The coolant void reactivity (CVR) values, which are calculated by an assumption that all of sodium in the active core is disappeared, are negative for both cases at beginning of life (BOL). However, they are turned to be positive values since the spectrum hardening by void would be dominant due to the accumulation of Pu. Due to the slightly negative FTC and CTC values and small range reactivity variation, it is expected that the autonomous operations of fast reactor type, H-MMR, could be easily achievable.

TABLE 3. REACTIVITY FEEDBACK COEFFICIENTS DEPENDING ON BURNUP

Model	Burnup	FTC (pcm/K)	CTC (pcm/K)	CVR (pcm)
Homogeneous Type	BOL	-0.742 ± 0.07	-0.002 ± 0.08	-43.49 ± 10.17
	EOL	-0.714 ± 0.07	-0.133 ± 0.09	16.30 ± 10.60
Heterogeneous Type	BOL	-0.649 ± 0.07	0.003 ± 0.08	-47.00 ± 10.10
	EOL	-0.569 ± 0.07	-0.006 ± 0.12	32.53 ± 10.66

The group-wise kinetic parameters are tabulated in TABLE 4 for the point kinetic analysis of the autonomous operation. Note that the effective reactivity values are above 700 pcm at BOL and around 580 pcm at end of life (EOL). The six-group fraction of delayed neutrons and decay constant of delayed neutron precursor were obtained for both cases.

TABLE 4. KINETIC PARAMETERS OF H-MMR

Energy group	BOL		EOL	
	Beta (β_i)	Lambda (λ_i)	Beta (β_i)	Lambda (λ_i)
<i>Homogeneous Type</i>				
1st	2.01E-04 ± 0.0965	1.34E-02 ± 0.0006	1.68E-04 ± 0.1033	1.34E-02 ± 0.0006
2nd	1.10E-03 ± 0.0417	3.24E-02 ± 0.0006	9.57E-04 ± 0.0464	3.22E-02 ± 0.0009
3rd	1.22E-03 ± 0.0384	1.21E-01 ± 0.0003	9.31E-04 ± 0.0437	1.21E-01 ± 0.0008
4th	2.71E-03 ± 0.0265	3.10E-01 ± 0.0007	2.29E-03 ± 0.0293	3.10E-01 ± 0.0009
5th	1.35E-03 ± 0.0369	8.77E-01 ± 0.0010	1.09E-03 ± 0.0417	8.77E-01 ± 0.0011
6th	5.78E-04 ± 0.0547	2.95E+00 ± 0.0015	4.60E-04 ± 0.0651	2.94E+00 ± 0.0018
Effective	7.18E-03 ± 0.0161	5.50E-01 ± 0.0224	5.89E-03 ± 0.0179	5.41E-01 ± 0.0245
<i>Heterogeneous Type</i>				
1st	2.06E-04 ± 0.0993	1.34E-02 ± 0.0006	1.42E-04 ± 0.1160	5.66E-01 ± 0.0248
2nd	1.11E-03 ± 0.0412	3.24E-02 ± 0.0006	9.57E-04 ± 0.0469	1.34E-02 ± 0.0009
3rd	1.11E-03 ± 0.0394	1.22E-01 ± 0.0003	8.61E-04 ± 0.0454	3.20E-02 ± 0.0009
4th	2.80E-03 ± 0.0259	3.10E-01 ± 0.0008	2.09E-03 ± 0.0311	1.21E-01 ± 0.0008
5th	1.46E-03 ± 0.0361	8.76E-01 ± 0.0010	1.16E-03 ± 0.0400	3.11E-01 ± 0.0009
6th	5.99E-04 ± 0.0564	2.94E+00 ± 0.0015	4.67E-04 ± 0.0678	8.80E-01 ± 0.0010
Effective	7.29E-03 ± 0.0158	5.70E-01 ± 0.0224	5.67E-03 ± 0.0185	2.94E+00 ± 0.0019

The normalized axial and radial power distribution were evaluated as shown in FIG. 6 and 7, respectively. The results showed that the shape of the axial power distribution in case of the heterogeneous type is mitigated by enhancing the neutron leakage to axial direction due to the reducing core height compared to that of homogeneous type. In case of normalized radial power distribution at the centre, the shapes of the both cases are resembling due to the similar fraction of the graphite moderator and relatively long mean free path of the neutron.

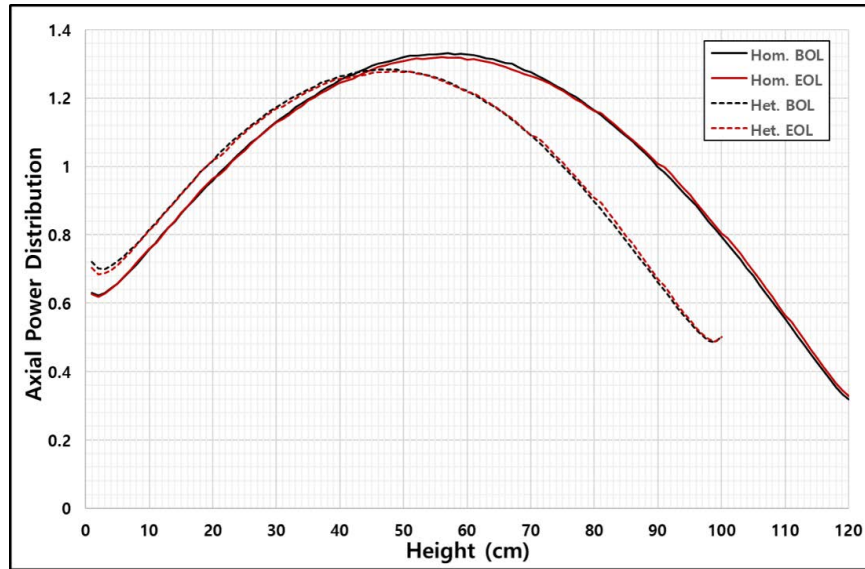


FIG. 6. Normalized axial power distribution of H-MMR

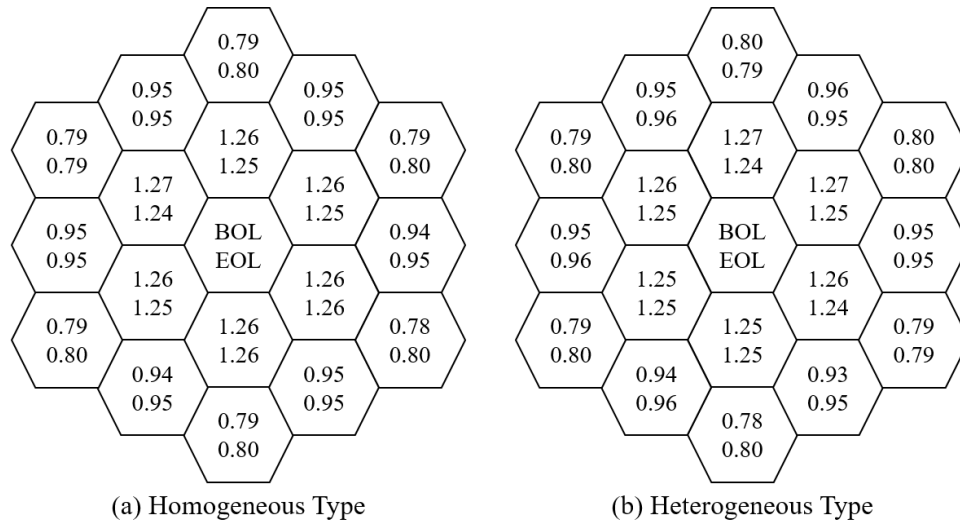


FIG. 7. Normalized radial power distribution of H-MMR

The primary reactivity control system has 98% B-10 enriched B₄C neutron absorber material with 98% theoretical density. By rotating the drum-type reactivity control system, the reactivity of the core can be adjusted as shown in Fig. 8. There is supplementary reactivity control system worked by gravity to ensure the safety margin since all of control drums are moved by electric power. The secondary reactivity control system consists of B₄C neutron absorber material with 98% theoretical density. The reactivity worth of both reactivity control system was evaluated as shown in TABLE 5. The results showed that the reactivity worth is enough to control the reactivity of the H-MMR core.

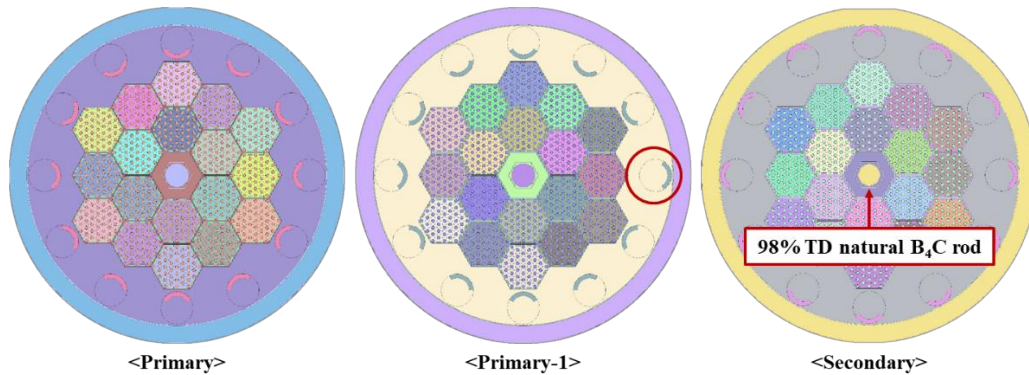


FIG. 8. Primary and secondary reactivity control system

TABLE 5. REACTIVITY WORTH OF PRIMARY AND SECONDARY REACTIVITY CONTROL SYSTEM OF HETEROGNEOUS TYPE

Worth	BOL (pcm)	EOL (pcm)
Primary	1822.67± 10.43	1571.11 ± 10.93
Primary-1	1690.65 ± 10.49	1441.83 ± 10.91
Secondary	2047.59 ± 10.53	1850.54 ± 10.96
Total	4167.12 ± 10.93	3784.79 ± 11.29

The H-MMR is the fast reactor, which has fast neutron spectrum as shown in Fig. 9. It was successfully achieved to get the optimized excess reactivity by introducing graphite moderator. The reproduction factor, eta value, could be steeply reduced if the neutron spectrum is softened at the fast energy region. Due to reduced eta value by graphite moderator, the neutron economy could be mitigated so the excess reactivity was obtained less than one dollar.

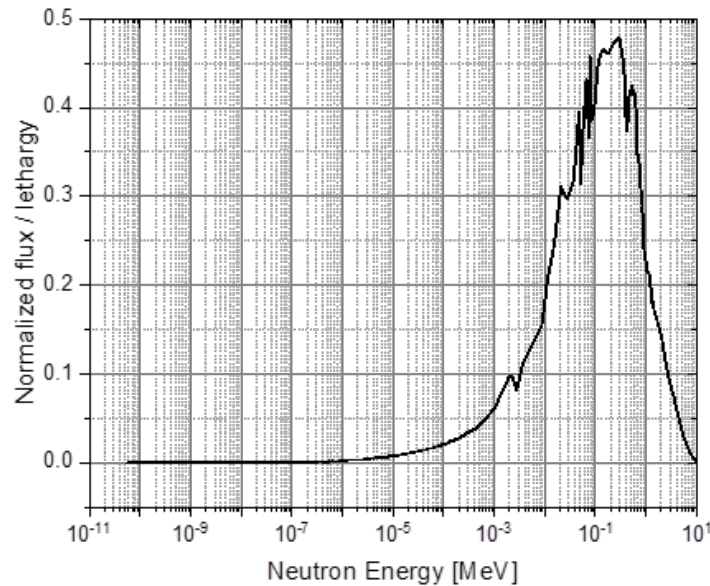


FIG. 9. Neutron spectrum in heterogeneous active core

The conversion ratio depending on EFPY were evaluated as shown in Fig. 10. It keeps increasing up to 0.85 due to the accumulation of Pu as shown in Fig. 11. The reason why the excess reactivity can be increased during lifetime though conversion ratio is less than 1.0 is that the UN fuel is loaded. By changing the fuel composition U-238 to Pu-239 during lifetime, the neutron economy evaluated by eta value of Pu is increased. This increased neutron economy due to the accumulation of Pu affect to the increase of excess reactivity along the EFPY. Therefore, it can be noted that the ultra-long lifetime could be achievable due to the characteristic of UN inverted fuel design which has proper neutron economy optimized by conversion ratio, composition of fuel material and neutron leakage.

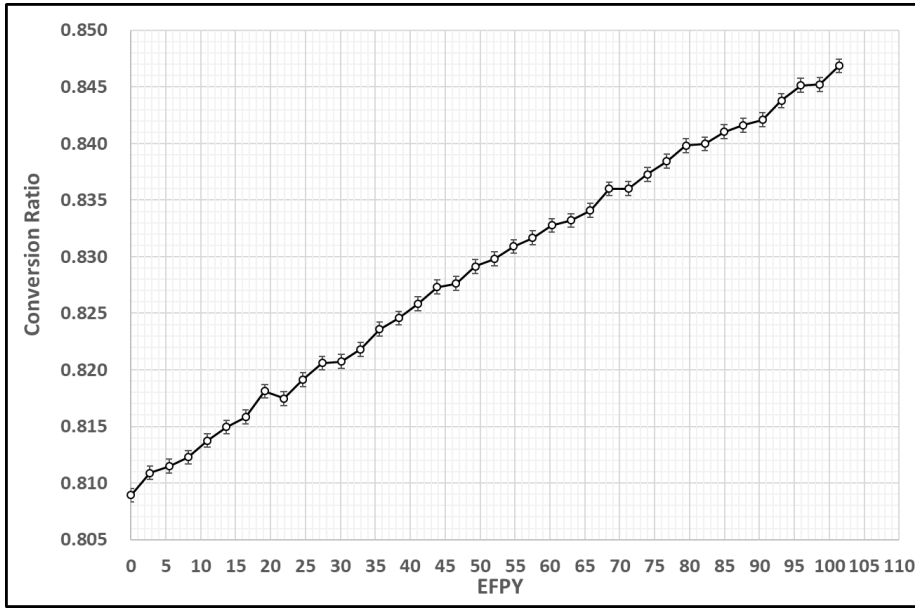


FIG. 10. Conversion ratio depending on EFPY in heterogeneous type

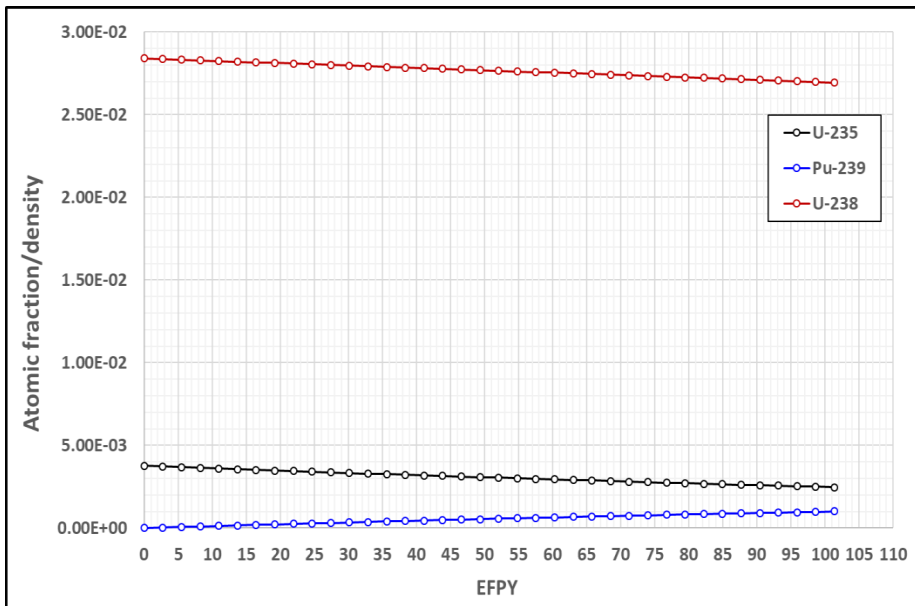


FIG.11 Composition change of major isotope in the fuel

4. CONCLUSIONS AND FUTUREWORKS

The preliminary study has been performed on the H-MMR aimed at autonomous and ultra-long life SMR design. The H-MMR has the unique FA design that inverted UN fuel type inserted homogeneous or heterogeneous graphite moderator and cooled by heat pipes. The study showed that the ultra-long lifetime, ~75 years for homogeneous type and ~100 years for heterogeneous type, is achievable with less than a one dollar reactivity swing when 99.9% ^{15}N and ~11.6 w/o ^{235}U enriched UN fuel is used with the graphite moderator. All of kinetics parameters were produced to conduct the point kinetic analysis. As the preliminary study, it can be concluded that ultra-long lifetime could be achievable within a one dollar excess reactivity swing thanks to the inverted UN fuel type cooled by sodium heat pipes.

In future works, the point kinetic analysis will be performed to evaluate applicability of the autonomous operation. After obtaining preliminary results of the H-MMR core analysis, it is needed to optimize the H-MMR design in terms of the FA manufacturing to realize practical H-MMR design. Moreover, the H-MMR core design optimization is also needed through the analysis combined with the secondary system design.

ACKNOWLEDGEMENTS

This work was supported by the National Research Foundation of Korea (NRF) grant funded by the Korean government (Ministry of Science and ICT) (No. NRF-2017M2B2B1071970)

REFERENCES

- [1] YU, DONNY HARTANTO, BONG SEONG OH, JEONG IK LEE, AND YONGHEE KIM, "Neutronics and Transient Analyses of a Supercritical CO₂-Cooled Micro Modular Reactor (MMR)", Energy Procedia, Vol. 131, pp. 21-28, December 2017.
- [2] HWANYEAL YU, DONNY HARTANTO, JANGSIK MOON AND YONGHEE KIM, "A Conceptual Study of a Supercritical CO₂-Cooled Micro Modular Reactor," Energies, Vol.8, Issue 12, p.139-13952, 2015. (1)
- [3] DONNY HARTANTO, YONGHEE KIM, AND FRANCESCO VENNARI, "Neutronics Evaluation of a Super-Deep-Burn with TRU Fully Ceramic Microencapsulated (FCM) Fuel in CANDU," Progress in Nuclear Energy, Vol. 83, p. 261-269, 2015. (3)
- [4] BONG SEONG OH, YOON HAN AHN, HWANYEAL YU, JANGSIK MOON, SEONG GU KIM, SEONG KUK CHO, YONGHEE KIM, YONG HOON JEONG, AND JEONG IK LEE, "Safety evaluation of supercritical CO₂ cooled micro modular reactor", Annals of Nuclear Energy, Vol. 110, pp. 1202-1216, December 2017
- [5] SEONGDONG JANG AND YONGHEE KIM, "Autonomous and Ultra-long Life Hybrid Micro-Modular Reactor Cooled by Heat Pipes," Proceedings of the Vietnam Conference on Nuclear Science and Technology, Ha Noi, Vietnam, August 7-9, 2019.
- [6] J. LEPPÄNEN, "Serpent—a continuous-energy Monte Carlo reactor physics burnup calculation code," VTT Technical Research Centre of Finland, 4 (2013).

SESSION II: HEAVY LIQUID METAL COOLED FAST SMRS

VALIDATION OF THERMAL HYDRAULIC DESIGN SUPPORT AND SAFETY METHODOLOGY AND APPLICATION SEALER

Paper ID #1

F. ROELOFS, K. ZWIJSEN, H. UITSLAG-DOOLAARD
NRG
Petten, the Netherlands
Email: roelofs@nrg.eu

F. ALCARO, M. STEMPIEWICZ
NRG
Arnhem, the Netherlands

J. WALLENIS
LeadCold
Stockholm, Sweden

Abstract

SEALER (Swedish Advanced Lead Reactor) is a passively safe lead-cooled reactor designed for commercial power production in the smallest possible format, under design by the LeadCold company. Support with respect to safety analyses is provided for the SEALER design based on advanced thermal hydraulic simulations covering various scales in advanced code systems. The paper describes the safety support activities for steady-state conditions and transients, e.g. an Unprotected Transient OverPower (UTOP), which are being carried out using the SPECTRA system thermal hydraulics code and a Computational Fluid Dynamics code. In addition to the SEALER support, the paper discusses the efforts that are being taken to validate the codes for application to lead cooled fast reactors by means of comparisons to experimental data as well as by means of code-to-code comparisons.

1. INTRODUCTION

SEALER [1] is a passively safe small lead-fast reactor under design for commercial operation in remote regions by LeadCold Reactors. In the design and safety evaluation process, NRG is currently providing support to LeadCold Reactors with respect to thermal-hydraulic safety analyses utilizing the unique SPECTRA system thermal-hydraulics code [2] complemented by Computational Fluid Dynamics (CFD) competences. Using this combination of simulation tools, preliminary evaluations have been made with respect to steady-state conditions and a selected transient. The goal of the presented work is to show the efforts undertaken to validate the design support and safety analyses of a lead-cooled reactor and their application to the SEALER reactor design. To this purpose, preliminary safety and design support analyses are presented using the SPECTRA system thermal hydraulics code and CFD codes. Where possible validation is based on comparison to experimental data but in addition also code-to-code comparisons are used and presented. In the following chapter, first the SEALER design will be introduced. Chapter 3 will explain the validation efforts, after which chapter 4 will describe the preliminary safety analyses that have been performed using the SPECTRA and CFD codes. Finally, chapter 5 presents conclusions and an outlook.

2. SEALER

In remote areas without connection to the national power grid, electricity is often produced using diesel generators. Such diesel power plants today account for 3% of global CO₂ emissions. In Arctic regions, diesel supplies are expensive to transport and store, leading to

very high costs for electricity and heat. The average cost of electricity for the consumer in Nunavut (Canada) is more than five times higher than that charged in southern Canada. Small nuclear power plants may potentially replace diesel generators in such regions at competitive costs. Currently, SEALER (Swedish Advanced Lead Reactor) is under design by LeadCold Reactors to meet such Arctic demands in Canada.

The SEALER design foresees in 8 MW(th) during normal operation. The primary system is laid out such that heat is transferred from the core to eight steam generators by forced circulation using eight primary coolant pumps. These pumps each provide 164 kg/s. The resulting temperature increase over the core is 42 K with a peak surface cladding temperature of about 717 K. The total pressure drop in the primary system is estimated at 140 kPa, out of which 127 kPa is over the core. For the purpose of removing decay heat by natural convection, the thermal centre of the steam generators is located 2.2 meters above the thermal centre of the core, providing a buoyancy head of more than 2 kPa resulting from a maximum temperature difference between the cold and the hot legs of 100 K over the core. SEALER relies mainly on passive safety:

- Gravity assisted shutdown of the reactor
- Decay heat removal from the core by natural convection of the lead-coolant
- Decay heat removal from the primary system by radiation from the vessel to the concrete pit

The aim of the design is that the only safety classified systems will be the shut-down system and the post-accident monitoring system. The design does not rely on a safety function of the steam generators, although these may contribute if they are still operational. Severe accident management relies on the ability of the lead coolant to retain volatile fission products through formation of compounds with low vapour pressure and to the very high lead boiling temperature. This is sufficient to prevent any off-site emergency measures. The conceptual design of SEALER was completed in 2017. The completion of basic and final design of SEALER is expected to be feasible within one or two years after an investment decision is taken. An elaborate description of the Canadian Arctic SEALER design depicted in Fig. 1 can be found in [1].



FIG. 1. Conceptual design of the Canadian Arctic SEALER [1]

3. VALIDATION EFFORTS IN SUPPORT OF LATER APPLICATION TO SEALER

3.1. Validation for SPECTRA Simulations

Validation for SPECTRA for the specific application of SEALER being cooled by pure lead is not straightforward, as the authors do not have access to relevant component or integral experimental data in pure lead. Consequently, the validation work is focused on application to heavy liquid metals, since there are relevant experimental data available from lead-bismuth eutectic (LBE) experiments. It meant to be noted that also the validation work for other liquid metal, like e.g. sodium is relevant. However, these efforts will not be described in detail here. Nevertheless, it is worth mentioning the comparisons that have been made with EBR-II experimental data described in [3] and [4], the code-to-code comparisons with respect to the French sodium reactor program presented in [5] and [6], and the comparison to Phénix reactor data shown in [7].

3.1.1. *ELSY and ALFRED code-to-code comparison*

In the process of the design of the European Lead-cooled System (ELSY), and later the Advanced Lead Fast Reactor European Demonstrator (ALFRED), code-to-code comparisons were made on the system behaviour together with other partners.

The efforts on ELSY are reported in [8]. This was the first application of the SPECTRA code to a pure lead system. Steady-state results showed results consistent with those of other partners except for the fuel surface and centreline temperatures. This was due to different assumptions on the fuel properties and topology. This was solved in follow-up work on ALFRED reported in [9]. This report presents an elaborate code-to-code comparison including all major system thermal hydraulics codes applicable to lead fast reactors, i.e. RELAP5/MOD3.3, SIM-LFR, TRACE, SIMMER-III, and CATHARE V2.5_2. The main conclusion with respect to the code comparison was that the consistency of the various code results was good. For all Design Extension Conditions the codes predicted similar transient behaviour leading to similar conclusions.

3.1.2. *CIRCE experiments*

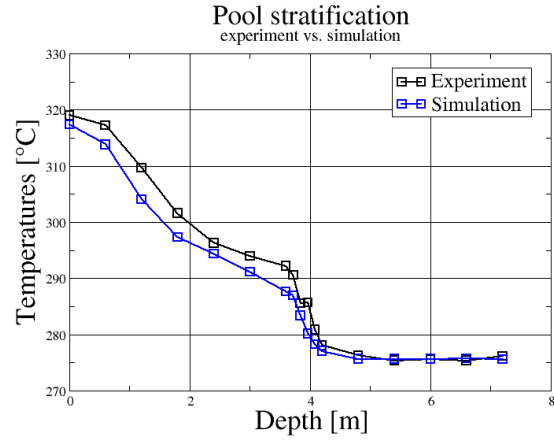
The CIRCE experiments conducted at ENEA in the Brasimone centre form a unique large-scale dataset for the validation of lead-based reactors. In fact, the CIRCE facility operates with liquid lead-bismuth eutectic. With respect to flow and heat transport, the behaviour of this eutectic mixture is assumed to be close to pure lead. During the recent European H2020 SESAME project, the facility was upgraded, and the so-called HERO 7-tube heat exchanger was installed. A pre-test comparison of simulations with RELAP5 and SPECTRA is reported in [10] showing good comparison. Post-test simulations are reported in [11]. Since the main goal of the work was to develop and validate a multi-scale simulation framework, no comparison of the system code stand-alone simulations is shown although they were performed. Again, they show a good comparison to the stand-alone RELAP simulations performed by ENEA. Apart from that, the system code simulations show a reasonable comparison with the experimental data, considering the fact that system codes can't capture 3-dimensional behaviour which was actually the reason for the development of the multi-scale simulation framework.

3.2. Validation for CFD Simulations

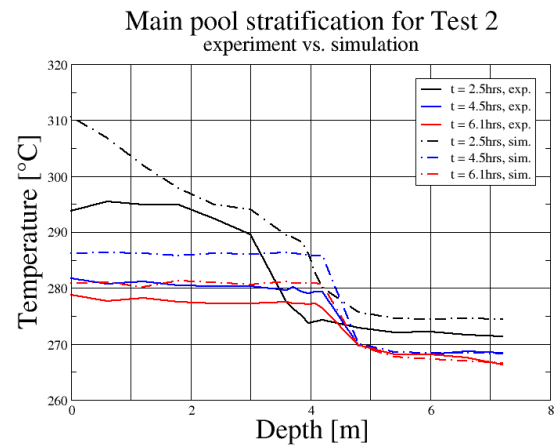
Like for the system codes, validation of CFD for the specific application of SEALER being cooled by pure lead is not straightforward, as the authors do not have access to relevant experimental data in pure lead. Consequently, the validation work is again focused on application to other heavy liquid metals, since there are relevant experimental data available from lead-bismuth eutectic (LBE) experiments. It is fitting to be noted that also the validation work for other liquid metal, like e.g. sodium is relevant. However, these efforts will not be described in detail here. The comparisons that have been made with EBR-II experimental data using a multi-scale coupled system code – CFD approach described in [3] showed good results. However, it supposed to be noted that the 3-dimensional flow behaviour in that particular case was not pronounced. The EBR-II case was basically used to test the multi-scale coupling approach. Later, comparisons for the Phénix dissymmetric test reactor data shown in [12] showed good performance of the multi-scale coupling framework for this dissymmetric test data which results in a highly 3-dimensional flow pattern in the liquid metal pool. The largest part of the reactor was modelled using CFD for this case. Therefore, this validation exercise confirms the applicability of the CFD framework to liquid metal pool reactor data.

3.2.1. CIRCE

As mentioned before, the Italian CIRCE facility provides a unique dataset for validation of heavy liquid metal simulation approaches. Comparisons for CIRCE in the so-called ICE configuration with a 91 tube heat exchanger with experimental steady state as well as transient data show reasonable correspondence [13]. The steady-state stratification in the pool was well predicted (see Fig. 2, left). Transient results however were more difficult to predict (see Fig. 2 right). A good agreement is found at the end of the experiment, after 6.1 hr. This indicates that during the transient part of the simulation, the total amount of heat removed by the decay heat removal system is very close to that of the experiment. At the other two times shown in the figure, the temperature profiles in the main pool of the experiment are below those of the model, indicating a stronger cooling in the experiment for the first part of the transient. At 4.5hr and later, the temperature in the bottom of the pool already agrees between the experiment and the simulation. Also, the location of the stratification inside the pool agrees well. Only the temperature calculated in the top part of the facility is lagging behind. Sensitivity studies performed show that the stratification prediction is sensitive on the modelling of the conjugate heat transfer between internal structures and the pool. Also, the influence of possible by-pass flows might play a role. Overall, modelling results of CIRCE-ICE served as valuable feedback to the experimentalists, leading to changes made to the facility and a better data acquisition for future experiments.



a)



b)

FIG. 2. Steady-state (a) and transient (b) comparison between experiments and CFD simulations for the CIRCE-ICE configuration [13].

3.2.2. E-SCAPE

Recently, the European SCAled Pool Experiment (E-SCAPE) was commissioned in Belgium as a 1:6 scale mock-up of the MYRRHA reactor [14]. First experimental data became available for validation of CFD codes. Design of this facility was supported by CFD, and the instrumentation was specifically selected for validation of CFD simulations. First comparisons with the new experimental data were shown in [15] and in more detail in [16].

The simulations show that the pressure drop from inlet to outlet of the E-SCAPE pool is about 20% over-predicted by the CFD model. Most likely this over-prediction of pressure results from differences in the geometry of the core inlet grid. A thorough comparison of the geometrical models and as-built geometry ought to be performed to resolve this pressure issue. The temperature distribution in different regions of the E-SCAPE pool is well predicted. Fig. 3 shows a comparison of simulation results versus experimental data for four different mass flow rates at one vertical line location in the pool. More comparisons are shown in [16]. Temperature profiles agree within 10% with the measurements, and with respect to the overall temperature

increase from inlet to outlet, in most regions and for most cases. Also, the effect of decreasing mass flow rate on the temperature in the E-SCAPE pool is captured well. Finally, it is concluded that the heat loss from the outer vessel wall of E-SCAPE to the environment is predicted with about 5% accuracy. This is a good demonstration of the applicability of CFD for thermal hydraulic studies of lead-based reactors.

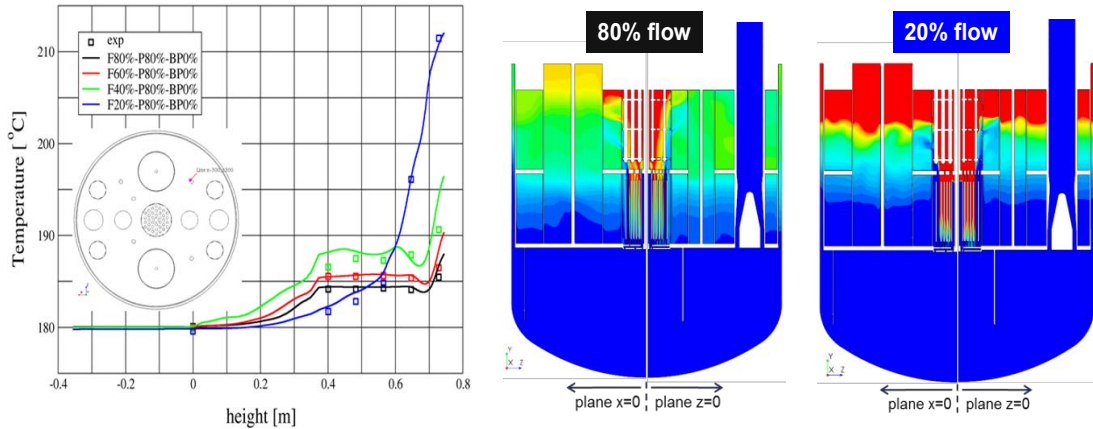


FIG. 3. E-SCAPE temperature comparisons for four experiments with different mass flow rates (left) and CFD cross-planes for two different flow rates (right) [16]

4. SEALER SAFETY ANALYSES

NRG has developed two complete models of the SEALER plant system. The first model was developed in the system thermal hydraulic code SPECTRA. Apart from that, a 3-dimensional CFD model of the primary system of SEALER was developed in the CFD code ANSYS Fluent 17.2. The two separate models are developed with the aim of performing both full system analysis, mainly addressed by the system thermal hydraulic model, and dedicated high-resolution simulations to investigate local phenomena through CFD analysis. Moreover, this also facilitates the development of a multi-scale simulation approach if this proves to be necessary.

4.1. SPECTRA Model

The system thermal hydraulics model was developed by means of the SPECTRA code and consists of the full primary system of SEALER and a simplified secondary system, where the complete Rankine cycle is discarded and fixed-conditions feedwater and steam header volumes are adopted to impose inlet and outlet boundary conditions for the secondary side of the steam generators. The model of the fuel assemblies in the core includes a point kinetic model of the reactor power. Reactivity feedback due to Doppler broadening, fuel pellet and cladding axial expansion, radial core support grid expansion and lead temperature effect (global core-wise) are implemented. Reactivity coefficients were provided by LeadCold Reactors. The main thermal hydraulic data of the fuel channels were tuned according to the design characteristics of SEALER provided by LeadCold Reactors and summarized in Table 1 for four typical fuel assemblies (central, middle, edge, and corner).

TABLE 1: THERMAL-HYDRAULIC CHARACTERISTICS OF SEALER FUEL ASSEMBLIES AT BEGINNING-OF-LIFE [1].

	Central	Middle	Edge	Corner
Q	0.66 MW	0.55 MW	0.37 MW	0.31 MW
\dot{m}_{Pb}	105 kg/s	88.3 kg/s	60.2 kg/s	49.9 kg/s
$v_{Pb}^{interior}$	1.41 m/s	1.19 m/s	0.81 m/s	0.67 m/s
v_{Pb}^{edge}	1.53 m/s			
ΔP_{bundle}	125 kPa	93 kPa	47 kPa	34 kPa
ΔP_{inlet}	1.0 kPa	33 kPa	80 kPa	93 kPa
ΔP_{outlet}	0.7 kPa	1.0 kPa	1.4 kPa	1.5 kPa
ΔP_{SA}	127 kPa	127 kPa	127 kPa	128 kPa </td

Fig. 4 presents the nodalization scheme of the primary SEALER system in SPECTRA. All the data adopted for the development of the NRG model were provided by LeadCold with the exception of the thermo-physical properties of lead in liquid state, which were obtained from [17].

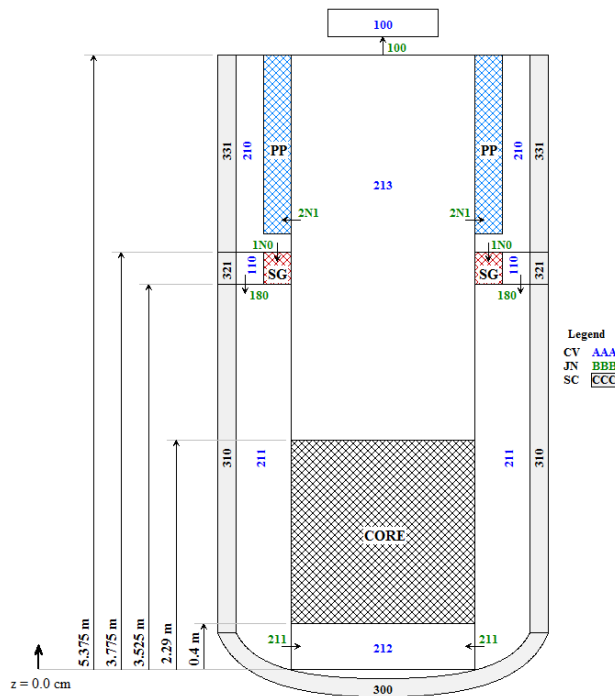


FIG. 4. Schematic representation of the SEALER vessel in SPECTRA

4.2. UTOP Analysis

An elaborate description of the Unprotected Transient Over-Power (UTOP) transient can be found in [1]. The transient consists of the inadvertently withdrawal of a control element occurring at beginning-of-life conditions. The reactivity insertion is 0.4 \$ and is completed in 1 second. The physical phenomena occurring in the reactor core are accounted for in the point kinetics model by means of the following reactivity equations:

$$\Delta\rho_{\text{tot}} = \Delta\rho_D + \Delta\rho_{\text{Pb}} + \Delta\rho_{\text{ax}} + \Delta\rho_{\text{rad}} \quad (1)$$

$$\Delta\rho_D = K_D \cdot \log(\bar{T}_{f,D}/\bar{T}_{f,D,0}) \quad (2)$$

$$\Delta\rho_{\text{Pb}} = K_{\text{Pb}} \cdot (\bar{T}_{\text{Pb}} - \bar{T}_{\text{Pb},0}) \quad (3)$$

$$\Delta\rho_{\text{ax}} = K_{\text{ax},f} \cdot (\bar{T}_f - \bar{T}_{f,0}) + K_{\text{ax},\text{cl}} \cdot (\bar{T}_{\text{cl}} - \bar{T}_{\text{cl},0}) \quad (4)$$

$$\Delta\rho_{\text{rad}} = K_{\text{rad}} \cdot (\bar{T}_{\text{LP}} - \bar{T}_{\text{LP},0}) \quad (5)$$

Eq. (1) represents the total reactivity term in the point kinetics model. Four different phenomena are considered, namely the Doppler effect described by Eq. (2), the coolant density effect described by Eq. (3), the axial rod expansion described by Eq. (4) and the radial grid expansion described by Eq. (5). The temperature terms appearing from Eq. (2) to Eq. (5) are explained in Table 2 (the subscript ‘0’ in the aforementioned equations refers to the value at steady-state conditions).

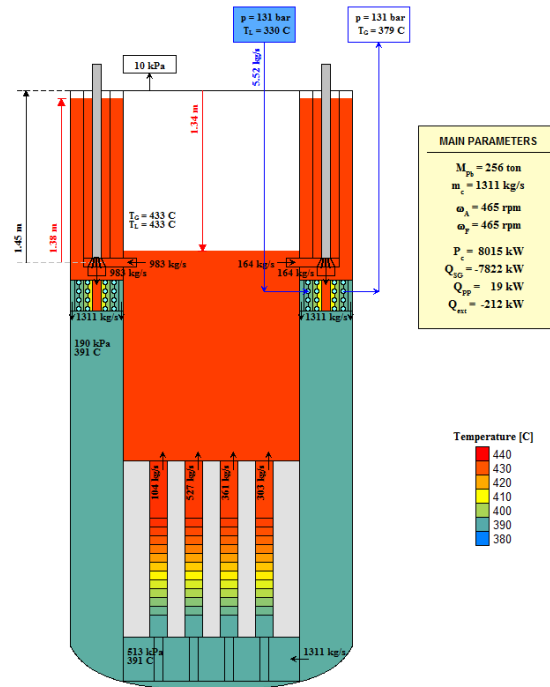


FIG. 5. Thermal-hydraulic state of SEALER at steady-state beginning-of-life conditions

TABLE 2: DESCRIPTION OF THE TEMPERATURE PARAMETERS IN THE POINT KINETICS MODEL

Property	Description
$\bar{T}_{f,D}$	Average core-wise temperature of the fuel pellets for the Doppler effect. The fuel pellet temperature is averaged on the radial peaking factor of the corresponding fuel assembly.
\bar{T}_f	Average core-wise temperature of the fuel pellets.
\bar{T}_{pb}	Average core-wise temperature of the lead coolant
\bar{T}_{cl}	Average core-wise temperature of the fuel cladding
\bar{T}_{LP}	Temperature of coolant in the lower plenum

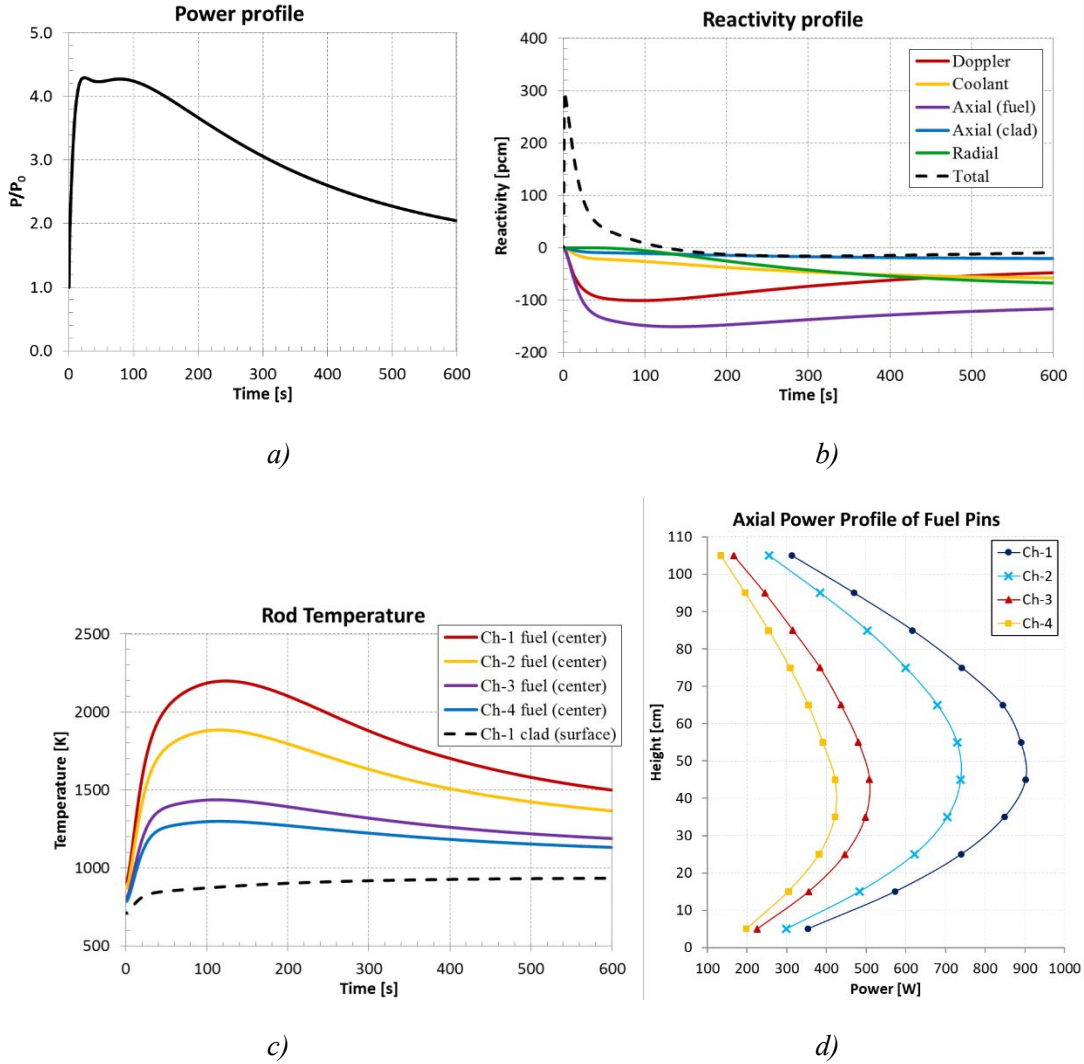


FIG. 6. Power profile (a), reactivity profile (b), rod temperatures (c) during the UTOP transient and axial power profile (d)

Fig. 5 graphically shows the thermal hydraulic state of SEALER at beginning-of-life conditions. Mass flow rate, pressures and temperatures are indicated in the figure. During the UTOP transient, power increases until negative reactivity feedback, mainly from fuel axial expansion and Doppler broadening, compensates for the reactivity insertion. Fig. 6 (top left) shows the evolution of the relative core power. A maximum value of 4.3 is observed after approximately 24 seconds from the occurrence of the control element withdrawal. Fig. 6 (top right) shows the profiles of the various contribution to the reactivity injected in the system during the transient. Finally, Fig. 6 (bottom left) presents the evolution of the four typical fuel pin maximum temperatures (central, middle, edge, and corner) as well as the peak cladding surface temperature. The axial power profiles of the fuel pins provided by the reactor designer are shown in Fig. 6 (bottom right), for the four fuel assembly types. Similar to the analyses shown in [1], the peak centreline fuel temperature is observed after about 100 seconds and provides a sufficient margin of about 700 K to fuel melting.

4.3. CFD Model

ANSYS Fluent 17.2 was used for the CFD simulations of SEALER. The CAD on which the simulation model is based is depicted in Fig 1. It contains most of the structural elements such as the fuel assemblies, steam generators, pumps, below-core structure and barrel and vessel walls. For future natural convection simulations, it is very important the walls are included, as they affect the heat transfer from the hot pool to the cold pool and also to the environment. For simplicity and computational efficiency, finer details such as fuel rods, steam generator tubes, pump impellers and the above core structure are not explicitly represented but modelled. The height of the lead free surface is fixed and modelled as a slip wall.

The meshing was done with the CAD and meshing tool Gambit. The non-wall resolved mesh has a total of 1.9M mainly tetrahedral cells, though where possible hexahedral cells are used. Mesh sensitivity studies, not reported in detail here, performed indicated that refining the mesh did not have much effect on the results, while strongly increasing the computational time. Hence it was deemed that the current mesh gives satisfactory results within a reasonable time.

Modelling approaches and numerical settings used for the simulations are listed in Table 6. The standard k - ϵ turbulence model with Enhanced Wall Treatment is used for the simulations. It is known that the heat transport modelling in liquid metals could be improved with more advanced heat transfer models which are currently under development [18] but as these developments are still ongoing, a constant turbulent Prandtl number approach has been applied with a fixed turbulent Prandtl number of 2, based on the recommendation for application to heavy liquid metals from [19]. Porous medium zones are used for the core and the steam generators, to represent the hydraulic resistances caused by the fuel rods and heat exchanger tubes. For the core, the inertial resistance coefficients are based on [1]. The core is divided in four different zones as indicated in [1], and an orifice model is applied to obtain a uniform outlet temperature. For the steam generators, correlations are used to determine the required value of the resistance coefficient. A volumetric heat source is prescribed over the active part of the core. A similar approach is used for the steam generators, though a more sophisticated model is used there, that allows better control over the outlet temperature of the steam generators. Finally, the lead is forced to flow by means of a volumetric momentum source applied to the relevant part of the pump.

TABLE 6. NUMERICAL SETTINGS AND MODELLING APPROACHES USED FOR THE CFD SIMULATION

Settings	
CFD code	ANSYS Fluent 17.2
Turbulence model	Realizable κ - ϵ model
Wall treatment option	Enhanced Wall Treatment
Liquid metal heat transfer	Turbulent Prandtl number = 2.0 (Bricteux et al. 2012)
Velocity-pressure coupling	SIMPLE algorithm
Gradient discretization	Least squares cell based
Spatial discretization	2 nd order
Linear system iterative method	Gauss-Seidel
Under relaxation factors	0.25 (mom.), 0.6 (pres.) and 0.95 (energy)
Core	Volumetric heat source and porous medium according to Table 1.
Steam generators	Modified volumetric heat sink and porous medium based on correlations (Idelchik, 1994).
Pumps	Volumetric momentum source.
Boundary conditions - flow	No-slip (except for free surface)
Boundary conditions - temperature	Conjugate Heat Transfer for internal walls. Radiative heat transfer on vessel outer wall.

4.4. Steady State at Beginning-of-Life

In first instance, the purpose of the CFD simulations is to get a better insight in the flow and temperature patterns of lead inside SEALER operating at beginning-of-life conditions. To this purpose, firstly, it was checked that the general design specifications were correctly reproduced by the simulations for mass flow rate, velocity, bundle pressure drop, inlet pressure drop and inlet and outlet temperature of the various type of core elements. The simulation values closely match those of the preliminary design, with most relative differences being less than a couple of percent.

Fig. 7 (left) shows a three-quarter cut of the geometry superimposed with a temperature field. As shown in this figure, the core outlet temperature is nearly uniform. The hot pool above the core also has a nearly uniform temperature, resulting in a heat-up to 706 K. The temperature field clearly shows that the heat source in the core is only applied to the active part of the core, as the lead in the lower part of the fuel assemblies is at a cooler temperature of 663 K. The thermal radiative boundary condition applied to the external vessel surface, along with the conductive resistance of the vessel wall, results in the wall temperatures being about 20 K colder when compared with lead temperatures in the rest of the cold pool.

Please note that there is a relatively cold patch in the bottom of the vessel, below the core. That particular region of the model is hydraulically separated from the rest of the reactor, resulting in more or less stagnant lead surrounded by solid steel. Hence the thermal radiative boundary condition will cool it more than the circulating lead in the rest of the reactor. The CFD results clearly reveal this cold spot, which was initially not anticipated. Hence the design was modified by adding 8 holes to the core grid as will be discussed in the next section.

Looking at the velocity magnitude field (Fig. 7 right), a jet coming out of the core is visible. This jet impinges on the fixed hot leg free surface, flows radially outward till it hits the barrel wall, moves downward along it and finally enters the pump inlets. A small part of the lead flowing downward along the barrel wall flows past the pump inlets and gets cooled by the colder lead on the other side of the barrel wall, resulting in a weak vortex.

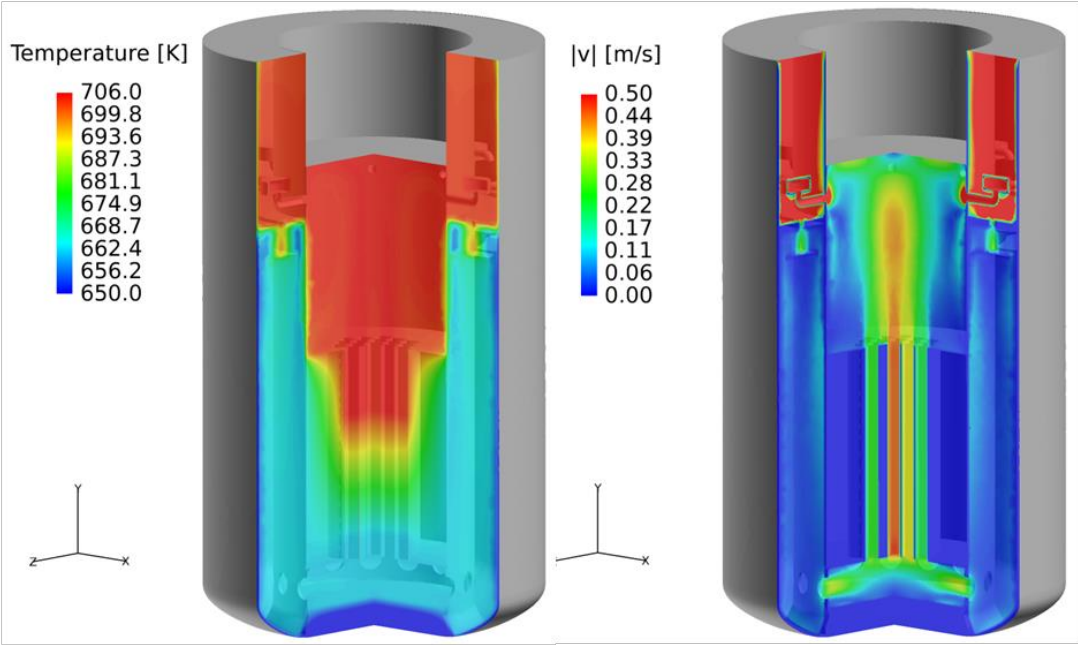


FIG. 7. Temperature (left) and velocity magnitude capped at 0.5 m/s (right) on a section of the CFD

4.5. Core Support Analysis

As mentioned before, the core support grid in the design depicted in Fig. 1 resulted in a cold spot with temperatures close to the solidification temperature of lead. Therefore, the design of the core support was modified including now 8 holes as can be seen in Fig. 8 (right). This leads to an inflow of liquid lead into the formerly hydraulically separated region and this way to an increase of the minimum temperature with about 17 K to 631 K, leaving sufficient margin to solidification.

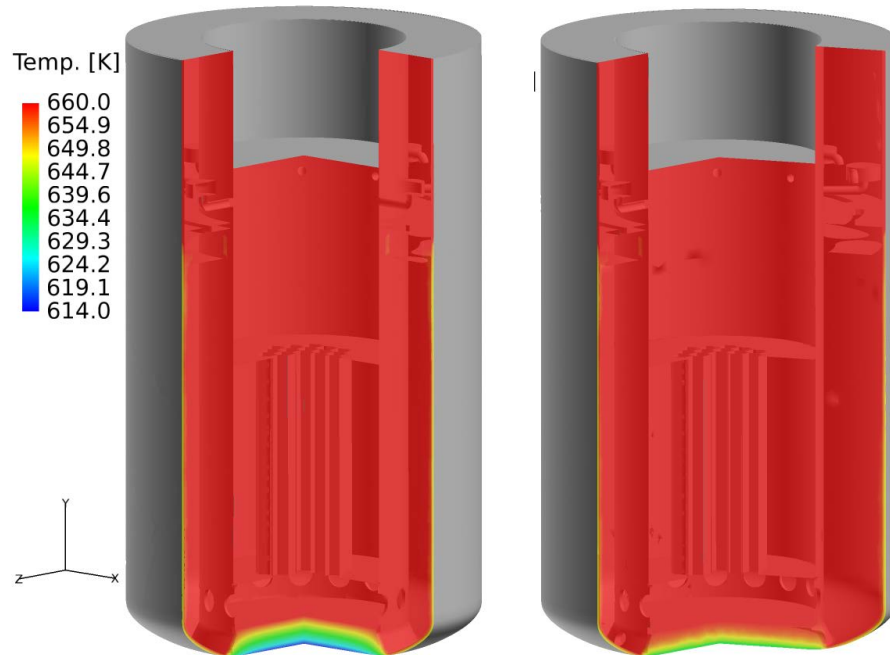


FIG. 8. Temperature capped at 660 K on a section of the CFD model for the original (left) and the modified (right) design of the core support

5. CONCLUSIONS AND OUTLOOK

Based on previous experience and validation efforts, briefly described here, for sodium cooled reactors, lead fast reactor code-to-code comparisons and lead-bismuth eutectic facilities (in particular the state-of-the-art E-SCAPE facility in Belgium), confidence was built in the simulation approach which allowed to construct simulation models at various scales for the safety assessment of SEALER.

Preliminary safety analyses are reported. In particular, the assessment of an unprotected transient over-power accident. This transient shows the forgiving nature of the SEALER design and sufficient margin to fuel melting. Apart from that, also preliminary 3-dimensional CFD analyses were performed to study the flow and heat transport in the primary system. From the analyses, an undesirable cold spot was observed in the core support leading to fluid temperatures close to the solidification point. Therefore, a design modification was proposed and analysed including 8 holes in the core support. The CFD analyses clearly show the benefits of this modification leading to a temperature increase of about 17 K providing sufficient margin to solidification.

ACKNOWLEDGEMENTS

Parts of this work have been performed within the ELSY, LEADER, ESNII+, MYRTE and SESAME European projects which have received funding from the Euratom research and training programs under grant agreements No. 036439, No. 249668, No. 605172, No. 662186 and No. 654935 respectively. All the work of NRG described in this paper was funded by the Dutch Ministry of Economic Affairs. The authors gratefully acknowledge the contributions of all colleagues involved in these projects.

REFERENCES

- [1] WALLENIUS, J., QVIST, S., MICKUS, I., BORTOT, S., SZAKALOS, P., EJENSTAM, J., Design of SEALER, a very small lead-cooled reactor for commercial power production in off-grid applications, *Nuclear Engineering & Design* **338** (2018) 23-33.
- [2] STEMPNIEWICZ, M., SPECTRA Sophisticated Plant Evaluation Code for Thermal-Hydraulic Response Assessment, Version 3.61, November 2017, Volume 1 – Program Description, Volume 2 – User’s Guide, Volume 3 – Subroutine Description, Volume 4 – Verification and Validation, NRG report K6202/MS-171112, Arnhem, the Netherlands (2017).
- [3] STEMPNIEWICZ, M., BREIJDER, P., DOOLAARD, H., ROELOFS, F., “Multi-scale Thermal Hydraulic Analysis of the EBR-II Loss of Flow Tests SHRT-17 and SHRT-45R”, NURETH17, Xi’an, China (2017).
- [4] BRIGGS, L., et al., “Benchmark Analyses of EBR-II Shutdown Heat Removal Tests”, FR17, Yekaterinburg, Russia (2017).
- [5] BUBELIS, E., et al., System codes benchmarking on a low sodium void effect SFR heterogeneous core under ULOF conditions, *Nuclear Engineering & Design* **320** (2017) 325-345.
- [6] STEMPNIEWICZ, M., DE GEUS, E., ROELOFS, F., NRG analysis of SFR heterogeneous core under ULOF conditions. *Nuclear Engineering & Design* **339** (2018) 65-74.
- [7] NARCISI, V., et al., “System Thermal-Hydraulic modelling of the Phénix dissymmetric test benchmark”, SESAME International Workshop, Petten, Netherlands (2018).
- [8] CASAMASSIMA, V., et al., Results of operational transient analysis. ELSY Del. 27, Milano, Italy (2010).
- [9] BANDINI, G., et al., Report on the results of analysis of DEC events for the ETDR (ALFRED). LEADER Del. 22, Bologna, Italy (2013).
- [10] ZWIJSEN, K., DOVIZIO, D., BREIJDER, P., ALCARO, F., ROELOFS, F., “Numerical Simulations at Different Scales for the CIRCE Facility”, ICAPP 2018, Charlotte, USA (2018).

- [11] ZWIJSEN, K., MARTELLI, D., BREIJDER, P., FORGIONE, N., ROELOFS, F., “Multi-Scale Modelling of the CIRCE-HERO Facility”, SESAME International Workshop, Petten, the Netherlands (2019).
- [12] UITSLAG-DOOLAARD, H., GEFFRAY, C., GERSCHENFELD, A., ALCARO, F., KRAUS, A., BRUNETT, A., WANG, X., “Results of the PHENIX dissymmetric test benchmark exercise”, ICAPP 2019, Juan-les-Pins, France (2019).
- [13] ZWIJSEN, K., DOVIZIO, D., MOREAU, V., ROELOFS, F., “CFD Modelling of the CIRCE Facility”, SESAME International Workshop, Petten, the Netherlands (2019).
- [14] SCK•CEN, Multi-purpose hYbrid Research Reactor for High-tech Applications; A research infrastructure for a new era, www.myrrha.be (2019).
- [15] VISSER, D., KEIJERS, S., LOPES, S., ROELOFS, F., VAN TICHELEN, K., KOLOSZAR, L., “CFD Analyses of the European Scaled Pool Experiment E-SCAPE”, SESAME International Workshop, Petten, the Netherlands (2019).
- [16] VISSER, D., ROELOFS, F., MIRELLI, F., VAN TICHELEN, K., “Validation of CFD analyses against pool experiments E-SCAPE”, NURETH-18, Portland, USA (2019).
- [17] OECD/NEA, Handbook on lead-bismuth eutectic alloy and lead properties, materials compatibility, Thermal-hydraulics and technologies. OECD/NEA Nuclear Science Committee, NEA No. 7268, Paris, France (2015).
- [18] SHAMS, A., et al., “A Collaborative Effort Towards the Accurate Prediction of Turbulent Flow and Heat Transfer in Low-Prandtl Number Fluids”, NURETH-18, Portland, USA (2019).
- [19] DUPONCHEEL, M., BRICTEUX, L., MANCONI, M., WINCKELMANS, G., BARTOSIEWICZ, Y., Assessment of RANS and improved near-wall modelling for forced convection at low Prandtl numbers based on LES up to $Re_{\tau}=2000$, *International Journal of Heat and Mass Transfer* **75** (2014) 470-482.

L. CINOTTI
Hydromine Nuclear Energy S. à r. l.
Luxembourg, Luxembourg
Email: lcinotti@hydromineinc.com

G. GRASSO
Agenzia Nazionale per le Nuove Tecnologie, l'Energia e lo Sviluppo Economico
Sostenibile (ENEA), Bologna, Italy

Abstract

Hydromine, in cooperation with ENEA is developing two projects: (I) the LFR-AS-200, where LFR stands for Lead-cooled Fast Reactor, AS stands for Amphora-Shaped, referring to the shape of the inner vessel and 200 is the electrical power in MW, and (II) the LFR-TL-X where TL stands for Transportable Long-lived core and X its power, ranging from 5 to 20 MW(e) or more, depending on the application. Hydromine has identified various innovative solutions to simplify and compact the Primary System of the LFR-AS-200, up to the achievement of a figure of merit of 1 MW(e)/m³, despite the low speed of circulation imposed by the use of lead as the coolant, thanks to the innovative reactor layout. The radically new solutions, which sometimes represent the reversal of traditional solutions applied to nuclear reactors, allow the elimination of many components of the primary system, which although typical of pool-type fast reactors, are no longer needed in the LFR-AS-200. The elimination of critical components, such as the in-vessel refuelling machine, the core support structures and the Above Core Structure, which would be immersed in lead and subject to thermal transients and fast neutron flux, reduces the need for in-service inspection and increases the reliability of the plant. Compactness of the Primary System, absence of intermediate loops, and, differently from LWRs, no significant, accidental pressurization of the Reactor building allow the design of a compact Reactor building with the associated economical advantage. Along with the predictable benefit to economics, compactness and simplification are important features for in-factory reactor assembling and the associated reduced construction costs and time schedule, both peculiar advantages of the small modular reactor segment. The flexibility in design, allowed by the physical properties of lead, permits to adjust the system performance to customer needs, extending therefore the market opportunities at low additional cost. Among the customized options, those related to the core are very interesting. Thus, for the LFR-AS-200, whose baseline design is MOX-fuelled core, a breeding ratio in the wide range 0.5 to 0.9 can be attained, thereby including a plutonium-burner option. Nevertheless, Hydromine is aware of the difficulties to overcome because of the socio-political and economical contest and the effort to license a new technology combined with the need of qualification of new steels. The LFR-TL-X helps to overcome these difficulties, with a gradual development, because of the reduced power and cost and the low operating temperature that allow the use of steel already used for SFRs. The same figure of merit of the Primary System compactness is also achieved in the LFR-TL-X that presents analogous simplifications and no on-site refuelling. This latter option makes the LFR-TL-X a plug-and-play battery reactor, i.e. modularization and factory reactor assembling pushed even further. For the LFR-TL-X, whose baseline design is a cassette core, the central channel is a convenient location for a test section or a special-purpose pin assembly, allowing the system to serve as an irradiation facility for testing new fuels and/or cladding steels. The paper provides details and discusses the merits and limits of both reactor versions.

1. INTRODUCTION

Present LWRs use less than 1% of the mined natural uranium, are limited in thermal efficiency and produce Pu and MA (Minor Actinides), which are among the long-lived waste.

Fast reactors can use almost the totality of the mined uranium, because they can breed fuel and burn all Pu isotopes, produce less amount of MA and can even recycle them, besides having higher thermal efficiency. Unfortunately, the development of the SFR technology has not yet devised a commercial reactor economically competitive with the LWRs. In fact, owing to the incompatibility of sodium with water and air, (i) the SFR requires a complicated, costly intermediate circuit, which reduces its efficiency and plant availability while complicating operation; and (ii) even a small sodium leak can initiate a serious accident.

The Fukushima accident has demonstrated the importance of ultimate, direct core cooling with water to recover a certain control of the plant in extreme situations, a possibility that is unthinkable for the SFR, if such an accident would occur.

The past, and in some Countries ongoing, experience on SFR is, nevertheless, precious because it has demonstrated the advantage of the fuel cycle of a fast reactor and contributed to the development of new fuels, namely the MOX fuel and other Pu- and also MA-bearing fuels. High-performance thermal cycle has been experienced in SFR together with the pool type configuration and a primary coolant operating at atmospheric pressure. The few SFRs operating in the world are valid instruments to test fuel and material irradiation at high fast neutron flux.

All this experience acquired with SFR can be almost entirely used for the development of the LFR, which uses the same fuel; behaves functionally similar; presents similar thermal-hydraulic and mechanical aspects, but is more promising in term of cost and safety as shown in the following chapters. The most important issues are related to the corrosive behaviour of lead, its high density and its high melting temperature.

Unlike the SFR, no LFR has been built yet and, to prove the technology, it is necessary to proceed in its development starting from small plants and proceeding to larger plants progressively with the gained experience as it was done in the past for the deployment of the other reactor types. It is a fortunate circumstance that an interesting market for micro reactors is looming, this allowing developer to seize two opportunities: to start the development of the LFR with modest financial commitment by starting the construction of micro reactors and immediately covering a market segment for which the LFR has unique advantages.

2. THE LFR-AS-200

The LFR-AS-200 concept is an innovative reactor cooled by molten lead; LFR stands for Lead-cooled Fast Reactor, AS stands for Amphora-Shaped, referring to the shape of the Inner Vessel and 200 is the electrical power in MW. It has been developed by Hydromine Nuclear Energy S. a r. l. (HNE), Luxembourg; ENEA has complemented the activity with core and shielding studies/optimization.

2.1. Description of the LFR-AS-200

The LFR-AS-200 is an integrated reactor [1], which means that all the primary components are installed in the Reactor Vessel. Among the key-components are: the Core, the Spiral-Tube Steam Generators (STSG), the Recirculation Pumps, the Dip Coolers of the Decay Heat Removal Systems (DHR), and the Amphora-Shaped Inner Vessel (ASIV), FIG.1.

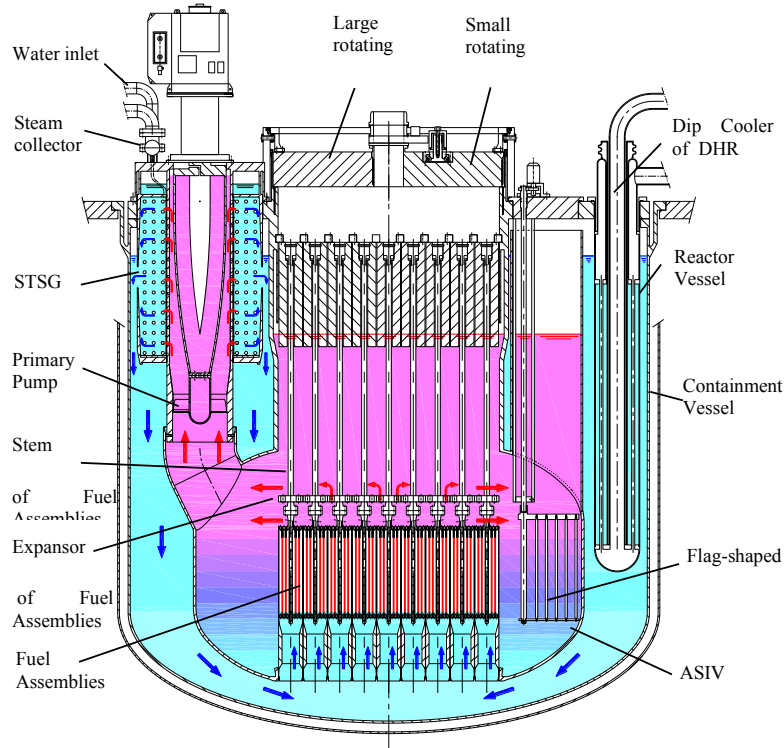


FIG. 1. LFR-AS-200 – Reactor assembly scheme

The roof is made of an annular, thick plate with penetrations for components of the primary system and a central opening, the edge of which is welded to an upstand that accommodates the rotating plugs. To be removable, all internals are hung from, and supported by, the fixed roof. No internal component is connected to the reactor vessel.

The LFR-AS-200 features an innovative, short Spiral-Tube Steam Generator (STSG) conceived for compactness and offering several advantages in terms of reactor cost, safety and reactor operability and simplicity of the lead flow path. The STSG tube bundle is composed of a stack of spiral-wound tubes arranged in the bottom-closed, annular space formed by the outer and inner shells of the STSG. The inlet and outlet end of each tube are connected to the feed water header and steam header, respectively, both arranged above the reactor roof.

The STSG tube bundle is partially raised above the lead-free level of the cold collector. The inner shell houses a primary lead pump with a short, large, hollow shaft filled with rotating lead, to provide additional mechanical inertia for enabling a smooth transition from forced to natural circulation during a loss of station service power. In contrast to traditional solutions, the STSG is fed from the bottom. Hot lead flows radially through the perforated inner shell and, once past the tube spirals, flows into the cold collector through a circumferential passage located just below the lead free level, thereby keeping the reactor vessel at the temperature of the cold collector, and minimizing the mass of lead displaced in case of a steam generator tube rupture accident.

Because the pump is installed in the hot collector, the reactor core is fed by the hydrostatic head, Δh , between the cold and hot collectors.

The short Pump-STSG assembly leaves a large free space in the lower part of the reactor vessel to allow widening the bottom of the Inner Vessel that is shaped like an ancient, greek amphora (hence, the terms Amphora-Shaped Inner Vessel, ASIV, and LFR-AS). The large width of the pool of lead interposed between the core and the ASIV contributes to the protection of the ASIV itself from neutron irradiation and thus allows the elimination of steel shielding assemblies. The core is therefore comprised of Fuel Assemblies (FAs) only, the weight of which is supported by buoyancy, with stems that extend upward to above the lead-free surface, i.e., into the cover gas space. Their heads can be interconnected, and the outer heads fixed also to the ASIV, by means of cams which are an integral part of each head. The result is a small, self-supporting core anchored to the inner profile of the ASIV that acts as a core barrel in the cover gas space. The FA heads are directly accessible for handling with an ex-vessel refuelling machine operating in the gas space under visual control in conjunction with rotating plugs of traditional design, as shown by Fig.2.

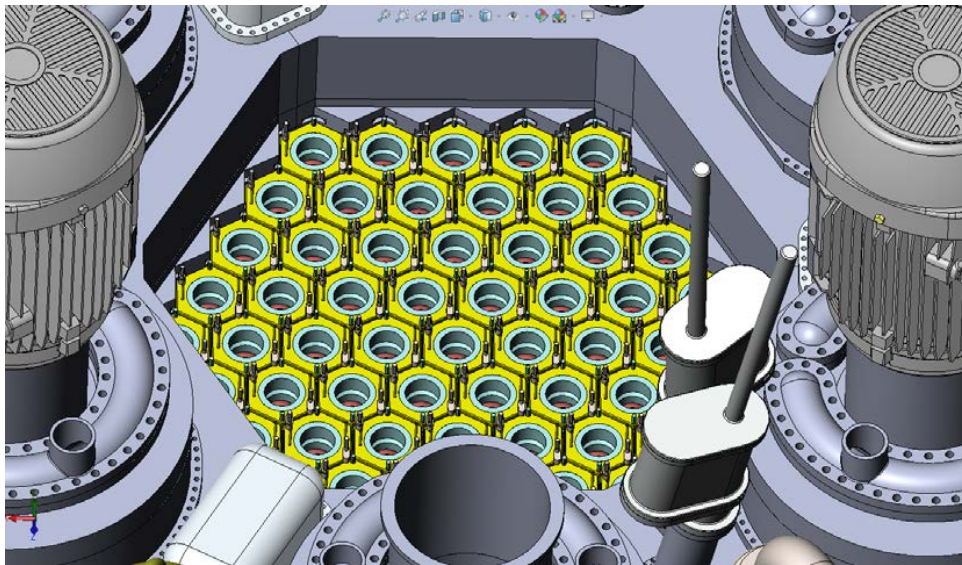


FIG. 2. Fuel Assembly top view

In a classical sodium-cooled, pool-type reactor configuration [2], the FAs are supported at their spikes by a grid plate (the Diagrid) and the Diagrid by a support structure (the Strongback, welded to the RV), while control rods are supported at their heads by the reactor roof. Thus, the collapse of the core support system would result in a control rod extraction. Consequently, the integrity of Diagrid and Strongback is of paramount safety importance and is submitted to a strict Surveillance Program. The support system of the core of the LFR-AS-200, instead, is located in the gas space under full visibility, is substantially free from thermal transients and neutron damage. The Diagrid and Strongback, with their associated difficult and time-consuming In-Service Inspection (ISI), are no more necessary.

The FA's stem supports the core instrumentation allowing the elimination of the Above Core Structure and the complicated, in-vessel refuelling machine is no more needed, too.

Having eliminated the shielding elements, an additional advantage, peculiar to the small fast core of the LFR-AS-200, is that it can be controlled by rods located outside the core [3]. This innovative solution has both advantages to further reduce the radial outline dimension of the core and to avoid disconnecting the Control and Shutdown (CSD) rods from their drives during refuelling.

The combined innovations have allowed the elimination of several systems/components, that are claimed by the designer to be no longer needed, and to achieve an unparalleled level of the reactor vessel compactness, reactor roof included, of about $1 \text{ m}^3/\text{MW(e)}$, being about 4 time less than that of SPX1 and of most of the previous LFR projects.

The LFR-AS-200 reactor is equipped with three kinds of ex-core CSD rods, one based on reversed-flag-shaped rotating bundles and two on more traditional cylindrical bundles with axial movement. The reactor is also equipped with mechanical core expanders, placed on the FA stems, foreseen in case of failure of all shutdown systems for the introduction of large negative reactivity and ultimate reactor shutdown during postulated, extended design basis accidents.

The core consists of 61 wrapped, hexagonal FAs. Power shaping or flattening has been achieved through the use of two radial zones with different levels of Pu-enrichment. In the inner zone, made of 37 FAs, the fuel stack is divided into three axial regions: the bottom and top ones fuelled with higher enrichment (21%) with respect to the central one (~15%). In the outer zone, made of the remaining 24 FAs, the fuel is axially homogeneous, and enriched with the highest plutonium content (~22%).

DHR (Decay Heat Removal) is performed by means of two diverse, redundant systems, each consisting of three identical loops. Two loops of either system are sufficient to remove the decay heat. Each loop of the first DHR system is set at 2.5 MW nominal power, is filled with lead and connects a lead-lead dip cooler with an air cooler. It is passively operated, and also passively actuated, thanks to the thermal expansion of the cold loop which actuates the louvers of the air cooler when its temperature exceeds $400 \text{ }^\circ\text{C}$ ¹. Each loop of the second DHR system is designed for 2.5 MW nominal power. It connects a lead-boiling water dip cooler, to a water storage.

¹ A small flow- rate natural circulation is always present, owing to the thermal loss of the circuit which is colder than the cold collector.

The extraction from the reactor vessel of the FA takes place via a flask that is connected to the Rotating Plugs and equipped with an argon cooling system and shielding materials. Inside the flask, the FA is then transferred into the storage pool.

The LFR-AS-200 operates with a primary system at nearly atmospheric pressure, so that the postulated, largest mass and energy releases assumed for the design of the Reactor building are only those associated with the main feed water or main steam line break accident. As a result, the RB size addressing the aforementioned functional design requirement will also be significantly smaller.

The operation of the primary system at atmospheric pressure, its modular and innovative concept (e.g. six Pump-STSGs assemblies) and the suppression of systems/components, no longer necessary, has allowed to drastically reduce the amount of structural material needed per unit power. In addition, the weight of the individual components is much lower than that of corresponding components of current nuclear facilities. For example, the weight of a STSG is just 12 tons against the hundred tons of typical SGs of current LWRs.

Gigantism being eliminated from the power plant, the component handling equipment can accordingly be reduced in size, and the transport of the components simplified. All components of the primary system can be manufactured in workshop and assembled with simple positioning and bolting operations.

The power conversion system has no safety grade function and produces superheated steam at 500°C and 180 bar (Table 1) typical of conventional plants, so that the use as much as possible of currently available technology is expected in that domain.

The selected power of 200 MW(e) follows an initial Hydromine design of 120 MW(e) and has been selected as the smallest power that, according to the designer, allows economic competitiveness, as a single unit, with large LWRs. It is worth considering that a higher power promises to be more economic, but at present is not considered because of the higher risk and the loss of some interesting features such as the control from outside the core. The modular configuration, studied only at very preliminary level, seems to provide additional economic benefits, in particular because of the common spent fuel pool and handling equipment.

TABLE 1. MAIN FUNCTIONAL PARAMETERS OF LFR-AS-200.

Core power (MW(th))	480	Turbine inlet (bar)	180
Electrical power (MW(e))	200	Feed water /steam temperature (°C)	340-500
Primary coolant	Pure lead	Primary coolant circulation (at power)	Forced
Core inlet/outlet temperature (°C)	420/530	Primary coolant circulation for DHR	Natural
Fuel	Mixed oxide	Reactor vessel height/diameter (m)	6,2/6
Fuel handling	One fifth every 16 months	Steam Generators	6
Inner Vessel	Amphora shaped	Primary Pumps	6

The main technological issue is related to corrosion of structural steels operating in lead. The reactor vessel is kept at a temperature sufficiently low to allow the use of 316LN, the same steel of the SFR, but for reactor internals and fuel cladding, new materials and/or protective coating are necessary.

AFA (Alumina-Forming Austenitic) steels developed by ORNL [4] appear resistant to corrosion in the operating temperature range of LFR-AS-200 and alumina coating developed by Istituto Italiano di Tecnologia [5] appears resistant to lead corrosion and to heavy ions irradiations, pending confirmation under neutron irradiation. A full qualification program of new materials and protective coating is required to be set up accordingly.

2.2. Performance of the LFR-AS-200

2.2.1. The LFR-AS-200 version nearly self-sustaining in Pu

The fuel pin is designed to achieve 100 MWd/kg_{HM} (per kg of Heavy Metal) average burn-up. Given the fuel inventory in the core, this turns out in a fuel residence time of about 2400 EFPDs (Equivalent Full-Power Days). To reduce the criticality swing during operation, the irradiation period is segmented in 5 cycles 480 EFPDs each long.

The design of the core has been oriented towards a system nearly self-sufficient in plutonium. A conversion ratio of about 0.9 is obtained without blankets (Table 2.). In the absence of fertile FA, a larger core would be necessary for complete autonomy in Pu, which is not a main objective of the project, given the surfeit of Pu available worldwide.

TABLE 2. URANIUM AND PLUTONIUM BALANCE IN THE FUEL DURING THE IRRADIATION PERIOD FOR THE LFR-AS-200 VERSION NEARLY SELF-SUSTAINING IN Pu.

Initial inventory	9139 kg _U	2148 kg _{Pu}
Final inventory:	8063 kg _U	2028 kg _{Pu}
Balance	-1076 kg _U	-120 kg _{Pu}

2.2.2. The LFR-AS-200 as a Pu burner

In Countries which have long been producing nuclear energy, the goal is sometimes to reduce the inventory of available plutonium. Such a capability could be, indeed, an added value of the LFR-AS-200.

Having this in mind, an additional core design activity has been performed in order to define a new core configuration that maximizes plutonium burning (LFR-AS-200 Burner), while maintaining all the main plant characteristics. The new configuration features an increased number (127) of smaller FAs with fuel pins reduced in diameter from 10.5 mm to 7 mm. The fuel residence time is therefore also reduced to 1080 EFPDs.

Uranium and plutonium balance in the fuel during the irradiation period is presented in Table 3. The higher enrichment in Pu and the higher reactivity swing to be compensated make the control from the outside the core problematic. To avoid removing FAs from the core to locate control and shut down rods, with the consequence of an increased core radius, the space inside the extended stem of selected FAs can be used. This space results from the suppression of 37 central fuel pins in every FA in order to locate a tube used to blow argon for cooling the spent FA being handled out-of-lead. During reactor operation, an absorber can be introduced into these FAs through the said tube.

TABLE 3. URANIUM AND PLUTONIUM BALANCE IN THE FUEL DURING THE IRRADIATION PERIOD FOR THE LFR-AS-200 BURNER.

Initial inventory	3900 kg _U	1651 kg _{Pu}
Final inventory:	3606 kg _U	1412 kg _{Pu}
Balance	-294 kg _U	-239 kg _{Pu}

3. THE MICRO LFR-TL

An important cost parameter to be considered when designing a vSMR (a very Small Reactor) is the plant cost per unit power (USD/W). It is possible, namely, to reduce the reactor size while reducing power, but the plant USD/W ratio is likely to become prohibitively high, owing to the cost of the fuel handling machines and the building facilities for storage of the fresh and spent fuel assemblies, which is relatively independent from the reactor power and hence increases the USD/W ratio. It is ought to be considered, too, that it is not wise, for risks of proliferation, to provide the predictably numerous vSMR plants with these fuel storage facilities.

A measure to overcome this proliferation and cost issue is to design vSMRs capable to be transported, complete of spent core, to a common facility for fuel handling and maintenance of main components. For this design approach to become viable, the vSMR ought to be provided with a long-life core and be capable of transport in upright position, in order not to affect its mechanical and thermal-hydraulic configuration while traveling.

The lead-cooled vSMRs derived from the LFR-AS-200 can be designed to comply with both features of long-life core and transportability in upright position. Long-life cores are possible owing to the high breeding capability of the fast reactor, and transportability, that is bound to the compact reactor assembly, in particular to the short outline height of the reactor vessel, is the result of the very compact Pump-Steam-Generator assembly.

The minimum power of Hydromine interest is 5 MW(e) of the LFR-TL-5 (Fig.3). The LFR-TL-5 has been conceived with a configuration able to operate continuously for 15 years. The core of a “cassette type” with just one large fuel assembly has been conceived in cooperation with ENEA [6].

The LFR-TL-5 is fuelled with enriched uranium in form of oxide and because of the non-proliferation issue, the enrichment is kept below 20% (19.75%). The mass of fuel to reach criticality and ensure a reactivity margin to compensate the reactivity swing during burn up is 2670 kg of which 2350 kg are uranium.

The LFR-TL-5 profits of the already outstanding layout compactness of the LFR-AS-200 and of the elimination of the fuel handling, to be carried out in a centralized facility to reduce proliferation risk. The result is a reactor (Table 4) with a reactor vessel about 3 m high and 2 m in diameter. All internals hang from the reactor roof and have no connection with the reactor vessel. The pump, STSG, and core are co-axial with the reactor vessel in a Matryoshka-type configuration, in which the upper part of the inner vessel, which supports the core, contains the STSG that, in turn, contains the circulation pump. All primary system components can be removed without having to lift off the core.

The reactor assembly presents a simple flow path of the primary coolant with a Riser and a Downcomer. The layout with heat source (the Core) located below the Riser, and heat sink (the Steam Generator) at the top of the Downcomer, allows for effective natural circulation of the coolant.

With respect to the LFR-AS-200, the steam pressure is reduced to 130 bar just enough to ensure a feedwater temperature of 330 °C, i.e. a temperature slightly above the melting point of lead.

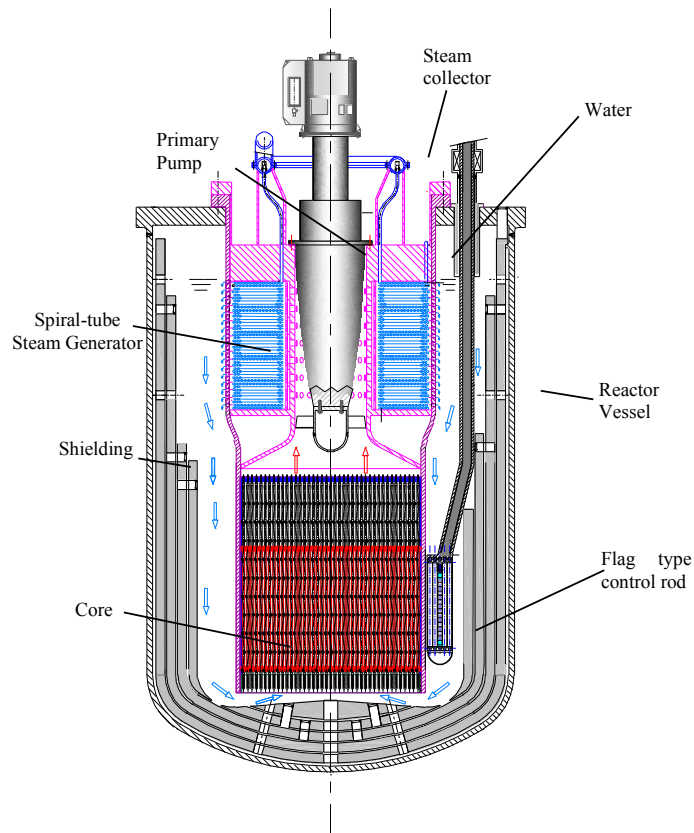


FIG. 3 LFR-TL-5 – Reactor assembly scheme

For vSMRs of power near to the lower limit of the investigated range, it is not important to further increase the steam pressure: a steam of 130 bar and 400°C is already a good improvement in comparison to that of LWRs. The cold lead in the downcomer keeps the Reactor vessel at uniform temperature all along its height.

Reactivity control is performed from outside the core with reversed-flag type rods similar to those of the LFR-AS-200. These rods also shut down the core. For diversification, a second, shutdown system is also located outside the core.

The LFR-TL type reactors operating at higher temperature than the LFR-TL-5, and the LFR-AS-200 need qualification of new materials. Considering the lack of irradiation facilities, the core of the LFR-TL-5 can be modified to provide locations for test sections in fast flux and lead environment. The more convenient location is directly beneath the primary pump, because access to either the test sections or/and to the special assemblies will be possible after removal of the primary pump that is not necessary for decay heat removal. A large region is also available between the core and the reactor vessel accessible from the roof for additional uses including the possibility of production of radio pharmaceuticals.

TABLE 4. BASIC PARAMETERS OF THE LFR-TL-5

Core Power (MW(th))	15	Turbine inlet pressure (bar)	130
Electrical power (MW(e))	5	Feed water /steam temperature (°C)	330-400
Primary coolant	Pure lead	Primary coolant circulation (at power)	Forced
Core inlet/outlet temperature (°C)	360/420	Primary coolant circulation for DHR	Natural
Fuel	Oxide, HALEU	Reactor vessel height/diameter (m)	2/3
Fuel handling	Whole core every 15 years	Steam Generator	1
Inner Vessel	Cylindrical	Primary Pump	1

4. POTENTIAL DEPLOYMENT OF LFR AT DIFFERENT POWER LEVELS

The innovations introduced into the LFR-AS-200 project have been conceived to demonstrate that it is possible to drastically reduce the volume of the primary system per unit power from about 4 m³/MW(e), typical of previous LFR projects, to about 1 m³/MW(e) which is even less than that of the most advanced SFR projects, which, in addition, have the cost linked to the intermediate circuits, unavoidable for them, and the associated larger Reactor building.

Research of LFR solutions much more compact than the LFR-AS-200 is likely to be useless not to excessively reduce the thermal capacity of the primary system, useful during operational and safety transients. Because of the scale effect, a power below 200 MW(e) constitutes an economic penalty, whereas a power above 200 MW(e) presents some economic interest, but involves the renunciation of salient features, such as the possibility of controlling the reactor from outside the core. To date, it is questionable if it is possible to design LFR reactors of power higher than 600 MW(e), typical power of the ELSY project [7], owing to the incidence of the large mass of lead on the mechanical design.

Important economic advantages, even with respect to large LWRs are expected rather than from the increase in unit power, from the sharing of expensive components, such as fuel transfer machines and the spent fuel storage pool, among more modules in a common building. In the previous chapter it has been shown that solutions with only one Pump-STSG assembly located above, and co-axially with, the core can give rise to a new series of micro reactors of the LFR-

TL-X type, which are extremely compact, i.e. more compact than their rated power would have otherwise allowed.

Several options have been investigated, so far, which are different regarding fuel type, power and thermal cycle (FIG.4).

Conveniently and traditionally, the development of a reactor type has been progressive, starting from low power for risk minimization. However, with use of the HALEU, the mass of U inside the core cannot be less than 2 to 3 tons, owing to the 20 % enrichment limit required by prevention of proliferation. The chemical nature of the fuel, either oxide or metal or nitride does not substantially affect this minimum fuel mass. Based on the two above considerations, the power selected for the first micro unit is 15 MW(th), i.e., 5 MW(e), for which, fortunately, a niche market is emerging, in remote places without interconnected grid as in Alaska or in the north of Canada, especially for mining applications.

Higher power units of 10-20 MW(e) can be designed with relatively low increase of the mass of fuel, with a volume per unit power typical of the larger LFR-AS-200 and can be deployed in short time, because of the available technology.

Increased compactness and efficiency can be obtained by a combination of higher coolant's temperature difference across the core and its mean higher core outlet temperature, and speed of coolant, provided that either new structural steels resistant to corrosion by lead at the higher temperatures of the thermal cycle become available or corrosion protection of the hottest structures by means of coating can be applied. A reactor with a thermal cycle similar to that of the LFR-AS-200, with the same Pump-STSG assembly, but only one assembly instead of six, and a small core can already deliver 33 MW(e).

This power level could open the potentially large market related to merchant ships, the decarbonization of which would result very expensive without nuclear propulsion.

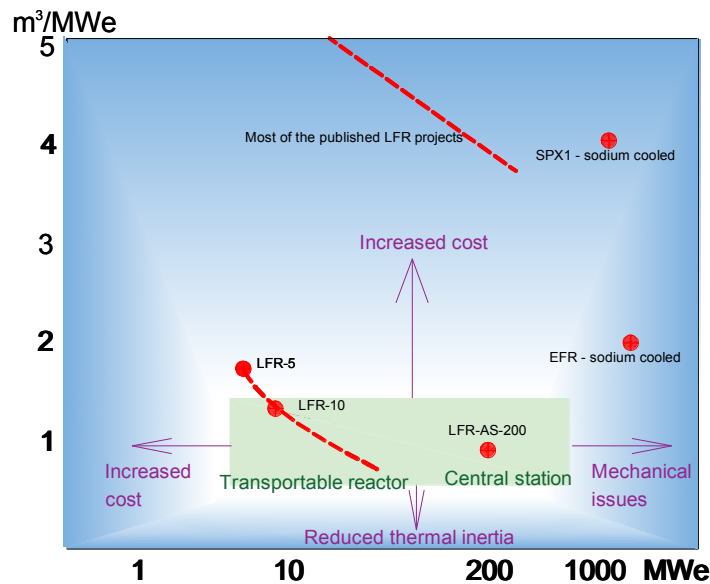


FIG. 4. The LFR-AS and the LFR-TL type reactors perspective deployment

Economics

Even at level of tens MW(e) power, the volume of the reactor vessel will remain at about $1 \text{ m}^3/\text{MW(e)}$ and even below as soon as high temperature resistant materials will be qualified as expected for the LFR-AS-200. Hydromine is not aware of other reactor types, which can reach this level of compactness that it considers a key figure of merit for economic competitiveness of a nuclear merchant ship, because:

- a loop-type PWR is bulky owing to circuits and steam generators outside the vessel.
- integrated PWRs have a bulky vessel because of the poor efficiency of the integrated steam generator owing to their unfavourable thermal cycle, which requires a volume of about five times more than that of the LFR-TL type operating with a thermal cycle typical of the LFR-AS-200.
- a gas cooled reactor has a bulky core, external loops and a steam generator about ten times bulkier.

The long-life core of about 15 years, predictably extendible to the entire life of the ship, dramatically simplifies the operation of the reactor which does not need shutdown periods for refuelling, but only limited periods for turbine maintenance.

Cleanness

The steady decline of polar sea ice over the last few decades has led to predictions that the North Polar regions will be open to regular marine traffic by at least the middle of the century (sooner, if specially constructed ice-breaking vessels are built). However, there are challenges and environmental aspects that needs to be considered. The production of soot from oil- and gas-burning engines will be caught in the circumpolar winds of the Arctic atmosphere and eventually be deposited on the snow and ice. Research has shown that even miniscule amounts of soot can increase the deposited energy into snow and ice, leading to increased melting [8]. A nuclear reactor does not produce soot.

Safety

Because no refuelling is required, the reactor will remain sealed during its lifetime with no risk of release of radioactive materials. Similarly to the LFR-AS-200, the LFR-TL exploits lead properties, which include a margin of hundreds K between the operating temperature and the mechanical limits of the core and the primary system, for actuation of passive shutdown and passive decay heat removal systems, which do not need power sources, operator intervention and logics, and hence are also free from cyber-attacks. A temporary rise in temperature to allow the intervention of passive systems is also admissible with regard to the corrosion of steels in lead because corrosion is a slow process.

Human intervention has concurred to mitigate effects of severe accidents occurred to ground reactors, instead the crew of any nuclear-powered ship has to be able to shut down the reactors and abandon the ship. The LFR has unique characteristics because, in case of shipwreck, frozen lead it is expected to constitute a confinement for all radionuclides for nearly unlimited time, without precluding the eventual recovery.

5. CONCLUSION

The 200 MW(e) LFR-AS-200 has been developed with the aim of producing a modular reactor economically competitive with the large LWRs, in addition to presenting the typical advantages of fast reactors.

The expected economy is based on (i) the properties of lead that allow the elimination of the intermediate circuits typical of SFRs, (ii) the compactness of the primary system, (iv) the compactness of the Reactor building, and (iii) the modular approach, which presents the advantage at the same time of standardization of critical components and the pooling of expensive plant parts. Although the LFR can take full advantage of the SFR experience, the need to qualify new materials and the numerous innovations require an important development program that it is wise to carry out starting from a smaller plant size.

Hydromine believes that the developed solutions could lend themselves to economic applications, even in the field of micro reactors for which a niche market is emerging for areas without interconnected grid.

Recently, a new important market of a few tens MW(e) nuclear reactors in the field of merchant ships is also emerging. Hydromine is convinced that for this application the micro LFR-TL is the best solution, because it combines the unique safety features due to the use of lead as the coolant to the extreme compactness of the conceived solutions.

REFERENCES

- [1] CINOTTI, L., BRIGER, P., GRASSO, G., Simplification, the atout of LFR-AS-200, Fast Reactors and Related Fuel Cycles: Next Generation Nuclear Systems for Sustainable Development (FR17) (Proc. Int. Conf. Yekaterinburg, 2017), IAEA, Vienna (2018) Paper CN245-140.
- [2] GUIDEZ J., PRELE G., Superphénix: Les acquis techniques et scientifiques. Atlantis Press 2016.
- [3] GRASSO G., BANDINI G., LODI F. and CINOTTI L., The core of the LFR-AS-200, Fast Reactors and Related Fuel Cycles: Next Generation Nuclear Systems for Sustainable Development (FR17) (Proc. Int. Conf. Yekaterinburg, 2017), IAEA, Vienna (2018) Paper CN245-185.
- [4] EJENSTAM J., SZAKÁLOS P., Long term corrosion resistance of alumina forming austenitic stainless steels in liquid lead, *Journal of Nuclear Materials* 461 (2015) 164–170
- [5] GARCÍA F. F., ORMELLESE M., DI FONZO F., BEGHI M.G., Advanced Al₂O₃ coatings for high temperature operation of steels in heavy liquid metals: a preliminary study. *Corros. Sci.* 77 (2013) 375-378.
- [6] CINOTTI, L., GRASSO, G., AGOSTINI, P., Flexibility of the LFR: an ASSET for Novel, Affordable LFR-AS-200-Based SMRs, *ANS Transactions* 117 (2017) 1464.
- [7] L. CINOTTI, G. LOCATELLI, H. AIT ABDERRAHIM, S. MONTI, G. BENAMATI, K. TUCEK, D. STRUWE, A. ORDEN, G. CORSINI, D. LE CARPENTIER, “The ELSY Project”, International Conference on the Physics of Reactors, *Nuclear Power: A sustainable Resource*, Interlaken, Switzerland, September 14-19-,2008.
- [8] HAAS B. S., Strategies for the Success of Nuclear-Powered Commercial Shipping, Presented to the Connecticut Maritime Association March 2014.

**INHERENT SELF-PROTECTION, PASSIVE SAFETY AND
COMPETITIVENESS OF SMALL POWER MODULAR FAST REACTOR
SVBR-100**

Paper ID #4

GEORGY TOSHINSKY
JSC “AKME-engineering”, JSC “SSC RF IPPE”
Moscow, Russia
Email: toshinsky@ippe.ru

OLEG KOMLEV, ALEXANDER DEDUL
JSC “AKME-engineering”
Moscow, Russia

Abstract

One of the ways to rehabilitate the population confidence to the nuclear power is construction of reactors with high level of inherent self-protection and passive safety such as modular fast reactors SVBR-100 with heavy liquid metal coolant lead-bismuth eutectic (LBE) alloy. Due to natural properties of LBE, in those reactors the causes of the severest accident with coolant loss, which require population evacuation, have been eliminated deterministically. Those reactors could be used for generation of electricity and heat, could be located near cities and replace coal electric plants. High safety of reactors SVBR-100 makes possible their location in the centres of power consumption or close to the regions, in which raw and mineral mining is performed. Thus, there is no necessity in construction of expensive extended electric transmission lines. Use of LBE is forming the backgrounds for simplification of reactor design due to elimination of the certain safety systems required in the reactors with other coolants. Thus, it is possible to construct the nuclear power plants (NPPs) based on SVBR-100 reactors not only safer, but more competitive, as compared with NPPs based on traditional type reactors. In the closed nuclear fuel cycle those reactors will operate in a mode of fuel self-breeding without consumption of natural uranium.

1. INTRODUCTION

The current state of the nuclear power (NP) and prognoses of world NP development do not correspond its mission both from the standpoint of natural uranium energy potential while operating in the closed fuel cycle, and from the standpoint of opportunities to realize sustainable development of the NP (the NP is one of those few power technologies generating power without releases of greenhouse gases). For instance, according to the data presented by IAEA, the current share of NP in the world consumption of electricity is about 11 %, whereas its prognosis can be reduced to 6 % by 2050 (according to the pessimistic estimation). Such situation for the NP is resulting both from the certain external factors, and existing internal needs of technological development.

The major external factors are the following: 1) very high frequency of severe accidents at NPPs, namely: Three Mile Island Unit 2 accident (1979, the USA), Chernobyl disaster at Unit 4 (April 26, 1986, the former USSR), disaster at NPP Fukushima 1 (2011, Japan), occurred during the life of one generation, 2) existence of developed alternative technologies for generating of electricity (fossil electric power plants on natural gas at low values of specific capital costs), 3) entering the market by renewable energy sources with an anticipated level of costs for the certain sites of their location, for example, solar electric plants about 0.03 \$/kW-h. In its turn, the obtained lessons and measures on enhancing of reliability and safety of the NPP equipment are resulting at present in increase of specific capital costs for their construction (specific capital costs for the NPPs planned to be constructed are considerably higher as compared with similar costs in contracts, which were made prior to the accident at NPP Fukushima 1).

At the same time, further increase of safety requirements (the value of probability of the severe accident requiring population evacuation is one of the vital quantity criteria for NPPs with traditional type reactors) can result in loss of competitiveness of NP based on water cooled reactors. For the purpose to reduce the specific capital costs and cost of produced electricity, it is required to increase a unit capacity of reactors, which, in its turn, is leading to growth of total costs of NPP construction and growth of construction terms. Thus, the financial risks are growing. An example is experience of construction of power-units EPR in Finland (Olkiluoto NPP) and France (Flamanville NPP with power of 1650 MW(e)). Their terms of construction have increased almost twice, and the cost has raised two or three times more. So, the profitableness of the project is sharply reduced that, depending on the tariff, can cause unprofitability of that project.

Very low probability of severe accident, calculated by the probabilistic safety analysis (PSA) methods, are not convincing for the population with radiophobia. Use of probabilistic safety analysis methods makes no sense when the initial events of severe accidents are not caused by chance (such as equipment failures, personnel's errors), but they are the results of ill-intended people's actions (such as sabotage, terrorists' actions). In those cases, all safety systems, which are in a standby mode, can be disabled deliberately, and the transport apertures in the protective shell are opened. Those NPPs can be used by terrorists as an instrument of political blackmail, and for that reason that problem was considered in the IAEA [2]. The PSA methods were and are useful. Often, they are the only instruments for quantitative assessment of safety parameters. However, their application in the existing types of reactors cannot deterministically eliminate the possibility of occurrence of the severe accident, which has a very small probability. And that fact does not contribute to lowering of population's radiophobia including those countries, where electricity is in deficit, and which are the potential market for construction of NPPs.

Along with this, in future the NP role will be very important as it makes possible generating of electricity and thermal power without limitations in fuel resources, releases of harmful substances into the environment and consumption of oxygen, which are resulting in global changes in the earth climate. Development of renewable energy sources, which eliminate carbon releases, is possible provided the governmental support covering their still low efficiency is assured.

The Global Agreement on Climate, that was accepted by 196 parties on 12.12.2015 and signed on 22.04.2016 at UN Climate Change Conference held in Paris and purposed to replace the Kyoto Protocol, will come into force in 2021 and does not specify the concrete ways of lowering of carbon releases into the atmosphere. It does not provide establishment of a mandatory tax on carbon exhaust as well. Moreover, the nuclear option is not provided in the Agreement, and that

is conditioned mainly by radiophobia of the population, whose opinion is accounted by politicians. Along with that, upon large-scale NP development, that is the NP that assures the opportunity of considerable lowering of carbon exhaust into the atmosphere.

These are the reasons, which provide the necessity for future changeover to the reactors with much higher level of inherent self-protection and passive safety. In such reactors the severe accidents requiring the population evacuation has to be deterministically eliminated² because there are no initiating events to cause those sequences.

First, the necessity for development of such reactors was specified in paper [3] in 1985. In that paper those class reactors were named “inherently safe reactors”. The more detailed justification of the necessity to develop those reactors and general principles of their construction were given in paper [4] in 1990 after the Chernobyl accident happened. In that paper it is highlighted that for the population the possibility of catastrophic consequences of the nuclear accident is much more important than the low probability of its realization. That is radiophobia phenomenon. Nevertheless, in accordance with the reliably received statistical data [5], the man-caused risks caused by operation of industrial enterprises and their fuel-energy infrastructure are many orders greater than the corresponding risks from the NP.

From the standpoint of the nuclear community and educated part of the population, that perception of the NP is not reasonable. However, that factor supposed to be taken into consideration as an objective one and the high safety level of the NPP is expected to be validated for the population, whose opinion is crucial and final, by convincing arguments without use of PSA methods, if possible. It is much easier to convince the population in the NPP safety if it is provided by nature laws (e.g. absence of pressure in the reactor, lack of hydrogen release assure that explosion cannot occur and so on). It is more clearly understood for the people, who consider the events on the basis of their own experience, but not on the results of probabilistic safety analysis.

That is resulting in the higher level of social acceptability of NPPs with reactors, which has a high level of inherent self-protection and passive safety. For that reason, under the equal costs, the projects of NPPs with a higher (and more “transparent”) level of inherent self-protection will stand a better chance to gain the tender on construction in the region.

² There are currently no such reactors, but they should appear in the future.

2. INHERENT SELF-PROTECTION AND PASSIVE SAFETY OF SVBR-100

2.1. Reactor self-protection against loss of coolant type accident

Use of the monoblock type reactor with forced circulation of LBE in the primary circuit that is provided by two pumps with gas-proof electric motors. The reactor monoblock vessel is provided by a protective casing. There are no pipelines and valves in the primary circuit (Fig. 1).

Due to the monoblock reactor design, the natural properties of LBE resulting from very high boiling point (1670 °C) and chemical inertness while contacting with water and air, that is possible in accidental conditions, eliminate the risk of LBE loss with core melting, reactor explosion and fires (no hydrogen release), which could be caused by internal reasons.

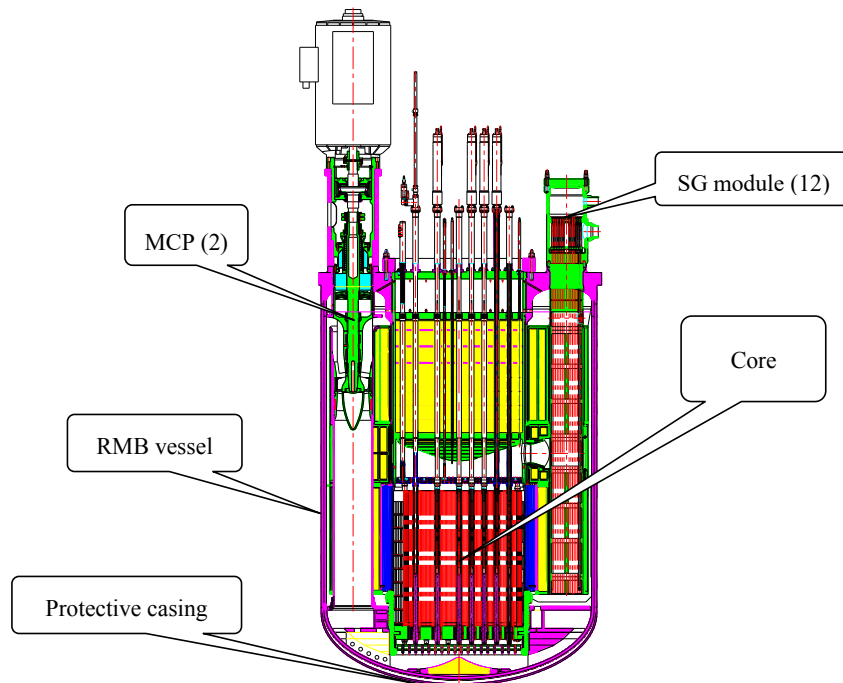


FIG.1. Reactor monoblock

2.2. Coolant compatibility with working medium in the secondary circuit and fuel

Realization of the RF design is based on a dual-circuit scheme. The steam generator (SG) is operating with multiple forced circulation with generation of dry saturated steam. LBE chemical inertness regarding to water eliminates the necessity of the intermediate circuit. Compatibility of oxide fuel with LBE is eliminating the event that the accidental situation with untightness in the fuel element cladding is developing in the accident with high release of radioactivity into the coolant.

2.3. Self-protection against accidents with SG tube rupture

To localize the accident with leak in SG tubes, the steam condensers are provided in the primary circuit gas system. In an event of their failure the steam-gas mixture is passively discharged into the bubbler via the rupture membranes (bursting disk). The scheme of LBE circulation in

the reactor monoblock (RMB) is providing effective gravitational separation of steam bubbles at the LBE free level under the RMB lid. Experience of operating the LBE cooled reactors at nuclear submarines³ has revealed that in an event of small leak in the SG (up to 10 kg/h) there is no necessity reactor shutdown. Excess oxidation of lead is not happening as simultaneously hydrogen formed.

2.4. Reactor self-protection against loss of heat sink, unprotected loss of heat sink (ULOHS) type accidents

In all heat-removal circuits the level of coolant natural circulation sufficient enough for removal of residual heat release is provided. Heat removal via the SG is provided by four independent channels of the passive heat removal system due to evaporation of water in the passive heat removal system tanks with steam discharge into the atmosphere, grace period is 72 hours (Fig. 2). Cut valves are obliged to be closed for prevention loss of water out of SG. They have the passive divers. In an event of postulated failure of four channels, it is provided that the RMB pit is flooded by water. Removal of residual heat going on via the RMB vessel is facilitated by large specific surface of RMB vessel that is typical for small power reactors. Management of that accident that is considered as the accident being beyond the design basis is provided by feeding of passive heat removal system tanks or RMB pit from emergency sources of water and electricity supply (for example, fire engines and so on).

2.5. Passive protection against reactivity accidents and unprotected transient over power type accidents

The reactor possesses a negative void reactivity effect and negative temperature reactivity coefficient. In addition to emergency protection rods actuated by electric signals, the reactor is equipped with directly acting addition passive emergency protection without electric drives, which rods are actuating by increase in LBE temperature (fusible locks).

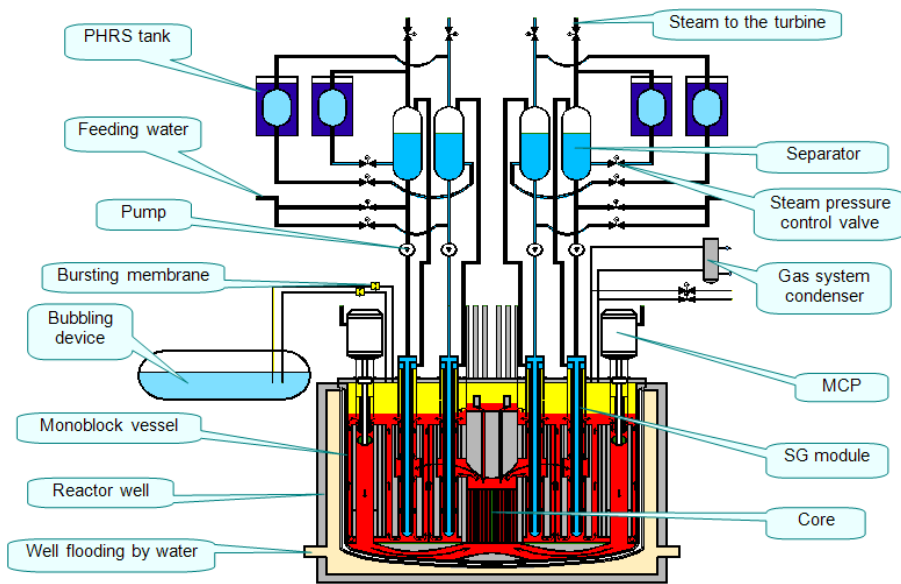


FIG. 2. Hydraulic diagram of RF SVBR-100

³ Experience of operating the LBE cooled reactors at NSs is presented in Ref. [7].

2.6. Passive protection against unprotected loss-of-flow type accidents

In an event of simultaneous shutdown of both pumps and failure of the main emergency protection system, protection of the reactor is provided passively due to actuation of the additional emergency protection rods, inertial rundown of pumps and natural circulation of coolants in heat-removal circuits.

2.7. Radio-ecological safety

At the stage of storage of spent nuclear fuel elimination of radioactivity release is provided as follows: after removal from the reactor the fuel sub-assembly is imbedded in a steel case filled with liquid lead, which then is put into the storage cell where removal of residual heat is realized passively due to natural circulation of atmospheric air. At this point, there are four safety barriers on the way of radioactivity release into the environment, namely: fuel pellet, fuel element cladding, solidified lead and leakproof case. Fuel subassembly is transported from reactor to steel case in container equipped a cooling system.

Actually, in the process of operation no liquid radioactive wastes are produced as refuelling is performed without removal of coolant from the primary circuit and its further decontamination, which is a cause of liquid radioactive wastes formation in large quantities.

2.8. Self-Protection against unauthorized “freezing” of LBE in the reactor

In an event of the shutdown reactor and low level of residual heat, the self-protection against unauthorized LBE “freezing” in the RF is provided by zero change of the LBC volume upon transition from a liquid state into solid one [8]. Maintenance of the equipment operability while “freezing-unfreezing” of LBE is performed, is verified not only experimentally at large-scale prototypes but in conditions of operation of the nuclear submarine RFs.

2.9. Defence-in-Depth Barriers

Elimination of radioactivity release into the environment is provided by the system of disposed defence-in-depth barriers, which includes:

- Fuel pellet UO_2 that is chemically compatible with LBE, which are retaining the main part of accumulated fission products excluding gaseous ones.
- Fuel element cladding made of ferrite-martensitic type steel EP-823 that is corrosion-resistant in LBE and withstands emergency overheating up $900\text{ }^\circ\text{C}$ without damage for 5 minutes and is eliminating formation of hydrogen in the accidental conditions.
- LBE retaining polonium, which is defining the radiation situation in an event of tightness failure in the reactor gas system and requires providing of corresponding radiation safety measures. Those measures were developed and realized in the process of operating the LBE cooled reactors at the nuclear submarines. They were very effective as nobody of the personnel (both military and civilian ones), who took part in elimination of accident consequences (about 20 t of radioactive LBE leaked in the reactor compartment of the 27/VT facility), got the polonium in-take dose that exceeded the permitted one [9]. Such favorable results were facilitated by the fact that the concentration of polonium-210 formed in LBE under irradiation by bismuth neutrons is very low (10^{-6}) and it forms thermodynamically resistant intermetallic compound with lead. Those factors reduce evaporation of polonium from LBE by a factor of 10^9 .
- The tight vessel of the RMB equipped with a protective casing (see point 2.1) and gas system pipelines eliminating release of radioactivity into the reactor box.
- The tight reactor box is protected against external impacts by reinforced concrete overlapping of 1.5 m in thickness. The air in the box is slightly rarefied relatively to that in the central hall (CH), rarefaction is produced with the help of a ventilation system discharging the air into the atmosphere via the ventilation tube through the system of filters. Additionally
- The protective reinforced concrete shell of the building has, which thickness is 1.5 m, and which is purposed for protection against external impacts (such as aircraft fall).

2.10. Tolerance to extreme initial events

To assess the safety potential of reactor SVBR-100, the preliminary calculation analysis [10] of the consequences caused by the postulated severe accident was performed under combination of such events as:

- (a) Destruction of the protective shell of the reactor building.
- (b) Damage of the reinforced concrete ceiling of the reactor box.
- (c) Rupture of gas system pipelines of the RMB installed in the concrete pit below the ground level with direct contact of the free surface of LBE under the RMB lid and atmospheric air.
- (d) Total blackout of the NPP.

That combination of initial events is only possible in extreme occasions, such as military actions, terroristic attacks, nature disasters, which occur very rarely, and so on. The results of the performed calculation analysis have revealed that even in an event of extremely unfavourable atmospheric conditions, no population evacuation beyond a three-kilometre zone

is required. For reactors with water or sodium coolants such combination of initial events can result in catastrophic consequences.

The performed analysis has revealed that RF SVBR-100 is not an amplifier of external impacts and, therefore, the scale of damages will be only determined by the energy of external impacts. Those type reactors assure their high resistance not only in events of single failures of the equipment and personnel errors, but in events of deliberate ill-intentioned actions when all special safety systems operating in a standby mode can be intentionally disabled. At those reactors such catastrophic accidents as Chernobyl or Fukushima disasters as well as fires similar to that occurred at reactor “Monju” are impossible in principle” [10]. This is extremely viable for realization of NPP construction in some countries where the level of terroristic threat is high. The obtained results are conditioned mainly by a low value of potential energy accumulated in the LBE. For water, sodium and heavy liquid-metal coolants this energy is 20, 10 and 1 GJ/m³ [11].

3. COMPETITIVENESS OF NPPS BASED ON REACTORS SVBR-100

The task of supporting and enhancing of economic competitiveness of the NP in conditions of growing safety requirements and alternative competitive power technologies available at markets is very important. It is impossible to assure large-scale NP development without finding the solution to this issue. For that purpose, it is necessary to provide economic competitiveness of some NPPs with fossil power plant on natural gas and electric power plants on the basis of renewable energy sources and also provide the conditions for attraction of investments for development of the NPP fleet.

With regards to that, the small and medium modular reactors (SMRs), which share in the future NP is expected to be at the level of not less than 30 %, need to meet the highlighted requirements of competitiveness and investment attractiveness. It is evident that meeting of those requirements for the SMPs is complicated as there is a tendency, which is resulting from experience of construction of the first SMR projects, to increase the specific capital costs (concerning the large power NPPs) at lowering of reactor module’s power. It can be expected that those negative tendencies will be overcome by the modular principle of NPP construction and considerable lessening of costs of the equipment of serial SMRs. And, in its turn, that is possible to be obtained by the effect of production scales and learning curve in the process of manufacturing of the equipment and SMR construction.

The additional barrier to provide the investment attractiveness of innovative SMR projects is the initial expenditures for development and demonstration of reference solutions at first such NPPs. In its turn, it is resulting in postponement of the phase of commercialization of those SMRs. Overcoming of those barriers by economical (market) methods can be only realized for technologies, which provide high profitability of the single NPP and with available market of sufficient volume.

Along with highlighted factors of enhancing the competitiveness and investment attractiveness, the serial NPPs with reactors SVBR-100 use the additional opportunities based on application of the following:

- (a) The space-saving equipment that can be compared with that for large power NPPs by labour expenditures in its manufacturing.
- (b) Sizeable lowering of the number of safety systems due to the high level of inherent self-protection.

(c) The reactor module is entirely factory manufactured and transported to the NPP site in readiness by different kinds of transport including railway. The small power and dimensions of those reactors makes possible organization of their conveyor production that enhances the quality of works and lessens the costs. On the basis of the same tested module, it is possible to construct the modular nuclear steam supplied systems (NSSS) of different power capacities of 100 MW(e)-fold for NPPs of different purposes without performs of additional research and development works (R&D). The effect of serial production is shown by Japanese organizations Central Research Institute of Electric Power Industry and TOSHIBA concerning to modular sodium fast reactor 4S of 80 MW(e). Those researchers have revealed [12] that the cost of a single module is reduced three times for their conveyor production in the specialized factory shop in the quantity of twelve modules per year (Fig. 3).

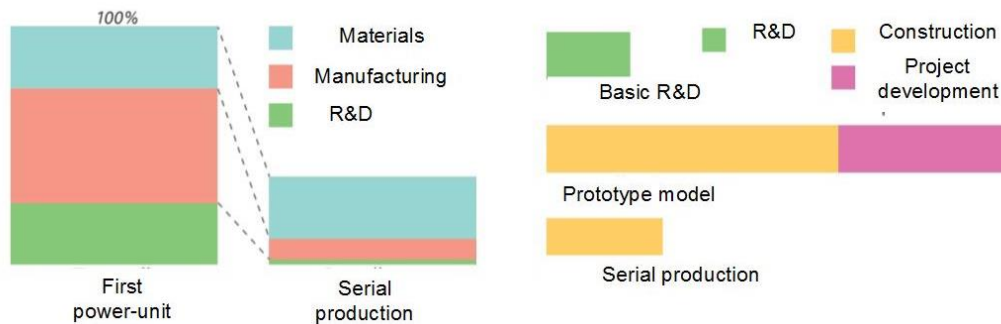


FIG. 3. Effect of serial production

(d) Modular structure of the power-unit NSSS [13] providing the following:

- The higher level of reliability (failure-resistance of the power-unit as a system of separate RFs) and safety (lessening of the potential radiation risk) as compared with a power-unit based on the single large capacity reactor;
- The opportunity not to provide the standby power-unit of large capacity in the areas of decentralized power supply;
- Under long operation of the reactor without refuelling (7-10 years), the loading factor is not less than 90 %, the loading factor will be determined by reliability indices of the turbine installation. When the RF is shutdown in turn for refuelling or technical maintenance, the power-unit's capacity is reduced noticeably less as compared with that of the power-unit based on a single reactor of large unit capacity;
- Continuous loading of engineering plants that considerably reduces the expenditures for manufacturing. Due to the fact that the unique engineering equipment is not required for manufacturing of the RMB, as it is required for the high-pressure vessels of thermal reactors, the opportunity to form the competitive market of manufacturers is arising;
- Use of the methods of standardized designing of different capacity power-units and production line methods of organization of building and construction works. Thus, together with a high level of serial production of RFs, reduction in terms and costs of power-units construction is provided;
- Location of small and medium capacity modular NPPs in the energy consumption centres that eliminates the expenditures for construction of powerful electric transmission lines;

- Power-unit's implementation in operating in turns with stepped raising of capacities as assembly and pre-commissioning works have been completed for the group of modules. This is lowering the term for pay-back of capital investments due to the earlier output of products and starting of pay off a credit as compared with that of the power-unit based on the reactor of large unit capacity.

Due to all listed points the competitiveness of reactors SVBR-100 is considerably increased.

The expected reduction of the investment cycle of NPP construction that is provided by modular structure of the NSSS and factory supply of ready modules is of major importance for nearing the technical and economical parameters of the NPP to corresponding parameters of modern steam-gas plants with short investment cycles and, thus, allowing considerably reduce the financial risks.

As there are only two states of reactor functioning, namely, operating and shutdown, control of the modular NSSS is carried out by one operator using the common power master unit. If there is any fault in a single reactor, it is automatically shut down and is cooled down autonomously, away from the turbine installation systems.

On expiring of the reactor lifetime (50...60 years) and unloading of the spent nuclear fuel and LBE, the basic reactor element – RMB – will be decommissioned and placed in a storage of solid radioactive wastes. A new RMB will be installed instead. The other elements of the reactor and power-unit can be decommissioned and replaced as well, i.e. the renovation can be performed [14]. At this point, the lifetime of the modular NPP will be only limited by that of reinforced-concrete construction structures and can be expanded up to 100...120 years while the lower costs as compared with those required for construction of the new power-unit. When the power-unit has been completely decommissioned, practically no radioactive materials are remaining in the NSSS building after the RMBs have been dismantled. Thus, the cost of decommissioning is considerably reduced.

The innovative Project of the NPP with reactors SVBR-100 is in fact the First Generation design based on a conservative approach. It has predetermined a high potential for further improvement of the Project, which will be realized as the corresponding R&D have been accomplished and operating experience has been gained.

In particular:

- Increasing of LBE temperature at the reactor outlet, while the maximal temperature of the fuel element's cladding (steel EP-823) is increased from 600 to 650 °C. There are the necessary backgrounds of that, – 16672 hours test by 650 °C in lead without of corrosion [15]. It will provide (as the computations have revealed) the growth of the reactor thermal power by about 10 % without change of the reactor design and cost.
- Use of the once-through SG generating the super-heated steam assures that the efficiency of the thermodynamic cycle will be heightened by about 10 %, capital costs will be lowered, reactor design will be simplified.
- Use of nitride fuel can provide twice increase of the reactor lifetime (the operability of fuel elements is to be verified) and correspondingly reduce the fuel costs.

4. R&D KEY RESULTS TO SUBTANTIATE THE REACTOR SVBR-100 PROJECT

At present the following results can be related to the key results of R&D on the RF SVBR-100 project:

- The RF design has been developed in a scope required for launching of production of the equipment, which manufacturing cycle is long.
- The commercial production of all basic components and semi-finished products, which required for manufacturing of the basic equipment, including experimental melting and fabrication of large blank parts for vessel structures, has been renewed.
- The corrosion resistance of fuel elements cladding (steel EP-823) has been grounded for 50135 of hours, i.e. for full lifetime, by temperature 600 °C [16].
- The tests of the structure of fuel elements prototypes in research reactor BOR-60 have been performed, experimental prototypes of the fuel elements with standard dimensions for conducting the tests in reactor BN-600 in radiation conditions, which are maximal close to those of SVBR-100, have been manufactured.
- The physical model of the SVBR-100 core has been constructed, and its neutron-physical features have been investigated at the BFS critical facility (IPPE).
- The mechanical tests of the separate units and devices of the refuelling system, flange connector, and unit of sealing of the reactor cover, CPS element drives.

The final part of the R&D program is oriented mainly to such long-time works as:

- Reactor tests of experimental lots of factory supplied fuel elements.
- Construction of the facility and tests of the prototype models of main circulation pump.
- Construction of the facility and tests of full-scale (1 loop) passive heat removal system, delivery tests of flow regulator of the passive heat removal system with passive feedback.
- The life tests of the steam generator scale model.
- The complex of works on construction and implementation of the normative base of reactor facilities with heavy liquid-metal coolant including certification of materials.

5. CONCLUSION

The stated materials enable to make the following conclusions:

- (e) Reactors SVBR-100, in which there is no accumulated in the primary coolant potential energy that is capable to cause damage of the protection barriers under the certain initial events, make possible deterministical elimination of severe accidents with catastrophic release of radioactivity requiring the population evacuation. Those reactors are not amplifiers of external effects and, therefore, the scale of damages will be only defined by energy of the external effect. Such type reactors possess the robustness properties, which assure their high resistance not only in events of single failures of the equipment and personnel's errors (human factor effect), but in events of deliberate ill-intended actions. Those properties of SVBR-100 reactor have to make possible overcoming of the population's radiophobia that has increased again after the accident happened at NPP Fukushima 1. And that is very important for development of the large-scale NP and sustainable development.
- (f) Implementation of reactors SVBR-100 in the NP makes possible elimination of the existing conflict between safety and economics requirements, which is typical for traditional type reactors because enhancement of safety is not reached due to the increase of the number of safety systems and protection barriers, but due to the higher level of inherent self-protection and passive safety, i.e. without detriment to economical parameters.
- (g) Reactors SVBR-100, which require a stage for their mastering including of real operating experience in the NPP conditions, can be used first for construction of SMRs operating in the local or regional energy-systems and generating the heat together with electricity and making possible replacement of the coal fossil power plant, which are the main pollutants of the environment.
- (h) It is planned that the technology of reactors SVBR will be realized at the experimental-industrial power-unit. The project is realized by JSC "AKME-engineering" established by State Corporation "Rosatom" and JSC "Irkutskenergo" in the form of state-private partnership. At present JSC "AKME-engineering" has obtained the "Rostehnadzor" license for location of the experimental-industrial power-unit in city Dimitrovgrad (Ulianovsk region).

ACKNOWLEDGEMENTS

The authors would like to thank Ms. S.V. Budarina and Mr. I.V. Tormyshev, for the assistance in preparation of the present Paper.

REFERENCES

- [1] Proatom.ru 12.03.2015 (2015).
- [2] Advanced nuclear plant design options to cope with external events, IAEA-TECDOC-1487 (February 2006).
- [3] SPIEWAK, I., WEINBERG, A., "Inherently Safe Reactors", Annual Review of Energy, **10**, (1985) 431-462, <http://dx.doi.org/10.1146/annurev.eg.10.110185.002243>.
- [4] FORSBURG, C., WEINBERG, A., "Advanced Reactors, Passive Safety and Acceptance of Nuclear Energy", Annual Review of Energy, **15**, (1990) 133-152, <http://dx.doi.org/10.1146/annurev.eg.15.110190.001025>.
- [5] ARUTYUNYAN, R.V., "Have We Got Safety Culture?", ATOMNAYA STRATEGIYA XXI, **83**, (October 2013), 9-11. (<http://www.proatom.ru/>).

- [6] PETROCHENKO, V.V., TOSHINSKY, G.I., KOMLEV, O.G., “SVBR-100 Nuclear Technology as a Possible Option for Developing Countries”, *World Journal of Nuclear Science and Technology*, **5**, 221-232 (2015), (<http://dx.doi.org/10.4236/wjnst.2015.53022>).
- [7] TOSHINSKY, G.I., STEPANOV, V.S., NIKITIN, L.B. *et al.* “The Analysis of Operating Experience of Reactor Installations Using Lead-Bismuth Coolant and Accidents Happened”, *Heavy-Liquid Metal Coolants in Nuclear Technologies (HLMC-98)* (Proc. of 1st Int. Conf., Obninsk, Russia, 1999), **1**, 63-69 (1999). See also in the book: Georgy I. Toshinsky. *Lead-Bismuth Cooled Fast Reactors (Collection of Selected Articles and Papers)*. LAMBERT Academic Publishing.
- [8] Handbook on Lead-bismuth Eutectic Alloy and Lead Properties, Materials Compatibility, Thermal-hydraulics and Technologies, Table 2.4.1. 2015 Edition (OECD – NEA).
- [9] PANKRATOV, D.V., YEFIMOV, YE.I., TOSHINSKY, G.I., RYABAYA, L.D., “Analysis of Polonium Hazard in Nuclear Power Installations with Lead-Bismuth Coolant”, *Advances in Nuclear Power Plants (Proc. Int. Congress)*, CD-ROM, Paper № 5497, Seoul, Korea (2005). See also in the book: Georgy I. Toshinsky. *Lead-Bismuth Cooled Fast Reactors (Collection of Selected Articles and Papers)*. LAMBERT Academic Publishing.
- [10] BOLHOVITINOV, V.N., PANKRATOV, D.V., YEFIMOV, YE.I., TOSHINSKY, G.I. *et al.*, “Assessment of Radiation Consequences Caused by Large Tightness Failure in the Primary Circuit Gas System of RF SVBR-75/100 with Simultaneous Coolant Overheating up to 600 °C”, *Heavy-Liquid Metal Coolants in Nuclear Technologies (HLMC-2003)* (Proc. of 2nd Int. Conf., Obninsk, Russia, 2003), CD-ROM, Paper No. 2203 (2003). See also in the book: Georgy I. Toshinsky. *Lead-Bismuth Cooled Fast Reactors (Collection of Selected Articles and Papers)*. LAMBERT Academic Publishing.
- [11] TOSHINSKY, G.I., KOMLEV, O.G., TORMYSHEV, I.V., PETROCHENKO, V.V., “Effect of Potential Energy Stored in Reactor Facility Coolant on NPP Safety and Economic Parameters”, *World Journal of Nuclear Science and Technology*, **3**, No. 2, 59-64 (2013), (www.scirp.org/journal/wjnst).
- [12] HATTORI, S., MINATO, A. “A Large Modular LMR Power Station which Meets Current Requirements”, *Reports of 4S (Super Safe, Small and Simple LMR)*, CRIEPI, Tokyo, Japan, 787-790 (1994).
- [13] TOSHINSKY, G.I., PETROCHENKO, V.V., “Modular Lead-Bismuth Fast Reactors in Nuclear Power”, *Sustainability* 2012, **4**, 2293-2316; doi:10.3390/su4092293, ISSN 2071-1050 (2012).
- [14] TOSHINSKY, G.I., KOMLEV, O.G., STEPANOV, V.S., KRUSHELNITSKY, V.N. *et al.* “Renovation of the “Old” NPP Units as a Way to Increase Cost Effectiveness of Nuclear Power”, *Proceedings of GLOBAL 2005*, Tsukuba, Japan, Oct. 9-13, 2005, Paper No. 276. See also in the book: Georgy I. Toshinsky. *Lead-Bismuth Cooled Fast Reactors (Collection of Selected Articles and Papers)*. LAMBERT Academic Publishing.
- [15] A.P. DEMISHONKOV, O.E. LEVIN, E.N. PYANKOVA *et al.*, “Behavior of protective oxide films by long-term corrosion test in HLMC”, Paper 2106 in *Proceeding of 3rd Conference “Heavy Liquid Metal Coolant in Nuclear Technology (HLMC-2008)”*, Vol. 2, p. 327 (in Russian).
- [16] A.E. RUSANOV, O.E. LEVIN, A.G. GUSHCHINA *et al.*, “Investigation of corrosion resistance of fuel element claddings of EP823 steel after test in Pb-Bi coolant flow”, *Proceeding of Fourth Conference “Heavy liquid metal coolants in nuclear technologies (HLMC-2013)”* Russia, Obninsk, September 23-26, 2013.

CLFR-300, AN INNOVATIVE LEAD-COOLED FAST REACTOR BASED ON NATURAL-DRIVEN SAFETY TECHNOLOGIES

Paper ID #7

Jiming LIN
Xiuan SHI
Chengjie DUAN
Zhao CHEN*
Dawei CUI
Lei SONG

China Nuclear Power Technology Research Institute Co., Ltd.
Shenzhen, China

E-mail: chen-zhao@cgnpc.com.cn

Abstract

New market requirement for nuclear power has emerged, which require to improve nuclear power safety and economic performances simultaneously. It is required to develop advanced nuclear reactor technologies to satisfy the new market requirement for nuclear power. During the past several years, China General Nuclear Power Corporation (CGN) had made an adequate comparative analysis of all alternate potential advanced reactor technologies and selected the Lead-cooled Fast Reactor (LFR) as the preferred technology for the next generation nuclear power development. Besides the selection of the LFR technology, CGN are proposing a new safety concept named Natural-Driven Safety (NDS) to solve conflicting requirements of safety and economy, which will make it possible to improve reactor safety and economics performances simultaneously then to meet the new market requirement. The paper presents the conceptual design of an innovative LFR based on NDS technologies named CLFR-300, including reactor core, primary system and related auxiliary system and safety system. Two specific NDS systems are applied in the design of CLFR-300, including the Natural Driven Shutdown System (NDSS) and the Natural Driven Decay Heat Removal System (NDDHRS). With the NDSS, it can virtually eliminate risks of unprotected accident, and with the NDDHRS, it can virtually eliminate risks of core damage and large release of radioactivity. These excellent safety features can help CLFR-300 to improve nuclear power safety and economic performances simultaneously and rule out the requirement of evacuation of the local population.

1. INTRODUCTION

Nuclear power is an important low-carbon energy source, but its development status is not going very well in the last decade, especially after the Fukushima NPP accident. According to the BP world energy report, through the past 10 years, the share of consumed electricity generated by renewables grew by 8.4%, while the share of a nuclear power decreased by 3.4% [1]. One reason for this result is that the market requirement for nuclear power has changed. On the one hand, the public demand for nuclear power safety has increased, which results in an increase in capital expenditures for current NPPs technologies, on the other hand, the technologies of renewables develop rapidly, which require nuclear power to be more economical. Therefore, there is an urgent need to develop advanced nuclear reactor technologies to satisfy the new market requirement for nuclear power.

During the past several years, China General Nuclear Power Corporation (CGN) had made an adequate comparative analysis of all alternate potential advanced reactor technologies and selected the Lead-cooled Fast Reactor (LFR) as the preferred technology for the next generation nuclear power development. Besides the selection of the LFR technology, CGN are proposing a new safety concept named Natural-Driven Safety (NDS) to solve conflicting requirements of safety and economy, which will make it possible to improve reactor safety and economics performances simultaneously then to meet the new market requirement.

In this paper, the conceptual design of an innovative LFR based on NDS technologies named CLFR-300 is presented, including reactor core, primary system and related auxiliary system and safety system. The NDS safety concept is defined and its application in CLFR-300 is presented and discussed.

2. CONCEPTURAL DESING OF CLFR-300

2.1. General description

The CLFR-300 is a lead-cooled pool-type fast reactor incorporating advanced design ideas such as integral arrangement, modular design, whole core refuelling and intelligent operation and maintenance. The development objectives of CLFR-300 are:

- (i) Demonstrate the technical feasibility of LFR with a target that ready for operation by 2030.
- (j) Demonstrate the economic competitiveness of LFR with a target that the construction costs per unit of power generated can below current LWR designs.
- (k) Qualify and standard fuel and materials for commercial LFR.
- (l) Provide operating experience with pumps, steam generations and other key components that are prototypic for commercial LFR.

The schematic of CLFR-300 is shown in Fig. 1 and main design parameters are presented in Table. 1.

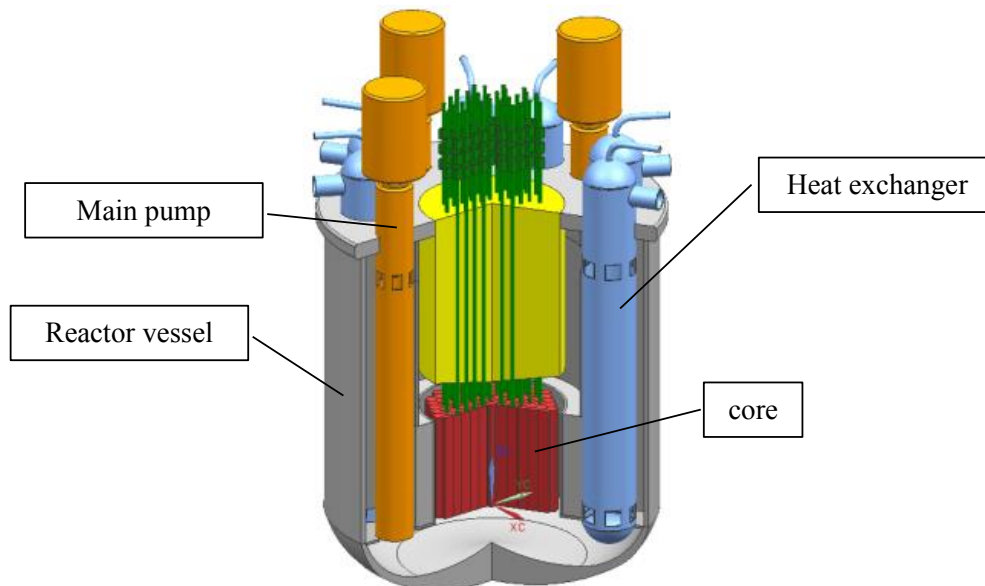


FIG. 1. The schematic of CLFR-300

TABLE 1 MAIN DESIGN PARAMETERS OF CLFR-300

Parameter	Value
Thermal power	740 MW(th)
Electric power	300 MW(e)
Plant net efficiency	40.5%
Fuel	UO ₂ (11.7%/15.6%)
Refuelling interval	3 years
Core inlet/outlet temperature	400/500°C
Primary system	Integral pool-type with forced circulation
Primary coolant	Liquid lead
Steam generators	8×Once through steam generator (OTSG)
Reactor coolant pump	4×Mechanical pump
Secondary cooling system	Water/steam forced circulation

2.2. Reactor core

The CLFR-300 core consists of 163 hexagonal fuel assemblies (FAs), including 114 fuel assemblies and 49 control rod assemblies. The fuel assembly consists of 217 fuel pins, which are placed in a triangular lattice and fixed by wires. The control rod assembly consists of 198 fuel pins and a central tube, where the central tube is used as the guide tube for absorber rods.

To ensure criticality throughout the irradiation cycle and flatten the power distribution, the core is divided in two enrichment zones: an inner region includes 126 assemblies with 11.7% ²³⁵U enrichment UO₂ pellet, and an outer region includes 37 assemblies with 15.6% ²³⁵U enrichment UO₂ pellet.

Reactivity control is ensured by 3 groups of absorbing rods, independent from each other and with different function. These absorbing rod groups are regulation rods (A rods), control rods (B rods), safety rods (S rods).

The core map of CLFR-300 is shown in Fig.2.

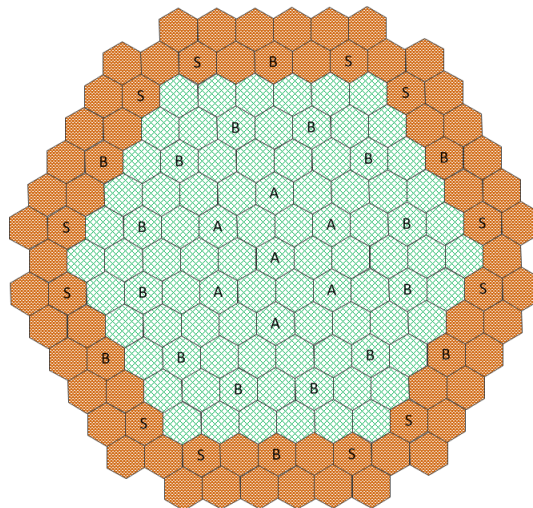


FIG. 2. CLFR-300 core map

2.3. Primary system and related auxiliary systems

The CLFR-300 primary system is an integral pool-type concept with all primary components are arranged in the Main Vessel (MV), including the reactor core, steam generators (SGs), reactor coolant pumps (RCPs) and the internal structure. The integral pool-type design can provide safety benefits of eliminating penetration assemblies the main vessel and thereby largely reducing the occurrence possibility of loss of coolant accidents (LOCA), and economic benefits of simplifying the primary system. All primary components are designed to be extractable from the primary system to ease maintenance and replacement, which benefits system reliability. The lead coolant is heated through the core and flows upward to the SGs drawn by the RCPs, and then cooled through SGs and flows downward back into the core.

CLFR-300 auxiliary systems including lead chemical control system, cover gas control system, lead heating system and lead filling system. The lead chemical control system is designed to provide the continuous monitoring and control of lead purity and oxygen content for the primary cooling system. The cover gas control system is designed to provide the continuous monitoring and purifying of the argon gas used as cover gas in the primary cooling system. The monitoring function can also provide an indirect indication of the presence of any fuel cladding failure. The lead heating system and the lead filling system are designed to provide auxiliary heat and filling of lead during the start-up and shut-down operations.

2.4. Safety systems

CLFR-300 safety systems including the emergency decay heat removal system and the overpressure protection system. The emergency decay heat removal system is designed to provide emergency decay heat removal when secondary cooling system failed. The emergency decay heat removal system consists of four independent loops connected to the SGs and isolation condensers immersed in water pools. When the valve open, the natural circulation of water/steam will be established to removing heat from the primary lead circulating across the SGs. Two of four loops can provide 100% cooling capability for decay heat removal. The water pool is designed to ensure seven days of grace time in decay heat removal mode, and easy to connect to the locally available water, such as the equipment cooling water and the firefighting water. The overpressure protection system and the containment system are designed to provide protection function of overpressure when the steam generator tube rupture (SGTR) accident occurs.

The system configuration of CLFR-300 is shown in Fig. 3.

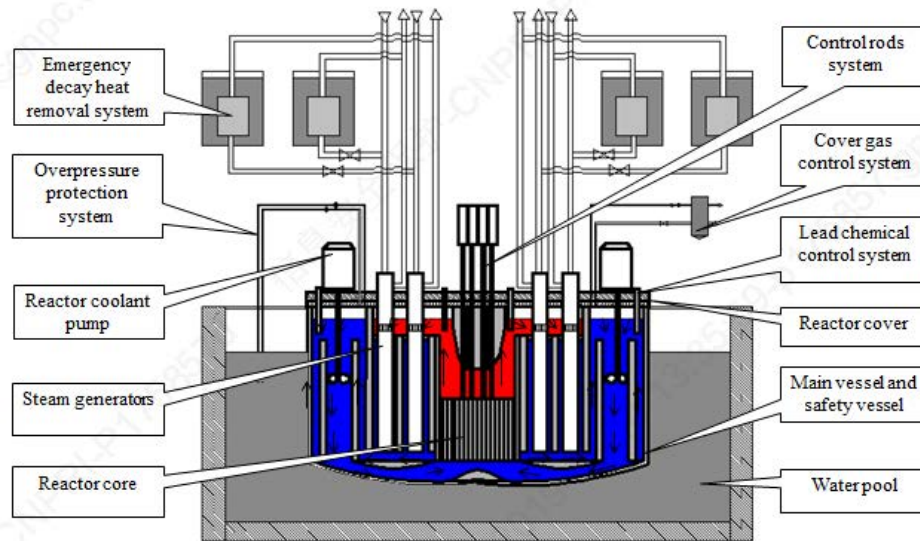


FIG. 3. The system configuration of CLFR-300

3. NATURAL-DRIVEN SAFETY TECHNOLOGY AND ITS IMPLEMENTATIONS IN CLFR-300

3.1. Definition of natural-driven safety technology

According to traditional safety concepts, the requirements of safety and economy are conflict in most cases, such as the redundant design requirement, the conservative margin requirement and the backup power (emergency diesel engines) requirement. Therefore, it is necessary to explore a new safety concept to reconcile the conflict so that we can improve the safety and economy simultaneously.

A new safety concept named Natural Driven Safety (NDS) has been defined and applied to the design of CLFR-300. The NDS means the start-up and operation of reactor safety systems are entirely driven by nature laws and without any non-natural means, such as batteries and electronic devices. This new concept is the extension of the passive safety and belongs to philosophy of inherent safety.

The benefits of NDS technology are:

- (a) improve reactor safety performance by providing self-protection capacity during all credible initiation events and their combinations and providing long term cooling capacity for decay heat by nature laws.
- (b) improve safety systems reliabilities by eliminating electric power requirements and any operator intervention.
- (c) improve reactor economic performance by simplifying equipment units and operation procedures of safety systems.
- (d) improve public acceptability by virtually eliminating risks of core damage and large release of radioactivity and ruling out the requirement of evacuation of the local population.

Some specific technological means to realize NDS can be:

- natural circulation cooling technique
- thermal expansion or thermal contraction technique
- selective fuse or quick fuse technique
- burst pressure technique
- high quality and high performance materials

3.2. NDS technology implementations in CLFR-300

Two specific NDS systems are applied in the design of CLFR-300. The first one is the Natural Driven Shutdown System (NDSS), and the second one is the Natural Driven Decay Heat Removal System (NDDHRS).

3.2.1. Natural-driven shutdown system (NDSS)

The Natural Driven Shutdown System (NDSS) is designed as the ultimate reactivity control mean for CLFR-300, which will provide shutdown protection when the safety rod system fails to actuate. The NDSS consists of absorber rods, guide tubes and controllers. The absorber rod is similar to that in the safety rod system, which is made of high enrichment boron carbide. The controller is a temperature based two-position (on-off) automatic controller. When the coolant temperature reaches a set value, the two-position controller actions and then the absorber rod will enter the core by gravity to shut down the reactor. There are several temperature based technologies can be used in NDSS, such as fusible locks and bimetallic strips.

The action of NDSS is based on the temperature change, which is the nature law of material properties and has the extremely high reliability. Therefore, with the NDSS, the CLFR-300 can virtually eliminate the risk of unprotected accident and make it possible to prevent anticipated transients without scram (ATWS) accidents.

3.2.2. Natural-driven decay heat removal system (NDDHRS)

The Natural driven decay heat removal system (NDDHRS) is designed as the ultimate decay heat removal mean for CLFR-300, which will provide cooling capability when the emergency decay heat removal system fails to actuate. The NDDHRS is composed of a water pool, pipelines and an isolation condenser immersed in a water tank, as shown in Fig.4.

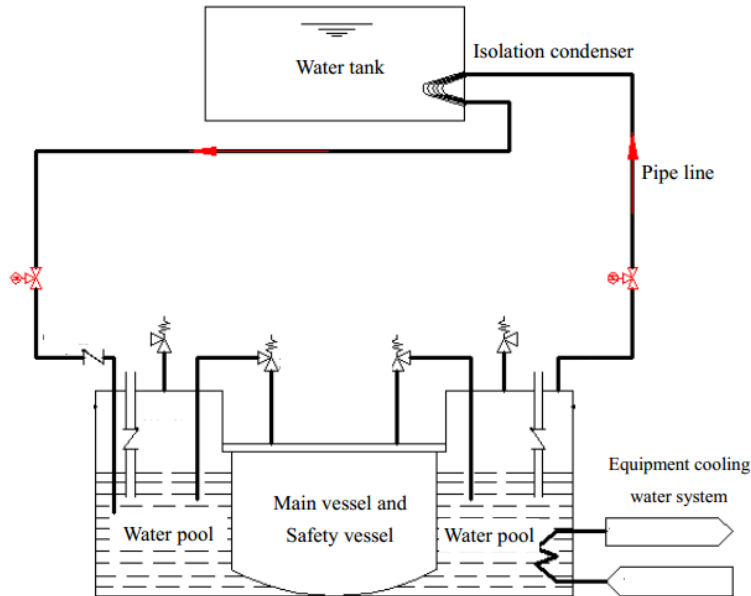


FIG. 4. The system configuration of NDDHRS

The NDDHRS removes the decay heat by thermal radiation from the reactor vessel to the water pool, and further due to the water boiling with steam removal through the pipeline to the isolation condenser. The water tank is the ultimate heat sink and the water inventory in the water tank can prevent fuel damage for at least 3 days without any source of power and operator action. After 3 days, the local available water, including the equipment cooling water and the firefighting water, can be filled into the water tank in an easy way through dedicated lines. If the local available water is failed to be filled into the water tank in 3 days, the pressure release valve in the pipe will be open and the steam from the water pool will be released. In this operation model, the cooling time can be extended to 7 days. In theory, it can provide an unlimited cooling capacity by NDDHRS, but it will require a very large water tank or water pool, which will increase cost. In our opinion, 7 days is an enough time to find and provide external supplement water to be filled into the water tank to provide the long-term cooling. The local available water or external supplement water will provide more than 30 days decay heat removal. After 30 days, the NDDHR will transition to long-term air cooling.

In normal condition, the temperature of the reactor vessel is 400°C. With this temperature, the heat transfer from the reactor vessel to the water pool through thermal radiation is about 1.5 MW(th), which is a kind of thermal waste. To solve this problem, the unique designed insulating layer is used in CLFR-300. The insulating layer is wrapped around the outside of the safety vessel by a temperature based connector. When the safety vessel temperature reaches a set value, the connector actions and then the insulating layer will fall off. With the insulating layer the heat transfer from the reactor vessel to the water pool will be very small and can be negligible. When the insulation layer falls off, the water will direct contact with the safety vessel and the heat transfer from the reactor vessel to the water pool will increase significantly.

In NDDHRS, the action is based on temperature and the operation is based on the thermal radiation, the water boiling and the water-steam natural circulation. All these operations entirely depend on nature laws and without battery and electronic devices. With the local available water or external supplement water, the NDDHRS can provide more than 30 days cooling capacity and then switch into long-term air cooling. With the NDDHRS, the CLFR-300 can practically eliminate risks of core damage and large release of radioactivity and rule out the requirement of evacuation of the local population.

4. CONCLUSIONS

New market requirement for nuclear power has emerged, which require to improve nuclear power safety and economic performances simultaneously. It is required to develop advanced nuclear reactor technologies to satisfy the new market requirement for nuclear power. CGN has proposed a new safety concept named Natural-Driven Safety (NDS) and conducted the conceptual design of an innovative LFR based on NDS technologies named CLFR-300.

The NDS means the start-up and operation of reactor safety systems are entirely driven by nature laws and without any non-natural means, such as batteries and electronic devices. This new concept is the extension of the passive safety and belongs to philosophy of inherent safety. Two specific NDS systems are applied in the design of CLFR-300, including the Natural Driven Shutdown System (NDSS) and the Natural Driven Decay Heat Removal System (NDDHRS). With the NDSS, it can virtually eliminate risks of unprotected accident, and with the NDDHRS, it can virtually eliminate risks of core damage and large release of radioactivity. These excellent safety features can help CLFR-300 to improve nuclear power safety and economic performances simultaneously and rule out the requirement of evacuation of the local population.

The detail design of the CLFR-300 conceptual, as well as the NDSS and the NDDHRS are ongoing, and key simulation analysis and validate tests will be conducted in near later.

REFERENCES

- [1] BP Statistical Review of World Energy, 67th edition, June 2018 <https://www.bp.com/content/dam/bp/business-sites/en/global/corporate/pdfs/energy-economics/statistical-review/bp-stats-review-2018-full-report.pdf>.

CONCEPTUAL DESIGN OF CHINA LEAD COOLED MINI-REACTOR CLEAR-M10D

Paper ID #15

Yican Wu

Institute of Nuclear Energy Safety Technology, Chinese Academy of Sciences
Hefei, Anhui, 230031, China

Email: yican.wu@fds.org.cn

Chao Liu, Ming Jin, Tao Zhou, Jieqiong Jiang, Fang Wang, Yong Song, Zhumin Zhao,
Liqin Hu, FDS Team

Institute of Nuclear Energy Safety Technology, Chinese Academy of Sciences
Hefei, Anhui, 230031, China

Abstract

Lead cooled reactors have significant advantages on inherent safety, economy and feasibility. Due to the long refuelling cycle and safety properties, lead-based reactors have attracted more and more attention in recent years. China Lead cooled Mini-Reactor (CLEAR-M) is developed by the Institute of Nuclear Energy Safety Technology of Chinese Academy of Sciences (INEST, CAS). It is an advanced power-supply installation with an electric power ranging from 1 to 100 MW(e) and can be flexibly combined and loaded by containers. With the inherent safety and well sustainability with minimized nuclear waste production, CLEAR-M can meet various needs, demonstrating broad application prospects. The typical design of CLEAR-M is named CLEAR-M10d, which is a small modular lead cooled reactor to demonstrate small-scale energy supply of 10 MW(e) level, with the features of small modular, inherent safety concept and long refuelling period. CLEAR-M10d is a pool-type reactor. The natural circulation heat transport has been adopted to reduce maintenance requirements of main equipment and enhance the reliability and safety of system. The use of average 18.5% enriched UO₂ has been chosen to realize long refuelling period while three radial regions with different fuel enrichments were designed to decrease the power peaking factor. CLEAR-M10d incorporates two independent and redundant residual heat removal systems, and the Reactor Vessel Air Cooling System (RVACS) is designed as the emergency heat removal system. In the meantime, a prototype mini-reactor named CLEAR-M10a is being carried out to support CLEAR-M10d, the engineering design is underway, and the existing technology has been used to accelerate the implementation progress.

1. INTRODUCTION

Lead cooled reactors have significant advantages on inherent safety, economy and feasibility [1-6]. Due to the long refuelling cycle and safety properties, lead-based reactors have attracted more and more attention in recent years [7-10]. As an advanced power-supply installation, CLEAR-M with the electric power ranging from 1 to 100 MW(e), can be flexibly combined and loaded by containers. With the inherent safety, small modular and compact, good economy with mass energy production and large-scale widely application, and well sustainability with minimized nuclear waste production, CLEAR-M can flexibly meet various needs, and demonstrating broad application prospects. CLEAR-M can also meet various electric needs, e.g. electric supply of islands, desalination of sea water, independent distributed power supply of remote region and combined heat and power of industrial park [11, 12].

The typical design of CLEAR-M is named CLEAR-M10d, which is a small modular lead cooled reactor to demonstrate small-scale energy supply of 10 MW(e) level, with the features of small modular, inherent safety and long refuelling period.

In the meantime, a prototype mini-reactor named CLEAR-M10a is being carried out to support CLEAR-M10d, the engineering design is underway, and the existing technology has been used to accelerate the implementation progress. Based on the continuously R&D activities of lead cooled reactors, CLEAR-M implementation and foundation of industrialized bases are going on, in order to finish the construction of the CLEAR-M10a in the near future.

2. CHINA LEAD COOLED REACTOR DEVELOPMENT STRATEGY

Due to its attractive features, lead cooled reactor is remarked as a promising reactor type for Generation-IV reactor and ADS system [13-15]. The Chinese government has provided a continuous national support to develop lead cooled reactors technology since 1986. In the last 30 years' research on lead cooled reactor, Institute of Nuclear Energy Safety Technology (INEST/FDS Team) has been working on the design and analysis of China LEAd cooled Reactor (CLEAR), developing key technologies and components, and has also proposed a roadmap for CLEAR. The designs of small LFR CLEAR-M for energy, ADS system CLEAR-I for transmutation and CLEAR-A for breeding and burning have been carried out [16].

In order to support the CLEAR lead cooled reactor projects, a multi-functional lead-bismuth experiment loop platform-KYLIN-II has been built and operated for more than 30,000 h. Various tests have been conducted, including corrosion test, LBE thermal-hydraulic experiment, components prototype proof test etc. [17,18]. In addition, three integrated test facilities were constructed to test the integrated properties of lead cooled reactor. The three facilities are CLEAR-S (an integrated non-nuclear test facility), CLEAR-0 (a zero-power critical/subcritical reactor), and CLEAR-V (a virtual reactor) [19-21].



FIG. 1. Multi-functional lead-bismuth loop KYLIN-II [16]

Based on a systematic R&D studies on LFR technologies, CLEAR-M project aiming at construction of small module energy supply system has been launched. The main purpose of this system is to provide a flexible power system for wide application such as islands, remote districts and industrial park etc. CLEAR-M with integrated modular design can operate more than 10 years without refuelling. The low enriched uranium (<20% enriched UO_2) is chosen as fuel and austenitic stainless steel is selected as the structural and fuel cladding material because of its good compatibility with lead.

3. DESIGN DESCRIPTION OF CLEAR-M10D

TABLE 2 lists the main parameters of CLEAR-M10d (Fig. 1). The natural circulation heat transport has been adopted to reduce maintenance requirements of main equipment and enhance the reliability and safety of system. The use of average 18.5% enriched UO₂ has been chosen to realize long refuelling period while three radial regions with different fuel enrichments are designed to decrease the power peaking factor. CLEAR-M10d incorporated two independent and redundant residual heat removal systems, and the Reactor Vessel Air Cooling System (RVACS) is designed as the emergency heat removal system.

TABLE 2. DESIGN PARAMETERS OF CLEAR-M10D

Item	Value
Thermal power	35 MW(th)
Electrical power	14 MW(e)
Fuel	Ave. 18.5% UO ₂
Coolant	Lead
Refuelling time	20 years
Core inlet / outlet temperatures	375/495 °C
Reactor vessel dimensions	Φ2.2m×8.5m(H)
Reactor vessel length-to-diameter ratio	4:1

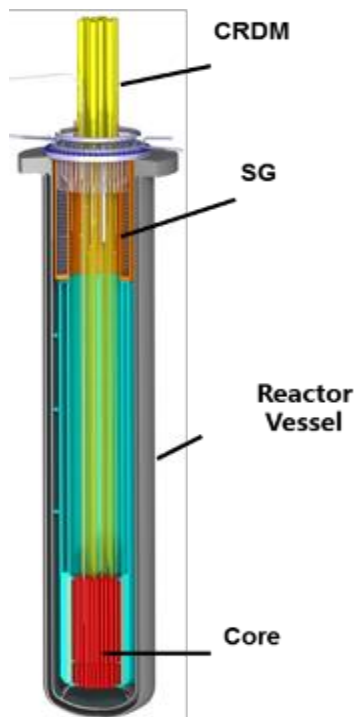


FIG. 2. Overall view of CLEAR-M10d reactor

3.1. Core design

3.1.1. Reactor core design

There is no fuel assembly for the M10d reactor. The core is an integrated structure, composed of fuel rods, reflector and control rods. There are in total ~3500 fuel rods with triangular arrangement. The core includes three active zones, and ²³⁵U enrichment of UO₂ in each zone is 19.75%, 19%, and 18%, respectively. In this way the power distribution is flattened, which is beneficial to temperature requirement of the fuel rods. The thermal power is 35 MW with core dimensions $\Phi 1200$ mm(D) \times 790 mm(H), active zones length 790 mm, diameter of fuel pin 16mm, pitch to diameter 1.2 and cladding thickness 1mm. The cladding material is 15-15Ti with FeCrAlY coating. The self-developed Super Multi-functional Calculation Program for Nuclear Design and Safety Evaluation (SuperMC) is used for the design and optimization of the core configuration. The active zones are enclosed by reflector. The initial keff is 1.097.

TABLE 3. PARAMETERS OF REACTOR CORE

Item	Value
Fuel type	UO ₂
Enrichment of fuel	19.75% / 19% / 18%
Cladding material	15-15Ti with FeCrAlY coating
cladding thickness	1mm
Number of fuel pins	3500
Diameter of fuel pin	16mm
Pitch to diameter	1.2
Fuel load	~4600kg
K _{eff}	1.097
Burnup	~62000 MWd/tU
Refuelling time	20 years
Reactor core dimensions	$\Phi 1200$ mm(D) \times 790 mm(H)

Two shutdown systems are designed with different control methodologies in the core. The primary shutdown system consists of 6 shim rods and 2 regulation rods, and the second shutdown system is composed of 4 safety rods. Each shutdown system is able to force the reactor to shut down even if the rod with maximum worth is hung-up.

Both coolant temperature coefficient and fuel Doppler coefficient have negative values, which are -392 pcm and -92 pcm respectively. The overall reactivity coefficient has large negative values, which ensures the inherent safety for the reactivity control.

Fig. 2 shows the effective multiplication factor behaviours over 20 years. The excess reactivity at BOC is 9700 pcm, which declines continuously to 700 pcm at EOC. During 20 years operation, the change of reactivity is 9000 pcm. The burnup is ~62000 MWd/tU.

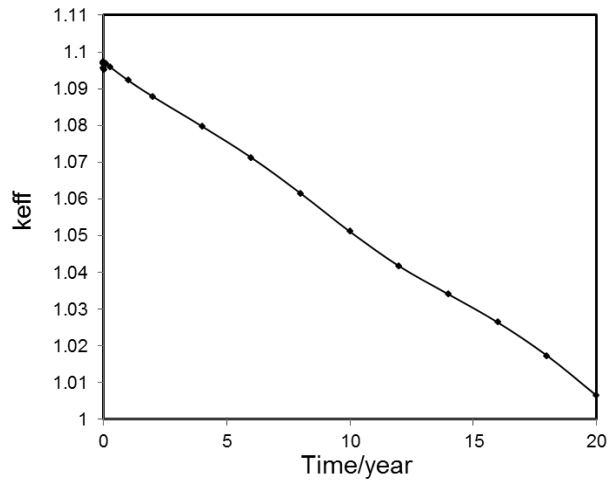


FIG. 3. Evolution of k_{eff} during 20 years

3.1.2. Fuel element design

The fuel element consists of upper end plug, plenum, upper reflector, active zone, down reflector and Down end plug. UO_2 has been chosen as the fission material and 15-15Ti with FeCrAlY coating has been chosen as the cladding. The fuel elements are fixed to the upper and the lower grids of the core, and the core is fixed to the cover of the vessel. The maximum temperature of the cladding under the normal condition is no more than 550 °C.

3.1.3. Thermal hydraulics design

The maximum thermal power of 35 MW(th) is evacuated by the primary coolant and secondary coolant systems. The average core coolant temperature rising is 120 °C under nominal operating conditions. There is no main pump in the primary system to simplify the mechanical structure and reduce maintenance requirement. Only natural circulation is designed to transport heavy liquid metal coolant. One single-layer spiral type steam generator with the annular mode is laid out in the main vessel. A barrier with insulation layer is located in the primary system to separate the hot pool and cold pool regions.

The power density is only 47.6 MW/m³, much lower than other reactors' ~100 MW/m³ (like PWR). In order to keep core pressure drops low, the open assembly geometry has been designed to realize large coolant volume fraction. The pitch-to-diameter ratio is 1.2. Thus, the average core coolant speed is 0.46 m/s. The thermal centres of gravity between core active zone and steam generator is 6.4m which provides enough natural circulation capacity of the primary system. With no moving parts in the primary coolant system, the whole primary system circulation can be more stable and safety.

TABLE 4. PARAMETERS OF THERMAL HYDRAULICS DESIGN

Item	Value
Thermal power	35 MW(th)
Core inlet / outlet temperatures	375/495°C
Natural circulation height difference	6400mm
Power density	47.6 MW/m ³
Average velocity of core	0.46m/s
Maximum cladding temperature	540.6°C
Maximum fuel temperature	1559°C

The fuel cladding hot spot and maximum fuel pellet temperature has been estimated by single channel analysis code. Fig.3 shows that the maximum cladding hot spot temperature as 540.6 °C which is lower than the material temperature limits of 550 °C. The central fuel temperature is 1559 °C which is under the limits as well.

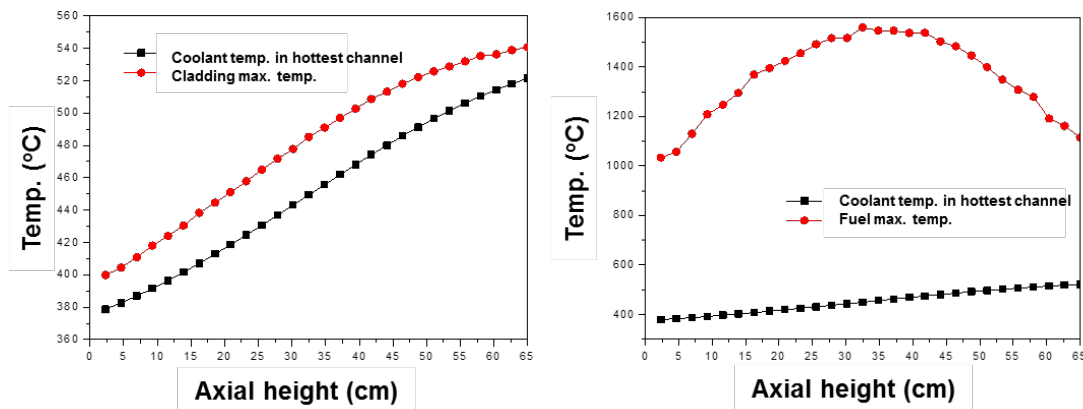


FIG. 4. The cladding hot spot and central fuel temperature

3.2. Reactor System design

CLEAR-M10d reactor is a pool reactor with compact structure, including reactor pressure vessel, internals, steam generator (SG), CRDM, reactor core, thermal-couple instrumentation, oxygen sensors, level measurements, safety valve, filling and draining pipe, cover gas pipe, etc. The reactor integrates the main important components. All primary coolant system's main components are immersed in the pool, and the reactor pressure vessel, reactor cover, SG and other equipment constitute the primary coolant system's pressure boundary. Without the driven pump in the primary system, the natural circulation capacity is sufficient enough to take away the heat of the core.

The reactor pressure vessel is designed as a pool vessel with double walls, and the inner vessel represents main vessel, while the outer vessel represents the safety vessel. The reactor pressure vessel acts as a physical barrier and a boundary constrain of the primary system. It acts as a vital barrier to prevent the leakage of radioactive waste. The reactor vessel adopts hanging support, that is, the main flange is installed on the foundation support, and the bottom head of the vessel and the cylinder can expand freely. The top part is designed with double concentric covers. The outer cover is assembled and welded with spiral coil heat exchanger, and then installed on the main flange of the vessel. The inner cover, the control rod drive mechanism and the guide cylinder are installed on the outer cover after assembly.

CLEAR-M10d reactor vessel adopts large length-to-diameter ratio structure (4:1), which has a large response to seismic response and is easy to be unstable. In this case, the vessel support of CLEAR-M10d adopts top-lower double support structure. The top support is fixed, and the lower support is used for radial constraint. The support of inner vessel adopts the structure similar to the lower support. Thus, the radial sloshing of inner vessel is limited, but the axial expansion of the inner vessel is free. The requirements of reactor vessel are met through the seismic analysis with response spectrum and the corresponding acceleration time-history input.

Reactor internals consist of upper internals structure, lower internals structure (core support structure) and radiation shielding. Upper support structure is designed to a double-layer cylinder with large heat resistance and small heat expansion inertia gas-argon in the gap, and it separates the coolant in the pool into two regions: the cold region and hot region. The lower internals are seated on bottom head, used to support and install the core assembly and the reflector assembly. From inside to outside, radiation shielding consists of Be-reflector, austenitic stainless steel and lead coolant.

TABLE 5. PARAMETERS OF REACTOR SYSTEM

Item	Value
Reactor vessel type	Pool vessel with double walls
Cover type	Flat cover
Cover gas	Argon gas
Reactor vessel support	Top-lower double support structure
Reactor vessel length-to-diameter ratio	4:1
Reactor vessel dimensions	$\Phi 2.2\text{m} \times 8.5\text{m(H)}$

3.2.1. Key components design

The steam generator is shell and tube type with spiral tube structure (STSG). There is only one STSG placed in the annular space of the reactor vessel. The tube bundle is ring-shaped and supported by two cylindrical shells. Both the outer shell and inter shell are welded on the cover.

The spiral tubes are passed through the cover using seal welding technology. Each spiral tube is a horizontal coil annular. The water inlet is placed at the outer diameter of horizontal coil annular, and the steam outlet is placed at the inner diameter of horizontal coil annular. There are two feedwater collectors and two steam collectors above the top of cover. The tubes are welded on the collectors with the active length of the tubes 21.2m.

The steam generator is fed from the outer of tube bundle. The liquid lead flows from the inner of tube bundle. The spiral tubes are used aiming to enhance the heat transfer in the both lead side and water side. The spiral structure could greatly reduce active length of tube bundle and enhance the natural circulation of the liquid lead flow [22].

Each spiral tube could be plugged above the cover and reduce maintenance cost and time for the SGTR condition.

TABLE 6. PARAMETERS OF STEAM GENERATOR

Item	Value
Number of steam generator	1
Type of steam generator	shell and tube type with spiral tube structure (STSG)
Number of tubes	132
Outer diameter of tubes	17mm
Active length of tubes	21200mm
Tube bundle active height	~1460mm
Outer diameter of steam generator	Φ1750mm

3.2.2. Engineering safety features

To ensure CLEAR-M10d safety under the accident conditions, special safety measures were designed, including passive decay heat removal system (DHR), confinement system and primary loop overpressure protection system.

The passive Reactor Vessel Air Cooling System (RVACS), as independent DHR, can be used to take away the core decay heat to deal with loss of all the power supply accident and steam generator failure. The RVACS is mainly composed by air rising and down-comer channels with air channel width 0.15m, a 10m height chimney, thermal insulating layer, main and safety vessels. The RVACS take away heat by heat radiation and convection with the power 525 kW (1.5%FP) and natural circulation. Firstly, the primary loop coolant transfers heat to the main vessel by convection. Secondly, the main vessel transfers heat to the safety vessel by heat radiation and convection. Thirdly, the safety vessel transfers heat to air by convection and heat radiation. The ultimate heat sink is atmospheric air. The RVACS can take away the heat by natural circulation without energy supply, so the RVACS has the advantage of high safety to prevent Fukushima-like accident.

TABLE 7. PARAMETERS OF RVACS

Item	Value
Coolant circulation	Natural circulation
Heat sink	atmosphere
Power	525 kW (1.5%FP)
Air channel width	0.15m
Chimney height	10m

3.3. Heat and Power Cogeneration System

The design object of Heat and Power Cogeneration System is to supply 10 MW(e) electric power and 17 MW heat power in Combined Heat and Power Generation (CHP) condition and supply 14 MW(e) electric power in power generation condition.

The power generation method is the Rankine cycle with a multistage condensing steam turbine. The heat supply method is extracting steam with certain temperature and pressure from the inside of steam turbine and then supplying to the heating heat exchanger. The temperature and pressure of main steam are 450 °C and 13 MPa, while the temperature and pressure of exhaust steam are 46 °C and 0.01MPa. The temperature and pressure of extraction steam are 121 °C and 0.2MPa. The maximum cycle efficiency is 40% in power generation condition, but in CHP condition, the maximum cycle efficiency is 77%.

Power generation with condensing steam turbine is a mature technology, and the thermodynamic calculation indicates that the design parameters can fit the 40% maximum cycle efficiency.

TABLE 8. PARAMETERS OF HEAT AND POWER COGENERATION SYSTEM

Item	Value
Thermal power	35 MW(th)
Electric power	10 MW(e)
Thermal supply	17 MW(th)
The system efficiency	78%
The inlet temperature of turbine	450°C
The inlet pressure of turbine	13MPa

4. CONCLUSION

Lead cooled reactor has many attractive features and China has launched several LFR/ADS projects including CLEAR-M. One typical design of CLEAR-M is named as CLEAR-M10d, which is a small modular lead cooled reactor to demonstrate small-scale energy supply of 10 MW(e) level, with the features of small modular, inherent safety and long refuelling period. The natural circulation heat transport has been adopted, and average 18.5% enriched UO₂ has been chosen in the system. Two independent and redundant residual heat removal systems are incorporated with RVACS as the emergency heat removal system. As a pool-type reactor, reactor internals, steam generator, CRDM, reactor core and other parts of primary system are integrated in the main reactor vessel. For the power generation, the Rankine cycle with a multistage condensing steam turbine is selected. A prototype mini-reactor named CLEAR-M10a is carrying out to support CLEAR-M10d, the engineering design is underway, and the existing technology has been used to accelerate the implementation progress.

ACKNOWLEDGEMENTS

The presented work is part of the National Key R&D Program of China (2018YFB1900601), the Strategic Priority Research Program of Chinese Academy of Sciences (Grand No. XDA22010504), and the Key Research Program of the Chinese Academy of Sciences (Grand No. ZDRW-KT-2019-1-0202). The authors would like to thank for all the support and contribution by FDS Team.

REFERENCES

- [1] IAEA, Accelerator driven systems: Energy generation and transmutation of nuclear waste. IAEA-TECDOC-985, 1997.
- [2] ALEMBERTI A, SMIRNOV V, ET AL., Overview of lead-cooled fast reactor activities. *Progress in Nuclear Energy*, 2014, 77:300–307.
- [3] Wu, Y., FDS TEAM, Conceptual design and testing strategy of a dual functional lithium-lead test blanket module in ITER and EAST. *Nuclear Fusion*, 2007, 47(11):1533–1539.
- [4] WU, Y., FDS TEAM, Design analysis of the china dual-functional lithium lead (DFLL) test blanket module in ITER. *Fusion Engineering and Design*, 2007, 82(15):1893–1903.
- [5] ZHAN W., XU H., Advanced fission energy program-ADS transmutation system. *Bulletin of Chinese Academy of Sciences*, 2012, 27(3):375–381.
- [6] WU Y., THE FDS TEAM, Design status and development strategy of China liquid lithium-lead blankets and related material technology. *Journal of Nuclear Materials*, 2007, 367:1410–1415.
- [7] GULEVICH, A.V., MARTYNOV, P.N., GULEVSKY, V.A., ET AL., Technologies for hydrogen production based on direct contact of gaseous hydrocarbons and evaporated water with molten Pb or Pb–Bi. *Energy Conversion and Management*, 2008,49:1946–1950.
- [8] HUANG, Q., FDS TEAM, Development status of CLAM steel for fusion application. *Journal of Nuclear Materials*, 2014, 455(1-3): 649–654.
- [9] GIACCO, M., WEISENBURGER, A., MUELLER, G., Fretting corrosion of steels for lead alloys cooled ADS. *Journal of Nuclear Materials*, 2014, 450 (1–3): 225–236.
- [10] WANG M., HUANG H., LIAN C., ET AL., Conceptual design of lead cooled reactor for hydrogen production, *International Journal of Hydrogen Energy*, 2015, (40):15127-15131.
- [11] WU Y., ET AL., Development Strategy and Conceptual Design of China Lead-based Research Reactor. *Annals of Nuclear Energy*, 2016, 87:511-516.
- [12] WU Y., BAI YQ, ET AL., Conceptual design of China lead-based research reactor CLEAR-I. *Chinese Journal of Nuclear Science and Engineering*, 2014, 34(2):201–208.
- [13] WU, Y., LI, J., LI, Y., ET AL., An integrated multifunctional neutronics calculation and analysis code system: VisusalBUS. *Chinese Journal of Nuclear Science and Engineering*, 2007, 27 (4):365–373.
- [14] OECD/NEA, Accelerator-driven Systems (ADS) and Fast Reactors (FR) in Advanced Nuclear Fuel Cycles: A Comparative Study. NEA, 2002.
- [15] WU Y., FDS TEAM, Development of High Intensity D-T Fusion Neutron Generator HINEG. *International Journal of Energy Research*, 2018, 42(1):68-72.
- [16] WU Y., FDS TEAM, Design and R&D Progress of China Lead-based Reactor for ADS Research Facility. *Engineering*, 2016, 2(1):124-131.
- [17] WU, Y., HUANG, Q., ZHU, Z., ET AL., R&D of dragon series lithium lead loops for material and blanket technology testing. *Fusion Science and Technology*, 2012, 62(1):272–275.
- [18] WU, Y., FDS TEAM, CAD-based interface programs for fusion neutron transport simulation. *Fusion Engineering and Design*, 2009, 84 (7–11):1987–1992.
- [19] WU Y., FDS TEAM, CLEAR-S: An Integrated Non-nuclear Test Facility for China Lead-based Research Reactor. *International Journal of Energy Research*, 2016, 40(14):1951-1956.
- [20] WANG M., LIAN C., LI Y., ET AL., Preliminary conceptual design of a lead-bismuth cooled small reactor (CLEAR-S). *International Journal of Hydrogen Energy*, 2015, (40):15132-15136.
- [21] YANG M., SONG Y., WANG J., XU P., ZHANG G., Temperature control characteristics analysis of lead-cooled fast reactor with natural circulation. *Annals of Nuclear Energy*, 2016, 90:54-61.
- [22] YU P., Nuclear Reactor Thermal hydraulic Analysis[M], Atomic Energy Press, 1986

**LEAD FAST REACTOR TECHNOLOGY:
A PROMISING OPTION FOR SMR APPLICATION**

Paper ID #24

G. GRASSO

Italian National Agency for New Technologies, Energy and Sustainable Economic
Development
Bologna, Italy
Email: giacomo.grasso@enea.it

M. FRIGNANI and A. ALEMBERTI

Ansaldo Nucleare
Genova, Italy

M. TARANTINO

Italian National Agency for New Technologies, Energy and Sustainable Economic
Development
Brasimone, Italy

M. CONSTANTIN and I. TURCU

Technologies for Nuclear Energy State Owned Company - Institute for Nuclear
Research
Pitesti, Romania

Abstract

Nuclear reactors in the small-modular segment are gaining more and more international consensus, leveraging the anticipated reduced investment risk expected from lower realisation costs and shorter construction schedules. Market opportunities have been identified worldwide, opening to systems falling in the entire range encompassed in the SMR segment: from few to few hundreds MW. However, for this opportunity to be actually seized, improved economics (to compensate the lack of economy of scale) and enhanced safety (not only to better protect people and the environment, but also the neighbouring modules in multi-unit plants) are to be demonstrated. In this context, lead-cooled fast reactors emerge as a promising option for SMR application, also adding the benefits of a fast-spectrum to the resulting plant. The favourable features of lead cooling, due to the inherent characteristics of lead, promise for significant design simplification, to the benefit of both safety and economics. The state-of-the-art on the LFR technology is presented and referenced as justification for the technical and design solutions supporting the claims for the opportunity of LFR applicability to the SMR segment. The planned steps for the remaining development and qualification challenges in a European context are also discussed, with focus on ALFRED in its twofold mission of demonstrator of the LFR technology and prototype of a commercial lead-cooled fast-spectrum SMR

1. INTRODUCTION

Small and Medium Modular Reactors (SMRs) are in the spotlight of nuclear deployment, mainly thanks to the reduced financial risk allowed by the lower capital investment (per unit), the shorter construction schedule and the dilution of the cash flow, which overlaps with early incomes resulting from the operation of first units while others are being realized. All these elements are boosters to bridge the gap towards new market segments, being acknowledged as key arguments to enlarge the basin of utilities embarking nuclear. Relevant opportunities are sought indeed for competitive SMRs, not only in replacing old units close to retirement, but also in representing a credible alternative to fossil-fuelled plants in a carbon-gentle energy scenario.

In the quest to demonstrate all these attracting elements, main challenges have to be addressed in order to materialise such opportunities. In this perspective, competitiveness is the password: due to the lack of economy of scale, only those solutions with clear economics can have an actual chance. Hyperbolically, SMRs with a capital cost as high as large reactors have no future; analogously, SMRs so complex to hinder the certainty of on-time construction will be excluded as well.

Moreover, additional challenges result from the will to enlarge the deployment basin. The inherent multi-unit nature of SMR-based plants requires such reactors to minimize the impact of accidents to one unit on the neighbouring ones, so as to not impair their operation nor emergency measures should all units be affected by a common initiating event.

In this promising scenario still to be materialized, fast-spectrum reactors are also considered, thanks to the perspective of adding fuel cycle features to those of an SMR.

2. COMPLIANCE OF THE LFR TO THE SMR CONCEPT

Among the fast-spectrum options for deployment in the SMR segment, is the lead-cooled one (namely, lead-cooled fast reactor, LFR). LFRs are gaining broader and broader international consensus as an interesting Generation-IV-compliant candidate for future nuclear energy systems capable of competing economically not only with nuclear plants powered with current-generation reactors, but also with fossil-fuelled plants. Leveraging on the features allowing for this, LFRs appear as promising candidates also for deployment in the SMR segment, as discussed in the following.

2.1. Technology-specific features

Several SMR-enabling features follow from the choice of lead coolant technology.

2.1.1. Neutronics

The low capture of neutrons by lead [1], along with the particularly hard spectrum, allows for an enhanced breeding, which reduces the reactivity swing to be managed along an irradiation sub-cycle. Besides high burnups, for the sake of economics this also permits considering very long refuelling intervals, or even cassette cores in battery-type units, which are of particular interest for micro-reactors.

The low neutrons capture permits the fuel pins to be much spaced apart, with clear benefits to the natural circulation in case of accidents (or even in normal operation, mostly for micro-reactors) for reducing the peak temperatures achieved in the system without the need for large heights nor complex solutions. The temperatures in the new regimes set in case even of unprotected transients [2] are low enough to relieve the structures from excessive creep, easily extending the grace time of the plant.

2.1.2. *Physics and chemistry*

The practical inertness of lead with air, the low vapor pressure of lead and the ease of cleaning components that have been immersed in the melt permit simple out-of-pile handling of components, and notably refuelling.

The practical inertness of lead with water/steam also permits locating the steam generators and dip coolers of the decay heat removal systems within the reactor vessel, eliminating the need for an intermediate circuit.

Both these elements are seen as key enablers for the economics of any LFR; both are therefore essential features for LFR-based SMRs to compete with current generation reactors and fossil-fuelled plants.

A main safety advantage of lead cooling derives from the minimal sources of potential energy that is stored in the primary system [3]. The lack of violent exothermic chemical reaction with water and air (in normal or decay-heat-removal mode), with the fuel (in case of core damage) and with concrete (in case of coolant leakage from the main and safety vessels), as well as the lack of chemical reactions potentially generating hydrogen on the plant, reduce the potential energy to the sole heat that is stored in the primary system, which can be therefore easily managed in full safety.

Conversely, the ease of chemical bonding of lead with almost all elements, and notably with iodine and caesium, provides a very effective means for reducing the source term that – upon core damage – is released from the coolant, hence from the primary system to the containment. This argument is the trailing one in claiming the reduction of the emergency preparedness zone, possibly to the site boundary.

2.2. **SMR-specific features**

Additional key features emerge in the specific perspective of SMR application.

2.2.1. *Plant integration*

Primary system integration is the general approach for SMRs based on light water reactor technology, in order to enhance safety while reducing costs. As most of the fast-spectrum systems built in the past, LFRs are (usually) meant for integral design (pool-type). This enables cost savings and robustness of the primary system while excluding (along with the primary system operating at ambient pressure) LOCA-type accidents

2.2.2. *Flexibility*

An LFR has a significant advantage in its flexibility of operation, deriving from the broad margins between nominal and limiting conditions⁴. These margins provide the basis to fully exploit the inherent feedbacks (driven by the reactivity coefficients, which in an SMR are also generally more effective than in a large reactor) in full safety, thereby facilitating manoeuvrability of the plant.

⁴ Light water reactors indeed are limited in operation by departure from nucleate boiling and critical heat flux, while sodium fast reactors have limitations imposed by coolant boiling.

Under a different perspective, the broad margins allow for different systems, each tuned to specific customer needs, to be realized around a reference design with minor modifications. This would add to an LFR-based SMR huge opportunities in responding to a wider market.

2.2.3. *Simplicity, compactness and sharing*

In an LFR, the absence of complex treats opens to the use of simple engineered solutions, which can therefore be optimized for compactness (including their arrangement). This provides an LFR-based SMR with robustness (i.e., lower maintenance costs), ease of manufacturing and small volumes (the latter two securing lower overnight costs). Additionally, compact nuclear islands and associated buildings provide more chances for the sharing of systems, e.g., by smaller common areas and/or simpler paths and layouts.

3. A COMMERCIAL SM-LFR

All these opportunities acknowledged, an LFR-based SMR (or SM-LFR) emerges as a very promising option for a brand-new generation of plants, potentially capable of serving present and future needs while ensuring the highest levels of safety and sustainability. In the European context, efforts are being put since 2017 to materialize a design of a commercial SM-LFR, standing on the experience gathered within EURATOM co-funded research projects such as ELSY [4] and LEADER [5], and within the Fostering ALFRED Construction (FALCON) international consortium.

The general strategy points to the use of simple solutions, as far as practicable off-the-shelf (or with the highest technology readiness levels otherwise), to secure an economic design is achieved in a time frame (i.e., mid 2030s - early 2040s) compatible with the market opportunities that are expected from the retirement of old nuclear units or the replacement of fossil-fuelled plants (envisaged by the carbon-neutral policies aimed worldwide).

The reactor layout presently representing the reference for design and market studies is shown in Fig. 1 [6]. The specific design shown refers to the advanced LFR European demonstrator (ALFRED) which, with a predicted electric output of 125 MW, is prototypic of an SM-LFR. It features:

- A main vessel (MV) with cylindrical body and hemispherical lower head, hung from above by the outermost branch of a “Y” forging and closed by a domed cover bolted to the other branch of the same forging;
- A safety vessel (SV) enveloping the MV, at a distance from the latter such to allow inspection while preventing the lead level to drop below the entrance to the heat exchangers in case of MV breach;
- An inner vessel (IV) providing support and lateral restraint to the core;
- An internal structure (IS) to guide lead flow from heat source to heat sink and back, while separating the hot and cold legs; it therefore defines a hot pool (HP) and a cold pool (CP) within the MV volume;
- Multiple shell-and-tubes steam generators (SGs), made of single-walled tubes of bayonet or helicoidal type, immersed in the melt to receive hot coolant from the HP and distributing cold lead into the CP;
- Multiple reactor coolant pumps (RCPs), mechanical with axial design, receiving hot lead from core outlet to feed the HP;

- Multiple shell-and-tubes heat exchangers of the decay heat removal system (DHR-HXs), made of double-walled bayonet tubes and placed in parallel with the SGs;

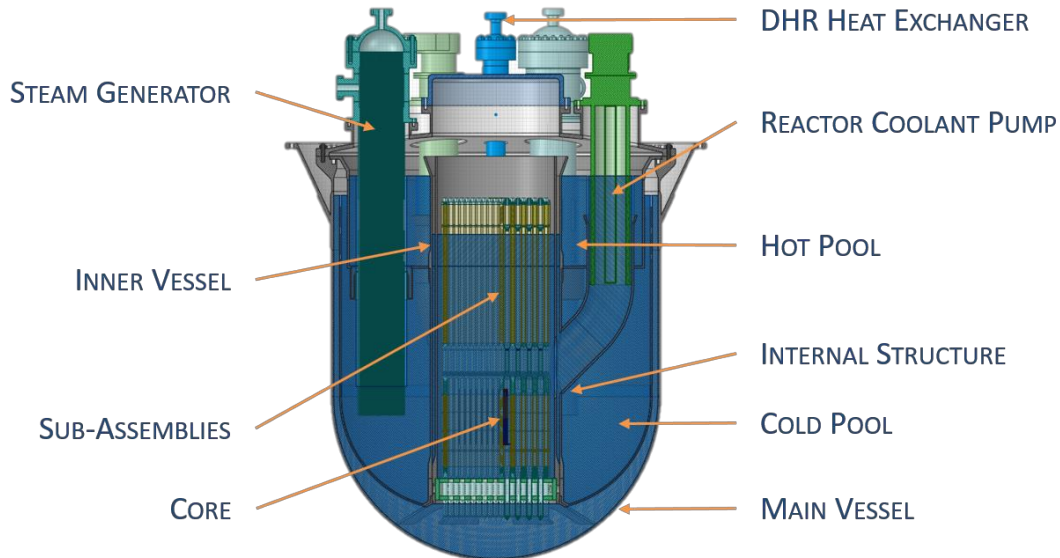


FIG. 1. Overview of the ALFRED primary system layout (reproduced from Ref. [6] with permission courtesy of Ansaldo Nuclcare)

- A core made of sub-assemblies (S/As) of active type (i.e., fuel assemblies, FAs), absorber type (for both control and shutdown, i.e., control rods, CRs, and safety devices, SDs, respectively) and dummy type (for reflection and shielding), extended up to the cover gas space i.e., above the lead free level.

All design choices allow for ease in solving typical FR (and LFR issues) while enhancing safety, effectiveness, compactness and economics.

The IS permits involving in the reactor circulation all the primary coolant (Fig. 2 [6]), thereby avoiding stagnation and associated thermal stratification for the protection of the MV without the need for complex structures (e.g., the “redan” of sodium-cooled FRs); moreover, being separated from the IV, which has core support and restraint safety functions, it is not safety classified.

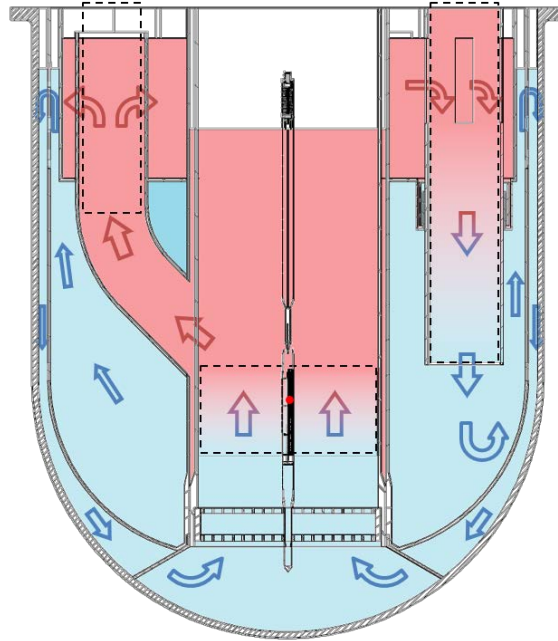


FIG. 2. Flow path in the reactor coolant system (reproduced from Ref. [6] with permission courtesy of Ansaldo Nucleare)

The RCPs in the hot leg simplify the reactor coolant system layout by eliminating complex structures otherwise required to feed the core; moreover, being connected to the core, such structures would have introduced additional potential safety threats in case of leakage or breach, which are instead avoided by the adopted configuration.

The choice of the components and of their arrangement allows for a compact design. Specifically, for ALFRED, 3 “loops” (i.e., 3 RCPs, 3 SGs and 3 DHR-HXs) were identified as optimal, whilst for the commercial SM-LFR – whose final size will depend on economics and shop-manufacturability considerations, options being considered up to about 250 MW(e) – more loops could be sought, still maintaining the same general layout. The option for a higher power would permit exploiting the non-scalability of some components (such as the dummy elements, hence the core dimensions), thereby allowing to reduce the specific volume per unit power, to the sake of economics. As an example, the inner vessel diameter could be predicted to increase from 3 m (ALFRED case) to 3.7 m for a 250 MW(e) system.

All options being investigated are based on the criterion of maintaining the power density in the core as high as practicable, to leverage the generalized compactness of the primary system allowed by a small core. In the ALFRED-type SM-LFR, a power density in the active core of about 98 kW/l is achieved, which is increased to about 105 kW/l for the 250 MW(e) option.

However, scoping studies are being performed to evaluate the impact of derated cores, which are therefore long-lasting. Economic advantages may result indeed by the increase of the plant availability factor (outages for refuelling being diluted in time), the lower fuel enrichments (due to the higher fuel inventory) and by financial aspects of the fuel cycle (e.g., anticipated return of investment).

At whole plant level, generally speaking an LFR can be expected to provide significant savings, with respect to an LWR, mainly thanks to:

- A lower amount of high-grade steel [7], in the order of 2 kg/kW(e) against 3 kg/kW(e)⁵;
- A lower amount of concrete, not only as proportionally dictated by the reduction in volume of the reactor coolant system thanks to the integral design (i.e., no footprint of spreading loops), but also, and probably mainly, to the lower inventory of pressurized water (in the secondary system only for an LFR; also in the primary system for an LWR) to cope with in case of sudden vaporisation upon coolant boundary breach.

Conversely, the only system that in an LFR (and more generally in FRs) is predicted to cost more than in an LWR is the refuelling one. The traditional solution standing on rotating plugs, fully remote handling machine(s) and all associated transfer and storage provisions is indeed much more complex, hence expensive, than the one employed in LWRs.

To this regard, the SM-LFR proposed at European level for commercial deployment benefits of a novel refuelling system, based on an ex-vessel fuel handling machine (FHM), reaching the heads of the S/As by opening a flanged port on the reactor cover, and on the use of transfer flasks, one per each FAs⁶, to secure passive cooling by lead during all phases of handling and transfer. The simplicity of the FHM results from the extension of the S/As, which emerge from the melt and can therefore be identified and handled in full visibility. The choice of transfer flasks – kept as simple as possible in their design – permits also to simplify meeting the safety and shielding requirements during transfer, and to eliminate the need for a spent fuel pool, with all associated systems and related complexities, since the flasks act as storage as well.

The projections on the capital component of the levelized unit electricity cost (LUEC) for a commercial SM-LFR sized 125 MW(e), made starting from ALFRED as a basis, led to a figure of about 46 EUR/MWh. Considering that the design of ALFRED was made greatly conservative, due to its demonstration nature (see next Section), and projecting the scale effect of increasing the size, it is suggested that an SM-LFR sized around 250 MW(e) could allow the cost of electricity to become competitive in the present energy market. Other estimates, made by SM-LFR vendors employing more aggressive design philosophies based on less technically ready options, indicate the possibility to further reduce the cost up to being competitive with currently operating large LWRs.

From a safety point of view, the SM-LFR – borrowing the same general design – would inherit from ALFRED also the safety characteristics. After years of extensive analyses, including benchmarks and – as much as practicable – experimental evidence, no credible scenario was found for ALFRED, leading to extended core damage [2]. Due however to the unavoidable uncertainties, and the potential impact of core degradation of a reactor on the neighbouring ones in a multi-units site, it was decided to improve the reference design by two main actions.

The first modification regarded the DHR. The concept of isolation condenser (IC) was kept, but improved by connecting, to the lower head, a storage tank for pressurized incondensable gases.

⁵ For an LWR of SMR type, this figure can be anticipated to increase further.

⁶ The S/As of all other types can be handled in gas for cooling by natural circulation, as their residual heat is sufficiently low to prevent their damaging during handling and transfer, even in case of failure of the FHM.

The presence of these gases within the IC, in normal operation, inhibits heat exchange with the water of the pool the IC is immersed in. However, as soon as the pressure in the IC loop increases (driven by the temperature increase in the primary system where the DHR-HX is installed), the vapor purges the gases away from the IC into the storage tank, allowing steam to be condensed. The different specific gravity of steam (in the hot leg of the DHR from the HX to the IC) and water (in the cold leg closing the loop) will drive natural circulation for the full passive operation of the system. The addition of the incondensable gases also permits a self-regulation of the removed power by the DHR system, the migration of gases from the IC to the storage tank being reversible: this also permits, in the very long term into an accident, to prevent coolant freezing almost indefinitely without the need for operators' intervention.

The shutdown system was the second to be modified. Also in this case, a redesign of the previous device allowed to achieve a system that is still engineeringly simple, but also extremely resilient even to large deformations (thereby guaranteeing insertion), fully passive in its operation and capable of both commanded (active) and spontaneous (passive) actuation. Notably, thanks to the addition of a second latch held by a Curie-point magnet, a failure in its commanded actuation – if happening simultaneously with the failure of the diverse control/shutdown system – would no more determine an indefinitely lasting unprotected scenario.

Thanks to the simplicity of the new solutions adopted, and the already excellent performance of ALFRED, it can be anticipated that the SM-LFR will secure unparalleled safety, as strong argument in favour of a significant reduction of the emergency preparedness zone, thereby materializing full compliance with the SMR philosophy and allowing siting close to final users.

4. CHALLENGES TO DEPLOYMENT AND ROLE OF ALFRED

The key challenges to materialize the SM-LFR are the demonstration of its technological viability, and the proof of the economic competitiveness of the proposed system. Expanding these concepts, included are mainly the qualification of the solutions used, the verification of the inherent plant behaviour, the assessment of the actual margins (for further optimization) and the consolidation of operating procedures.

In the European context, research on the heavy liquid metals (HLMs) technology started about twenty-five years ago, in the mainstream of accelerator-driven systems (ADSs), for which lead (or lead-bismuth eutectic, LBE) could have provided both reactor cooling and spallation target functions. Within ENEA, pioneering facilities were realized in the 1990s, including LECOR (an LBE loop for materials corrosion and components testing) and CIRCE (a large pool, mainly for system thermal hydraulics and integral testing). The experimental bases gathered through the operation of these facilities unlocked the doors for viability, proving no showstoppers for an HLM-cooled reactor.

Since then, many other European laboratories constructed and operated HLM facilities, quickly extending the knowledge bases for an informed design of a credible system. The key phenomena (dissolution of alloying elements to the melt and penetration of the HLM into the steel) ruling corrosion (originally thought as the killing point) were understood, and two alternative strategies for protecting structural materials found (namely: oxygen control at low temperatures and surface coating otherwise). The dynamics of HLM thermal hydraulics in a pool configuration was explored, and solutions to all associated issues (e.g., stratification) verified. Many components up to prototypical scale were tested and preliminarily qualified for use in a nuclear system.

However, several challenges still remain, which require additional effort. The roadmap defining the reference for R&D activities on the LFR in Europe top ranks the qualification of the coating under neutrons irradiation, of the RCP at significant scale and of the oxygen monitoring/control system in a pool. Whilst the latter can be addressed in new facilities, planned for construction at RATEN-ICN's premises in Mioveni with the support of the Romanian Government, the former might represent an issue due to the shortage of irradiation facilities that are capable of reproducing a representative environment (i.e., fast neutron spectrum and high temperature).

For this reason, and since before commercial deployment the LFR technology requires demonstration, ALFRED – originally conceived in the frame of the LEADER research project and since 2013 further developed and promoted by FALCON – was recently reviewed with a twofold objective:

- (a) To be prototypical of the commercial SM-LFR;
- (b) To provide irradiation testing capabilities for the progressive qualification of the coating.

The first goal was achieved by adjusting the original configuration in order to represent the reference one, selected for the commercial units because of its simplicity, economic potential and elevated safety performance.

The achievement of the second goal required to segment the operation of ALFRED in stages [8], with increasing power levels and core outlet temperatures, so that during the early stages – for which the low temperatures allow for corrosion protection by maintaining oxygen at low levels typical of previous FRs – special fuel elements provided with coatings can be irradiated in dedicated positions at significant doses under representative conditions [9]. This strategy is better detailed in Table 1.

TABLE 1. OVERVIEW OF MAIN PARAMETERS, OBJECTIVES AND PROVISIONS OF ALFRED OPERATION STAGES

Stage	Reactor thermal power [MW]	Coolant inlet/outlet temperatures [°C]	Peak cladding temperature (with uncertainties) [°C]	Provisions	Objectives
1	100	390 / 430	450	Corrosion protection of cladding and FA structures by oxygen control	Qualification of coating for the cladding
2	200	400 / 480	550	Corrosion protection of cladding by coating, and of FA structures by oxygen control	Qualification of coating for the FA structures
3	300	400 / 520	600	Corrosion protection of cladding and FA structures by coatings	Demonstration of LFR technology and validation of prototypical LF-SMR design

The adoption of this staged operation, and complementing ALFRED with a coordinated network of experimental facilities performing the complementary R&D programme in parallel, will permit Europe to achieve, by mid 2030s, the technological readiness that is required for commercial deployment of a new generation of nuclear reactors, excelling in safety and sustainability and with competitive economic potential.

5. CONCLUSIONS

The market opportunities for safe and competitive nuclear systems in the SMR segment oriented the efforts being spent at European level on the LFR towards the idea of an SM-LFR. The possibilities offered by the inherent properties of lead, when used as coolant, permit indeed to achieve a very safe design (as required to any SMR for compliance with the multi-units logics and for close siting to the final users) with simple – hence robust, reliable and cheap – engineering solutions.

The claims of unparalleled safety and competitive economics, preliminarily supported by extensive analyses, experimental evidence and projections, need however to be demonstrated through the successful construction and operation of ALFRED in Romania. For this, an ambitious – yet feasible – supporting programme was drafted by the FALCON consortium to materialize its vision for a commercial SM-LFR deployment in 2035-2040.

REFERENCES

- [1] CINOTTI, L., SMITH, C.F., ARTIOLI, C., GRASSO, G., CORSINI, G., “Lead-cooled fast reactor (LFR) design: safety, neutronics, thermal hydraulics, structural mechanics, fuel, core, and plant design”, Handbook of Nuclear Engineering, Springer, New York (2010).
- [2] BANDINI, G., BUBELIS, E., SCHIKORR, M., STEMPNIEWICZ, M.H., LÁZARO, A., TUCEK, K., KUDINOV, P., KÖÖP, K., JELTSOV, M., MANSANI, L., “Safety analysis results of representative DEC accidental transients for the ALFRED reactor”, Fast Reactors and Related Fuel Cycles: Safe Technologies and Sustainable Scenarios (FR13) (Proc. Int. Conf. Paris, 2013), IAEA, Vienna (2015) Paper CN199-260.
- [3] TOSHINSKY, G.I., KOMLEV, O.G., TORMYSHEV, I.V., PETROCHENKO, V.V., Effect of potential energy stored in reactor facility coolant on NPP safety and economic parameters, World J. Nucl. Sci. Technol. **3** 2 (2013) 59–64.
- [4] CINOTTI, L., LOCATELLI, G., CORSINI, G., AIT ABDERRAHIM, H., MONTI, S., BENAMATI, G., TUCEK, K., STRUWE, D., ORDEN, A., LE CARPENTIER, D., “The ELSY project”, International Conference on the Physics of Reactors: Nuclear Power: A Sustainable Resource (PHYSOR'08) (Proc. Int. Conf. Interlaken, 2008).
- [5] DE BRUYN, D., ALEMBERTI, A., MANSANI, L., GRASSO, G., BANDINI, G., ARTIOLI, C., BUBELIS, E., MUELLER, G., WALLENIUS, J., ORDEN, A., “Main achievements of the FP7 LEADER collaborative project of the European Commission regarding the design of a lead cooled fast reactor”, International Congress on Advances in Nuclear Power Plants (ICAPP 2013) (Proc. Int. Conf. Jeju Island, 2013) Paper FF052.
- [6] MERLI, F., “ALFRED primary system layout”, paper presented at ESNII European workshop on liquid metal fast reactors: progress and synergies, Brasimone, 2019.
- [7] GRASSO, G., “A safe and competitive lead-cooled small modular fast reactor concept for a short-term deployment”, Fast Reactors and Related Fuel Cycles: Next Generation Nuclear Systems for Sustainable Development (FR17) (Proc. Int. Conf. Yekaterinburg, 2017), IAEA, Vienna (2018).
- [8] FRIGNANI, M., ALEMBERTI, A., TARANTINO, M., GRASSO, G., “ALFRED staged approach”, International Congress on Advances in Nuclear Power Plants (ICAPP 2019) (Proc. Int. Conf. Juan-Les-Pins, 2019).
- [9] GRASSO, G., SAROTTO, M., LODI, F., CASTELLUCCIO, D.M., “An improved design for the ALFRED core”, International Congress on Advances in Nuclear Power Plants (ICAPP 2019) (Proc. Int. Conf. Juan-Les-Pins, 2019).

PRELIMINARY CONCEPTUAL DESIGN OF LEAD-COOLED SMALL FAST REACTOR CORE FOR ICEBREAKER

Paper ID #29

T.D.C. NGUYEN, J. CHOE, X. DU, S. CHOI & D. LEE

Department of Nuclear Engineering, Ulsan National Institute of Science and
Technology,

50 UNIST-gil, Ulju-gun, Ulsan, 44919, Republic of Korea

Email: tungnguyen@unist.ac.kr, chi91023@unist.ac.kr, dxndxnwww@unist.ac.kr,
csy0321@unist.ac.kr, deokjung@unist.ac.kr

Abstract

A preliminary conceptual core design of the ultra-long life and small modular lead fast reactor (SMLFR) for icebreakers has been introduced in this work. The primary design constraint for this fast reactor is the transportation capability in spent nuclear fuel cask (SNF) that can be used as the power propulsion for icebreakers. An innovated feature of this suggested SMLFR is all the core components are included within a small reactor vessel enabling immediate transfer into the SNF cask after its entire operation time. It is also designed to target the ultra-long cycle without refuelling and a small reactivity swing by adopting a breed and burn concept. The target thermal power of the SMLFR is 37.5 MW, with an assumption of 40% thermal efficiency. The vital challenge of this long-life, small, and portable reactor is a neutron economy requirement. Therefore, the uranium nitride and lead-bismuth eutectic are selected as fuel and coolant materials, respectively. The core inlet and outlet temperatures are set at 300°C and 400°C, respectively. The 15-15Ti stabilized steel is used as cladding and structure material as a result of its excellent swelling resistance and stability in LBE. The performance in design and analyses of this core are conducted with the fast reactor analysis code system MC²-3/TWODANT/REBUS-3 developed by Argonne National Laboratory and the UNIST in-house Monte Carlo code MCS with ENDF/B-VII.0 cross-section library. It is confirmed through depletion calculations that the designed reactor is capable of operating for more than 40 years without refuelling and a reactivity swing less than 500 pcm. The SMLFR core is further evaluated the characteristics of various significant neutronics, thermal-hydraulics and safety parameters, including criticality, power and temperature profiles, control rod worth, effective delayed neutron fraction, fuel temperature coefficient, coolant density coefficient and integral reactivity parameters for quasi-static reactivity balance.

1. INTRODUCTION

Recently, the lead-cooled fast reactor (LFR), one of the six advanced nuclear energy systems, is selected for further development in Generation IV International Forum (GIF) [1]. The primary interest in this reactor system originates from the fact that characteristics of lead-bismuth eutectic (LBE) [2], such as a low melting point, a very high boiling temperature, and chemical inertness. It can provide an abundant degree of flexibility in design and enables the enhancement of the inherent safety features of LFR. Other arguments presented in GIF-IV suggest the general features of a long-life core and small reactor size, significantly yielding to the concept of long-life, safe, simple, small, and portable reactors. In the recent past, “a once-for-life fast breeder core Encapsulated Nuclear Heat Source (ENHS) [3] has been designed by the University of California at Berkeley with 125 MW(th) power, lead or lead-bismuth coolant, and nearly zero burnup reactivity swing throughout 20 years of full-power operation. Another lead-bismuth fast reactor is the SVBR-100 [4], developed by AKME Engineering, the Russian Federation, which can achieve 7-8 years of the fuel cycle” [3,4]. Based on the preceding, a preliminary design for the long-life Small Modular Lead-bismuth eutectic Fast Reactor (SMLFR) has been performed in this work. The primary design constraint in this study is that

the core is expected to be transportable in a Spent Nuclear Fuel (SNF) cask to be used as a single or cluster power plant for icebreakers. Another advanced feature of this suggested SMLFR is all the core components are included inside a small reactor vessel, which can be immediately transferred into a SNF cask after its full operation time. The thermal power of the SMLFR is 37.5 MW, with an assumption of 40% thermal efficiency by using an advanced energy conversion system based on supercritical carbon dioxide (S-CO₂) [5] as a working fluid. It is also designed to achieve 40 years of a lifetime without refuelling. For such a long-life, small, and portable reactor, the key requirement is an excellent neutron economy. A recent study [2] has reported that the LBE cooled fast reactor demonstrates better performance in neutron economy, burnup reactivity swing, and void coefficient compared to a sodium fast reactor (SFR). In addition, uranium nitride (UN) [6] with high thermal conductivity is chosen as one of the primary fuel candidates for the LFR due to better compatibility with the LBE coolant and providing an immense improvement in neutron economy compared to uranium oxide fuel. The core inlet and outlet temperatures are 300 °C and 400 °C, respectively. An electromagnetic pump drives the primary coolant circulation. The 15-15Ti [7] stabilized steel is selected as cladding material due to its excellent swelling resistance and stability up to 550°C or even 570°C in LBE. This temperature is well above the operating temperature of this suggested core.

In summary, the conceptually designed core, SMLFR consists of the UN as fuel material, LBE as coolant material, and 15-15Ti as a cladding material. The neutronic design and analysis of this core are performed with the fast reactor analysis code suite MC²-3/TWODANT/REBUS-3, developed by Argonne National Laboratory (ANL) with ENDF/B-VII.0 cross-section library. It is confirmed through depletion calculations that the designed reactor can be operated for more than 40 years without refuelling. Furthermore, core performance characteristics were analysed for isotopic inventory, criticality, and radial and axial power profiles using the inhouse Monte Carlo (MC) code MCS. A preliminary thermal-hydraulic (T-H) analysis is investigated by a T-H one-dimensional module using a single-phase closed-channel model. Pin-by-pin temperature profiles are obtained as receiving the pin-wise power profiles from MCS. The SMLFR core is also evaluated in terms of various significant safety parameters, including control rod worth, fuel temperature coefficient, coolant void reactivity, and integral reactivity parameters for quasi-static reactivity balance.

2. COMPUTER CODES

2.1. Fast reactor analysis code system ARC

“A suite code package for fast reactor analysis, called Argonne Reactor Computation (ARC) [8], and developed by ANL, was used in this work. The package consists of three main modules: (a) a Multigroup Cross-section generation Code (MC²-3) which prepares problem-dependent ultrafine group cross-sections [9]; (b) TWODANT which generates ultrafine group flux from the Boltzmann transport equation solution using the discrete ordinate method [10]; and (c) REBUS-3 which performs nodal diffusion and depletion calculations for fast reactor fuel analyses [11]. In the first step of fast reactor analysis, TWODANT generates the ultrafine group region-wise flux spectra using the ultrafine group cross sections (XS) from MC²-3. After the flux generation is completed” [8-11], MC²-3 condenses the ultrafine group cross sections into broad-group cross-sections. Finally, the nodal diffusion and depletion calculations are carried out by REBUS-3, using these broad-group cross sections. Fig. 1 shows the fast reactor analysis flow.

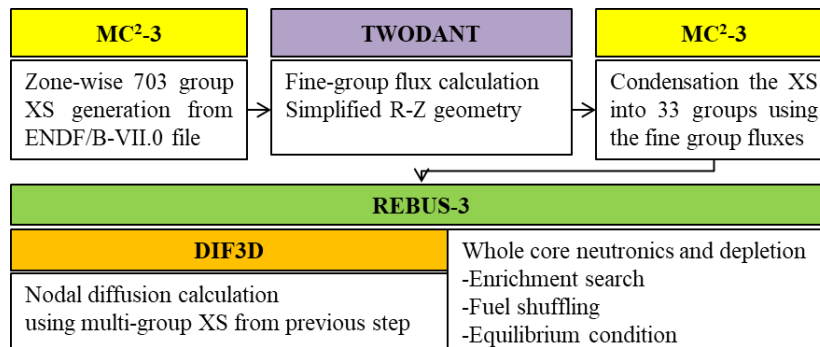


FIG. 1. Fast reactor analysis flow

2.2. Monte Carlo code MCS

MCS is a 3D continuous-energy neutron-physics code for particle transport based on the MC method, under development at UNIST since 2013 [12]. Two kinds of calculations are allowed by MCS: criticality runs for reactivity calculations and fixed source runs for shielding problems. MCS neutron transport capability is verified and validated with many benchmark problems, including BEAVERS benchmarks, the International Criticality Safety Benchmark Experimental Problem (ICSBEP), and the Jordan Research and Training Reactor (JRTR).

3. THE DESIGN STRATEGY OF THE CONCEPTUAL CORE

3.1. Core design requirements and primary parameters

The design parameters of the SMLFR core are presented in Table 1. The output power designed for SMLFR is 37.5 MW(th)/15 MW(e) with an assumed thermal efficiency of 40%. This SMR is suggested to power nuclear icebreakers, the target average lifetime is hence 40 years [13]. Besides, the hexagonal-lattice pin concept is employed for the SMLFR because of its higher fuel-to-coolant volume fraction, allowing for increasing average power density compared to the square-lattice pin. The fuel enrichment supposed to be lower than 20 w% ²³⁵U - low-enriched uranium (LEU) - due to the limit on uranium enrichment for civilian use (uranium enriched

above 20w/o is considered military grade uranium). In this work, the maximum enrichment is not higher than 19.75w/o due to the fuel fabrication uncertainties. Uranium nitride fuel (UN) [6] is considered as the nuclear fuel in this study because it exhibits several favourable properties in comparison to oxide fuel. Uranium nitride has a higher thermal conductivity, melting temperature, and fissile density than oxide fuel. Nonetheless, UN also presents some drawbacks, such as the high neutron capture cross section of ^{14}N , the production of the radioactive ^{14}C isotope through neutron absorption by ^{14}N with a subsequent proton emission, and significant swelling under irradiation. The fuel fabrication to enrich the fuel in ^{15}N to reduce the amount of ^{14}N can mitigate the first two drawbacks. Despite these challenges, the choice of UN fuel enables a significant improvement in the fuel efficiency. Lead-bismuth Eutectic (LBE) [5] is selected as the coolant due to its low melting point, high boiling temperature, outstanding capacity of heat transmission, neutronic features (such as low neutron absorption and good neutron scattering/shielding), and chemically inertness. The selection of LBE as a reactor coolant brings up two specific concerns: (i) the production of alpha-active and radiotoxic ^{210}Po during irradiation, and (ii) the small scales of bismuth production capabilities and insufficiently explored bismuth resources. Overall, if these issues are under control, LBE can be used as an asset to improve the economics of a Small Modular Reactor (SMR) power plant. LBE coolant velocity is however limited to less than 2m/s due to corrosion and erosion concerns of primary loop pipes. The harsh neutron irradiation in a fast reactor core region raises a special concern for structural and cladding materials. 15-15 Ti, a Ti-stabilized austenitic steel, has therefore been chosen as the cladding material because of its outstanding thermal conductivity, irradiation resistance, and superior swelling resistance compared to the other alloys [7]. The inlet and outlet in-core coolant temperatures are chosen according to the material properties of martensitic steels, which can be used in contact with LBE if the operating temperature is not beyond 550 °C [14]. Based on the selection of these design parameters, the optimization of the core, fuel design, and loading patterns will be performed to satisfy all the design criteria and to improve the economic benefits and safety of the SMLFR.

TABLE 1. PRIMARY CORE DESIGN PARAMETERS

Parameter	Unit	Value
Thermal/Electric power	MW	37.5/15.0
Target cycle length	EFPY ^a	>40
Fuel material	-	UN
- Smear density	%TD ^b	85
- Maximum ^{235}U enrichment	w/o	19.75
Cladding material	-	15-15 Ti
Coolant	-	LBE
- Inlet/Outlet temperature	°C	300/400
- Maximum coolant velocity	m/s	2.0
- Pressure	MPa	0.1

^aEffective full power year

^bTheoretical Density

3.2. Pin design parameter

Three types of pins (fuel pin, reflector pin, and control pin) are employed as shown in Fig. 2. Zirconium oxide (ZrO_2) has been chosen as a reflector material instead of stainless steel (SS) to improve the neutron economy in the fast reactor [15]. Zirconium (Zr) has a large neutron scattering cross section with a low neutron capture cross section compared to the major nuclides of the SS, such as iron (Fe) and chromium (Cr). In case of the control rods, they move together to control the core reactivity. Absorber material is B_4C with natural ^{10}B isotopic enrichment [16]. The spiral wire can be applied for each rod to avoid collisions between adjacent rods. Table 2 presents the pin design parameters, including the fuel pin data and the volume fraction at manufacture.

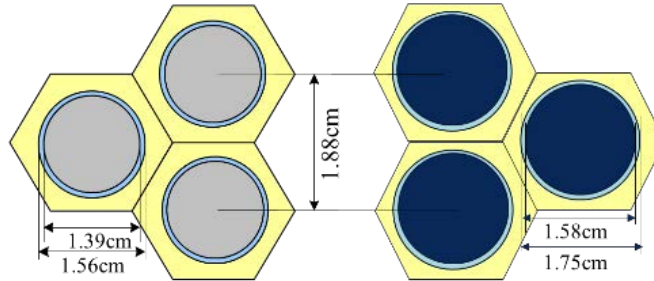


FIG. 2. Pin design geometry: fuel pin (left) and control/reflector pin (right)

TABLE 2. DESIGN PARAMETER FOR SMLFR PIN

Parameter	Fuel	Reflector	Control
Pin data			
- Pin material	UN	ZrO_2	B_4C
- Diameter, cm	1.56	1.75	1.75
- Cladding thickness, cm	0.085	0.085	0.085
- Pin pitch, cm	1.88	1.88	1.88
- Pin pitch-to-diameter ratio	1.21	-	-
Volume fraction at manufacture, %			
- Fuel/Reflector/Absorber	49.58	64.06	64.06
- Cladding	12.87	14.53	14.53
- Coolant	37.56	21.42	21.42

3.3. Core configurations

The core type considered in this paper is the uniform core. In SMLFR, the main nuclear fuel cycle is a uranium cycle. In order to design a small-size core capable of operating for more than 40 years without refuelling, the preliminary sensitivity analyses are carried out on the following parameters: enrichment of ^{235}U and active core height. The initial core has dimensions equal to $D_{\text{eq}} \times H = 150\text{cm} \times 100\text{cm}$ (diameter excluding 9-cm radial reflector equivalent thickness) surrounded by a layer of LBE (circulation loop down-comer section) [17]. Throughout the analyses, the equivalent core diameter combined with the LBE layer is intended not to exceed 183 cm, due to the limit in size of the SNF cask – TN-40 [18]. The first candidate is analysed in terms of k_{eff} trends during depletion for different values of enrichment in the fuel region, while the next analysis focuses on enlarging the core to achieve the target cycle length. These sensitivity analyses are conducted with ARC code system. Table 3 summarizes the core parameters of the core candidates proposed for the optimization study.

TABLE 3. CORE CANDIDATES PARAMETER

Core type	Equivalent core diameter, cm	Core height, cm	LEU enrichment, w/o	
A	A1	150	100	12.0
	A2	150	100	13.5
	A3	150	100	15.0
B	B1	150	100	12.0
	B2	150	125	12.0
	B3	150	150	12.0
	B4	150	175	12.0

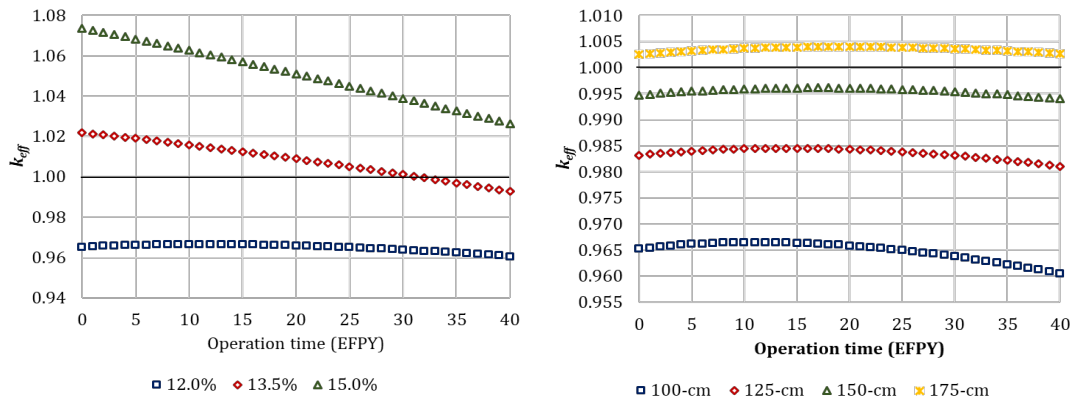
For type A core, three different ^{235}U enrichments are applied to the fuel region. The multiplication factors k_{eff} at Beginning-of-Cycle (BOC), Middle-of-Cycle (MOC, $t = 20$ EFPYs) and End-of-Cycle (EOC, $t = 40$ EFPYs) are presented in Table 4. Fig. 3a illustrates the behaviours of k_{eff} over time with all control rods out. The k_{eff} trend is more flatten during the depletion as using the lower ^{235}U enrichment due to the more amount of ^{238}U transmuted to fissile ^{239}Pu . For the type B core, the enrichment is reduced and fixed at 12.0w/o to minimize the excess reactivity during 40 EFPY operation. Four different active core heights are tested. The multiplication factor k_{eff} at BOC, MOC, and EOC, and the cycle length obtained are summarized in Table 5. Fig. 3b shows the behaviours of k_{eff} and core breeding ratio over time with all control rods out for the type B core. This type of core with the active core height of 175 cm can achieve the target cycle length with the lowest excess reactivity. Based on these results, the proposed optimized core is the type B4 core.

TABLE 4. k_{eff} FOR THE TYPE A CORE

Parameter	A1-12.0 w/o	A2-13.5 w/o	A3-15.0 w/o
k_{eff}			
- BOC	0.96522	1.02180	1.07362
- MOC	0.96585	1.00890	1.05104
- EOC	0.96049	0.99270	1.02626
Cycle length, EFPY(s)	0	31	>40

TABLE 5. k_{eff} FOR THE TYPE B CORE

Parameter	100-cm	125-cm	150-cm	175-cm
k_{eff}				
- BOC	0.96522	0.98320	0.99474	1.00259
- MOC	0.96585	0.98435	0.99609	1.00401
- EOC	0.96049	0.98107	0.99402	1.00270
Cycle length, EFPY(s)	0	0	0	>40



(a)

(b)

FIG. 3. Evolution of k_{eff} versus time for the (a) type A core and (b) type B core

3.4. Optimization of the conceptual core

The optimized core design is shown in Fig. 4 (depiction of the active core region only). This core achieves a lifetime of 40 EFPYs and a small burnup reactivity swing. The summary of fuel pin parameters for this new core is in Table 2. The optimization of the core size and the enrichment of the fuel region is conducted by sensitivity analyses of k_{eff} trends over 40 EFPYs cycle. The fuel enrichment is 12.0 w/o ^{235}U . In total, the core consists of 5,550 fuel pins, 211 control rods, and 1,440 reflector pins. The control rod system is compartmental in two independent systems, a primary control rod system (PCRS, 133 control rods) and a secondary control rod system (SCRS, 78 control rods) [19]. “The purpose of the PCRS is to bring the reactor from any operating condition to a “cold” subcritical state. The SCRS provides an alternate shutdown capability. Its task is to bring the reactor from any operating condition to hot standby condition, leading to an improvement in overall shutdown reliability.”[19] Finally, the equivalent active core diameter and height are 1.50 m and 1.75 m, respectively, resulting in an H/D (height/diameter) ratio of 1.16.

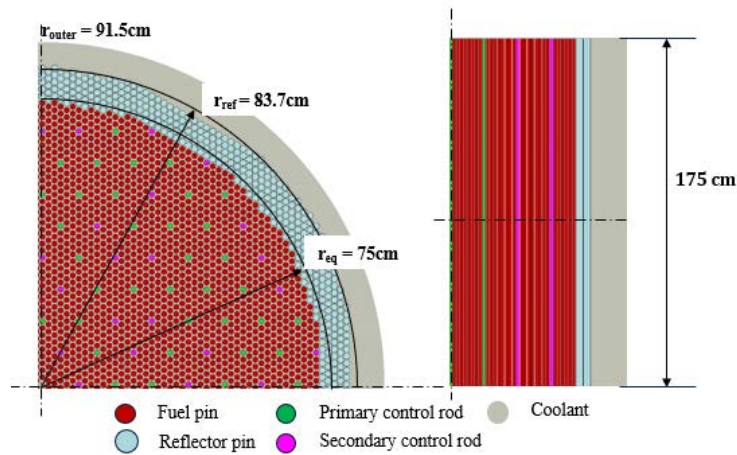


FIG. 4. Radial and axial view of the quarter active core layout for conceptual design

4. PERFORMANCE ANALYSES

4.1. Neutronic performance

The performance analyses are conducted by the MC code, MCS. The results of MCS are expected to have better accuracy due to the use of a heterogeneous core model and continuous-energy cross-sections. The summary of the core multiplication factor, power, and coolant parameters are presented in Table 5. The average specific power density, average volumetric power density, linear power density, coolant total mass, fluid velocity and, flow rate in the active core region are calculated from the design data. The k_{eff} as a function of time is illustrated in Fig. 5. Core reactivity swing is less than 500 pcm. The average standard deviation for MCS k_{eff} is 20 pcm. As shown in Fig. 5, compared to MC code MCS, the ARC code system shows a higher k_{eff} for an average k_{eff} difference of 31 pcm. The fluid velocity (0.360 m/s) is less than the design limit of 2 m/s for the coolant velocity. The average discharge burnup of the core is 32,25 MWd/kgHM.

Figs. 6 and 7 show the radial and axial power distributions at BOC, MOC, and EOC (normalized so that the average power equals 1.0 over the active core region) by MCS. The maximum relative standard deviation for power profiles is less than 0.2%. The radial power peak at the BOC, MOC and EOC are 1.58, 1.58, and 1.57, respectively, located in the centre region of the core due to the utilization of uniform fuel. Overall, the axial power rate decreases at the centre and increases at the bottom and the top of active core height during the depletion. As shown in Fig. 7, a high power-generating region tends to move to the periphery at MOC and EOC from the centre at BOC.

TABLE 5. SUMMARY OF PRIMARY CORE PARAMETERS

Parameter	Value
Cycle length, EFPYs	40
Reactivity swing, pcm	411
Power	
- Average specific power density, MWd/kgHM	32.25
- Average power density, W/cm ³	25.44
- Linear power density, W/cm	39.81
Coolant (in active core region)	
- Total mass, kg	12,629
- Fluid velocity, m/s	0.36
- Flow rate, kg/s	2,590

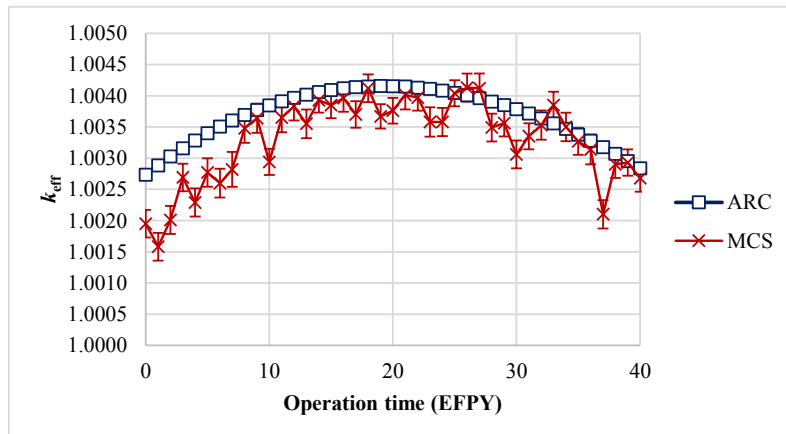


FIG. 5. Core multiplication factor, ARC and MCS

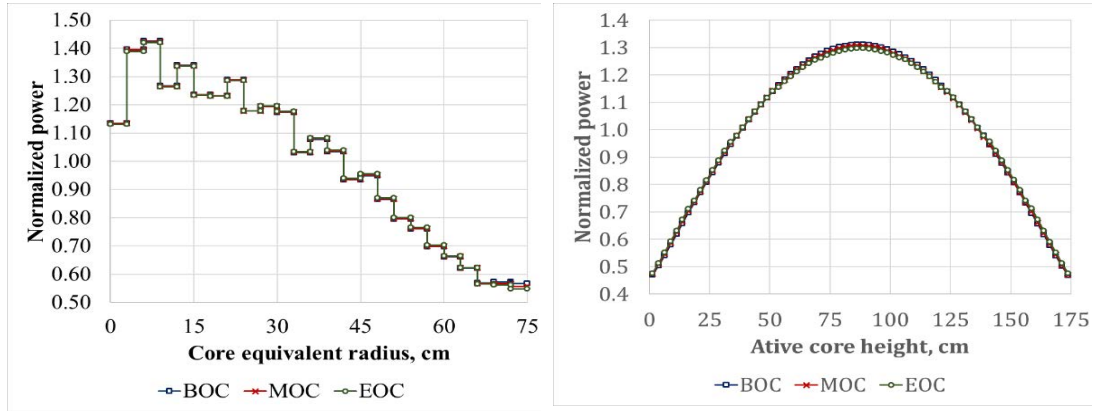


FIG. 6. Radial and axial normalized power distribution at BOC, MOC and EOC

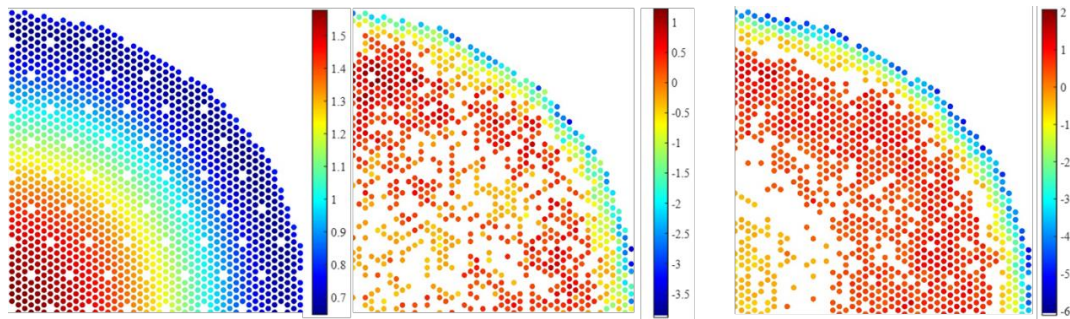


FIG. 7. Normalized pin-wise power distributions at BOC (left), the MOC and EOC power difference vs. BOC (middle to right, in: %)

4.2. Thermal-hydraulic performance

A preliminary one-dimensional (1D) T-H analysis is performed for the SMLFR core using a single-phase closed-channel model. The pin-wise power profiles from MCS contributes to pin-by-pin temperature profiles. In this analysis, a single pin is considered as 1D domain, and cylindrical and hexagonal channels have equivalent diameters. The core height is divided into 70 axial meshes (2.5 cm per mesh). The coolant has an assumed inlet temperature of 573K and an assumed pressure of 0.1MPa. The maximum and average fuel temperatures and the peak cladding temperature, and several coolant parameters at BOC, MOC, and EOC are summarized in Table 6. Figure 8 shows the radial pin-wise average fuel temperature distributions and the axial fuel, cladding, and coolant temperature distributions at BOC since the temperature profiles do not have significant changes over the full cycle.

Meanwhile, the axial fuel, cladding, and coolant temperatures increase from the bottom to the top of the active core (coolant flows from bottom to top). The calculated average outlet coolant temperature is 673K. The maximum fuel temperature is 692K, as shown in Table 6. The study by Shornikov et al. [20] shows that the UN does not interact with steel below 873K, ~181K is higher than the maximum fuel temperature. The peak cladding temperature over the full cycle is 682K, ~140K lower 15-15 Ti corrosion limit temperature.

TABLE 6. SUMMARY OF TEMPERATURE PROFILES AT BOC, MOC AND EOC

Parameter	BOC	MOC	EOC
Avg./Max. fuel temperature, K	646/692	646/692	646/692
Max. cladding temperature, K	682	682	682
Avg./Outlet coolant temperature, K	623/673	623/673	623/673

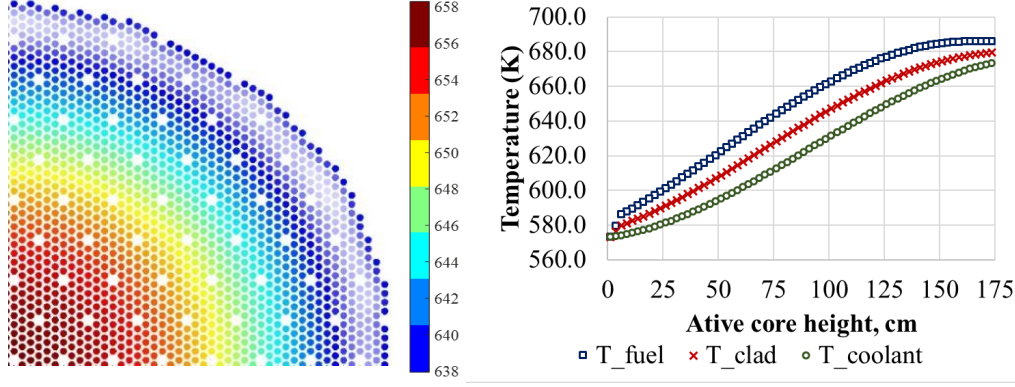


FIG. 8. BOC normalized pin-wise temperature distributions (left) and the axial temperature profiles (right)

4.3. Control rod worth and reactivity feedback coefficients

Table 7 shows the effective delayed neutron fraction (β_{eff}) and control rod worth during the core lifetime as calculated by MCS (β_{eff} is calculated with the adjoint-weight kinetic parameter calculation module of MCS [21]). The rod worth of the PCRS and SCRS is higher than the core reactivity swing of ~ 411 pcm.

TABLE 7. CONTROL ROD WORTH

Parameter	BOC	MOC	EOC
Effective delayed neutron fraction (β_{eff}), pcm	809 \pm 1	760 \pm 1	715 \pm 1
Primary control rod worth, pcm	6,498 \pm 7	6,517 \pm 7	6,523 \pm 7
Secondary control rod worth, pcm	4,200 \pm 7	4,229 \pm 7	4,247 \pm 7
Total control rod worth, pcm	10,667 \pm 7	10,687 \pm 7	10,716 \pm 7

The reactivity feedback coefficients of the SMFLR are computed by employing the direct approach with MCS, as shown in Table 8. The coefficients considered in this work include the coolant density coefficient, the fuel Doppler coefficients, the axial core expansion coefficient, the radial core expansion coefficient, and the control rod driveline expansion coefficient. These coefficients are determined by direct eigenvalue differences between the base configuration and the perturbed state of the reactor. A feedback coefficient (α) over a particular parameter X is calculated as shown in Eq. (1):

$$\alpha_X = \frac{\rho_{ref} - \rho_{perturbed}}{\delta X}, \quad (1)$$

where α_X is the feedback coefficient over the parameter X , ρ_{ref} is the reference state reactivity, $\rho_{perturbed}$ is the perturbed state reactivity, and δX is the perturbation of the parameter X . All the reactivity feedback coefficients are negative, which demonstrates that the core is inherently safe.

TABLE 8. REACTIVITY FEEDBACK COEFFICIENTS

Parameter	BOC	MOC	EOC
- Doppler coefficient, pcm/K	-0.743±0.034	-0.740±0.036	-0.735±0.035
- Axial expansion coefficient, pcm/K	-0.339±0.009	-0.340±0.009	-0.338±0.009
- Radial expansion coefficient, pcm/K	-0.508±0.011	-0.522±0.009	-0.576±0.010
- Coolant temperature coefficient, pcm/K	-0.179±0.069	-0.208±0.071	-0.204±0.071
- Control rod driveline thermal expansion coefficient, pcm/K	0.0693±0.0001	0.0695±0.0001	0.0697±0.0001

4.4. Integral reactivity parameters for quasi-static reactivity balance

“The quasi-static reactivity balance (QSRB) method [22] proposed by ANL is an efficient approach to evaluate the inherent safety of the SMLFR core in terms of the passive self-controllability under unprotected transient conditions. This self-controllability means that a reactor leads to a passive safe shutdown state solely through the reactivity feedback effects [23]. To attain self-controllability, prior research [24] points to the idea that a given number of various criteria needs to be satisfied. These criteria depend on the values and the ratio of three integral reactivity parameters (A , B , and C), which can be computed by using the QSRB approach. A is the net power reactivity decrement corresponding to the reduction of reactivity as a result of a rise in fuel temperature from the average coolant temperature to the average fuel temperature;”[3,4,8-12] B is the power-to-flow reactivity decrement, defined as the variation of reactivity as the coolant temperature rises across the core; and C is the coolant inlet temperature coefficient. Those parameters are defined as:

$$A (pcm) = (\alpha_D + \alpha_{Ax})\Delta T_f, \quad (2)$$

$$B(pcm) = (\alpha_D + \alpha_{Ax} + \alpha_{Co} + 2\alpha_{Cr} + 2\alpha_{Ra})\frac{\Delta T_c}{2}, \quad (3)$$

$$C(pcm/K) = \alpha_D + \alpha_{Ax} + \alpha_{Co} + \alpha_{Ra}, \quad (4)$$

where α_D is the fuel Doppler coefficient [pcm/K], α_{Ax} is the fuel axial expansion coefficient [pcm/K], α_{Ra} is the core radial expansion coefficient [pcm/K], α_{Co} is the coolant density coefficient [pcm/K], α_{Cr} is the control rod driveline thermal expansion coefficient [pcm/K], ΔT_f is the average fuel temperature increment in comparison with the average coolant temperatures [K], ΔT_c is the positive average coolant temperature rise across the core [K].

“By applying the QSRB method, the self-controllability and inherent safety for LFR core are ensured if the following criteria are satisfied [24]:

- A , B , and C are all negative values, which guarantees the power and temperature control in the core;
- $A/B < 1$, which guarantees control of the asymptotic temperature rise under ULOF condition;
- $1 < C\Delta T_c < 2$, which guarantees an appropriate balance between ULOHS and the chilled inlet temperature and maintains the balanced state of a plant; and
- $\Delta \rho_{TOP}/|B| < 1$ to ensure the reactivity control in UTOP scenarios, where $\Delta \rho_{TOP}$ is the ratio of the reactivity that control systems need to compensate for the number of operation control groups in the reactor core.” [3,4,8-12]

“From the T-H analysis, the average inlet and outlet coolant temperatures are 300 and 400°C, respectively, so the coolant temperature rise across (ΔT_c) the core is 100K.” [3,4,8-12] Besides, the average temperature of the fuel is calculated and approximately equals 646K. Table 14 summarizes the integral reactivity parameters of the QSRB and the several criteria required for the SMLFR inherent safety features as calculated MCS. The first criterion for the SMLFR core is satisfied because all the integral reactivity parameters are negative. Furthermore, using the calculated integral reactivity parameters, it is shown that the next three required criteria are also satisfied. The QSRB analysis demonstrates that, if given a sufficient amount of time, the SMLFR core will return to a safe stationary state even after an unprotected transient accident.

TABLE 9. INTEGRAL REACTIVITY PARAMETERS AND INHERENT SAFETY CRITERIA

Parameter	BOC	MOC	EOC
A: power coefficient, pcm	-25.98±0.85	-25.92±0.89	-28.07±0.86
B: power-to-flow coefficient, pcm	-120.79±5.22	-123.55±5.37	-133.49±5.34
C: inlet temperature coefficient, pcm/K	-1.77±0.08	-1.81±0.08	-1.95±0.08
$\Delta\rho_{TOP}$: transient over-power initiator, pcm	19.1±0.5	38.7±0.5	27.7±0.5
Required criteria for inherent safety			
$A/B < 1$	0.22±0.01	0.21±0.01	0.21±0.01
$1 < C\Delta T_c/B < 2$	1.46±0.09	1.47±0.09	1.46±0.08
$\Delta\rho_{TOP}/ B < 1$	0.16±0.01	0.31±0.01	0.21±0.01

5. CONCLUSION

An innovative SMLFR core cooled by LBE has been designed which possibly satisfies advanced reactor requirements. The power level and the assumed thermal efficiency is 37.5 MW(th)/15 MW(e) and 40%, respectively. The SMLFR adopts UN fuel to improve fuel efficiency. The small size allows the active core to be transported in an SNF cask to meet the electricity demand in remote areas, off-grid locations, and to power the nuclear icebreakers or submarines. The reactor uses 12.0 w/o enriched uranium nitride fuel. The core depletion calculations using the deterministic code system ARC confirms that operation at full power for 40 years without refuelling and has a reasonable excess reactivity is feasible. Several reactor core design parameters have been analysed, such as the behaviour over time of the core multiplication factor, normalized power distribution, and T-H results. Preliminary safety assessment for this advanced LFR core was evaluated by employing the MC code MCS to calculate the control rod worth, reactivity coefficient, and integral parameters. The primary and secondary control rod worth can manage the excess reactivity. The reactivity feedback coefficients are calculated to be a negative value during the full lifetime. Some preliminary accident analyses of the SMLFR show that the new conceptual core can attain self-controllability even in cases of primary accident scenarios under unprotected transient conditions. Several essential points for the feasibility of the reactor were left out as future work and require rigorous studies. In order to increase the design reliability of this SMLFR, a more rigorous uncertainty evaluation is also important and will be analysed in the future.

ACKNOWLEDGEMENTS

This work was supported by the National Research Foundation of Korea (NRF) grant funded by the Korea government (MSIT) (No.NRF-2017M2A8A2018595). This work was also supported by the National Research Foundation of Korea (NRF) grant funded by the Korea government (MSIT) (No.NRF-2019M2D1A1067205).

REFERENCES

- [1] BEHAR, C., Technology Roadmap Update for Generation IV Nuclear Energy Systems, In OECD Nuclear Energy Agency for the Generation IV International Forum, accessed Jan (Vol. 17, No. 2018, pp. 2014-03)
- [2] TUČEK, K., CARLSSON, J., WIDER, H., Comparison of sodium and lead-cooled fast reactors regarding reactor physics aspects, severe safety and economical issues, *Nuclear Engineering and Design* (2006), 236(14-16), 1589-1598.
- [3] GREENSPAN, E., HONG, S. G., LEE, K. B., ET AL., Innovations in the ENHS reactor design and fuel cycle. *Progress in Nuclear Energy*, (2008) 50(2-6), 129-139.
- [4] ZRODNIKOV, A. V., TOSHINSKY, G. I., KOMLEV, O. G., ET AL., Innovative nuclear technology based on modular multi-purpose lead–bismuth cooled fast reactors, *Progress in Nuclear Energy* (2008), 50(2-6), 170-178.
- [5] DI MAIO, D. V., BOCCITTO, A., CARUSO, G., Supercritical carbon dioxide applications for energy conversion systems, *Energy Procedia* (2015), 82, 819-824.
- [6] PUKARI, M., Experimental and theoretical studies of nitride fuels, Doctoral dissertation, KTH Royal Institute of Technology (2013).
- [7] CAUTAERTS, N., DELVILLE, R., DIETZ, W., ET AL., Thermal creep properties of Ti-stabilized DIN 1.4970 (15-15Ti) austenitic stainless steel pressurized cladding tubes, *Journal of Nuclear Materials* (2017), 493, 154-167.
- [8] JUST, L. C., HENRYSON, I. I., KENNEDY, A. S., ET AL., System Aspects and Interface Data Sets of the Argonne Reactor Computation (ARC) System (No. ANL--7711), Argonne National Laboratory, 1971.
- [9] LEE, C. H., & YANG, W. S., MC2-3: Multigroup Cross Section Generation Code for Fast Reactor Analysis (No. ANL/NE-11-41 Rev. 2), Argonne National Laboratory, 2013.
- [10] ALCOUFFE, R. E., BAKER, R. S., BRINKLEY, F. W., ET AL., DANTSYS: A Diffusion Accelerated Neutral Particle Transport Code System (LA-12969-M), Los Alamos National Laboratory, 1995
- [11] TOPPEL, B. J., User's Guide for the REBUS-3 Fuel Cycle Analysis Capability (No. ANL--83-2). Argonne National Laboratory, 1983.
- [12] LEE, H., KIM, W., ZHANG, P., ET AL., MCS – A Monte Carlo particle transport code for large-scale power reactor analysis, *Annals Nuclear Energy*, Under review (2019).
- [13] Review of UK Shipping Emissions, Tech. Rep., The Committee on Climate Change (CCC), 2011.
- [14] KONDO, M., TAKAHASHI, M., SAWADA, N., ET AL., Corrosion of steels in lead-bismuth flow, *Journal of Nuclear Science and Technology* (2006), 43(2), 107-116.
- [15] FUKUSHIMA, M., KITAMURA, Y., ANDOH, M., ET AL., Measurement and analysis of reflector reactivity worth by replacing stainless steel with zirconium at the fast critical assembly (FCA), *Journal of Nuclear Science and Technology* (2012), 49(10), 961-965.
- [16] ZHAO, H., GAO, R., BAI, P., Advances in boron isotope separation by ion exchange chromatography, *Asian Journal of Chemistry* (2014), 26(8), 2187.
- [17] SAMOKHIN, D. S., KHORASANOV, G. L., TORMYSHEV, I. V., ET AL., Low-power lead-cooled fast reactor for education purposes, *Nuclear Energy and Technology* (2015), 1(3), 191-194.
- [18] BOHACHEK, R., PARK, C., WALLACE, B., WINSTON, P., MARSCHMAN, S., Viability of Existing INL Facilities for Dry Storage Cask Handling (No. INL/EXT-13-29035), Idaho National Laboratory, 2013.
- [19] MCKEEHAN, E. R., SIM, R. G., Clinch River Breeder Reactor Secondary Control Rod System (No. CONF-771217-3), Energy, Inc., Idaho Falls, Idaho, 1977.
- [20] SHORNIKOV, D. P., S. N. NIKITIN, B. A. TARASOV, ET AL., “The Interaction Between Nitride Uranium and Stainless Steel,” In IOP Conference Series: Materials Science and Engineering (2016), 130(1), 012037. IOP Publishing.
- [21] JO, Y., LEE, D., “Verification of Adjoint-Weight Kinetics Parameter Calculation Capacity in MCS,” Proc. Int. Conf. of PHYSOR, 2018 April 22 – 26; Cancun, Mexico (2018). [USB]

- [22] WADE, D. C., WIGELAND, R. A., HILL, D. J., The safety of the IFR, *Progress in Nuclear Energy* (1997), 31(1-2), 63-82.
- [23] QVIST, S. A., Safety and core design of large liquid-metal cooled fast breeder reactors, University of California, Berkeley, 2013.
- [24] HYUN, H., HONG, S. G., A sodium-cooled ultra-long-life reactor core having improved inherent safety with new driver-blanket burning strategy, *International Journal of Hydrogen Energy* (2016), 41(17), 7082-7093.

SEALER-UK: A 55 MW(E) LEAD COOLED REACTOR FOR COMMERCIAL POWER PRODUCTION

Paper ID #30

J. WALLENIOUS, S. QVIST, I. MICKUS, P. SZAKALOS

LeadCold Reactors

Stockholm, Sweden

Email: janne@leadcold.com

Abstract

SEALER-UK is a 55 MW(e) lead-cooled reactor using uranium nitride fuel. The purpose of the design is to produce base-load power on the UK grid. In a reference configuration of four units, a SEALER-UK power plant may produce 220 MW of electricity at an estimated cost of £47-55/ MWh. A single fuel load will last 22.5 full power years, corresponding to 25 calendar years of operation. Five years after shut-down, the primary system is transported as a single package to Sellafield for safe surface storage until the UK high level waste repository becomes operational. The integrity of steel surfaces exposed to liquid lead is ensured by use of alumina forming steels, containing 3-6 wt% aluminium. These steels are applied either as weld overlay, as a surface alloy, or as bulk material, depending on the radiation damage dose tolerance and mechanical strength required for a particular component. Passive safety of the reactor is ensured by removal of decay heat from the core by natural convection of the lead coolant. Transport of the decay heat from the primary system is accomplished by dip-coolers, or ultimately by radiation from the primary vessel to a reservoir of water surrounding the guard vessel. In the event of a core disruptive accident, volatile fission products are retained in the lead coolant and no evacuation of persons residing at the site boundary will be required.

1. INTRODUCTION

LeadCold designs SEALER-UK (Small, Economic and Agile Lead-Cooled Reactor for the United Kingdom) to produce electricity at a competitive cost on the UK power grid, with the added value of a significantly reduced investment risk, as compared to large scale nuclear new-build.

LeadCold expects to reduce capital and operational expenditures for the reactor owner/operator through:

- automated factory assembly of primary systems featuring minimized physical dimensions;
- a reduced time for on-site construction activities;
- a nuclear battery design, eliminating fuel reloading systems/operations and maximising availability;
- passive safety features, reducing the number of safety classified systems to a minimum.

The choice of lead coolant ensures passive safety in a format as compact as possible. The selection of uranium nitride fuel minimizes the volume of the fuel required to operate the reactor. Manufacturing the fuel with 11.8% enriched ^{235}U minimizes the reactivity swing and the number of control assemblies, and hence the volume of the core for a given power.

Applying alumina forming alloys to protect all steel surfaces in contact with the primary lead-coolant results in strongly reduced corrosion rates and permits a larger variation in permissible oxygen concentration.

The primary system is designed so that decay heat will be possible to remove from the core by natural convection of the lead coolant. Thereafter, the decay heat is evacuated to the environment, either by dip coolers, or by radiation from the primary vessel to a reservoir of water surrounding the guard vessel.

In the case of a core disruptive event, volatile fission products are retained through forming stable compounds with the coolant. Full release of the end-of-life inventory of noble gases does not require evacuation of any population residing outside the site boundary.

In this contribution, we present the major technical parameters of the plant and reactor design, as well as its performance during design basis and beyond design basis accidents. We also discuss the economic performance necessary to achieve in order to make SEALER-UK competitive on the UK electricity market.

2. PLANT, FUEL AND CORE DESIGN

Figure 1 shows the conceptual layout of a four-unit SEALER-UK site. Each reactor produces a net electric power of 55 MW and the total power output of the plant is 220 MW(e). A single reactor unit, its safety-related and primary-auxiliary equipment is located underground, while one control-room and other auxiliary equipment is shared between two units. All four units share a common turbine building. The target availability of the plant is 96%, allowing for preventive maintenance and quality inspection to be carried out during two weeks for each of the units. No fuel reload is foreseen during the life of the plant.

Figure 1 also shows a bank of cooling towers, which provide the ultimate heat sink for the condenser cooling system. Each reactor building is equipped with four stacks for Reactor Vessel Auxiliary Cooling (RVAC) by means of radiation of decay heat to a guard vessel immersed in a water pool, and Direct Reactor Auxiliary Cooling (DRAC) dip-cooler systems. The footprint of the site is 150 x 200 meters.



FIG. 1. Conceptual layout of a 4x55 MW(e) SEALER-UK plant

The 140 MW(th) reactor core of SEALER-UK is designed to achieve an average fuel burn-up of 60 MWd/ton of uranium without any fuel reload while minimising the ratio between the number of control-rod and fuel assemblies. To achieve the latter objective, the 19.9% enriched uranium oxide fuel of SEALER-Arctic [1] has been substituted with 11.8% enriched uranium nitride, which features a breeding ratio equal to 1.0. Figure 2 shows the hexagonal core map of SEALER-UK, including 85 fuel assemblies, six B₄C control assemblies, six (W, Re)¹⁰B₂ shutdown assemblies and 72 yttria-stabilised zirconia reflector assemblies.

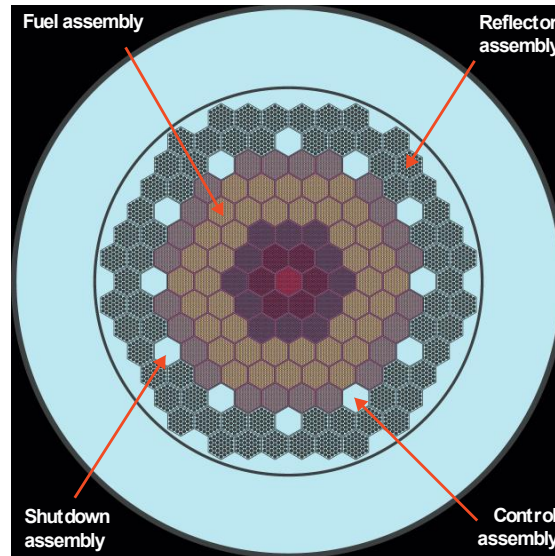


FIG. 2. Core map of SEALER-UK. Six shutdown and six control assemblies located at the periphery are shown withdrawn.

It may be noted that nitrogen used for the fuel fabrication is foreseen to be 99.5% enriched in ¹⁵N. Each fuel assembly contains 271 fuel rods. Operating at a modest average linear rating of 4.4 kW/m, the end-of-life core averaged burn-up is 6.0 % and burn-up reactivity swing of the SEALER-UK core is about 540 pcm over 22.5 equivalent full power years of operation.

Axial and radial power distributions are flattened during burn-up, leading to a peak pellet burn-up of 11% fission in actinides, and a peak clad radiation damage dose of 160 dpa. The latter corresponds to the threshold for swelling of the best lot of 15-15Ti irradiated by CEA in the Phénix reactor [2]. The plutonium inventory at End of Life (EoL) is 850 kg, or 4.4% of the actinide mass.

The fuel rod is dimensioned so that the cold swelling rate of uranium nitride fuel of 1.5% per percent burn-up [3] can be accommodated without any risk for pellet-clad mechanical interaction at End-of-Life. Fuel rod design parameters are listed in Table 1.

TABLE 1: FUEL ROD DESIGN PARAMETERS FOR SEALER-UK

Item	Value
Fuel composition	$(^{235}\text{U}_{0.118}, ^{238}\text{U}_{0.882})^{15}\text{N}$
Pellet diameter	8.12 mm
Pellet porosity	4 %
Clad inner/outer diameter	8.56/9.60 mm
Fuel column height	1305 mm
Clad bulk material	15-15Ti
Clad surface alloy	Fe-10Cr-6Al-RE

The core inlet- and outlet temperature of SEALER-UK are set to be 420°C and 550°C. As the latter is significantly higher than the core outlet temperature of SEALER-Arctic [1], additional measures for corrosion protection are foreseen. Namely, every single surface of metal exposed to liquid lead will be protected by aluminium oxide. E.g., 15-15Ti fuel cladding tubes will be surface alloyed with Fe-10Cr-6Al-RE, and the SS316L primary vessel may be protected by a weld-overlay of Fe-10Cr-4Al-RE. Recent experiments conducted at KTH have shown that optimized RE (Reactive Element) compositions make this alloy corrosion resistant in liquid lead up to a temperature of at least 750°C [4]. Whereas the primary vessel will not be exposed to temperatures above 420°C during nominal operation, its surface will be protected in order to reduce the requirement for oxygen supply, as well the inventory of corrosion products in the coolant.

3. SAFETY

Table 2 lists neutronic safety parameters calculated with Serpent [5] at Beginning-of-Life (BoL) and End-of-Life (EoL).

TABLE 2: SAFETY PARAMETERS OF THE SEALER-UK CORE

Parameter	BoL	EoL
β_{eff}	731 pcm	543 pcm
Λ_{eff}	7.6 μs	7.5 μs
K_D	-615 pcm	-500 pcm
$\alpha_{\text{pb}}(\text{core})$	+0.07 pcm/K	+0.11 pcm/K
α_{axial}	-0.12 pcm/K	-0.13 pcm/K
α_{radial}	-0.36 pcm/K	-0.39 pcm/K
$\Delta\rho_{\text{void}}(\text{core})$	+ 560 pcm	+960 pcm

In spite of a positive coolant temperature coefficient, the total temperature and power coefficients of the core are negative, leading to a benign behaviour of the core and primary system during transients.

3.1. Safety performance

The safety approach adopted by LeadCold is to design SEALER-UK so that events initiated by simultaneous failure of two reliable safety systems (classically defined as design extension condition, or DEC) will have the same consequence as permitted for design basis accidents (DBA). That is, such events are in the case of SEALER-UK included in the design basis. This is expected to lead to a reduction in estimated frequencies of core melts and large radiological releases.

Figure 3 shows results from a SAS4A-SASSYS-1 [6] simulation of an un-protected loss-of-flow (ULOF) transient at BoL, where a half-life of 10 s was adopted for the pump head. The major approximation made is a constant fuel-clad gap conductance of $1285 \text{ W/m}^2/\text{K}$, which was applied throughout the simulation. As can be observed, the system reaches an asymptotic equilibrium after two hours (relying on the function of the steam generators), in which the peak fuel cladding temperature and corresponding Hoop stress are low enough to ensure integrity of the cladding and zero release of fission products for an indefinite amount of time. As a matter of fact, the failure temperature of the cladding at BoL is nearly equal to its solidus temperature of 1680 K.

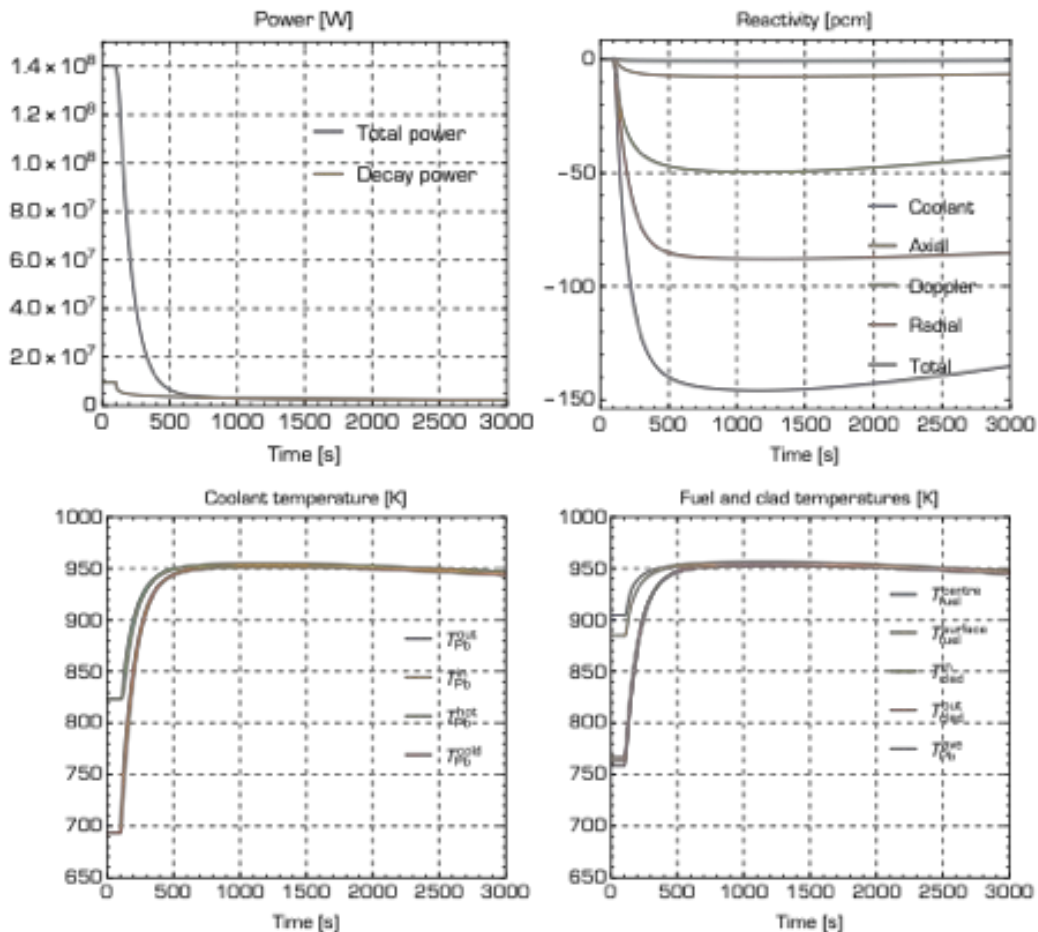


FIG. 3. Evolution of fuel and clad temperatures, reactivity feedback, power and coolant mass flow in SEALER-UK during an un-protected loss-of-flow accident at beginning of life.

During the first 70 seconds, the peak clad temperature increases, reaching a maximum of 1095 K (822°C). At BoL, when there is no fission gas inventory, this is much below the creep rupture limit of the clad. A net negative feedback renders the reactor sub-critical, and power decreases towards decay heat levels until positive feedback from falling fuel temperatures leads to re-criticality 1400 seconds into the transient. A damped oscillation follows, stabilizing the core at a power level of 12% of the nominal level after two hours.

Preliminary EoL simulations of the ULOF transient indicate about 50°C lower peak cladding temperatures but exhibit a larger element of uncertainty due to a less well determined physical and chemical state of the fuel at this point in time. E.g., gas release from the UN fuel is expected to be very small at $T_{fuel} < 1200$ K [7], but this assumption needs to be verified.

BELLA [8] is applied to simulation of un-protected loss of heat sink transients. Figure 4 shows the predicted evolution of system temperatures, power and reactivity following a postulated loss of the secondary system at BoL, without activation of dip-coolers. The RVAC system is postulated to ensure a constant guard vessel temperature of 100°C by means of condensation and recirculation of boiling water in the emergency cooling pool. Also, one may note that the negative coolant temperature reactivity coefficient of the upper plenum (-0.07 pcm/K) cancels out the positive reactivity coefficient of the coolant in the active zone of the core.

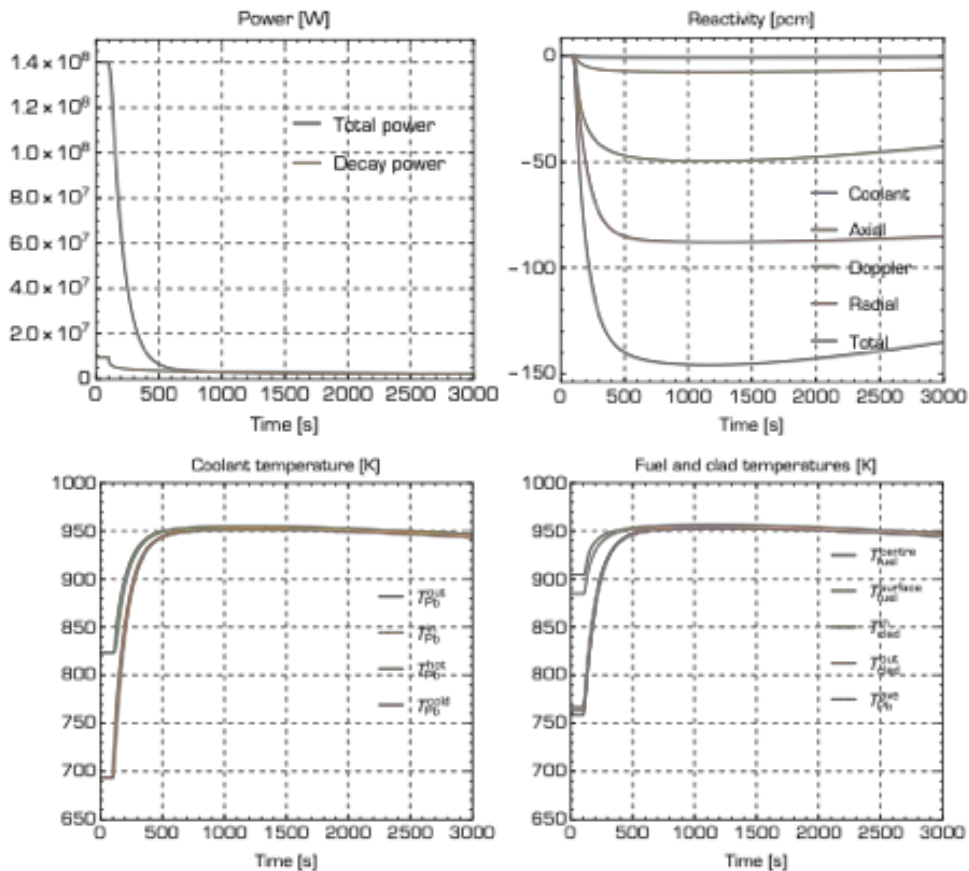


FIG. 4. Evolution of power, reactivity feedback, coolant, fuel and clad temperatures in SEALER-UK during an un-protected loss-of-heat-sink accident at beginning of life.

A negative reactivity insertion is resulting from rising temperatures in fuel assembly diagrid and the fuel itself, and a maximum coolant temperature of 955 K (682°C) is observed 900 seconds into the transient. At this time, fission product decay is responsible for the entire production of heat (3.3 MW). The primary vessel temperature is determined by the cold leg coolant temperature, and the 1% creep strain limit of this component is respected by a wide margin, even for hold times exceeding 1000 hours. Fuel and cladding temperatures remain below 956 K (683°C), maintaining a sufficient margin to creep rupture during an indefinite time. In order to evaluate the performance of SEALER-UK at EoL, fission gas release models of UN have to be implemented into BELLA.

4. ECONOMIC PERFORMANCE

The specific cost of staffing a small reactor plant is likely to be higher than for a conventional LWR plant, simply due to the need for a minimum amount of security staff. The increase in specific number of control rooms required to operate the plant may also contribute to a larger operational expenditure. The approach taken by LeadCold to compensate for the increase in OPEX is to design SEALER-UK so that the primary system ought to be possible to manufacture by automated procedures in a serial manner. The aim is to be able to deliver and commission a reactor unit within two years following a commercial order, which reduces expenditures for cost of capital to less than 10% of the overnight cost. The feasibility of this objective remains to be verified. Moreover, the nuclear battery approach adopted by LeadCold means that a SEALER-UK plant has zero capital cost for fuel reloading systems as well as zero OPEX for fuel reloading procedures, in addition to the potential for reduced outage time.

TABLE 3: TARGET ECONOMIC INDICATORS OF SEALER-UK

Item	Value
Plant configuration	4 x 55 MW(e)
Overnight cost per 55 MW(e) unit	GBP 140 M
Specific overnight cost	GBP 2500/kW(e)
Time from order to operation	2 years
Cost of capital	9 %
OPEX	GBP 20/MWh
LCOE	GBP 55/MWh

5. CONCLUSIONS

A 4x55 MW(e) SEALER plant design adapted to the UK market needs has been developed, based on the use of lead-coolant and uranium nitride fuel. An essential key to the viability of the concept is the protection of all steel surfaces exposed to liquid lead by means of alumina forming steels developed at KTH. It is shown that the heat capacity of the primary coolant inventory, in conjunction with a sufficiently large vessel surface area to power ratio makes the reactor to behave well under un-protected transients at BoL, while transients at MoL and EoL remain to be assessed. The estimated LCOE for this plant is GBP 55/MWh, under the condition that the time from order to commercial operation is two years and that the reactor factory produces 200 units during its economic life. It may be noted that this corresponds to a total capacity of 11 GW(e). This roughly corresponds to the gap in carbon-free base-load capacity in the UK once the existing fleet of AGRs have been shut-down and the large LWRs currently under construction or being planned in the UK have been taken into operation. Thus, the 200 unit sales target of the factory could be satisfied if SEALER-UK catches 100% of the domestic market. If this, admittedly optimistic, target is not realised, one or several export markets would have to be identified, where units produced in the UK can be deployed. One such potential market is Canada, considering that the UK and Canadian regulatory bodies are conducting discussions on harmonizing their respective regulations.

REFERENCES

- [1] J. WALLENIUS ET AL., Design of SEALER, a very small lead-cooled reactor for commercial power production in off-grid applications, Nucl. Eng. Des. 338 (2018) 23.
- [2] P. YVON ET AL., Structural materials for next generation nuclear systems: challenges and the path forward. Nucl. Eng. Des. 294 (2015) 161–169 .
- [3] J. WALLENIUS, Nitride fuels, In Comprehensive Nuclear Materials, edited by R.J.M. Konings, in Press (2019).
- [4] P. DÖMSTEDT ET AL, Corrosion Studies of Low-Alloyed FeCrAl Steels in Liquid Lead at 750 ° Oxidation of metals 91 (2019) 511.
- [5] J. LEPPÄNEN ET AL., The serpent Monte Carlo code: status, development and applications in 2013. Ann. Nucl. Energy 82 (2015) 142.
- [6] T. FANNING ET AL., The SAS4A/SASSYS-1 Safety Analysis Code System, ANL/NE-16/19, Argonne National Laboratory, 2017.
- [7] E.K. STORMS, An equation which describes fission gas release from UN reactor fuel, J. Nucl. Mater. 158 (1988) 119.
- [8] S. BORTOT ET AL., BELLA: a multi-point dynamics code for safety-informed design of fast reactors, Ann. Nucl. Energy 85 (2015) 228. AUTHOR, A., "Paper title in sentence case", Conference Title in Title Case (Proc. Int. Conf. Place of Conference, year), Publisher, Place of Publication (Year).

SESSION III: SAFETY ASPECTS OF FAST SMRS

EXPERIENCE IN THE PHYSICS DESIGN AND SAFETY ANALYSIS OF SMALL AND MEDIUM SIZED FBR CORES

Paper ID #3

A. Riyas, T. Sathiyasheela, Abhitab Bachchan and K. Devan
Indira Gandhi Centre for Atomic Research
Kalpakkam, India 603 102
Email: rias@igcar.gov.in

Abstract

It is envisaged that, faster growth of nuclear power in India is possible by the use of metallic-fuelled fast breeder reactor (FBR) cores with higher breeding ratio (BR) and lower doubling time (DT). It is well known that, such core designs compromise on safety parameters mainly due to the higher positive sodium void reactivity worth and its impact on transient behaviour. Also, the possible design modifications that enhance safety of such cores will have the drawback of economic penalties. The choice of metallic-fuelled FBRs is thus challenging, additionally due to the lack of worldwide operating experience of metallic fuelled fast reactors, other than experimental reactors. Giving more importance to safety, core designs are proposed with sodium void reactivity lower than 1 \$. The core physics parameters and safety performance during loss of flow accident of such an FBR core is described in this paper. For comparison, the results of a medium sized FBR core are also given.

1. INTRODUCTION

Commercialization of the fast breeder reactor (FBR) fuel cycle in India have been planned through the use of metallic fuel, which offers a higher breeding ratio and lower fuel doubling time, along with the pyro-process recycling [1][2][3]. Metal fuels considered here are the alloy of uranium, plutonium and zirconium that have experience in EBR-II experimental reactor during 1980's. Also, the selection of this alloy was the fundamental reason for the superior safety characteristics shown in EBR-II [4][5]. Initial difficulties of attaining high burn-up using these fuels are rectified using modified fuel pin designs and a maximum burn-up of 18 % could be obtained [6][7]. The implementation of metallic fuel in fast power reactors is advantageous with respect to its high breeding ratio [8] and lower fuel doubling times. Also, its merits can be extended with actinide incineration [9][10] and nuclear non-proliferation [11]. The benefits are possible only when its safety concerns are addressed realistically. The first concern is from the choice of sodium cooled fast reactors itself and next is from the extra challenges by the use of metallic fuel in these power reactors.

The important safety concerns can be addressed through the response of few rare possible transients the core undergoes during its operation. The fuel in a fast reactor is not in the most reactive configuration, re-criticality in an accident is possible unlike in the case of thermal reactors and hence safety analysis of FBR cores is important. The safety can be ensured by active and passive safety systems, as well by inherent characteristics. SCRAM through active systems requires an activation signal to function. But passive systems do not depend on activation signal and function automatically based on some physical criteria like temperature, magnetic property etc. Even though, it does not rely on any activation signals, safe shutdown may further prevent by additional failures of the system. In depth safety of a fast reactor can be ensured by inherent safety phenomenon, as they are the result of inherent physical phenomenon like thermal expansion and gravity that don't have a probability of failure [12]. It is important to analyse the capability of a FBR core to shutdown inherently during severe accidental conditions. Among the three FBR accidents, the severity of unprotected transient over power (UTOPA) can be minimized by control rod design optimization such that the reactivity insertion

due to uncontrolled withdrawal can be restricted within allowed safety limits [13]. This is especially true for metallic fuelled FBR cores which have low excess reactivity, low control rod worth and favourable thermo-physical properties. The severity of unprotected loss of heat sink (ULOHS) accident can be minimized by pool type designs which provide longer time constants.

The unprotected loss of flow accident (ULOFA) is assumed to be initiated by a total loss of offsite power and the resulting failure of both primary and secondary pumps. The resulting coast down of pumps is decided by a flow halving mechanism of flywheels. It is also assumed that the SCRAM systems are not available in the event and the reactor power varies in accordance with the feedback reactivity only. The effect of change in pressure drop across the coolant channel on the flow is considered negligible compared to the flow reduction, which is defined through a flow halving time. Now the reactivity feedback is a function of flow coast down of pumps, which depends on their inertial characteristics only [14]. During a ULOFA, the core will undergo through 3 phases of pre-disassembly, transition and disassembly [15]. In the pre-disassembly phase, reactor power decreases due to the dominating negative feedback from core radial expansion. In the transition phase, reactor power starts to increase due to the initiation of positive feedback from sodium voiding. Once the voiding spreads to more core regions (channels), power excursion and rapid temperature rise happens, and ultimately leads to core meltdown. It constitutes the dis-assembly phase. The value of the sodium void worth hence has an important impact on the transient in sodium cooled fast reactor cores [16][17].

Various studies are reported on the inherent safety properties of FBR cores. Inherent safety performance of oxide and metal fuels during transients are studied on a large sized FBR core [18][14][19]. In these studies, the net reactivity of the core is calculated as the sum of feedback reactivities. Flow coast down due to pump failure is represented by a flow halving time – the time required for flow reduction by 50%. The net reactivity and temperatures are obtained as a function of time after the initiation of the event. These studies ensure the better inherent safety performance of metal fuels over oxide and other ceramic fuel types. The shutdown capability of a medium sized (500 MW(e)) liquid-metal FBR during ULOFA as a function fuel type has been reported using static and dynamic analysis methods from IGCAR scientists [20][21][22][23]. Better performance of metallic fuels during ULOF transients is due to the preferable thermo-dynamic properties of metallic fuels, even though such fast reactors having very high sodium void worth. Such transients are proved benign in EBR-II experimental fast reactor. Regardless of these facts, no fast power reactors in world are realized with metallic fuels.

At the same time, future Indian sodium cooled fast reactors are planned with advanced design features to enhance the level of safety to meet the emerging Gen-IV criteria. The general trend is towards enhancing the safety level which seeks to prevent severe core damage and large radioactivity release to the public and practical elimination of severe accident scenarios involving energy release and public evacuation. It translates to the design of fast reactor core designs with zero or near-zero sodium void worth, in line with the international fast reactor community. In this regard, the basic core physics design of a 120 MW(e) small metallic fuelled FBR core with sodium void worth $<1\%$ and its safety performance during ULOFA is briefly described in this report and the results are compared with those of a medium sized FBR.

2. CALCULATION SCHEME AND REFERENCE CORES

The scheme of calculations is described in this section. The self-shielded cross-sections are calculated using the CONSYST/EFCONSY code system [24] from the basic cross-section set of ABBN-93 [25]. Core multiplication factor (k_{eff}) is calculated using the two-dimensional diffusion theory code ALCIALMI, which uses R-Z geometry for calculations. The code ALEX computes the power densities, reaction rates, breeding ratio etc, the reactor doubling time is obtained by neglecting fuel cycle length and processing losses [26].

The core excess reactivity and hence the effective multiplication factor are decided mainly based on the possible reactivity losses due to burn-up, power decrement and temperature decrement. These parameters are determined by breeding ratio and coefficients of temperature and power respectively. The material void worths, delayed neutron fraction, boundary movement worth and kinetic parameters are obtained by 1st order perturbation theory code PERTX [27], which is an extended version of the perturbation code NEWPERT [28][29].

The radial configuration of the reference 120 MW(e) core used in this analysis is shown in Fig. 1. Configuration of medium sized 500 MW(e) core used for comparison is shown in Fig. 2 [30]. In these figures, CSR and DSR are the two types of control rods used. CSR is control and safety rods used for reactivity regulations and shutdown, DSR is diverse control rods used only for shutdowns.

The common core design parameters are mentioned in Table 1 and the basic thermo-physical parameters of U-Pu-Zr (6%) fuel are given in Table 2 [21][30]. The choice of this fuel is justified by the following facts. First, this particular fuel composition is also having irradiation experience, though limited, from EBR-II reactor [31]. Second, few pins made of this fuel is undergoing irradiation in an indigenous test reactor. Additionally, this fuel can provide better breeding ratio than the classical metallic fuel type U-Pu-Zr(10%) due to the hardened spectrum in the former [8].

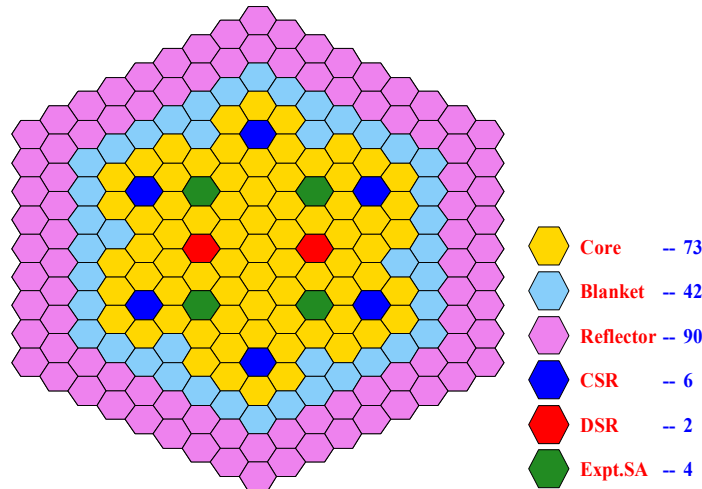


FIG. 1. Core Configuration of 120 MW(e) FBR Core

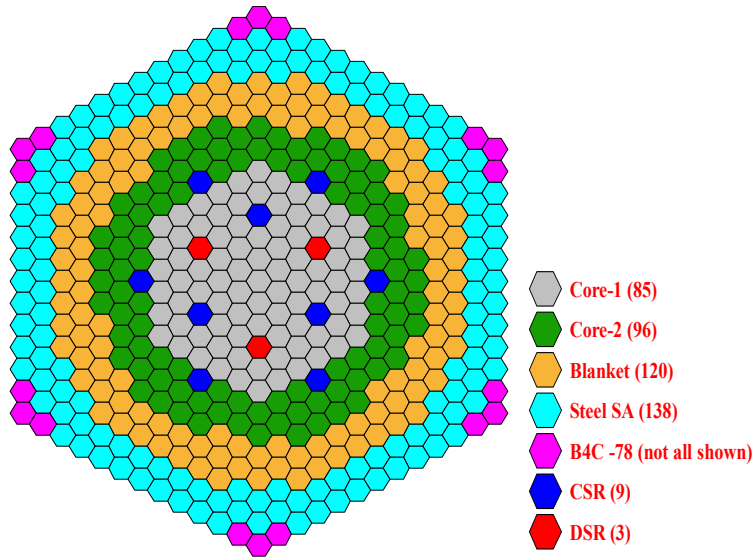


FIG.2. Core Configuration of 500 MW(e) FBR Core

TABLE 1. BASIC CORE DESIGN PARAMETERS

Parameter	Value
Maximum Allowed Linear Heat Rating	450 W/cm
Fuel Pin Diameter	6.6 mm
Clad Thickness – Fuel	0.45 mm
Assembly Pitch	135 mm
Number of Pins per Sub-assembly –Fuel	217
Number of Rows of Radial Blanket	2
Pin Diameter - Blanket	14.3 mm
Clad Thickness-Blanket	0.55 mm
Number Pins per Sub-assembly- blanket	61
Volume Fractions of	Core 26/24/50
Fuel/ Steel/ Sodium (%)	
Number of Fuel Enrichment Zones	1 for small, 2 for medium core
Total Height Core Fuel Region	100
Total Heights of axial Blankets (cm)	30/30

Pre-disassembly part of the ULOF is analysed using the code PREDIS [32]. PREDIS is a multi-channel, single pin model code, where each flow channel is represented by a representative single pin with its associated coolant flow and surrounding structure. Code PREDIS has two inputs; one is the material void and Doppler worth distributions in the reactor zones. Other input contains mainly the thermo-physical properties of the fuel used and the boundary movement worths. The boundary movement worth is used for the estimation of core expansion feedback along the axial and radial directions. The static power coefficients and isothermal temperature coefficients are calculated in the steady state mode of PREDIS code. During a loss of flow accident, it is assumed that the coolant flow coasts down in the form,

$$V(t) = \frac{V(0)}{1 + \frac{t}{\tau}} \quad (1)$$

Where $V(0)$ is the initial flow velocity, τ is the flow halving time and t is the time. Flow halving time of 8s is considered for the present analysis. The code uses point kinetics approximation for the calculation of reactor power. Net reactivity is the sum of input reactivity and feedback reactivity.

TABLE 2. THERMO-PHYSICAL PROPERTIES OF METALLIC FUELS

Number	Parameter	Value
1	Fuel Type	U-Pu-6%Zr
2	Fuel Density (g/cm ³)	17.1
3	Smeared Density (g/cm ³)	12.8
4	Plutonium Isotopic Composition: Pu239/Pu240/Pu241/Pu242 (%)	68.8/24.6/5.3/1.3
5	Melting Point (°C)	1067
6	Boiling Point (°C)	3932
7	Thermal Conductivity (W/cm/°C)	0.25
8	Linear Expansion Coefficient (oC-1)	19.7×10-6
9	Gap Conductance (W/cm ² /°C)	27
10	Specific Heat (J/g/°C)	0.2
11	Latent Heat of Fusion (J/g)	38
12	Latent Heat of Vaporization (J/g)	1641

The main feedbacks considered are from the axial expansion of fuel, clad, coolant expansion, Doppler effect, core radial expansion and coolant voiding. It has to be noted that, 2-dimensional diffusion calculations in RZ geometry has been chosen for the analysis as it is compatible with the safety analysis codes used. The schematic of total calculation is shown in Fig. 3 [30].

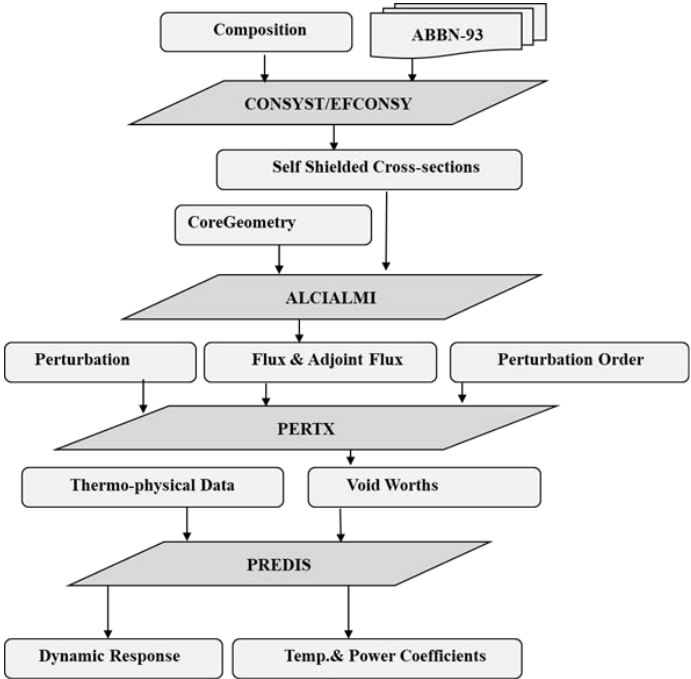


FIG. 3. Scheme of Calculation Method

3. CORE PHYSICS PARAMETERS – A COMPARISON

The basic core physics parameters of the small FBR core chosen for analysis is given in Table 3 [30]. The results of 500 MW(e) core is also given for comparison. From this table, 120 MW(e) FBR core can provide a BR of 1.1 and have a sodium void worth less than 1 \$. The 500 MW(e) core have higher BR in the cost of high void reactivity more than 4 \$. The 120 MW(e) have a slightly lower Doppler constant, due to higher enrichment and low U-238 content in the core.

TABLE 3. BASIC CORE PHYSICS PARAMETERS- A COMPARISON

Parameter	Reactor Power – MW(e)		
	120	500	
1. Core Excess Reactivity (pcm)	7000	4500	
2. Number of Core Enrichments	1	2	
3. Plutonium Enrichment (wt %)	19.6	13.6/18.2	
4. Total Number of Fuel SA	73	181	
5. Number of Radial Blanket SA	42	120	
6. Breeding Ratio	Internal	0.63	0.83
	External	0.47	0.53
	Total	1.10	1.36
7. Simple Reactor Doubling Time (years)	60	10.5	
8. Delayed Neutron Fraction (value of 1 \$ in pcm)	385	403	
9. Sodium Void Worth (pcm)	+164	+1830	
10. Doppler Constant (pcm)	-336	-470	

4. RESPONSE TO UNPROTECTED LOSS OF FLOW ACCIDENT (ULOF)

The transient behaviour of the reference FBR core during an ULOF event with a flow halving time of 8 sec and with the results of first order perturbation methods are discussed in this section. Voiding of steel, sodium, fuel and the Doppler constant in the operating range is used. The reactivity change produced by 100% voiding and its spatial distribution is considered in the first order method, and it is scaled linearly for the actual expansion or void undergone by different materials of the core during the transient. The validity of this approximation is justified in pre-disassembly phase in which the core undergoes lower material movements [30]. The Doppler constant is estimated in the range 200 °C to 827 °C, the latter close to sodium boiling temperature and it is sufficient for transient in the pre-disassembly phase. The Doppler feedback due to an actual temperature fluctuation during a transient is estimated by integrating dk/dT using the estimated Doppler constant which is computed for the operating temperature range.

Reactivity is a measure of the deviation of core multiplication factor from its critical value of 1.0. Reactivity change is the change in core multiplication factor due to any change in the core. As flow reduces, the core reactivity and hence the reactor power varies due to the reactivity feedbacks caused by the changes in temperature and the associated changes in the geometry and composition of the core. The first and abrupt feedback is from the Doppler effect of neutron absorption cross-section in reactor materials. Among the different reactor materials, the main contribution to this feedback is from fuel and its magnitude depends on fuel choice. The net reactivity feedback due to Doppler effect is governed by the value of Doppler constant and the temperature gradient during a transient and hence depends indirectly on other properties like fuel thermal conductivity and sodium flow rate. The feedback contribution from coolant is due

to the density changes that alter its moderating, leakage and capture properties. As the coolant temperature is immediately affected by the transient, this feedback is also quick. The magnitude of this reactivity feedback is highly space dependent for a particular core and the net value is decided by the size and compactness of core. The reactivity feedback due to dimensional changes along the axial direction during a transient will be decided by the thermal expansion coefficient of fuel and cladding along with the temperature changes. As fuel SA worth shows a clear radial dependence in FBR cores, core dimensional changes during a transient also lead to reactivity feedbacks. The net feedback due to this effect can be further divided into the effects of SA bowing and grid plate expansion, the latter shows a slower response. Two long time delay feedback mechanisms are from vessel expansion and control drive line expansion. The former provides +ve feedback, while the latter gives -ve feedback. For the present calculations, the above mentioned feedbacks have been not been included by assuming the net effect is negligible, and because of the relative safety comparison attempted in this study. Of course, the inclusion of these feedback mechanisms is essential for an accurate assessment of safety performance during transients for a particular core.

The estimated material void worths are given in Table 4. It has to be noted that the mentioned material void worths are given in the unit of dollar (1 dollar = 385 pcm for small core and 403 pcm for medium core). First order perturbation theory code has been used for the estimation of material void worth corresponds to 100 % void from core. The estimated fuel void worth of 120 MW(e) core estimated using first order perturbation theory is 43736 cm (-113.6 \$) and for 500 MW(e) core, its value is -95.4 \$.

TABLE 4. VOIDING WORTH OF CORE MATERIALS

Parameter	Core Power (MW(e))	
	120	500
Sodium Void Worth (\$)	+0.43	+4.54
Fuel Void Worth (\$)	-113.6	-95.4
Steel Void Worth (\$)	+2.5	+10.2

Fuel void worth of -113.6 \$ reported in Table 4 is the reactivity change obtained by the removal of the 100 % fuel from the reference core and is highly conservative (less negative compared to the actual reactive change with removal of 100 % fuel) as it is estimated through 1st order approximated methods. The actual fuel removal worth during a transient (provided the core is in the pre-dis-assembly phase) which is used in the analysis is obtained by the scaling down of the above 100 % removal worth, and the method is justified through the previous studies [30].

Isothermal temperature coefficient is the reactivity change produced due to an isothermal change of temperature by 1°C. Power coefficient is the reactivity change caused by the change of power by 1 MW(th). Both the coefficients are calculated by the feedback reactivities caused by the corresponding change in temperature and power using the code PREDIS. The values of the estimated coefficients and their components are also given in Table 4. From the table it is clear that, both the temperature and power coefficients are more negative for smaller core. It is due to the increase in net negative contributions from, fuel axial expansion and radial expansions with reduction in core size [30]. The values of different contributions to give the final coefficient are given in Table 5.

TABLE 5. STATIC TEMPERATURE COEFFICIENT (PCM/OC) AND POWER COEFFICIENT (PCM/MWT) OF TWO CORES

Components of Reactivity coefficient (pcm)	Temperature Coefficient ($pcm/^{\circ}C$)		Power Coefficient ($pcm/MW(th)$)	
	Small (120 MW(e))	Medium (500 MW(e))	Small (120 MW(e))	Medium (500 MW(e))
Doppler	-0.881	-0.632	-0.165	-0.092
Fuel axial expansion	-0.586	-0.466	-0.244	-0.074
Clad axial expansion	+0.019	+0.083	+0.009	+0.008
Coolant expansion	+0.047	+0.522	+0.021	+0.038
Core Radial Expansion	-1.197	-1.056	-0.237	-0.093
Total	-2.598	-1.549	-0.616	-0.213

As the coolant temperature changes during a transient, all the components of feedback changes and provides a net reactivity feedback. The net feedback is the sum of individual feedbacks considered and mentioned above. The response during ULOF will be different for 120 MW(e) core and 500 MW(e) core due to the fact that all the input parameters that leads to the feedback is different for both the cores. The components of reactivity and net reactivity of the small and medium sized cores during the transient are given in Fig. 4 and Fig. 5 respectively.

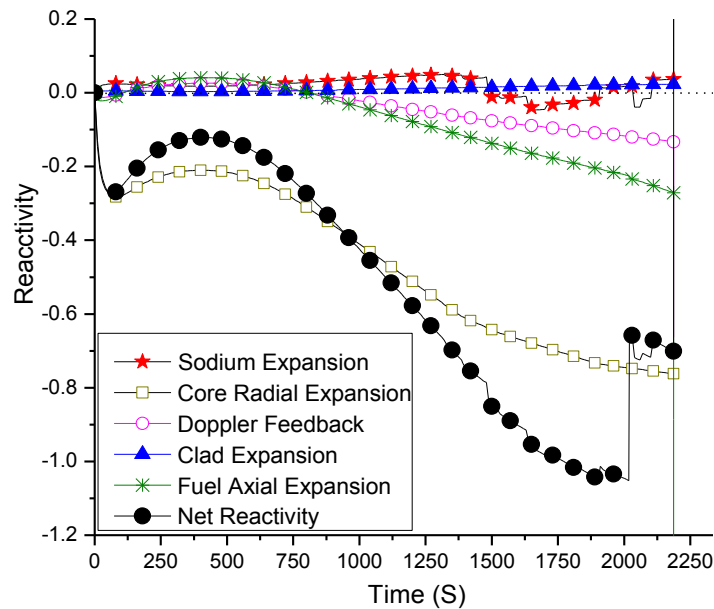


FIG. 4. Time Dependence of Net Reactivity and its Components during ULOFA of 120 MW(e) FBR Core

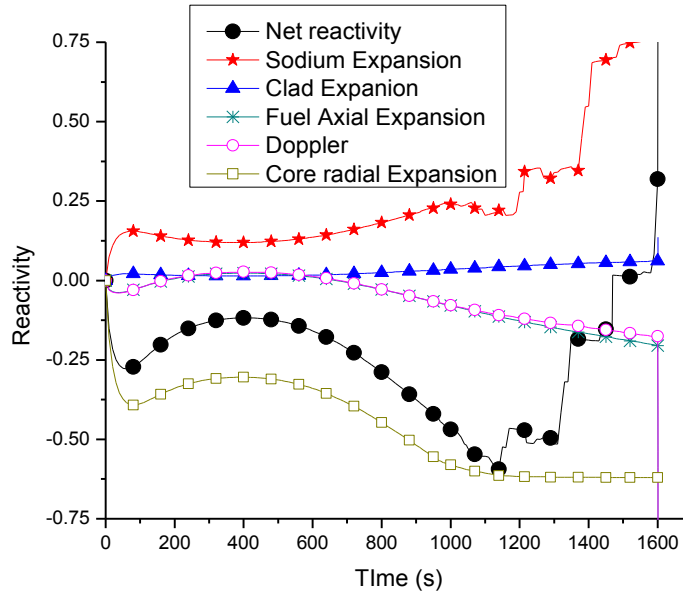


FIG. 5. Time Dependence of Net Reactivity and its Components during ULOFA of 500 MW(e) FBR Core

From the above figures it is clear that the main positive feedback during an ULOFA of metal fuelled FBR's is due to the expansion and voiding of sodium and the main negative feedback is from core radial expansion even though they are different for cores of different sizes. However, at the beginning of ULOFA, the positive feedback is only from sodium expansion as there is no initiation of sodium voiding. Also, the negative core radial expansion overwhelms the positive contribution from sodium expansion and causes the net reactivity feedback negative. As this difference is more for smaller cores, 120 MW(e) FBR core shows slightly more sub-criticality during ULOFA. Steel expansion feedback is small positive throughout the event. Fuel and Doppler feedbacks are small negative, but both the cores show a positive contribution initially due to the decrease of temperature.

As already mentioned, the net reactivity is the sum of the feedback reactivity and therefore will vary with core size. Its variation with respect to time for the two FBR cores is compared in Fig. 7 [30]. It can be observed from the figure that the pre-disassembly phase of sodium small reactors will be longer. This is caused by the lower positive reactivity addition from sodium density fall. Compared to the other reactor cores this phenomenon results in safer pre-disassembly phase of ULOFA accidents for the 120 MW(e) FBR core. The prompt critical transient indicates the end of the pre-disassembly phase in both reactors. The driving force of this prompt critical transient is the large-scale sodium voiding in the core. In these scenarios only indication for a large positive reactivity insertion are the reactivity plots since the perturbation results are not very accurate. It has to be noted that, the relative safety claimed for 120 MW(e) core is with respect to the available time for the introduction of other safety systems like safety grade decay heat removal systems, introduction of active safety measures like forced insertion of Control Rods etc.

As given in Fig. 6, the FBR cores go to subcritical state during the initial times of transient and cause a reduction in fission power. Total power is the sum of fission power and decay power. For a flow coast down time of 8 sec assigned to the present analysis, power reduction of the cores during ULOFA is shown in Fig. 7. It is seen from the figure that the total power decreases and asymptotically reaches to a value before entering in the dis-assembly phase. The asymptotic power value, time at which the power attains the asymptotic value and the time interval at which it retains in the asymptotic value are functions of core size. These asymptotic power values are 8 MW(th) and 33 MW(th) for the small and medium reactor cores respectively. It means that by providing decay heat removal systems having capacities equal to the asymptotic power levels, the power excursion and dis-assembly phase can be eliminated in these cores.

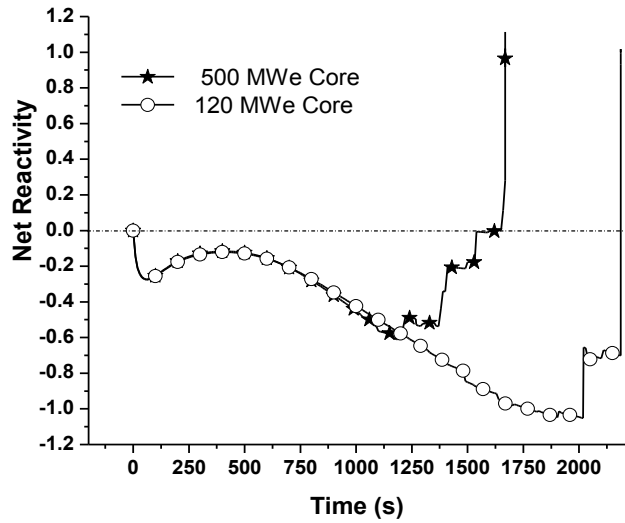


FIG. 6. Variation of Net Reactivity with Time

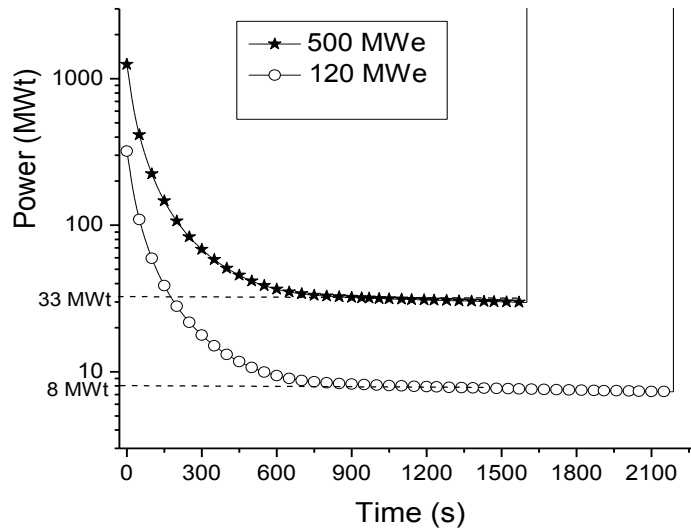


FIG. 7. The Variation of Reactor Power with Time during ULOFA

It has to be noted that, even both the feedbacks from sodium and core radial expansion is due to the changes in sodium temperature, different material movements are contributing to these. Feedbacks from sodium are caused by its density changes during transient, but the feedbacks from core radial expansion are mainly provided by the fuel density changes and boundary movement worths.

The core behaviour during ULOF transient and the shape of reactivity curves depicted in Fig. 4, Fig. 5 and Fig. 6 can be further explained with the changes of temperatures experienced by the core materials. This has been illustrated through Fig. 8, which shows the temperature variation of 500 MW(e) core during ULOFA. The associated reactivity change and power variation are also given for better understanding. Pump coast down during ULOFA causes continuous flow reduction and rise in temperature of sodium, steel and fuel. This causes positive insertion of reactivity from sodium and steel and negative reactivity insertion from fuel axial expansion, core radial expansion and Doppler effect. Out of these, the major negative contribution is from core radial expansion and the major positive contribution is from sodium expansion and voiding. As the total negative contributions are more compared to the total positive components, net reactivity becomes negative and becomes more negative with further flow coast down. Further, the insertion of negative reactivity causes power reduction, but the power to flow ratio (P/F) shows an increase as the power reduction is less compared to flow reduction. As the negative reactivity insertion increases, power reduces to still smaller values so that the P/F ratio saturates and then decreases leading to reduction of sodium, steel and fuel and temperatures.

With reduction of temperatures, feedbacks show decrease in its values (both +ve and -ve contributions), but the net reactivity continues to be negative. But the net -ve reactivity shows a reduction in its value as the reduction in -ve components are more than the reduction in +ve components and causes a slow-down of power reduction. As further flow coast down happens, P/F increases and causes a temperature hike. This causes increase in both +ve and negative reactivity components and the net becomes more -ve. But as the time elapses, the main -ve grid-plate expansion saturates, the main +ve sodium component continues to increase and the net reactivity increases again. It causes further sodium voiding, boiling and a saturation of sodium temperature, but the positive insertion of reactivity continues to increase with time. These causes increase in clad and fuel temperatures hence leads to an initiation of core disruptive accident (CDA). The step increases in reactivity shown in the figure represents the propagation of sodium voiding within a radial channel from top periphery to lower periphery in the axial direction and towards radial outward direction from channel to channel. The positive contribution from sodium voiding in the centre of a radial channel can be possible to be nullified with the negative contribution from the peripheries of the same channel and responsible for the flatness of the reactivity curve. The increase of reactivity between the flat variations is due to the addition of reactivity worths as sodium voiding propagates from one radial zone to another. It has to be noted that the net sodium void worth of the 500 MW(e) core is positive (+4.5 \$). The same arguments with differences in feedbacks and time dependence are valid for 120 MW(e) core also, with a better time margin for the introduction of possible safety systems to avoid CDA.

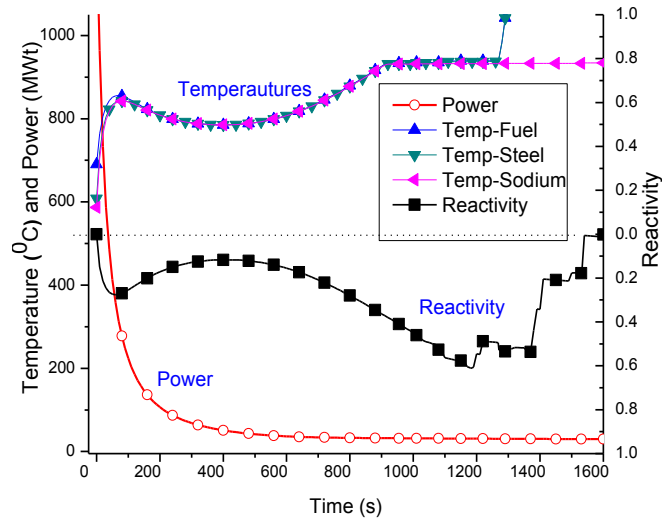


FIG. 8. Time Dependence of Material Temperatures, Reactor Power and Reactivity during ULOFA of 500 MW(e) FBR Core

5. CONCLUSION

It is planned to have a future use of metallic fuels in fast reactors of India for a faster growth of nuclear energy. The deployment of such fuels is challenging with respect to economics and safety, proper optimization studies have to be carried out before installations. The merits and possible challenges of such fuels in sodium cooled FBR cores are discussed in this paper.

The relative merits and demerits of a small metallic fast breeder core compared to a medium sized core in terms of safety is described. A conceptual fast reactor core of power 120 MW(e) is presented with a breeding ratio of 1.1 and void reactivity less than 1 \$. The transient response of this reactor core during ULOFA is studied and compared to that of 500 MW(e) core. With a flow halving time of 8 sec and with the results of first order perturbation methods, the study shows that small reactor will be in pre-disassembly phase for longer time due to the lower positive reactivity addition from sodium density fall. If a passive safety grade heat removal system is able to remove the decay heat, the reactor can be brought to safe shutdown state with better time margins. Therefore, a small FBR core is recommended for the commencement of metallic fuelled FBR cores with the advantage of better ULOFA performance but with a small compromise on breeding.

ACKNOWLEDGEMENT

We are thankful to Mr. V. L. Anuraj, IGCAR, for the valuable suggestions that help to improve and revise this paper with reviewer comments.

REFERENCES

- [1] GROVER, R. B., CHANDRA, D., 2006. Scenario for Growth of Electricity in India, *Energy Policy*, 34, pp.2834-2847.
- [2] CHETAL, S.C. ET AL., 2011. Current Status of Fast Reactors and Future Plans in India, *Energy Procedia*, 7, pp.64-73.
- [3] VASUDEVA RAO, ET AL., 2013. A Perspective on the Indian Programme on Fast Reactors and Associated Fuel Cycles, International Conference on Fast Reactors and Related Fuel Cycles: Safe Technologies and Sustainable Scenarios, FR13, Paris, France.
- [4] PAHL, R.G. ET AL., 1992. Irradiation Behaviour of Metallic Fast Reactor Fuels, *Journal of Nuclear Materials*, 188, pp.3-9.
- [5] PLANCHON, H.P. ET AL., 1987. Implications of the EBR-II Inherent Safety Demonstration Test, *Nuclear Engineering and Design*, 101 (1), pp.75-90.
- [6] CHANG, Y.I., 2007. Technical Rationale for Metal Fuel in Fast Reactors, *Nuclear Engineering and Technology*, 39 (3), pp.161-170.
- [7] WALTERS, L.C., 1999. Thirty Years of Fuels and Materials Information from EBR-II, *Journal of Nuclear Materials* 270, pp.39-48.
- [8] RIYAS, A., MOHANAKRISHNAN, P., 2008. Studies on Physics Parameters of Metal (U-Pu-Zr) Fuelled FBR Cores, *Annals of Nuclear Energy*, 35, pp.87-92.
- [9] IAEA-TECDOC-693, 1993. Use of fast reactors for actinide transmutation, Proceedings of a Specialists Meeting held in Obninsk, Russian Federation, 22-24 September 1992, IAEA.
- [10] BARBARA VEZZONI ET AL., 2015. Plutonium and Minor Actinides incineration options using innovative Na-cooled fast reactors: Impacting on phasing-out and on-going fuels, *Progress in Nuclear Energy*, pp.58-63.
- [11] AVRORIN, E.N AND CHEBESKOV, A.N, 2015. Fast reactors and nuclear nonproliferation problem, *Nuclear Energy and Technology* 1, pp.1-7.
- [12] WIGELAND, R., CAHALAN, J. 2011. Inherent Prevention and Mitigation of Severe Accident Consequences in Sodium-Cooled Fast Reactors. *Journal of Nuclear Science and Technology*. 48. Pp.516-523.
- [13] YOKOO, T., OHTA, H., 2001. ULOF and UTOP Analyses of a Large Metal Fuel FBR Core Using a Detailed Calculation System, *Journal of Nuclear Science and Technology*, 38, No.6, pp.444-452.
- [14] CAHALAN, J.E. ET AL., 1990. Performance of Metal and Oxide Fuels during Accidents in a Large Liquid Metal Cooled Reactor, International Fast Reactor Safety Meeting, Snowbird, USA, Vol. IV, 73.
- [15] CHELLAPANDI, P., 2013. Severe Accident Scenarios: Indian Perspective, FR13, Paris.
- [16] FUJITA, E.K., WADE, D.C., 1990. The Neutronic and Fuel Cycle Performance of Interchangeable 3500 MWth Metal and Oxide Fuelled LMRs, International Conference on the Physics of Reactors, Marseille, France.
- [17] KHALIL, H.S., HILL, R.N., 1991. Evaluation of Liquid-Metal Reactor Design Options for Reduction of Sodium Void Worth, *Nuclear Science and Engineering* 109, pp.221-266.
- [18] ROYL, P. ET AL., 1990. Influence of Metal and Oxide Fuel Behaviour on the ULOF Accident in 3500 MWth Heterogeneous LMR Cores and Comparison with Other Large Cores, International Fast Reactor Safety Meeting, Snowbird, USA.
- [19] OTT, K.O., 1988. Inherent Shutdown Capabilities of Metal-fueled Liquid Metal Cooled Reactors during Unscrammed Loss of Flow and Loss of Heat Sink Incidents, *Nuclear Science and Engineering*, 99 (1), pp.13-27.
- [20] SINGH, O.P., ET AL., 1994. Analysis of Passive Shutdown Capability for a Loss of Flow Accident in a Medium-Sized Liquid-Metal Fast Breeder Reactor, *Annals of Nuclear Energy*, Vol. 21. Iss. 3. Pp.165-170.
- [21] HARISH, R. ET AL., 2009. A Comparative Study of Unprotected Loss of Flow Accident in 500 MWe FBR Metal Core with PFBR Oxide Core, *Annals of Nuclear Energy*, 36, pp. 1003-1012.
- [22] SATHIYASHEELA, ET AL., 2011. Comparative study of Unprotected Loss of Flow Accident Analysis of 1000 MWe and 500 MWe Fast Breeder Reactor Metal (FBR-M) Cores and their Inherent Safety, *Annals of Nuclear Energy*, 38, pp.1065-1073.
- [23] SATHIYASHEELA, ET AL., 2013. Inherent Safety Aspects of Metal Fuelled FBR *Nuclear Engineering and Design*, 265, pp.1149-1158.
- [24] Devan, K., 2003. An Interface between CONSYST/ABBN-93 and IGCAR Diffusion Theory Codes. RPD/NDS/90, IGCAR Report.
- [25] MANTUROV, G.N., 1997. ABBN-93 Group Data Library Part I: Nuclear Data for the Calculation of Neutron and Photon Radiation Functions INDC (CCP-409), IAEA, Vienna.

- [26] WYCKOFF, H.L., 1974. GREEBLER, P., Definitions of Breeding Ratio and Doubling Time, Nuclear Technology, 21, Number 3, pp.158-164
- [27] RIYAS, A., DEVAN, K., MOHANAKRISHNAN, P., 2013. Perturbation Analysis of Prototype Fast Breeder Reactor Equilibrium Core using IGCAR and ERANOS Code Systems, Nuclear Engineering and Design, 255, pp.112-122.
- [28] MCMURRY, H.L., 1956. Perturbation Theory and Applications, AEC Research and Development Report, UK.
- [29] JOHN T.M., 1984. NEWPERT–Perturbation Code for Two-Dimensional Diffusion Equations. REDG/01150/RP-253, REDG/01150/RP-253, IGCAR Report.
- [30] RIYAS, A., MOHANAKRISHNAN, P., 2014. ULOF Transient Behaviour of Metal Fuelled FBR Cores as a Function of Core and Perturbation Method, Nuclear Engineering and Design, 278, pp.141-149.
- [31] PAHL, R.G. ET AL., 1990. Experimental Studies of U-Pu-Zr Fast Reactor Fuel Pins in EBR-II, Metallurgical Transactions A, 21, Issue 7, pp.1863-1870.
- [32] HARISH, R. ET AL., 1999. KALDIS: A Computer Code System for Core Disruptive Accident Analysis of Fast Reactors, IGC-208, IGCAR Report.

INNOVATIVE MODELLING APPROACHES FOR MOLTEN SALT SMALL MODULAR REACTORS

Paper ID #8

E. CERVI
Politecnico di Milano
Milan, Italy
Email: eric.cervi@polimi.it

S. LORENZI
Politecnico di Milano
Milan, Italy

L. LUZZI
Politecnico di Milano
Milan, Italy

A. CAMMI
Politecnico di Milano
Milan, Italy

M.E. RICOTTI
Politecnico di Milano
Milan, Italy

Abstract

The aim of the paper is to present a multiphysics approach for the analysis and the development of molten salt small modular reactors. Particular focus is devoted to the investigation of gas bubbling systems (employed for the removal of gaseous fission products and as a possible option for reactivity control) and of their effect on reactivity. In addition, fuel compressibility effects during fast, reactivity-driven transients are studied.

Both compressibility and the bubble motion in the liquid fuel cannot be described by standard single-phase, incompressible thermal-hydraulics models. To address this issue, a multiphysics OpenFOAM solver is developed, coupling a Euler-Euler model for two-phase, compressible thermal-hydraulics with a multi-group neutron diffusion model. Transport equations for the moving precursors are also implemented, to describe their motion through the system.

The proposed model is applied to the analysis of a molten salt small modular reactor, highlighting the effect of fuel compressibility and of gas bubbles on reactivity and on system dynamics. In particular, the impact of (smaller) size on these phenomena is put in evidence and the safety implications are discussed. This work constitutes a step forward in the multi-physics analysis of small modular molten salt reactors, in the optimization of their main design characteristics as well as in the assessment of the safety and feasibility of these innovative systems.

1. INTRODUCTION

Small modular reactors, deployable for single or multi-unit plants, offer the possibility to fulfil the need of a more flexible power generation for a larger basis of users and applications. In this regard, the adoption of molten salt fuel instead of conventional solid fuel can be an interesting option to achieve a higher modularity, thanks to the design simplicity of molten salt systems. In addition, molten salt reactors offer interesting characteristics of safety and sustainability, such as the possibility to be operated at atmospheric pressure (due to the high boiling temperature of molten salts), and an actinide inventory with lower radiotoxicity.

At the same time, the presence of a circulating fuel arises completely new design and technological challenges. Notably, the delayed neutron precursors are not static, as in conventional nuclear systems, but they are dragged by the circulating fuel through the reactor and the external circuits. As a consequence, the coupling between neutronics and thermo-fluid-dynamics is even stronger than in traditional reactors, since the fuel velocity field has a direct impact on the precursor distribution.

Moreover, gas (e.g., helium) bubbling systems are being considered as a possible option for the removal of gaseous fission products and for reactivity control. Being a completely new design choice, that would replace traditional control rods, accurate investigation is needed to assess the safety and the feasibility of this option. In addition, the compressibility of the liquid fuel is expected to have a strong influence on fast, reactivity-driven transients, where the finite propagation velocity of pressure waves can lead to delays in the thermal expansion reactivity feedbacks.

In the development of the SMR technology, it is relevant to highlight the possible scaling effects that may impact both the operation and the safety of the reactor. Once these effects are well-defined, provisions and innovative solutions can be undertaken in order to improve the SMR design, fully exploiting the benefits of the small modular concept. In this view, the aim of this paper is analysing the scaling effect on a molten salt reactor related to the presence of the bubbling system and to the compressibility. Although these phenomena have been studied in larger-scale molten salt reactors [1, 2, 3, 4, 5, 6, 7, 8], there is no detailed analysis of their impact in smaller reactors. Compared to larger systems, these phenomena are expected to be particularly important in small modular reactors, in which thermal expansion and void reactivity effects are more significant due to the larger neutron leakages.

Both compressibility and the bubble motion in the liquid fuel cannot be described by standard single-phase, incompressible thermal-hydraulics models. To address these peculiarities of molten salt systems, a multiphysics OpenFOAM [9] solver is developed, coupling a two-fluid model for two-phase, compressible thermal-hydraulics with multi-group neutron diffusion model. Transport equations for the moving precursors are also implemented, to describe their motion through the system.

The remainder of the work is organized as follows. In Section 2, the main design features of the investigated system are briefly described, while in Section 3 the multiphysics OpenFOAM solver for small modular molten salt reactors is presented. In Section 4, the impact of a gas bubbling system on reactivity is studied, highlighting the importance of an accurate description of the two-phase flow inside the reactor. Finally, in Section 5, fuel compressibility effects in super-prompt-critical transients are investigated. In both Sections 4 and 5, the selected small modular reactor is compared to a larger-scale molten salt reactor, to point out the impact of the system size on the investigated phenomena. Conclusions are provided in Section 6.

2. THE INVESTIGATED SYSTEM

Void and compressibility effects have been studied in a 3000 MW molten salt reactor in [1, 2, 3, 4, 5, 6]. In the paper, a rescaled version of this system is considered as representative of a small modular molten salt reactor (Fig. 1), while the 3000 MW reactor is chosen as a reference for comparison. In more details, the volume and the power of the reactor are reduced by a factor 10, keeping unchanged the operating temperature and the fuel composition (even though in a final design these specifications need to be optimized in order to reach criticality). This choice has the purpose of minimizing the differences between the small modular system considered in this work and the reference 3000 MW reactor used as comparison. In this way, the impact of the system size on void and compressibility effects can be isolated from other factors that may also have an influence (e.g., the fissile enrichment). In both cases, the gas bubbles are injected at the bottom of the system and they are removed at the top, before they can enter the heat exchanger. The main design features of the 300 MW reactor are listed in Table 1.

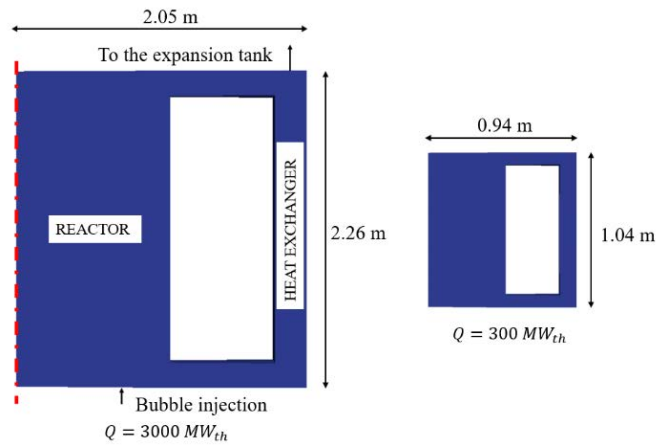


FIG. 1. 3000 MW molten salt reactor from [1, 2, 3] (left) and rescaled version investigated in the paper (right)

TABLE 1. MAIN PARAMETERS OF THE CONSIDERED SYSTEM

Nominal thermal power	300 MW(th)
Composition of the fuel (% mol.)	LiF (77.5) - ThF ₄ (20.0) - ²³³ UF ₄ (2.5)
Fuel temperature (inlet)	923 K
Fuel temperature (outlet)	1023 K
Total volume of the salt	1.8 m ³
Multiplication factor at zero void fraction	300 MW: 0.78130 - 3000 MW: 0.97629

3. THE MODELLING APPROACH

The proposed multiphysics model solves, at each time step, the system thermal-hydraulics and neutronics in two different cycles, as sketched in Fig. 2. The thermal-hydraulics sub-solver is based on the standard OpenFOAM solver “twoPhaseEulerFoam” for the compressible fluid and the bubble modelling, while neutronics are described by means of a multi-group neutron diffusion or, in alternative, to an SP3 transport [2, 3, 6, 10, 11, 12] model (in the paper, the diffusion model is selected for simplicity). The thermal-hydraulics solver finds the phase fractions, the velocity of both phases, the pressure and the temperature. Picard iterations are performed until convergence is reached for the solution of the thermal-hydraulic part of the problem. Then, the neutronics solver finds the flux, the delayed neutron precursors and the decay heat. Once the flux (and the fission power in turn) and the decay heat are known, the volumetric power source field is updated, and the energy equation is solved again. Once the new temperature and density fields of the fuel are calculated, the cross sections are updated, and the cycle is repeated with Picard iterations until convergence is reached. In addition, a certain number of external iterations between the thermal-hydraulics and the neutronics sub-solvers is performed. The external iterations are particularly important in fast transients, in which the large thermal expansions due to steep power excursions have a strong impact on the fuel velocity field.

This model can be used in two different modes:

- (a) A time-independent, criticality mode, in which the system multiplication factor is evaluated at steady-state conditions. To this aim, a power iteration routine, based on the k-eigenvalue method is implemented into the neutronics module. In this case, the main output is represented by the multiplication factor.
- (b) A time-dependent mode, for the analysis of operational as well as accidental transients. The main output provided by the transient mode is the reactor thermal power.

In both cases, the temperature and velocity fields of the fuel and of the gas bubbles, the void fraction distribution, the pressure fields and the precursor density distributions are provided as output. More details on the thermal-hydraulics and neutron diffusion models are provided in the following sections.

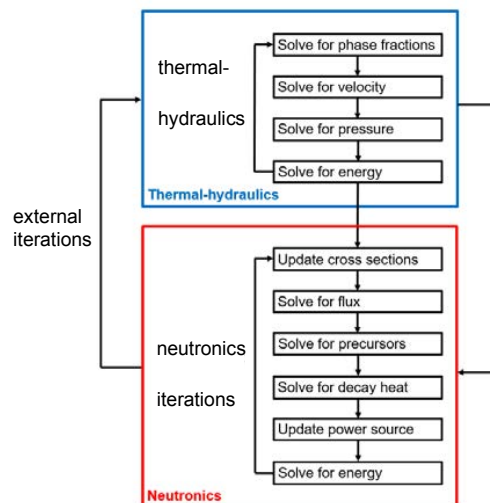


FIG. 2. The solver structure

3.2. Thermal-hydraulics model

The need for a two-phase thermal-hydraulics solver is due to the presence of gaseous fission products inside the reactor. To this aim, the “*twoPhaseEulerFoam*” solver available in the OpenFOAM library is used, which implements an Euler-Euler approach [13]. This model is widely verified and validated in many scientific and industrial applications and with different materials (not only water and air) [14, 15]. Each phase is treated as a continuum interpenetrating each other and is described with averaged conservation equations. Due to the averaging process, phase fractions are introduced into the governing equations.

The mass and momentum conservation equations for the two phases read:

$$\left\{ \begin{array}{l} \frac{\partial(\rho_j \alpha_j)}{\partial t} + \nabla \cdot (\rho_j \alpha_j \mathbf{u}_j) + S_j = 0 \\ \frac{\partial \rho_j \alpha_j \mathbf{u}_j}{\partial t} + \nabla \cdot (\rho_j \alpha_j \mathbf{u}_j \mathbf{u}_j) = \nabla \cdot \alpha_j \left[-p \mathbf{I} + (\mu + \mu_t)(\nabla \mathbf{u} + (\nabla \mathbf{u})^T) - \frac{2}{3} \mu \mathbf{I} \operatorname{div} \mathbf{u} \right] + M_j \end{array} \right. \quad (1)$$

A mass source term S_j is considered in the continuity equation to model gas injection and extraction in the reactor. The term M_j appears in the averaged momentum equations of each phase due to non-linearity, which requires closure equations. This term takes into account the momentum transfer between the two phases, due to the forces acting at the liquid-gas interface, namely the lift, the drag, virtual mass forces and turbulent dispersions. Several models are implemented into the solver to describe the inter-phase terms and to close the momentum equation [16, 17].

The energy equations for the two-phases for the “*twoPhaseEulerFoam*” read:

$$\begin{aligned} \frac{\partial \rho_j \alpha_j h_j}{\partial t} + \nabla \cdot (\rho_j \alpha_j \mathbf{u}_j h_j) + \frac{\partial \rho_j \alpha_j k_j}{\partial t} + \nabla \cdot (\rho_j \alpha_j \mathbf{u}_j k_j) = \\ = \alpha_j \frac{\partial p}{\partial t} + \frac{\alpha_j}{\rho_j c_{p,j}} \nabla \cdot ((K + K_t) \nabla h_j) + L \Delta T + \rho_j \alpha_j \mathbf{g} \cdot \mathbf{u}_j + Q_f + Q_d \end{aligned} \quad (2)$$

where L is an inter-phase heat transfer coefficient resulting from the averaging process and ΔT is the temperature difference between the two phases. Also in this case, different models are implemented in the solver and can be chosen to describe L , closing the energy equation [18].

In addition, the Lahey k- ϵ turbulence model [19] has been adopted to account for the contribution of the dispersed gaseous phase on eddy viscosity. A preliminary sensitivity analysis pointed out that the choice of different closure correlations and turbulence models has a negligible impact on results.

3.3. Neutronics model

Multi-group neutron diffusion equations are selected for the evaluation of the flux:

$$\frac{1}{v_i} \frac{\partial \varphi_i}{\partial t} = \nabla \cdot D_i \nabla \varphi_i - \Sigma_{r,i} \varphi_i + \frac{\bar{v}}{k_{eff}} \Sigma_{f,i} (1 - \beta) \chi_{p,i} \varphi_i + S_{n,i} (1 - \beta) \chi_{p,i} + S_d \chi_{d,i} + S_{s,i} \quad (3)$$

The macroscopic cross sections are evaluated by assuming a logarithmic dependence on temperature and a linear dependence on density and on the void fraction due to the helium bubbles, according to the following relation:

$$\Sigma_{i,j} = \left[\Sigma_{i,j}^o + A_{i,j} \log \frac{T_{fuel}}{T_{ref}} \right] \frac{\rho_{fuel}}{\rho_{ref,fuel}} (1 - \alpha_b) \quad (4)$$

The source terms represent the fission neutrons, the scattering neutrons and the delayed neutrons, respectively, and are evaluated as follows:

$$S_{n,i} = \frac{1}{k_{eff}} \sum_{j \neq i} \bar{v} \Sigma_{f,j} \varphi_j \quad S_d = \sum_k \lambda_k c_k \quad S_{s,i} = \sum_{j \neq i} \Sigma_{s,j \rightarrow i} \varphi_j \quad (5)$$

Due to these explicit terms, an iterative procedure among the several groups is required to achieve convergence for the neutronics description. Albedo boundary conditions are adopted at the top and bottom walls of the reactor (axial reflectors) and at the radial wall (blanket salt), in order to limit the domain of the equation set of neutronics to the fuel salt circuit only [20, 21].

The precursor balance equations include the diffusion and the transport term to allow for the fuel motion (neglecting the precursor mass transfer from the liquid to the gas phase):

$$\frac{\partial \rho_l \alpha_l c_k}{\partial t} + \nabla \cdot (\rho_l \alpha_l \mathbf{u}_l c_k) = \nabla \cdot \left(\rho_l \alpha_l \left(\frac{v}{Sc} + \frac{v_t}{Sc_t} \right) \nabla c_k \right) + \beta_k \sum_i \bar{v} \Sigma_{f,i} \varphi_i - \lambda_k \rho_l \alpha_l c_k \quad (6)$$

The Schmidt and the turbulent Schmidt numbers, Sc and Sc_T , are set to 20 and 0.85 for every group respectively, even if no data are specifically available for the diffusion of species in the MSR salt [20]. Analogous equations are provided for the decay heat precursors. In addition, a power iteration routine, based on the k-eigenvalue method, is implemented in the neutronics module of the solver for the calculation of the multiplication factor. For a more detailed description, the reader is referred to [4]. This model is verified against Monte Carlo simulation in [2, 3].

4. ANALYSIS OF THE VOID REACTIVITY EFFECT

A helium bubbling system is envisaged in the MSFR as a possible option for reactivity control, replacing the traditional control rods. Even if other control systems will be preferred, the helium bubbling will still be employed for the online removal of gaseous fission products. Therefore, the effect of the bubbly flow on reactivity needs to be carefully investigated, in order to assess the safety and the feasibility of this design choice. This is particularly true for a SMR design due to the expected greater influence of neutron leakage.

In more details, the presence of gas bubbles in the reactor causes a negative reactivity insertion into the system, due to the negative void feedback coefficient. A preliminary estimation of this contribution can be made assuming a uniform void fraction. On the other hand, the real distribution of the bubbly flow inside the reactor is not uniform, since the bubbles are transported by the fluid flow. Therefore, the void reactivity coefficient needs to be calculated accounting for the spatial and importance dependence of the void feedback, i.e., considering the real bubble spatial distribution. The developed model, thanks to the coupling between neutronics and two-phase fluid-dynamics, is suitable to this purpose.

Table 2 present the void coefficients for the 3000 MW and the 300 MW systems, evaluated with two different approaches: (i) considering the bubble spatial distribution calculated by the multiphysics solver (Fig. 3); and (ii) assuming a uniform bubble distribution with the same core-average value (i.e., modelling the void fraction as a uniform density effect). In both the cases, the void reactivity coefficient is calculated with the following formula:

$$\alpha_{void} = \frac{k(\bar{\alpha}_b) - k(0)}{\bar{\alpha}_b} \quad (7)$$

where $\bar{\alpha}_b$ is the core-average percent void fraction. These calculations are carried out with six neutron energy groups, using homogeneous group constants evaluated with the continuous energy Monte Carlo code SERPENT 2 [22]. A 2D axial-symmetric mesh with 43484 cells is used, ensuring that results are not significantly affected by further mesh refinements. The first cell wall distance y^+ is kept between 30 and 300 with typical values around 100-200, which is compatible with the adoption of wall function boundary conditions for turbulence.

TABLE 2. VOID COEFFICIENT VS. VOID FRACTION

Core average void fraction (%)	α_v in pcm/% – 3000 MW system (absolute effect in pcm)			Core average void fraction (%)	α_v in pcm/% – 300 MW SMR (absolute effect in pcm)		
	<i>Uniform bubble distribution</i>	<i>Real bubble distribution</i>	<i>bubble distribution</i>		<i>Uniform bubble distribution</i>	<i>Real bubble distribution</i>	<i>bubble distribution</i>
0.288	-154.2 (-44.4)	-341.7 (-98.4)		0.264	-363.6 (-104.7)	-735.2 (-211.7)	
0.635	-155.0 (-98.4)	-312.9 (-198.7)		0.597	-361.8 (-229.7)	-662.1 (-420.4)	
1.030	-155.7 (-160.4)	-292.9 (-301.7)		0.980	-364.9 (-375.8)	-619.6 (-638.2)	
1.468	-156.5 (229.7)	-277.4 (-407.2)		1.406	-365.7 (-536.8)	-584.6 (-858.2)	

Significant differences arise between the two approaches, pointing out that the void reactivity feedback is strongly dependent on bubble spatial distribution as well as on neutron importance effects. In more details, when the calculated bubble distribution is considered, the major part of the bubbles is concentrated in the centre of the reactor (Fig. 3), where neutron importance is higher, leading to a stronger feedback, compared to the uniform case. Moreover, it is interesting

to observe that with the “uniform” approach, the void coefficient increases at higher void fractions. In fact, higher void fractions result in more neutron leakages which in turn lead to a strong void reactivity effect. On the other hand, when the calculated bubble distribution is considered, the void coefficient decreases as the void fraction increases. This is due to the fact that higher bubble concentrations in the centre of the system reduce the neutron importance in that region, thus leading to a decrease of the marginal reactivity effect.

As expected, in the downscaled small modular reactor, the higher neutron leakages lead to a much stronger void effect. In particular, the void coefficient is about a factor 2 higher than in the 3000 MW system. In this regard, particular care supposed to be taken to operate small modular molten salt reactors at low void fractions, as a failure of the bubbling system (and the subsequent removal of the bubbles from the fuel mixture) may lead to a prompt-critical reactivity insertion. In more detail, a sudden decrease of the void fraction from 1% to 0 would result in a more than 600 pcm reactivity injection. Conversely, operation at small void fraction is expected to be feasible in a small modular reactor due to the smaller quantity of fission products in the fuel mixture. Again, it is stressed that with the considered fuel composition (see Table 1) the system is strongly subcritical and that an increase of the fissile enrichment is needed to achieve criticality at nominal conditions. Nevertheless, using the same enrichment in both the systems allows to isolate the size effect on the void coefficient, prescinding from other factors that may have an additional impact.

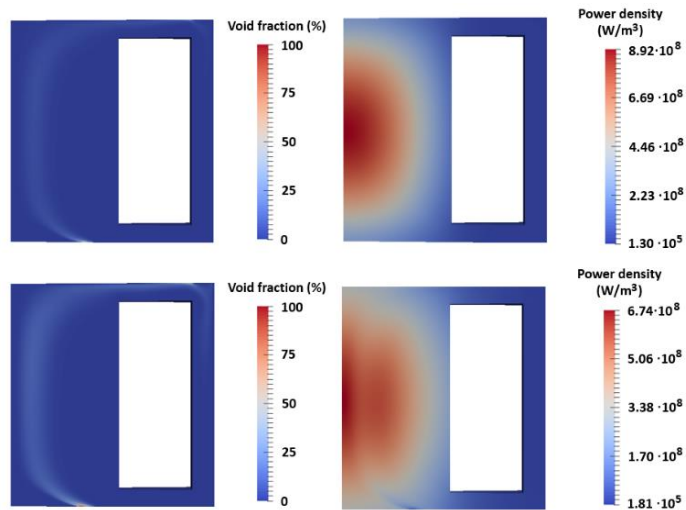


FIG. 3. Void fraction and power density distribution at 1.406% core average void fraction

5. ANALYSIS OF FUEL COMPRESSIBILITY EFFECTS

Together with the Doppler effect, the thermal expansion of fuel outside the reactor is one of the most important reactivity feedback effects in fast-spectrum MSRs [23]. While the former increases neutron absorptions by the fertile nuclei, the latter increases neutron leakages, introducing a negative reactivity into the system.

If the fuel mixture is assumed as incompressible (i.e., its density is not dependent on pressure), salt expansion is “instantaneous” (i.e., there is no delay between temperature increase and density decrease), and the expansion feedback acts promptly to reduce reactivity. On the other hand, if fuel is treated as a compressible fluid (i.e., its density is influenced by pressure), a pressure/density wave propagates through the reactor with a finite velocity, introducing a delay in the thermal expansion feedback. This effect is believed to be particularly important in fast, super-prompt-critical transients, whose characteristic times, in the order of a few milliseconds, are comparable to the propagation times of pressure waves through the system [23].

To investigate these effects, a 500 pcm reactivity insertion (which for the considered fuel composition is super-prompt-critical, since static $\beta = 310$ pcm while circulating $\beta = 120 - 150$ pcm [7]), is simulated in two different cases (gas bubbling is not considered for simplicity):

- (a) Fuel is treated as a compressible fluid, with a density given by the following relation:

$$\rho_{fuel} = \rho_0 - \beta_{th}(T - T_{ref}) + \psi(p - p_{ref}) \quad (8)$$

where $\rho_0 = 4125$ kg/m³, $\beta_{th} = 0.882$ kg/m³K and $T_{ref} = 973$ K [24]. The isothermal compressibility ψ is evaluated as:

$$\psi = \frac{\rho_{fuel}}{K_{fuel}} \quad (9)$$

where K_{fuel} is the bulk modulus of the pure salt, for which a value of 6.3 GPa can be adopted [23], while at 923 K $\rho_{fuel} = 4169$ kg/m³. In addition, it is assumed that $p_{ref} = 2$ bar in Eq. (10).

- (b) Fuel is treated as an incompressible fluid; density is evaluated with Eq. (8) assuming $\psi = 0$.

The resulting power transients are presented in Fig. 4. In the incompressible case, the power excursion is strongly underestimated with respect to the compressible case. In fact, when compressibility is considered, the thermal expansion feedback is delayed, leading to an overall weaker feedback and, as a consequence, to a stronger energy release. In more details, due to the sudden heating following the reactivity insertion, a pressure wave in the order of 10⁸ Pa is generated, leading to density increases between 2.5% and 10% of the nominal value, depending on the system size. This density increase delays the thermal expansion of the fuel. Consequently, the peak power is 7 GW in the incompressible case and 14.4 GW in the compressible case, yielding a 106% difference between the two cases.

The same effect has been studied in the 3000 MW reference system in [1], pointing out a 28% difference between the compressible and the incompressible cases. Again, the higher neutron leakages occurring in the downscaled small modular system lead to a magnification of the compressibility effect. Therefore, compared to large-scale systems, the proper modelling of fuel compressibility is even more important in small modular reactors. In fact, the incompressible approximation leads to strong underestimations of the energy release in reactivity insertion accidents, turning out to be non-conservative for the analysis of these scenarios.

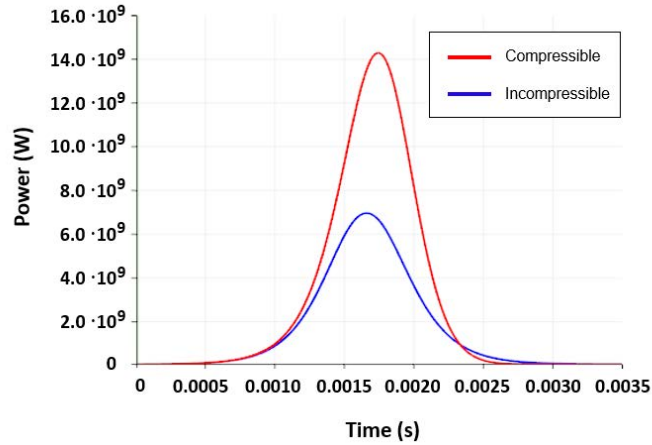


FIG. 4. Power transient in the compressible (red curve) and incompressible (blue curve) cases

6. CONCLUSIONS

In the paper, void and compressibility effects in a small modular molten salt reactor are investigated. Particular care is taken to highlight the impact of the system size on these phenomena and to put in evidence the safety concerns that may arise in small modular reactors. To this purpose, a multiphysics OpenFOAM model is proposed, coupling a two-phase, compressible thermal-hydraulics model with a multi-group neutron diffusion model.

The void reactivity coefficient of gas bubbles in a 300 MW small modular reactor is evaluated on the basis of the bubble spatial distribution calculated by the multiphysics solver. Important differences are highlighted with respect to simulations carried out with uniform bubble distributions. These results point out that the void reactivity feedback is strongly dependent on spatial as well as on neutron importance effects.

In addition, a super-prompt-critical transient is simulated i) considering the fuel mixture compressibility, and ii) approximating the fuel mixture as incompressible. This analysis shows that approaches neglecting the fuel compressibility may significantly underestimate the energy release resulting from super-prompt-critical reactivity insertions.

The investigated 300 MW small modular reactor is compared to a larger 3000 MW system, in order to point out the impact of the reactor size on the described effects. Even though these phenomena are observed in molten salt reactors in general, in small modular reactors they are significantly magnified by the larger neutron leakages, that lead to stronger void and density reactivity feedbacks.

As a consequence, the bubble distribution in the fuel mixture and the liquid fuel compressibility needs to be modelled and described with accuracy. In fact, standard single-phase and compressible fluid-dynamics models would be strongly non-conservative for the analysis of many accidental scenarios, such as failures of the gas bubbling system or super-prompt-critical reactivity insertions. This is particularly true in smaller systems, where reduced size magnifies both void as well as compressibility effects. Therefore, compared to simpler state-of-art-approaches, the proposed tool constitutes a significant improvement in the modelling of molten salt SMRs. In the light of these results, the present work constitutes a step forward in the multi-physics analysis of small modular molten salt reactors, allowing for more reliable assessment of the safety and feasibility of these innovative systems.

REFERENCES

- [1] CERVI, E., LORENZI, S., CAMMI, A., LUZZI, L., Development of a multiphysics model for the study of fuel compressibility effects in the Molten Salt Fast Reactor, *Chem. Eng. Sci.* **193** (2019) 379-393.
- [2] CERVI, E., LORENZI, S., CAMMI, A., LUZZI, L., Development of an SP3 neutron transport solver for the analysis of the Molten Salt Fast Reactor, *Nucl. Eng. Des.* **346** (2019) 209-219.
- [3] CERVI, E., LORENZI, S., LUZZI, L., CAMMI, A., Multiphysics analysis of the MSFR helium bubbling system: A comparison between neutron diffusion, SP3 neutron transport and Monte Carlo approaches, *Ann. Nucl. Energy* **132** (2019) 227-235.
- [4] CERVI, E., LORENZI, S., CAMMI, A., LUZZI, L., “An Euler-Euler multi-physics solver for the analysis of the helium bubbling system in the MSFR”, NENE 2017 26th International Conference Nuclear Energy for New Europe, Bled, Slovenia (2017).
- [5] CERVI, E., LORENZI, S., CAMMI, A., LUZZI, L., “Analysis of the effect of fuel compressibility on super-prompt-critical dynamics of the Molten Salt Fast Reactor”, International Conference on Reactor Physics paving the way to more efficient systems (PHYSOR 2018), American Nuclear Society, Cancun, Mexico (2018).
- [6] CERVI, E., LORENZI, S., LUZZI, L., CAMMI, A., “Analysis of the Void Reactivity Effect in the Molten Salt Fast Reactor: Impact of the Helium Bubbling System”, Fourth International Conference on Physics and Technology of Reactors and Applications (PHYTRA4), Marrakech, Morocco (2018).
- [7] AUFIERO, M., BROVCHENKO, M., CAMMI, A., CLIFFORD, I., GEOFFROY, O., HEUER, D., LAUREAU, A., LOSA, M., LUZZI, L., MERLE, E., RICOTTI, M.E., ROUCH, H., Calculating the effective delayed neutron fraction in the Molten Salt Fast Reactor: Analytical, deterministic and Monte Carlo approaches, *Ann. Nucl. Energy* **65** (2014) 78-90.
- [8] HU, T., CAO, L., WU, H., DU, X., HE, M., Coupled neutronics and thermal-hydraulics simulation of molten salt reactors based on OpenMC/TANSY, *Ann. Nucl. Energy* **109** (2017) 260-276.
- [9] OpenFOAM Documentation, available at <http://www.openfoam.org/docs/> (2013).
- [10] CERVI, E., LORENZI, S., LUZZI, L., CAMMI, A., An OpenFOAM solver for criticality safety assessment in dynamic compression events, *ANS Transactions* 119 (2018) 855-858.
- [11] CERVI, E., CAMMI, A., An Arbitrary Lagrangian Eulerian solver for shock imploding fissile materials, *ANS Transactions* 121 (2019) 763-766.
- [12] CERVI, E., CAMMI, A., A Coupled Neutronics Shock Physics Solver: Implementation of an SN Neutron Transport Module, *ANS Transactions* 121 (2019) 767-770.
- [13] RUSCHE, H., Computational Fluid Dynamics of Dispersed Two-Phase Flows at High Phase Fractions, PhD thesis (2002).
- [14] PANDA, S.K., SINGH, K.K., SHENOY, K.T., BUWA, V.V., Numerical simulations of liquid-liquid flow in a continuous gravity settler using OpenFOAM and experimental verification, *Chem. Eng. J.* **310** (2017) 120-133.
- [15] KOPSCH, T., MURNANE, D., SYMONS, D., Computational modelling and experimental validation of drug entrainment in a dry powder inhaler, *Int. J. Pharm.* **553** (2018) 37-46.
- [16] GIDASPOW, D., 1994. Multiphase flow and fluidization, Academic Press, New York.
- [17] ENWALD, H., Peirano, E., Almstedt, A.E., Eulerian Two-Phase Flow Theory Applied to Fluidization, *Int. J. Multiphase Flow* **22** (1996) 21-66.
- [18] RANZ, W.E., MARSHALL, W.R., Evaporation from droplets, *Chem. Eng. Progress* **48** (1952) 173-180.

- [19] LAHEY, R.T., The simulation of multidimensional multiphase flows, Nucl. Eng. Des. **235** (2005) 1043-1060.
- [20] AUFIERO, M., CAMMI, A., GEOFFROY, O., LOSA, M., LUZZI, L., RICOTTI, M.E., ROUCH, H., Development of an OpenFOAM model for the Molten Salt Fast Reactor transient analysis, Chem. Eng. Sci. **111** (2014) 78-90.
- [21] FIORINA, C., HURSIN, M., PAUTZ, A., Extension of the GeN-Foam neutronic solver to SP₃ analysis and application to the CROCUS experimental reactor, Ann. Nucl. Energy **101** (2017) 419-428.
- [22] LEPPÄNEN, J., PUSA, M., VIITANEN, T., VALTAVIRTA, V., KALTIAISENAHO, T., The Serpent Monte Carlo code: Status, development and application in 2013, Ann. Nucl. Energy **82** (2015) 142-150.
- [23] AUFIERO, M., RUBIOLO, P., FRATONI, M., 2017. Monte Carlo/CFD coupling for accurate modelling of the delayed neutron precursors and compressibility effect in Molten Salt Reactors, ANS Transaction 116 (2017).
- [24] IGNATIEV, V.V., FEYNBERG, O., MERZLYAKOV, A., TOROPOV, A., "Progress in development of MOSART concept with Th support", Proceedings of ICAPP '12, Chicago, USA, (2012).

T. TAKATA
 Japan Atomic Energy Agency
 Narita/O-arai, Japan
 Email: takata.takashi@jaea.go.jp

M. AOYAGI
 Japan Atomic Energy Agency
 Narita/O-arai, Japan

M. SONEHARA
 Japan Atomic Energy Agency
 Narita/O-arai, Japan

Abstract

Sodium fire is one of the key issues for plant safety of sodium-cooled fast reactor (SFR) regardless of its size. In general, a concrete structure, which includes free and bonding water inside, is used in a reactor building. Accordingly, water vapor will release from the concrete during sodium fire incident due to temperature increase resulting in a hydrogen generation even in a dry air condition. Since a surface area ratio of concrete wall per compartment volume will increase in accordance with a decrease of the dimension of the compartment, which corresponds to a small and medium sized or modular reactor (SMR), the probability of hydrogen generation may increase due to an increase of a concentration of water vapor that will be released from the concrete. A numerical investigation of a small leakage sodium pool fire has been carried out by changing a dimension of compartment. Furthermore, numerical challenges to enhance a prediction accuracy of hydrogen generation during sodium fire has also been discussed in the paper.

1. INTRODUCTION

A chemical reactivity of liquid sodium, such as sodium fire and sodium-water reaction, is one of the key issues for plant safety of sodium cooled fast reactor (SFR). In Japan Atomic Energy Agency (JAEA), both experimental and numerical researched of the chemical reactivity have been carried out. Figure 1 shows numerical tools developed in JAEA for sodium fire investigation.

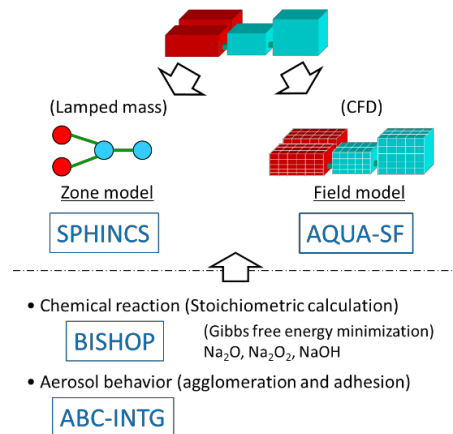


FIG. 1. Numerical tools for sodium fire developed in JAEA

A lamped mass model (zonal approach) is applied in SPHINCS code [1] for fast running and design tool. In AQUA-SF code [2], a coupling of multi-dimensional CFD and sodium fire has been carried out. The same concept of spray and pool combustion models are implemented to SPHINCS and AQUA-SF codes. Both codes include subprogram of BISHOP and ABC-INTG. A chemical equilibrium is calculated based on the Gibbs free energy minimization method in BISHOP [3]. An aerosol behaviour, such as an agglomeration and adhesion, is evaluated in ABC-INTG [4].

A chemical reaction of water vapor and liquid sodium has also been considered in the spray and pool combustion model due to existence of moisture in a typical Japanese climate. Furthermore, a concrete includes free and bonding water and water vapor will release to a circumjacent atmosphere when it is heated up. Accordingly, water vapor release model has been implemented in the codes as well.

In sodium fire incident, hydrogen will be generated when water vapor reacts with sodium. If there are plenty of oxygen in a compartment where sodium fire occurs, a recombination with oxygen will take place to form water vapor resulting in a low concentration of hydrogen. However, it remains when oxygen concentration decreases due to sodium fire. In a small and medium sized or modular reactor (SMR) of sodium-cooled fast reactor (SFR), a compact compartment will be designed. Accordingly, hydrogen risk may increase caused by a water vapor release from concrete even in a dry air condition.

In the paper, a sodium pool fire under a comparative small leakage, which is a most probable scenario regardless of reactor size, has been investigated numerically using SPHINCS code and challenges for enhancing a prediction accuracy of hydrogen concentration has been discussed.

2. NUMERICAL MODELS IN SPHINCS

2.1. Pool combustion model

As a pool combustion model, a flame sheet concept (Fig.2), in which an infinite thin flame is assumed and mass and energy balance at the flame is considered, is applied in SPHINCS code.

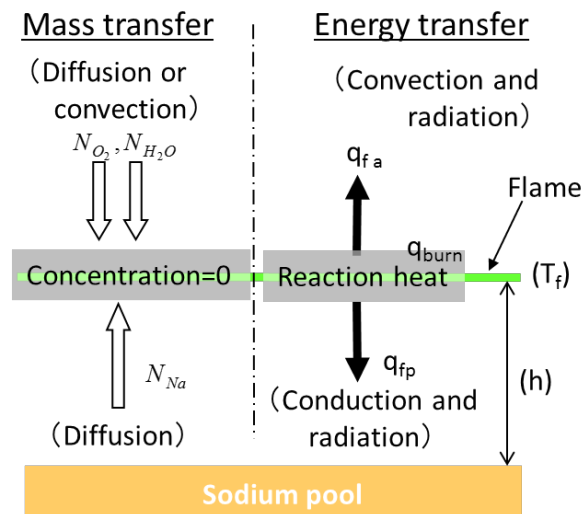


FIG. 2. Flame sheet concept

The mass and energy conservations are obtained as below.

$$N_{Na} = \sum_j \frac{N_j}{i_j} \text{ (formassflux)} \quad (1)$$

$$q_{burn} = q_{fa} + q_{fp} \text{ (forenergyflux)}$$

Here, N is mass flux, and q is energy flux. The subscripts b, g and p mean the burning, the atmospheric gas and the sodium pool respectively, i is the stoichiometric coefficient that is calculated using BISHOP. The subscript j means oxygen (O_2) or water vapor (H_2O). The mass flux of sodium and the reactant can be estimated by

$$N_{Na} = \frac{C_{Na}D_{Na}}{l} \ln \frac{P}{P - P_{Na}^{sat}} \quad (2)$$

$$N_j = \left(\frac{x_j}{1 - x_j} \right) \frac{C_g D_j}{l} Sh_j$$

Here, C, D are the molar concentration and the diffusivity respectively. P and P^{sat} is the absolute pressure and the saturation pressure respectively. l is the height of flame from the pool surface, and x is the molarity of the reactant. Sh is the Sherwood number and can be estimated by Eq. (3) based on the analogy between heat and mass transfers in natural convection [5] and the height of the compartment is used as a characteristic length in Eq. (3) considering the consistency in the natural heat transfer between the flame and an ambient gas.

$$Sh_j = 0.14(Gr \times Sc_j)^{1/3} \quad (3)$$

Energy fluxes from the pool to flame and from an ambient gas to flame are respectively determined by

$$q_{fa} = q_{fa}^{conv} + q_{fa}^{rad} = \frac{Nu\lambda}{d} (T_f - T_g) + \sigma \varepsilon_g (T_f^4 - T_g^4) \quad (4)$$

$$q_{fp} = q_{fp}^{cond} + q_{fp}^{rad} = \lambda \left. \frac{dT}{dz} \right|_{flame} + \sigma \varepsilon_p (T_f^4 - T_p^4)$$

Here, ε is the emissivity, and σ is the Stefan-Boltzmann constant. The emissivity is set as an input condition ($\varepsilon_g=0.65$ and $\varepsilon_p=0.5$, defined from results of previous studies). The Nusselt number in Eq. **Error! Reference source not found.** are determined by Eq. **Error! Reference source not found.** (the same analogy of heat and mass transfer). Note that, in addition to this, the rate of generated aerosol dropping onto the pool is also needed as an input (The initial rate is set to 0.75, according to previous work [6]). This is because a heat transfer evaluation of energy flux (q_{fp}) from flame to the pool (the right side in Eq. **Error! Reference source not found.**) takes energy transferred by the aerosol dropping into account [2]. Finally, Eq. **Error! Reference source not found.** will be the functions of the flame height l and the flame temperature T_f , which are solved by using Newton-Raphson method.

An enlargement of sodium pool area is also considered in the code. The pool area (part of floor) can be segmented into several mesh with one dimensional cylindrical coordinate. The pool area is evaluated so as to keep a height of liquid sodium constant in each mesh. The height is set based on a constant input or calculated from a contact angle of liquid sodium. In the paper, a constant value of 0.01m is applied based on the previous work [1]. It is also noted that sodium pool will not be enlarged when liquid sodium in each cell becomes short in height of 0.01m because of the combustion.

2.2. Chemical reaction and recombination ratio of hydrogen

In SPHINCS code, an infinite reaction rate is assumed and a chemical equilibrium of Na, O₂, N₂, H₂, H₂O, NaOH, Na₂O, Na₂O₂ under a constant pressure is calculated based on the Gibbs free energy minimization method (BISHOP subprogram). In an equilibrium state, hydrogen (H₂) never co-exists with oxygen (O₂) because of the chemical potential of water (H₂O). On the other hand, an energetic barrier of the reaction (H₂ + 1/2O₂ -> H₂O) is comparatively high resulting in co-existence of H₂ and O₂ in an actual phenomenon. In the present investigation, a recombination ratio (=0.9) is applied empirically in SPHINCS. It is also mentioned that hydrogen reaction with oxygen is omitted in an atmospheric reaction model, where reactions of sodium oxide aerosol, oxygen and water vapor are calculated, in the code.

2.3. Water vapor release from concrete

Considering the previous research [7], the following release fraction is set in the paper.

Concrete temperature (°C)	Release fraction (wt%)
30	0.0
80	0.1
200	1.5
1000	3.0

In Table 1, a release fraction of steady state is estimated. An instantaneous water vapor release to an adjacent atmosphere is assumed in SPHINCS code as well and the release fraction is calculated based on Table 1 by applying a linear interpolation.

3. NUMERICAL INVESTIGATION OF SODIUM POOL FIRE INCIDENT

In the numerical investigation, a comparative small pool fire with different volume of compartment (1000m³ and 500m³) is carried out with/without water vapor release from concrete structures (side wall and ceiling) in order to evaluate hydrogen risk in SMR of SFR.

3.1. Numerical condition

Figure 3 shows a schematic of compartment. Two type of dimension (1000 m³:10 mW×20 mD×5 mH, 500 m³:10 mW×10 mD×5 mH) is applied as a compartment. As shown in Fig. 3, a steel liner is covered on the floor to eliminate sodium-concrete reaction and thus no water vapor release is assumed from the floor to the compartment in each computation. A dry air (volumetric fraction of N₂ and O₂ are 0.79 and 0.21 respectively) condition is assumed and the initial temperature is set to 35°C both at the atmosphere and the concrete structure. No ventilation is assumed for simplicity.

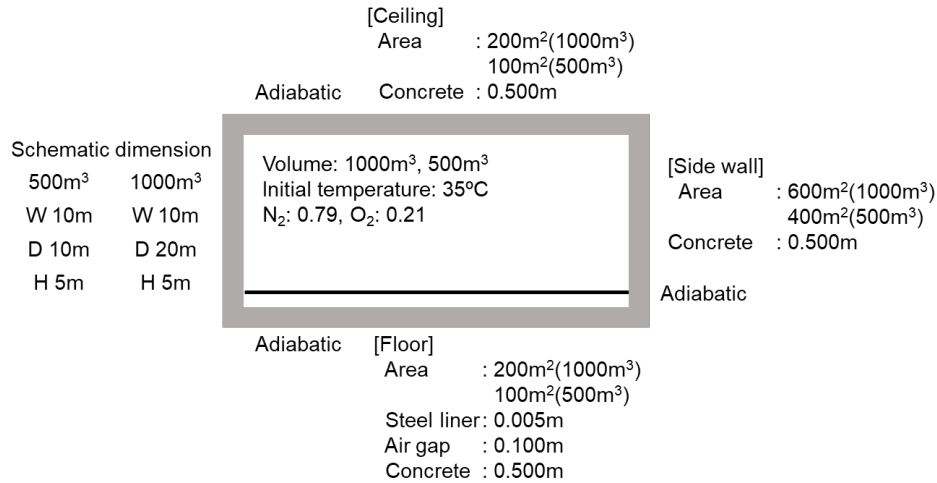


FIG. 3. Schematic of compartment

With regard to a sodium leakage, a comparative small leakage rate of 0.05kg/s with leakage temperature of 500°C is assumed. The leakage duration is set to 2hr and total amount of leakage is 360kg. The leakage rate is similar, but the total amount is about half comparing with that in Japanese prototype fast breeder reactor MONJU accident in 1994 [8]. In the analysis, leaked sodium piles upon the steel liner directly and thus only the pool combustion is considered. The total analytical duration is set to 10hr. Table 2 summarizes the numerical condition.

TABLE 2. NUMERICAL CONDITION

	No water vapor release		Water vapor release	
Volume (m ³)	1000	500	1000	500
Side wall (m ²)	600	400	600	400
Ceiling (m ²)	200	100	200	100
Floor (m ²)	200	100	200	100
Initial temperature (°C)	35			
Volume fraction of N ₂ , O ₂ (-)	N ₂ :0.79, O ₂ :0.21			
Sodium leakage rate (kg/s)	0.05			
Temperature (°C)	500			
Duration (hr)	2.0			
Water vapor release from concrete	off		on	

3.2. Result and Discussion

3.2.1. No water vapor release from concrete

The computational result is shown in Fig. 4 and the maximum and minimum values are summarized in Table. 3. As shown in Fig. 4 (a) and (b) and Table 3, the maximum gas temperature and pressure increase slightly as the compartment becomes small. In both cases, the maximum values of the gas temperature and pressure seems to be lower than enough from structural integrity's viewpoint.

Since the total amount of oxygen in 500m² volume is insufficient to run out all leaked sodium (Fig. 4(e)), approximately 100kg of sodium remains unburnt (Fig. 4(d)). Therefore, the pool area is larger in case of 500m³ than that in 1000m³ and the average pool temperature decreases in the small compartment case (500m³). As a result, a slight increase of the maximum values is investigated. The maximum surface temperature of the concrete structures is lower than 70°C (Fig. 4(f) and Table 3) and thus it will be concluded that the structural integrity is confirmed in both compartments.

TABLE 3. SUMMARY OF RESULT (NO WATER RELEASE FROM CONCRETE)

	1000 m ³	500 m ³
Maximum values		
Gas temp. (°C)	114.8	127.0
Gas pressure (kPa gage)	15.9	17.9
Concrete surface temp. of side wall (°C)	65.3	66.2
Concrete surface temp. of ceiling (°C)	67.4	68.3
Pool area (m ²)	10.2	18.4
Average pool temperature (°C)	641.7	615.2
Minimum value		
Oxygen concentration (vol%)	7.5	0.002

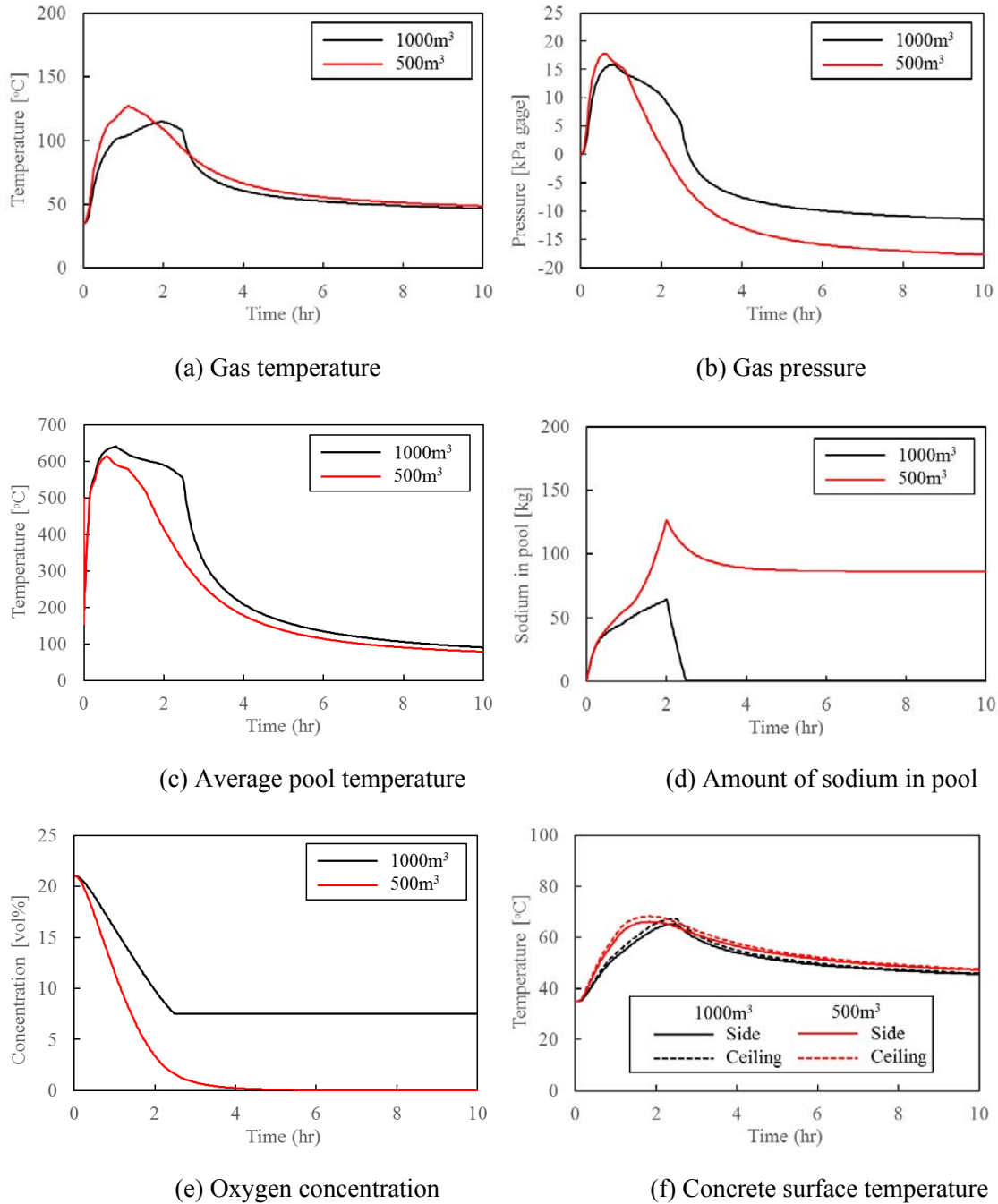


FIG. 4. Computational result (no water vapor release from concrete)

As seen in Fig. 4(b), a negative pressure (gage) is evaluated approximately 2hr after the leakage in both cases. In a practical compartment, a ventilation caused by the pressure difference will take place and sodium fire may continue in the small compartment (500m³). However, the maximum values appear at less than one hour from the leakage. Hence, the ventilation will not affect the maximum values significantly.

3.2.2. Water vapor release from concrete

Table 4 and Fig. 5 summarize the computational result. Comparing with no water vapor release (Table 3), the maximum values of temperature and pressure increases due to water vapor release. On the other hand, the pool area decreases in size because of the reaction with water vapor. As seen in Fig. 5(d), the leaked sodium runs out in the small compartment case.

TABLE 4. SUMMARY OF RESULT (WATER RELEASE FROM CONCRETE)

	1000 m ³	500 m ³
Maximum values		
Gas temp. (°C)	120.4	136.1
Gas pressure (kPa gage)	18.2	21.1
Concrete surface temp. of side wall (°C)	68.5	73.2
Concrete surface temp. of ceiling (°C)	70.8	75.6
Pool area (m ²)	9.5	14.7
Average pool temperature (°C)	647.0	621.2
Concentration of water vapor (vol%)	6.69	5.88
Concentration of hydrogen (vol%)	0.15	4.11
Total amount of released water vapor (kg)	84.0	66.8
Minimum value		
Oxygen concentration (vol%)	9.19	0.52

As concerns the maximum temperature and pressure, the structural integrity of the compartment seems to be confirmed although the additional water vapor is released from the concrete. However, the hydrogen concentration increases significantly in the small compartment case as seen in Table 4 and Fig. 5(f). This is attributed to the fact that the recombination of hydrogen suppresses when oxygen concentration decreases a certain level. In addition to the recombination of hydrogen, oxygen reacts with sodium in a sodium fire incident. And alkali metal has higher reactivity with oxygen than hydrogen. When oxygen exists sufficiently enough to react with sodium, the recombination will also take place resulting in a low concentration of hydrogen like the 1000m³ compartment case. As seen in Fig. 5 (f), hydrogen diminishes due to the recombination before 1.5hr from the leakage in the small compartment case. However, hydrogen increases significantly because of the suppression of the recombination caused by rapid decrease of oxygen concentration (see Fig. 5(e)).

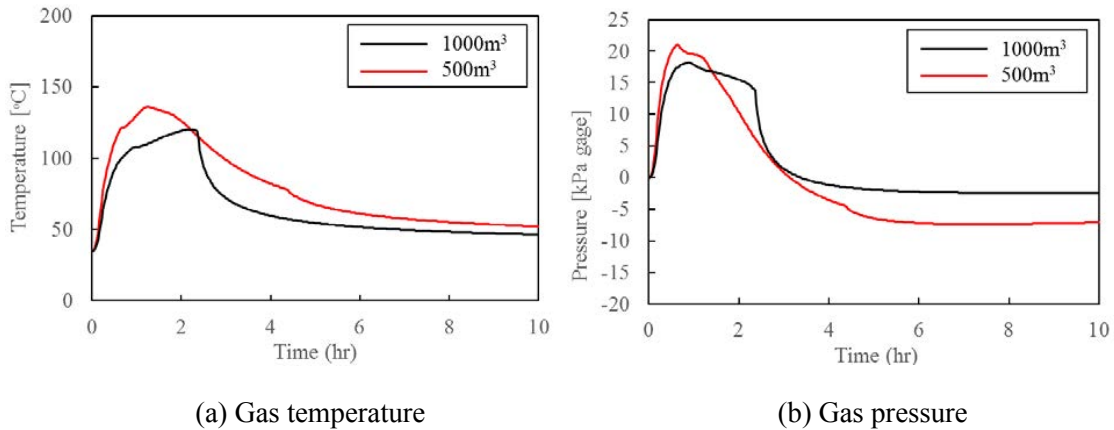
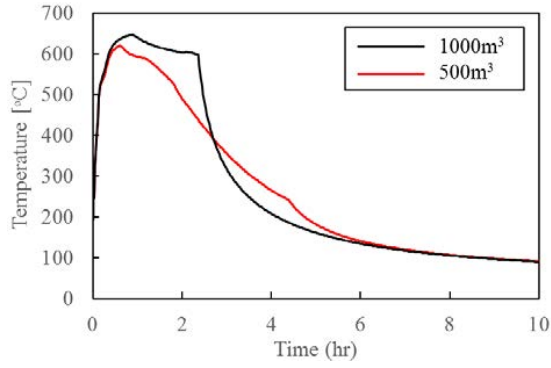
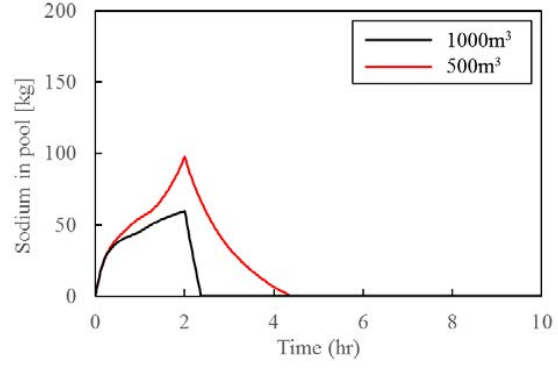


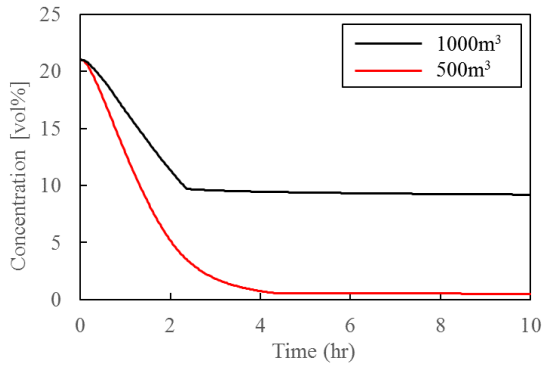
FIG. 5. Computational result (water vapor release from concrete) (1/2)



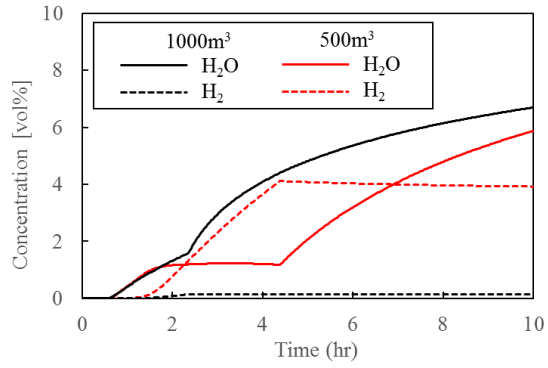
(c) Average pool temperature



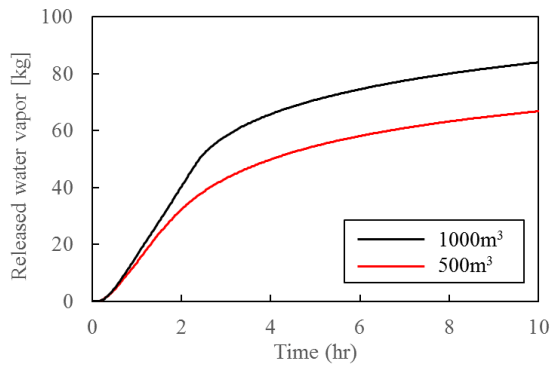
(d) Amount of sodium in pool



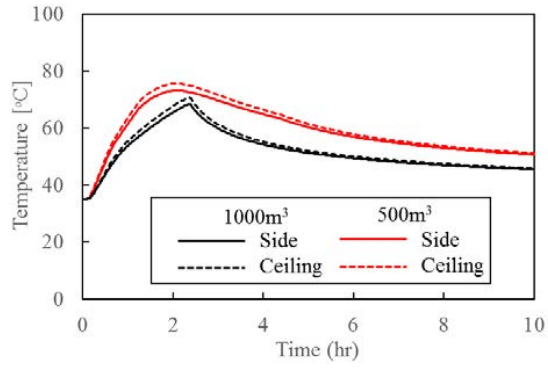
(e) Oxygen concentration



(f) Water vapor and hydrogen concentration



(g) Total amount of released water vapor



(h) Concrete surface temperature

FIG. 5. Computational result (water vapor release from concrete) (2/2)

As shown in Table 4, 4.11 vol% of hydrogen concentration will not be negligible, and one has to take care a hydrogen risk such as a hydrogen spreading and combustion in other compartments. In general, oxygen concentration decreases faster as the volume of compartment decreases. Accordingly, it might be said that the hydrogen risk with a small compartment with concrete structure is an additional key issue in a sodium fire incident of SMRs.

It is also mentioned that the following countermeasure will be effective to suppress an increase of hydrogen.

- Limitation of pool area and sodium drain;
As seen in Fig. 5(f), hydrogen will generate until sodium runs out and the generation rate is proportion to the pool area. Hence, a segmentation of floor liner into small partitions and put a drain line will be efficient.
- Injection of inert gas or ventilation;
An injection of inert gas to the compartment has an advantage of decreasing gas temperature and diluting hydrogen and water vapor concentrations as well as suppression of chemical reaction. In general, ventilation is prohibited in case of sodium fire. However, it will be effective from the viewpoint of decrease of hydrogen concentration.
- Thermal insulation coverage or isolation of water vapor;
A thermal insulation coverage on the concrete structure decreases a water vapor release. However, the coverage will result to an increase of gas temperature. Therefore, a partial coverage has less effective to the suppression. An isolation of water vapor using such as a steel liner is quite effective.

4. CHALLENGES IN SMR

As mentioned in Chap. 3, hydrogen generation due to water vapor release from concrete structure will be an additional key issue in sodium fire incident of SMRs. However, current numerical models and validation of them has some challenges.

- Water vapor release model;
As mentioned in Cahp.2, a simplified steady state release model is applied based on an experimental database of the release fraction. A development of transient model, in which a diffusion of water vapor inside a concrete structure is also taken into account, will be necessary to enhance the prediction accuracy. Furthermore, experimental database of the release fraction with various types of concrete will be required. As shown in the paper, hydrogen generation is much affected by the water vapor release although the maximum concrete temperature is lower than 80°C that corresponds to lower than 0.1wt% of the release fraction (Table 1). A detail database including uncertainty will be necessary.
- Recombination ratio;
Although the recombination ratio has less effective when oxygen concentration decreases to a certain level, it is still key parameter to evaluate the hydrogen concentration. Especially, it is an essential factor in a lamped mass model. An experimental database of the ratio under a sodium fire condition will be required as well as a development of mechanistic and theoretical model.

- Integrated test of sodium fire with high concentration of water vapor;
Currently, there is a little experimental research of sodium fire with high concentration of water vapor. When water vapor releases from concrete structure, a high concentration of water vapor may appear even in a dry air condition. From the viewpoint of code V&V for various sodium fire phenomenon, carrying out of an integrated sodium fire test with high concentration of water vapor and sharing the information internationally will be of importance.

5. CONCLUSION

In sodium fire incident, hydrogen will be generated when water vapor reacts with sodium. If there are plenty of oxygen in a compartment where sodium fire occurs, a recombination with oxygen will take place to form water vapor resulting in a low concentration of hydrogen. However, it remains when oxygen concentration decreases due to sodium fire. In a small and medium sized or modular reactor (SMR) of sodium-cooled fast reactor (SFR), a compact compartment will be designed. Accordingly, hydrogen risk may increase caused by a water vapor release from concrete even in a dry air condition.

In the paper, a sodium pool fire under a comparative small leakage, which is a most probable scenario regardless of reactor size, has been investigated numerically using SPHINCS code. As a result, it is demonstrated that a significant increase of hydrogen concentration occurs in case of the small compartment when water vapor is released from concrete structure, although a structural integrity seems to be confirmed in terms of the maximum temperature and pressure. It might be said that the hydrogen risk with a small compartment with concrete structure is an additional key issue in a sodium fire incident of SMRs.

Since the numerical approach related to hydrogen behaviour has not been well established in sodium fire incident, challenges in SMRs has also been discussed in terms of the water vapor release model, the recombination ratio and the necessity of integrated sodium fire test with high concentration of water vapor.

REFERENCES

- [1] YAMAGUCHI, A., AND TAJIMA Y., “Validation study of computer code SPHINCS for sodium fire safety evaluation of fast reactor”, *Nuclear Engineering and Design*, 219(1), (2003), 19-34.
- [2] TAKATA, T., YAMAGUCHI, A., MAEKAWA, I., “Numerical investigation of multi-dimensional characteristics in sodium combustion”, *Nuclear Engineering and Design*, 220(1), (2003), 37-50.
- [3] OKANO, Y., “Development of Bi-Phase Sodium-Oxygen-Hydrogen Chemical Equilibrium Calculation Program (BISHOP) using Gibbs Free Energy Minimization Method”, JNC TN9400 99-071, 1999 (in Japanese).
- [4] MIYAHARA, S., MITSUTUKA, N., AND OBATA, H., “Development and Validation of ABC-INTG code”, PNC TN943 84-08, 1984.
- [5] FISHENDEN, M., SAUNDERS, O.A., “Introduction to Heat Transfer”, Clarendon Press, p.180, (1959).
- [6] TAKATA, T AND YAMAGUCHI, A., “Development and Validation of Multi-Dimensional Sodium Combustion Analysis Code AQUA-SF”, JNC TN9400 2000-065, 2000 (in Japanese).
- [7] OKABE, A., OHNUKI, K., KIKUCHI, H., ET AL., “Sodium Combustion Analysis for the detail design of prototype fast breeder reactor MONJU”, JNC TN2400 2003-005, 2004 (in Japanese).
- [8] UCHIYAMA, N., TAKAI, T., NISHIMURA, M., ET AL., “Investigation for the sodium leak in Monju – sodium fire test-II–”, PNC TN9410 97-051, 1997 (in Japanese).

ALFRED PROTECTED LOSS OF FLOW ACCIDENT EXPERIMENT IN CIRCE FACILITY

Paper ID #26

FABIO GIANNETTI, PIERDOMENICO LORUSSO, VINCENZO NARCISI,
GIANFRANCO CARUSO
CIRTEN - “Sapienza” University of Rome
Rome, Italy
Email: fabio.giannetti@uniroma1.it

ANTONIO NAVIGLIO, ULISSE PASQUALI
Servizi di Ricerche e Sviluppo (SRS)
Rome, Italy

MICHELE FRIGNANI, ALESSANDRO ALEMBERTI
Ansaldo Nucleare
Genova, Italy

MARIANO TARANTINO, DANIELE MARTELLI
Italian National Agency for New Technologies, Energy and Sustainable Economic
Development,
FSN-ING
C.R. ENEA Brasimone
Camugnano, Italy

Abstract

Lead cooled Fast Reactors (LFR) are one of the most promising nuclear technologies, able to meet the goals set out by the Generation IV International Forum (GIF) and playing an important role in the international context. ALFRED (Advanced Lead-cooled Fast Reactor European Demonstrator) is the European Technology Demonstration Reactor for the LFR technology and aims to bridge the gap between the research and development effort and the industrial deployment.

Fostering ALFRED CONstruction, an international consortium under the leadership of Ansaldo Nucleare with ENEA (IT) and ICN (Ro), is pursuing the re-design of the European Technology Demonstration Reactor in addition to the definition of an R&D and licensing roadmap. Fostering ALFRED CONstruction gathers European organizations who share the objective of making ALFRED the prototype of a viable competitive LFR commercial unit in the small modular reactors segment, by 2035-2040. Among these organizations, CIRTEN (IT) and SRS (IT) takes part as Supporting Organization to Fostering ALFRED CONstruction to enhance the R&D activities devoted to ALFRED. In this frame an R&D activity has been carried out at the ENEA Brasimone Research Center, aiming at investigating the thermal-hydraulic behaviour of an innovative Steam Generator (SG) based on a double wall bayonet tubes concept.

For this purpose, a dedicated Test Section (TS) named HERO (Heavy liquid mEtal pRessurized water cOoled tubes) has been developed and installed in the pool-type integral effect facility, LBE (Lead-Bismuth Eutectic) cooled, named CIRCE (CIRcolazione Eutettico). The HERO steam generator is a mock-up (full length and scaled in volume) which represents the ALFRED Steam Generator (SG), and it consists of seven double wall bayonet tubes.

In this configuration, the CIRCE-HERO facility has been involved in a set of experimental tests in the framework of the HORIZON2020 SESAME (Simulations and Experiments for the Safety Assessment of MEtal cooled reactors) European project. An integral test experiment has been designed and realized to reproduce a Protected Loss of Flow Accident (PLOFA) occurring with the facility operated in nominal steady-state conditions for both primary and secondary side.

The transient test is obtained reducing the thermal power supplied by the Fuel Pin Simulator (FPS), accordingly to a characteristic heat decay curve, while the loss of the primary pump is simulated by the reduction of the argon injection in the primary loop. The loss of the heat sink is simulated reducing the HERO feedwater in the secondary loop, simulating the activation of the decay heat removal system.

The aim of the paper is to discuss the main results achieved from the performed experimental test, investigating on the thermal-hydraulic performances of the HERO SG in operating conditions and characterizing the system behaviour during this reference accidental scenario, using all obtained data to assess the RELAP5-3D[©] system code for Heavy Liquid Metal (HLM) reactors focused on the ALFRED design. The paper summarizes the post-test activity performed for the experimental test, respecting the main trend for all thermal-hydraulics phenomena analysed and highlighting a good agreement between simulations and experiment for all the primary circuit physical quantities monitored.

1. INTRODUCTION

As part of the R&D experimental program developed by ENEA in the frame of the liquid metal technologies development for GEN-IV LFR [1], an experimental and numerical activity has been completed, involving the CIRCE facility at ENEA Brasimone Research Centre. One of the scopes of the CIRCE facility is to support the HLM technology development, and, in particular, the ALFRED design. As explained in [2], ALFRED could be considered as a prototype for a LFR commercial unit in the small modular reactor segment. The facility was refurbished with the implementation of a mock-up of a Steam Generator Bayonet Tube (SGBT), in a relevant configuration for ALFRED steam generator (SG) [3] (scaled 1:1 in length). In the framework of the Fostering ALFRED CONstruction consortium activities, into the definition of an R&D and licensing roadmap, an important need is the validation of the tools used for the safety analysis (SA). In this frame an R&D activity has been carried out at the ENEA Brasimone Research Center, aiming at investigating the thermal-hydraulic behaviour of the SGBT concept and the pool thermal-hydraulic, both in nominal and transient conditions. The experimental data was also used for the validation of the thermal-hydraulic safety analysis tools, with a focus for one of the codes probably adopted for the future ALFRED reactor SA, RELAP5-3D[©] [4].

2. CIRCE-HERO EXPERIMENTAL TEST PLOFA #1

A test matrix consisting of three PLOFA scenarios has been performed on CIRCE facility in HERO configuration, in the framework of H2020 SESAME EU Project [5], in order to obtain experimental data relevant for the ALFRED SG [6]. In the paper, one of the three experimental tests (Test N°1), is presented and discussed.

2.1. Facility description

CIRCE (CIRColazione Eutettico) is an integral test pool-type facility using LBE as primary coolant, designed and realized at the ENEA Brasimone Research Centre [7]. A 3D view of the facility is reported in FIG. 1. The facility is mainly composed by a main vessel (S100), a storage tank (S200), a transfer tank (S300). S100 hosts the test section and during the normal operations it is partially filled with about 70 tons of LBE. The main parameters of CIRCE are listed in TABLE 1.

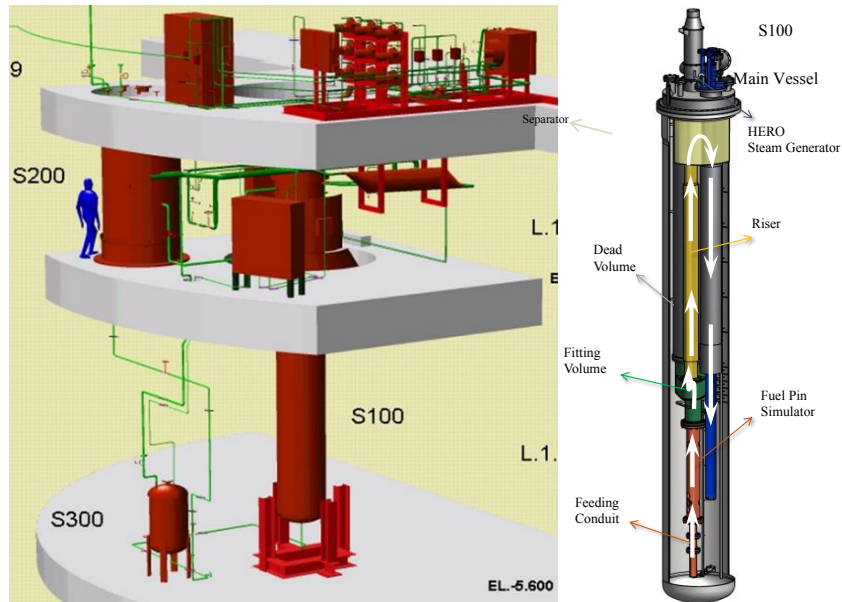


FIG. 1. 3D view of the CIRCE facility (left) and HERO TS implemented in the S100 main vessel (right)

TABLE 1. MAIN GEOMETRICAL AND OPERATIVE PARAMETERS OF THE CIRCE FACILITY

CIRCE Parameters	Value
S100 outer Diameter [mm]	1200
S100 height [mm]	8500
Max LBE Inventory [kg]	90000
Electrical Heating [kW]	47
Temperature Range [°C]	200 to 500
Operating Pressure [kPa]	15 (gauge)

The HERO (Heavy liquid metal pressurized water cooled tubes) test section [8] is mainly composed of the following components (see FIG. 1): Fuel Pin Simulator (FPS, in red in FIG. 1), with a maximum thermal power of ~1 MW; fitting volume (green); riser (yellow); separator (gold); SGBT (blue), acting as primary heat sink during the normal operative conditions and as decay heat removal system during the transients; argon injection device; dead volume, which encloses and maintains insulated the power supply rods feeding the FPS. When the facility is in operation, the LBE flows upwards through the FPS (see flow path in FIG. 1) where it is heated,

it passes the fitting volume and flows up along the riser, where argon could be injected for performing Gas-Enhanced Circulation (GEC) of the primary coolant, working instead of the primary pump. Then, LBE flows down crossing the shell side of the tube bundle for six meters, leaving the component from the bottom. The SGBT unit is composed by 7 double wall bayonet tubes, with an active length of 6 m, arranged with triangular pitch in a hexagonal shell, as reported in (FIG. 2, left). Each Bayonet Tube (BT) is composed of four coaxial tubes (FIG. 2, right): the feedwater enters from the top of the slave tube, flowing downward and then rising through the annular riser between the first and second tube, where the steam is produced. The gap between slave and first tube is filled by air (slight vacuum) as insulator in order to avoid steam condensation. The gap between second and third tube is filled with AISI316L stainless steel powder pressurized by helium at ~ 8 bar, for monitoring possible ruptures of both mentioned tubes, maintaining a good heat exchange capability, thanks to the metallic powder.

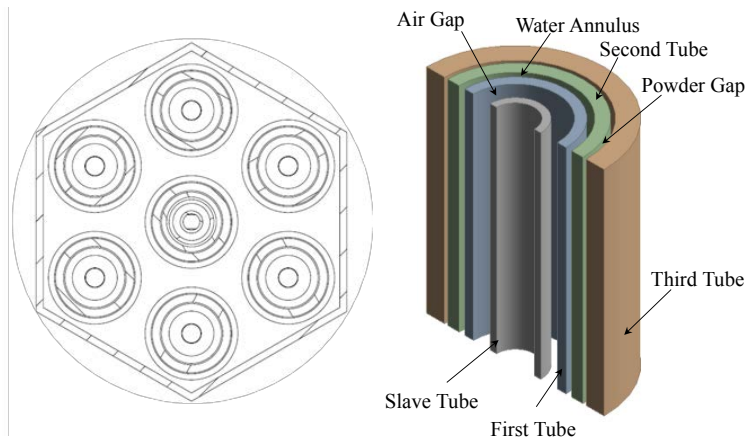


FIG. 2. Sketch of the tube bundle geometry (left) and internal view of the double wall bayonet tube (right)

A dedicated once-through secondary circuit has been designed and realized to provide feedwater to the HERO SGBT at 335°C and ~ 172 bar [9], consistent with operative conditions of ALFRED SG.

The instrumentation installed in the primary and secondary loop and relative details of the instrumentation positions are reported in [9][10].

2.2. Experimental test PLOFA #1 description

TABLE 2 reports the experimental boundary conditions for primary and secondary systems achieved during the test. At the beginning of the test, power supplied by the FPS is about 352 kW, as reported in FIG. 3, balancing power removed by the SG and the heat losses from S100 to the environment. The GEC regime is performed by injection in the riser of an argon flow rate of about 2.75 NI/s (see FIG. 3), achieving a LBE mass flow rate of about 35 kg/s.

In the secondary loop, the water mass flow rate is acquired by three mini-turbine flow meters (TFM) installed upstream the inlet section of tubes 4, 5 and 6 (respectively TFM-T4, TFM-T5 and TFM-T6 in FIG. 4) and a Coriolis flow meter.

The PLOFA scenario is reproduced reducing the FPS power according to a characteristic heat decay curve and achieving the trend shown in FIG. 3, while the loss of the primary pumping system is simulated by reducing the argon flow rate from 2.75 NI/s to 0 with a linear trend (FIG. 3) in a time lapse of 10 s. Simultaneously, the loss of the primary heat sink is simulated reducing the feedwater to the SG setting to 30% the pump RPM in a time lapse of 2 s (FIG. 4) and reaching the final value of ~ 0.095 kg/s measured by mini- TFM's. The loss of signals of TFM-T5 and TFM-T6 is due to the low flow rate achieved after the transient, which is close to the lower limit of the measure range of the instruments. The water temperature at the inlet section of the BTs is maintained at about 336°C , managing the power of the heater component. In this scenario, it is possible to evaluate the performances of the HERO SGBT acting as Isolation Condenser decay heat removal system [11].

TABLE 2. EXPERIMENTAL BOUNDARY CONDITIONS OF TEST #1

Parameter	Unit	Value (Before Transient)	Value (After Transient)
FPS Power	[kW]	352	20
Argon Flow Rate	[NI/s]	2.75	0
H2O mass flow rate	[kg/s]	0.274	0.095
H2O T inlet SG	[$^{\circ}\text{C}$]	~ 336	~ 336

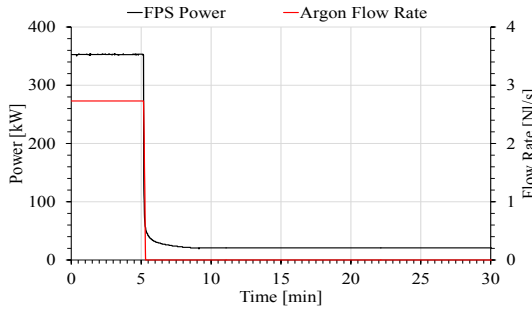


FIG. 3. FPS Power and argon Flow Rate trends during the PLOFA Test #1

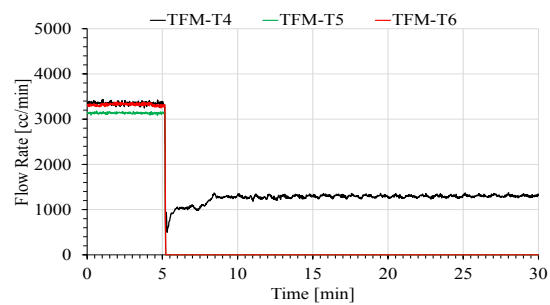


FIG. 4. H₂O mass flow rate trends measured by TFMs during the PLOFA Test #1

The LBE mass flow rate is reported in FIG. 5: the initial value of ~ 35 kg/s is subjected to a sudden decrease due to the argon flow rate reduction, reaching a minimum of 2 kg/s immediately after the gas transition and assuming the final value of about 6 kg/s when the natural circulation regime is established.

2.3. Experimental results

The temperatures are reported in FIG. 6 and FIG. 7 for the FPS and the SG, respectively. In particular, inside the FPS the outlet temperature decreases significantly because of the power decrease, passing from the initial value of $\sim 495^{\circ}\text{C}$, reached before the transient, to a minimum of 442°C , followed by a subsequent maximum peak of 478°C . Then, it reaches in few minutes $\sim 460^{\circ}\text{C}$, from which it starts to decrease slowly, when natural circulation regime of the LBE is established. The temperatures at the FPS inlet section remain almost the same during the test at $\sim 420^{\circ}\text{C}$, with a low decrease after the transient. A particular trend can be noticed for the thermocouple (TC) T-FPS-33, which measures a higher temperature before the transient. This can be probably due to a stagnation point near the thermocouple. The pin clad temperatures (FIG. 6) decrease from $\sim 530^{\circ}\text{C}$ before the transient, to $\sim 450^{\circ}\text{C}$, passing through a minimum of 445°C and a subsequent maximum peak of 486°C , corresponding to the minimum of LBE mass

flow rate. Concerning the SG, before the transient, the LBE inlet temperature is about 480°C, while after the cooling it is about 460°C. When the transient occurs, the inlet LBE temperature starts to decrease slowly, without abrupt changes. The outlet temperature decreases of about 20°C in 2 minutes, then it starts to decrease slowly. It can be noticed that the temperature measured at the inlet by TC-SG-01 suffers of an instability in GEC respect to the other two TCs, because of its position in the separator. In fact, this TC is directly exposed to the rising LBE, mixed to the argon injected at the bottom of the riser and this turbulence affects the measure acquired. The water temperature (FIG. 7, right) is kept constant at ~336 °C for the entire test, excepting for few seconds of oscillations, when the transient occurred, due to the re-balancing of the heater power, when the water mass flow rate is reduced. At the BTs outlet, the steam temperature is subjected to a sudden variation, passing from an average value of ~390°C before the transient to a maximum value of ~450°C immediately after, due to the reduction of the water mass flow rate. From this value, the temperature starts to decrease slowly, because of the lower thermal field in the primary system (lower LBE SG inlet temperature).

FIG. 8 shows the temperatures measured by the 119 TCs placed in the LBE pool, as function of their vertical position on the supporting bars (A-I) [10], before and after the transient. The stratification in the pool occurs between the positions at 5000 mm and 6000 mm, assuming 0 mm the bottom part of the separator.

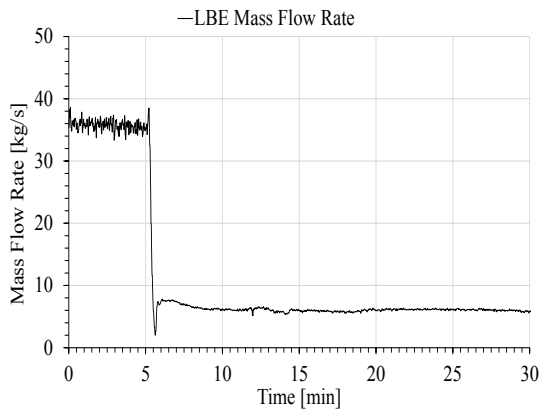


FIG. 5. LBE mass flow rate during PLOFA Test #1

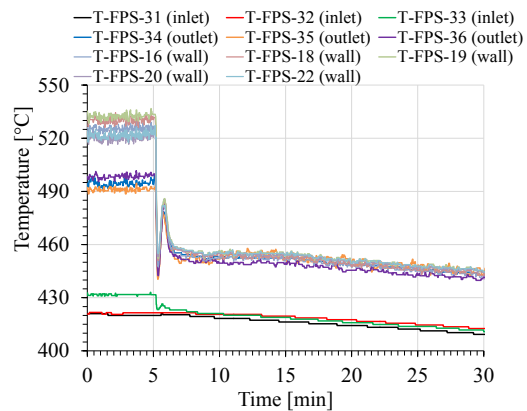


FIG. 6. LBE temperatures at the FPS inlet/outlet sections

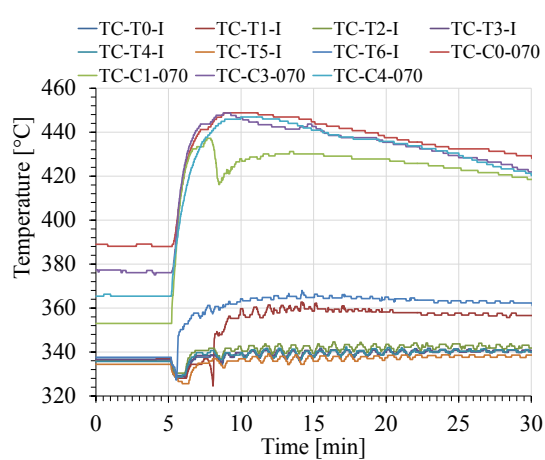
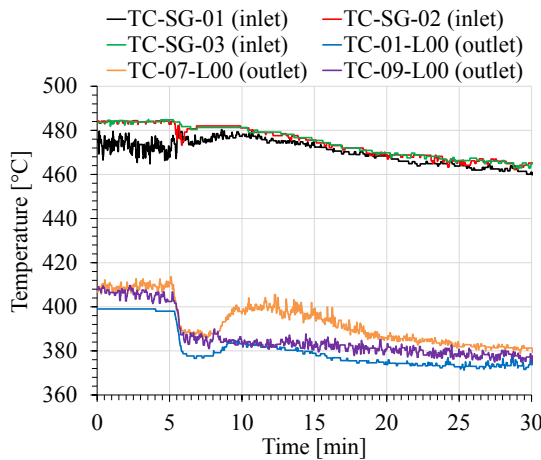


FIG. 7. LBE (left) and H2O (right) temperatures at the HERO SGBT inlet/outlet sections during PLOFA Test #1

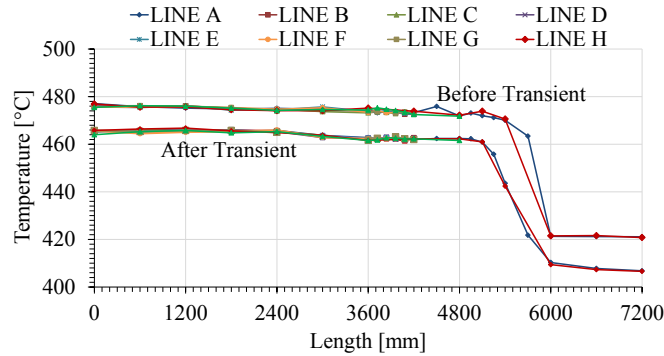


FIG. 8. LBE axial temperature profile inside the S100 vessel before and after the transient

3. SIMULATION ACTIVITY

The simulation activity has been performed with RELAP5-3D[®] v. 4.3.4 [12], developed at Idaho National Laboratory (INL). It is a generic thermal-hydraulic system code used in a large variety of nuclear and non-nuclear system analysis. The purpose to use RELAP5-3D (R5-3D) as safety tool for the ALFRED reactor makes necessary the improvement of the code validation in HLM, mainly for the large pool convection and the natural circulation, relevant phenomena for many transients.

The nodalization scheme of the facility, developed by “Sapienza - University of Rome”, consists of two main regions: a mono-dimensional scheme, reproducing HERO TS and the secondary loop, and a multi-dimensional component, simulating the pool volume between S100 and TS.

FIG. 9 shows the nodalization scheme of the CIRCE HERO TS. The inlet section of the TS is modelled with a PIPE component, simulating the feeding conduit. A detailed model of the FPS was developed and tested during the post-test activity performed in the previous configuration of CIRCE, which was operated in Integral Circulation Experiment configuration [13]. It consists in a subchannel modelling approach (represented in the hexagon into the lower part of the figure), simulating the single FPS assembly present in CIRCE, with 72 vertical PIPE components (from 801 to 872 in FIG. 9): 54 inner subchannels, 6 edge subchannels and 12 corner subchannels. Each one is axially divided in 16 control volumes, allowing the comparison of the temperature calculated by the code in the actual position of the thermocouples. Mass transfer between adjacent subchannels is taken into account with several cross junctions. A detailed description of the nodalization approach is reported in the ref. [14].

Thermal power supplied by the electrically heated pins is reproduced by 5760 heat transfer active nodes, which provide to each control volumes of the FPS active region a fraction of the total power proportional to their heat transfer area. According to the experiment, a flat power distribution within the heat source (HS) is considered. The HS model is completed with

- 3456 passive heat transfer nodes, reproducing the heat conduction within the fluid on the radial direction (see ref. [13]);
- 3600 passive heat transfer nodes, simulating the rods cold tails;
- 1728 passive nodes, reproducing the heat losses towards the pool.

Three PIPE components connect the FPS with the separator, simulating the fitting volume and the riser. At the inlet section of the riser, a time dependent junction injects the argon flow rate, reproducing the gas injection system. Inlet conditions of the gas are set with a time dependent volume. The separator is simulated with two parallel vertical pipes connected with five cross junctions to reproduce buoyancy effect within the large volume. The separator is connected with the gas plenum, where the cover pressure is imposed with a time dependent volume, and with the SG primary side.

A detailed model of the secondary loop was developed to reproduce a possible asymmetrical operation of the SG (Ref.[14] and [10]). The nodalization scheme is presented in FIG. 9. Feedwater temperature, steam pressure and total secondary mass flow rate are inserted as boundary conditions. The seven Double Wall Bayonet Tubes (DWBT) are separately simulated; each DWBT is modelled with two vertical PIPE components, reproducing the descending side and the annular riser of the unit.

The pool of the facility is reproduced with a multi-dimensional component (in the left part of the FIG. 9), consisting of 51 axial levels (z- coordinate), 4 radial meshes (r- coordinate) and 8 azimuthal intervals (theta- coordinate). The nodalization scheme on r- and theta- coordinates was developed according the geometry of the facility, considering the asymmetries of the system. The meshing on the z- coordinate was imposed equal to the axial discretization of the mono-dimensional region, according with the sliced modelling approach. The volume filled by the TS is considered with specific porosity factors, in order to match the actual volume of LBE contained within the pool. High equivalent diameter is considered into the pool, limiting the wall friction (typical for large volumes such as HLM pool), The multi-dimensional component allows the comparison of the LBE temperature calculated by R5-3D in the positions of the TCs in each support rods [14].

The heat losses are completely reproduced with heat structure that connects each control volumes of the primary flow path with the pool. The heat losses towards the environment are also simulated, considering the outside temperature of 20°C and a constant heat transfer coefficient on the external surface of the S100 insulation. For the rest of the heat structures, the heat transfer coefficient is evaluated with Seban-Shimazaki correlation for non-bundle geometries and Westinghouse correlation for bundle geometries. Westinghouse correlation was developed in the range of $1.1 < p/d < 1.4$, out of range for the application in FPS and SG of HERO TS. In addition, this correlation was reported to be in good agreement with experimental data for p/d lower than 1.2, underestimating the Nusselt number (Nu) when p/d exceeded 1.2 [4]. For this reason, constant multiplicative factors are applied to the bundles geometries heat transfer coefficient (1.3 for FPS and 1.02 for SG) to modify the coefficient according with Ushakov correlation [15], that offers a better estimation of the heat transfer coefficient for p/d higher than 1.2 [16].

The local pressure losses were proved to play a crucial role in the simulation of the first seconds after a transition event in CIRCE-HERO test facility [14][10]. For a good evaluation of the pressure drops in both GEC and natural circulation operations, k-loss coefficients dependent on flow conditions are considered for flow meters and grids [14].

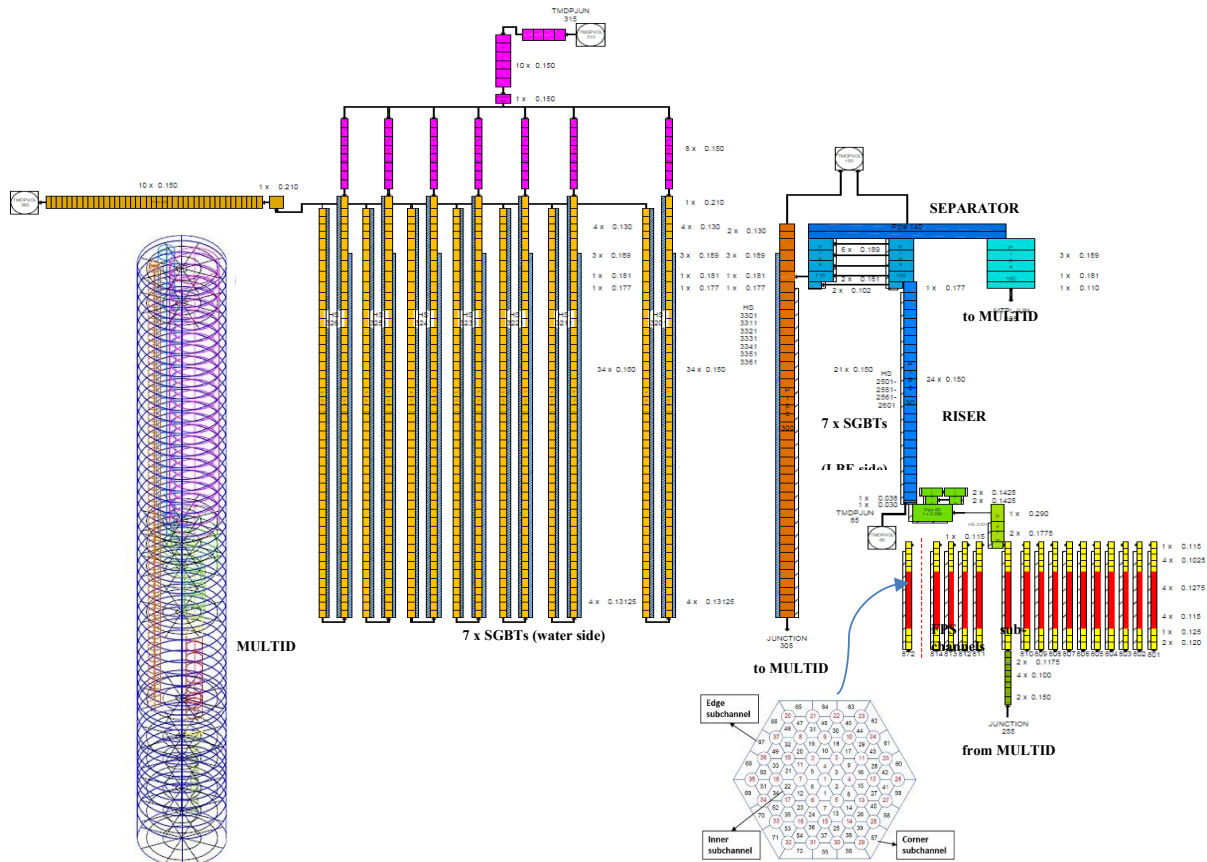


FIG. 9. CIRCE-HERO nodalization scheme

Calculations have been performed adopting the most recent thermophysical properties correlations recommended by NEA for LBE [17] and integrated in R5-3D as presented in [18]. Within the multi-dimensional component, the three-dimensional momentum equations are used.

3.1. Steady state results

A preliminary full power calculation has been carried out in order to obtain the initial conditions for the transient analysis, assuming the boundary conditions presented in section 2.2. The main results are summarized in Tab. 3, comparing them with experimental data. Globally, the simulation results are in good agreement with experimental outcomes. The largest discrepancies are observed at the SG LBE side. As presented in section 2.3, the experimental acquisition at the SG inlet is affected by instabilities due to the position of TC-SG-01. This could explain the large discrepancy observed. A similar behaviour is observed at the outlet section, where it is difficult to evaluate an average temperature due to the large discrepancies acquired by the TCs.

On the secondary side, the experiment is well reproduced by R5-3D. the main discrepancies are due to the lack of information of the feedwater mass flow rate per each DWBT.

TABLE 3. FULL POWER CALCULATION: MAIN RESULTS

Parameter	Unit	Experiment	Uncertainty	R5-3D	Error
LBE MFR	kg/s	34.0	10 - 25%	31.7	-6.7%
Av. FPS inlet T	K	420.0	2.0	418.4	-1.6
Av. FPS outlet T	K	493.5	2.0	495.0	1.5
Av- SG inlet T	K	480.0	5.0	485.1	5.1
Av. SG outlet T	K	403.7	8.0	413.9	10.2
TFM-T4	kg/s	0.036	0.0044	0.039	0.003
TFM-T5	kg/s	0.033	0.0044	0.039	0.006
TFM-T6	kg/s	0.035	0.0044	0.034	-0.001
TC-C0-O70	K	387.9	2.0	387.9	0.0
TC-C1-O70	K	353.0	2.0	353.9	0.9
TC-C3-O70	K	376.1	2.0	366.1	-10.0
TC-C4-O70	K	365.4	2.0	366.1	0.7

3.2. Transient results

Starting from the full power steady state conditions, the transient analysis has been carried out, applying the boundary conditions described in section 2.2. The following plots compare the simulation results with experimental data, reported with the associated uncertainty bands (dotted line).

FIG. 10 shows the LBE mass flow rate, experimentally measured by the Venturi flow meter. The initial decrease of the flow rate, occurring after the transition event, is well predicted by R5-3D, reaching the minimum value of 1.5 kg/s. After that, the code underestimates primary flow rate in natural circulation operation, even if the calculated trend is maintained within the experimental uncertainty bands over the whole test. The experimental and computational trends are compared with the LBE mass flow rate obtained applying the energy balance equation to the HS (see FIG. 10). For the calculation, the power supplied by the FPS and LBE temperature acquired at the inlet and outlet sections of the active length are considered. In both full power steady state condition and quasi steady state condition after the transient, the energy balance trend approaches very well the calculated value. Discrepancies with experimental data are justified by the large uncertainties related to the Venturi operation at low value of mass flow rate.

FIG. 11 compares the LBE temperature acquired at the FPS inlet (T-FPS-31) and at the outlet section (T-FPS-35 and T-FPS-36) with the simulation results. R5-3D provides a good estimation of the temperature trend over the whole test. At the inlet section of the active length, the code well reproduces the cooling down derivative trend, matching the experimental acquisition up to the end. At the outlet section, the quick decrease of the LBE temperature is well predicted, even if some discrepancies are observed at the minimum peak, where R5-3D overestimates the minimum temperature of about 6 degrees. After that, the temperature rapidly increases up to the maximum value; the code approach very well the acquisition of the TC T-FPS-35, whereas the T-FPS-36 provides a measurement few degrees higher. Then, the temperature decreases following the cooling down trend of the whole system and the calculation predictions are in good agreement with experimental data.

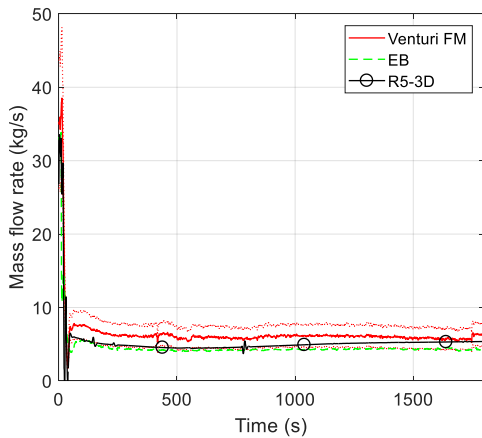


FIG. 10. LBE mass flow rate

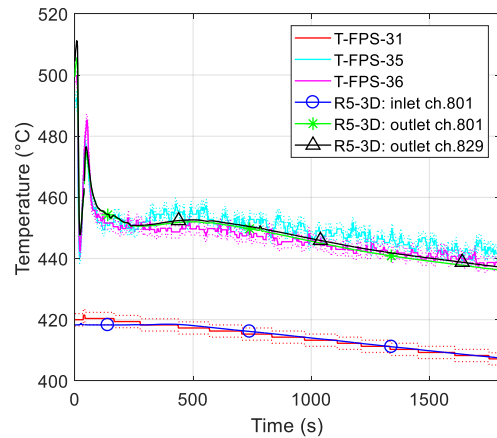


FIG. 11. FPS inlet and outlet temperature

FIG. 12 shows inlet and outlet temperature of the LBE flowing through the SG. The separator operates as a hot pool, reducing the quick cooling trend seen at the FPS outlet section. This effect is well reproduced by the code, that provides a good estimation of the heat losses occurring through the hot leg, confirmed by the good evaluation of the SG inlet temperature. At the outlet section, the quick temperature decrease is well reproduced in the first instants after the transition event. This is due to the rapid reduction of the primary flow rate. After that, new quasi steady state conditions (long-term natural circulation decay heat removal) are obtained and the LBE maintains quite constant temperature at the outlet section of the unit. This is confirmed by the experimental data, except for the acquisition of T-C-07-L00 that shows some instabilities.

On the secondary side, the quick reduction of the feedwater flow rate causes the rapid steam temperature to increase at the outlet of the DWBTs. FIG. 13 compares the experimental acquisitions at the outlet of tubes 0, 1, 3 and 4 with simulation results. R5-3D predicts the sharp increase, even if the maximum temperature is overestimated of about 30 degrees. After that, the cooling down derivative trend is well predicted by the code. Discrepancies are probably due to the thermal conductivity of the powder, that represent one of the most relevant uncertainties of the calculations. It is possible to note in the experimental results the different behaviour of the tube 1. In this tube the turbine flow meter was not present for this test and then this is considered in the numerical simulation in terms of local pressure drops. For this also the numerical results are different for the tube 1 and it follows the trend of the experimental results.

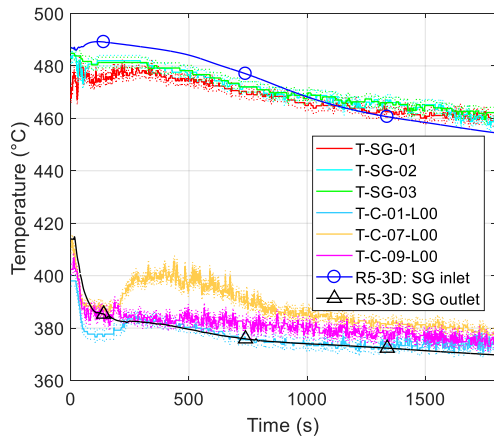


FIG. 12. LBE temperature through the SG

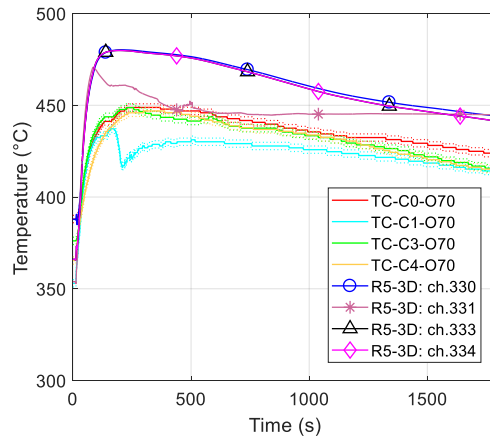


FIG. 13. Steam outlet temperature

FIG. 14 and FIG. 15 analyse the pool thermal stratification respectively at the beginning and at the end of the test. As presented in section 2.3, the experimental acquisition shows a relevant stratification phenomenon along the vertical direction and a quite uniform temperature at the same axial level. This is well reproduced by the code. The calculation results are acquired at the same position of the TCs, along the support rods A and H. As presented in FIG. 14 and FIG. 15, R5-3D predicts uniform temperature at the same quote, and the vertical temperature trend approaches very well the experimental data: almost uniform temperature in the upper part of the pool, relevant stratification phenomenon (about 50 degrees) in between -5 m and -6 m, and uniform temperature at the lower part of the pool. In addition, the transition from GEC to natural circulation is well reproduced.

The relevant stratification phenomenon occurs at the SG outlet level. This is due to the heat losses between the hot leg and the main pool that warms the upper part of the pool. Downstream the SG outlet, the cold fluid exiting the heat exchanger cools the lower pool, causing the characteristic thermal stratification.

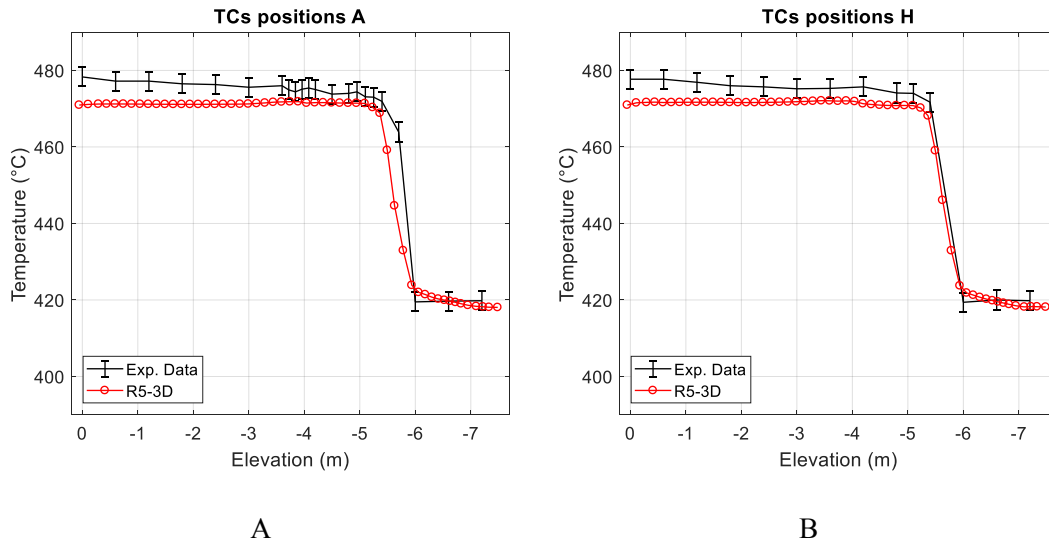


FIG. 14. Pool thermal stratification: initial conditions

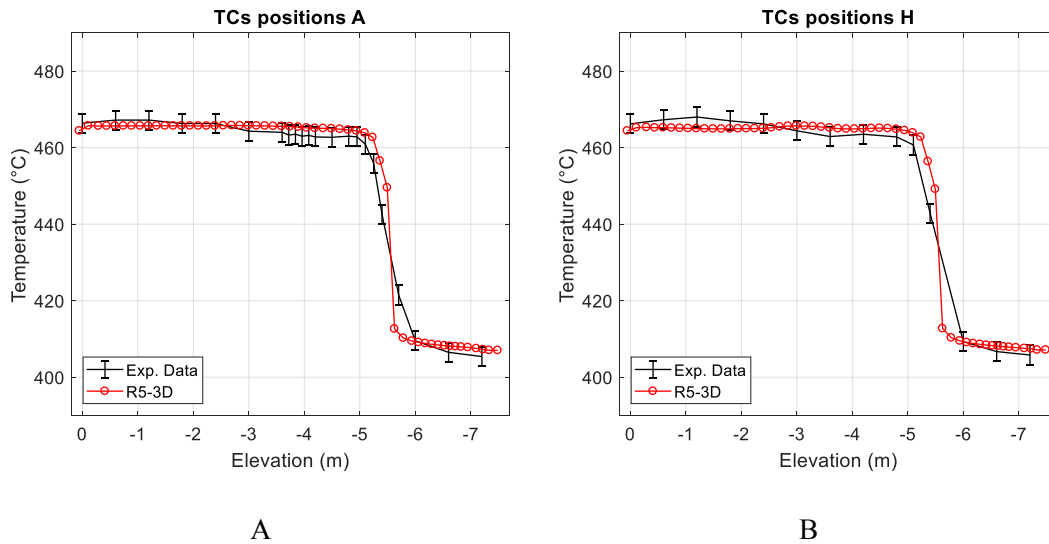


FIG. 15. Pool thermal stratification: final conditions

4. CONCLUSIONS

The PLOFA experiment #1, performed in CIRCE-HERO facility at ENEA Brasimone, provided a useful data for the analysis in support to the HLM safety demonstration and for the validation of the thermal-hydraulic transient analysis codes. In the second aspect, the paper shows a detailed analysis of the natural circulation characteristic parameters during the transient and the evolution of the thermal stratification in a large HLM pool.

The comparison of the experimental data and the numerical results (obtained with R5-3D) make know a good agreement. Regarding the thermal stratification, as in CIRCE- Integral Circulation Experiment [13] and in another CIRCE-HERO test [14], R5-3D with a multi-dimensional nodalization in the pool is capable to well predict the stratification quota, and to have an agreement in the temperature evaluation into the pool, with a large part of the points within the experimental error bars. The prediction in natural circulation is good for the mass flow rate and the FPS inlet and outlet temperatures, but in this test is present an overestimation of the temperatures in the HERO TS both in the primary and secondary side in the central part of the transient, with a good long-term prediction. This needs additional analysis to investigate the HERO behaviour at low mass flow rate for the secondary side.

ACKNOWLEDGMENTS

This work was performed in the framework of H2020 SESAME project. This project has received funding from Euratom research and training program 2014-2018 under grant agreement No 654935.

REFERENCES

- [1] LORUSSO P., BASSINI S., DEL NEVO A., DI PIAZZA I., GIANNETTI F., TARANTINO M., UTILI M., 2018, GEN-IV LFR development: Status & perspectives, *Progress in Nuclear Energy* 105 (2018) 318–331, <https://doi.org/10.1016/j.pnucene.2018.02.005>.
- [2] G. GRASSO, M. FRIGNANI, A. ALEMBERTI, M. TARANTINO, M. CONSTANTIN E I. TURCU. “Lead Fast Reactor technology: a promising option for SMR application”, IAEA TM on Fast SMRs, 24-27 September 2019, Milan (this conference).
- [3] M. FRIGNANI, A. ALEMBERTI, G. VILLABRUNA, R. ADINOLFI, M. TARANTINO, G. GRASSO, A. PIZZUTO, I. TURCU, S. VALECA, ALFRED: A Strategic Vision for LFR Deployment. ANS Winter Meeting 2017, Washington, D.C., October 29-November 2, 2017.
- [4] The RELAP5-3D© Code Development Team, 2015. RELAP5-3D Code Manual Vol. IV: Models and Correlations. INL/MIS-15-36723, vol. 4, rev. 4.3.
- [5] SESAME Project, EURATOM H2020, Grant Agreement N. 654935, April 2015.
- [6] LORUSSO P., PESETTI A., TARANTINO M., NARCISI V., GIANNETTI F., FORGIONE N., DEL NEVO A., 2019, Experimental Analysis Of Stationary And Transient Scenarios Of ALFRED Steam Generator Bayonet Tube In CIRCE-HERO Facility, *Nucl. Eng. Des.* 352 (2019) 110169, <https://doi.org/10.1016/j.nucengdes.2019.110169>.
- [7] TARANTINO, M., et al., 2011. Integral Circulation Experiment: Thermal-hydraulic simulator of a heavy liquid metal reactor. *J. Nucl. Mater.*, 415 (3), pp. 433-448. DOI: 10.1016/j.jnucmat.2011.04.033.
- [8] ROZZIA, D., PESETTI A., DEL NEVO A., TARANTINO M., FORGIONE N., 2017. HERO test section for experimental investigation of steam generator bayonet tube of ALFRED. *Proceedings ICONE-25* Doi: 10.1115/ICONE2567422.
- [9] LORUSSO P., PESETTI A., TARANTINO M., 2019, ALFRED Steam Generator Assessment: design and pre-test analysis of HERO experiment, *Proceedings of the 26th International Conference on Nuclear Engineering*, July 22-26, 2018, London, England, ICONE26-81824, DOI: 10.1115/ICONE26-81824.

- [10] LORUSSO P., PESETTI A., TARANTINO M., NARCISI V., 2019. Protected loss of flow accident simulation in CIRCE-HERO facility: experimental test and system code assessment, Proceedings of the 2019 27th International Conference on Nuclear Engineering, May 19-24, 2019, Ibaraki, Japan.
- [11] MARINARI, R., ALEMBERTI, A., CARMELLO, M., RIZZO, E., GIANNETTI, F., TARANTINO, M., NITTI, F.S., ACHILLI, A., FERRI, R. SIRIO: An experimental facility for a new heat removal system passively controlled by non-condensable gases (2018) Proceedings ICONE-26, DOI: 10.1115/ICONE26-82379.
- [12] The RELAP5-3D© Code Development Team, 2015. RELAP5-3D Code Manual Vol. I: Code Structure, System Models and Solution Methods. INL/MIS-15-36723, vol. 1, rev. 4.3.
- [13] NARCISI V., GIANNETTI F., CARUSO G., 2019. Investigation on RELAP5-3D© capability to predict thermal stratification in liquid metal pool-type system and comparison with experimental data. Nucl. Eng. Des., vol. 352, 110152, <https://doi.org/10.1016/j.nucengdes.2019.110152>.
- [14] NARCISI V., GIANNETTI F., DEL NEVO A., TARANTINO M., CARUSO G., 2019, Post-test simulation of a PLOFA transient test in the CIRCE-HERO facility, Nucl. Eng. Des. 355 (2019) 110321, <https://doi.org/10.1016/j.nucengdes.2019.110321>.
- [15] USHAKOV P.A., ZHUKOV A.V., MATYUKHIN N.M., 1977. Heat transfer to liquid metals in regular arrays of fuel elements. High Temp. vol. 15, pp. 868–873 translated from Teplofizika Vysokikh Temperatur, vol. 15 (1977), pp. 1027–1033.
- [16] GIANNETTI, F., DI MAIO, D.V., NAVIGLIO, A., CARUSO, G., 2016. Thermal-hydraulic analysis of an innovative decay heat removal system for lead-cooled fast reactors. Nucl. Eng. Des. 305, 168-178. <http://dx.doi.org/10.1016/j.nucengdes.2016.05.005>.
- [17] OECD/NEA Nuclear Science Committee, 2015. Handbook on Lead-bismuth Eutectic Alloy and Lead Properties, Materials Compatibility, Thermal-hydraulics and Technologies
- [18] BALESTRA P., GIANNETTI F., CARUSO G., ALFONSI A., 2016. New RELAP5-3D lead and LBE thermophysical properties implementation for safety analysis of Gen IV reactors. Sci. Technol. Nucl. Install., vol. 2016. <http://dx.doi.org/10.1155/2016/1687946>.
- [19] MEMMOTT, M., BUONGIORNO, J., HEJZLAR, P., 2010. On the use of RELAP5-3D as a subchannel analysis code. Nucl. Eng. Des. 240, 807-815. DOI: 10.1016/j.nucengdes.2009.11.006.
- [20] IDELCHIK, I.E., 1986. Handbook of Hydraulic Resistance. Second ed. Hemisphere Publishing Corporation.

A PASSIVE SAFETY DEVICE FOR SFERS WITH POSITIVE COOLANT TEMPERATURE COEFFICIENT

Paper ID #28

CHIHYUNG KIM

Korea Advanced Institute of Science and Technology
Daejeon, Republic of Korea

YONGHEE KIM

Korea Advanced Institute of Science and Technology
Daejeon, Republic of Korea
Email: yongheekim@kaist.ac.kr

Abstract

The advantages of fast reactor based SMR (small modular reactors) are most pronounced when the neutron economy of the core is maximized with hard neutron spectrum. However, the SFR cores with low neutron leakage and hard neutron spectrum have the noticeable disadvantage that the coolant temperature reactivity feedback tends to be positive, which is not preferable in terms of inherent safety. A passive safety device concept that inserts negative reactivity as coolant temperature rise is a good way to improve the safety of SFR cores without significant loss of the neutron economy. In this regard, the paper presents FAST (floating absorber for safety at transient) for the improved safety of SMFRs (small modular fast reactors). The performance of FAST in metallic and oxide fuelled cores is analysed considering three representative ATWS (anticipated transient without scram) scenarios, which are ULOF (unprotected loss of flow), ULOHS (unprotected loss of heat sink) and UTOP (unprotected transient overpower). All the transient simulations are performed using in-house thermal hydraulics coupled point kinetics code, and time-dependent reactor power and resulting temperatures of core components are evaluated for the quantitative performance analysis of FAST. It is confirmed that FAST can very successfully mitigate the consequences of ULOF, ULOHS and UTOP in typical SFRs with positive coolant temperature coefficient.

1. INTRODUCTION

SMR is an attractive reactor concept for its modularity and it can be used to supply the electricity in remote isolated areas. However, frequent refuelling is not preferable for the SMRs located in isolated areas, since refuelling necessitates transport of nuclear fuels and management of spent nuclear fuels. In this regard, SMRs based on fast reactor concept is preferable with its low TRU (Transuranic) production, high fuel utilization and long-time operation without refuelling.

Fast reactors take advantage of high fission-to-capture ratio in hard neutron spectrum. Fast neutrons are likely to leak from the core, the core with less neutron leakage usually has superior performance by utilizing the conversion of nuclear fuel effectively. However, the core with low neutron leakage may have less negative or even positive coolant temperature reactivity feedback, which is not preferable in terms of inherent safety.

Small modular fast reactor (SMFR) with dense and compact fissile loading for low neutron leakage is desirable for long term operation without refuelling, but high neutron leakage is also required for negative reactivity feedbacks. In this regard, a passive safety device concept, which can improve safety maintaining high fissile loading density, is well suited for SMFRs. This study suggests FAST (Floating Absorber for Safety at Transient) [1] which can passively insert the negative reactivity in case of coolant temperature rise or coolant voiding.

In this study, performance of FAST is investigated assuming ATWS scenarios for 300 MW(th) metallic fuel-loaded SFR (sodium-cooled fast reactor), 1000 MW(th) oxide fuel-loaded SFR, and 250 MW(th) metallic fuel-loaded B&BR (breed-and-burn fast reactor) core. Reference cores are a compact B&BR [2] for metallic-fuel-loaded B&BR, ABTR (advanced burner test reactor) [3] for metallic-fuel-loaded burner core and ABR (advanced burner reactor) [4] for oxide-fuel-loaded burner core. Three ATWS scenarios, which are ULOF (unprotected loss of flow), ULOHS (unprotected loss of heat sink) and UTOP (unprotected transient overpower), are considered and transient analyses are carried out using in-house thermal hydraulics coupled point kinetics code. The performance of FAST is evaluated in terms of reactor power and resulting temperature of coolant and fuel.

2. DESCRIPTION OF FAST

FAST consists of absorber module and guide thimble containing it. The appearance of the FAST guide thimble is exactly same as the fuel rod so that it can be easily installed in the fuel assembly replacing the fuel rod. There are several coolant bypass holes at the top and bottom of the guide thimble to fill the inside of it with primary coolant. It needs to be noted that the bypass holes are designed such that coolant flow inside the guide thimble is nearly zero.

Absorber module located in the coolant inside guide thimble is composed of absorber part and void part. The basic principle of FAST is that the absorber module sinks or floats due to the change of buoyancy in accordance with the temperature and density change of coolant. Therefore, length, thickness and density of absorber part and void part of absorber module are determined considering the required magnitude of buoyancy force. The proper magnitude of buoyancy force makes the absorber module to float above the active core in nominal state and to sink down to the active core in case of temperature rise of primary coolant. It needs to be noted that the absorber part and void part are not connected but only contact each other by buoyancy. In a similar sense, the absorber part can be made of several pieces contacting each other if it is necessary to improve the freedom of sinking path.

B₄C is considered as an absorber material and reactivity worth of the FAST is easily controlled by adjusting the density or enrichment of the B₄C. Reactivity worth of FAST is maximum when absorber module is located near the centre of the active core, and hence, sinking limit of the absorber module is determined considering the required maximum reactivity worth of FAST. SiC/SiC composite, which is helium permeable [5], is chosen for the cladding material of absorber since it can vent out the helium produced by (n, alpha) reaction of ¹⁰B.

FAST is installed in place of fuel pins in fuel assembly, so it can be easily applied to conventional or existing SFR concepts. Another advantage of FAST is that it can effectively cope with local accidents such as coolant flow blockage since FAST works interacting with temperature of surrounding primary coolant.

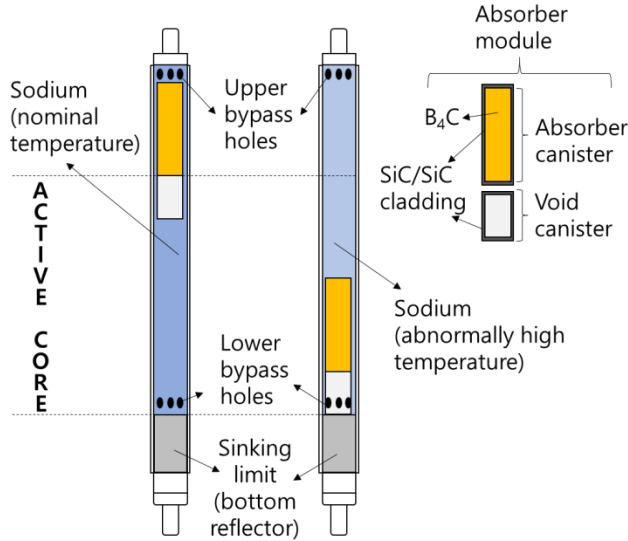


FIG. 1. Concept of FAST (Floating Absorber for Safety at Transient)

3. REFERENCE CORES

Reference core for metallic-fuel-loaded B&BR is a compact advanced B&BR developed in KAIST, and ABTR and ABR developed by ANL are chosen for the metallic-fuel-loaded burner SFR and oxide-fuel-loaded burner SFR, respectively. Table. 1 summarizes the design parameters of reference cores. Thermal powers of metallic-fuel-loaded B&BR and metallic-fuel-loaded burner SFR are in the range of SMR defined by IAEA and oxide-fuel-loaded SFR with 1000 MW thermal power is at the boundary of SMR.

Axial power distributions of reference cores for the temperature calculations are shown in Fig.2. In case of metallic-fuel-loaded B&BR, power distribution evaluated in Ref. 2 is used, and chopped cosine shapes are assumed for the others. It has to be noted that perturbation of power distribution during the transient is neglected since the impact of reactivity insertion in fast reactor hardly affects the power distribution. One may recall that conventional transient analysis codes for fast reactors are using point kinetics equation which works well when time and shape function of flux is well-separable.

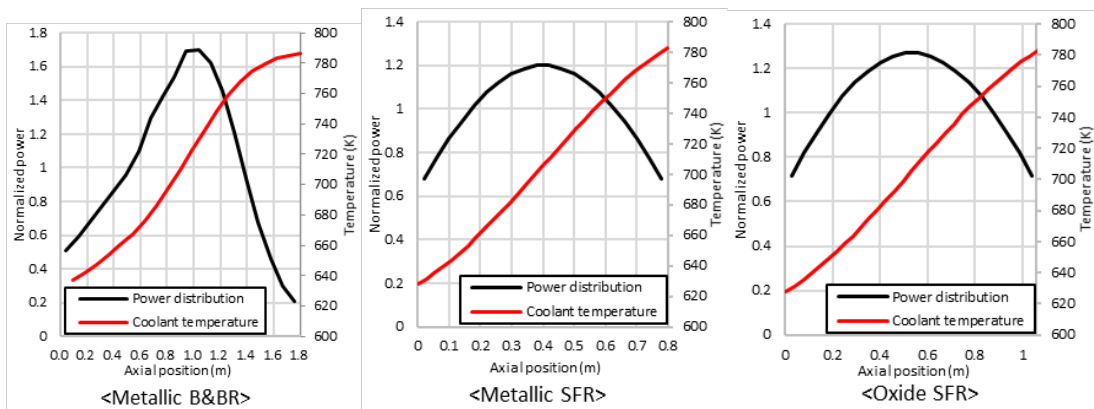


FIG. 2. Whole core average axial power distribution of reference cores

Table. 2 shows the reactivity feedback coefficients and kinetic parameters of the reference cores. It ought to be noted that EOC condition of equilibrium core is considered for the metallic fuel-loaded and oxide-fuel-loaded burner cores since they do the multi-batch fuel management. One can note clearly positive coolant temperature coefficients in all reference cores.

Design parameters of FASTs adopted to the reference cores for the transient analyses are tabulated in Table. 3. Outer radii of the FASTs are same as that of fuel rod in each reference core, and configurations of absorber modules are determined considering the active core height. Maximum reactivity worth of FAST is assumed to be 1\$ for all cases. It has to be noted that void part of absorber module in each core is fully inserted, and absorber part is located just above the active core region at nominal state. In this way, a positive reactivity insertion by void insertion can be avoided.

TABLE 1. MAIN DESIGN PARAMETRES OF THE REFERENCE CORES

Parameter	Value		
	Metallic-fuel-loaded B&BR	Metallic-fuel-loaded burner	Oxide-fuel-loaded burner
Thermal power (MW(th))	400	250	1000
Fuel material	U-Zr (driver) SNF-Zr (blanket)	U-TRU-Zr	TRU/SNF oxide
Average power density of active core (W/cm ³)	57.1	258	231
Coolant inlet/outlet temperature (K)	633 / 783	628 / 783	628 / 783
Average discharge burnup (GWd/MTHM)	160	97.7	111
# of batches / cycle length (month)	1 / 624	(12/15/12)* / 4	5 / 12

* inner / outer / test assembly

TABLE 2. REACTIVITY FEEDBACK COEFFICIENTS AND KINETIC PARAMETERS OF THE REFERENCE CORES

Parameters		Value		
		Metallic-fuel-loaded B&BR	Metallic-fuel-loaded burner	Oxide-fuel-loaded burner
Reactivity feedback coefficients (pcm/K)	Fuel temperature	-0.163	-0.33	-0.372
	Coolant temperature	0.952	0.099	0.496
	Radial expansion	-0.561	-1.947	-0.93
	Axial expansion	-0.243	-0.198	-0.155
Delayed neutron fraction		0.00362	0.0033	0.00264
Prompt neutron lifetime (μ s)		0.34	0.33	0.59

The FAST configurations presented in Table. 3 are definitely realistic. However, it is advised to be noted that they may not be the optimal for each reference core, and the FAST configurations can be further optimized if necessary. For example, absorber module can be longer, shorter, thinner or thicker depending on the required moving velocity or required reactivity worth. Reactivity worth of FAST is assumed to be similar in shape to the S-shaped reactivity worth curve of control rods and maximum reactivity worth is assumed to be 1\$ as shown in Fig. 3.

TABLE 3. DESIGN PARAMETERS OF THE REFERENCE FASTS

Design parameters	Value		
	Metallic-fuel-loaded B&BR	Metallic-fuel-loaded burner	Oxide-fuel-loaded burner
Reactivity worth, \$	1	1	1
Absorber / void height, cm	90 / 50	40 / 20	60 / 20
B ₄ C density, g/cm ³	1.178	1.248	1.109
Absorber module average density, g/cm ³	0.832	0.832	0.832
Absorber module radius, cm	0.3	0.2	0.2
FAST radius, cm	0.95	0.4	0.3775
Guide thimble thickness, cm	0.06	0.052	0.05

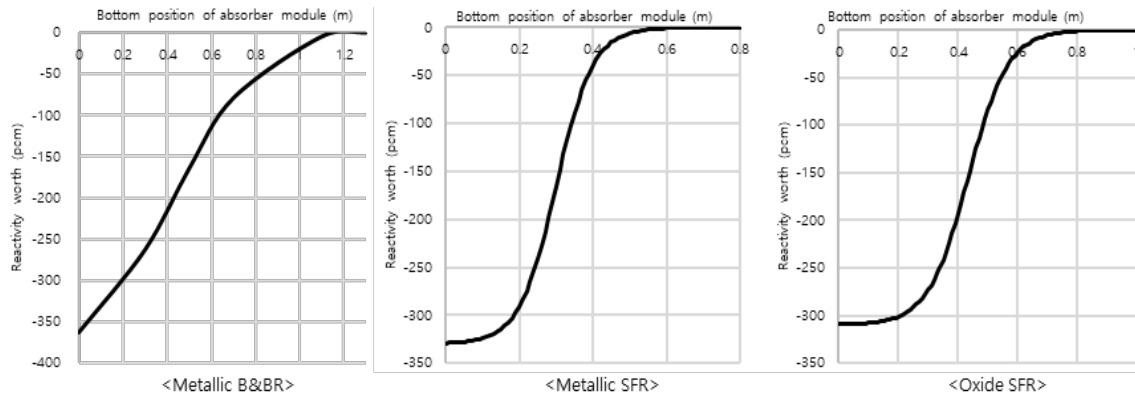


FIG. 3. Position-wise reactivity worth of FASTs in reference cores

4. ATWS ANALYSES

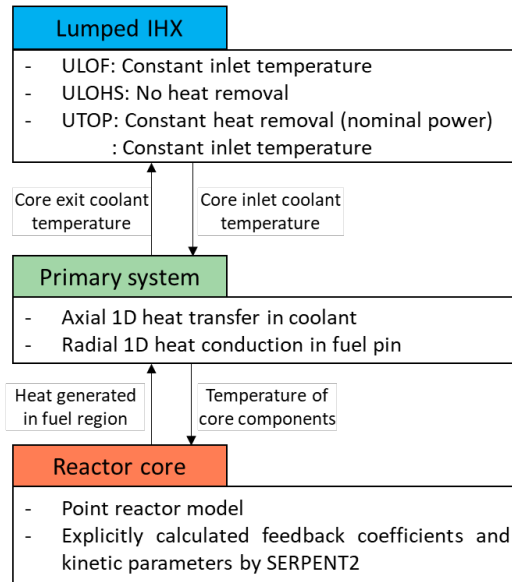


FIG. 4. Overall flow of the code for the transient analysis of FAST

ATWS simulations are performed using in-house thermal hydraulics coupled point kinetics code [6]. The codes consist of a temperature calculation module, point kinetics module and FAST simulation module. Temperatures of fuel, cladding and coolant are calculated in temperature calculation module and the temperatures are used to calculate the reactivity feedbacks and position of absorber module. The reactivity information including reactivity feedbacks and reactivity inserted by FAST is used to calculate the reactor power in point kinetics module. Overall flow of the program is shown in Fig. 4.

Failure limit of the fuel is 1350 K for metallic fuel and 3100 K for oxide fuel, which are lower than melting point of each fuel material with margin. Failure temperature of coolant is assumed to be 1150 K which is about the boiling point of sodium at atmospheric pressure. It is compelled to be noted that realistic failure limit of coolant in pool-type SFRs can be higher than 1150 K if pressure in sodium pool is considered. The transient simulations are not interrupted even when temperatures of core components exceed the failure limit due to difficulties and uncertainties in modelling of fuel melting and coolant boiling.

4.1. ULOF

In ULOF, loss of primary coolant flow with 5 seconds of pump halving time is assumed, and core inlet coolant temperature is assumed to be a constant same as nominal condition [6]. Figures 5 to 7 show the results of ULOF simulations. The most dramatic improvement of safety in metallic-fuel-loaded B&BR with the most positive CTC (coolant temperature coefficient) is observed, and the rest of the cases also show better safety with FAST. One can note a slight re-floating of absorber module in all cases due to the power suppression and resulting coolant temperature decrease, while the impact of re-floating is almost negligible.

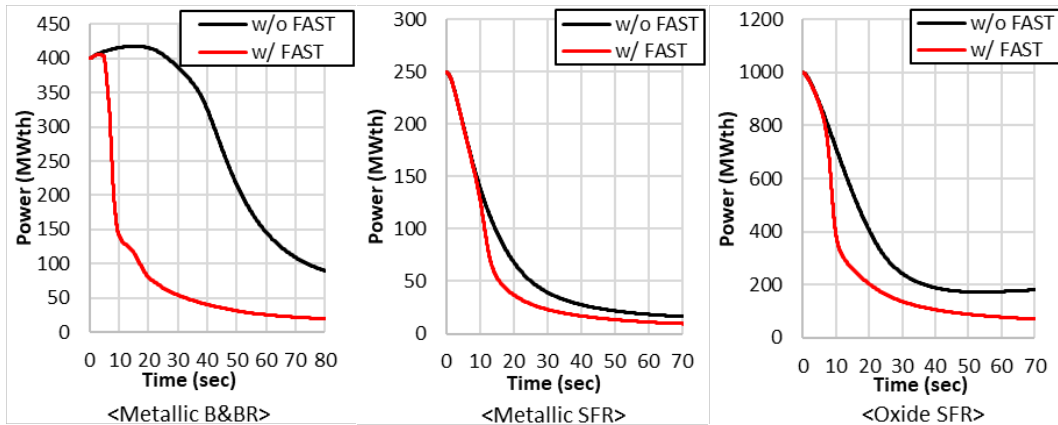


FIG. 5. Time evolution of reactor power during the ULOF

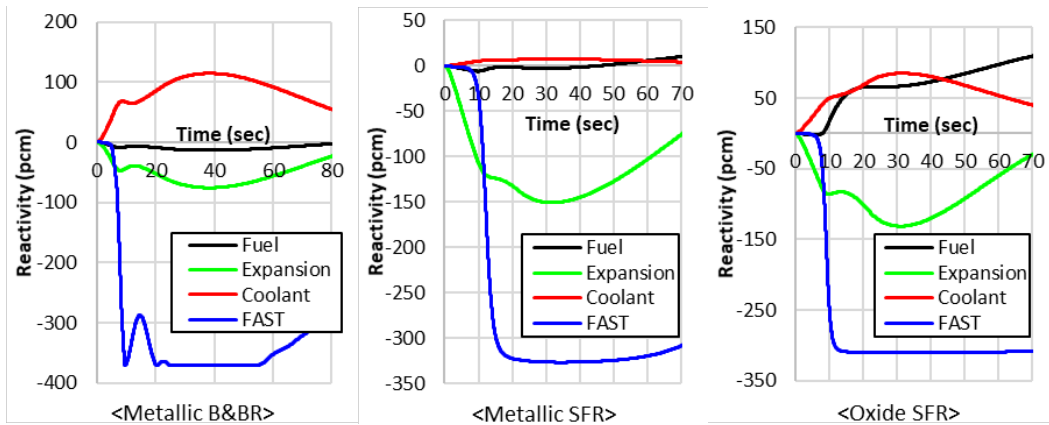


FIG. 6. Reactivity components during the ULOF

In case of the oxide-fuel-loaded core, coolant temperature exceeds the failure limit in absence of the FAST even though net reactivity feedback is negative and power decreases from the beginning of ULOF (see Fig. 6). This result indicates that core failure can occur if power suppression rate is slow even though the net reactivity feedback is negative. In this regard, the performance of FAST to suppress the power in case of coolant rise is clearly shown.

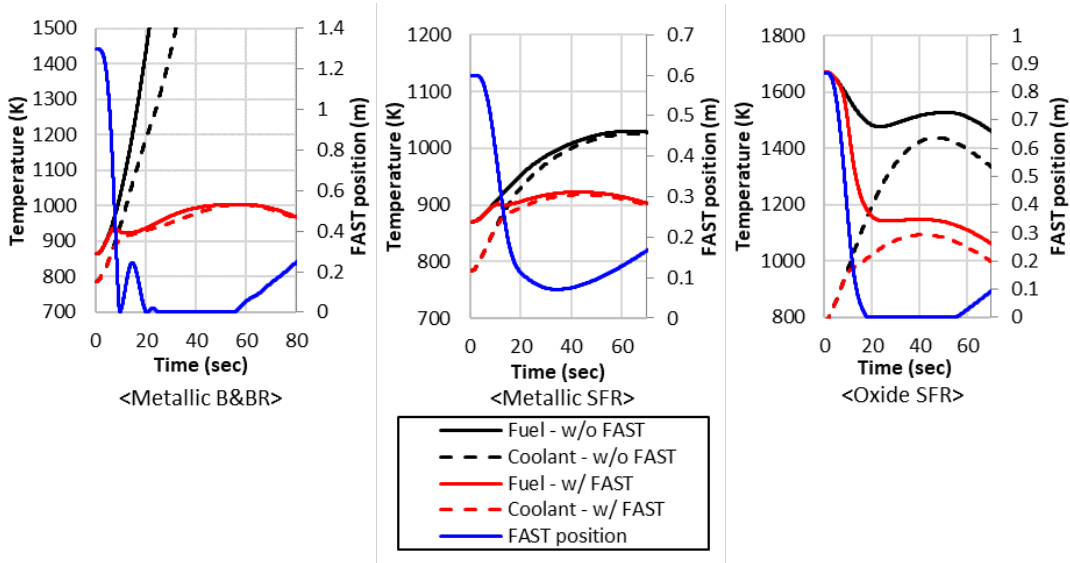


FIG. 7. Maximum temperatures of the core components and corresponding FAST position during the ULOF

4.2. ULOHS

In ULOHS, loss of heat removal capacity in IHX in 20 seconds is assumed, and core inlet coolant temperature is calculated using core outlet coolant temperature considering heat balance equation. Figures 8 to 10 show the results of ULOHS simulations. Quick suppression of reactor power during the ULOHS is observed in all cases. However, similarly to the ULOF cases, slow suppression of reactor power in absence of FAST causes the core failure in oxide-fuel-loaded core at about 40 seconds from the beginning of ULOHS. Re-floating of absorber module is not observed at all since coolant temperature only increases during the ULOHS.

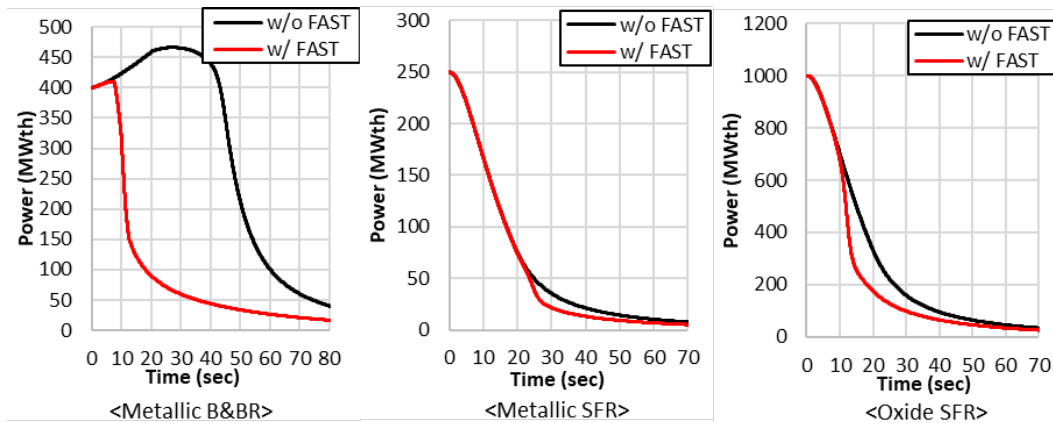


FIG. 8. Time evolution of reactor power during the ULOHS

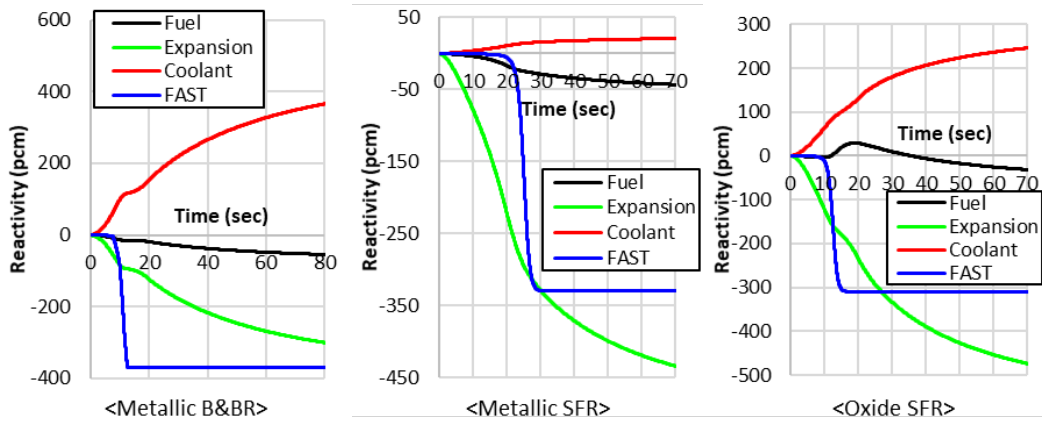


FIG. 9. Reactivity components during the ULOHS

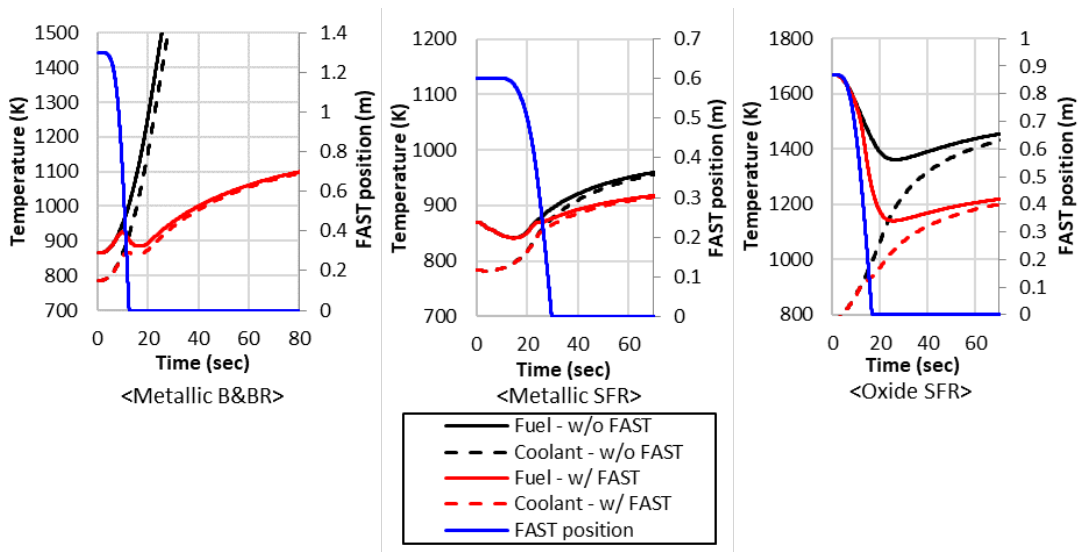


FIG. 10. Maximum temperatures of the core components and corresponding FAST position during the ULOHS

4.3. UTOP

In UTOP, external reactivity insertion of 1\$ over 50 seconds is assumed considering ramp up rate of 0.02 \$/sec. The coolant flow rate is kept same as that in nominal state, and two heat removal scenarios are considered for the calculation of core inlet coolant temperature, which are constant temperature drop in IHX (CDI) and constant core inlet coolant temperature (CIT). The CDI scenario assumes that the amount of heat removal in IHX is always the same as nominal full power, and CIT scenario considers constant inlet temperature same as that of nominal full power regardless of core outlet coolant temperature.

Figures 11 to 13 show the results of UTOP simulations with CDI scenario. Increase of power at the initial stage of UTOP is observed in all cases due to external reactivity and coolant temperature induced positive reactivity feedback. As UTOP continues, net reactivity feedback decreases and becomes negative due to the temperature rise of fuel and core expansion. However, initially increased power makes temperatures of core components increase, and

failure of coolant is observed in case of metallic-fuel-loaded B&BR core if FAST is not adopted. In cases with FASTs, reactor powers of reference cores are quickly suppressed by FAST from the initial stage of UTOP, and thus, core failure is not observed in any cases with FAST.

Quite sudden decrease of reactor power and resulting quick decrease of coolant temperature by the FAST causes the oscillation of absorber module as shown in Figs. 11 and 13. Oscillatory behaviour of FAST is mainly due to the re-floating of absorber module due to the coolant temperature decrease, which causes overshoot of reactor power and temperature. In spite of the oscillations, core failure is not observed in all cases.

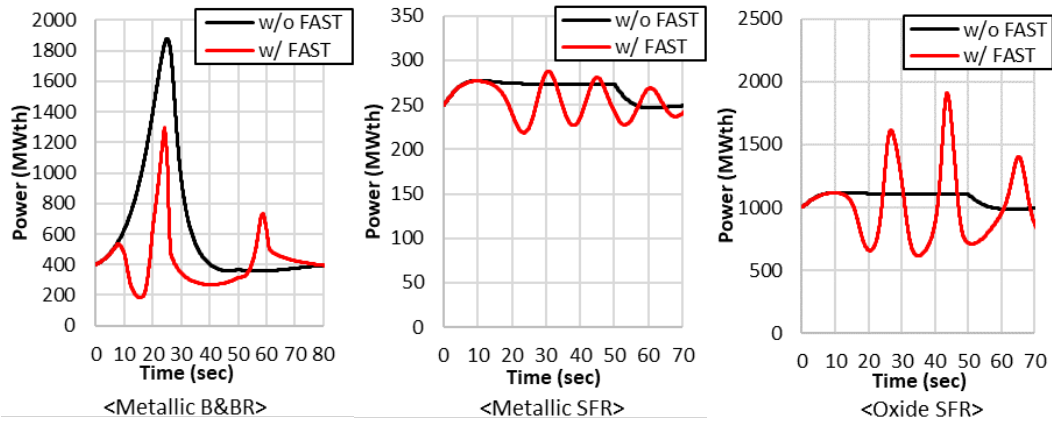


FIG. 11. Time evolution of reactor power during the UTOP with CDI scenario

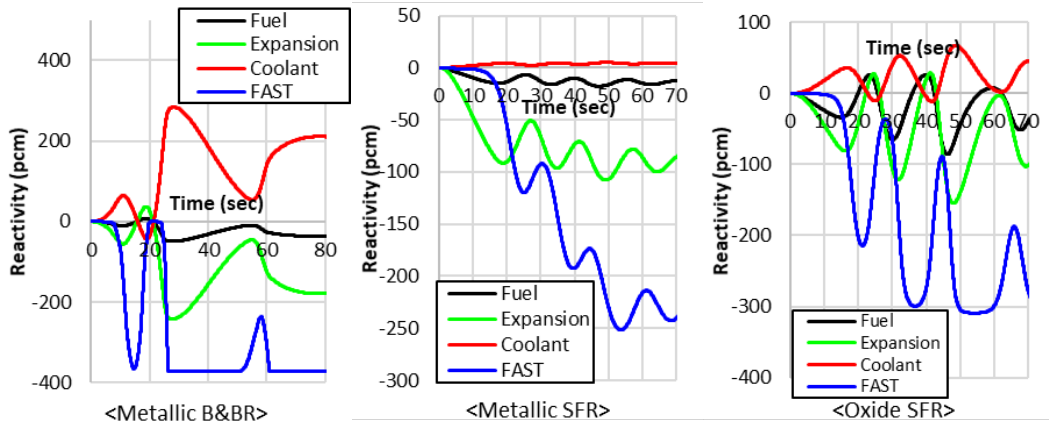


FIG. 12. Reactivity components during the UTOP with CDI scenario

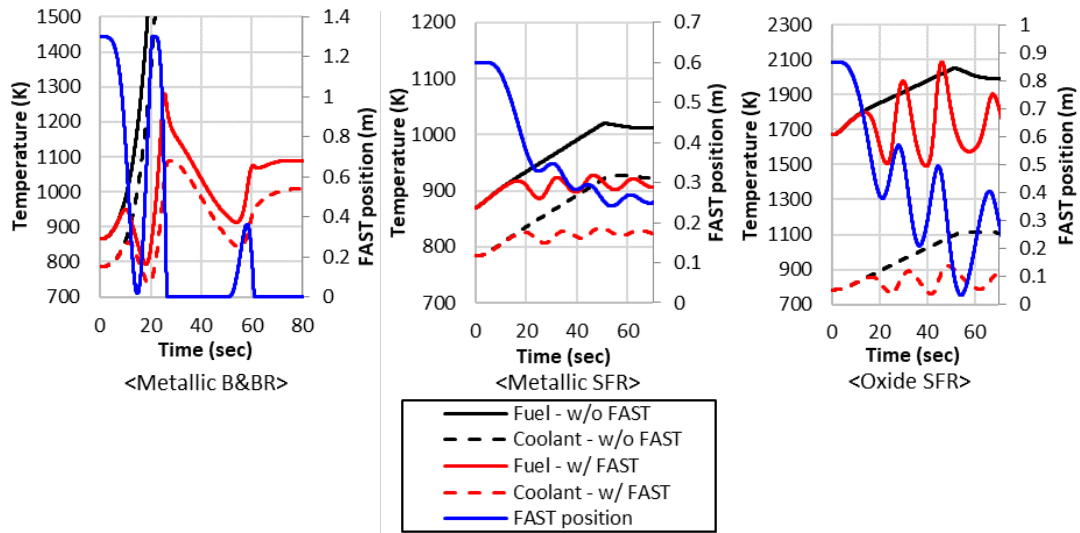


FIG. 13. Maximum temperatures of the core components and corresponding FAST position during the UTOP with CDI scenario

Figures 14 to 16 show the results of UTOP simulations with CIT scenario. Similar to the UTOP cases with CDI scenario, quick suppression of power by FAST and also oscillatory behaviour of FAST are observed during the UTOP in all reference cores. Coolant temperatures with CIT scenario are lower than those with CDI scenario since core inlet temperatures of reference cores are fixed as those of nominal conditions.

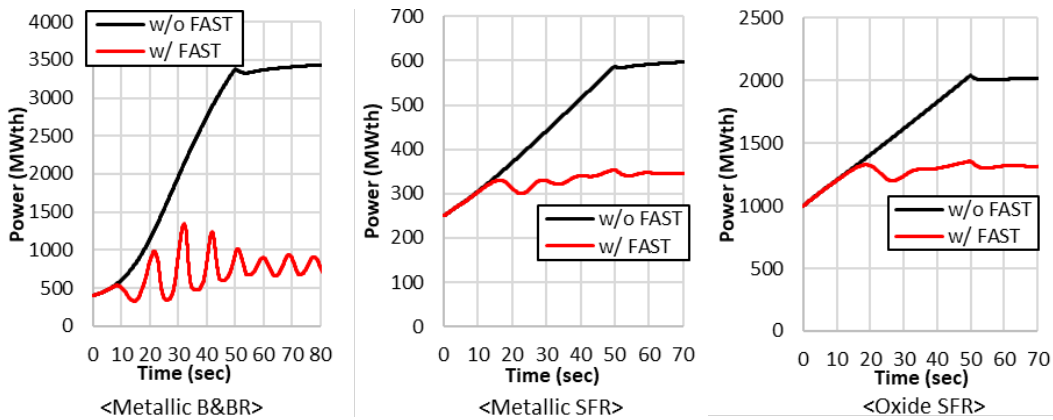


FIG.14 Time evolution of reactor power during the UTOP with CIT scenario

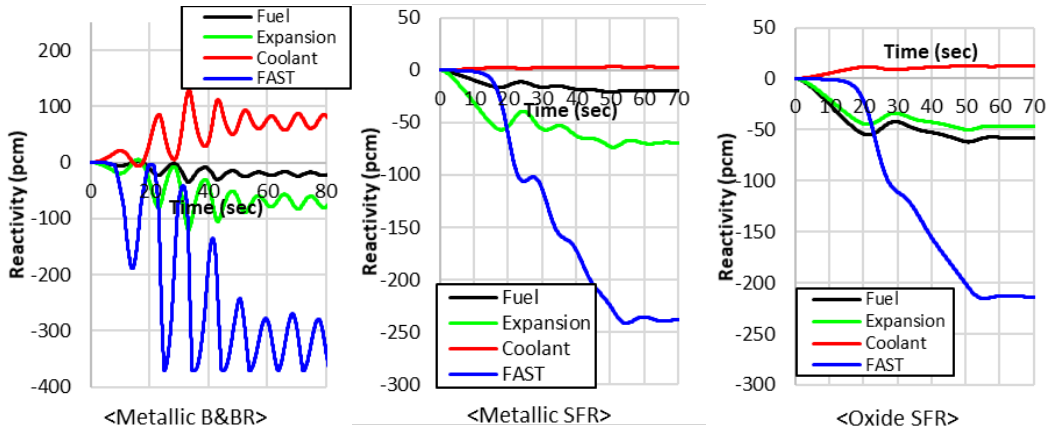


FIG.15 Reactivity components during the UTOP with CIT scenario

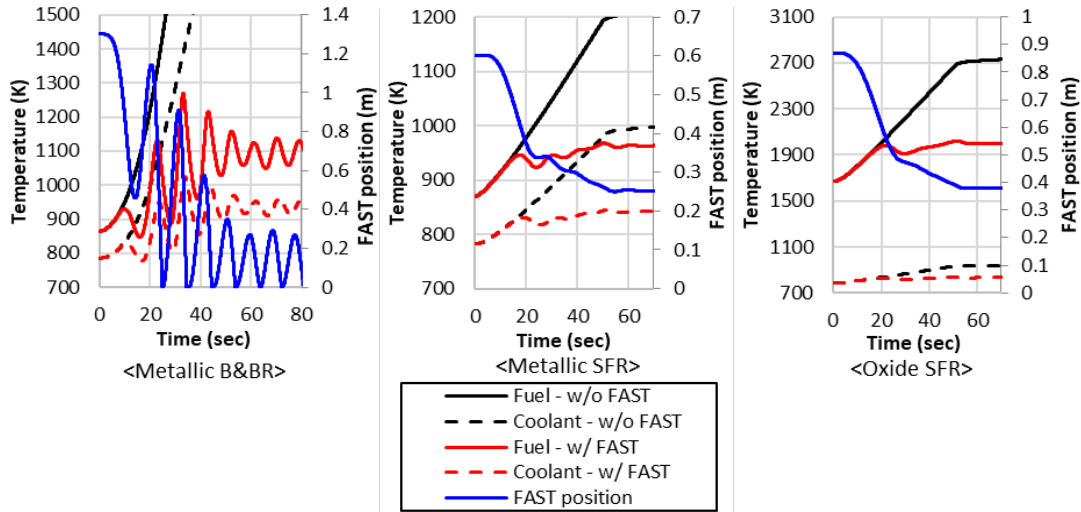


FIG.16 Maximum temperatures of the core components and corresponding FAST position during the UTOP with CIT scenario

5. CONCLUSIONS AND FUTURE WORKS

This study has investigated the application of FAST in SFRs. It is shown that the FAST effectively prevents the core failure or meltdown by inserting negative reactivity in response to the coolant temperature rise during the ULOF and ULOHS. Although oscillation of reactor power is observed in all reference cores during the UTOP, much lower temperatures of core components are observed due to the quick initial suppression of power by FAST. In conclusion, the feasibility of FAST is shown assuming serious ULOF, ULOHS and UTOP transients, although the progress of ATWS is different depending on fuel type and core design.

The transient analyses in this paper are carried out assuming very simplified and lumped IHX model. In this regard, ATWS transient analyses using an accurate system simulation code needs to be performed for a more concrete performance evaluation of the FAST device. In addition, further study to reduce or remove the oscillatory behaviour of the FAST in case of UTOP can be considered as a valuable future work.

ACKNOWLEDGEMENTS

This work was supported by the National Research Foundation of Korea Grant funded by the Korean government NRF-2016R1A5A1013919.

REFERENCES

- [1] DONNY HARTANTO, CHIHYUNG KIM, INHYUNG KIM, AND YONGHEE KIM, "FAST and SAFE Passive Safety Devices for Sodium-cooled Fast Reactor," Transactions of the Korean Nuclear Society Spring Meeting (2015).
- [2] DONNY HARTANTO, A design and physics study of a compact sodium-cooled breed-and-burn fast reactor, PhD Dissertation, KAIST (2015).
- [3] Y.I. CHANG, P.J. FINCK AND C. GRANDY, Advanced Burner Test Reactor Preconceptual Design Report, ANL-AFCI-173, Argonne National Laboratory, 2006.
- [4] CAHALAN, JAMES E. ET AL., Advanced Burner Reactor 1000MWth Reference Concept, ANL-AFCI-202, Argonne National Laboratory, 2007.
- [5] Y. KATOH, ET AL., Mechanical Properties of Chemically Vapor-Infiltrated Silicon Carbide Structural Composites with Thin Carbon Interphases for Fusion and Advanced Fission Applications, Materials Transactions 46 (3), 527-535 (2005).
- [6] C. Kim and Y. Kim, Potential of FAST (floating absorber for safety at transient) as a solution for positive coolant temperature coefficient in sodium-cooled FAST reactors, Annals of Nuclear Energy (2019)
- [7] HOUSIADAS, C., Simulation of loss-of-flow transients in research reactors. Annals of Nuclear Energy, 27(18), 1683-1693 (2000).

**SESSION IV: TECHNOLOGY AND RESEARCH IN SUPPORT OF SMR
DEVELOPMENT**

MYRRHA TECHNOLOGY AND RESEARCH FACILITIES IN SUPPORT OF HEAVY LIQUID METAL SMR FAST REACTORS

Paper ID #5

R. FERNANDEZ
Belgian Nuclear Research Centre (SCK•CEN)
Mol, Belgium
Email: Rafael.fernandez@sckcen.be

K. VAN TICHELEN, A. AERTS, E. STERGAR,
M. SCHYNS, D. DE BRUYN, H. AÏT ABDERRAHIM
Belgian Nuclear Research Centre (SCK•CEN)
Mol, Belgium

Abstract

The MYRRHA reactor (Multi-purpose hYbrid Research Reactor for High-tech Applications), currently developed at SCK•CEN, will allow the demonstration of transmutation of high-level nuclear waste, fuel developments for innovative reactor systems, material developments for GEN IV and fusion reactors, and radioisotope production for medical and industrial applications. Since MYRRHA is based on heavy liquid metal technology with Lead Bismuth Eutectic (LBE) coolant, it can significantly contribute, during its development and in its operational phase, to the development of Lead Fast Reactor (LFR) technology for both large and SMR systems cooled with Lead Bismuth Eutectic or with Lead. To support the MYRRHA development, SCK•CEN has launched a strong R&D programme to address the main design and licensing challenges, in particular those related to the use of liquid Lead-Bismuth Eutectic as reactor coolant. In this frame SCK•CEN has constructed and commissioned various LBE test facilities for heavy liquid metal chemistry and conditioning research, the heavy liquid metal corrosion research for materials for advanced fast reactors, the testing of mechanical rotating components in heavy liquid metals, reactor component testing in a heavy liquid metal loop and a facility for the validation of complex flows in liquid metal pool systems. These facilities are used for the qualification of the key materials and components of MYRRHA and can also be used for the development of materials and components for fast reactors of all power ranges, including SMR type, working with LBE or Lead as coolant.

The paper describes the SCK•CEN concept roadmap for lead SMR type power reactors based on MYRRHA technology developed from the ongoing R&D programme. The existing research facilities and their applicability for the development of lead SMR type systems are presented.

1. INTRODUCTION

MYRRHA, the Multi-purpose hYbrid Research Reactor for High-tech Applications developed at SCK•CEN [1], will demonstrate the accelerator driven system (ADS) concept by coupling the three components, the accelerator, the spallation target and the subcritical reactor, at power levels capable of providing experience feedback which is scalable to an industrial demonstrator and to allow the study of efficient transmutation of high-level nuclear waste (FIG 1). The MYRRHA-facility is conceived as a subcritical flexible irradiation facility fulfilling the requested application catalogue in subcritical mode. It will also be able to work in critical mode albeit with different performance characteristics. Both modes of operation have their specific energy and flux distributions which permit a wide range of applications: from fuel development for innovative reactor systems; material development for GEN IV systems and fusion reactors, to radioisotope production for medical and industrial applications. As such, MYRRHA will be the successor to the materials testing reactor BR2. Since MYRRHA is based on heavy liquid metal technology with lead-bismuth eutectic (LBE) as coolant, it can also significantly

contribute to the development of Lead Fast Reactor Technology and will therefore play the role of the European Technology Pilot Plant in the roadmap for Lead Fast Reactors (LFR) [2,3].

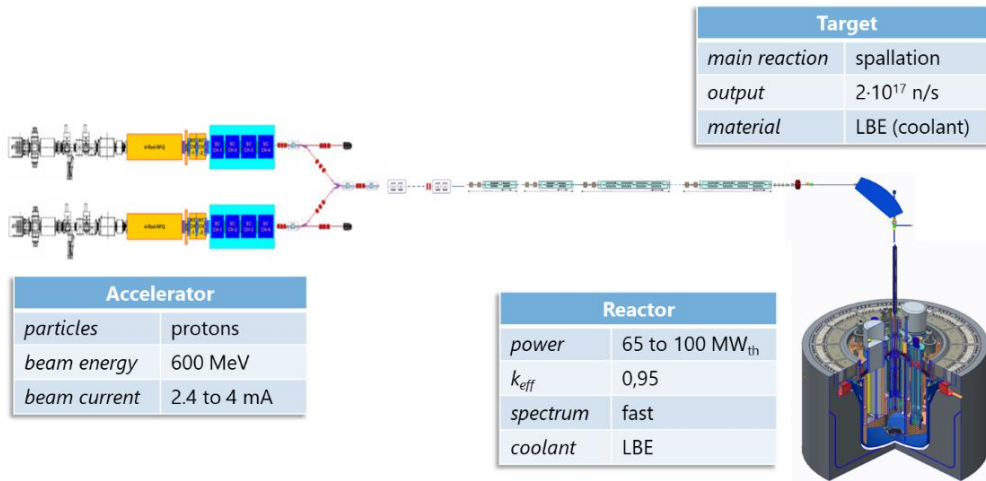


FIG.1. MYRRHA - an Accelerated Driven System: the coupling of the accelerator, the spallation target and the reactor

The application catalogue which MYRRHA has to fulfil to meet the objectives are listed below [1].

- (a) The system will demonstrate the complete ADS concept in representative conditions scalable to an industrial ADS.
- (b) Transmutation studies in representative conditions are ought to be possible. The study of the efficient technological transmutation of high-level nuclear waste, in particular of minor actinides, requires a high intensity of fast flux intensity.
- (c) The system is required to, in ADS mode, also incorporate a provision for material development for fusion reactors which need irradiation with high constant fast flux level, at representative irradiation temperatures and a representative ratio appm He/dpa(Fe).
- (d) Radioisotope production for medical and industrial applications ought to be considered in standard irradiation channels in the core.
- (e) The system needs to be able to be used as a fast spectrum research reactor for material and for fuel.
- (f) MYRRHA is intended to be a technology test platform for Heavy Liquid Metal (HLM)-cooled reactor technology for Gen IV systems and HLM-based SMR's. HLM reactor components such as heat exchangers and pumps and even fuel assemblies can be tested directly in MYRRHA. Although, these components have to be compatible with MYRRHA for what concerns the operational specifications such as dimensions, required mass flow rates, temperature limits, flow paths and for what concerns safety.
- (g) The accelerator of MYRRHA will also be used for fundamental and applied research.

The Belgian government took the decision on September 7th, 2018 to support the construction of MYRRHA at the site of Mol, Belgium in a phased approach. A budget of 558 M€ is allocated for the period 2019 to 2038 divided in three parts [4]:

- 287 M€ is allocated for the construction of the first part of the accelerator up to 100 MeV including an ISOL (Isotope Separator On Line) and a proton target facility. This first phase, called MINERVA, has to be finalised in 2026.
- 115 M€ is reserved for the further design, R&D and licensing for the second part of the accelerator from 100 MeV to 600 MeV (phase 2) and for the reactor (phase 3). The objective is to obtain the construction permit in 2026.
- The remaining 156 M€ will be used for the operation of the MINERVA installation for the period of 2027 to 2038.

To assure the remaining funding of the MYRRHA project the Belgian government requests the foundation of an international non-profit organization welcoming international partners. The most recent version of the high-level planning of the MYRRHA programme is shown in FIG 2.

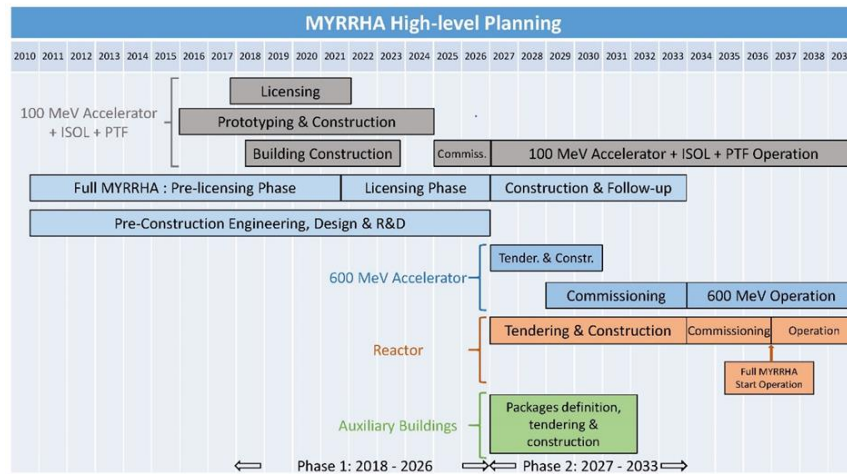


FIG. 2. MYRRHA high-level planning (reproduced from Ref. [4] with permission courtesy of ICAPP)

To achieve the objective of obtaining a construction license in 2026, SCK•CEN conducts since the beginning of the programme an ambitious R&D programme to address the main design and licensing challenges. In this frame SCK•CEN has constructed and commissioned various LBE test facilities which are used for qualification of the key materials and components of MYRRHA. These facilities can also be used for the development of materials and components for fast reactors of all power ranges, including SMR type systems, working with LBE or Lead as coolant.

2. APPLICABILITY OF MYRRHA R&D FACILITIES

The main challenges of the MYRRHA development are in particular related to the use of liquid Lead-Bismuth Eutectic as reactor coolant. Consequently, various LBE test facilities for research on

- heavy liquid metal chemistry and conditioning,
- heavy liquid metal corrosion of materials,
- thermal hydraulics in heavy liquid metals,
- instrumentation in heavy liquid metals, and
- testing of components in heavy liquid metals

have been constructed and commissioned. These research facilities and their applicability for the development of lead SMR type systems are elaborated in the next sections.

2.1. Component testing and thermal hydraulics

2.1.1. ESCAPE

The E-SCAPE facility [4,5], European SCAle Pool Experiment, is a thermal hydraulic 1/6-scale model (FIG. 3.,4.) of the MYRRHA reactor and has been commissioned in spring 2017. The main objective of this installation is the study of the thermal hydraulic behaviour of liquid metal in a complex pool geometry. The characterization of the pool thermal hydraulic phenomena is needed for the code qualification of computational fluid dynamics (CFD) and other system tools used for the safety assessment of a reactor system. The installation uses 27 tons of LBE as working liquid at temperatures between 200°C and 350°C (

TABLE 1). The core is simulated by means of electrical heating elements of 100 kW. The system can work in forced and in natural circulation and is cooled by a secondary system using thermal oil as heat transfer medium. The facility is heavily instrumented with 300 thermocouples, level sensors, ultrasonic Doppler velocimetry and pressure sensors to have a good characterization of the thermal hydraulic phenomena in view of the validation of system thermal hydraulic and computational fluid dynamics (CFD) codes.

Because of the integral system behaviour, the thermal mixing, stratification and flow distribution in plena will be similar in LBE as in lead, this installation can be used, as is, for the code validation of other lead SMR type reactors. Still, if needed, the installation can be equipped with an internal structure, geometrically similar to the studied SMR type and can be upgraded for temperatures of around 400°C allowing the utilization of lead as working liquid.



FIG. 3. The overview of the E-SCAPE facility

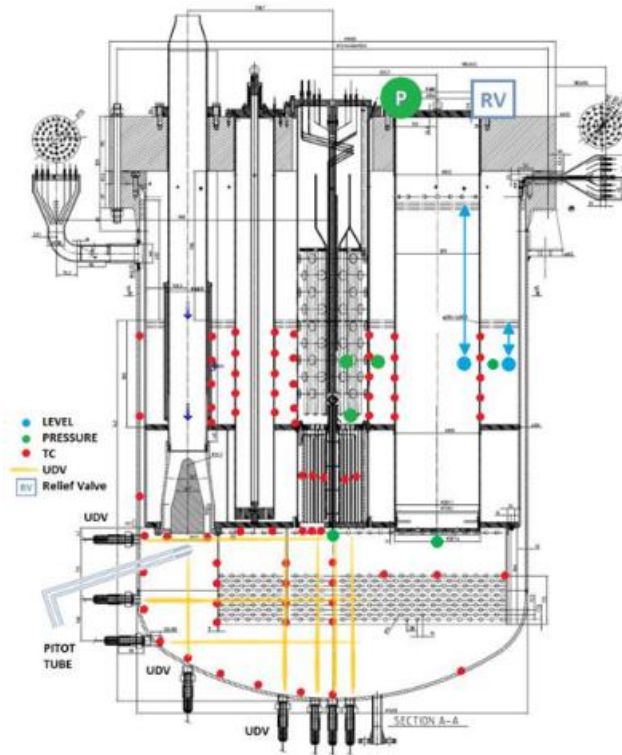


FIG. 4. The E-SCAPE facility: the cross section of the pool indicating the measurement locations

TABLE 1. CHARACTERISTICS OF E-SCAPE

Coolant inventory	27 tons LBE
Additional heating and cooling power	100 kW
Flow range	Up to 120 kg/s
Coolant chemistry control	Is possible
Temperature range	200 °C – 350 °C
Possible upgrade to lead	Up to 400 °C

2.1.2. COMPLIT

The COMPLIT [4,5], **COMP**onents **LO**op **T**esting, facility is a large-scale, closed loop isothermal experimental loop (FIG. 5.) in operation since 2014, used for hydraulic experiments of full-scale reactor components in flowing LBE. The goal of COMPLIT is to simulate a full-scale hydraulic flow path through the MYRRHA core allowing the characterisation of hydraulic and hydrodynamic behaviour of full-scale MYRRHA core components such as the fuel assembly, the spallation target, the control and safety rod systems and other in-pile instrumentation, systems and experiments. The facility operates at a constant temperature in the range of 200 °C – 400 °C with a mass flow range of 3.5 kg/s to 104.8 kg/s (TABLE 2). Due to the size of MYRRHA, the two vertical test sections can accommodate experimental devices up to 12 m tall. The loop is equipped with thermocouples, level sensors, ultrasonic velocimetry, pressure gauges, flow meters and fibre Bragg gratings to measure the pressure drop, flow induced vibration and other relevant parameters of the test sections. Besides the characterisation of the In-Pile Sections (IPS) also the performance and the reliability will be assessed. The results will be also employed for the validation of system codes and CFD. Recently COMPLIT

was equipped with an active coolant chemistry control system to accurately control the oxygen concentration of the nine tons of LBE to study the possible relation between drag and oxygen concentration in the coolant. Due to the modularity of the installation, the test sections can be modified in function of the dimensions of the reactor core component to be tested. Also this installation can be upgraded to lead as working fluid.



FIG. 5. The COMPLIT facility: principal layout and a picture of the installed facility

TABLE 2. CHARACTERISTICS OF COMPLIT

Coolant inventory	9 tons LBE
Additional heating and cooling power	-
Flow range	3.5 kg/s to 104.8 kg/s
Coolant chemistry control	Yes
Temperature range	200 °C – 400 °C
Possible upgrade to lead	Up to 400 °C

2.1.3. HEXACOM

The HEXACOM, Heat EXchanger at COMplot, steam loop [6] is a two-phase water-steam cooling circuit that provides temperatures and flow conditions representative of the MYRRHA Secondary Cooling System (16 bar, nearly saturated water inlet) [1] and is able to reject 100 kW of heat to the environment. The test section is at the interface between an upgraded COMPLIT with a heating capacity of 100 kW and HEXACOM and hosts a single double-walled heat exchanger tube at full scale. The LBE-channel dimensions are chosen to provide flow conditions as close as possible to the MYRRHA configuration. The HEXACOM steam loop is part of the development of the innovative double wall MYRRHA heat exchanger. The steam/water part of the loop represents the MYRRHA secondary system while LBE from the COMPLIT loop represents the reactor LBE side. The facility is currently in commissioning and is expected to be operational in 2020.

The main objectives of the facility (FIG. 6.) is to investigate the heat transfer performances of different PHX configurations within the operational ranges relevant to MYRRHA, to develop and validate heat transfer correlations specific to bayonet tube applications in flowing LBE, to improve the level of knowledge on the phenomena that occur in the steam/water side of double wall bayonet tube heat exchangers operated at low pressure (less than 20 bar), to obtain experimental data suitable for model development and/or the validation and verification of system codes. Since HEXACOM is a small version of the MYRRHA secondary and tertiary system, additional phenomena, typical for steam/water, natural circulation cooling and anti-freezing strategies can be studied in support to the design of these systems in MYRRHA. By design the secondary system can be easily modified to different layouts to test different arrangements and their impact on stability, natural circulation and anti-freezing strategies. The facility is limited by the design parameters of 25 bar, 250 °C and a water flow rate of 1.1 m³/h. The liquid metal parameters are limited by the COMPLIT specifications (TABLE 3).

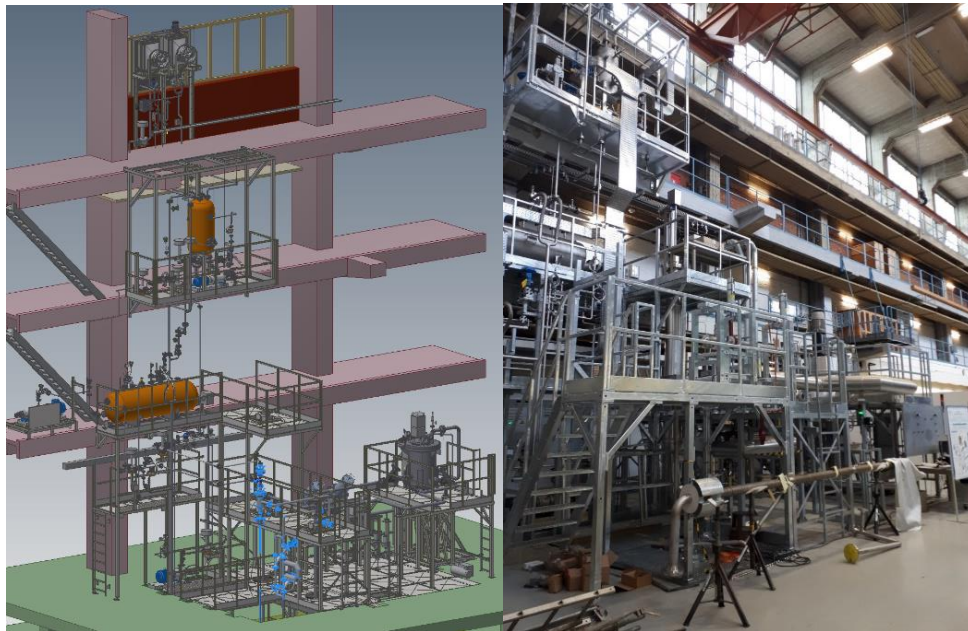


FIG. 6. The HEXACOM facility: principal layout and a picture of the installed facility

TABLE 3. CHARACTERISTICS OF HEXACOM

Coolant inventory	9 tons LBE
Additional heating and cooling power	100 kW
Limit of water/steam cooling system	25 bar, 250 °C, 1.1 m ³ /h
Flow range LBE	3.5 kg/s to 104.8 kg/s
Coolant chemistry control	Yes
Temperature range	200 °C – 400 °C
Possible upgrade to lead	Up to 400 °C

2.1.4. RHAPTER

RHAPTER, the **R**emote **H**Andling **P**roof-of-principle **T**Est **R**ig, in operation since 2011, is designed to test and validate mechanical components submerged in LBE [4,7]. MYRRHA incorporates several machines that work within the liquid LBE such as submerged pumps, the fuel loading system, control and safety rods.

All these machines depend on precise and reliable components like bearings, gears, springs or moving electrical cabling to perform their functions. The main challenge for mechanical components in liquid metals are temperature, compatibility of the materials with liquid metals and lubrication. High temperatures not only limit the choice of materials but also pose problems with thermal expansion, especially in the tight tolerances between the mating parts of mechanical systems. Material problems include corrosion, erosion, dissolution of soft metals and alloying elements, and specific phenomena like liquid metal embrittlement (LME). These can be worsened by the mechanical movement, which hampers the formation of a protective oxide layer on metals or damages protective coatings.

The primary focus for RHAPTER (FIG. 7.) is feasibility testing, to demonstrate the usability and reliability of the required mechanical components in MYRRHA. This involves screening tests of a wide variety of materials and design variations for each component type and detailed testing of promising candidates.

RHAPTER is designed to test mechanical components up to a diameter of 445 mm and a height of 350 mm submersed in liquid metal with a temperature range of 150 to 450 °C which allows a conversion to lead (TABLE 4). Two shafts can be used to power the mechanical component and create different loading situations. This installation is not equipped with a conditioning system but can be upgraded if a controlled oxygen concentration is required.

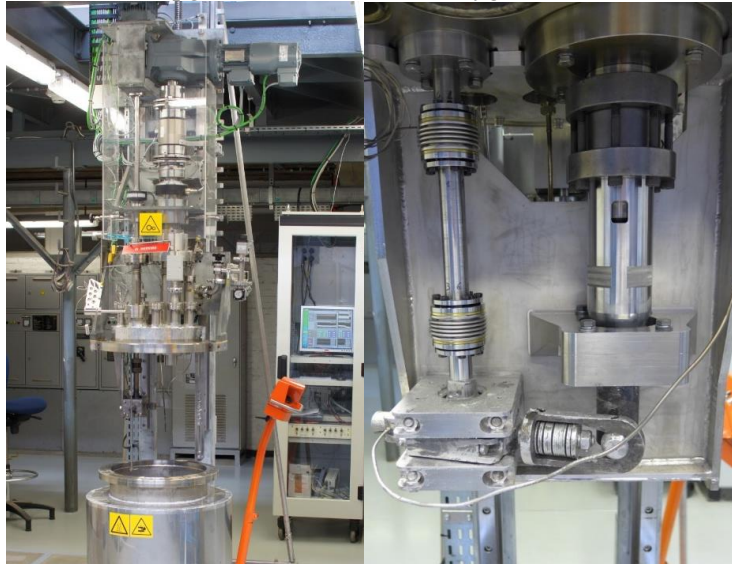


FIG. 7. The RHAPTER facility: the installed facility and a close-up of a bearing testing module

TABLE 4. CHARACTERISTICS OF RHAPTER

Coolant inventory	0.5 tons LBE
Additional heating and cooling power	-
Flow range	-
Coolant chemistry control	Is possible
Temperature range	150 °C – 450 °C
Possible upgrade to lead	Up to 450 °C

2.2. LBE chemistry and conditioning

2.2.1. MEXICO

The MEXICO, **Mass EXchanger In Continuous Operation**, loop (FIG. 8.) is used to test different oxygen control systems, such as the gas phase, solid oxide phase and electrochemical oxygen pumping systems for regulating dissolved oxygen in liquid lead-bismuth eutectic [4]. It is also used to evaluate the efficiency and expected lifetime of filtration systems for purifying the LBE of oxides and possible impurities from the liquid metal flow while minimizing the created heavy metal waste stream. For these two filter housings are located in the lowest temperature zone of the loop to separate not only suspended solid impurities but also dissolved impurities from the liquid LBE by cold trapping. Finally, the data of the 23 potentiometric oxygen sensors will be used to validate numerical models of oxygen mass transfer in LBE. The facility which is in operation since 2014 contains 7 tons of LBE and runs in a temperature range from 200 to 450 °C. For lead reactors this installation could run, after small modifications, in the temperature range from 350 to 450 °C and preferably has to be upgraded to reach 550 °C (TABLE 5).

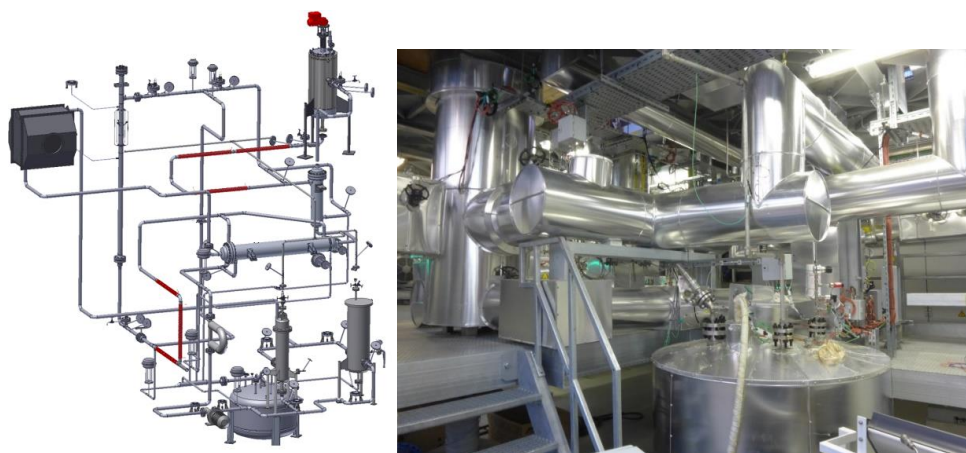


FIG. 8. The MEXICO facility: principal layout and a picture of the installed facility

TABLE 5. CHARACTERISTICS OF MEXICO

Coolant inventory	7 tons LBE
Additional heating and cooling power	120 kW
Flow range	up to 10 kg/s
Coolant chemistry control	Yes
Temperature range	200 °C – 450 °C
Possible upgrade to lead	From 350 °C to 450 °C, upgradable to 550 °C

2.2.2. HELIOS

HELIOS, **HE**avy **L**iquid metal **O**xygen conditioning **S**ystem, is a LBE conditioning and storage setup (FIG. 9.) which is used to investigate LBE conditioning schemes [4]. It can also serve to study calamity mitigation strategies after a possible steam ingress due to a tube rupture in a heat exchanger or exposure to air. The conditioning in this installation is based on the method of gas bubbling with a given composition of Ar:H₂:H₂O through the liquid metal implemented using removable sparger/impeller inserts. The sparger injects small bubbles which are redistributed in the liquid metal by the impellers to improve the gas-liquid interaction. A gas recirculation system allows minimizing the conditioning gas consumption. This installation is in operation since 2013 and can be operated up to 450 °C which allows a conversion to lead and can be adapted to other conditioning schemes (TABLE 6).

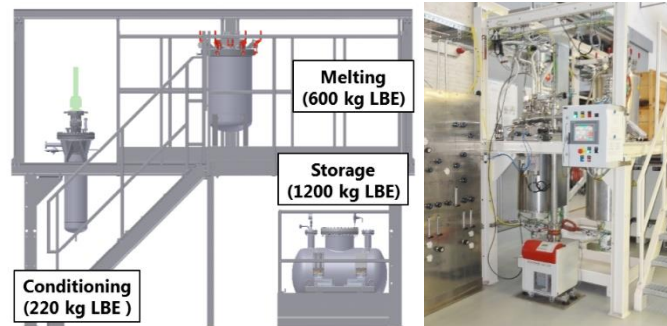


FIG. 9. The HELIOS facility: principal layout and a picture of the installation

TABLE 6. CHARACTERISTICS OF HELIOS

Coolant inventory	220 kg LBE
Additional heating and cooling power	-
Flow range	-
Coolant chemistry control	Yes
Temperature range	Up to 450 °C
Possible upgrade to lead	Up to 450 °C

2.2.3. LILIPUTTER-II

LILIPUTTER, **L**iquid **L**ead alloy **I**nnovative **P**ump **T**echnology **T**est **R**ig, was a small loop (FIG. 10.) in operation from 2010 to test different small LBE pumps and was modified in 2013 to test several filter media to remove solid impurities. More recently an oxygen control system was installed, and this installation is being used as a test bench for cold trap development. Due to the used screw spindle pump the loop temperature is limited to 200 °C but the system can be upgraded to work at 400 °C (TABLE 7), allowing the use of lead as working medium.

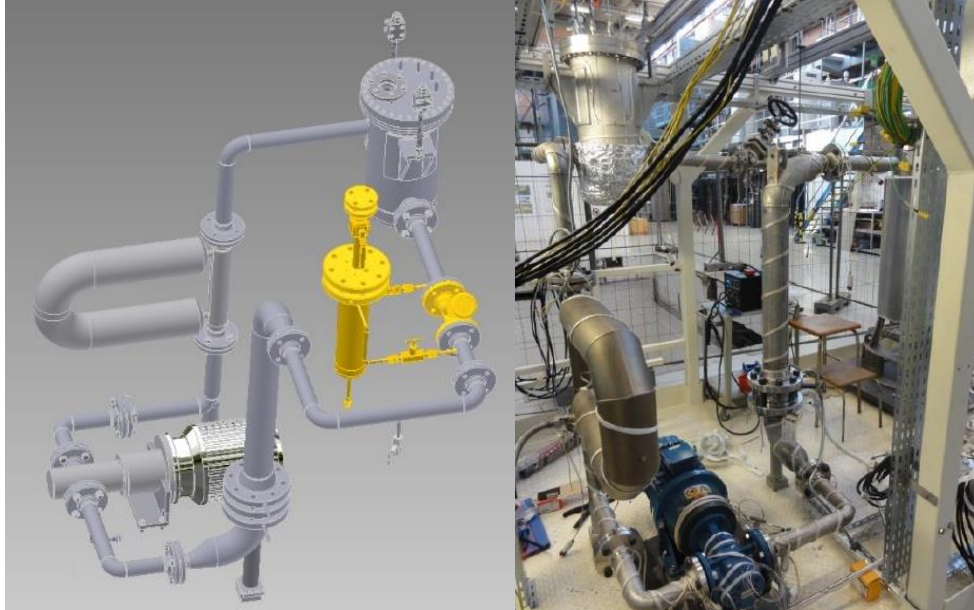


FIG. 10. The LILIPUTTER facility: principal layout and a picture of the installed facility

TABLE 7. CHARACTERISTICS OF LILIPUTTER

Coolant inventory	0.855 tons LBE
Additional heating and cooling power	-
Flow range	up to 100 kg/s
Coolant chemistry control	Yes
Temperature range	200 °C
Possible upgrade to lead	Up to 400 °C

2.2.4. Heavy Metal Lab (HLM)

The Heavy Metal Lab (HML) operational since 2012, is equipped to perform chemistry experiments with heavy metals in a controlled environment. The HML accommodates an inert gas glove box which contains evaporation setups to study the evaporation of impurities from heavy metals under various conditions of temperature and gas atmosphere composition (FIG 11FIG.). Typical impurities under investigation include fission products such as iodine and caesium which are important for the safety assessment of reactor systems. Recently a triple filter quadrupole mass spectrometer is connected to the evaporation setup to study the gas-phase chemistry of evaporated molecules. Specific for accelerated driven systems, a dedicated setup to study the evaporation of mercury from LBE has been developed and implemented. These evaporation setups can work up to 1000 °C allowing the study of all types of heavy metals.

Besides these evaporation setups also autoclaves for oxygen sensor and oxygen-pump testing, a setup for electronic impedance spectroscopy studies of sensor membranes and autoclaves with oxygen control for corrosion studies under stagnant and stirred conditions are available. These autoclaves are designed for a temperature of 500 °C and can be used with lead.

A setup named CHEKMATE (**CHEMical Kinetics and MAss transfer Experiment**) is used to study chemical reactions with oxygen and impurities in LBE whereas with the OSCAR setup (**Oxygen Sensor CALibration Rig**) nucleation, growth, dissolution and deposition of lead oxide particles in LBE is currently studied. Both setups can be used for studies with lead.

In a dedicated lab, polonium release from LBE or lead up to 1000 °C under flowing Ar, H₂ and H₂O can be performed and the deposition of volatile polonium-species on different media can be studied.



FIG. 11. The Heavy Metal Lab: picture of the lab with the different set-ups

2.3. Materials

2.3.1. CRAFT

CRAFT, Corrosion Research for Advanced Fast reactor Technology, [4] is an installation for long term corrosion experiments on MYRRHA candidate materials in liquid LBE. The loop type installation operates at representative conditions of temperatures, LBE velocities and dissolved oxygen concentrations of MYRRHA. The loop (FIG 12), in operation since 2014, consists of a cold leg running at 200 °C (designed for 450 °C) and a hot leg equipped with two materials-test sections which can run up to 550 °C. The system (TABLE TABLE 8) is filled with 4 tons of LBE and equipped with a magneto hydrodynamic pump that delivers up to 10 kg LBE/s by which flow velocities of up to 5 m/s can be reached in the test section. The facility is equipped with an oxygen control system, 12 oxygen sensors, a Coriolis flowmeter and pressure measurements to accurately control and monitor the process parameters of the long term experiments. This facility can easily be converted to lead to perform corrosion and erosion tests on candidate materials of future SMR reactor systems with lead. The CRAFT loop is also equipped with a glove box which allows to conduct stagnant corrosion tests in oxygen free highly purified environment. In total 12 test stations can be easily adapted for tests in PbBi, Pb, PbLi and Li.

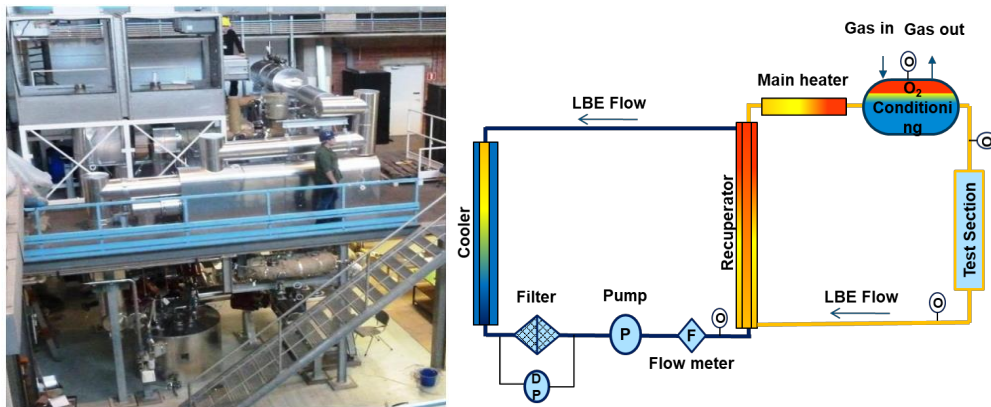


FIG. 12. The CRAFT facility: overview picture of the installed facility and principal layout

TABLE 8. CHARACTERISTICS OF CRAFT

Coolant inventory	4 tons LBE
Additional heating and cooling power	60 kW
Flow range	Up to 10 kg/s (5 m/s)
Coolant chemistry control	Yes
Temperature range	200 °C – 550 °C
Possible upgrade to lead	Up to 550 °C

2.3.2. LIMETS

LIMETS, **L**iquid **M**etals **T**est **S**tands, [4] are experimental set-ups designed for mechanical testing of materials in a stagnant LBE environment in order to investigate mechanisms and kinetics of material-liquid metal interactions that influence the mechanical properties of materials. Currently 4 installations are in operation and consist of an autoclave in which experiments are performed (FIG. 13.). The oxygen concentration in LBE is controlled via gas mixture and continuously monitored by oxygen sensors. The autoclave houses a mechanical testing device that can operate either in a gas atmosphere or in stagnant liquid metal. The temperature range of all the facilities is from room temperature up to 550 °C (TABLE 9). The 4 installations differ by the tests that can be performed. LIMETS 1 is equipped to perform tensile tests, fracture toughness tests, slow strain rate tests, constant load tests and crack growth rate experiments. LIMETS 2 is identical to LIMETS 1 regarding the testing capabilities but is installed in a hot-cell in the Laboratory for High and Medium Activity allowing for testing of irradiated (including alpha contamination) samples. LIMETS 3 is designed for fatigue tests with a load of up to 15 kN and a frequency of 0.3 Hz in liquid metal with an extensometer on the sample [8]. LIMETS 4 is based on LIMETS 1 but the range of possible experiments is increased. All four set-ups can be easily converted to lead.

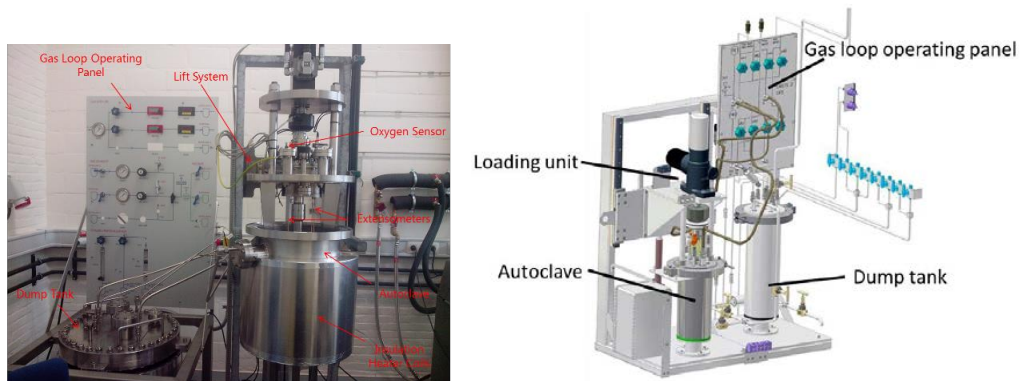


FIG. 13. The LIMETS facility: overview picture of LIMETS 3 and the design layout of LIMETS 1

TABLE 9 CHARACTERISTICS OF LIMETS 1, 2, 3 AND 4

Coolant inventory	From 35 kg to 150 kg LBE
Additional heating and cooling power	-
Flow range	-
Coolant chemistry control	Yes
Temperature range	Up to 550 °C
Possible upgrade to lead	Up to 550 °C

3. IMPLEMENTATION STRATEGY OF A LEAD FAST REACTOR SMR BASED ON THE MYRRHA TECHNOLOGY

The objective of the MYRRHA Reactor Programme for the period of 2019 – 2026 is to obtain at the end of 2026 the necessary permits from the licensing authority to be able to start the construction of the MYRRHA Reactor (phase 3). The MYRRHA reactor programme consists of the reactor primary system design, the licensing and the R&D in support of the design and the licensing.

In the first phase until end 2020 (FIG 14) a coherent concept design is developed answering the issues found in the previous design. In this first phase the pre-licensing will be closed. In the second phase the conceptual design will be developed further to a basic design which is, amongst others necessary to establish the Preliminary Safety Analysis Report (PSAR) to request a license. In parallel of the basic design, the needed safety studies are performed and reported to the federal safety authority in the licensing process. At the end of this process in 2024 the final report including the PSAR will be delivered to the safety authority. In this second phase the licensing is formally initiated. In the last phase the safety authority will finalize the review of the documents. During this period some details of the design are elaborated in function of the requests of the safety authority. It is expected that the necessary license needed to start construction is obtained at the end of 2026.

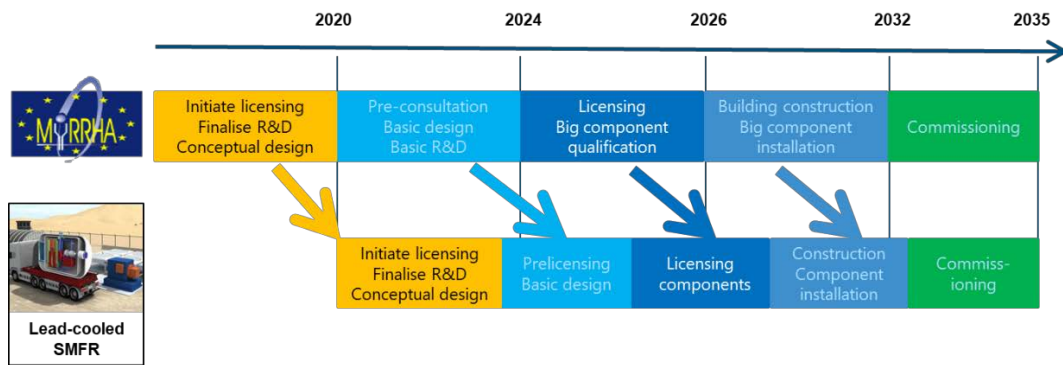


FIG.14. Deployment strategy

Using the MYRRHA technology platform, licensing experience and R&D facilities which can be converted to lead, could support the development of lead based fast reactor SMR. As shown in FIG. the deployment could be phased according to the development of the MYRRHA project to limit the research effort and allow a fast implementation. This fast implementation is possible if MYRRHA key components such as the fuel assembly concept, MYRRHA candidate materials, limited power densities, limited temperatures and coolant velocities are considered. These disadvantages can be partly compensated by long operation cycles. In a later phase the power density can be increased by an update of materials and/or the use of coatings, relaxing the temperature and velocity limits.

4. CONCLUSION

The MYRRHA reactor programme with its associated R&D and licensing experience can support the development of SMR working with LBE or Lead as coolant. The R&D facilities can be converted or upgraded to the specific needs of lead and contribute to the qualification of materials and components of these systems. Furthermore, the design and licensing experience gained during the MYRRHA development can help to accelerate the deployment of lead fast reactors of the SMR type. By using MYRRHA components, a fast deployment of lead based SMR's could be considered. In a second phase MYRRHA can be used for the further qualification of materials, fuel and components which will help to improve these first and later generation of lead based SMR's. This forms the basis of MYRRHA as technology test platform for Heavy Liquid Metal (HLM)-cooled reactor technology for Gen IV systems and HLM-based SMR's.

REFERENCES

- [1] FERNANDEZ R., DE BRUYN D., BAETEN P., AÏT ABDERRAHIM H., The Evolution of the Primary System Design of the MYRRHA Facility, Fast Reactors and Related Fuel Cycles: Next Generation Nuclear Systems for Sustainable Development (FR17) (Proc. Int. Conf. Yekaterinburg, Russian Federation, 2017), IAEA, Vienna (2018) Paper CN245-358.
- [2] SNETP – SUSTAINABLE NUCLEAR ENERGY TECHNOLOGY PLATFORM, ESNI – THE EUROPEAN SUSTAINABLE NUCLEAR INDUSTRIAL INITIATIVE, A contribution to the EU Low Carbon Energy Policy: Demonstration Programme for Fast Neutron Reactors, October 2010.
- [3] SNETP – SUSTAINABLE NUCLEAR ENERGY TECHNOLOGY PLATFORM, Strategic Research and Innovation Agenda, February 2013.
- [4] DE BRUYN D., AÏT ABDERRAHIM H., SCHYNS M., Recent progress and perspectives in the Belgian MYRRHA ADS programme, International Congress on Advances in Nuclear Power Plants (ICAPP 2019), Juan-les-Pins, France, May 12 – 15, 2019, Paper 64.
- [5] VAN TICHELEN K., GRECO M., KENNEDY G., MIRELLI F., COMPLIT and E-SCAPE: Facilities for Liquid-Metal, Pool-Type Thermal Hydraulic Investigations and their Associated R&D Program in the Frame of the MYRRHA Project, The 10th International Topical Meeting on Nuclear Thermal-Hydraulics, Operation and Safety (NUTHOS-10), Okinawa, Japan, December 14 – 18, 2014.
- [6] ROZZIA D., KENNEDY G., MIRELLI F., VAN TICHELEN K., Development of the HEXACOM facility for characterizing the heat transfer performance of the MYRRHA PHX in LBE, SESAME International Workshop, Petten, The Netherlands, March 19 – 21, 2019.
- [7] CAERS B., The RHAPTER test rig, Internal Report SCK•CEN-I-236, April, 2013.
- [8] MARMY P., GONG X., LIMETS 3, a novel system for high strain fatigue testing in lead-bismuth eutectic, Journal of Nuclear Materials, vol. 450, pp. 256-261, 7 2014.

M. LANCONELLI

University of Bologna, DIN, Lab. of Montecuccolino
Via dei Colli, 16, Bologna, 40136, Italy
Email: marco.lanconelli@studio.unibo.it

M. SUMINI

University of Bologna, DIN, Lab. of Montecuccolino
Via dei Colli, 16, Bologna, 40136, Italy
Email: marco.sumini@unibo.it

S. MANSERVISI

University of Bologna, DIN, Lab. of Montecuccolino
Via dei Colli, 16, Bologna, 40136, Italy
Email: sandro.manservisi@unibo.it

Abstract

A preliminary hexagonal geometry of the SMR model of the ALFRED (Advanced Lead Fast Reactor Demonstrator) concept design for a lead cooled reactor is analysed with a computational platform that integrates different computational tools into the common framework given by the SALOME platform software. The purpose of the paper is to investigate the multiphysics (thermal-hydraulic-neutronic) approach to this SMR model by coupling the DRAGON-DONJON codes, for lattice calculations and full core simulation, with a 3D-porous media thermal-hydraulic code, FEMUS. In particular, the lattice code, DRAGON, is used to evaluate the macroscopic cross sections over the hexagonal lattice devised for ALFRED, collapsing the microscopic cross section data into 33 groups, parametrized on fuel and moderator temperature, density and power distribution. With the macroscopic cross sections for the various lattice cells of the reactor defined, the distribution of neutron flux in the core is obtained by the full core simulation with the DONJON code, that may be used in the simulation of fuel management, reactor operation or accident scenarios. In transient simulations (in a quasi-static approach), at each time step, the neutron flux is computed with the corresponding thermal source while the thermal-hydraulic module (FEMUS) computes the distribution of the coolant velocity, pressure and temperature fields in the reactor core. Then the neutron modules can receive all the feedback variables, as fuel temperature, moderator temperature and density that can be cast in input to the DRAGON code, where macroscopic cross sections are interpolated, and total neutron fluxes evaluated. In this way, one can obtain an iterative process for studying the transient evolution of the model of the ALFRED fast lead cooled reactor as SMR case-study and preliminary results about his time-dependent behaviour can be fully analysed.

1. INTRODUCTION

In recent times, with challenges associated to anthropic activities environmental impact and global climate changes more and more evident, nuclear energy has been considered able to play a long-term role for meeting the world's increasing energy demand. An interest in small and simple units able to generate electricity from nuclear power is growing due to the need of reducing the impact of capital costs and provide power to larger and smart grid systems.

The International Atomic Energy Agency (IAEA) defines “Small Modular Reactors (SMRs) as nuclear reactors, generally 300 MW(e) equivalent or less, designed with modular technology using module factory fabrication, pursuing economies of series production and short construction times” [1]. The World Nuclear Association 2015 report on SMR standardization of licensing and harmonization of regulatory requirements, wrote that the enormous potential of SMRs is based on features such as small power and compact architecture that allow building of SMR units directly at factory, improving the level of construction quality and efficiency [1].

TABLE 1. ALFRED SMR CORE MAIN PARAMETERS (REPRODUCED FROM REF. [3,4])

Parameters		Unit	Value	
PIN	Thermal Power	MW	300	
	Pellet hollow diameter	mm	2.0	
	Pellet radius	mm	4.5	
	Gap thickness	mm	0.15	
	Clad thickness	mm	0.6	
	Pin diameter	mm	10.5	
	Bottom plug length	mm	50	
	Gas plenum height	mm	550	
	Bottom insulator height	mm	10	
	Active height	mm	600	
	Upper insulator height	mm	10	
	Spring length	mm	120	
	Upper plug height	mm	50	
Fuel Assembly	Lattice pitch (hexagonal)	mm	13.86	
	Pins per FA	-	126	
	Wrapper thickness	mm	4.08	
	Distance between to wrappers	mm	5.0	
	Average coolant velocity	m/s	1.28	
	CORE	Inner/Outer FAs number	-	56/78
Inner Vessel Radius		m	1.475	
Cycle length		month	12	
Number of batches		-	5	
FUEL	Pu vector	²³⁸ Pu	atom%	2.348
		²³⁹ Pu		57.015
		²⁴⁰ Pu		26.951
		²⁴¹ Pu		6.069
		²⁴² Pu		7.616
	U vector	²³⁴ U	atom%	0.003
		²³⁵ U		0.409
		²³⁶ U		0.010
		²³⁸ U		99.578
		Inner/Outer enrichment (Pu+ ²⁴¹ Am)/(Pu+ ²⁴¹ Am+U)	atom%	20.5%/26.2%

Furthermore, the small size and passive safety system could drive to massive use of SMRs in countries with small grids and less experience of nuclear power due to a more flexible financing policy. The lower power reduces the reactor radioactivity inventory, minimizes costs for a specific SMR design and during decommissioning, at the end of the core lifetime, the small size makes easier to remove reactor modules. There are different options for SMR's technology since these technologies allow the construction of a large range of small and simple reactors with long operational period before refuelling.

This paper is devoted to the analysis of a fast neutron lead cooled reactor with a core in hexagonal geometry. In particular the multi-physics approach, described in this paper, is focused on the conceptual design of ALFRED (Advanced Lead Fast Reactors European Demonstrator) [2,3,4], that is based on the sustainability of the nuclear energy source in the long term and on the high level of reactor safety design due to the intrinsic features of the lead coolant. The features of ALFRED in terms of thermal power and core size (small core sizes are more suitable for a joint neutronic-thermo-hydraulic modelling) makes it an interesting case-study that can be eventually extended to other SMR of the same class.

The details of the ALFRED core main parameters are reported in Table 1 [2,3,4] and a core configuration in Figure 1.

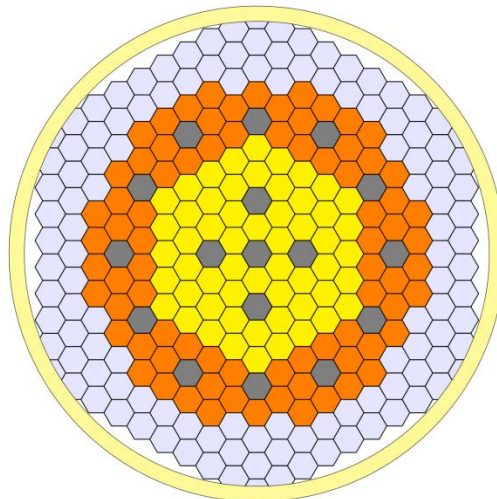


FIG. 1. Core geometry for ALFRED where inner MOX fuel with 20.5% in plutonium (yellow) and outer MOX fuel with 26.2% in plutonium (orange) (reproduced from Ref. [4]).

2. THE APPLICATION OF THE DRAGON LATTICE CODE

The hexagonal geometry, as shown in Figure 2, has been built by following symmetry criteria in order to save computational time. The first step of a multi-scale neutronic approach consists of the creation of data structures containing macroscopic cross sections about the elements that form the nuclear reactor fuel.

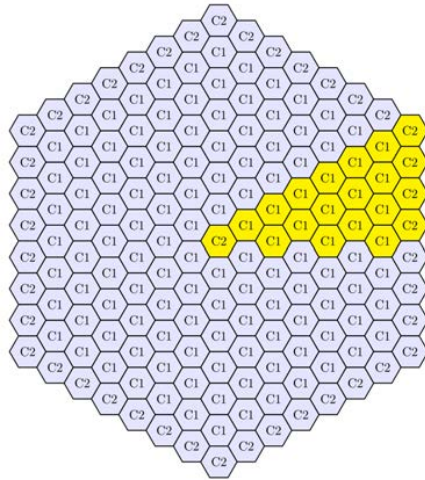


FIG. 2. Hexagonal geometry of the fuel assemblies used by Dragon-Donjon-FEMUS

This is obtained by using the lattice code DRAGON, version 5, released by Ecole Polytechnique of Montreal, a computer code designed around solution techniques of the neutron transport equation, which can simulate the neutronic behaviour of a fuel assembly in a nuclear reactor [5]. Based on the work in [2,3,4] for the project data of ALFRED, we use three kind of macroscopic cross sections: two for fuel assemblies with different enrichment in plutonium and one for structural and control materials such control rods, safety rods and plenum lead. The lattice code DRAGON obviously starts from the microscopic cross sections libraries of nuclear data. In this case we used JEFF 3.1.2 cross section library with 315 energy groups (as reworked by Santamarina, Hebert and Hfayed) that, by setting nuclei properties, creates the needed micro-libraries. Elementary nuclei are chosen taking into consideration fuel, coolant and cladding temperature together with nuclei density in order to consider Doppler and material expansion effects.

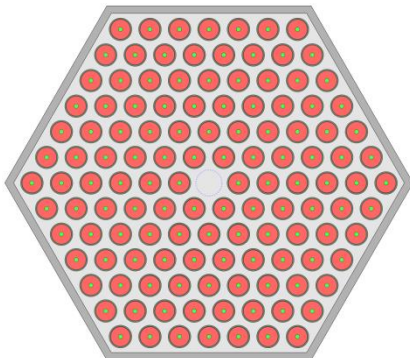


FIG. 3. Fuel assembly with 126 fuel pins, fuel pin (Ref. [4])

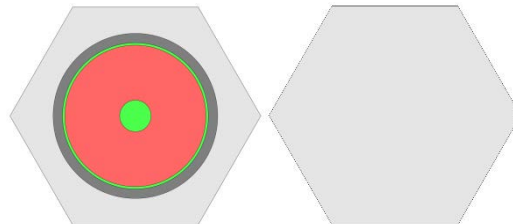


FIG. 4. Cell C1(left) composed by lead, helium gap, cladding and cell C2 (right) only composed by lead

The neutron transport equation in the lattice, is solved with the collision probability method [6] using a hexagonal geometry according to model geometry of the fuel assembly as defined in [2,3,4] (see Figures 3 and 4). The cell C1, shown in Figure 4, constitutes the fuel pin which is composed by lead, cladding, helium gap and nuclear fuel, while the cell C2 constitutes the structural parts of the fuel assembly. Then, the data structures of the macroscopic cross sections have been created using a series of calculations that take into account self-shielding, fuel burn-up, temperature and concentration changes. These data structures, called multi-compo, are condensed in 33 energy groups in order to reduce computation time while maintaining a high level of accuracy.

3. THE FULL CORE ANALYSIS (DONJON CODE)

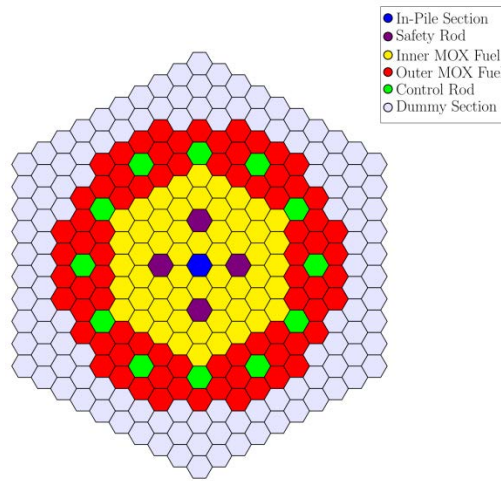


FIG. 5 Core map of reactor composed by assembly of In-Pile section (blue), Safety rods (violet), Control rods (green), Inner MOX Fuel (yellow), Outer MOX Fuel (red) and Dummy elements (grey) (Ref. [4])

The comprehensive neutronic behaviour of this nuclear reactor is investigated with the full core simulation by using the DONJON, version 5, code and the group cross sections from the previous lattice code step in order to obtain the reactor characteristics as flux and power distribution. ALFRED (Advanced Lead-cooled Fast Reactor European Demonstrator) [2,3,4] is a demonstrator of the lead fast reactor technology, with a foreseen thermal power of 300 MW and his composition of U and PU vectors is a typical MOX fuel but with enrichment different for inner (yellow FA) and outer (red FA) core zones, with the purpose of a more uniform (flat) flux distribution on the whole core. Some parameters of the reference model used in this work have been reported in Table 2 [3].

TABLE 2. Reference data used to model the ALFRED reactor (Ref. [4]).

Parameters	Value
Thermal Power [MW]	300
Total Fuel Assembly	134
Inner Fuel Assembly	56
Outer Fuel Assembly	78
Control Rods	12
Safety Rods	4
In-Pile Section	1
Inner vessel inner/outer radius [m]	1.475/1.525
Total Height Vessel [m]	3.50
Active Height [m]	0.60 </td
Average Core Flow [m/s]	1.28
Coolant inlet/outlet Temperature [°C]	400/520

The core map has a hexagonal geometry as shown in Figure 5. The geometry of the whole reactor core has been considered as a hexagonal prism, as in Figure 5, comprising 10 rings and 16 floors with different level of accuracy, in particular in the core zones. The full core simulation employs finite elements methods to resolve neutron diffusion and simplified PN equations [7]. The fuel bundles have a distinct set of properties that are recovered from the reactor database, obtained from lattice calculations, and then interpolated according to the specified global or local parameters.

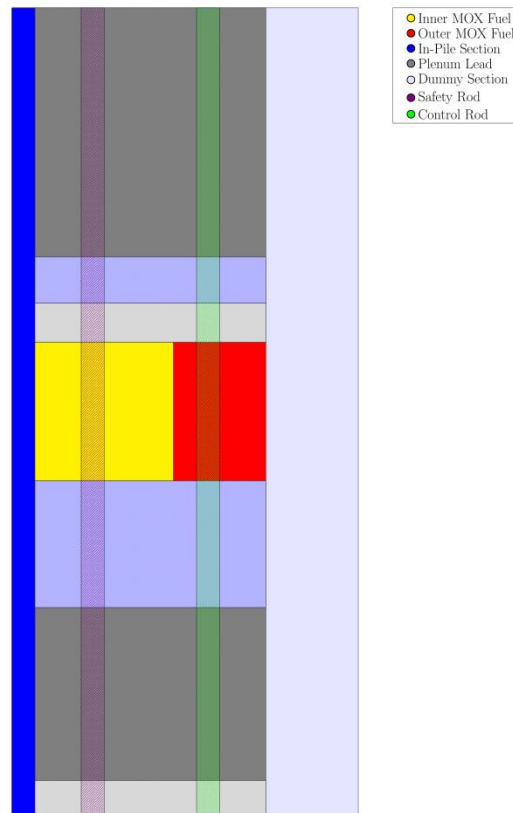


FIG. 6. Axial profile of reactor used during the full core simulation

In this way, it is possible to interpolate the values of fuel and coolant temperatures that are obtained from the thermal-hydraulic analysis, and set an iterative approach producing values for both neutronic and thermal-hydraulic codes. Flux distribution, power distribution, peak power factor and effective multiplicative factor are computed by full core simulation code. In order to validate the obtained computations, we take into account the reference multiplication factor and compare the results with other works [3]; in Table 3 we show the results from computation Monte Carlo code, MCNP [9], considering BOC at 2 years and EOC at 3 years about the study in reference [3]. Therefore, in these works the cycle swing in one year (evaluated between BOC and EOL) is $\Delta k_{\text{eff}}/k_{\text{eff}} = -2580$ pcm for MCNP code and about -2500 pcm for ERANOS code [8]; these values are closed enough with DONJON code, where the burn-up swing is about -2300 pcm.

Anyway, the difference of k-effective between computational codes is wide. However, the results are inside a reasonable range of values since this computational design is an ALFRED-like model and so some dimensional parameters are not up to date, some are a little different and others are not available.

TABLE 3. K-EFFECTIVE WITH CONTROL RODS WITHDRAW FROM DIFFERENT COMPUTATIONAL APPROACHES. [3]

Time (days)	DONJON	MCNP
0	1.11403	1.0804
365	1.08531	1.0510
730 (BOC)	1.05929	1.0247
1095 (EOC)	1.03549	0.9988

4. THE NUMERICAL PLATFORM

The principal purpose for code coupling in the wrapping numerical platform is to couple the solution of a multi-physics and multi-scale three-dimensional problem inside a simplified and more comprehensive framework. The Salomé project facilitates the coupling of scientific mesh-based codes [10], in our case between the full core simulations by the DONJON code and the open source code FEMUS, thanks to its architecture and suite of tools that provide several data interfaces and exchange across the different codes.

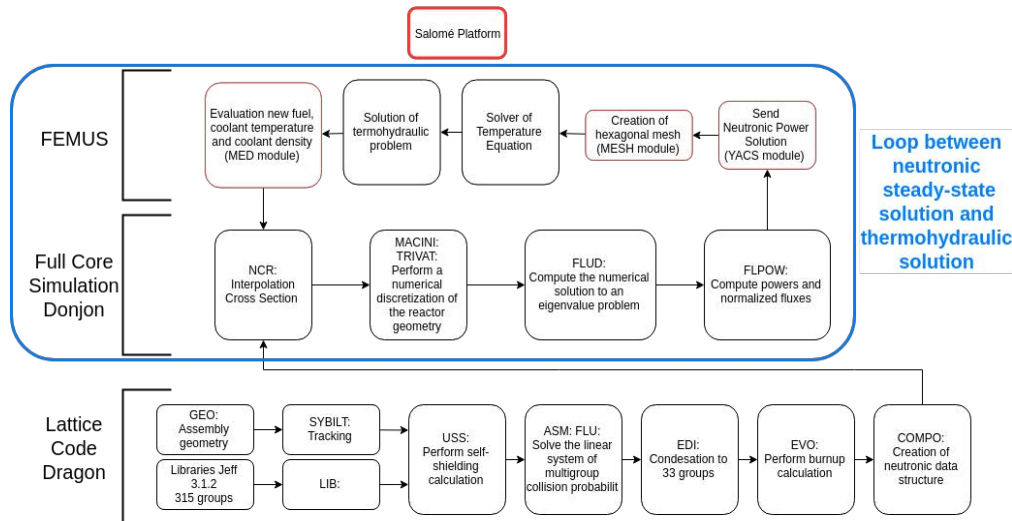


FIG. 7 Flowchart of the coupled neutronics-thermal hydraulics problem

Inside Salomé there are libraries, called MED (Modélisation et Echanges de Données, i.e. Data Modelization and Exchanges) modules, that provide a library for storing and recovering computer data in a suitable format. The MED data transfer is based on the association of numerical meshes with fields and allows the data exchange between solvers and codes. The GEOM and MESH modules of the Salomé platform have the main function to draw and create meshes in MED format, respectively.

Other Salomé module such as the YACS module is a tool to supervise execution of complex interconnected scientific applications as object structure available during execution of DONJON code. The integration of a code on the Salomé platform is obtained by generating an interface with functions available in the MEDMem library that allows a data transfer from the platform to the code and then from the code to the interface.

In addition to neutronic codes, previously described, CFD modules [11,12] have the function to solve energy and temperature equations starting from a given neutronic power density distributions. Temperature fields, evaluated with CFD codes, FEMUS or OPEN-FOAM, may be introduced into the DONJON neutronic code with the purpose of interpolating macroscopic cross sections according to the local temperature fields and local coolant (lead) density distributions. As result of this temperature distribution the neutron flux changes and defines a new power density distribution inside these CFD modules. In particular, the nuclear reactor is modelled as a *porous* medium where we consider the real assembly geometry and the effective mass flow: this approach allows us to consider that the lead cooling is effective only on a part of the assemblies, being the available cooling channels limited by fuel assemblies and structural materials. A flowchart that summarizes the behaviour of this multi-physics approach with the Salomé platform is shown in Figure 7.

5. RESULTS AND CONCLUSION

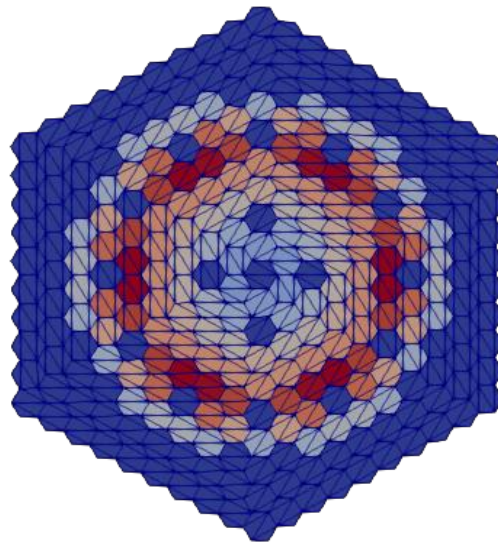


FIG. 8. Finite element solution for the neutronic power of reactor ALFRED with a mesh optimized for the neutron transport equation.

In both CFD and neutron transport codes, the various fields have been computed using a FE method over different refined meshes. The coarse mesh, as shown in Figure 8, consists of

hexagonal assemblies. Each assembly element is divided in such a way that each sub elements have quadrangular surfaces. This coarse mesh is then refined by using midpoint refinement algorithm several times. Each hexagonal element has constant properties but several field points.

In conclusion a collection of images for the flux distribution, power distribution and temperature field are reported in Figures 9-13, that describe the behaviour of the core model on different sections at different heights.

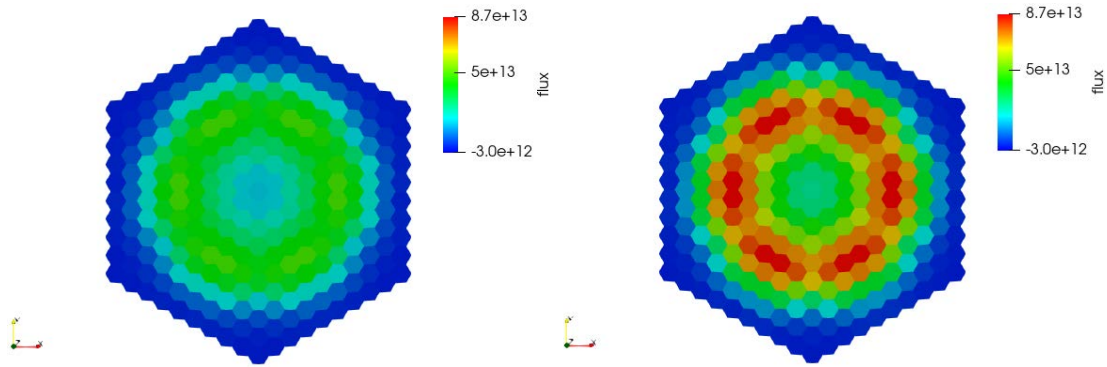


FIG. 9. Flux distribution over a section of core reactor at 150 cm (left) and 175 cm (right).

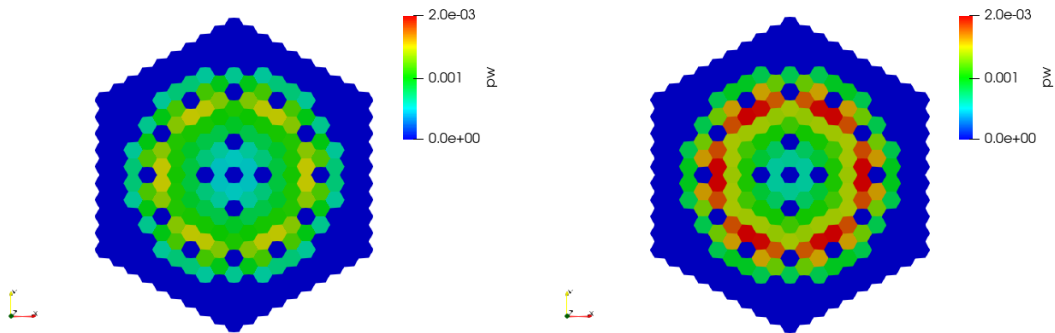


FIG. 10. Normalized power distribution over a section of core reactor at 150 cm (left) and 175 cm (right), i.e. at the top and at the middle of the core active zone.

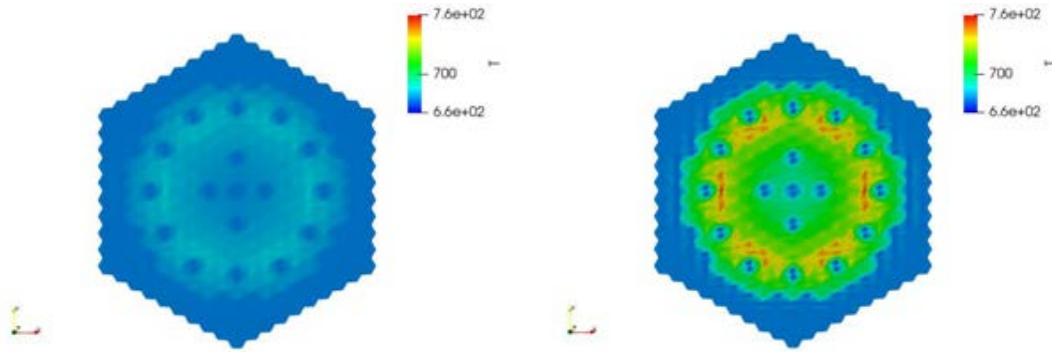


FIG. 11. Temperature field over a section of core reactor at 150 cm (left) and 175 cm (right).

In particular Figure 9 shows the total neutronic flux over two different planes of the reactor. On the left we have the distribution on the section at 150 cm while on the right the section is located at 175 cm from the bottom. It is important to recall that the neutron flux is computed using 33 groups and this is the integral over all energy values. Figure 10 shows, from the left to the right, the normalized power distribution over a section of core reactor at 150 cm and 175 cm, respectively. The thermal power is computed based on the peak factors which represent the ratio between the assembly thermal source and the average assembly power. The thermal source contributes by advection thanks to the velocity field of each assembly and is diffused by solving the 3D energy equation of the porous media core model. Figure 11 shows the temperature over the same section of core reactor at the same heights as before. The temperature distribution resembles the thermal power distribution and shows cooled area in the assemblies where there is no heat generation.

In Figure 12 we show a summary for neutron flux, thermal power distribution and temperature field. The neutron flux, the power distribution and the temperature field are reported on the left, centre and right over the sections of core reactor defined by the z-value of 150 cm (top), 175 cm (centre) and 200 cm (bottom), respectively.

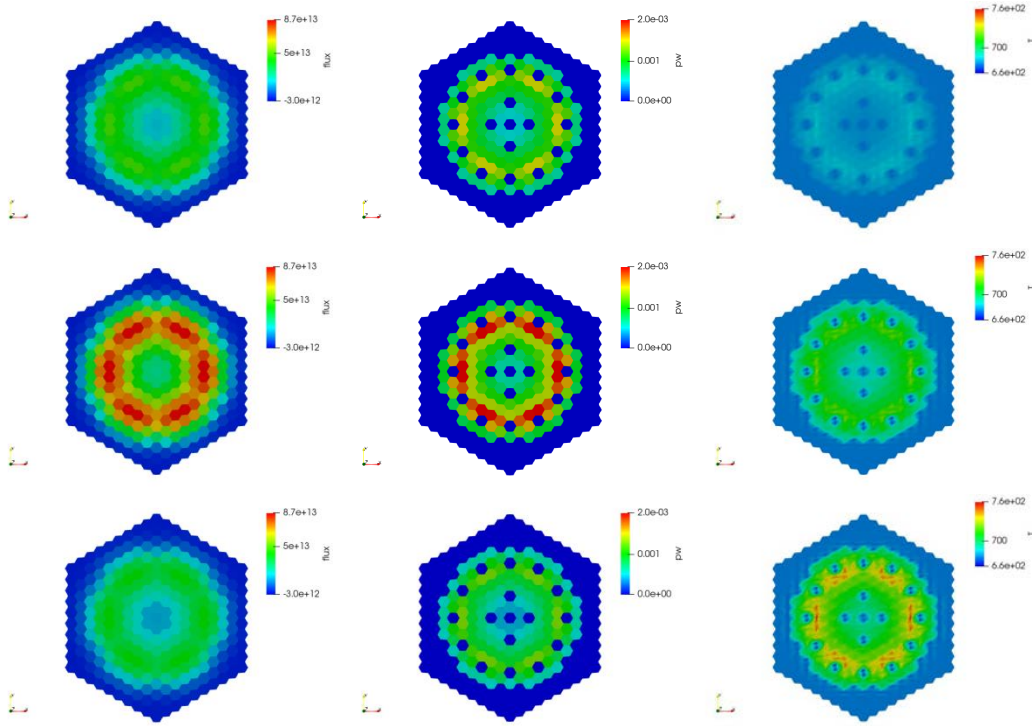


FIG. 12. Flux distribution (left), Power distribution (middle), Temperature field (right) at section of core reactor at 150 cm (top), 175 cm (centre) and 200 cm (bottom).

The solution is obtained after several iterations between the thermal-hydraulic and the neutron code with temperature and density feedback corrections. In Figure 13 the neutron flux and the thermal power field over a vertical section of the reactor are shown. The neutron flux along y-axis is showed in Figure 14. The DONJON code can compute the neutron flux for different burn-up inventory and a large range of control rod movement. This allows a detailed analysis of the reactor and its large capability in term of fuel available from different models of this fourth generation fast reactor.

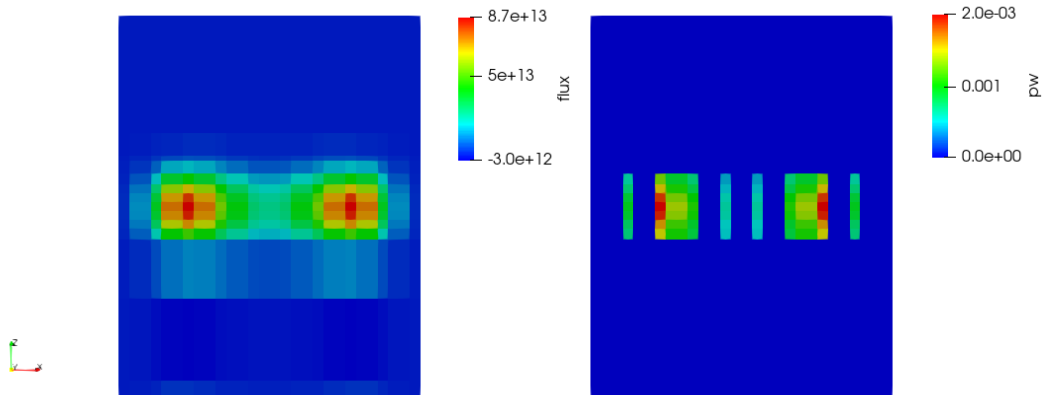


FIG. 13. Neutron flux and thermal power field over a vertical section of the reactor

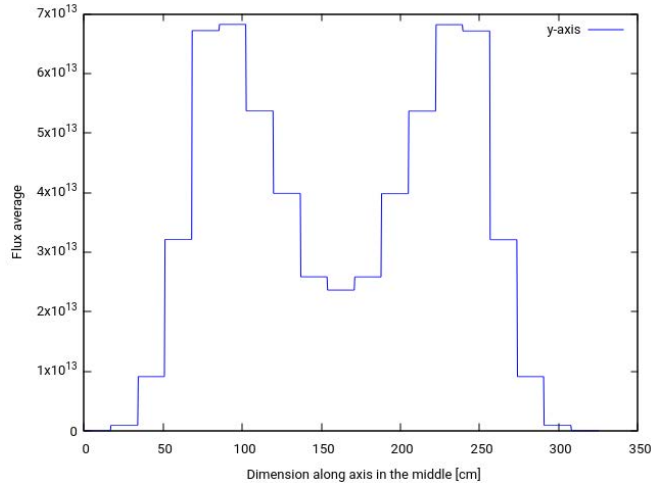


FIG. 14. The distribution of neutron flux average (piecewise constant in each cells) along y-axis

The results obtained in this simple case study, open a perspective of an extensive similar approach to other models: SMRs look as ideal candidates due to their size and compactness (mainly in terms of core dimensions in the FR case).

Finally this work need more time for refine data modelling about the model of ALFRED and has the aim to present the numerical platform for coupling the neutronic codes and thermal-hydraulic code; anyway we are sure that the numerical platform is a good help to analysis the physics behaviour of nuclear reactor in project phase on terms of reliability.

REFERENCES

- [1] Facilitating International Licensing of Small Modular Reactors, Cooperation in Reactor Design Evaluation and Licensing (CORDEL) Working Group of the World Nuclear Association, Report No. 2015/004, August 2015.
- [2] G.GRASSO, A.ALEMBERTI, ALFRED core. Summary, synoptic table, conclusions and recommendations, Lead-cooled European Advanced DEMonstration Reactor (LEADER), UTIFISSM-P9SZ-002 (ENEA), DEL027-2013 rev.0
- [3] C.PETROVICH, G.GRASSO, A.ALEMBERTI, D07-Definition of the ETDR core and neutronic characterization, Lead-cooled European Advanced DEMonstration Reactor (LEADER), UTIFISSM-P9SZ-002 (ENEA), DEL007-2012 rev.1
- [4] G.GRASSO, ALFRED v.2.00 Data for modeling, Private Technical Report – FSN-SICNUC-PSSN, ENEA, April 2018.
- [5] A. HÉBERT, Applied Reactor Physics, Presses Internationales Polytechnique, ISBN 978-2-553-01436-9, 424 p., Montréal, 2009.
- [6] G. MARLEAU, R. ROY AND A. HÉBERT, “DRAGON: A Collision Probability Transport Code for Cell and Supercell Calculations”, Report IGE-157, École Polytechnique de Montréal (1993).
- [7] A. HÉBERT, Applied Reactor Physics, Second Edition, Presses Internationales Polytechnique, ISBN 978-2-553-01698-1, 396 p., Montréal, 2016
- [8] G.RIMPAULT. The ERANOS code and data system for fast reactor neutronic analyses. International conference on the PHYSICS Of Reactors (PHYSOR2002), Seoul, Korea, 2002.
- [9] D.B. PELOWITZ ET AL., MCNPX 2.7.E Extension. Technical Report LA-UR-11-01502, Los Alamos, March 2011
- [10] V.BERGEAUD, M. TAJCHMAN, Application of the SALOME software architecture to nuclear reactor research, CEA/DEN.
- [11] A. CERVONE AND M. MANSERVISI, “A three-dimensional cfd program for the simulation of the thermo-hydraulic behaviour of an open core liquid metal reactor,” tech. rep., Report RSE/2009/85, 2008.
- [12] S. BNÀ, S. MANSERVISI, AND O. LE BOT, “Simulation of the thermo-hydraulic behaviour of liquid metal reactors using a three-dimensional finite element model,” tech. rep., Report RdS/2010/107, 2010.

ESTIMATION OF MINIMAL CRITICAL SIZE OF BARE ISO-BREEDING CORE FOR EIGHT SELECTED FAST REACTORS IN TH-U AND U-PU CYCLES

Paper ID #21

J. KREPEL
Paul Scherrer Institut
Villigen, Switzerland
Email: jiri.krepel@psi.ch

E. LOSA
Czech Technical University
Prague, Czechia

Abstract

Small and medium sized modular reactors (SMRs) ought to provide increased safety and economy. The modularity can provide reduced capital cost and the reduced reactor power additional passive safety features. Fast spectrum SMRs can also provide high fuel cycle sustainability in the closed fuel cycle. In this study, eight fast spectrum systems have been analysed from the perspective of equilibrium U-Pu and Th-U fuel cycle. The equilibrium fuel composition was evaluated on infinite lattice and fission products were neglected. The equilibrium fuel composition actually represents an Eigen vector of the respective Bateman matrix. The resulting system parameters as infinite multiplication factor, Fermi age, and Migration area represent inherent core characteristics. They were used to estimate the minimal critical bare core size. Several other performance parameters were also compared. The obtained minimal core size can be in reality bigger, because the fission products are neglected in this study. At the same time, the bare core assumption is used and in reality, application of reflector or blanked can reduce the core size. Even though the enumerated minimal iso-breeding core size represents only rough estimate, the results are still sufficiently indicative to compare the performance and size of different fast SMR cores.

1. INTRODUCTION

Small and medium sized modular reactors (SMRs) are expected to provide increased safety and economic performance. In comparison to the classical big sized reactors, the safety of SMRs can profit from the reduced reactor power and size. The related safety systems can thus rely on passive heat removal and can be simplified and/or integrated into the reactor vessel. Furthermore, the more compact reactor systems can be designed as modular. The simplification, integration, and modularity can help to reduce the capital costs. The capital cost reduction is probably the major motivation for SMRs deployment in countries with developed electric grid. The justification for SMRs deployment may differ in countries without developed grid or for remote areas application. Furthermore, even in the grid operation mode there exist a niche for combined electricity and heat production. This covers not only the district heating, which is conditioned by public acceptance, but also some technologies which demand process heat at temperatures much above the level that water based technology can provide.

The deployment of non-water SMRs and especially of fast SMRs can be thus driven by higher available temperature of the process heat or by the competitive capital cost and safety features. Moreover, fast SMRs can also help to increase both aspects of the fuel cycle sustainability: higher fuel utilization and waste reduction. As such fast SMRs can be sustainable in a general sense. The general sustainability consists from three pillars: environment, economics, and social [1]. Fast SMRs can address all of them because of their prospective features. These features relate to one or more sustainability pillars (see Fig. 1) and are:

- (1) High fuel utilization: breeding in fast spectrum.
- (2) Waste minimization in fast spectrum: less own waste and capability to burn legacy waste.
- (3) Criticality safety: the positive coolant density effect can be mitigated by fuel composition in burners and/or by higher neutron leakage from smaller core in breeders.
- (4) Absence of driving forces: especially in liquid metal cooled fast reactors and in molten salt reactors the strong driving forces are absenting.
- (5) Reduced decay heat: the reduced reactor power also means reduced decay heat. The respective decay heat removal system can be thus designed as passive and/or integral.
- (6) Simpler safety system: can be enabled by the reduced decay heat and absence of driving forces.
- (7) Modularity: integral design and/or compact component size can allow modularity and ex-situ fabrication.
- (8) Reduced material mass: based on integral and modular layout.

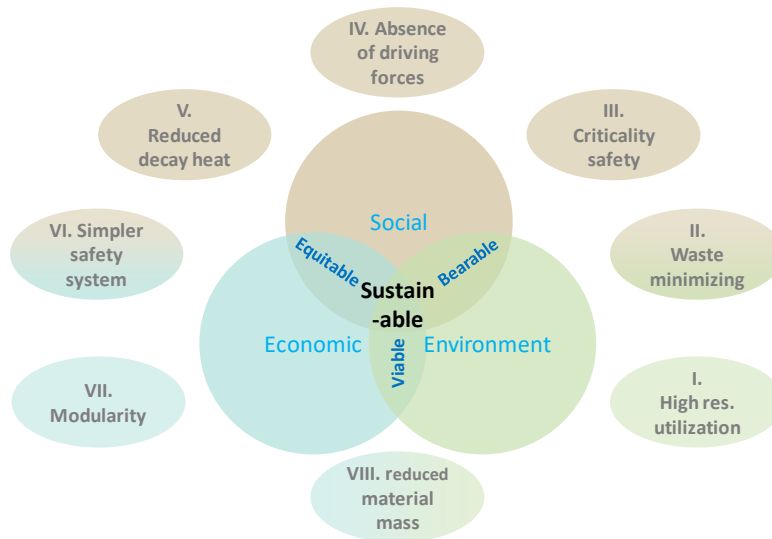


FIG. 1. Potential advantages/features of fast SMRs for the three general pillars [1] of sustainability.

This paper focuses on the minimal core size of iso-breeding fast reactors. As such, it is not directly relevant for the fast SMRs. However, both these features: iso-breeding capability and compact core size are important and can be advantageous for fast SMRs. At the same time, they are obviously in conflict.

The minimal iso-breeding core size in this study is estimated with several strongly simplifying assumptions and approximations. The minimal core size can be in reality bigger, because the fission products are neglected in this study. Nonetheless, the bare core approximation is used in this study and in reality, an application of reflector or blanked can reduce the core size. Even though it is only rough estimation, the results are sufficiently indicative to compare the size of different fast SMRs cores. This statement is not valid only for iso-breeding cores. In case of smaller cores, the difference between the actual core size and minimal iso-breeding core size can indicate the conversion ratio of the design. Obviously, extremely small cores will be strong burners with negligible conversion ratio. The results presented in this paper focus on the core size and are a subset of bigger study already presented in [2, 3, and 4].

2. SELECTED REACTORS, APPLIED TOOLS AND ASSUMPTIONS

2.1. Selected reactors

The eight fast reactors selected in this study are described in [2, 3, and 4], for readers convenience they are recapitulated in Tab. 1. Four solid fuel fast reactors and four liquid fuel fast reactors were selected. The four solid fuel fast reactors represent the most typical: lead, sodium and gas cooled systems. In the case of sodium cooled reactor, the option with metallic fuel was also considered. Its higher specific power was adopted from the preliminary safety analysis report [5]. The down-selection of four liquid fuel fast reactors was more challenging. There are basically two general fast Molten Salt Reactor (MSR) classes: homogeneous and heterogeneous fast MSR (see Fig. 2). Furthermore, many MSR designs are only pre-conceptual. Since not enough data was found during the study for heterogeneous cores, it was limited to the homogeneous cores. Two cases have been selected for both chloride and fluoride salt MSRs. Since the study is limited to infinite geometry, each homogeneous MSR is actually represented by the fuel salt composition. In the fluoride case, the two most often used carrier salt have been selected: the LiF-BeF₂ eutectic and the LiF standalone in eutectic mixture with actinides fluorides. In chloride case the NaCl in eutectic with actinide chlorides was chosen. The second salt consist only from actinide chlorides and it is rather extreme hypothetical option with high melting temperature. At the same time, it is considered in some heterogeneous designs as the fuel salt. Performance of other salts was evaluated in [6].

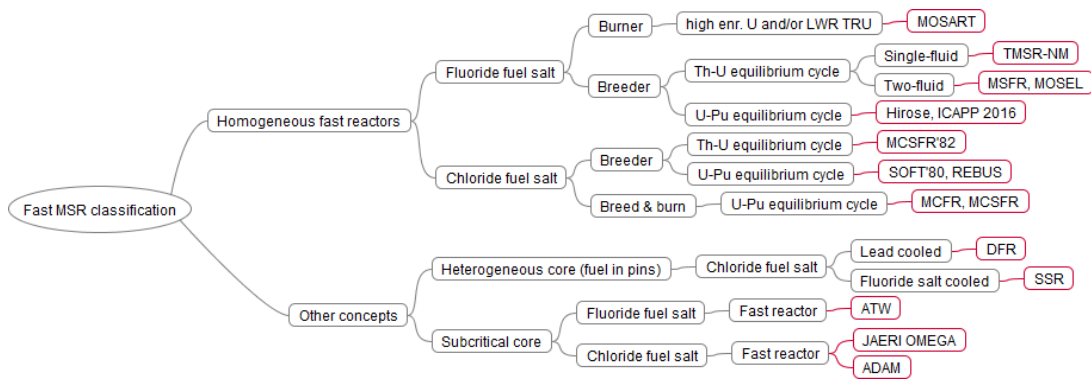


FIG. 2. Classification of fast MSR concepts available from literature.

2.2. Applied tools and assumptions

The major objective of this study in broader sense is the Bateman matrix eigenstate. It represents an equilibrium state for the respective fuel cycle type. It was evaluated for both Th-U and U-Pu fuel cycle options. The actual simulation tool is the EQL0D Matlab script [17, 18, 19] which steers the Serpent 2 code [20] calculations and simulates the burnup. For more details about the simulation, script flow chart, and assumptions and approximations refer to [2]. Since, the assumptions used to achieve the equilibrium state are crucial for the result understanding, they are repeated here:

- (1) Infinite lattice or geometry simulation (neglecting leakage).
- (2) Fissioned actinide atom is immediately replaced by new fertile atom (neglecting fission products and reprocessing losses).
- (3) Constant specific power is imposed during the convergence process (irradiation is independent from super- or sub- criticality).

The first two assumptions obviously cause overestimation of the resulting equilibrium core multiplication factor. It is important to understand that the third assumption enables equilibrium states for subcritical cores. This would be the case for majority of the thermal reactors [2]. In this study only one case has negative equilibrium reactivity, the MSFR with FLIBE salt in the U-Pu cycle. The relationship between k_{eff} and k_{inf} or actually the neutron leakage was estimated in the second part of this study using the Fermi's theory of bare thermal reactor. It represents the last strong assumption in this study:

- (4) Neutron leakage from a given core geometry is estimated from migration area M^2 .

The neutron non-leaking probabilities during slow-down p_1 and diffusion p_2 were approximated as follows:

$$k_{eff} = k_{inf} p_1 p_2 = k_{inf} \frac{e^{-\tau B^2}}{1 + L^2 B^2} \cong k_{inf} \frac{1}{1 + (\tau + L^2) B^2} = k_{inf} \frac{1}{1 + M^2 B^2}, \quad (1)$$

where τ is the Fermi age, L^2 is the diffusion area, M^2 is the migration area, and B is the buckling. The Fermi age and the migration area were enumerated by Serpent code using following formulas:

$$\tau = \frac{\bar{D}_F}{\Sigma_1} = \frac{\bar{D}_F}{\xi \Sigma_s} \ln \frac{E_0}{E_T} \quad \text{and} \quad L^2 = \frac{\bar{D}_T}{\Sigma_a}, \quad (2)$$

where \bar{D} is the average diffusion coefficient for fast F and thermal T neutrons, Σ represents the macroscopic cross-section for scattering s , removal l , and absorption a , ξ is the average logarithmic decrement of energy E of fast 0 and thermal T neutrons. The diffusion area in fast reactors is zero. Nonetheless, there is one exception caused by very soft fast spectrum in the MSFR-FLIBE case, refer to the discussion in [2]. Assuming cylindrical reactor shape the buckling in Eq. 1 can be enumerated from the core height h and radius r as follows:

$$B^2 = \left(\frac{\pi}{h} \right)^2 + \left(\frac{2.405}{r} \right)^2. \quad (3)$$

For fixed buckling value a cylindrical reactor with minimal volume has the height to radius ratio equal to:

$$\frac{h}{r} = \frac{\sqrt{2}\pi}{2.405} \cong 1.85, \text{ where } h = \frac{\sqrt{3}\pi}{B} \text{ and } r = \frac{2.405\sqrt{3}}{\sqrt{2}B}. \quad (4)$$

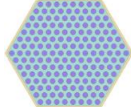
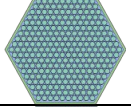
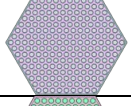
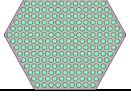




Accordingly, the minimal core volume is:

$$V_{\min} = \pi hr^2 = \pi \frac{\pi\sqrt{3}}{B} \frac{2.405^2 * 3}{2B^2} \cong \frac{148.3}{B^3}. \quad (5)$$

Using the Eq. 1-5 above the minimal core size and volume can be estimated. This approximation was verified by direct calculation of minimal critical core for SFR and acceptable agreement between the estimate and direct Serpent 2 code calculation was found for bare core.

To quantify the impact of the second assumption on the core radius, the results from full core calculation in [7] can be used. The fission product build-up in this study resulted in reactivity loss of 6% for GFR and of 3% for SFR and LFR. The radial neutron loss in pancake SFR core can be estimated from [21] to be around 2.5%. The fourth assumption of bare core overestimate the neutron leakage; nonetheless the assumption of high to diameter ratio close to 1 reduces the leakage. For the same volume, pancake core will have by 33% bigger radius and by 10% higher buckling. Overall, the applied assumptions are compensating to certain level and the results are indicative enough to compare the size of different fast SMR cores.

TABLE 1. OVERVIEW OF EIGHT SELECTED REACTORS.

Solid fuel fast reactors			
Reactor name (label)	Fuel design adopted from [reference]	Specific power (W/gHM)	Lattice geometry
European lead system (LFR)	Consortium of EU FP7 LEADER project [7, 8]	54.8	
European sodium fast reactor (SFR)	Consortium of EU FP7 ESFR project [7, 9]	48.8	
Gas cooled fast reactor (GFR)	Consortium of EU FP7 GoFastR project [10, 11]	40.1	
Metal fuelled fast breeder reactor (MFBR)	IGCAR, Kalpakkam [5, 12]	178.6	
Liquid fuel fast reactors			
Reactor name (label)	Fuel design adopted from [reference]	Specific power (W/gHM)	
Fast MSR: LiF-BeF ₂ -AcF ₄ salt* (MSFR-FLIBE)	MSBR fuel salt properties [13]	41.1	
Fast MSR: LiF-AcF ₄ salt* (MSFR-FLI)	Consortium of EU FP7 EVOL project [14]	41.1	
Fast MSR: NaCl-AcCl ₄ salt* (MCFR-NaCl)	Salt eutectic comp. and density from [15, 16]	54.8	
Fast MSR: AcCl ₄ salt* (MCFR-AcCl)	Salt density adopted from [16]	54.8	

* Li and Cl used in this study was enriched to 99.995 % of ⁷Li and ³⁷Cl.

3. OBTAINED RESULTS

3.1. Infinite multiplication factor and migration area

Major equilibrium results adopted from the general study [2, 3] are the infinite multiplication factor k_{inf} and the migration area M^2 (see Tab. 2). The k_{inf} strongly differ between the cycles, being higher for the U-Pu cycle. As discussed in [2] it is mainly based on the higher neutron production per ^{239}Pu fission. At the same time, the U-Pu cycle suffers strongly from spectrum softening, because of the increasing ^{239}Pu parasitic capture. This is actually the reason why MSFR-FLIBE performs better in the Th-U cycle. The differences in migration area between the two fuel cycles are almost negligible.

TABLE 2. INFINITE MULTIPLICATION FACTOR K_{INF} AND THE MIGRATION AREA M^2 (= FERMI AGE T + DIFFUSION AREA L^2) FOR EIGHT SELECTED REACTORS AND EQUILIBRIUM U-PU AND TH-U FUEL CYCLES.

Reactor type	Th-U cycle				U-Pu cycle			
	k_{inf}	Fermi age [cm ²]	Diffusion area [cm ²]	Migration area [cm ²]	k_{inf}	Fermi age [cm ²]	Diffusion area [cm ²]	Migration area [cm ²]
MSFR-FLIBE	1.03872	184.9	8.6	193.6	0.98453	190.4	0.8	191.2
MSFR-FLI	1.06920	167.2	0.0	167.2	1.07032	176.5	0.0	176.5
LFR	1.09446	272.1	0.0	272.1	1.20220	282.0	0.0	282.0
SFR	1.13408	195.3	0.0	195.3	1.27046	202.0	0.0	202.0
GFR	1.10004	422.4	0.0	422.4	1.21835	434.9	0.0	434.9
MFBR	1.11684	357.7	0.0	357.7	1.31404	370.9	0.0	370.9
MCFR-NaCl	1.16013	1383.8	0.0	1383.8	1.28892	1205.2	0.0	1205.2
MCFR-AcCl	1.19756	1768.5	0.0	1768.5	1.43767	1873.7	0.0	1873.7

The different k_{inf} are caused partly by parasitic captures of structural materials. However, the inherent equilibrium actinides composition plays stronger role. Fig. 3 shows the relative fuel composition for all eight reactors and nicely illustrates the fact that in the U-Pu fuel cycle the fuel composition degrades faster with spectrum softening. This is also the reason, why MSFR-FLIBE case with softest fast spectrum provides negative equilibrium reactivity in the U-Pu cycle, whereas in the Th-U cycle not. The ^{233}U capture probability is less sensitive to the spectrum changes. This is also the reason, why the Th-U cycle can be operated in thermal spectrum.

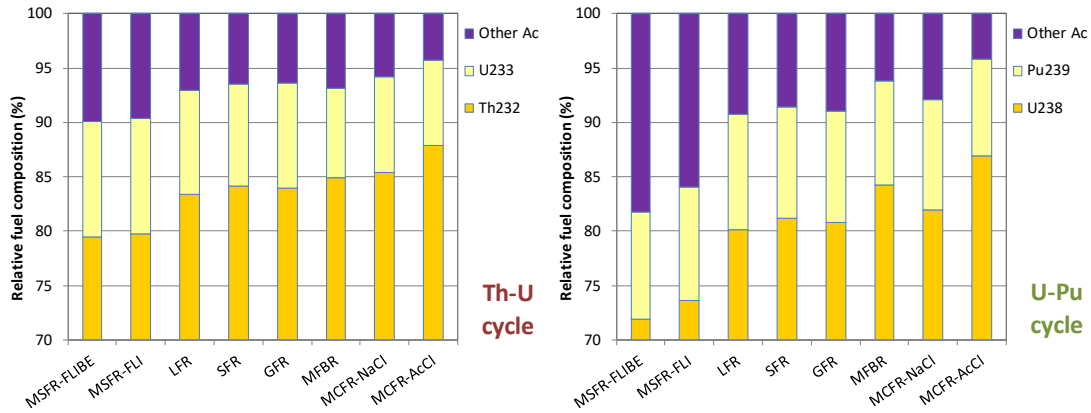


FIG. 3. Relative equilibrium fuel composition for eight selected reactors in the Th-U and U-Pu fuel cycles.

3.2. Bare core criticality line

The Eqs. 1-4 can be used to relate k_{inf} with the critical core radius. The assumed critical core has a cylindrical shape with minimal buckling for given volume. The height to radius ratio is 1.85. This may be unnatural for the solid fuel fast reactors, which usually have pancake shape. However, pancake cores would strongly suffer from the applied bare core assumptions. The k_{inf} as a function of core radius is shown in Fig. 4.

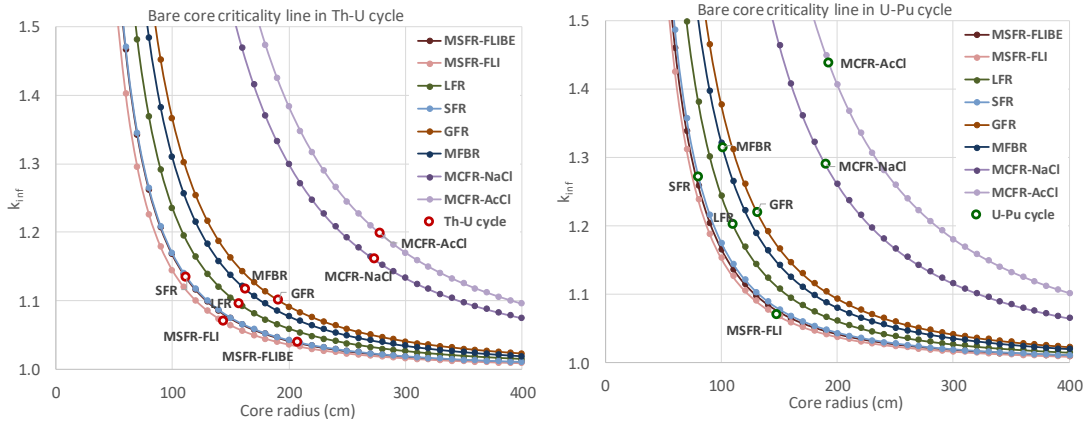


FIG. 4. k_{inf} as a function of the core radius for eight selected reactors in the Th-U and U-Pu fuel cycles.

It is obvious that the bare core criticality lines are similar for both fuel cycles; nonetheless, the equilibrium k_{inf} strongly differ between the Th-U and U-Pu cycle. Therefore, the resulting core size is always bigger in the Th-U cycle. The only exception is MSFR-FLIBE with very soft neutron spectrum and MSFR-FLI with almost equal core size for both cycles.

3.3. Radius of bare critical core

The differences between the Th-U and U-Pu fuel cycles in bare core critical radius are highlighted in Fig. 5, where the respective points are connected by line. The two cases with strongest k_{inf} drop and core radius increase are MFBR and MCFR. In case of MFBR the Th-U fuel cycle suffers from substantial ^{233}Pa capture rate, which is proportional to the specific power. For detailed explanation refer to [2]. The MCFR core has the hardest neutron spectrum and profits, in the U-Pu fuel cycle, from high neutron production per fission, low ^{239}Pu parasitic capture and ^{238}U direct fission. The respective effects are much weaker in the Th-U cycle.

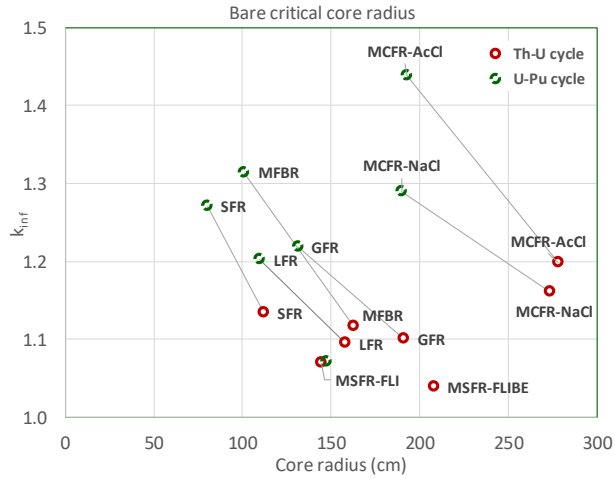


FIG. 5. Core radius difference between the Th-U and U-Pu fuel cycles for eight selected reactors.

Based of Fig. 5 it can be concluded that the Th-U cycle provides more bulky critical cores that the U-Pu cycle. Furthermore, the enormous migration area in both MCFR cases results in big cores. The three most compact cores are provided by liquid metal cooled reactors in the U-Pu cycle (SFR, LFR, and MFBR). The SFR has quite compact core also in the Th-U cycle. The GFR core in the U-Pu cycle and the MSFR-FLI core in both cycles represent the next three most compact cores.

3.4. Core radius and breeding gain

Not all fast SMRs will be designed as iso-breeder. It is probable that majority of them will acts as convertors and the most compact designs will act as burners. To assess the core size impact on breeding performance the relationship between k_{inf} and Breeding Ratio (BR) was derived. The derivation was based on the fact that in equilibrium cycle all creation and destruction rates are in balance. The nominal equilibrium state is represented by a standard neutron balance equation where $k_{eff} \neq 1$ and $BR=1$ by definition. For the purpose of this derivation the BR is defined as a production to destruction ratio of other than main fertile isotopes and the two nominal state equations have the following form:

$$k_{eff} = \frac{P^{total} + 2(n, 2n)^{total}}{F^{total} + C^{total} + (n, 2n)^{total}} \neq 1 \quad (6)$$

$$BR = \frac{C^{fertile} + (n, 2n)^{fertile}}{F^{total} - F^{fertile}} = 1$$

where P , F , C , and $(n,2n)$ stands for the respective production, fission, capture, and $n,2n$ reactions. Since the fuel composition is constant in equilibrium, it is obvious that the equilibrium BR is per definition equal to one. The nominal state can be perturbed by increasing or decreasing the capture rate of the main fertile isotope by $\Delta C^{fertile}$ so that a criticality is obtained from the neutron balance. The respective perturbed equations are:

$$k_{eff,pert} = \frac{P^{total} + 2(n,2n)^{total}}{F^{total} + C^{total} + \Delta C^{fertile} + (n,2n)^{total}} = 1$$

$$BR_{pert} = \frac{C^{fertile} + \Delta C^{fertile} + (n,2n)^{fertile}}{F^{total} - F^{fertile}} \neq 1$$
(7)

The Eq. 6 and 7 can be combined to obtain two new relations:

$$\frac{\Delta C^{fertile}}{F^{total} + (n,2n)^{total}/\bar{\nu}} = \bar{\nu} \cdot \frac{k_{eff} - 1}{k_{eff}}$$

$$BR_{pert} = 1 + \frac{\Delta C^{fertile}}{F^{total} - F^{fertile}}$$
(8)

The final relationship between BR and k_{eff} can be expressed from Eq. 8 as:

$$BR_{pert} = 1 + \bar{\nu} \cdot \frac{k_{eff} - 1}{k_{eff}} \cdot \frac{F^{total} + (n,2n)^{total}/\bar{\nu}}{F^{total} - F^{fertile}} \cong 1 + \bar{\nu} \cdot \frac{k_{eff} - 1}{k_{eff}},$$
(9)

where $F^{fertile}$ and $(n,2n)^{total}/\bar{\nu}$ were neglected in the second part of the equation. The corresponding Breeding Gain (BG) is equal to:

$$BG_{pert} = BR_{pert} - 1 \cong \bar{\nu} \cdot \frac{k_{eff} - 1}{k_{eff}},$$
(10)

The relationship from Eq. 9 and 10 was used to relate the potential BG with the multiplication factor for the infinite lattice. The adjusted multiplication factor for infinite lattice was then used to calculate the critical core radius. The influence of critical core radius on the BG is shown in Fig. 6 for five BG values ranging from -0.2 to +0.2. The core radius sensitivity is proportional to the initial k_{inf} value. The lower nominal k_{inf} results in higher BG sensitivity to the core radius variation. Accordingly, the Th-U cycle is more sensitive to the BG changes. The trend lines from Fig. 6 are similar to the trend lines from Fig. 4.

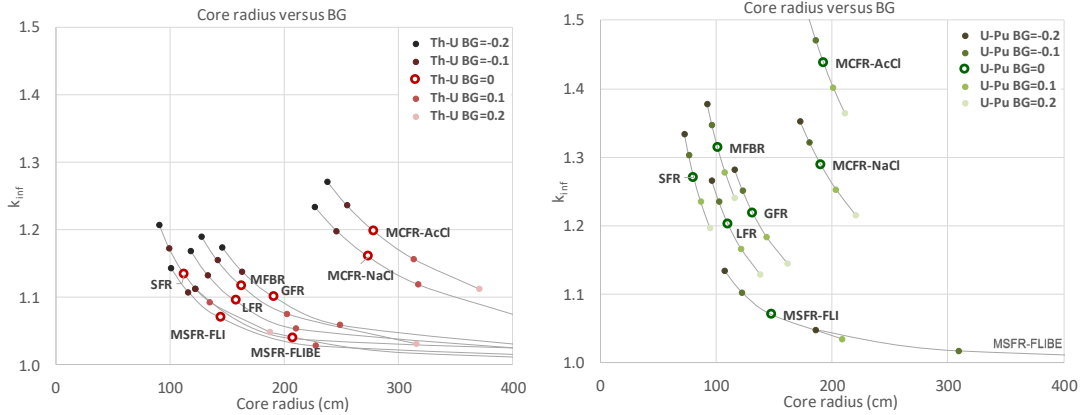


FIG. 6. Dependency of the core radius for different BG values for eight selected reactors and both fuel cycles.

4. SUMMARY AND CONCLUSION

Fast SMRs can have several prospective features which increase their general sustainability. One of these features relates to the specific fuel cycle sustainability. Fast SMRs are capable to produce less own waste and utilize legacy waste. Furthermore, they can be designed as breeders with high natural resources utilization. In this paper the conflict between the breeding capability and core size is analysed. Physical core size can be advantage for SMRs which can enable their integral and modular design.

Minimal critical radius for iso-breeding core was evaluated for eight selected fast reactors. The fission products were neglected in the study and the equilibrium Th-U and U-Pu cycles were calculated at infinite lattice level. The equilibrium cycle results were used to estimate the minimal critical core size for iso-breeding reactor and to assess the impact of breeding ratio variation on the core size. Neglecting of fission products leads to the overestimation of infinite multiplication factor. On the other, the bare core approximation is applied, and the blanket or reflector can make the real core smaller. Overall, the results are only indicative, but sufficiently characterize the potential of each selected reactor.

The major results of the study are coherent with the common knowledge. The Th-U fuel cycle requires bigger cores than U-Pu cycle. The three liquid metal cooled reactors (SFR, LFR, and MFBR) have the most compact core. The SFR has quite compact core also in the Th-U cycle. The GFR core in the U-Pu cycle and the MSFR-FLI core in both cycles are the next three most compact cores.

In general, the liquid fuel fast reactors are bulkier than the solid fuel fast reactors. This is valid especially for MCFR, the MSFR core size is still acceptable. At this point, it is important to note that the power density in solid fuel reactors is limited by the lattice design. This limit is absent in homogeneous MSR. Accordingly, the liquid fuel reactors will be bigger than the solid

fuel reactors; however, they can have equal or even higher power density if needed. Hence, MSR can be potentially modular also at higher installed powers. This statement, however, neglects several technological requirements for actual core design and it is thus rather academic.

In the last simulation the influence of breeding gain or actually of conversion ratio on the core size was evaluated. It is stronger for reactors with low infinite multiplication factor. Accordingly, it has higher influence on the critical core size in the Th-U cycle. This statement can be also inverted. Small core size changes have strongest impact on most compact cores especially in the U-Pu cycle.

Finally, even though the minimal iso-breeding core size enumerated in this study represents only rough estimate, it is still indicative enough to compare the size of different fast SMR cores.

REFERENCES

- [1] <http://www.circularecology.com/sustainability-and-sustainable-development.html#.XOUBmWeP5Hg>
- [2] KŘEPEL, J., LOSA, E., Ann. Nucl. Energy, Closed U-Pu and Th-U cycle in sixteen selected reactors: evaluation of major equilibrium features, 2019.
- [3] KŘEPEL, J., LOSA, E., "Comparison of fast reactors performance in the closed U-Pu and Th-U cycle," Proceedings of FR17, International Conference on Fast Reactors and Related Fuel Cycles, Yekaterinburg, Russian Federation, June 26 – 29, 2017.
- [4] KŘEPEL, J., LOSA, E., "Enumeration of static and dynamics neutron consumption D-factor for several selected reactors at equilibrium closed fuel cycle," Proceedings of ICAPP 2016, San Francisco, USA, April 17-20, 2016.
- [5] IGCAR, "Prototype Fast Breeder Reactor Preliminary Safety Analysis Report." 2004.
- [6] HOMBOURGER, B.A., 2018. Ph.D. Thesis. EPFL Lausanne, Switzerland.
- [7] KREPEL, J., PELLONI, S., MIKITYUK, K., "Comparison of open and closed U–Pu equilibrium fuel cycles for Generation-IV fast reactors with the EQL3D procedure," Nuclear Engineering and Design, vol. 250, pp. 392–402, 2012.
- [8] ARTIOLI, C., ET AL., "ELSY Neutronic Analysis by deterministic and Monte Carlo methods: an innovative concept for the control rod systems," ICAPP'09, Tokyo, Japan, 2009.
- [9] BUIRON, L., ET AL., "Innovative Core Design for Generation IV Sodium-Cooled Fast Reactors," ICAPP'07, Nice, France, 2007.
- [10] BOSQ, J. C., ET AL., "Fine 3D neutronic characterization of a gas-cooled fast reactor based on plate-type subassemblies," PHYSOR 2006, Vancouver, BC, Canada, 2006.
- [11] PERKÓ, Z., ET AL., "Core neutronics characterization of the GFR2400 Gas Cooled Fast Reactor," Progress in Nuclear Energy, vol. 83, pp. 460–481, 2015.
- [12] MOHAPATRA, D. K., ET AL., "Physics aspects of metal fuelled fast reactors with thorium blanket," Nuclear Engineering and Design, vol. 265, pp. 1232–1237, Dec. 2013.
- [13] ROSENTHAL, M. V., ET AL., "Advances in the development of MSBR," 4th International Conference on the Peaceful Uses of Atomic Energy, Geneva, 1971.
- [14] HEUER, D., ET AL., "Towards the thorium fuel cycle with molten salt fast reactors," Annals of Nuclear Energy, vol. 64, pp. 421–429, 2014.
- [15] DESYATNIK, V. N., ET AL., "Density, surface tension, and viscosity of uranium trichloride-sodium chloride melts," At Energy, vol. 39, no. 1, pp. 649–651, 1975.
- [16] MOUROGOV, A., BOKOV, P. M., "Potentialities of the fast spectrum molten salt reactor concept: REBUS-3700," Energy Conversion and Management, vol. 47, no. 17, pp. 2761–2771, 2006.
- [17] HOMBOURGER, B., ET AL., "Parametric Lattice Study of a Graphite-Moderated Molten Salt Reactor," ASME J of Nuclear Rad Sci, vol. 1, 2015.
- [18] HOMBOURGER, B., ET AL., "The EQL0D procedure for fuel cycle studies in molten salt reactors," Proceedings of ICAPP 2016, San Francisco, USA, 2016.
- [19] HOMBOURGER, B., KŘEPEL, J., PAUTZ, A., "The EQL0D Procedure for Fuel Cycle Studies in Molten Salt Reactors and its Application to the Transition to Equilibrium of Selected Designs," Submitted to Ann. Nucl. Energy. 2019

- [20] LEPPÄNEN, J., "Serpent a Continuous-Energy Monte Carlo Reactor Physics Burnup Calculation Code," VTT Technical Research Centre of Finland, Finland, 2013.
- [21] KREPEL, J., RAFFUZZI, V. Mapping of sodium void effect and Doppler constant in ESFR-Smart core with Monte Carlo code serpent and deterministic code ERANOS. PHYSOR2020, Cambridge, United Kingdom, March 29th-April 2nd, 2020

INTRODUCTION OF THE U.S. DOE VERSATILE REACTOR PROJECT

Paper ID #18

F. HEIDET

Argonne National Laboratory
Lemont, IL, United States of America
Email: fheidet@anl.gov

J. ROGLANS-RIBAS

Argonne National Laboratory
Lemont, IL, United States of America

Abstract

The Versatile Test Reactor is a major endeavour led by the U.S. Department of Energy, Office of Nuclear Energy, aiming at designing and building a fast reactor in order to provide enhanced irradiation testing capabilities to the advanced reactor community by means of a high flux fast neutron source, a capability that currently does not exist in the U.S. Bridging this capability gap will allow moving forward various reactor technologies which are in need of accelerated fuel and material testing. The Versatile Test Reactor is currently in the conceptual design phase. A comprehensive team of experts has been put together, pulling talents and skills from the U.S. National Laboratories, industrial partners, and academia. The reactor plant is being designed based on the small modular fast reactor PRISM, which has previously been developed by GE Hitachi Nuclear Energy. The reactor core is a new concept enabling achievement of very attractive irradiation conditions.

The paper discusses the current state of the Versatile Test Reactor project and provides a short overview of preceding activities which enabled initiating this project. A description of the preliminary core designed is included alongside with a summary of the core performance characteristics and testing conditions achievable.

1. INTRODUCTION

The Versatile Test Reactor (VTR) is a program supported by the United States Department of Energy (US-DOE) aiming at designing and building a fast-spectrum test reactor to bridge capability gaps related to accelerated fuels and materials testing and qualification for nuclear applications. In its current conceptual design stage, the VTR is a 300 MW(th) sodium-cooled fast reactor of the pool type. It will not generate electricity as to avoid competing secondary missions which could divert it from its primary mission, that is irradiation testing. The heat generated will be released to the air through several air-dump heat exchangers, conceptually similar to those used for the Fast Flux Test Facility (FFTF). The overall plant design for the VTR is based on the PRISM Mod-A reactor, designed by GE Hitachi Nuclear Energy. The DOE process includes an Analysis of Alternatives to select the preferred technology and potential siting.

Based on the small and medium sized or modular reactors (SMRs) definition provided by the International Atomic Energy Agency, the VTR does not qualify as SMR given that it is not intended to produce electricity. However, with respect to power level, at 300 MW(th) the VTR is well within the power range of SMRs. With respect to modularity, the VTR is not designed with the purpose of being modular but being based on PRISM Mod-A it will have some modular components such as the reactor vessel. While we could argue that VTR is a SMR from all perspectives except from the point of view of electricity-generation, this is of little relevance. The importance of the VTR to the fast spectrum SMR community is that it will be able to support development of several of these reactor technologies by providing a wide range of irradiation services. In particular, VTR will allow for use of coolants types different from the

primary coolant in designated test locations, allowing it to provide value to a wide range of advanced reactors designs.

The motivation, objectives and current state of the VTR project are discussed in this paper. This includes a discussion of previous efforts which enabled the VTR project, and a summary of the current VTR design activities. A summary of the preliminary VTR core design, of its performance characteristics and of the resulting testing capabilities are presented.

2. VTR PROJECT

2.1. Overview

The VTR program started in 2017 under the auspices of the US-DOE Office of Nuclear Energy (DOE-NE). The objectives are to bridge a capability gap (high-flux fast spectrum neutron irradiation) for the nuclear industry in the U.S. While the U.S. had been pioneering the demonstration of fast-spectrum reactors in the early age of nuclear energy, notably with EBR-II and FFTF, no reactor currently operating in the U.S. can offer significant fast flux levels. Fast flux is very important for irradiation testing as it allows achieving material damage much faster and can reduce the irradiation time needed to study new materials by over one order of magnitude. With the growing interest in new types of reactors, including SMRs and micro-reactors of various types of advanced reactors, irradiation needs are increasing, making having the capability to perform accelerated fuels and materials testing of the upmost importance.

The mission of the VTR program is to help accelerate the testing of advanced nuclear fuels, materials, instrumentation, and sensors. It will also allow DOE to modernize its essential nuclear energy research and development infrastructure, and conduct crucial advanced technology and materials testing necessary to re-energize the U.S. nuclear energy industry. The timeline envisioned by the VTR program is to complete the construction of the reactor and start its operation by 2026. The reason for this accelerated schedule is to enable establishing this much-needed capability in time to support most advanced reactor technologies being currently developed.

The VTR objectives are to offer the following capabilities:

- Fast flux in excess of 4×10^{15} n/cm²-s;
- Very high dpa level, in excess of 30 dpa/year;
- Test volumes in excess of 7 litres per test location;
- Large number of potential test locations;
- Effective testing heights of at least 60 cm;
- Ability to test fuel and material in prototypical environments other than sodium. This includes, but is not limited to, lead, lead-bismuth, helium and molten salts.

In 2018 the VTR program became a design project under the DOE Order 413.3B [1] that governs the management of capital acquisition projects. This directive is the process through which the DOE can enable the acquisition or construction of capital assets. This reflects the intent to ensure the VTR program is being managed in accordance with the expectation set forth for a construction project. In particular, the purpose of this directive is “to provide the DOE with program and project management direction for the acquisition of capital assets with the goal of delivering projects within the original performance baseline, cost and schedule, and fully capable of meeting mission performance, safeguards and security, and environmental, safety, and health requirements unless impacted by a directed change”.

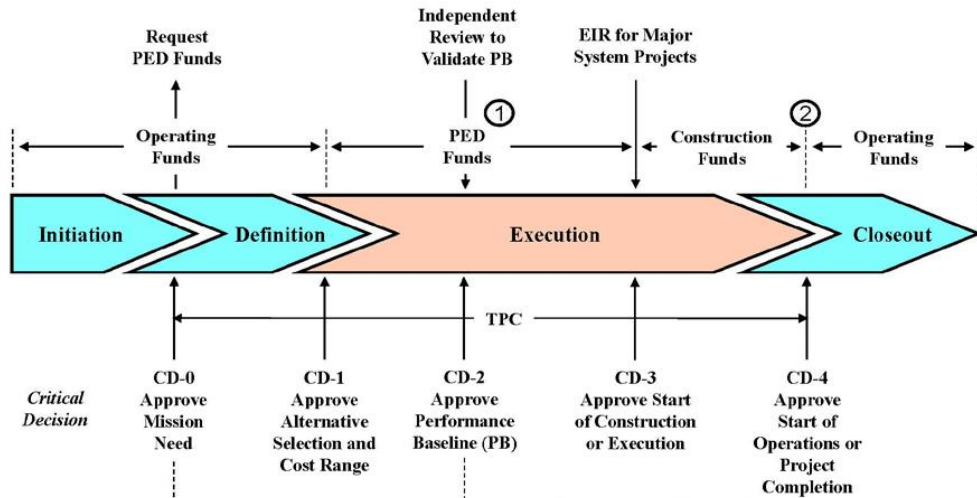


FIG. 1. Critical decision chart as part of DOE directive 413.3B (Source: DOE)

In practice, by becoming a project, the VTR program has to deliver on a number of critical decision (CD) points to approve the project from the design stage to final construction and operation. The five required CD points are presented in Fig. 1. CD-4 is the last one and would correspond to the start of operations for the VTR. The VTR program has successfully completed the CD-0 phase in February 2019 [2] and is now aiming at CD-1 which is planned to be completed during US fiscal year 2020. Three important pieces of the CD-1 package are the conceptual design of the entire reactor plant, the conceptual safety design report, and the corresponding cost range estimate.

2.2. Organization

When initiated in 2017, the main contributors to the VTR program were Idaho National laboratory (INL), Argonne National Laboratory (ANL) and Oak Ridge National Laboratory (ORNL). With the fast pace of the program and the accelerated schedule, the team supporting the development of the VTR quickly grew and is now including 36 contributing institutions, as shown in Fig. 2. Overall, the VTR program is led by INL.



FIG. 2. VTR team map

In order to tackle the current phase of the project, the VTR program is organized around several areas of expertise. Most of them are being led by the U.S. National Laboratories, with support from a number of contributors, with the notable exception of the plant design activities which are handled by GE Hitachi Nuclear Energy (GEH) and Bechtel National, Inc. (BNI). GEH and BNI have been selected in this role with the intent to leverage the PRISM Mod-A plant design for VTR, without having to incorporate too many major modifications. The PRISM reactor design is one of the most mature advanced reactor designs existing in the U.S. [3], which is key to meeting the accelerated VTR schedule.

2.3. Preceding activities and highlights

The initiation by DOE of the VTR program is the result of many years of research & development (R&D) activities in the domain of advanced reactors and was made timely as evidenced by several U.S. House of Representative bills supporting advancing nuclear energy, and bridging capability gaps being passed in the last few years. All these elements made it possible to engage in the VTR project with a credible end goal in sight.

R&D activities supported by the DOE-NE Advanced Reactor Campaign throughout the years led to the completion of the “Advanced Demonstration and Test Reactor options study (ADTR)” in 2016 [4]. This study was carried by a diverse group of experts representing the various U.S. stakeholders (academia, industry and national laboratories) and focused on assessing different reactor technologies against four postulated representative strategic objectives. For the strategic objective related to developing testing capabilities in support of advanced reactors, the study found that a sodium-cooled fast reactor would be the most credible type of reactor in order to offer the desired testing capabilities. The point design reactor concept used to assess potential performance of SFR against the targeted strategic objective was the FASt TEst Reactor (FASTER) developed by Argonne National Laboratory [5]. While differing from the current VTR design in several ways, FASTER provided a thorough assessment of the potential capabilities, and coincidentally the VTR featured similar fuel type, core materials, power level, and performance characteristics to FASTER.

At the same time as the ADTR study was on-going, DOE-NE tasked its Nuclear Energy Advisory Committee (NEAC) with forming a team to assess the user needs for irradiation testing. In particular, this task force was charged to identify the testing needs of advanced non-light-water reactors, to determine the requirements and overall capabilities (*e.g.*, neutron spectrum/spectra, testing environments, etc.) for a new irradiation test reactor and compare these requirements with alternate existing facilities, methodologies, and approaches for meeting these needs. Among the several findings identified by this task force [6], they clearly identified the lack of testing capabilities for fast-neutron systems, as well as salt-cooled systems, as well as the aging of existing testing facilities. They pointed out that a new domestic fast flux test reactor could address missions such as accelerated fuel and material irradiations for fast-spectrum reactors and other reactors, large volume irradiations, and advanced instrumentation testing, while re-constituting a domestic capability. The key recommendation of the NEAC report was that “*DOE-NE proceed immediately with pre-conceptual design planning activities to support a new test reactor*” to fill the domestic need for a fast-neutron test capability, pursuant to DOE order 413.3B.

2.4. Current status

In the early stages of the VTR program, efforts have been focused on narrowing down the design space for a fast test reactor. A sodium-cooled reactor was selected as reference because of the higher level of maturity and experience with the technology. A trade-off study [7] was performed in order to determine the relationship between the maximum achievable peak fast flux ($E_n > 0.1$ MeV) as a function of the core power, while respecting basic thermal-hydraulics and temperatures limits. The analysis was performed for several types of metallic fuel, and the major trends established by this study are shown in Fig. 3. The metallic fuel systems were selected with the objective of meeting the performance requirements while using fuels that had previously undergone extensive irradiation that would facilitate qualification for their use in the VTR.

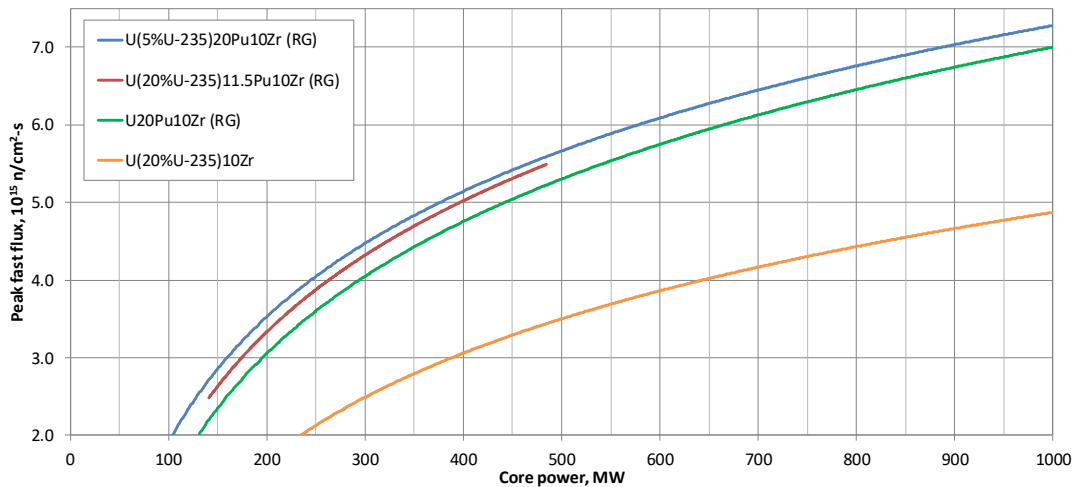


FIG. 3. Trade-off of achievable peak fast flux as a function of the core power for various fuels

These early results indicated that in order to achieve the desired flux levels ($>4.0 \times 10^{15}$ n/cm²-s) without resorting to highly enriched uranium and without resorting to very large power levels, use of plutonium-based fuel is necessary. With a target core power level of 300 MW(th), the envisioned plutonium-based fuel forms would allow to achieve the desired flux.

Based on these results, the VTR team is working on the conceptual design of the VTR. The core design efforts, discussed in Section 3, are primarily supported by the National Laboratory contributors, and the plant design by the GEH and BNI contributors. The plant design is based on the PRISM Mod-A reactor developed by GEH in the 90's through the Advanced Liquid Metal Reactor program. The general vessel arrangement of PRISM is shown in Fig. 4, and a detailed view of the cover-head is shown in Fig. 5. Modifications of the PRISM Mod-A design are underway to accommodate the VTR core. For instance, compared to PRISM Mod-A, the VTR core is using different assembly dimensions, leading to a different positioning of the core in the vessel, as well as a lower power level (300 MW(th) vs. 471 MW(th)) which leads to scaling of some of the vessel components. The cover head design also needs modifications in order to allow for the various testing locations requiring head penetrations.

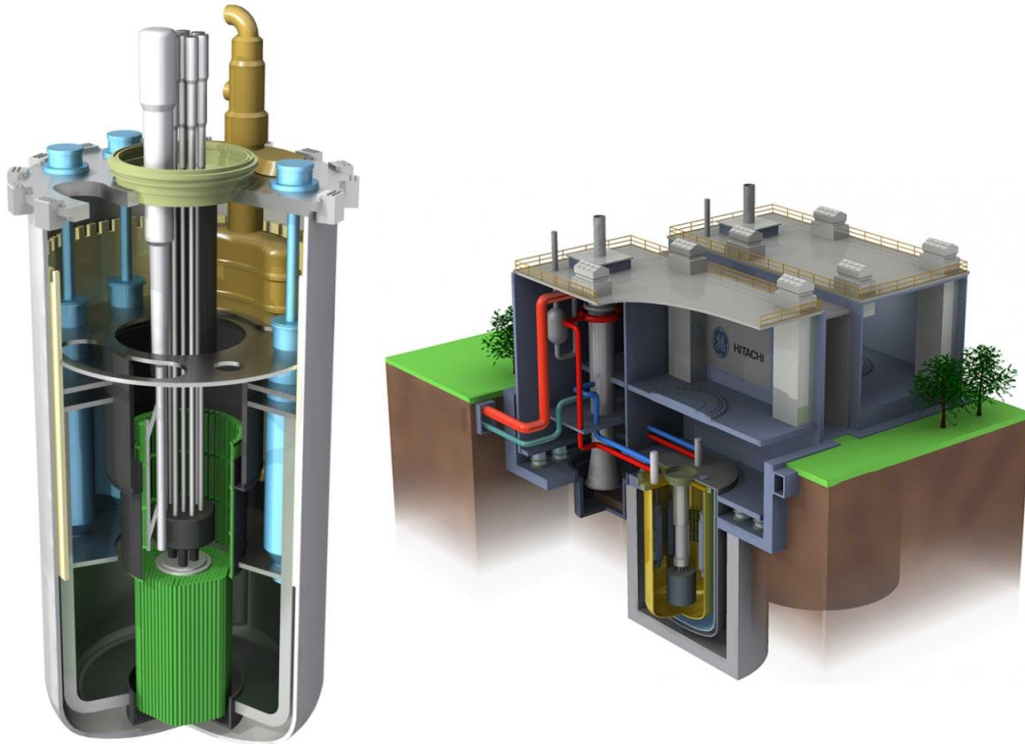
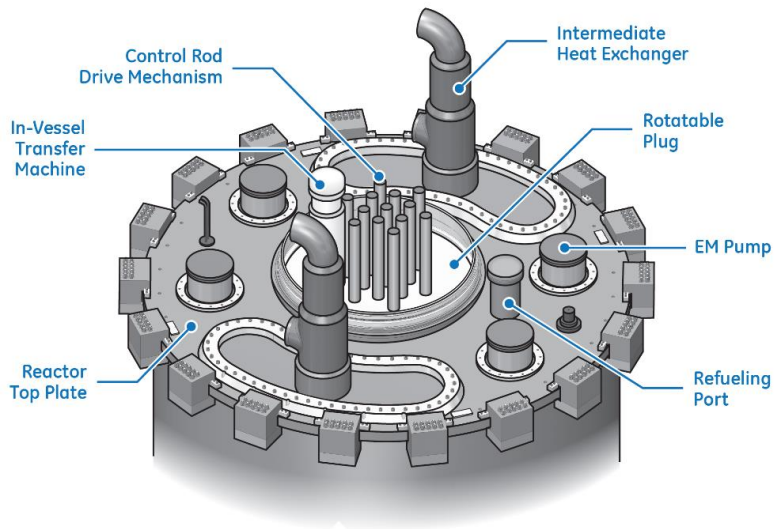


FIG. 4. General Vessel Arrangement for PRISM Mod-A (Source: GEH)



39518408-31_r0

FIG. 5. Cover head view for PRISM (Source: GEH)

As stated in Section 2, the VTR program is in the conceptual design phase, which includes the development of a credible cost estimate for the VTR facility. This requires considering all aspects of the VTR, from the core to the general site layout, including the vessel, the primary and secondary systems and other major components of the plant.

In August 2019, an announcement was made by the DOE about the preparation of an Environmental Impact Statement (EIS) to examine the impacts of building the VTR [8]. This is part of the process respondent to the National Environmental Policy Act (NEPA). Several DOE sites are being evaluated as part of the NEPA process.

3. CORE DESIGN

The VTR core layout designed as part of the CD-0 phase of the project is shown in Fig. 6 and generates 300 MW(th). It is composed of 66 fuel assemblies, six control rods, three safety rods, 114 radial reflectors, 114 radial shield reflectors, and 10 test locations. Some of the test assembly locations will be designed to enable accommodating instrumented test assemblies, and therefore will have a corresponding penetration through the cover head shown in Fig. 5 (additional penetrations not shown on this figure). The overall length of each assembly from the bottom of the lower shield to the coolant outlet is 3.53 m. The representative performance characteristics, at equilibrium, for this configuration are provided in Table 1. Detailed description of the core geometry and performance characteristics is available in referenced paper [9].

All assembly ducts are made of HT-9 and have a pitch of 12 cm. The fuel assemblies contain 217 fuel pins having an 80cm-tall column of fuel and an 80cm-tall fission gas plenum above the fuel. The fuel is contained in a HT-9 cladding wrapped in a thin wire. These assemblies also contain a 90cm-tall lower reflector region and a 60cm-tall upper reflector region. The fuel is the U-10Pu-10Zr ternary metallic fuel, using reactor-grade plutonium and low-enriched uranium with 5% ^{235}U .

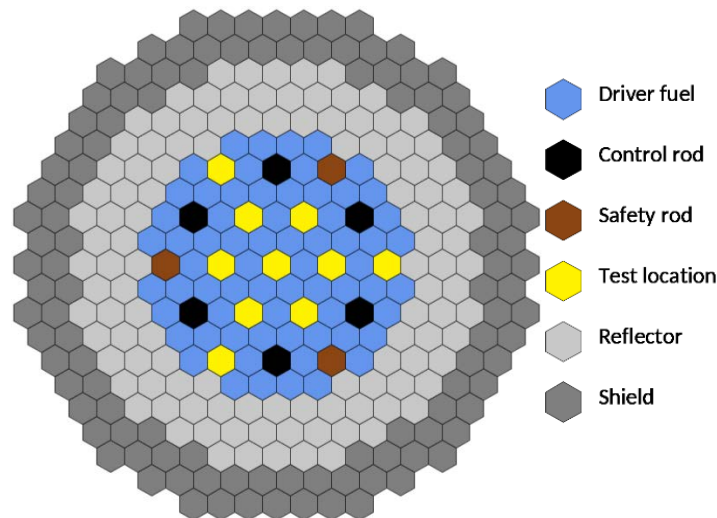


FIG. 6. Preliminary VTR core layout

TABLE 1. PRELIMINARY VTR CORE PERFORMANCE CHARACTERISTICS

Parameter	Value
Power	300 MW(th)
Fresh Fuel Height	80 cm
# Fuel Assemblies	66
Cycle Length	100 EFPD
# Batches	5
Plutonium Weight Percent	19.4%
Test Peak Fast Flux	4.17×10^{15} n/cm ² -s
Absolute Peak Fast Flux	4.35×10^{15} n/cm ² -s
Maximum Assembly Power	6.1 MW(th)
Burnup Reactivity Swing	2124 pcm
Fuel Charge/Cycle	551.4 kg HM
Average Discharge Burnup	54.4 GWd/t

The reflector assemblies are made of an array of HT-9 pins running through the entire length of the assembly duct. The shield assemblies are made of an array of absorber pins also running through the entire length of the assembly duct. The absorber pins consist of HT-9 cladding containing B₄C pellets, using natural boron. The control and safety rods are of a double duct, with the inner duct containing an array of absorber pins. The control and safety absorber pins have a similar design as those of the shield assemblies but use different dimensions. They are also using natural boron. As details of the test assemblies would vary based on experiments, these assemblies are currently modelled as sodium-filled duct assemblies.

Extensive design analyses have been performed to characterize the major aspect of the reactor to ensure feasibility from all perspectives. This includes a thermal-hydraulic assessment of the core [10], determination of the reactivity coefficients [9] and of the required shutdown worth, assessment of the control and safety rods performance [11], in-vessel shielding calculations for secondary sodium activation [12], and preliminary safety analyses [13].

4. TESTING CHARACTERISTICS

In the layout shown in Fig. 6, 10 test locations are shown as an illustration. In practice, non-instrumented test assemblies could be placed anywhere in the VTR core, selecting regions with irradiation conditions relevant to the test to be conducted. Only the instrumented test or cartridge loops will have to be placed in pre-defined locations, allowing head access. Cartridge loops, schematically shown in Fig. 7, are test vehicles with an independent closed loop allowing for different coolant to be used locally. If only few or no instrumented testing is being conducted, then these locations would be filled with non-instrumented test, driver assemblies, or dummy assemblies. The VTR is designed with a relatively large radial reflector region in order to allow additional irradiation testing to take place there. While the flux level is smaller in the reflector than at the centre of the core, it could offer another 30 test locations with a peak fast flux above 10^{15} n/cm²-s.

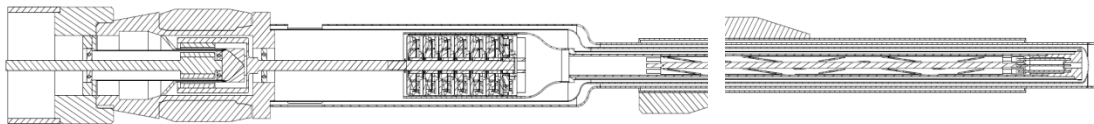


FIG. 7. Pre-conceptual representation of a cartridge loop system

A summary of a few metrics related to testing capabilities are provided in Table 2. The values provided for the test locations shown in Fig. 6. The values are provided per one assembly, and were obtained for an equilibrium cycle, with no materials loaded in the test locations. As such, the numbers will be affected by the actual test loading of VTR. Compared to existing research and test reactors in the U.S., the values predicted for VTR are significantly larger than what these other reactors can offer.

TABLE 2. SUMMARY OF IRRADIATION PERFORMANCE CHARACTERISTICS

Test assembly location	Row 1	Row 3	Row 5	Reflector
Peak fast flux, n/cm ² -s	4.17E+15	3.70E+15	2.26E+15	1.0-1.5E+15
Volume with fast flux above 1e15 n/cm ² -s, litre	17.7	17.1	13.8	-
Volume with total flux above 1e15 n/cm ² -s, litre	22.2	21.3	18.7	-
Peak fast fluence/year, n/cm ²	1.32E+23	1.17E+23	7.13E+22	3.0-4.5E+22
Estimated dpa/year in Fe	65	60	35	10-20

The 33-group flux spectrum achieved in the innermost test location and in the furthest radial reflector location are shown in Fig. 6 to illustrate the small variation in spectrum. While the spectrum could be tailored in the reflector region by proper selection of materials in the test assembly, the spectrum available by default is ideally suited for fuel and material testing for any type of fast reactor, including for molten-salt or gas-cooled fast reactors.

5. SUMMARY

The VTR project is a major initiative supported by the U.S. Department of Energy aiming to design and build a fast flux test reactor at one of the U.S. DOE sites by 2026. This project has been enabled by many years of work in support of advanced reactors development as well as by the recognition by the government of important capability gaps that would hinder the development of nuclear energy in the U.S. A team composed of many collaborators has been pulled together to support this project and ensure its success. The project is currently in the conceptual design phase.

Currently, the reference VTR is a 300 MW(th) pool-type sodium-cooled fast reactor fuelled with ternary fuel bearing plutonium. The core fits into the PRISM Mod-A plant layout, which will require some modifications to meet the mission of the VTR. It will offer peak fast fluxes in excess of 4.3x10¹⁵ n/cm²-s, with up to 30 test locations concurrently available, each having several litres of available testing space. All these test locations will enable achievement of over 30 dpa/yr, with a maximum of 65 dpa/year. Furthermore, the VTR will enable irradiation testing with coolants other than sodium through the cartridge loop systems without requiring any modifications. The specific technology and siting of the VTR will be selected as the result of an Analysis of Alternatives and the NEPA process that are part of the DOE approach to capital acquisition projects.

ACKNOWLEDGEMENTS

The submitted manuscript has been created by UChicago Argonne, LLC, Operator of Argonne National Laboratory (“Argonne”). Argonne National Laboratory’s work was supported by the U.S. Department of Energy, Office of Nuclear Energy under contract DE-AC02-06CH11357.

The work reported in this summary is the results of R&D studies supporting a VTR concept, cost, and schedule estimate for DOE-NE to make a decision on procurement in the future. As such, it is preliminary.

REFERENCES

- [1] U.S. DEPARTMENT OF ENERGY, DOE O 413.3B Chg 5 (MinChg), Program and Project Management for the Acquisition of Capital Assets, Department of Energy, Office of Management, April 2018
- [2] U.S. DEPARTMENT OF ENERGY, “Secretary Perry Launches Versatile Test Reactor Project to Modernize Nuclear Research and Development Infrastructure”, <https://www.energy.gov/articles/secretary-perry-launches-versatile-test-reactor-project-modernize-nuclear-research-and>, February 28, 2019
- [3] B. S. TRIPLETT, E. P. LOEWEN, B. J. DOOIES, PRISM: a competitive small modular sodium-cooled reactor, *Nuclear Technology*, 178, 186-200, May 2012
- [4] D. PETTI, ET AL., A Summary of the Department of Energy’s Advanced Demonstration and Test Reactor Options Study, *Nuclear Technology*, 199:2, 111-128, July 2017
- [5] C. GRANDY, ET AL., FASTER Test Reactor Preconceptual Design Report, Argonne National Laboratory, ANL-ART-86, March 2016
- [6] NUCLEAR ENERGY ADVISORY COMMITTEE, Assessment of Missions and Requirements for a New U.S. Test Reactor, Department of Energy, February 2017
- [7] F. HEIDET, ET AL., Tradeoff Studies for a Versatile Fast Spectrum Test Reactor, 2018 Pacific Basin Nuclear Conference, October 2018
- [8] U.S. DEPARTMENT OF ENERGY, “Notice of Intent to Prepare an Environmental Impact Statement for a Versatile Test Reactor”, <https://www.federalregister.gov/documents/2019/08/05/2019-16578/notice-of-intent-to-prepare-an-environmental-impact-statement-for-a-versatile-test-reactor>, August 2019
- [9] F. HEIDET, Current status of the Versatile Test Reactor core design, European Research Reactor Conference 2019 (RRFM/IGORR), March 2019
- [10] F. HEIDET, Preliminary Thermal-Hydraulic Assessment of the Versatile Test Reactor, Transactions of the 2019 ANS Annual Meeting, American Nuclear Society (2019)
- [11] Z. ZHONG, A. ABOU-JAOUDE, F. HEIDET, Preliminary Control Rod Lifetime Assessment for the Versatile Test Reactor, Transactions of the 2019 ANS Annual Meeting, American Nuclear Society (2019)
- [12] T. FEI, S. BAYS, F. HEIDET, Preliminary In-Vessel Shielding Analyses for the Versatile Test Reactor, Transactions of the 2019 ANS Annual Meeting, American Nuclear Society (2019)
- [13] T. SUMNER, T. FEI, N. STAUFF, T. FANNING, F. HEIDET, Versatile Test Reactor Preliminary Safety Analysis, Transactions of the 2019 ANS Annual Meeting, American Nuclear Society (2019)

**A CHARACTERIZATION OF THE FINANCIAL RISK PROFILE OF
FAST SMRS**
Comparison with SMRs of the PWR type

Paper ID #22

S. BOARIN
Politecnico di Milano
Milano, Italy
Email: sara.boarin@polimi.it

K. TUČEK
European Commission, Joint Research Centre
Petten, The Netherlands

C.F. SMITH
Naval Postgraduate School
Monterey, USA

Abstract

The capability of attracting investors' financing is essential for the deployment of a new technology. Financial risk and low generating costs are the two key axes of an investment decision in a power technology. After focusing on the estimation of generating cost and relying on the economy-of-scale paradigm, nuclear economics research is now turning to the investment risk issue.

The risk perception of an investment in the nuclear industry is notoriously high, especially due to the high capital cost element and its associated long pay-back time, uncertainties in the investment scenario conditions, and construction schedule delays and cost overruns. The realization of these adverse conditions tends to undermine the original estimate of the investment rate of return. Additionally, the scale of the asset value at stake makes the risk unbearable for many investors.

Financial risk is one of the reasons why Small Modular Reactors (SMRs) are becoming more and more attractive in energy markets, despite a higher estimated Levelized Unit of Energy Cost. Lower Total Capital Investment Cost⁷ reduces the financial risk of a project and makes the consequences of the risk manageable. Simplification, standardization and reduced size of components are expected to streamline the supply-chain and make the construction schedule more predictable and controllable.

These considerations hold in general for SMRs, but are there specific benefits that Fast SMRs can add to the SMR business case? In this context, the present research work investigates the financial risk profile of Fast SMRs. The study is broken down into risk components specific to the different phases of the project lifetime, from licensing to decommissioning; each risk area is then analysed in light of the design features and innovations brought in by the advanced, Generation-IV technologies. The analysis is carried out by means of an analytical hierarchy process, which is suitable to the evaluation of factors with different metrics and/or which are not fully quantifiable. Information is derived from expert elicitation and supported by strong rationales; the elaboration defines a proper characterization of the Fast SMRs risk profile. Finally, the strengths and weaknesses of Fast SMRs compared to Generation-III/III+

⁷ According to Ch.1.4 of: GIF/EMWG/2007/004, "COST ESTIMATING GUIDELINES FOR GENERATION IV NUCLEAR ENERGY SYSTEMS, Revision 4.2", September 26, 2007.

Pressurised Water Reactor SMRs (PWR-SMRs) are discussed. Risk mitigation factors are outlined, as well as areas of improvement, in order to foster a rational approach to the risk, reduce the barrier to the nuclear investment and enable a level playing field with other low carbon energy projects to attract public and/or private financing.

1. INTRODUCTION

Financial risk is fundamentally linked to the likelihood of financial loss. It is associated with uncertainty and refers to the variability of returns of an investment project (M. Bernadete Junkesa, 2015). The concept of financial risk can be typically broken down into a cascade of components at different levels, specific to the type of project, such as “market risk”, “operating risk”, “environmental risk”, etc.

An increase in financial risk will increase the cost of capital and will be charged to the cost of the final product (e.g., electricity). Beyond a certain level of risk, which is a subjective evaluation, investors are not willing to put their financing at stake, and the project becomes infeasible. This is especially true in free market conditions, where little or no protection for the fate of a private investment is granted. This is particularly applicable to a nuclear investment project, due to peculiarities that are discussed in section 2.

Reducing financial risk is therefore an enabling condition for the deployment of a new nuclear technology. This aspect is complementary to the economic analysis that traditionally focuses on the assessment of costs.

The purpose of the work is therefore the analysis of the financial risk associated with Fast SMRs, to understand its sources. Risk measurement on an absolute scale is not straightforward, and its perception is very subjective. Therefore, the financial risk of Fast SMRs has been broken down into a cascade of components at different levels, specific to the nature of the project, and quantified according to the comparative methodology described in section 4. This is i) based on the opinion and the perception of recognized experts in the nuclear sector (cf. also Section 3.3 for details on the qualifications and selection process of these experts), and ii) assumes an alternative SMR technology as a reference (i.e., PWR-based SMRs).

This comparative analysis highlights the issues and opportunities of Fast SMRs in terms of investment attractiveness, as discussed in the Conclusion section. The results provide hints to facilitate mitigation of the factors with higher impact on the financial risk of the project.

2. RISK IN NUCLEAR POWER INVESTMENT

According to its definition in safety analysis, risk is the combination of the probability and impact magnitude (a measure of consequence) of an adverse event.⁸

A nuclear investment project presents a considerable scale of magnitude from the financial point of view, and a very specific combination of potentially unfavourable factors that are rarely encountered in other type of projects.

⁸ According to the IAEA Safety Glossary (IAEA, “IAEA Safety Glossary - 2018 Edition”. Publication 1830, Vienna, 2019), risk assessment normally includes consequence assessment, together with some assessment of the probability of those consequences arising.

- Nuclear projects are characterized by a considerable amount of capital invested and a long-term period of capital recovery; the potential for construction project mismanagement, realization of bottlenecks, or unanticipated schedule delay, may have very large consequences. Research considers these factors as commonalities with mega-projects such as infrastructures (Brookes, 2015).
- The size of the plant and the complexity of design are likely to increase the probability of unanticipated problems in the construction process while also increasing the burden on project management. Some studies argue that there is a correlation between increased complexity and construction cost overruns and delays (Grubler, 2010).
- Nuclear power plants are capital-intensive projects that have to act as “price-taker” on the electricity markets. In the electricity generation market, the price is usually made in a bid-and-offer or pay-as-clear mechanisms, by power technologies with low variable costs. Wind and solar photovoltaics (PV) have virtually no variable costs and, over the last decades, they benefited from large subsidies to stimulate demand in the hope that their initially high generation costs would decline.
- On another side, natural gas-related technologies such as Combined Cycle Gas Turbine (CCGT), with low capital and fixed operation and maintenance costs, are experiencing the lowest wholesale price of gas in some countries and regions (e.g., the USA). Due to their consequent low energy generation costs, these technologies have the chance of displacing conventional technologies with higher variable generation costs.
- Besides market risks, the nuclear industry experiences considerable opposition in public opinion, from some political factions as well as very stringent regulatory activity and requirements. These factors may translate into changes in boundary conditions, additional costs and delays in project schedules that may compromise the expected investment return.

3. ASSUMPTIONS AND FRAMEWORK

3.1. Fast SMRs

Several Fast spectrum reactors are currently under development worldwide (World Nuclear Association, 2019); they rely on innovative reactor coolant technologies, including, but not limited to, sodium, lead, lead-bismuth eutectic, molten salt and helium. Many of them fall in the Gen-IV design types. Their electric outputs range from small sizes (up to 300 MW(e)) to medium sizes (300–700 MW(e))⁹. They can operate either as breeders, or as burners of plutonium and/or long-lived minor actinides, reducing the radio-toxicity and volume of the final waste, and delivering a highly efficient use of fuel resources; however, the benefits of a fully closed fuel cycle can only be realized when the related reprocessing technology becomes available at a commercial scale.

These innovative technologies require extensive research and qualification programmes on existing and new structural materials to demonstrate their ability to operate at high temperatures and, in some cases, to accommodate corrosive coolant media. Fast SMRs under current

⁹ Some of these new fast reactor concepts are also envisioned at large or very large sizes (more than 700 MW(e) and up to 1200 MW(e) or greater).

development have different technology readiness levels and different features and benefits in terms of fuel cycle and waste management.

Fast SMRs generally incorporate coolant temperature cycles that are higher than current conventional reactors or, in particular, Generation-III/III+ SMRs of the PWR type. This not only enables higher energy conversion efficiencies, but it also may allow more flexible operational modes for energy storage as well as other non-electric applications. For example, higher operating temperatures would allow delivery of higher quality process heat for production of clean energy products such as Hydrogen through industrial processes requiring temperatures well above 300°C (Fig. 1). As an example, demand of oil refineries for process heat is in the temperature range of 300-750°C, with most of the demand at temperatures below 500°C, well within operation regimes of liquid metal cooled Fast SMRs [5] [6]. Applications above 500°C include for example high temperature steam electrolysis and steam reforming of natural gas to produce hydrogen and syngas, respectively. Additional advantages, compared to traditional Giga-Watt scale plants, is the expected enhancement of inherent and passive safety features, and the suitability for a distributed and flexible power/energy generation system.

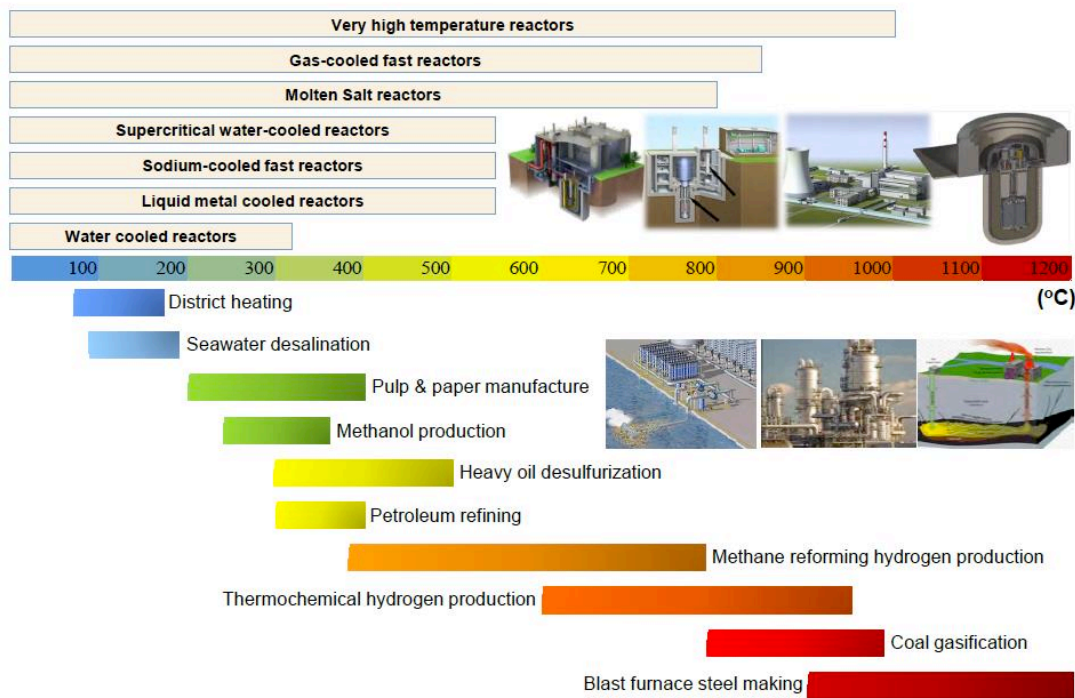


FIG. 1. Summary of SMR designs for non-electrical applications [6].

3.2. PWR SMRs

PWR SMRs represent today a new interesting nuclear investment paradigm, that matches the operating experience of well-established reactor technology, with the benefits of a small output scale, such as: enhanced passive safety, reduced upfront capital investment, wider range of non-electric applications than large PWRs due to more flexible sizing to the exiting demand, and suitability for a distributed and flexible power generation system. With respect to conventional Giga-Watt plants, the SMR paradigm is conceived to exploit the economy of series, i.e., cost

savings that arise from standardisation, modularisation, factory-fabrication, layout simplification, transportability, etc. The interest in SMRs lies in the promise to cope with the risk factors and potential for project mismanagement of stick-built complex plant concepts, supply-chain bottlenecks, long pay-back times, etc. [7].

The readiness level of PWR SMRs is higher than that of Fast SMRs. To set the same investment scope for the two plant types, this research assumes that they are both already available for commercial deployment. Design certification is assumed as already obtained from the nuclear regulatory authorities for both SMR types. Any possible investor could choose one or the other plant category, as if the prototype phase was already been accomplished. The investment time horizon spans from the construction licensing to the Decommissioning & Decontamination (D&D) phase.

3.3. The panel of experts

Thirty-five experts in the nuclear industry were contacted and requested to express their opinions about the risk factors of the two SMR technologies. Each of the authors of this study prepared lists of candidate experts who are highly respected in their fields, and cover a range of the desired backgrounds and expertise. The lists were combined and refined by the authors to assure an appropriate mix to cover a diversity of roles and competencies related to nuclear energy development. Nineteen of these experts provided their responses for this study; three of them participated in tandem with another expert such that the total number of separate responses was sixteen. The panel included experts with different roles in the industry: from engineering, to safety and licensing, and energy/nuclear economics. Some experts are entrepreneurs and design developers; some of them are involved in fast reactor technology, some others are generalists. Fig. 2 provides a breakdown of the panel composition in terms of role and competencies.

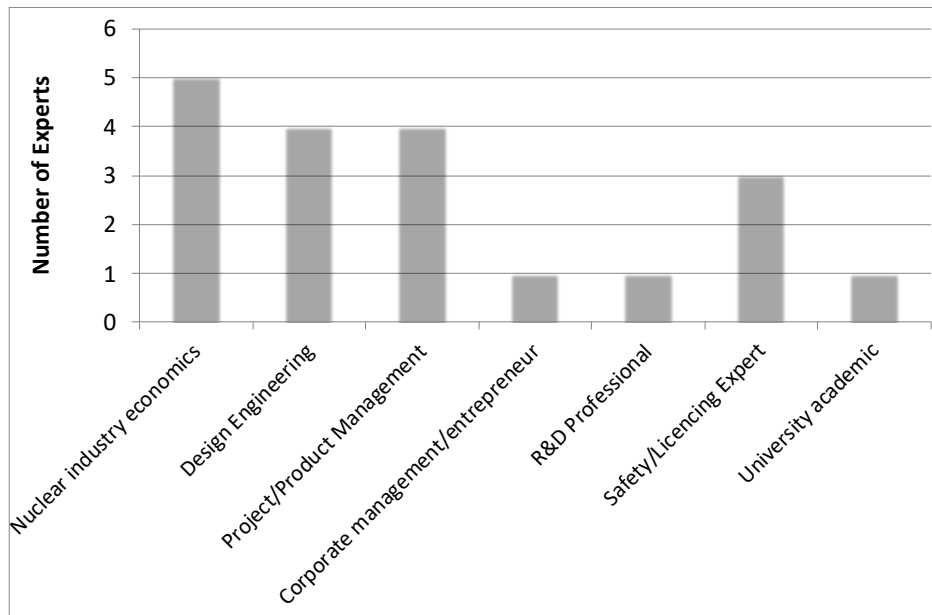


FIG. 2. Chart with the roles of the panel of experts that provided responses to the elicitation

4. METHODOLOGY

4.1. The issue of risk measure

The *a priori* risk measurement of an innovative project on an absolute scale is not feasible, due to the subjective nature of the risk perception by possible investors and of the specific boundary condition of each investment case. Innovative projects do not have historical financial information available for the calculation of financial indicators. Financial risk of an innovative technology investment is based on forecasts, expectations and judgments developed in the face of uncertainty. The elicitation of expert opinion was chosen as the appropriate approach in this context.

When an absolute measurement is not practically achievable, it is still possible to give a relative-one: the experts are asked to consider two alternative hypothetical investment options and evaluate their risk on a comparative basis. They have to state if Fast SMRs or PWR SMRs are more or less risky, in relation to different factors. The opinion is given on a discrete scale of levels, and experts provide a rationale to justify their opinion.

4.2. The financial risk break-down

To understand the sources of risk and their contribution to the overall financial risk, the latter has been organized into a set of factors, according to two criteria:

- The first level corresponds to the different phases of the lifetime of the investment project; each-one represents a “risk area”, in line with the risk classification given by [8], that identifies the risk of Licensing, Delivery/Construction, Operational and D&D.
- For the second level, each of these life-cycle risk areas is further broken-down into risk factors that trace the key sources of uncertainty during a specific lifetime phase.

The result is a two-level breakdown of the financial risk, as summarized in Fig. 3.



FIG. 3. Chart with the risk breakdown structure at two levels

The second level risk factors are not meant to be exhaustive but to catch the key risk sources

that are influenced by the different Fast or PWR SMR technology concepts. Accordingly, electricity price risk is not mentioned in the operation phase, since it is technology independent.

Licensing

The licensing phase concerns the project feasibility on a specific site and its approval for construction and operation prior to the construction phase (combined construction and operation licence); in other cases, the construction phase is performed first, and the operation licence is filed during the plant construction. In this phase investors raise and commit their capital: they have already made the decision to invest in the specific plant on a specific site that they are applying for, and therefore they must keep their capital available for the eventual construction phase. Such a financial effort cannot be set in place overnight, and the investment decision implies an opportunity cost for not employing capital in an alternative investment project. The Regulatory activity is particularly solicited and active during this phase: any possible setback would translate in deployment delay and/or design modification. During the licensing phase, public opposition and “not in my backyard” behaviour could be a serious barrier to the site selection and plant realization. Any delay or drawback translates into a loss in terms of the cost of money. On the other hand, political support may create a favourable legislative framework for the project’s economic viability.

4.2.4. Construction

Risk factors related to this phase represent any occurrence that translates into a delay or a cost increase. Public opposition, changes in the political climate and revisions to safety standards and requirements can materialize at any time resulting in a source of risk for the nuclear project schedule and cost. On the other hand, political support in this phase may translate into some forms of financial backing of the project, decreasing the capital cost and becoming a fundamental risk mitigating factor.

Supply chain management is a sensitive aspect when suppliers are few and very specialized; on the other hand, supply chain management may also become complex when it is highly fragmented into a considerable number of different suppliers.

Project management is a critical practice for the timely and proper project execution; it concerns the management of time, costs, resources, goals and quality constraints. Mismanagement may increase with project complexity.

On-site work has been identified as a risk factor based on the results of scientific research about nuclear economics: the stick-build construction paradigm (piece-by-piece on the construction site) is considered riskier than the factory-fabrication paradigm, in that it relies on standardization, modularity and pre-construction, increase in automation content and assembling on site by human resources. The reasons for this lie in the better work setting at the factory, its controlled environment, automation, higher precision and quality control, as opposed to the adverse weather conditions, high variability, customization and uniqueness of layout solutions, higher labour content (and risk of human error) encountered in on-site construction [9, 10, 11, 12]. The degree of on-site work in the construction process is therefore considered as a risk-increasing factor, while the factory-fabrication content is considered as a risk-mitigating factor.

4.2.5. Operation

The risk factors or the risk-mitigating factors relevant to this phase are many and are listed in Fig. 3. They have been identified as those factors potentially having a financial impact on the investment project. For instance, safety issues are considered in terms of their impact on the plant profit and loss, for example in determining unplanned outages. Waste management and spent management issues from the point of view of the non-proliferation have been included in the security risk factor, while the spent fuel issues in the wide perspective of the environmental sustainability have been included in the risk factors specific to the D&D phase.

Regulatory activity, political support and public acceptance have an influence throughout the plant lifecycle, with the possibility for imposition of more stringent safety requirements and consequent design interventions, documentation, stress-tests, etc.

Planned and unplanned outages are risk factors since the higher their number and duration, the higher the impact on the revenue stream: missed income is equivalent to financial loss.

Plant flexibility consists of the combination of plant manoeuvrability and fit with cogeneration or energy storage options. Plant manoeuvrability is the capability of performing power ramping up and down, in a safe and reliable way, changing the power output on request, to fit with variable electricity demand. This feature can help to compensate the variability of demand in an integrated system with renewable power generation. A core designed to offer a prompt response to the load change will have limited structural stress from the power ramping and will not risk an operating lifetime decrease.

But on the other hand, any power output reduction means lower revenues. For this reason, the fit with cogeneration options is a risk-mitigating factor, since the revenues from the electricity sale may be replaced by revenues from the sale of complementary products (district heat, desalinated water, hydrogen, industrial process heat for other applications, etc.). Fit with energy storage technologies is a risk-mitigating factor as well, since the revenue stream from the sale of electricity can be shifted in time, i.e., to peak hours (even if in the conversion and storage processes, some energy loss needs to be taken into account).

In a once through, traditional fuel cycle, the main source of price volatility (unexpected variation) is the uranium natural resource (that represents 14% of levelized cost of energy [13]). Innovative fuel cycles, with multi-recycling of uranium and plutonium, partitioning and transmutation of minor actinides, and new fuel matrices and compositions (e.g., nitrides, thorium-based fuels, etc.) will have to be supported by new fuel production facilities and might necessitate new or further developments of existing spent fuel reprocessing technologies (e.g., electro-metallurgical). Their cost and final product price (nuclear fuel) are not known today. On the one hand, reprocessing costs will represent a relevant component of the nuclear fuel price, but on the other hand the impact of the natural resource price will be lower for fast reactors than Light Water Reactors (LWRs), due to a more efficient use of fissile and fertile materials and therefore a lower content of uranium ore in the final product. The benefit of this lower content in raw material might be limited by a potential uranium price decrease following a possible demand reduction, but this speculation depends on the deployment pace of worldwide nuclear energy production.

Finally, robustness to natural events and security are risk-mitigating factors: flooding, seismic events as well as intrusion, diversion of fissile materials, tampering and terrorist attacks may have catastrophic effects without a proper protection of the nuclear plant, with consequent private and public/social costs. The degree of robustness and security has a strong influence on the public opinion and acceptance, as well as on regulatory and other government officials. The

sensitivity and response to external risks depends both on the type of reactor (meaning the coolant technology) and on the design and safeguards implemented in a specific plant concept. For instance, at the level of the reactor type, a sodium plant bears the risk of an exothermic reaction of the coolant with air and water. Liquid metal reactors have higher seismically induced loads to be addressed, but also have higher decay heat removal capability, etc.

4.2.6. Decommissioning & Decontamination (D&D)

The decommissioning of a nuclear plant is a project that encompasses the same phases as its construction: engineering, cost estimation, project management, project execution. Very often the D&D project execution results in time and costs that are higher than predicted. The decommissioning liabilities can be more volatile with increases or decreases in the cost of decommissioning, which is sensitive to changes in regulations, waste disposal policy, politics and plant conditions as the generating facility ages. Consequently, a funding plan developed for decommissioning a nuclear facility needs to be more responsive than for plans designed for the retirement of conventional assets [14]. The higher the D&D costs with respect to the provisional fund, the higher is the financial impact on the plant's owner profit margin. There is a significant cost uncertainty in this phase, and this is a source of financial risk.

The nuclear regulator oversees the D&D process with continuous permission release activity. Public acceptance and political support are critical in this phase, since they can ease or complicate the process (e.g., the identification and realization of waste repository). As in the plant operation phase, the level of security and safety of the plant during the D&D process has a favourable impact on public opinion, on the government and on the regulator, easing the process and the licensing of the dismantling procedures.

On the D&D execution side, modular design is expected to facilitate both construction and dismantling of the plant, reducing time and costs, just as it does in the construction phase. Plant layout to facilitate dismantling is a risk-mitigation factor that refers to this situation, while on-site work refers to the opposite situation, when the plant has not been designed to be dismantled in a modular way; it is considered as a risk-increasing factor, due to the need of tailor-made solutions and more complex project management [15].

Finally, the amount and type of high-level waste has an impact on the D&D costs, as well as the need of special dismantling/cutting/decontamination techniques. Fast reactors may require special/additional decommissioning strategies, coolant removal, storage and treatment methods (e.g., the technology for sodium residue neutralization after draining). New technologies and strategies for the D&D of the primary circuits of fast reactors are under development; their cost and effectiveness bring uncertainty to the business plan with an impact on costs.

4.3. The analytical hierarchy process

In the Analytical Hierarchy Process, the experts are first asked to give their opinion about the impact that each risk area at the 1st level has on the overall financial risk. This opinion (hereafter referred to as the “weight”) has the meaning of weighting a specific lifetime phase on the overall risk. The sum of the weights has to be equal to 100%.

Secondly, the risk factors at the 2nd level breakdown are assigned a “score” by each expert that indicates the contribution of each factor to the risk of a given lifetime phase. The score ranges on a scale from 1 to 5; the meaning of values is summarized in TAB. 1: the higher the value, the higher the contribution of the factor to the risk of a given lifecycle phase.

TABLE 1. SCALE OF SCORES ASSIGNED TO THE 2ND LEVEL RISK FACTORS IN THEIR RESPECTIVE LIFECYCLE PHASE

Score	Meaning
1	Not at all important
2	Slightly Important
3	Important
4	Fairly Important
5	Very Important

Finally, Fast SMRs are “rated” by the experts, compared to PWR SMRs, against each 2nd level risk factor. This information states how good is the performance of one SMR type in comparison to the alternative one, in terms of reduction of the risk impact (hereafter referred to as the “rating”). Ratings are assigned according to the scale in TAB. 2.

TABLE 2. SCALE OF RATING VALUES FOR THE COMPARATIVE RISK ASSESSMENT OF FAST AND PWR SMRS, RELATED TO EACH 2ND LEVEL RISK FACTOR, AND THEIR MEANING

Rating	Meaning	Complementary meaning for alternative SMR option
1	PWR SMR much better	Fast SMR much worse
2	PWR SMR fairly better	Fast SMR fairly worse
3	PWR SMR slightly better	Fast SMR slightly worse
4	Equal	Equal
5	Fast SMR slightly better	PWR SMR slightly worse
6	Fast SMR fairly better	PWR SMR fairly worse
7	Fast SMR much better	PWR SMR much worse

Each expert assigns a value on the rating scale shown in TAB. 2 (1st column); by calculating its complement to eight, it is possible to derive the rating value for the SMR type (3rd column).

4.4. Data elaboration

Weights assigned to the different lifecycle phases are aggregated and averaged over the expert panel to provide a result on the 1st level risk breakdown: the averaged weights represent the contribution of each plant lifecycle phase to the overall financial risk.

Going further into the detail of the 2nd level breakdown, the scores assigned to the risk factors are aggregated and averaged to give the measure of their risk impact in each lifecycle phase.

If the scores are weighted by the 1st level weights, they become comparable with each other, across the different lifecycle phases. The weighted average scores provide an indicator of the impact of the risk factors on the whole financial risk, independently and prior to a specific SMR technology.

Different risk performances between the two SMR technologies come into play at the 3rd level, when risk factors are rated according to the potential of Fast SMRs or PWR SMRs for increasing or reducing the risk.

Then, the average ratings are multiplied once by the score of the risk factor and then by the weight of the lifecycle phase concerned. The result is a risk indicator that allows comparison of

the risk performance of the two SMR technologies and that is proportional to the risk impact of the different risk factors (2nd level) in the different lifecycle phases (1st level).

The value of these risk indicators has a comparative meaning only and does not lie on any absolute scale. The relevant information is the ratio between the risk values of the two SMR types; the risk indicators have a numeric meaning in the context of the comparative assessment only, given the above-defined methodology framework.

5. RESULTS

5.1. First level: lifecycle phases

Figure 4 presents the weights assigned by the panel of experts to each lifecycle phase. Percentages are calculated as the arithmetic average of data and represent the risk contribution of each phase to the overall financial risk of the project. All the experts agree that construction is the most sensitive phase from the point of view of risk; this critical phase represents 43.3% of total risk, on average. Plant operation is the second-ranked, with 29.3% of total risk. The average weight given to the licensing phase is 17.5%, while D&D represents 9.9% of total financial risk.

The construction phase has the highest impact in terms of financial risk, since during this phase the investment cost becomes a sunk cost.

The results are in agreement with historic evidence and with the scientific literature [3, 10, 12, 16] that identifies the construction phase as the most critical phase from the point of view of the financial risk. Extra costs and delays that may arise in this phase have a considerable financial impact, due to the huge scale of the investment cost. Beyond a certain threshold, the nuclear plant investment might be withdrawn, since it would not be able to generate an adequate profit anymore (e.g., V.C. Summer, units 2 and 3, in the US [16]).

The risks during the plant operation phase may affect the revenue stream (e.g., lower electricity demand, or plant unavailability), or costs (e.g., extra-costs for maintenance, repair, safety improvements). The risk impact is therefore relevant, since the net operating cash inflow allows profit gathering and investment remuneration.

The risk associated with the licensing phase is lower as are the sunk costs at this stage of the project lifetime.

D&D has been assigned the lowest risk; this is due to the actualization of future values (i.e., the calculation of the present value of a future amount of money). Another way of seeing this effect is that plant operation allows the provision of dedicated funds during a long period of time, to face a long-term expenditure. The longer the period, the lower the incidence of the annual provision; moreover, very often it is possible to invest the provision fund in risk-free assets, decreasing the annual provision needed. In this way, the financial impact of a very long-term expenditure has a low risk at present.

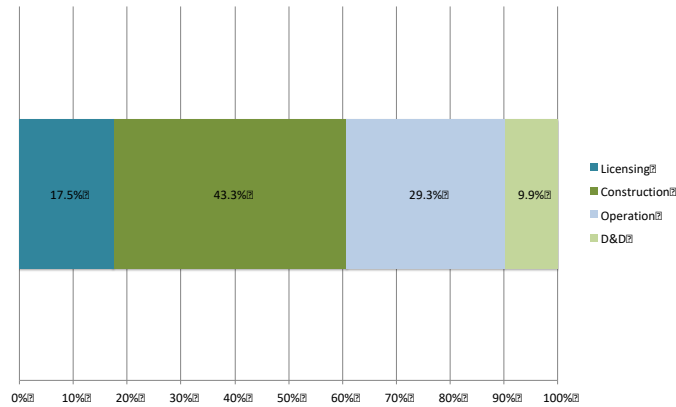


FIG. 4. Chart with the 1st level breakdown of the financial risk

5.2. Second level: risk factors

Looking inside each lifecycle phase, the average opinion of the experts about the risk breakdown in the different lifecycle phases is shown in Figs. 5 to 8. Besides regulator activity, whose outcome determines the chances for the project realization, public acceptance is considered by the experts as an *a priori* enabling factor: without it an NPP project would hardly be feasible. Political support is considered a critical factor for the deployment of a first-of-a-kind, by means of funding, risk sharing, policies and regulations, etc. [17] [18].

Supply chain management, project management and on-site work are the key cost drivers during construction and therefore represent the key risk factors in this phase (Fig. 6). Even if both Fast and PWR SMRs evolve towards modularity, managing on site work will still be important to reduce the risk of cost overrun. One expert highlight that on-site work risks may be controllable by project management. In one opinion, factory-fabrication cost savings might be overestimated, while on average, this paradigm is given a lot of importance by the expert panel as a risk-mitigating factor.

Financial risk during plant operation is driven by the planned and unplanned outages and by their duration (Fig. 7).

The fit with energy storage or cogeneration options is considered an important complement to the plant manoeuvrability.

Robustness to natural events is considered critical and linked to the public acceptance. Resilience against hazard impact is a precondition for operation and might generate the need for back-fitting with associated costs. Some experts highlight that robustness to natural events is also relevant to the licensing and the D&D phases. The importance of security is perceived as country dependent: in some countries (e.g., in the US) the cost to ensure security is not negligible.

Uncertainty on fuel cost has a minor role in the opinion of experts, compared to the other operating risk factors: although Fast SMR fuels are expected to be more expensive (due to reprocessing, specialized fabrication, etc.), the fuel cost is still expected to represent a small fraction of the levelized cost of energy.

High Level Waste (HLW) management¹⁰ and special decommissioning techniques are key cost drivers in the D&D phase (Fig. 7); nevertheless, innovative reactors are expected to simplify the waste management, compared to present reactors. Plant layout to facilitate dismantling is perceived as an important cost-reducing factor (and therefore risk-mitigating) by the average of the panel of the experts, with simple dismantling layout being also linked to simple construction.

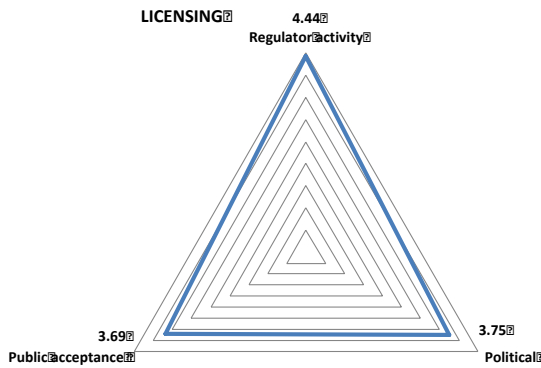


FIG. 5. 2nd level breakdown of the financial risk in the licensing phase

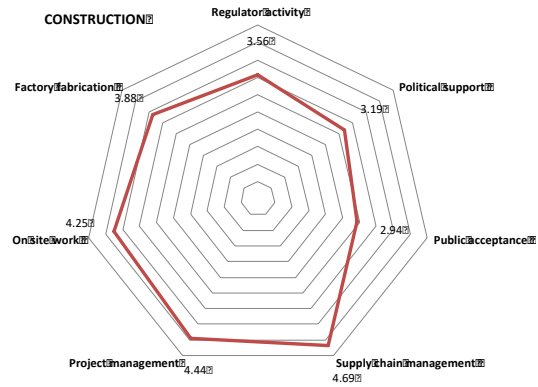


FIG. 6. 2nd level breakdown of the financial risk in the construction phase

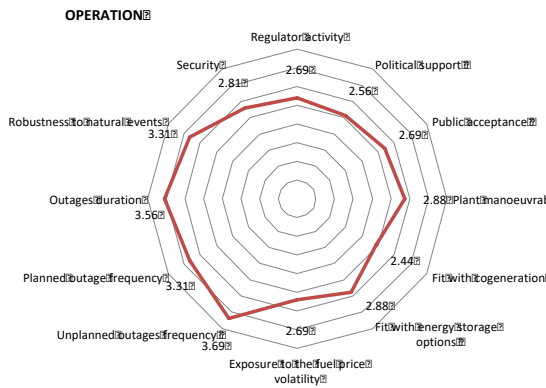


FIG. 7. 2nd level breakdown of the financial risk in the operation phase

DECOMMISSIONING AND DECONTAMINATION

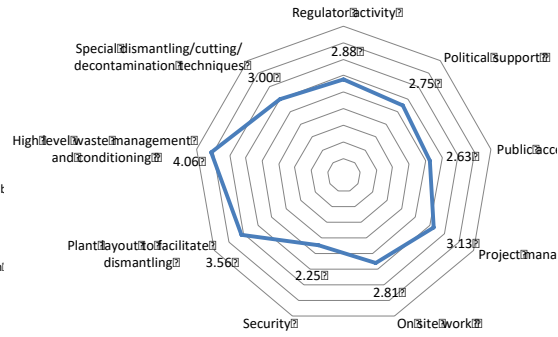


FIG. 8. 2nd level breakdown of the financial risk in the D&D phase

5.3. Third level: Fast SMR and PWR risk evaluation

Licensing

Figure 9 shows the average ratings assigned by the experts to the Fast and PWR SMRs in the licensing phase. According to the opinion of the experts, regulators have limited knowledge of advanced Gen-IV systems, while they are familiar with traditional water-cooled technologies

¹⁰ High Level Waste is considered either the waste from reprocessing of spent fuel or the spent fuel itself when it is directly disposed of.

of Generation III/III+. They might require additional experimental demonstrations (including fuel demonstrations), which would increase the licensing risk and costs, especially for Fast SMRs. In section 3.2 it is assumed that both Fast and PWR SMR types have obtained the plant design certification; nevertheless, according to the expert panel, the amount of reactor operating years, accumulated over the decades by PWR Gen II, III and III+ plants, would increase the confidence of the regulators towards PWR SMRs, in contrast with that of Fast SMRs, during construction and operation licensing.

On the other hand, no significant difference emerges in the political support risk indicator. This factor will depend on overall national benefits, including capacity building for local industries, job creation, climate change goals, etc. The advantage of higher sustainability (i.e., the reduced volume and radiotoxicity of radioactive waste and more efficient use of fuel when implementing a closed fuel cycle) will be a plus for Fast SMRs. On the other hand, according to some experts, PWR SMRs technology readiness is a better match to the short term needs of the electricity market. Moreover, there might be more political support for established vendors of PWRs and a psychological barrier against new technologies. All this considered, the average opinion is well balanced.

According to the experts, the performance of Gen-IV technologies is expected to positively influence the public perception, due to the better use of resources, enhanced safety and higher sustainability (reduced environmental impact). In the average opinion of the experts, fast reactors are expected to be more inherently safe and consequently should be favoured considering the public acceptance. Of course the relevance of these factors varies considerably depending on the design type, but the expert panel was asked a general opinion about the Fast SMRs category, all averaged, in comparison to PWR SMRs: in their evaluation they focused on the common features of the new fast technologies. This work could be a starting point for further analysis on a breakdown level of the different Fast SMRs designs.

It is noted that some of the experts disagree, considering that general negative opinion on nuclear power ought to lead to greater trust in PWRs as an established technology.

5.3.8. Construction

Figure 10 shows at a first glance a better risk performance of PWR SMRs with respect to Fast SMRs in the construction phase.

The dominant opinion is that PWR SMR needs to be able to exploit the supply chain established for Gen-III PWR plants. Moreover, the experience from building recent PWRs will help in better planning and reduce the project management risk in PWR SMRs. No experience feedback exists on Fast SMRs construction, even if some experts believe that there is no difference in complexity between the two SMR types. Concerning the potential for factory-fabrication, experts generally agree that, at the moment, there is a perspective for short-term factory-fabrication of PWR SMR modules, while no factory has been identified for Gen-IV innovative components.

Some experts believe that PWR SMRs can also benefit from more experience about on-site work, from large plant construction, inheriting some degree of learning, while some others think that the two technologies will be equivalent from this point of view; the average opinion put PWR SMRs in a slightly better position. As for regulator activity, the rationale is the same of the licensing phase: PWR SMRs can exploit the actual experience with the construction of commercial PWRs.

Fast SMRs keep their advantage in terms of public acceptance, while political support during construction is similar, due to a similar impact of the two SMR technologies on the economic environment.

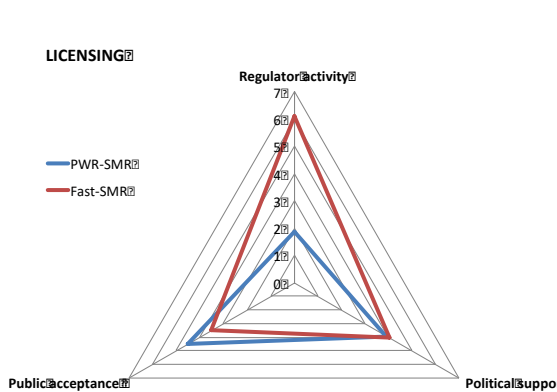


FIG. 9. Rating of Fast SMRs versus PWR SMRs in licensing

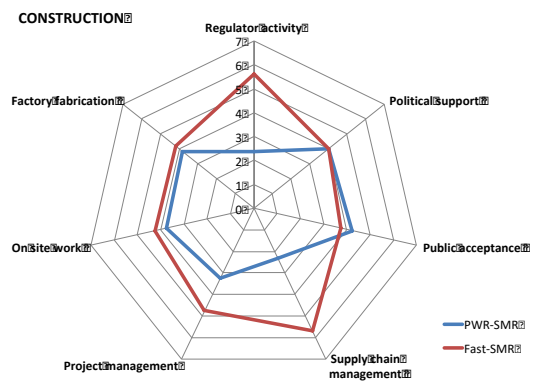


FIG. 10. Rating of Fast SMRs versus PWR SMRs in construction

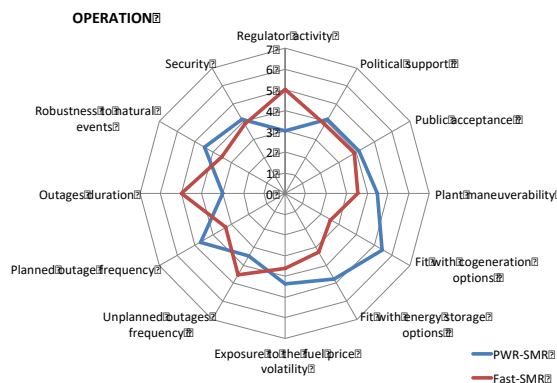


FIG. 11. Rating of Fast SMRs versus PWR SMRs in operation

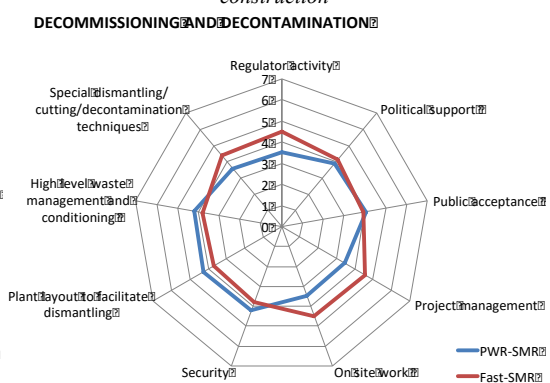


FIG. 12. Rating of Fast SMRs versus PWR SMRs in D&D

5.3.9. Operation

In the operation phase, the risk profile of Fast SMRs is globally perceived as lower than that of PWR SMRs. Experts expect Fast SMRs to offer higher plant manoeuvrability on account of the goals set for the Generation IV systems compared to current technologies: the Generation IV International Forum is progressing toward a system approach to flexibility in a broad sense, addressing operational flexibility (manoeuvrability, compatibility with hybrid systems, island mode operation, diversified fuel use), deployment flexibility (scalability, siting, constructability), and product flexibility (electricity, process heat) [19]. For instance, the Gas-cooled Fast Reactor (GFR) has better manoeuvrability because of helium flow control; it does not compromise reactor integrity and cycle efficiency when regulating the power [20]. The Molten Salt Reactor (MSR) has a significant load-following capability where reduced heat removal through the boiler tubes leads to increased coolant temperature, or greater heat removal reduces coolant temperature and increases reactivity. Primary reactivity control can be achieved by adjusting the secondary coolant salt pump or circulation which changes the temperature of

the fuel salt in the core, thus altering reactivity due to its strong negative reactivity coefficient [21].

The flexible operation of advanced water-cooled SMRs and of fast Generation-IV concepts is still under investigation and design, but the experience and the studies conducted on a French PWR operated in flexible mode show us that this capability is restrained after a planned periodic refuelling outage in a PWR or Boiling Water Reactor (BWR). During this period, it is necessary to increase the power slowly in a planned manner for fuel conditioning and for recalibration of instruments. Hence, it is not possible to operate the unit flexibly for several days, or even weeks. In addition, towards the end of the fuel cycle, the capability for flexible operation may be diminished, up to several weeks prior to the end of the cycle, because of the reduced reactivity margin in the core, the reduced boron concentration in the coolant or the conditioning of the fuel [22].

Scientific reports about PWR operated in a flexible mode show that for a PWR, changing from baseload to load following and frequency control operations puts the components under new kinds of stress. This mainly concerns the control rod drive mechanism (CRDM) and control rods, as well as the mechanical structures of the reactor coolant pressure boundary [22].

Besides, PWRs generally have a basic minimum capability of self-control: variations of temperature act on the moderation capability of the reactor coolant water in a self-controlled way. This property may lead to a perception that PWRs have some inherent capability to perform frequency control without a need for additional features. However, this self-control has limitations: as said, it is almost 0% of full rated thermal power for new fuel and, more on the long term, it depends on the boron concentration in the reactor coolant water. Another effect limiting the flexible operation of existing PWR is the Xenon accumulation during low power periods that counteract the eventual power ramp-up.

All this said, the ability of PWRs to load follow improves with low core power densities and shorter cores. Most PWR-based SMRs exhibit these characteristics. They can therefore be considered to offer the potential for an improved load following ability in comparison with large PWRs: they are expected to be stable against axial Xenon oscillations for core heights $< \sim 2.5$ m and local core power conditions may be less of an issue for SMRs, allowing load following over a wider power range and for the whole fuel lifetime. Further load following analysis is required on specific designs to expand the SMR load following capability compared with large reactors; if required to achieve faster ramp rates, an SMR's capability will have to be confirmed through more analysis and testing, covering fuel and controls. Furthermore, while large components have not been observed to experience fatigue failure due to load following within current limits, if the rate and magnitude of power changes were to increase or the number of cycles was to increase, there is the risk that large components may require more frequent replacement [23].

Regarding liquid metal SMRs, such as sodium- and lead-cooled reactors (SFRs and LFRs, respectively), they are expected to feature higher safety margins when operated in a flexible mode: they may have near zero burnup reactivity swing and strong negative temperature reactivity coefficients, can potentially withstand the potential for a wide range of core coolant temperature rises, and benefit from an absence of poisoning effects (such as Xenon poisoning) followed by positive reactivity insertion [4]. The strong negative temperature coefficient provides the basis for automatic load following in many new designs [24].

Further analysis and demonstration of flexible capability is required for Fast Generation-IV concepts as well as for PWR SMRs, but the experts' opinions converged on trusting the former as more capable of withstanding power cycling.

Regarding cogeneration options, PWRs are well suited to lower temperature applications only, while Fast SMRs have higher enthalpy in the secondary loop, and therefore have a wider market potential for cogeneration. The higher temperatures and alternative cycles of Fast SMRs (in terms of primary coolant technology) allow more efficient thermal storage of energy and are better suited to integrate with existing thermal storage systems (e.g., molten salt for thermal solar applications can be used as a coolant and energy storage medium at the same time).

More efficient use of fuel will decrease the exposure of Fast SMRs to fuel price volatility. Nevertheless, some experts point out that PWR fuel technology is well established and the risks of fuel fabrication cost are lower compared to those of Fast SMRs.

PWRs use a more established a technology, with probably fewer unforeseen outages than Fast Generation-IV designs. Light water SMRs have the lowest technological risk, but fast neutron reactors can be smaller, simpler and with longer operation before refuelling. Some lead-cooled reactors are designed to operate 15-20 years without refuelling, and are suitable for remote site or distributed generation while supporting alternative energy-intensive processes such as desalination (e.g., SSTAR, LeadCold) [25].

On the other hand, unplanned outages and their duration are perceived by the experts as relevant risk factors in Fast SMR operations (Fig. 11). Both SMR types (Fast and PWR) have a reduced number of active safety-related components, but still have a number of active/rotating components relevant for their operation (primary pumps, turbine, etc.). In this respect, corrosion of structural materials in Pb-alloy cooled nuclear reactors and in molten chloride and fluoride salts is a major aspect to consider for plant operations. The chemical control of sodium is an important issue as well: it is necessary to control oxygen (corrosion control), hydrogen (detection of the sodium-water reaction), and to a lesser degree carbon (carburization, decarburization phenomena) [26]. Finally, the fast neutron spectrum is expected to cause more damage (displacements-per-atom) in fuel and structural materials. Nevertheless, some experts highlight that the unplanned outages are expected to be reduced with operating experience in n^{th} -of-a-kind units of Fast SMRs.

Outage duration depends on the ease of repair (e.g., lead or sodium opaqueness and temperature complicate the task; opening for fuel handling is easy with PWRs while cleaning of LFR and SFR fuel is an issue) and of finding spare components (easier for PWRs, due to supply chain depth). Experts expect longer outage durations for Fast SMRs.

Fast SMRs are likely to offer higher robustness to natural events, with the possible exception of GFRs that may present the difficulty of ensuring sufficient cooling (decay heat removal) in extreme event conditions. The heat transfer coefficients of liquid metals in accident conditions are considered to be a risk-mitigating factor that has been highlighted by the expert panel. Additionally, for liquid metal cooled SMRs of the pool-type, large inventory of the primary coolant combined with its high volumetric heat capacity provides high thermal inertia, contributing to slow down of any heat-up transient.

On the other hand, heavy liquid metal cooled reactors are more sensitive to seismicity, due to the coolant density and SFRs have the risk of sodium reactions with air and water. In a pool type primary circuit LFR, seismic isolation systems can be used to reduce the structural stresses,

but its effect on sloshing of liquid metal requires separate evaluation to prevent structural failures, gas entrapment and potential core voiding; specific mitigation solutions need to be designed [27].

Security related to material diversion is particularly sensitive in reactors designed as breeders: on the one hand, fuel breeding reduces or eliminates the need of fuel enrichment facilities, thus enhancing proliferation resistance, but on the other hand, there are risk increases associated with the reprocessing facility necessitated by the closed fuel cycle goal. Other issues to be balanced and managed are high burn-up and plutonium production and core design: to be intrinsically more proliferation resistant and avoid potential diversion of separated plutonium, designs should ideally foresee core concepts without fertile blankets. The created Pu should be inside the fissile fuel and recycled by co-extraction with other actinides, without separation. Nevertheless, many fast Generation-IV concepts show advantages in terms of PR&PP (Proliferation Resistance and Physical Protection):

- the Molten Salt Fast Reactor (MSFR) has interesting characteristics from the viewpoint of proliferation resistance. Its fissile inventory is low due to a high-power density and the absence of excess fuel reactivity for operations. The fissile material is dissolved in small quantities in the fuel salt. To obtain the critical mass of fissile material would require a reprocessing system designed for a large amount of salt.
- In LFRs, the use of a mixed-oxide (MOX) fuel containing minor actinides (MAs) increases proliferation resistance; the long-life sealed core of some designs eliminates possibility of access by the operators. In addition, the small size of some “nuclear battery” concepts enables a small operational and security footprint. Suitable strategies can be implemented to allow safeguards: for instance, no dismantling activities of the active part of the European Lead-cooled System (ELSY) and European Lead Fast Reactor (ELFR) fuel assemblies are foreseen on the site. Likewise, for SSTAR, no dismantlement or fuel handling activities are anticipated at the reactor site, and furthermore the specialized equipment and trained staff required for refuelling would be retained by the reactor supplier organization and would not be present at the reactor location during normal operations [28].

PR&PP is a very complex issue that has to be evaluated in a comprehensive way, inside and beyond the plant fences and depends more on the very specific plant design rather than on the coolant type. In this first attempt to explore the opinion of an expert panel on the subject, without the chance of focusing on more precise information, experts have set security risk of Fast SMRs comparable to that of PWR SMRs.

The expert panel expectation on political support and public acceptance is higher for Fast SMRs, on account of more sustainable and efficient operation performance in terms of a closed fuel cycle, better resource exploitation and reduced inventory and lifetime of HLW.

5.3.4 D&D

On account of the experience accumulated with large PWRs, PWR SMRs are believed to present lower risk in the D&D phase, linked to regulatory issues, project management, on-site work and special dismantling techniques. Experience from the recent decommissioning of PWRs will help in better planning and reducing the project management risk for PWR SMRs. Conversely, there is no decommissioning experience on an industrial scale for Gen-IV technology. Cleaning of structures is not easy with LFRs or SFRs; project management and

decontamination strategies will be needed depending on the unique wastes created by special materials in Fast SMRs.

The majority of experts indicates that Fast SMRs entail lower risk in high level waste management (Fig. 12), which has been rated by the panel as the most relevant financial risk factor in the D&D lifecycle phase. As said, in the whole D&D phase, the need of unexpected solutions and options and unforeseen events might translate into extra costs. The back-end phase of the fuel cycle is perceived as a very sensitive one in this respect, especially considering that the plant owner liability has different extent in different countries. In a closed fuel cycle, the counterpart of higher costs for the fuel recycling is a reduced final stock of HLW from spent fuel, with lower and more controllable expenses for management and disposal. Differently from PWR SMRs, Fast SMRs will have reduced spent fuel inventory and lower long-term radiotoxicity (e.g., lower content of minor actinides in LFRs) that is expected to favour the economics of this phase.

It has to be said that many experts expressed their indecision in the rating of the two SMR technologies (rating = 4) with respect to several D&D risk factors, due to the lack of detailed information on the design of Fast SMRs, to the differences in the fast reactor types that may translate into different D&D practices and aspects, and to the general lack of experience in the D&D of commercial fast plants.

6. CONCLUSIONS AND FURTHER DEVELOPMENTS

This research focuses on the financial risk performance of Fast SMRs. In the liberalized electricity market, the realization of an investment project is based on the free initiative and willingness of investors to put their capital at risk. Any risk that prevents capital recovery and adequate remuneration is a threat. Over a given risk threshold, a project becomes infeasible for financial reasons, despite its technical feasibility. The issue is a very critical one for the successful transition of nuclear technology toward innovative concepts like Fast SMRs.

Since risk cannot be measured on an absolute scale, through direct quantitative indicators, a comparative assessment of Fast SMRs risk is done with the PWR SMR alternative technology and is based on the solicitation of the opinion of an expert panel.

The general results of the study show that Fast SMRs pay for the novelty of their concept in terms of higher financial risk perception.

Stakeholders such as the general public, government and regulatory authorities all have very limited knowledge of Fast SMR design features or phenomenology. New Generation-IV systems are expected to implement a closed fuel cycle, enhanced environmental sustainability, increased efficiency and fit with cogeneration options; these are factors in favour of general public acceptance and of potential government support. However, in the opinion of the expert panel regulatory activity and focus might be more intense on Generation-IV plants than on PWR SMRs with a direct consequence in terms of extra-time and cost of the project implementation. The same experts judge that Fast SMRs might experience a higher incidence of unexpected plant outages with an unfavourable impact on the financial risk during the plant operation.

Some options offer near-term technology solutions; some others are based on more innovative concepts and fuel cycles; the latter have to solve specific technology issues or decide between alternative technology options. For the purpose of this analysis, the technology readiness level

of Fast and PWR SMRs has been assumed to be equal, with both technologies ready for commercialization and first-of-a-kind deployment. Nevertheless, even in this hypothetical situation, the opinion of experts is that PWR SMRs can rely on the experience of conventional PWR technology and keep a competitive advantage in terms of operating risk perception over Fast SMRs. A certain degree of learning and supply chain infrastructure is believed to be transferable from Gen-III PWR plants to PWR SMRs.

On the other hand, fast nuclear power technology proposes innovations in core cooling, and for long-term applications, also in terms of fuel and fuel cycle technology. This translates in higher risk during the licensing process and higher variance of the expected construction cost, schedule, and procedures.

Concerning plant operations, according to the experts, Fast SMRs will be favoured in general public opinion, thanks to their intrinsic safety and sustainability, involving better use of resources and lower waste inventory, benefitting from the implementation of a closed fuel cycle. The operation of Fast SMRs supposed to ensure higher plant availability, efficiency, flexibility and lower exposure to fuel price, with an overall lower financial risk than PWR technology.

The above-mentioned risk-mitigating factors globally compensate higher expected risks of unplanned outages and outage duration, linked to the technology challenges of Fast SMR.

The risks of Fast SMRs are mainly related to the licensing and construction phase. These risks need to be overcome to lead to successful adoption and a virtuous operation phase.

The results of this preliminary financial risk assessment provide some indications to deal with the financial risk perception of Fast SMRs. Key recommendations focus on the information and communication effort, and on the technology demonstration program to increase the knowledge of these innovative systems performance. In particular, stakeholders are likely to be reassured about the unplanned outage probability and about the capability to tackle such outages with prompt repairs.

The higher risk perception associated with Fast SMRs in the critical construction phase is essentially motivated by “soft issues” such as supply chain planning, scarce knowledge/trust and lack of experience in project management.

In this situation, design soundness, communication and information can be part of the solution, but appropriate risk-compensation measures are needed to fill the gap with traditional nuclear plants. Free market rules are not efficient to allocate resources on long-term, strategic projects with high innovation content; market strategy always favours short-term return and lower risk projects. The high scale of the investment and the consequent long-term payback time involve too much risk, especially when operating performance has no track record to show. Public policies have started to reflect this consideration in countries that foster the nuclear power technology. Appropriate regulatory frameworks and government support packages are being envisaged to mitigate the investment risk in nuclear projects, in order to raise the amount of financing required.

Government protection/guarantee might offset low probability but high impact risk events (e.g., cost overruns beyond a certain cap, risks for which insurance is not available in the market, political risks, etc.).

New business models are envisaged to decrease the financial risk and secure the cash inflows [18, 29], such as Contract for Difference, Regulated Asset Base (RAB), the Mankala approach implemented at Olkiluoto-3, etc. These public policy instruments would be essential to reduce the financial risk perception of an investment in Fast SMRs, at least for the deployment of the first units of this new technology.

Finally, it has to be highlighted that this work is a preliminary exercise that presents a method for financial risk assessment and leads to general conclusions about Fast SMRs as a whole category. Nevertheless, each fast reactor system has its own specific benefits and challenges that has a different impact on the financial risk perception. This risk assessment method is intended to be better implemented in the compared analysis of the different specific Fast SMR designs, to draw more specific results and address the development and communication efforts in a more effective way.

ACKNOWLEDGEMENTS

The authors want to acknowledge the experts who supported the research with their contributions, for the time that they dedicated to provide their valuable opinions. This work was supported by the EU-US International Nuclear Energy Research Initiative (INERI) project 2016-002-E: Small Modular Lead-Cooled Fast Reactors in Regional Energy Markets: Safety, Security, and Economic Assessments.

REFERENCES

- [1] M. BERNADETE JUNKES, ANABELA P. TERESO, PAULO S.L.P. AFONSO, "The Importance of Risk Assessment in the Context of Investment Project Management: a Case Study", *Procedia Computer Science*, Vol. 64, Pages 902-910, 2015.
- [2] BROOKES, N., LOCATELLI, "Power plants as megaprojects: Using empirics to shape policy, planning, and construction management", *Utilities Policy*, vol. 36, pp. 57–66, 2015.
- [3] GRUBLER, A., "The costs of the French nuclear scale-up: A case of negative learning by doing", *Energy Policy*, vol. 38, pp. 5174–5188, 2010.
- [4] WNA. (2019, April) "Fast Neutron Reactors" [Online]. <https://www.world-nuclear.org/information-library/current-and-future-generation/fast-neutron-reactors.aspx> ; Updated December 2020.
- [5] AIDEN PEAKMAN, ROBERT GREGG, "The Fuel Cycle Implications of Nuclear Process Heat", *Energies* 2020, 13, 6073; November 2020.
- [6] IAEA, "Advances in Small Modular Reactor technology developments", 2020 Edition, a supplement to: "IAEA Advanced Reactors Information System (ARIS) ", Vienna, 2020.
- [7] DAHLGREN, E., LACKNER, K.S., GOCMEN, C., VAN RYZIN, G., "Small Modular Infrastructure", Columbia Business School, Decision, Risk & Operations Working Papers Series DRO-2012-03 , 2012.
- [8] EXPERT FINANCE WORKING GROUP, "Market framework for financing small nuclear", Department for Business, Energy and Industrial Strategy (BEIS), UK Government, A report to Her Majesty's Government by the Expert Finance Working Group on Small Nuclear Reactors 2018.
- [9] BOARIN, S., LOCATELLI, G., MANCINI, M., RICOTTI, M.E., "Financial Case Studies on Small- and Medium-Size Modular Reactors", *Nuclear Technology*, vol. 178, pp. 218-232, May 2012.
- [10] PETROVIC, B., MYCOFF, C.W., TRUCCO, P., RICOTTI, M.E., LOCATELLI, G., CARELLI, M.D., "Smaller sized reactors can be economically attractive", in *International Congress on Advances in Nuclear Power Plants (ICAPP)*, Nice (France), 2007.
- [11] KESSIDES, N., KUZNETSOV, V., "Small modular reactors for enhancing energy security in developing countries", *Sustainability*, vol. 4, no. 8, pp. 1806–1832, 2012.
- [12] LOCATELLI, G., MANCINI, M., RICOTTI, M.E., BOARIN, S., "Economics and financing of Small Modular Reactors (SMRs)", in *Handbook of Small Modular Nuclear Reactors*, MD and Ingersoll, DT Carelli, Ed. Cambridge, UK: Woodhead Publishing, 2014, pp. 239-277.
- [13] WNA, "Economics of Nuclear Power". [Online]. <https://www.world-nuclear.org/information-library/economic-aspects/economics-of-nuclear-power.aspx>; Updated March 2020.
- [14] LOCATELLI, G., MANCINI, M., "Competitiveness of Small-Medium, New Generation Reactors: A Comparative Study on Decommissioning", *Journal of Engineering for Gas Turbines and Power*, vol. 132, October 2010.
- [15] IAEA, "Financial aspects of decommissioning", TECDOC-1476, November 2005
- [16] World Nuclear News, "US nuclear construction project to be abandoned," *World Nuclear News*, August 2017.
- [17] Canadian Small Modular Reactor (SMR) Roadmap Steering Committee, "A Call to Action: A Canadian Roadmap for Small Modular Reactors," 2018.
- [18] ROQUES, F., FINON, D., "Contractual and financing arrangements for new nuclear investment in liberalized markets: Which efficient combination?", in *Security of Energy Supply in Europe: Natural Gas, Nuclear and Hydrogen*, Jean-Michel Glachant, Julián Barquin, Christian von Hirschhausen, Franziska Holz, William J. Nuttall François Lévêque, Ed. Cheltenham, UK: Edward Elgar Publishing Limited, 2010, pp. 117-135.
- [19] Nice Future initiative, "Flexible nuclear energy for clean energy systems", Technical Report, NREL/TP-6A50-77088, September 2020

- [20] ARNOLD GAD-BRIGGS, PERICLES PILIDIS, THEOKLIS NIKOLAIDIS, “Analyses of the Load Following Capabilities of Brayton Helium Gas Turbine Cycles for Generation IV Nuclear Power Plants”, *Journal of Nuclear Engineering and Radiation Science* 3(4), June 2017, DOI: 10.1115/1.4036983.
- [21] WNA, “Small Nuclear Power Reactors”, website ((URL: <https://www.world-nuclear.org/information-library/nuclear-fuel-cycle/nuclear-power-reactors/small-nuclear-power-reactors.aspx>), Updated December 2020
- [22] IAEA, “Non-baseload Operation in Nuclear Power Plants: Load Following and Frequency Control Modes of Flexible Operation”, 2018, Nuclear Energy Series No. NP-T-3.23, Vienna
- [23] Ernst & Young LLP, “Small modular reactors Can building nuclear power become more cost-effective?”, March 2016
- [24] IAEA, “Liquid Metal Cooled Reactors: Experience in Design and Operation”, Tecdoc-1569, 2007 Vienna
- [25] WNA, “Generation IV Nuclear Reactors”, website (URL: <https://www.world-nuclear.org/information-library/nuclear-fuel-cycle/nuclear-power-reactors/generation-iv-nuclear-reactors.aspx>), Updated December 2020
- [26] IAEA, “Challenges for Coolants in Fast Neutron Spectrum Systems”, Tecdoc-1912, Vienna 2020
- [27] Jeltsov, M., Villanueva, W., Kudinov, P. “Seismic Sloshing Effects in Lead-Cooled Fast Reactors”, International Conference on Fast Reactors and Related Fuel Cycles: Next Generation Nuclear Systems for Sustainable Development (FR17), report number IAEA-CN—245, 2017
- [28] GIF, “Proliferation Resistance and Physical Protection of the Six Generation IV Nuclear Energy Systems”, GIF/PRPPWG/2011/002, July 15, 2011
- [29] OECD/NEA, "Nuclear New Build: Insights into Financing and Project Management," Paris, NEA No. 7195, 2015.

MEETING PROGRAMME

MEETING ORGANIZATION

General Chair	Pietro Agostini
Honorary Chair	Georgii Toshinskii
Chair of Local Organizing Committee	Marco Ricotti
	Vladimir Kriventsev
Scientific Secretaries	Frederik Reitsma
	Chirayu Batra

METING SESSIONS

The contributions to the meeting are classified into four major areas, and the meeting was divided into following four session:

Session I: Sodium cooled fast SMRs

PaperID	Title	Presenter	Country	Org
6	Large Eddy Simulation of Thermal Striping in the Upper Internal Structure of the Prototype Gen-IV Sodium-cooled Fast Reactor	Mr Dehee Kim	Korea, Rep. of	KAERI
10	SMR CADOR: an inherently safe small SFR as a response to the dilemma 'safety vs cost'	Mr Paul Gauthé	France	CEA/GIF
23	Feasibility study of small sodium cooled fast reactors	Mr Hiroki Hayafune	Japan	JAEA
27	A preliminary study of autonomous and ultra-long life hybrid micro-modular reactor cooled by sodium heat pipes	Mr Seoungdong Jang	Korea, Rep. of	KAIST
16	Evaluation of potential safety and economic benefits and challenges of modular sodium-cooled fast reactors	Mr Iurii Ashurko	Russia	IPPE

Session II: Heavy Liquid Metal Cooled Fast SMRs

PaperID	Title	Presenter	Country	Org
1	Validation of thermal hydraulic design support and safety methodology and application to sealer	Mr Ferry Roelofs	Netherlands	NRG
2	LFR-SMR: Affordable solutions for multiple needs	Mr Luciano Cinotti	Luxembourg	Hydromine
4	Inherent Self-Protection, Passive Safety and Competitiveness of Small Power Modular Fast Reactor SVBR-100	Mr Georgii Toshinskii	Russia	AKME-Engineering
7	CLFR-300, an Innovative Lead-cooled Fast Reactor Based on Natural-driven Safety Technologies	Mr Zhao Chen	China	CGN
15	Conceptual design of china lead-based mini-reactor clear-m10d	Mr Chao Liu	China	INEST
24	Lead fast reactor technology: A promising option for SMR application	Mr Giacomo Grasso	Italy	ENEA
29	Preliminary conceptual design of lead-cooled small fast reactor core for icebreaker	Mr Deok Jung Lee	Korea, Rep. of	UNIST
30	SEALER-UK: a 55 MW(e) lead-cooled reactor for commercial power production	Mr Janne Wallenius	Sweden	KTH

Session III: Safety aspects of fast SMRs

PaperID	Title	Presenter	Country	Org
3	Experience in physics design and safety analysis of small and medium sized FBRs	Mr Riyas Abdul Salim	India	IGCAR
8	Innovative modelling approaches for molten salt small modular reactors	Mr Eric Cervi	Italy	POLIMI
25	Numerical assessment of sodium fire incident	Mr Takashi Takata	Japan	JAEA
26	ALFRED protected loss of flow accident experiment in CIRCE facility	Mr Fabio Giannetti	Italy	La Sapienza
28	A Passive Safety Device for SFRs with Positive Coolant Temperature Coefficient	Mr Chihyung Kim	Korea, Rep. of	KAIST

Session IV: Technology and Research in Support of SMR Development

PaperID	Title	Presenter	Country	Org
5	MYRRHA technology and research facilities in support of heavy liquid metal SMR fast reactors	Mr Rafael Fernandez	Belgium	SCK•CEN
9	A multiphysics approach to LFR analysis	Mr Marco Sumini	Italy	University of Bologna
18	Introduction of the U.S. DOE Versatile Test Reactor Project	Mr Florent Heidet	USA	ANL
21	Estimation of minimal critical size of bare iso-breeding core for 8 selected fast reactors in Th-U and U-Pu fuel cycles	Mr Jiri Krepel	Switzerland	PSI
22	A characterization of the financial risk profile of fast SMRs	Ms Sara Boarin	Italy	POLIMI

GROUP DISCUSSIONS

<i>Group Discussion</i>	<i>Title</i>	<i>Chair</i>
Group Discussion I	In-factory construction	Janne Wallenius
Group Discussion II	Technological challenges to be resolved	Vladimir Kriventsev
Group Discussion III	Benefits of fast SMRs including market needs	Marco Ricotti

INTERNATIONAL ADVISORY GROUP

<i>Name</i>	<i>Organization</i>	<i>Country</i>
Mr Alessandro Alemberti	Ansaldo Nucleare S.p.a	Italy
Mr Didier DE BRUYN	SCK•CEN	Belgium
Mr Donghui Zhang	CIAE	China
Mr Ferry Roelofs	NRG	Netherlands
Mr Georgy Toshinsky	IPPE	Russia
Mr Giacomo Grasso	ENEA	Italy
Mr Haileyesus Tsige-Tamirat	JRC	EC
Mr Jaehyuk Eoh	KAERI	Korea, Rep. of
Mr Joel Guidez	CEA/GIF	France
Mr Kamil Tucek	JRC	EC
Mr Karl-Fredrik Nilsson	JRC	EC
Mr Luciano Cinotti	Hydromine	Luxembourg
Mr Mariano Tarantino	ENEA	Italy
Mr Paul Schuurmans	SCK CEN	Belgium
Mr Pietro Agostini	ENEA	Italy
Mr Sergii Fomin	KIPT	Ukraine
Mr Yican Wu	INEST	China
Mr Zhao Chen	CGN	China
Mr Zoltan Szaraz	JRC	EC

LIST OF PARTICIPANTS

BELGIUM

Fernandez, R.	SCK•CEN
De Bruyn, D.	SCK•CEN
Anton, G. R.	Bel V
Malicki, M.	Tractebel (ENGIE)

CHINA

Liu, Y.	China Institute of Atomic Energy (CIAE)
Ren, L.	China Institute of Atomic Energy (CIAE)
Chen, Z.	China General Nuclear Power Group (CGNPG)
Liu, C.	Institute of Nuclear Energy Safety Technology, Chinese Academy of Science (INEST CAS)

EUROPEAN COMMISSION

Tucek, K.	Joint Research Centre, European Commission (EC/JRC)
-----------	---

FRANCE

Gauthé, P.	Commissariat à l'énergie atomique et aux énergies alternatives (CEA)
------------	--

GERMANY

Klein-Hesling, W.	Gesellschaft für Anlagen und Reaktorsicherheit (GRS)
Rineiski, A.	Karlsruher Institut für Technologie (KIT)

INDIA

Salim, R.A.	Indira Gandhi Centre for Atomic Research (IGCAR)
-------------	--

ITALY

Grasso, G.	Italian National Agency for New Technologies, Energy and Sustainable Economic Development (ENEA)
Agostini, P.	Italian National Agency for New Technologies, Energy and Sustainable Economic Development (ENEA)
Ricotti, M.	Politecnico di Milano (POLIMI)

Meloni, P.	Italian National Agency for New Technologies, Energy and Sustainable Economic Development (ENEA)
Cammi, A.	Politecnico di Milano (POLIMI)
Boarin, S.	Politecnico di Milano (POLIMI)
Sumini, M.	Università di Bologna (UNIBO)
Lanconelli, M.	Università di Bologna (UNIBO)
Cervi, E.	Politecnico di Milano (POLIMI)
Lorenzi, S.	Politecnico di Milano (POLIMI)
Giannetti, F.	La Sapienza University of Rome (UNIROMA)

JAPAN

Yamaguchi, A.	The University of Tokyo
Takata, T.	Japan Atomic Energy Agency (JAEA)
Hayafune, H.	Japan Atomic Energy Agency (JAEA)

REPUBLIC OF KOREA

Kim, Y.	Korea Advanced Institute of Science and Technology (KAIST)
Kim, D.	Korea Atomic Energy Research Institute (KAERI)
Kim, Ch.	Korea Advanced Institute of Science and Technology (KAIST)
Jang, S.	Korea Advanced Institute of Science and Technology (KAIST)

LUXEMBOURG

Cinotti, L.	Hydromine Nuclear Energy Sàrl
-------------	-------------------------------

NETHERLANDS

Zwijssen, K.	NRG
--------------	-----

RUSSIAN FEDERATION

Toshinskii, G.	JSC “AKME-engineering”
Rtishchev, N.	Rosatom Overseas
Levchenko, A.	Simulation Systems Ltd. (SSL)

SWEDEN

Wallenius, J.

Royal Institute of Technology (KTH)

SWITZERLAND

Krepel, J.

Paul Scherrer Institute (PSI)

USA

Heidet, F.

Argonne National Laboratory (ANL)

IAEA

Kriventsev, V.

International Atomic Energy Agency (IAEA)

CONTRIBUTORS TO DRAFTING AND REVIEW

Agostini, P.	Italian National Agency for New Technologies, Energy and Sustainable Economic Development (ENEA), Italy
Anton, G. R.	Bel V, Belgium
Ashurko [†] , Y.	Institute of Physics and Power Engineering (IPPE), Russia
Batra, C.	International Atomic Energy Agency (IAEA)
Boyer, B.	International Atomic Energy Agency (IAEA)
Boarin, S.	Politecnico di Milano (POLIMI), Italy
Cammi, A.	Politecnico di Milano (POLIMI), Italy
Cervi, E.	Politecnico di Milano (POLIMI), Italy
Chen, Z.	China General Nuclear Power Group (CGNPG), China
Cinotti, L.	Hydromine Nuclear Energy Sàrl, Luxembourg
De Bruyn, D.	SCK*CEN, Belgium
Fernandez, R.	SCK*CEN, Belgium
Gauthé, P.	Commissariat à l'énergie atomique et aux énergies alternatives (CEA), France
Giannetti, F.	La Sapienza University of Rome (UNIROMA), Italy
Grasso, G.	Italian National Agency for New Technologies, Energy and Sustainable Economic Development (ENEA), Italy
Hayafune, H.	Japan Atomic Energy Agency (JAEA), Japan
Heidet, F.	Argonne National Laboratory (ANL), USA
Jang, S.	Korea Advanced Institute of Science and Technology (KAIST), Republic of Korea
Calle Vives, P.	International Atomic Energy Agency (IAEA)
Kim, Ch.	Korea Advanced Institute of Science and Technology (KAIST), Republic of Korea

[†] Deceased

Kim, D.	Korea Atomic Energy Research Institute (KAERI), Republic of Korea
Kim, Y.	Korea Advanced Institute of Science and Technology (KAIST), Republic of Korea
Klein-Hesling, W.	Gesellschaft für Anlagen und Reaktorsicherheit (GRS), Germany
Korinny, A.	International Atomic Energy Agency (IAEA)
Krepel, J.	Paul Scherrer Institute (PSI), Switzerland
Kriventsev, V.	International Atomic Energy Agency (IAEA)
Lanconelli, M.	Università di Bologna (UNIBO), Italy
Levchenko, A.	Simulation Systems Ltd. (SSL), Russia
Liu, C.	Institute of Nuclear Energy Safety Technology, Chinese Academy of Science (INEST CAS), China
Liu, Y.	China Institute of Atomic Energy (CIAE), China
Lorenzi, S.	Politecnico di Milano (POLIMI), Italy
Mahanes, J.	International Atomic Energy Agency (IAEA)
Malicki, M.	Tractebel (ENGIE), Belgium
Meloni, P.	Italian National Agency for New Technologies, Energy and Sustainable Economic Development (ENEA), Italy
Reitsma, F.	International Atomic Energy Agency (IAEA)
Ren, L.	China Institute of Atomic Energy (CIAE), China
Ricotti, M.	Politecnico di Milano (POLIMI), Italy
Rineiski, A.	Karlsruher Institut für Technologie (KIT), Germany
Rtishchev, N.	Rosatom Overseas, Russia
Salim, R.A.	Indira Gandhi Centre for Atomic Research (IGCAR), India
Sumini, M.	Università di Bologna (UNIBO), Italy
Takata, T.	Japan Atomic Energy Agency (JAEA), Japan
Toshinsky, G.	JSC “AKME-engineering”, Russia
Tucek, K.	Joint Research Centre, European Commission (EC/JRC)

Wallenius, J.	Royal Institute of Technology (KTH), Sweden
Yamaguchi, A.	The University of Tokyo, Japan
Zeman, M.	International Atomic Energy Agency (IAEA)
Zwijnsen, K.	NRG, Netherlands



ORDERING LOCALLY

IAEA priced publications may be purchased from the sources listed below or from major local booksellers.

Orders for unpriced publications should be made directly to the IAEA. The contact details are given at the end of this list.

NORTH AMERICA

Bernan / Rowman & Littlefield

15250 NBN Way, Blue Ridge Summit, PA 17214, USA

Telephone: +1 800 462 6420 • Fax: +1 800 338 4550

Email: orders@rowman.com • Web site: www.rowman.com/bernan

REST OF WORLD

Please contact your preferred local supplier, or our lead distributor:

Eurospan Group

Gray's Inn House

127 Clerkenwell Road

London EC1R 5DB

United Kingdom

Trade orders and enquiries:

Telephone: +44 (0)176 760 4972 • Fax: +44 (0)176 760 1640

Email: eurospan@turpin-distribution.com

Individual orders:

www.eurospanbookstore.com/iaea

For further information:

Telephone: +44 (0)207 240 0856 • Fax: +44 (0)207 379 0609

Email: info@eurospangroup.com • Web site: www.eurospangroup.com

Orders for both priced and unpriced publications may be addressed directly to:

Marketing and Sales Unit

International Atomic Energy Agency

Vienna International Centre, PO Box 100, 1400 Vienna, Austria

Telephone: +43 1 2600 22529 or 22530 • Fax: +43 1 26007 22529

Email: sales.publications@iaea.org • Web site: www.iaea.org/publications

**International Atomic Energy Agency
Vienna**